

Technical University of Košice



Faculty of Electrical Engineering
and Informatics

SCYR

25th Scientific Conference of Young Researchers
Proceedings from Conference

ISBN 978-80-553-4826-1

2025

Sponsors & Organizers



Fakulta elektrotechniky
a informatiky



B/S/H/



SCYR 2025: 25th Scientific Conference of Young Researchers
Proceedings from Conference

Published: Faculty of Electrical Engineering and Informatics
Technical University of Košice
Edition I, 192 pages, Available Online

Editors: Assoc. Prof. Ing. Karol Kyslan, PhD.
Assoc. Prof. Ing. Emília Pietriková, PhD.
Ing. Lukáš Pancurák

ISBN 978-80-553-4826-1

Scientific Committee

General chair: Prof. Ing. Liberios Vokorokos, PhD.

Editorial board chairman: Assoc. Prof. Ing. Karol Kyslan, PhD.

Committee Members:

Ing. Martin Čertický, PhD., Caterpillar Slovakia
Ing. Tibor Gujdán, FPT Slovakia
Ing. Juraj Bujňák, PhD., Siemens Healthineers
Ing. Alexander Revák, Magna Electronics Slovakia
Ing. Ján Šepeľa, BSH Drives and Pumps
Prof. RNDr. Vladimír Lisý, DrSc.
Assoc. Prof. František Babič, PhD.
Assoc. Prof. Eva Chovancová, PhD.
Assoc. Prof. Jaroslav Džmura, PhD.
Assoc. Prof. Peter Feciľak, PhD.
Assoc. Prof. Stanislav Ondáš, PhD.
Assoc. Prof. Peter Papcun, PhD.
Assoc. Prof. Emília Pietriková, PhD.
Assoc. Prof. Matúš Pleva, PhD.
Assoc. Prof. Ing. Marek Pástor, PhD.
Assoc. Prof. Ján Papaj, PhD.

Organizing Committee

Members: Assoc. Prof. Ing. Karol Kyslan PhD.
Assoc. Prof. Ing. Emília Pietriková, PhD.
Ing. Ivana Olšiaková
Ing. Viliam Balara
Ing. Nikola Geciová
Ing. Matej Hric
Ing. Eva Kupcová
Ing. Richard Král
Ing. Peter Nemergut
Ing. Lukáš Pancurák
Ing. Simona Šaparová

Contact address: Faculty of Electrical Engineering and Informatics
Technical University of Košice
Letná 9
040 01 Košice
Slovak Republic

Proceedings Reviewers

Norbert Ádám	Vladimir Lisy
Ján Bačík	Lubomír Livovský
Michaela Bačíková	Oliver Lohaj
Anton Baran	Branislav Madoš
Lubomír Beňa	Ján Magyar
Matej Bereš	Marian Mach
Anna Biceková	Dusan Medved
Peter Bober	Miroslav Michalko
Samuel Bucko	Matus Molcan
Gabriel Bugar	Monika Molnárová
Marek Bundzel	Jozef Onufer
Peter Butka	Luboš Ovseník
Zsolt Čonka	Jan Paralic
Peter Drotár	Marek Pástor
Milos Drutarovsky	Marek Pavlík
Frantisek Durovsky	Daniela Perdukova
Jaroslav Džmura	Ján Perháč
Peter Fecilák	Emília Pietriková
Pavol Fedor	Marek Ružička
Ján Genči	Martin Sarnovsky
Peter Girovský	Peter Sincak
Peter Gnip	Natalia Smidova
Filip Gurbál	Ján Staš
Milan Guzan	William Steingartner
Renát Haluška	Matúš Sulír
Máté Hireš	Csaba Szabó
Daniel Hládek	Martina Szaboova
Sergej Chodarev	Slavomír Šimoňák
Eva Chovancova	Eugen Šlapak
Ondrej Kainz	Viktor Šlapák
Erik Kajáti	Róbert Štefko
Ján Kaňuch	Martin Tomášek
Jozef Király	Jana Tóthová
Mária Kladivová	Ján Vaščák
Štefan Korečko	Igor Vehec
Ondrej Kováč	Marcel Vološin
Jozef Kravčák	Jan Zbojovsky
Karol Kyslan	Ján Ziman
Milan Lacko	Iveta Zolotova
Tomáš Lenger	Jaroslava Žilková

Foreword

Dear Colleagues,

SCYR (Scientific Conference of Young Researchers) is a scientific event focused on exchange of information among young researchers from Faculty of Electrical Engineering and Informatics at the Technical University of Košice – series of annual events that was founded in 2000. Since 2000, the conference has been hosted by FEEI TUKE with rising technical level and unique multicultural atmosphere. The 25th Scientific Conference of Young Researchers (SCYR 2025) was held on April 11, 2025 at University Conference Centre, Technical University of Košice. The mission of the conference, to provide a forum for dissemination of information and scientific results relating to research and development activities at the Faculty of Electrical Engineering and Informatics, has been achieved. In total 56 participants presented their papers during the conference.

Faculty of Electrical Engineering and Informatics has a long tradition of students participating in skilled labor where they have to apply their theoretical knowledge. SCYR is an opportunity for doctoral and graduating students to train their scientific knowledge exchange. Nevertheless, the original goal is still to represent a forum for the exchange of information between young scientists from academic communities on topics related to their experimental and theoretical works in the very wide spread field of a wide spectrum of scientific disciplines like informatics sciences and computer networks, cybernetics and intelligent systems, electrical and electric power engineering and electronics.

Traditionally, contributions was divided in 3 categories:

- Electrical & Physical Engineering,
- Artificial Intelligence,
- Computer Science,

with approx. 56 technical papers dealing with research results obtained mainly in the University environment. This day was filled with a lot of interesting scientific discussions among the junior researchers and graduate students, and the representatives of the Faculty of Electrical Engineering and Informatics. This scientific network included various research problems and education, communication between young scientists and students, between students and professors. Conference was also a platform for student exchange and a potential starting point for scientific cooperation. The results presented in papers demonstrated that the investigations being conducted by young scientists are making a valuable contribution to the fulfillment of the tasks set for science and technology at the Faculty of Electrical Engineering and Informatics at the Technical University of Košice.

We want to thank all participants for contributing to these proceedings with their high quality manuscripts. We hope that conference constitutes a platform for a continual dialogue among young scientists.

It is our pleasure and honor to express our gratitude to our sponsors and to all friends, colleagues and committee members who contributed with their ideas, discussions, and sedulous hard work to the success of this event. We also want to thank our session chairs for their cooperation and dedication throughout the entire conference.

Finally, we want to thank all the attendees of the conference for fruitful discussions and a pleasant stay in our event.

Liberios VOKOROKOS
Dean of FEEI TUKE

April 11, 2025, Košice

Contents

Ladislav Hric

Object detection systems for unmanned aerial vehicles 10

Lukáš Tomaščík

Current Trends in Modeling and Simulation of Complex Physical Systems with Neural Networks 14

Tomáš Kormaník

Towards IoT Education Evolution 18

Tadeáš Kmecik

Analysis of Improvement Possibilities for Sensorless Control of a BLDC Motor Using AI 21

Marek Horváth

Programmer Identification Based on Source Code Stylometric Analysis and Behavioral Biometrics 23

Peter Pekarčík

Implementation of PQC algorithm for IoT devices 26

Nikola Geciová

Optimization of Discrete-event Systems 28

Antónia Kováčová

Sparse Wars: Nyquist Strikes Back 32

Tomáš Basarik

Decoupling Control of TAB Converter 34

Marek Bobček

Power System Protection Based on Virtual Protection and WAMS 36

Miroslav Jusko

Overview of Sensors for Biosignal Measurement 39

Richard Král

Design and Implementation of a Device for Supporting the Visually Impaired with a Focus on Spatial Orientation 43

Renáta Runsáková

Solving optimization and search problems using D-Wave Systems' Quantum Annealer 48

Dominika Líšková

Modelling and Analysis of Cyber-Physical Systems 52

Daniel Gordan

Achieving Maximum Efficiency: Critical Factors for Optimizing Phase-Shifted Full-Bridge (PSFB) Converter 56

Jozef Badár

Artificial Intelligence in Routing for Mobile Multi-Hop Networks in 6G: A Comprehensive Review 58

Kristián Eliáš

Research on the possibilities of increasing the integration of renewable energy sources into the electric power system 63

Július Šimčák

<i>Dynamic Allocation of Electric Power Capacities</i>	67
Simona Saporová	
<i>Effect of halloysite content on the quality and mechanical properties of thermoplastic starch-based material</i>	71
Matúš Dopiriak	
<i>Video Compression Using Radiance Fields for V2I Communication</i>	74
Miroslav Imrich	
<i>Optimizing Wireless Robotics Using NeRF and RIS</i>	76
Martin Nguyen	
<i>Correlation Between AMS-02 Data and Space Weather Parameters for Machine Learning Prediction</i> 80	
Peter Nemergut	
<i>Power Module Packaging Technology Trends</i>	83
Daniel Marcin	
<i>Hardware Construction of Capacitor-Based Active Cell Balancer</i>	87
Dmytro Miakota	
<i>Structural Transitions in Ferronematics Under Electric and Magnetic Fields</i>	90
Martin Eliáš	
<i>Effect of magnetic anisotropies on the properties of magnetic microwires</i>	93
Eva Kupcova	
<i>Applications of Homomorphic Encryption in Biometric Data Protection</i>	97
Jaroslav Marko	
<i>Intrusion Detection Systems and Attack Graphs</i>	99
Miroslava Matejová	
<i>Use of XAI methods and its evaluation in various domains</i>	103
Matej Hric	
<i>Digital twin of mechatronic system: An Overview</i>	106
Sylvia Maťašová	
<i>Research and development of artificial intelligence for document indexing and structuring</i>	110
Róbert Rauch	
<i>Split Computing and Early Exiting for Computer Vision Tasks in Autonomous Vehicles</i>	115
Lenka Bubeňková	
<i>Cybersecurity Awareness Through Gamification</i>	118
Tomáš Buček	
<i>Automated Knowledge Evaluation in Software Engineering Disciplines</i>	122
Kristian Sopkovic	
<i>Data Augmentation with Large Language Models for Minority Languages: A Review</i>	125
Samuel Novotný	
<i>Implementation Potential of Transparent Intensional Logic in Multi-Agent System Communication</i> 129	

Peter Popřík	
<i>Procedural Content Generation in Computer Graphics – A Survey</i>	131
Kamil Sevc	
<i>Photovoltaic Systems and Their Influence on Power System Management</i>	135
Ardian Hyseni	
<i>Effectiveness Limits of Benford’s Law</i>	139
Heidar Khorshidiyeh	
<i>CC 6D SVT: Child Node Mask Compression of 6Dimensional Sparse Voxel Trees</i>	142
Maroš Krupáš	
<i>Human-Machine Collaboration and Artificial Intelligence in Industry 5.0</i>	145
Viliam Balara	
<i>Multimodal Detection of Toxic Behavior in Social Media</i>	147
Lubomír Urblík	
<i>Exploring the Potential of Docker for Edge AI and IoT Applications</i>	151
František Margita	
<i>Calculation of Transient Dynamic Ampacity in the Conditions of the Slovak Electricity Transmission System</i>	153
Miroslav Murin	
<i>Phishing Vishing and Deepfake Attacks in the Context of Emerging Cyber Threats</i>	156
František Kurimský	
<i>Electricity price prediction: Overview, data analysis and future research</i>	159
Erika Abigail Katonová	
<i>Innovations and perspectives in Software-Defined Networking</i>	163
Kristián Glajc	
<i>High-Speed Imaging of Streamer Propagation in Nano-Functionalized Transformer Oils</i>	166
Kristina Zolocheska	
<i>Shielding properties and radiation modification of magnetic nanoparticle-functionalized textiles</i>	171
Lenka Kališková	
<i>Analysis of multiple machine learning approaches in astrophysics</i>	174
Leoš Ondriš	
<i>Thermal stability of thermoplastic starch blends with lignin</i>	177
Lukáš Pancurák	
<i>Experimental Validation of Direct Speed Predictive Control</i>	180
Dušan Čatloch	
<i>Malware threat detection using artificial intelligence and machine learning methods</i>	182
Ivana Nováková	
<i>Advanced Physical Approaches to Presenting Physical Phenomena Using AR</i>	187
Author’s Index	190

Object detection systems for unmanned aerial vehicles

¹Ladislav Hric (1st year),
Supervisor: ²Daniela Perduková

^{1,2}Dept. of Electrical Engineering and Mechatronics, FEI, Technical University of Košice, Slovak Republic

¹ladislav.hric@tuke.sk, ²daniela.perdukova@tuke.sk

Abstract—Object detection in unmanned aerial vehicles (UAVs) has gained significant attention due to its practical applications in various fields, including surveillance, reconnaissance, search and rescue, and infrastructure inspection. Advancements in convolutional neural networks (CNNs) have led to the development of relatively precise and fast detection algorithms that can be deployed in diverse scenarios. Despite these improvements, several limitations and challenges remain when implementing object detection systems in UAVs. This paper first examines the general challenges of object detection systems and then highlights the specific issues associated with their use in UAV applications. Additionally, the paper discusses dataset creation, data augmentation techniques, image preprocessing, and evaluation metrics used to assess object detection performance. Finally, potential future research directions in this field are considered.

Keywords—computer vision, convolutional neural network, unmanned aerial vehicle, object detection.

I. INTRODUCTION

This paper focuses on the challenges of object detection in unmanned aerial vehicle (UAV) systems. Object detection is a computer vision technique that utilizes convolutional neural networks to extract essential information from input images. Significant advancements have been made in this field over the past decades; however, there is still considerable room for improvement in addressing its limitations.

The importance of these systems is undeniable, as they are widely used in modern applications. This technique has achieved great success in military drones [1] for surveillance, reconnaissance [2], enemy tracking [3], and identifying potential threats. In civilian applications, UAVs equipped with object detection technology assist in search and rescue missions [4] by identifying people in remote or disaster-stricken areas, optimizing farming practices by monitoring crop health [5], and improving traffic flow analysis [6].

It is important to note that object detection from aerial perspectives differs from traditional ground-based detection. One of the main challenges is developing effective models capable of detecting very small objects from above, Fig. 1. As altitude increases, models must analyze progressively smaller objects that blend into the background. Additionally, densely packed objects can pose difficulties for convolutional neural networks. Hardware limitations also need to be taken into account. These challenges, along with many others, will be reviewed in this paper, summarizing key challenges, recent achievements, and potential directions for future research.

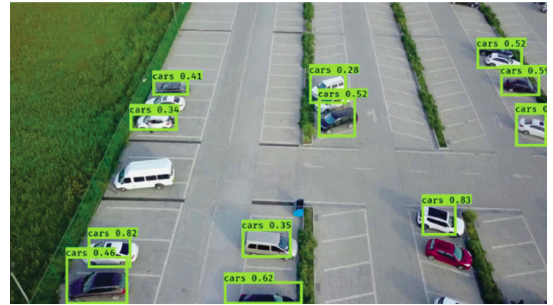


Fig. 1: Single-shot object detection [7].

II. OBJECT DETECTION

Object detection is a computer vision technique used for localizing and identifying objects. The inputs of these systems are images or video frames. These systems use machine learning and deep neural networks to accomplish these tasks. Over the years, many object detection models have been researched. The development of new detectors and the improvement of existing ones are essential for advancing object detection and classification tasks. The output of an object detector consists of a bounding box that defines the region of an image containing the detected object, a class label, and a confidence score, typically ranging from 0 to 1. Ground-truth annotations, which include manually labeled bounding boxes and class labels, serve as reference data for training and evaluating detection models.

A. Metrics

One of the most important aspects of object detector development is the assessment of its performance [9], considering various factors. This paper discusses one of the most widely used and popular detection evaluation metrics. Intersection over Union (IoU) measures the overlap between predicted and ground-truth bounding boxes,

$$IoU = \frac{\text{area of overlap}}{\text{area of union}}. \quad (1)$$

Precision assesses the model's detection accuracy and indicates how many detections were correct. It is calculated as follows:

$$Pr = \frac{TP}{TP + FP}, \quad (2)$$

where TP is the number of true positives, meaning the model correctly identifies an object as present, and this object actually exists according to ground-truth data.

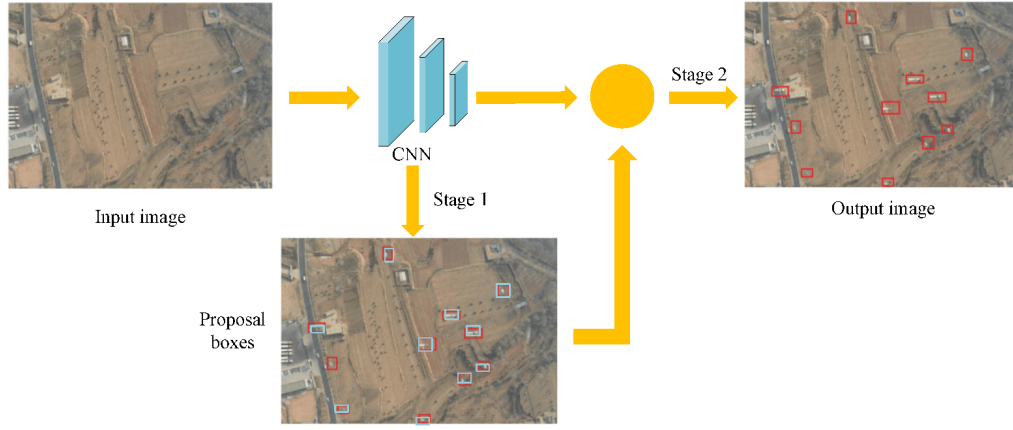


Fig. 2: Two-shot object detection [8].

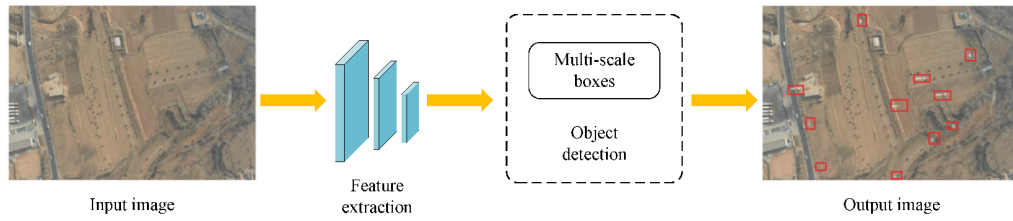


Fig. 3: Single-shot object detection [8].

FP is the number of false positives, meaning the detector identifies an object that is not actually present. Another essential metric is Recall, which measures the model's ability to correctly identify all instances of a given class. Recall is calculated using the following formula:

$$Rc = \frac{TP}{TP + FN}, \quad (3)$$

where FN is the number of false negatives, meaning the model missed objects.

The next metric discussed in this paper is the $F1$ Score, which calculates the harmonic mean of precision and recall, providing a balanced assessment of the model's performance:

$$F1 = 2 \frac{Pr \cdot Rc}{Pr + Rc} = \frac{TP}{TP + \frac{FN + FP}{2}}. \quad (4)$$

Another frequently used metric is Average Precision (AP), which computes the area under the precision-recall curve and encapsulates the model's precision and recall performance. For multi-class object detection scenarios, Mean Average Precision (mAP) is used. It calculates the AP values across all object classes the model can detect. A commonly used extended version of mAP is mAP50-95, which provides a more comprehensive evaluation. It assesses the model at multiple levels of IoU , ranging from 0.5 to 0.95.

Object detection algorithms

Object detectors can be classified into two main categories based on their approach to accomplishing the task. Two-shot detection models process an image in two stages, as shown in Fig. 2. The first stage focuses on proposing a series of bounding boxes that could contain an object, while the second stage classifies those regions and refines the location prediction. In general, these detectors are considered more precise than single-shot detectors but are slower. The most

well-known two-shot detection algorithms are R-CNN, Fast R-CNN [10], and Faster R-CNN, though various variants and alternatives exist.

In contrast, single-shot detectors omit the regional proposal stage and perform localization and classification simultaneously, Fig. 3. These models are generally faster than two-shot detectors but tend to have slightly lower accuracy. However, they are more suitable for real-time systems while still achieving good accuracy. The two most commonly mentioned single-shot detectors are SSD (Single Shot Detector) [11] and YOLO (You Only Look Once) [12].

Dataset

Object detection models must be trained on a set of images to learn how to extract features, accurately detect objects, and assign them to the proper class. The dataset is crucial, as the model's quality heavily depends on it. It must be designed according to the application and include a diverse set of images representing the objects the detector should recognize. Objects should be captured from various angles and under different lighting conditions. It is essential to train the model on diverse scenarios so it can generalize well and recognize objects even in conditions not explicitly covered by the dataset.

Data augmentation

In practice, it is difficult to capture objects in all possible conditions, especially for uncommon objects. In such cases, data augmentation becomes useful. Augmentation is a technique used to expand the original dataset by modifying images. Examples of augmentation techniques include rotation and shearing of existing images, allowing the model to learn how objects appear from different angles. Another beneficial approach is adding noise to images, helping the model handle sensor imperfections. This can be done by introducing random

black and white pixels into the images. There are many other augmentation techniques that can enhance datasets and better prepare the model for diverse real-world scenarios.

Image preprocessing

Another important step is image preprocessing. Unlike augmentation techniques, preprocessing does not expand the original dataset. Instead, it focuses on manipulating input data to improve efficiency and speed up model inference and training. One of the most common preprocessing techniques is resizing images, as models tend to learn faster with smaller inputs. Contrast adjustment is also crucial for object detection, as it enhances edges, making them easier for neural networks to recognize. If color information is not necessary, all images in the dataset can be converted to grayscale. This simplifies the training process by allowing the model to focus on shapes while reducing computational complexity. Since a grayscale image contains only one color channel instead of three, this preprocessing step makes the model more efficient and faster. There are many preprocessing techniques, and their choice should depend on the application.

III. UAV OBJECT DETECTION

Object detection technology has made remarkable progress, however, most research focuses on analyzing videos and images captured from the ground. When applied to unmanned aerial vehicles (UAVs), object detection introduces new challenges compared to conventional ground-based detection. Developing detection systems for UAV applications requires addressing not only software-related challenges but also hardware constraints. Some of the most important challenges are discussed in this section.

Computing resources

While ground-based devices can use powerful computing hardware without space constraints, drones must consider several limitations. The most limiting factors in UAV-based object detection include drone dimensions, battery capacity, and processor weight, making system design more complex. Drones can transmit data to external devices, such as ground stations, which provide greater computational power for higher accuracy and deeper analysis. However, this introduces latency due to data transmission. On the other hand, onboard detection is better suited for real-time systems where speed is a critical requirement, but limited computational resources often result in lower precision. In research [13], detection models like YOLO, SSD and Faster RCNN were optimized for cross-edge platforms such as the NVIDIA Jetson Xavier, NVIDIA Jetson Nano, and Intel's Neural Compute Stick 2. In paper [14], an approach is proposed to enhance the visual capabilities of a UAV system for recognizing landing spots using a YOLO detector and an NVIDIA JetsonTM Xavier NX.

Detection algorithms challenges

In real-time detection systems, the most commonly used detectors are one-stage models such as YOLO and SSD. The application and testing of these systems have highlighted three main challenges in their use for UAVs [15].

- 1) Object rotation In images obtained from drone cameras, objects of the same class can appear in any position and

orientation. Classical object detection assumes a horizontal object position, but UAV perspectives can rotate along any axis. Therefore, even the best model trained on common datasets with ground-level images may struggle with drone-captured images. Rotating objects lead to more false positives or missed detections. Researchers attempt to minimize these challenges using rotation-based object detection methods. In these methods, detection models work with oriented bounding boxes that can adapt to any object angle [15].

- 2) Small object increasing Detection models analyzing aerial photography must be robust enough to handle a wide range of object scales. As altitude increases, objects appear smaller, making it difficult to distinguish them from one another, which leads to false positives or missed detections. The research [16] addresses this challenge by proposing a detection network based on self-attention guidance and multiscale feature fusion (SGMFNet).
- 3) Complex background Another challenge arises when detectors struggle to distinguish patterns in densely populated object areas. Too many objects close together can confuse the system, leading to incorrect detections or missed objects. A similar issue is background noise, which refers to extra visual information in the background. Examples include trees, shadows, or reflections that the algorithm may misinterpret as objects. In [17], a semantic segmentation module is proposed to suppress background clutter and improve the accuracy of object proposals.

Drone-based datasets

In recent years, unmanned aerial vehicles (UAVs) systems have advanced rapidly, not only in research but also in commercial and entertainment sectors. This progress has made aerial data collection more convenient and affordable. However, assembling large-scale drone-based object detection datasets remains a significant challenge. These datasets include thousands of aerial images along with detailed annotations for training and evaluating detection models. Today, researchers have access to a wide range of public datasets, each tailored to address specific challenges and diverse scenarios.

The Video Satellite Objects (VISO) dataset was created using the Jilin-1 satellite constellation, comprising 47 high-quality videos with 1,646,038 instances of interest for object detection and 3,711 trajectories for object tracking [18].

The Dataset of Object Detection in Aerial Images (DOTA) contains 1,793,658 object instances across 18 categories, annotated with oriented bounding boxes from 11,268 aerial images. Additionally, the dataset includes a code library for object detection in aerial images (ODAI) and provides a website for evaluating different algorithms [19].

The Vision Drone (VisDrone) dataset consists of aerial images captured in 14 different cities, primarily focusing on urban and suburban areas. The process of collecting, annotating, and organizing this dataset for object detection and tracking algorithms required over 6,000 worker hours [20].

For researchers focused on detection algorithms, collecting a custom dataset is often time-consuming and inefficient. A more practical approach is to leverage existing public datasets, selecting the most suitable one to aid in model development and benchmark performance effectively.

IV. SUMMARY

The interest in UAV object detection systems has been growing rapidly, driving significant advancements over the past decades. These systems are widely utilized across various fields, including military operations, agriculture, surveillance, infrastructure inspection, and entertainment. Thanks to advancements in technology, including processors, GPUs, and other hardware components, more complex software solutions can now be deployed on various types of drones. This progress has driven engineers and researchers to develop and implement increasingly complicated software solutions, even for relatively small-sized drones. Despite these achievements, there are still many shortcomings that future research must address. While many modern GPUs on the market are suitable for processing AI tasks, limitations still exist and must be considered. Even the most powerful hardware can struggle with applications that are too complex and demand high computational power. This must be taken into account when designing object detection systems. As a result, different versions of object detectors are available ranging from more precise but slower models to less precise but faster alternatives. Ideally, research should aim to develop models that are both highly accurate and fast. Another important direction is hardware development, focusing on increasing computational power while addressing physical constraints. Even as more powerful processors and GPUs become available, factors such as heat dissipation, energy consumption, and power sources must be considered. In particular, small drones must account for battery size, weight, and efficiency. Advancements in battery technology are promising, and we can expect smaller batteries with higher capacities, which could significantly enhance UAV performance. Another challenge is related to datasets, which play a crucial role in training, evaluating, and testing object detection models. It is undoubtedly beneficial that many datasets for UAV systems are publicly available and easily accessible for research. However, these datasets still face the same fundamental issue: they cannot capture every object in all possible conditions. This is an unsolvable problem, but it can be partially mitigated using techniques such as data augmentation. Research should focus on developing more efficient augmentation techniques and frameworks to improve model performance and generalization. With the invention of convolutional neural networks (CNNs), object detection has made significant progress. Many researchers have proposed new neural network structures and modules to enhance model efficiency. However, these algorithms still struggle in UAV applications, primarily due to the need to handle a wide range of object scales, the varying angles from which UAVs capture objects, and the challenges of detecting objects in densely populated areas. Addressing these challenges and developing new approaches would make UAV-based object detection systems more robust and effective. To effectively work on these challenges, researchers can take advantage of the many frameworks and software libraries available for detection systems and deep learning. These resources simplify development and allow researchers to focus on solving critical problems rather than building models from scratch.

ACKNOWLEDGMENT

This work was supported by the Slovak Research and Development Agency under the Contract no. APVV-19-0210 and project VEGA 1/0363/23.

REFERENCES

- [1] Z. Xiaoning, "Analysis of military application of uav swarm technology," in *2020 3rd International Conference on Unmanned Systems (ICUS)*, 2020, pp. 1200–1204.
- [2] L. Wenguang and Z. Zhiming, "Intelligent surveillance and reconnaissance mode of police uav based on grid," in *2021 7th International Symposium on Mechatronics and Industrial Informatics (ISMII)*, 2021, pp. 292–295.
- [3] M. Wicaksono and S. Y. Shin, "Optimizing uav navigation through non-uniform b-spline trajectory for tracking uav enemy," in *2023 14th International Conference on Information and Communication Technology Convergence (ICTC)*, 2023, pp. 1075–1078.
- [4] S. Wang, Y. Han, J. Chen, Z. Zhang, G. Wang, and N. Du, "A deep-learning-based sea search and rescue algorithm by uav remote sensing," in *2018 IEEE CSAA Guidance, Navigation and Control Conference (CGNCC)*, 2018, pp. 1–5.
- [5] A. Kumar, S. S. T. N. P. Rajalakshmi, W. Guo, B. Naik, B. Marathi, and U. Desai, "Identification of water-stressed area in maize crop using uav based remote sensing," in *2020 IEEE India Geoscience and Remote Sensing Symposium (InGARSS)*, 2020, pp. 146–149.
- [6] M. Elloumi, R. Dhaou, B. Escrig, H. Idoudi, and L. A. Saidane, "Monitoring road traffic with a uav-based system," in *2018 IEEE Wireless Communications and Networking Conference (WCNC)*, 2018, pp. 1–6.
- [7] K. R. Akshatha, S. Biswas, A. K. Karunakar, and B. Satish Shenoy, "Anchored versus anchorless detector for car detection in aerial imagery," in *2021 2nd Global Conference for Advancement in Technology (GCAT)*, 2021, pp. 1–6.
- [8] W. Zhang, Z. Li, Y. Zhang, Y. Zhang, Y. Zhang, Y. Zhang, Y. Zhang, Y. Zhang, Y. Zhang, and Y. Zhang, "A survey of object detection for uavs based on deep learning," *Remote Sensing*, vol. 16, no. 1, 2024. [Online]. Available: <https://www.mdpi.com/2072-4292/16/1/149>
- [9] R. Padilla, W. L. Passos, T. L. B. Dias, S. L. Netto, and E. A. B. da Silva, "A comparative analysis of object detection metrics with a companion open-source toolkit," *Electronics*, vol. 10, no. 3, 2021. [Online]. Available: <https://www.mdpi.com/2079-9292/10/3/279>
- [10] R. Girshick, "Fast r-cnn," in *2015 IEEE International Conference on Computer Vision (ICCV)*, 2015, pp. 1440–1448.
- [11] W. Liu, D. Anguelov, D. Erhan, C. Szegedy, S. Reed, C.-Y. Fu, and A. C. Berg, "Ssd: Single shot multibox detector," in *Computer Vision—ECCV 2016: 14th European Conference, Amsterdam, The Netherlands, October 11–14, 2016, Proceedings, Part I 14*. Springer, 2016, pp. 21–37.
- [12] J. Redmon, S. Divvala, R. Girshick, and A. Farhadi, "You only look once: Unified, real-time object detection," in *2016 IEEE Conference on Computer Vision and Pattern Recognition (CVPR)*, 2016, pp. 779–788.
- [13] Z. Saeed, M. H. Yousaf, R. Ahmed, S. A. Velastin, and S. Viriri, "On-board small-scale object detection for unmanned aerial vehicles (uavs)," *Drones*, vol. 7, no. 5, 2023. [Online]. Available: <https://www.mdpi.com/2504-446X/7/5/310>
- [14] M.-Y. Ma, S.-E. Shen, and Y.-C. Huang, "Enhancing uav visual landing recognition with yolo's object detection by onboard edge computing," *Sensors*, vol. 23, no. 21, 2023. [Online]. Available: <https://www.mdpi.com/1424-8220/23/21/8999>
- [15] G. Tang, J. Ni, Y. Zhao, Y. Gu, and W. Cao, "A survey of object detection for uavs based on deep learning," *Remote Sensing*, vol. 16, no. 1, 2024. [Online]. Available: <https://www.mdpi.com/2072-4292/16/1/149>
- [16] Y. Zhang, C. Wu, T. Zhang, Y. Liu, and Y. Zheng, "Self-attention guidance and multiscale feature fusion-based uav image object detection," *IEEE Geoscience and Remote Sensing Letters*, vol. 20, pp. 1–5, 2023.
- [17] C. Li, C. Xu, Z. Cui, D. Wang, Z. Jie, T. Zhang, and J. Yang, "Learning object-wise semantic representation for detection in remote sensing imagery," in *Proceedings of the IEEE/CVF Conference on Computer Vision and Pattern Recognition Workshops*, 2019, pp. 20–27.
- [18] Q. Yin, Q. Hu, H. Liu, F. Zhang, Y. Wang, Z. Lin, W. An, and Y. Guo, "Detecting and tracking small and dense moving objects in satellite videos: A benchmark," *IEEE Transactions on Geoscience and Remote Sensing*, vol. 60, pp. 1–18, 2022.
- [19] J. Ding, N. Xue, G.-S. Xia, X. Bai, W. Yang, M. Y. Yang, S. Belongie, J. Luo, M. Datcu, M. Pelillo, and L. Zhang, "Object detection in aerial images: A large-scale benchmark and challenges," *IEEE Transactions on Pattern Analysis and Machine Intelligence*, vol. 44, no. 11, pp. 7778–7796, 2022.
- [20] P. Zhu, L. Wen, D. Du, X. Bian, H. Fan, Q. Hu, and H. Ling, "Detection and tracking meet drones challenge," *IEEE Transactions on Pattern Analysis and Machine Intelligence*, vol. 44, no. 11, pp. 7380–7399, 2022.

Current Trends in Modeling and Simulation of Complex Physical Systems with Neural Networks

¹Lukáš TOMAŠČÍK (1st year),

Supervisor: ²Norbert ÁDÁM

^{1,2}Department of Computers and Informatics, FEI TU of Košice, Slovak Republic

¹lukas.tomascik@tuke.sk , ²norbert.adam@tuke.sk 

Abstract—Modeling and simulation of complex physical systems have seen significant advancements with the integration of neural networks. Traditional computational methods, such as Eulerian and Lagrangian techniques, face challenges in computational efficiency and accuracy, particularly in fluid simulations and real-time hybrid systems. Recent approaches leverage deep learning, reinforcement learning, and data-driven models to enhance simulation accuracy, reduce computational costs, and improve scalability. This paper reviews current trends in neural network applications for physical system modeling, highlighting innovations in fluid simulation, photonic computing, and reinforcement learning-driven control methods. The discussion outlines key challenges, including training bottlenecks and generalization issues, and explores potential future research directions to address these limitations.

Keywords—neural networks, machine learning, simulation, physical systems, artificial intelligence

I. INTRODUCTION

The modeling and simulation of physical systems are crucial for scientific and engineering applications, enabling the study of dynamic behaviors across various domains. Traditional numerical approaches, such as solving Navier-Stokes equations for fluid dynamics or employing finite element methods for structural simulations, offer high accuracy but demand extensive computational resources. Recent advancements in artificial intelligence, particularly deep learning and reinforcement learning, have provided alternative data-driven methods that can accelerate simulations while maintaining accuracy. This paper explores the latest developments in using neural networks for modeling physical systems, examining their impact on computational efficiency and predictive capabilities. The study also discusses how AI-driven approaches integrate with existing methodologies and the challenges associated with their adoption.

II. RELATED WORK

Efficient fluid simulation has been an active area of research, with significant efforts directed at improving computational performance. Traditional methods for solving the Navier-Stokes equations can be categorized into Lagrangian methods, which track discrete particles as seen in work by Gingold and Monaghan [1], and Eulerian methods, which discretize the fluid domain using a fixed grid introduced by Foster and Metaxas [2]. While Eulerian methods are commonly used due to their ability to accurately simulate incompressible fluids, they suffer from high computational costs, particularly in

solving the pressure projection step, which requires solving a large sparse linear system.

To address this challenge, researchers have proposed a variety of acceleration techniques. Multi-grid methods such as in work by McAdams et al. [3] aim to improve convergence of iterative solvers by solving the problem at multiple resolutions, but they are difficult to parallelize on GPUs and can fail in complex boundary conditions. Approximate solvers, such as iterated orthogonal projections in Molemaker et al. [4] and coarse-grid corrections by Lentine et al. [5], reduce computational complexity at the cost of accuracy. However, these methods do not leverage the statistics of fluid data, leading to limited generalization.

A promising direction is data-driven simulation, where machine learning techniques are used to accelerate fluid solvers. Galerkin projection methods used by Treuille et al. [6] and De Witt et al. [7] reduce computation by operating on a lower-dimensional representation of the fluid state. Similarly, pre-computed simulations can be interpolated to generate complex fluid behavior as demonstrated by Raveendran et al. [8], and state-graph formulations used by Stanton et al. [9] exploit the observation that only a limited set of states are visited in certain simulations.

More recently, researchers have explored deep learning techniques to approximate fluid solvers. Ladický et al. [10] used random regression forests to predict the state of particles in smoothed particle hydrodynamics simulations, while Yang et al. [11] applied convolutional neural networks to Eulerian methods, training a patch-based neural network to approximate pressure projections. However, existing learning-based methods suffer from a supervised training bottleneck, as they require ground-truth pressure solutions from an exact solver. This discrepancy between training and inference can lead to error accumulation over time.

The work presented in a paper by Thompson et al. [12] builds upon these advances by introducing an unsupervised deep-learning framework that learns to solve the pressure projection step without requiring ground-truth labels. By formulating the training objective to minimize velocity divergence directly, their approach ensures better generalization and long-term stability. Furthermore, this architecture introduces domain-specific optimizations, such as multi-resolution processing and pressure bottlenecks.

Their work also aligns with broader efforts in intuitive physics modeling, where neural networks are trained to predict physical interactions as described in Lerer et al. [13] and

Kubricht et al. [14]. These approaches aim to develop AI systems capable of reasoning about fluid behavior, which could have implications for robotics, gaming, and virtual environments.

Liquid manipulation has been a growing area of interest in robotics as well, with research focusing on robotic pouring and liquid perception. Works by Kunze and Beetz [15] and Schneck and Fox [16] have also employed simulation-based techniques for predicting liquid behavior and tracking real-world liquids. One key area of research involves estimating fluid parameters such as viscosity and cohesion from observed data. Prior work by Elbrechter et al. [17] proposed methods for estimating fluid parameters through action-based differences between models and observations.

Schenck and Fox [18] employed particle-based representation for fluids, which is computationally efficient for modeling sparse fluid distributions. This model directly integrates particle states into deep learning frameworks. While previous research by Engelcke et al. [19] and Su et al. [20] have developed techniques for processing unordered point sets with neural networks, these methods primarily address object recognition and classification rather than fluid dynamics.

Schenck and Fox [18] introduced new layers specifically designed for interfacing neural networks with particle-based fluid representations. Their work leverages Position Based Fluids described by Macklin and Müller [21], which is optimized for modeling incompressible fluids like water. A critical advantage of this model is its differentiability, enabling the computation of analytical gradients that can be used for optimization and learning tasks. By integrating fluid dynamics into deep learning frameworks, their model enables end-to-end training of fluid control policies and facilitates learning from real-world observations pictured in Fig. 1. The differentiability of their approach allows for the optimization of fluid parameters and control strategies using gradient-based methods, bridging the gap between analytical fluid models and modern deep learning techniques.

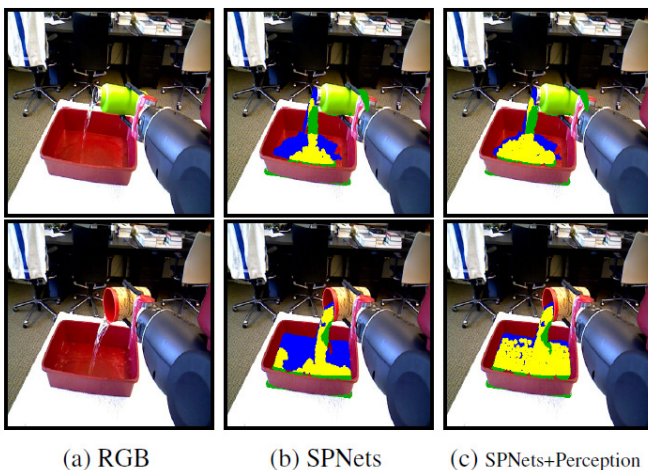


Fig. 1. Robot learning from real-world observation [18]

III. DEVELOPMENTS IN ARTIFICIAL INTELLIGENCE

The increasing computational demands of artificial intelligence models have led to significant research efforts in developing more efficient algorithms and hardware architectures. Several approaches have been explored to address the

scalability challenges of AI, including model compression techniques such as pruning, knowledge distillation, and quantization. Pruning methods identify and remove less critical neural network connections to reduce the overall model size while maintaining performance as explained by Setsma and Dow [22]. Hinton et al. [23] described knowledge distillation, which transfers knowledge from a large model to a smaller one, enabling similar accuracy with fewer parameters.

Alternative computational paradigms, such as Extreme Learning Machines described by Huang et al. [24] and reservoir computing by Schrauwen et al. [25], have also been proposed to achieve high efficiency with reduced trainable parameters. Extreme learning machines rely on fixed, randomly initialized hidden layers to minimize training complexity, whereas reservoir computing leverages dynamic systems to process input data with minimal parameter tuning.

Alongside algorithmic advancements, photonic computing has emerged as a promising approach to overcoming the limitations of traditional digital electronics. Integrated photonic circuits and spatial light modulators have enabled the development of photonic AI architectures with reduced energy consumption and increased bandwidth as described by Lin et al. [26].

Recent work has also explored the potential of photonic implementations of neural cellular automata, which utilize local interactions for computation. Inspired by classical cellular automata, neural cellular automata models operate based on differentiable update rules and have been adapted for photonic hardware by Randazzo et al. [27]. In a notable study, Li et al. [28] demonstrated a photonic implementation of NCA for classification tasks, achieving high-speed and high-accuracy performance through optoelectronic integration. Their approach leveraged nonlinear optical interactions and variable optical attenuators to perform computations in a massively parallel manner, significantly reducing inference time compared to conventional digital implementations.

These advancements underscore the potential of photonic computing in addressing the increasing resource demands of AI. By aligning AI algorithms with photonic capabilities as noted by Oguz et al. [29], future research can further enhance computational efficiency, enabling sustainable and scalable AI systems.

Real-Time Hybrid Simulation (RTHS) has been extensively studied in the field of structural engineering as an effective method to analyze the dynamic response of civil structures.

One of the major challenges in RTHS is the synchronization of numerical and physical components, as time delays introduced by actuators and computational processing can compromise simulation accuracy. To address this, various tracking controllers have been developed. Horiuchi et al. [30] introduced polynomial extrapolation as an initial delay compensation technique, which has been expanded into more robust methodologies, such as the adaptive inverse compensation by Chen et al. [31].

More recent studies have focused on adaptive and data-driven methods to enhance control strategies in RTHS. Chae et al. [32] developed an adaptive time-series compensator, while Palacio-Betancur and Gutierrez Soto [33] explored conditional adaptive time series compensation. Similarly, Najafi and Spencer [34] proposed an adaptive model reference control method for real-time hybrid simulation, demonstrating improved performance in tracking accuracy.

Reinforcement learning (RL) has emerged as a promising approach in control systems, including structural engineering applications. Li et al. [35] proposed an RL-based tracking controller for RTHS using the deep deterministic policy gradient algorithm, which combined an RL agent as a feedback controller with conventional time-delay compensation. The application of reinforcement learning in control systems has been widely studied in other domains, indicating its potential for RTHS applications.

Felipe Nino et al. [36] expanded on prior research by integrating deep reinforcement learning DRL into tracking control for RTHS. Unlike traditional model-based methods that require system identification and tuning, DRL offers a model-free approach, which is particularly advantageous for systems with high uncertainties. Their study explores various DRL-based controllers, including hybrid approaches combining conventional feedback and DRL agents, as well as fully DRL-based control policies. The findings contribute to the ongoing development of intelligent control methodologies for improving the accuracy and robustness of RTHS.

IV. DISCUSSION

The integration of neural networks into the modeling and simulation of complex physical systems presents a transformative approach to computational physics and engineering. The reviewed literature demonstrates the growing trend of leveraging machine learning to enhance traditional simulation methodologies, particularly in fluid dynamics, structural engineering, and reinforcement learning-based control systems.

One of the key observations from the study is the effectiveness of deep learning techniques in accelerating conventional numerical solvers. Traditional methods, such as Eulerian and Lagrangian approaches for fluid simulation, suffer from high computational costs, especially in pressure projection steps. By employing convolutional neural networks (CNNs) and unsupervised learning frameworks, recent studies have shown a significant reduction in computational complexity while maintaining accuracy. This shift from purely physics-based models to hybrid data-driven techniques has facilitated real-time simulations in various applications, such as gaming, robotics, and virtual environments.

Moreover, current research highlights the increasing reliance on differentiable physics models. Unlike black-box neural network solutions, differentiable models maintain physical interpretability and allow gradient-based optimization, making them more robust for real-world applications. Position-Based Fluids and neural network-integrated particle representations exemplify this paradigm shift, bridging the gap between theoretical physics and data-driven learning approaches.

Despite these advancements, several challenges remain. First, the training bottleneck in supervised learning approaches continues to be a limiting factor, requiring large-scale labeled datasets that may not always be available for complex physical simulations. Second, while unsupervised learning and reinforcement learning offer potential solutions, their generalization capabilities across different simulation scenarios need further exploration. Lastly, the integration of neural network-based models with existing physics-based solvers necessitates careful validation to ensure that the learned representations adhere to fundamental physical laws.

V. FUTURE RESEARCH

Overall, the convergence of machine learning and traditional simulation techniques holds immense promise for advancing computational modeling. Future research should focus on improving the interpretability of neural network-driven simulations, developing more efficient training methodologies, and exploring the full potential of alternative computing architectures to overcome current computational limitations. Traditional simulations, grounded in first principles and well-established numerical methods, offer transparency and robustness but often suffer from high computational cost, especially for high-dimensional or nonlinear systems. In contrast, AI-driven simulations—particularly those based on neural networks—enable rapid approximations and generalization from data but may sacrifice interpretability and physical fidelity.

A key future research direction will involve systematically quantifying the trade-offs between these paradigms in terms of accuracy, efficiency, scalability, and explainability. For instance, I intend to benchmark neural network-driven models against classical solvers for specific physical systems to evaluate where machine learning offers clear advantages and where traditional methods remain superior.

One critical area of exploration is the development of hybrid models that seamlessly integrate physics-based solvers with deep learning techniques. While neural networks have demonstrated significant speed-up in simulations, ensuring physical consistency remains a challenge. Future research should aim to incorporate physics-informed neural networks (PINNs) and differentiable physics frameworks to improve model reliability while retaining computational efficiency.

Another promising direction is the optimization of neural network architectures for simulation tasks. Current deep learning models require extensive computational resources, which can hinder their deployment in real-time applications. Advances in model compression techniques, such as pruning, quantization, and knowledge distillation, should be further investigated to develop lightweight, high-performance neural models suitable for large-scale simulations.

The role of reinforcement learning (RL) in simulation-based decision-making also presents an avenue for further research. RL has shown promise in optimizing control strategies for fluid dynamics and structural engineering, but its application in high-dimensional, uncertain environments remains under-explored. Future research should focus on improving RL-based controllers by incorporating uncertainty quantification methods, meta-learning, and transfer learning techniques to enhance adaptability across different simulation scenarios.

Moreover, alternative computational paradigms such as quantum computing and photonic AI could revolutionize the field. The feasibility of leveraging quantum-enhanced neural networks for complex physical simulations should be thoroughly investigated. Additionally, photonic computing, which has demonstrated energy-efficient AI acceleration, could be explored further to enable scalable and sustainable AI-driven simulations.

Finally, addressing the limitations of current data-driven models is crucial for advancing simulation technologies. Many neural network-based approaches rely on large labeled datasets for training, which may not always be available for certain complex systems. The scarcity of labeled data in complex systems remains a bottleneck. I intend to explore unsupervised

and self-supervised learning techniques, including contrastive learning and generative modeling, to reduce dependence on labeled datasets while retaining model accuracy.

In the longer term, I am also interested in evaluating alternative computational platforms, such as quantum computing and photonic AI, for specific simulation use cases. Although currently experimental, these technologies may offer breakthroughs in energy efficiency and computational speed in near future.

By pursuing these research directions, the field of AI-driven modeling and simulation can continue to evolve, leading to more efficient, interpretable, and scalable solutions across various domains, including engineering, physics, and robotics.

VI. CONCLUSION

The integration of neural networks into modeling and simulation has significantly improved computational performance and predictive capabilities for complex physical systems. Despite existing challenges, AI-driven methods offer a promising path toward scalable and efficient simulations across various scientific and engineering domains. Continued research into hybrid modeling techniques, advanced learning paradigms, and hardware optimizations will drive future innovations in this field. As AI continues to evolve, its application in physical simulations will expand, enabling more accurate, efficient, and real-time predictions for a wide range of applications.

REFERENCES

- [1] R. A. Gingold and J. J. Monaghan, "Smoothed particle hydrodynamics: theory and application to non-spherical stars," *Monthly notices of the royal astronomical society*, vol. 181, no. 3, pp. 375–389, 1977.
- [2] N. Foster and D. Metaxas, "Realistic animation of liquids," *Graphical models and image processing*, vol. 58, no. 5, pp. 471–483, 1996.
- [3] A. McAdams, E. Sifakis, and J. Teran, "A parallel multigrid poisson solver for fluids simulation on large grids," in *Symposium on Computer Animation*, vol. 65, 2010, p. 74.
- [4] J. Molemaker, J. M. Cohen, S. Patel, J. Noh *et al.*, "Low viscosity flow simulations for animation," in *Symposium on Computer Animation*, vol. 9, 2008, p. 18.
- [5] M. Lentine, W. Zheng, and R. Fedkiw, "A novel algorithm for incompressible flow using only a coarse grid projection," *ACM Transactions on Graphics (TOG)*, vol. 29, no. 4, pp. 1–9, 2010.
- [6] A. Treuille, A. Lewis, and Z. Popović, "Model reduction for real-time fluids," *ACM Transactions on Graphics (TOG)*, vol. 25, no. 3, pp. 826–834, 2006.
- [7] T. De Witt, C. Lessig, and E. Fiume, "Fluid simulation using laplacian eigenfunctions," *ACM Transactions on Graphics (TOG)*, vol. 31, no. 1, pp. 1–11, 2012.
- [8] K. Raveendran, C. Wojtan, N. Thuerey, and G. Turk, "Blending liquids," *ACM Transactions on Graphics (TOG)*, vol. 33, no. 4, pp. 1–10, 2014.
- [9] M. Stanton, B. Humberston, B. Kase, J. F. O'Brien, K. Fatahalian, and A. Treuille, "Self-refining games using player analytics," *ACM Transactions on Graphics (TOG)*, vol. 33, no. 4, pp. 1–9, 2014.
- [10] L. Ladický, S. Jeong, B. Solenthaler, M. Pollefeys, and M. Gross, "Data-driven fluid simulations using regression forests," *ACM Transactions on Graphics (TOG)*, vol. 34, no. 6, pp. 1–9, 2015.
- [11] C. Yang, X. Yang, and X. Xiao, "Data-driven projection method in fluid simulation," *Computer Animation and Virtual Worlds*, vol. 27, no. 3–4, pp. 415–424, 2016.
- [12] J. Tompson, K. Schlachter, P. Sprechmann, and K. Perlin, "Accelerating Eulerian fluid simulation with convolutional networks," in *Proceedings of the 34th International Conference on Machine Learning*, ser. Proceedings of Machine Learning Research, D. Precup and Y. W. Teh, Eds., vol. 70. PMLR, 06–11 Aug 2017, pp. 3424–3433. [Online]. Available: <https://proceedings.mlr.press/v70/tompson17a.html>
- [13] A. Lerer, S. Gross, and R. Fergus, "Learning physical intuition of block towers by example," in *International conference on machine learning*. PMLR, 2016, pp. 430–438.
- [14] J. Kubricht, C. Jiang, Y. Zhu, S.-C. Zhu, D. Terzopoulos, and H. Lu, "Probabilistic simulation predicts human performance on viscous fluid-pouring problem," in *CogSci*, 2016.
- [15] L. Kunze and M. Beetz, "Envisioning the qualitative effects of robot manipulation actions using simulation-based projections," *Artificial Intelligence*, vol. 247, pp. 352–380, 2017.
- [16] C. Schenck and D. Fox, "Reasoning about liquids via closed-loop simulation," *arXiv preprint arXiv:1703.01656*, 2017.
- [17] C. Elbrechter, J. Maycock, R. Haschke, and H. Ritter, "Discriminating liquids using a robotic kitchen assistant," in *2015 IEEE/RSJ International Conference on Intelligent Robots and Systems (IROS)*. IEEE, 2015, pp. 703–708.
- [18] C. Schenck and D. Fox, "Spnets: Differentiable fluid dynamics for deep neural networks," in *Proceedings of The 2nd Conference on Robot Learning*, ser. Proceedings of Machine Learning Research, A. Billard, A. Dragan, J. Peters, and J. Morimoto, Eds., vol. 87. PMLR, 29–31 Oct 2018, pp. 317–335. [Online]. Available: <https://proceedings.mlr.press/v87/schenck18a.html>
- [19] M. Engelcke, D. Rao, D. Z. Wang, C. H. Tong, and I. Posner, "Vote3deep: Fast object detection in 3d point clouds using efficient convolutional neural networks," in *2017 IEEE International Conference on Robotics and Automation (ICRA)*. IEEE, 2017, pp. 1355–1361.
- [20] H. Su, V. Jampani, D. Sun, S. Maji, E. Kalogerakis, M.-H. Yang, and J. Kautz, "Splatnet: Sparse lattice networks for point cloud processing," in *Proceedings of the IEEE conference on computer vision and pattern recognition*, 2018, pp. 2530–2539.
- [21] M. Macklin and M. Müller, "Position based fluids," *ACM Transactions on Graphics (TOG)*, vol. 32, no. 4, pp. 1–12, 2013.
- [22] Sietsma and Dow, "Neural net pruning-why and how," in *IEEE 1988 international conference on neural networks*. IEEE, 1988, pp. 325–333.
- [23] G. Hinton, "Distilling the knowledge in a neural network," *arXiv preprint arXiv:1503.02531*, 2015.
- [24] G.-B. Huang, Q.-Y. Zhu, and C.-K. Siew, "Extreme learning machine: theory and applications," *Neurocomputing*, vol. 70, no. 1–3, pp. 489–501, 2006.
- [25] B. Schrauwen, D. Verstraeten, and J. Van Campenhout, "An overview of reservoir computing: theory, applications and implementations," in *Proceedings of the 15th european symposium on artificial neural networks*. p. 471–482 2007, 2007, pp. 471–482.
- [26] Z. Lin, B. J. Shastri, S. Yu, J. Song, Y. Zhu, A. Safarnejadian, W. Cai, Y. Lin, W. Ke, M. Hammood *et al.*, "120 gops photonic tensor core in thin-film lithium niobate for inference and in situ training," *Nature Communications*, vol. 15, no. 1, p. 9081, 2024.
- [27] E. Randazzo, A. Mordvintsev, E. Niklasson, M. Levin, and S. Greydanus, "Self-classifying mnist digits," *Distill*, vol. 5, no. 8, pp. e00027–002, 2020.
- [28] G. H. Li, C. R. Leefmans, J. Williams, R. M. Gray, M. Parto, and A. Marandi, "Deep learning with photonic neural cellular automata," *Light: Science & Applications*, vol. 13, no. 1, p. 283, 2024.
- [29] I. Oguz, M. Yildirim, J.-L. Hsieh, N. U. Dinc, C. Moser, and D. Psaltis, "Resource-efficient photonic networks for next-generation ai computing," *Light: Science & Applications*, vol. 14, no. 1, p. 34, 2025.
- [30] T. Horiuchi, M. Inoue, T. Konno, and Y. Namita, "Real-time hybrid experimental system with actuator delay compensation and its application to a piping system with energy absorber," *Earthquake Engineering & Structural Dynamics*, vol. 28, no. 10, pp. 1121–1141, 1999.
- [31] C. Chen, J. Ricles, and T. Guo, "Improved adaptive inverse compensation technique for real-time hybrid simulation," *Journal of Engineering Mechanics*, vol. 138, pp. 1432–1446, 12 2012.
- [32] Y. Chae, K. Kazemibidokhti, and J. M. Ricles, "Adaptive time series compensator for delay compensation of servo-hydraulic actuator systems for real-time hybrid simulation," *Earthquake Engineering & Structural Dynamics*, vol. 42, no. 11, pp. 1697–1715, 2013.
- [33] A. Palacio-Betancur and M. G. Soto, "Adaptive tracking control for real-time hybrid simulation of structures subjected to seismic loading," *Mechanical Systems and Signal Processing*, vol. 134, p. 106345, 2019.
- [34] A. Najafi and B. F. Spencer Jr, "Adaptive model reference control method for real-time hybrid simulation," *Mechanical Systems and Signal Processing*, vol. 132, pp. 183–193, 2019.
- [35] N. Li, J. Tang, Z.-X. Li, and X. Gao, "Reinforcement learning control method for real-time hybrid simulation based on deep deterministic policy gradient algorithm," *Structural Control and Health Monitoring*, vol. 29, no. 10, p. e3035, 2022.
- [36] A. Felipe Niño, A. Palacio-Betancur, P. Miranda-Chiquito, J. David Amaya, C. E. Silva, M. Gutierrez Soto, and L. Felipe Giraldo, "Deep reinforcement learning-based control for real-time hybrid simulation of civil structures," *International Journal of Robust and Nonlinear Control*, 2025.

Towards IoT Education Evolution

¹Tomáš KORMANÍK (2nd year),
Supervisor: ²Jaroslav PORUBÄN

^{1,2}Dept. of Computers and Informatics, FEI TU of Košice, Slovak Republic

¹tomas.kormanik@tuke.sk, ²jaroslav.poruban@tuke.sk

Abstract—This article points out current issues in the Internet of Things and its education. These issues are directly and indirectly affecting related fields of ambient applications, pervasive computing, and ubiquitous computing. The majority of these issues became apparent during the continuation of our research for the previous volume of this conference, SCYR 2024. Presented analysis of currently utilized education curricula reveals fundamental shortcomings, which were not considered by their creators. However, these shortcomings are proving to be more significant due to the open and broad scope of all of these paradigms.

Keywords—Internet of Things, Education, Ambient Software, Higher Education

I. INTRODUCTION

Our previous work has proven that topics like the Internet of Things (abbr. IoT), ubiquitous computing, ambient software, and pervasive computing (and various synonyms to these phrases) have grown in popularity. This growth has stimulated their development in the industrial field and implementation in the education process. Various engineering or informatics-oriented study programs have been modified by their respective institutions to teach about these topics directly, with hopes of satisfying demand for experts educated in these fields. But most of these curricula don't match the definitions of these paradigms set by researchers or industry leaders. These discrepancies are further deepened by the fact that many of the presently available definitions are based on different models, ideas, and points of view, and often we consider these definitions outright incorrect and misleading.

We consider these findings a major issue, as students and educators are thinking they are learning and teaching IoT or related technologies, but in fact, they are expanding their knowledge with unclear or incorrect goals. This study leads us to the conclusion that it is crucial to address these issues and improve education curricula related to these technologies or paradigms. This improvement will lead to curricula whose contents are more in line with required knowledge, and therefore it will prepare students not only for working with these paradigms but also for developing them.

II. WHAT IS IoT ?

We consider that the paradigm of IoT originated in 1982 with the creation of an early network-connected smart device in the form of a vending machine at *Carnegie Mellon University*[1]. The first mention of IoT as a paradigm is publicly credited to *Kevin Ashton* during his presentation at *Procter & Gamble*[2]. Since then, this topic evolved, and the phrase IoT became more common. We can consider the company *Cisco*

as one of the largest industrial actors pushing this paradigm further, since their presence is highest in public articles relating to this topic. However, when we now look back, analyzing previous works becomes troublesome, since they are mostly steering away not only from the main idea but also from each other. Many researchers share similar opinions or conclusions. *Moreira et al.*[3] and *Ramlowat and Pattanayak* have highlighted the fact that there is no conceptual definition of this paradigm widely accepted. Their work confirms our assumption that authors and people often misinterpret IoT as a technology, concept, or even service. Overall, we believe that these discrepancies stem from the individual's understanding of the concept. Some think the Thing is a modified, ordinary item that became part of the Internet, while others think it's an existing device.

To clarify the meaning of IoT, we considered the thing as any device, object, living being, or data connected and actively contributing to the Internet. Bringing this consensus to the table helped refine the definition of the IoT paradigm. After an analysis of available materials, we deemed a single definition as most accurate. This definition is available in the IoT Strategic Research Roadmap[4], which states: "*The Internet of Things allows people and things to be connected Anytime, Anyplace, with Anything and Anyone, ideally using Any path/network and Any service.*"[4]. While the phrase might seem extremely broad since it can include almost anything, that is actually the point, since the Internet can benefit from the sheer amount of information available to its members. This aligns with the ideas and goals of many current open technologies, which are all part of Industry 4.0. This topic is further explored by *Khan and Javaid*[5], which also point out that IoT is part of this revolution. These works by researchers and leaders in industry further underline the relevance and importance of IoT now and in the future.

III. CURRENT STATE OF IoT EDUCATION

As mentioned in the previous section, IoT curricula vary by each institution and study program. At our university, students currently learn by creating small applications that interact with the Raspberry Pi and gather data from sensors or openly available sources. While this approach is not inherently flawed, there is definitely room for improvement. When exploring other curricula, we can observe examples that are even farther away from IoT. Work by *Gomez et al.*[6] utilizes digital twin technology to teach about parts of computers. This approach is definitely intriguing and innovative for students, but it considers itself IoT-enabled, which we consider misleading at least, since this technology is completely isolated and

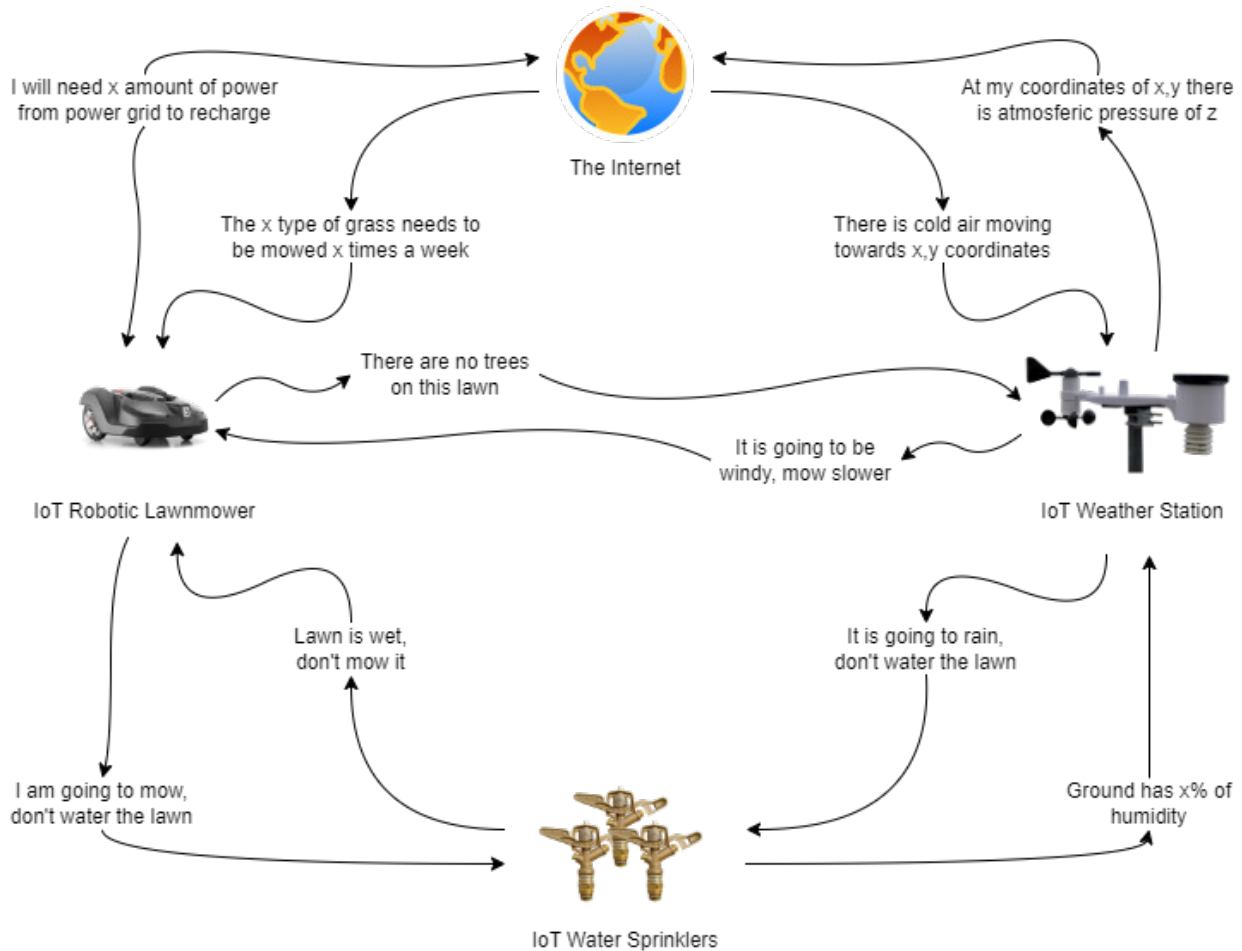


Fig. 1. Example of a garden enhanced by IoT-enabled devices.

detached from the Internet or any other distributed sources of data. This also highlights another common issue with IoT articles—62% of articles we sampled were implementing only a single application, service, sensor, module, or device—which means they created so-called Internet of Thing, dropping the critically important "s" letter.

There are many more examples of this misleading categorization or interpretation of IoT. From a different perspective, much better is the work by Dobrilović et al. [7], which utilizes the open-source platform Arduino and its many sensors. This approach is flawed because of the 5-layer IoT model, which they refer to. This model presents various services as actual layers, whether they are middleware or databases. This model itself is relevant, but only when interpreted correctly.

This led us to the conclusion that the course presented in our department is acceptable, but there is room for improvement, mainly when focusing on a theoretical understanding of IoT and practical examples. Silvis-Cividjian[8] provides an analysis of this landscape while also understanding the complexity of the IoT paradigm. She recommends teaching related knowledge from pervasive computing to enhance the understanding and potential of this paradigm. Naturally, we should discuss and properly demonstrate certain issues related to IoT, such as energy requirements or security. Hossain et al.[9] have their recent publication, which summarizes the current state of IoT security and prevalent challenges. These findings should be implementable to courses effortlessly, since many vulnerabilities of flawed designs can be demonstrated

by already existing issues. The work of Karthikeyan et al. [10] shows that their intrusion detection solution, designed specifically for IoT applications, can use machine learning or artificial intelligence to help solve these problems. Sadly, these new solutions also increase energy consumption when implemented, so when demonstrating to students, we must provide examples that do not conflict with the capabilities of IoT devices.

IV. CONCLUSION

Our research indicates that many institutions worldwide, including ours, need to update IoT curricula, education environments, and technologies. These changes should deepen understanding of IoT and ubiquitous computing. Mursid et al. [11] say that project-based learning is often used in these kinds of situations because it encourages students to be creative and try new things. Our department has several labs that are ideal for this type of comfortable education. Mainly, our OpenLAB (open laboratory), located in the corridor of our building, offers a unique and openly accessible space for students. This laboratory places computers, their peripherals, and sensors all the way around users, making it easier to demonstrate the ubiquitous computing paradigm.

Foundational work for these changes has already begun. To help students understand IoT more easily, we have already created several example scenarios. One of the examples we created as a demonstration is an IoT-enabled garden (Fig. 1), which shows the benefits of IoT as well as potential contents

of communication. This example also shows the fact that every device is providing some sort of information to the Internet, which is or can be beneficial to other IoT devices. This example is considered just a prototype for now, but we aim to utilize it during lectures, collect feedback, and observe changes in understanding of the IoT paradigm. We have analyzed several existing solutions, highlighting their strengths and weaknesses, and identifying the areas where they comply or violate the IoT paradigm. Our analysis of *Apple FindMy Network* is a good example; it wasn't made as an IoT solution, but it mostly fits the paradigm. The key drawback is the closed nature of this technology, further deepened by the need for connectivity to the official Apple servers and association with an account. This, however, mitigates the issue of privacy and security, serving as a reasonable tradeoff in this case.

Overall, we aim to create scenarios for practices and lectures that have a basic IoT and relevant software stack prepared. Utilizing already present knowledge of software engineering, which our students need to foster, we should lead them to creative solutions for this paradigm. Currently utilized solutions consisting of simple API calls, MQTT messages, or Zigbee solutions are interesting, but they are presented only as single use cases, which define smart devices, not IoT. Our next steps consist of analyzing currently available courses and curricula around the world and designing an improved approach if one does not already exist. Designing such a solution will likely utilize large simulation environments or IoT-enabled laboratories available at our department, which will serve as great practical examples, further deepening the potential understanding. Measuring understanding and engagement is harder, so it will be considered when designing the solution.

ACKNOWLEDGMENT

This work was supported by project APVV-23-0408 "Evolving Architectural Knowledge in the Edge-to-Cloud Continuum".

REFERENCES

- [1] C. S. of Computer Science. (1982) Network connected coke machine history. [Online]. Available: <https://www.cs.cmu.edu/~coke/coke.history.txt>
- [2] K. Ashton *et al.* (2009) That 'internet of things' thing. [Online]. Available: <https://www.itrc.jp/libraries/RFIDjournal-That%20Internet%20of%20Things%20Thing.pdf>
- [3] F. T. Moreira, A. Magalhães, F. Ramos, and M. Vairinhos, "The power of the internet of things in education: An overview of current status and potential," in *Citizen, Territory and Technologies: Smart Learning Contexts and Practices*, Ó. Mealha, M. Divitini, and M. Rehm, Eds. Cham: Springer International Publishing, 2018, pp. 51–63.
- [4] O. Vermesan, P. Friess, P. Guillemin, S. Gusmeroli, H. Sundmaeker, A. Bassi, I. S. Jubert, M. Mazura, M. Harrison, M. Eisenhauer *et al.*, "Internet of things strategic research roadmap," in *Internet of things: global technological and societal trends from smart environments and spaces to green ICT*. River Publishers, 2022, pp. 9–52.
- [5] I. H. Khan and M. Javaid, "Role of internet of things (iot) in adoption of industry 4.0," *Journal of Industrial Integration and Management*, vol. 07, no. 04, pp. 515–533, 2022. [Online]. Available: <https://doi.org/10.1142/S2424862221500068>
- [6] J. Gómez, J. F. Huete, O. Hoyos, L. Perez, and D. Grigori, "Interaction system based on internet of things as support for education," *Procedia Computer Science*, vol. 21, pp. 132–139, 2013, the 4th International Conference on Emerging Ubiquitous Systems and Pervasive Networks (EUSPN-2013) and the 3rd International Conference on Current and Future Trends of Information and Communication Technologies in Healthcare (ICTH). [Online]. Available: <https://www.sciencedirect.com/science/article/pii/S1877050913008120>
- [7] D. Dobrilović, Z. Čović, Ž. Stojanov, and V. Brtko, "Approach in teaching wireless sensor networks and iot enabling technologies in undergraduate university courses," in *Proceedings of the 2nd regional conference Mechatronics in Practice and Education, MechEdu*, 2013, pp. 18–22.
- [8] N. Silvis-Cividjian, "Teaching internet of things (iot) literacy: A systems engineering approach," in *2019 IEEE/ACM 41st International Conference on Software Engineering: Software Engineering Education and Training (ICSE-SEET)*, vol. 41, 2019, pp. 50–61.
- [9] M. Hossain, G. Kayas, R. Hasan, A. Skjellum, S. Noor, and S. M. R. Islam, "A holistic analysis of internet of things (iot) security: Principles, practices, and new perspectives," *Future Internet*, vol. 16, no. 2, 2024. [Online]. Available: <https://www.mdpi.com/1999-5903/16/2/40>
- [10] M. Karthikeyan, D. Manimegalai, and K. RajaGopal, "Firefly algorithm based wsn-iot security enhancement with machine learning for intrusion detection," *Scientific Reports*, vol. 14, no. 1, p. 231, 2024.
- [11] R. Mursid, A. H. Saragih, and R. Hartono, "The effect of the blended project-based learning model and creative thinking ability on engineering students' learning outcomes," *International Journal of Education in Mathematics, Science and Technology*, vol. 10, no. 1, pp. 218–235, 2022.

Analysis of Improvement Possibilities for Sensorless Control of a BLDC Motor Using AI

¹Tadeáš KMECIK (2nd year)
Supervisor: ²Peter GIROVSKÝ

^{1,2}Dept. of Electrical Engineering and Mechatronics, FEI TU of Košice, Slovak Republic

¹tadeas.kmecik@tuke.sk, ²peter.girovsky@tuke.sk

Abstract—In this article, we focus on the use of artificial intelligence in sensorless control of BLDC motors aiming for improving the quality of operating parameters during control and maintenance. We analyse the biggest disadvantages and problems associated with sensorless control of BLDC motors, while presenting the most promising solutions for the identified problems using elements of artificial intelligence.

Keywords— BLDC, artificial intelligence (AI), sensorless control, model predictive control (MPC), torque ripple reduction.

I. INTRODUCTION

BLDC motors are an integral part of industrial and consumer applications and their proper control is key to ensuring high reliability, accuracy and efficiency. Rapid advances in data collection and artificial intelligence (AI) are opening up new possibilities for optimizing the drive lifecycle from design to control to maintenance [1], [5].

This publication focuses mainly on optimizing the operation of BLDC motors, specifically on control and maintenance. BLDC motors are widely used in automotive, consumer electronics, robotics, medical devices, industrial applications, energetics and transportation due to their high efficiency, simple design, long lifespan and reliability. With increasing demands for efficiency, flexibility and cost reduction, the need to design new advanced control methods is also growing. AI plays a key role in the ability to analyse data, predict system behaviour and optimize its operation [1], [5].

Reducing manufacturing costs leads to the preference for sensorless control techniques that eliminate the need of hardware position sensors while maintaining the quality of traditional methods. Nevertheless, traditional control algorithms are still often used in current applications, which can suffer from insufficient accuracy, mainly due to simplifications. This factor limits the expansion of sensorless control in applications with high quality demands.

The goal of this work is to analyse the possibilities of improving sensorless control of BLDC motors through AI and moving their performance and operating characteristics closer to the level of sensor-based control [2], [3].

II. SENSORLESS CONTROL OF BLDC MOTOR

Sensorless control provides a way to eliminate the need for a position sensor, significantly reducing the cost of a BLDC motor drive, as quality sensors often exceed the cost of the motor itself.

In the first part of this chapter, we will focus on the theory behind BLDC motors and describe the main factors that affect the quality of operation of these drives. These factors are often associated with the motor design.

In the second part, we will address traditional sensorless control techniques, highlight their weak points and explore possibilities for their improvement using artificial intelligence.

A. Factors affecting the operation quality of BLDC motor

The performance of BLDC motors is affected by several factors that can reduce performance, efficiency and reliability. Key factors include higher harmonics, magnetic saturation, phase lag, cogging torque, mechanical and electrical faults [1].

The most prominent problem affecting the performance of BLDC motors is the presence of higher harmonics, which are caused by nonlinearities in the motor or non-optimized modulation. These higher harmonics significantly affect efficiency and increase the torque ripple of the motor too [1].

Another performance-affecting factor is magnetic saturation, which occurs due to a non-optimal motor current at a given moment. Magnetic saturation significantly affects the inductance and thus the efficiency of the motor. In addition to the performance and efficiency itself, saturation of the magnetic circuit significantly affects control dynamics. This creates an opportunity to integrate approximated magnetic circuits using AI models into control structures [1], [5].

Phase lag causes the electric current to be out of sync with the magnetic flux, leading to increased torque ripple and decreased efficiency, especially at higher speeds. This presents an opportunity to design new advanced AI prediction models capable of effectively observing and compensating for this lag [1], [5].

Cogging torque is a common phenomenon in all permanent magnet motors. It has a significant impact on the torque ripple of a BLDC motor. It is created by the interaction of the permanent magnets of the rotor with the iron slots of the stator. This parasitic torque is most pronounced in the low speed range and reaches up to 5-10% of the nominal torque. Currently, very few publications deal with the compensation of cogging torque in the field of BLDC motors. Although some works have addressed this issue with traditional methods, achieved results were not optimal over the entire range of motor operation. In some cases, incorrect compensation led to an increase in torque ripple. This parasitic phenomenon is difficult to describe and identify mathematically due to strong nonlinearities. This opens up the possibility of using AI models to identify and compensate for cogging torque more accurately. Their integration into control structures could ensure effective

compensation over the entire range of motor operation [1], [5].

In addition, mechanical and electrical failures also impact the quality of operation and reliability. Traditional mechanical failure detection techniques often rely on expert analysis or additional sensors. AI allows for the creation of models of the remaining useful life (RUL) of motors based on received data, enabling detection and also prediction of future failures.

Electrical faults on the motor include phase loss and inter-turn short circuits. These electrical faults have well-established methods. As for electrical faults on the converters, there is a whole spectrum of possibilities for integrating AI prediction models..

B. Traditional sensorless control techniques and their weak points

Traditional sensorless methods use mathematical and physical principles to estimate position and velocity. Despite their widespread use, they face several shortcomings that limit their accuracy and reliability, especially in low speeds, noise influence, and nonlinear regions of operation. Position detection techniques for sensorless BLDC motor control can be categorized as follows [1]:

- Detection based on back-EMF
- Detection based on magnetic flux
- Detection based on inductance changes

Detection based on back-EMF is the most widely used and is based on the measurement of zero crossings (ZCP) of the back electromotive force (back-EMF). The main disadvantages are the insufficient amplitude of the back-EMF in the low-speed range for reliable ZCP detection and the need to calculate the optimal commutation time by delaying the ZCP detection time. This is where the problem of calculating the optimal delay arises [1].

Detection based on magnetic flux is a method of estimating the rotor position using a flux linkage model dependent on the measured voltages and currents. The main disadvantages of this method are the need for an accurate motor model, the accumulation of errors caused by the integration of the measured signals and high sensitivity to variations in motor parameters. This opens up the possibility of integrating AI models that take the dependence of motor parameters on the current operating conditions (temperature, speed, load) into account [1].

Detection based on inductance changes is the only method intended primarily for the initial detection of the rotor position. The principle consists in measuring the amplitudes of currents after injecting short voltage pulses into individual stator windings. The disadvantage is again the sensitivity to variations in motor parameters, mainly depending on the temperatures of the winding and magnetic circuit [1].

C. Problems with traditional control strategies

Traditional control strategies can be divided into [1], [2], [3]:

- Control based on state observers
- Control based on Kalman filter (KF) with use of Extended KF (EKF)
- Control based on Sliding Mode Observer (SMO)

Control based on state observers often uses simplifications such as considering the back-EMF as a constant disturbance, which significantly reduces the computational complexity. However, the accuracy and dynamics are significantly limited due to the absence of consideration of nonlinear dynamic dependencies. With this type of control, disturbances in the measurement of currents and voltages have a significant presence [1].

Control based on KF and EKF combine mathematical models and corrections based on measured data. They provide more accurate estimates and eliminate random noise. EKF is more suitable for nonlinear systems [4].

Control based on SMO involves a robust strategy that is resistant to interference and noise due to its nonlinear characteristics, but the chattering effect, complicated process of setting SMO gains and thresholds and the complexity of the control strategy might create problems when using this strategy [1].

III. CONCLUSION

Based on an analysis of current research, we identified the greatest potential for AI in the area of sensorless control of BLDC motors, particularly in rotor position estimation, low speed control, torque ripple minimization, and efficiency enhancement.

Traditional sensorless control methods are problematic at low speeds, which, based on analysis, can be improved by using AI prediction models and third harmonic filtering for more accurate zero-crossing detection (ZCP).

Another challenge of the research is compensating for cogging torque, which negatively affects motor operation at low speeds.

The expected result is an increase in the accuracy, reliability and efficiency of sensorless BLDC motor operation by integrating AI.

ACKNOWLEDGMENT

This work was supported by the Scientific Grant Agency of the Ministry of Education of the Slovak Republic under the project KEGA 032TUKE-4/2024.

REFERENCES

- [1] XIA, Chang-liang. Permanent Magnet Brushless DC Motor Drives and Controls. Hoboken: Wiley-IEEE Press, 2012. ISBN 978-1-118-18833-0.
- [2] X. Song, B. Han, S. Zheng and J. Fang, "High-Precision Sensorless Drive for High-Speed BLDC Motors Based on the Virtual Third Harmonic Back-EMF," in IEEE Transactions on Power Electronics, vol. 33, no. 2, pp. 1528-1540, Feb. 2018, doi: 10.1109/TPEL.2017.2688478.
- [3] T. Li and J. Zhou, "High-Stability Position-Sensorless Control Method for Brushless DC Motors at Low Speed," in IEEE Transactions on Power Electronics, vol. 34, no. 5, pp. 4895-4903, May 2019, doi: 10.1109/TPEL.2018.2863735.
- [4] NAIR, Deepthi S.; JAGADANAND, G.; GEORGE, Saly. Torque estimation using Kalman filter and extended Kalman filter algorithms for a sensorless direct torque controlled BLDC motor drive: A comparative study. Journal of Electrical Engineering & Technology, 2021, 16.5: 2621-2634.
- [5] S. Zhao, F. Blaabjerg and H. Wang, "An Overview of Artificial Intelligence Applications for Power Electronics," in IEEE Transactions on Power Electronics, vol. 36, no. 4, pp. 4633-4658, April 2021, doi: 10.1109/TPEL.2020.3024914.

Programmer Identification Based on Source Code Stylometric Analysis and Behavioral Biometrics

¹Marek HORVÁTH (2nd year),
Supervisor: ²Emília PIETRIKOVÁ

^{1,2}Department of Computers and Informatics, FEI TU of Košice, Slovak Republic

¹marek.horvath@tuke.sk, ²emilia.pietrikova@tuke.sk

Abstract—This research focuses on source code authorship identification by combining behavioral biometrics, stylistic analysis, and machine learning techniques. The study explores the effectiveness of integrating static code features with dynamic behavioral patterns to improve identification accuracy. We present a methodology that captures both stylistic attributes of source code and programming habits, such as keystroke dynamics and interaction patterns, to build authorship profiles. The experimental evaluation is based on a dataset compiled from several academic years of student submissions at the Technical University of Košice. It includes thousands of source code files, with multiple assignments submitted by each student over time. The dataset was anonymized and features were extracted to represent both structural and behavioral aspects of programming. The initial experiments compare models trained on stylometric, behavioral, and combined feature sets. Among the evaluated methods, XG-Boost has shown promising results when applied to the integrated data. The study also addresses ethical and legal concerns related to behavioral monitoring in educational environments. Future research will focus on extending the dataset and exploring advanced classification techniques, including deep learning and alternative code representations.

Keywords—Authorship attribution, Behavioral biometrics, Code stylometry, Hybrid classification

I. INTRODUCTION

Authorship identification of source code has received attention across various fields, including software engineering, security, and education. As software projects grow in number, determining code authorship has applications in forensic analysis, plagiarism detection, and adaptive learning systems. Recognizing an individual's programming style can provide insights into their coding behavior and expertise, benefiting both academic and industrial settings.

Traditional methods for authorship attribution have relied on stylometric analysis, which examines lexical, syntactic, and structural features of code. Early approaches used statistical techniques, such as token frequency analysis and n-gram modeling, to differentiate authors based on their coding patterns. More advanced methods have incorporated abstract syntax trees (ASTs) and feature extraction techniques to improve classification performance. However, these approaches often face difficulties with code obfuscation, collaborative development, and structured projects, where stylistic differences become less distinct.

We believe that behavioral biometrics can complement static code analysis by incorporating real-time coding behaviors. This includes keystroke dynamics, code editing patterns, debugging habits, and interaction with development tools. By

integrating these behavioral aspects with traditional stylometric techniques, a hybrid approach can improve authorship attribution.

This research focuses on developing and evaluating a methodology that combines static code features with behavioral biometrics. The goal is to improve the accuracy of programmer identification. The study explores applications in academic integrity monitoring, software security, and talent identification. Integration of machine learning models, including deep learning architectures, presents potential improvements in authorship attribution systems.

This paper provides an overview of progress made in the past year, including dataset preparation, feature extraction, and preliminary classification results. The contributions of this work lie in combining static and behavioral aspects of programming. Future research will explore additional machine learning models, expand the dataset with behavioral indicators, and examine ethical considerations associated with programmer identification.

II. RELATED WORKS

Authorship identification in source code has been studied in software forensics, plagiarism detection, and cybersecurity. Early approaches relied on stylometric methods, which analyze lexical and syntactic features of source code to distinguish between authors. Studies such as [1] and [2] demonstrated that statistical models based on token distributions and n-grams could achieve reasonable accuracy in identifying authors across different programming languages.

More recent research has explored the use of ASTs and vector-based representations for improving classification performance. Caliskan-Islam et al. [3] proposed a methodology that extracts stylistic features from AST representations and applies machine learning classifiers for authorship attribution. This approach improved accuracy compared to purely lexical methods.

While these methods focus on static properties of code, behavioral biometrics have emerged as a complementary technique in authorship identification. Studies by Hayes and Offutt [4] and Gonçalves de Oliveira et al. [5] have explored behavioral patterns, including keystroke dynamics, code navigation habits, and editing speed. Their findings suggest that behavioral data can serve as an additional layer of authorship verification, particularly in cases where code has been obfuscated or heavily refactored.

TABLE I: Comparison of selected authorship identification studies

Study	Authors – Language	Method	Task Type	Reported Performance
Pellin [6]	2 – Java	Support Vector Machine	Classification	88.5%
MacDonell et al. [7]	7 – C++	Feedforward Neural Network	Classification	81.1%
Frantzeskou et al. [8]	8 – C++	K-Nearest Neighbors Similarity	Classification	100.0%
Burrows et al. [9]	10 – C	Probabilistic Retrieval Ranking	Classification	76.8%
Elenbogen & Seliya [10]	12 – C++	Decision Trees	Classification	74.7%
Krsul & Spafford [11]	29 – C	Discriminant Analysis	Classification	73.0%
Ding & Samadzadeh [12]	46 – Java	Canonical Discriminant Analysis	Classification	62.7%
Burrows et al. [13]	100 – C, C++	Neural Networks	Classification	79.9%
Caliskan-Islam et al. [3]	229 – Python	Random Forest	Classification	53.9%
Abuahmad et al. [14]	1,600 – C++	Convolutional Neural Network	Classification	96.2%
Abuahmad et al. [14]	1,500 – Python	Convolutional Neural Network	Classification	94.6%
Abuahmad et al. [14]	1,000 – Java	Convolutional Neural Network	Classification	95.8%
Abuahmad et al. [14]	566 – C	Recurrent Neural Network + Random Forest	Regression	$R^2 = 0.94$
Abuahmad et al. [14]	1,952 – Java	Recurrent Neural Network + Random Forest	Regression	$R^2 = 0.97$

Note. Classification results are reported using accuracy, while regression tasks report R^2 values. Metrics are taken as reported in the original studies and are not directly comparable across task types.

Table I provides an overview of selected studies that employed different machine learning methods for source code authorship identification. The table includes task types and reported metrics, highlighting whether the approach was classification-based or regression-based. A wide range of techniques has been used, including support vector machines (SVM), artificial neural networks, random forests, and convolutional neural networks (CNN), illustrating the diversity of approaches in the field.

Feature fusion approaches that integrate both stylistic and behavioral features have been explored as a direction in authorship attribution. Azcona et al. [15] combined static analysis with behavioral biometrics, demonstrating that a multimodal approach can outperform traditional methods. Similarly, deep learning models based on CNNs and long short-term memory networks (LSTMs) have been investigated for detecting stylistic variations in programmer writing style. Future research will likely focus on refining these approaches by integrating larger datasets and testing models on a broader range of programming environments.

III. SOURCE CODE DATASET AND PRELIMINARY EXPERIMENTS

To develop an authorship identification framework, we created a dataset consisting of source codes submitted by students of the Technical University of Košice between 2018 and 2024. The dataset includes submissions from two courses: *Fundamentals of Algorithmization and Programming* and *Programming in C*. Each course enrolls approximately 1000 students per year, resulting in a dataset of around 6000 individuals. To ensure data quality, we included only students who submitted at least 80% of the assigned tasks, leading to a collection where each student provided at least eight distinct source code submissions throughout the academic year. This sequential submission process reflects the natural development of programming skills over time. Additionally, the dataset was fully anonymized, considering ethical guidelines related to student data privacy.

For feature extraction, we developed a custom script that analyzes various stylistic and structural attributes of the collected source codes. The extracted features include fundamental statistics such as code length, average line length, and function sizes, as well as more advanced properties like variable naming conventions, the frequency of mathematical operations,

and the depth of nested conditionals. In total, approximately 40 different attributes are tracked, covering various aspects of programming style. Some features also reflect consistent stylistic preferences of individual programmers, such as the use of standard versus external libraries, the organization of variable declarations, and spacing around operators. These are not dynamic behavioral signals, but they may still encode habitual tendencies that are characteristic for an individual.

To evaluate the feasibility of authorship attribution, we conducted preliminary machine learning experiments using regression models. At this stage, we focused exclusively on stylistic features extracted from source code, as behavioral data collection is still in progress. We used a scikit-learn pipeline with standard preprocessing and evaluated models including linear regression, support vector machines, and gradient boosting. Among these, the XGBoost regressor was selected for further testing due to its early performance and flexibility. Hyperparameters were tuned using grid search with 5-fold cross-validation, optimizing for the coefficient of determination (R^2). The current results demonstrate the potential of stylistic analysis in this task. Future experiments will extend the evaluation to include behavioral metrics and multimodal feature combinations.

In addition to our dataset, we identified the *Google Code Jam* dataset as a suitable external benchmark [16]. The *Google Code Jam* competition, hosted by Google from 2008 to 2020, provides a vast collection of competitive programming submissions from a diverse set of programmers. The dataset includes solutions to algorithmic challenges written in multiple programming languages, allowing for an extensive analysis of programming styles across different skill levels. This dataset serves as a valuable resource for evaluating authorship attribution models in a broader and more diverse context.

Future work will focus on expanding the dataset by incorporating additional behavioral metrics, such as debugging habits, indentation styles, and function call patterns. In our educational setting, debugging behavior can be partially reconstructed from submission logs in the *Arena* system, which evaluates student solutions every three hours and captures intermediate revisions. Furthermore, students work on live assignments in the *Spartan* environment during lab sessions, where their edit sequences and command usage can be instrumented for research purposes. These data sources offer an opportunity to capture dynamic aspects of programming

behavior in a realistic setting.

IV. FUTURE WORK

Future research will focus on expanding the range of machine learning models applied to authorship attribution. Experiments will be conducted with both traditional classification methods, such as decision trees, support vector machines, and random forests, as well as deep learning techniques, including recurrent and convolutional neural networks. By evaluating various approaches, the goal is to determine the most effective models for accurately attributing source code to the correct programmer.

Additionally, more dynamic behavioral features will be incorporated into the analysis. In particular, tracking student interactions with version control systems, will allow for capturing coding workflow, commit frequency, and collaborative practices. These behavioral patterns could provide valuable insights into individual programming habits beyond static code analysis.

Another key direction involves exploring different ways to decompose and represent source code. ASTs, n-gram representations, and source code embeddings will be examined to assess their suitability for authorship identification. These methods could improve classification performance by capturing deeper structural and contextual characteristics of code.

The primary objective of this research is to develop models capable of accurately assigning a given piece of code to its correct author. Additionally, programmers will be classified into distinct categories based on their coding style, proficiency, and habits. This classification could be leveraged in talent acquisition processes, enabling recruiters to identify promising developers based on their unique programming signatures.

V. CONCLUSION

This research explores a hybrid approach to source code authorship attribution by integrating stylometric analysis and behavioral biometrics. The dataset, collected from thousands of students over multiple years, provides foundation for evaluating various machine learning techniques. Initial results demonstrate the effectiveness of combining static and dynamic features, with hybrid models showing promising accuracy. Next work will expand the range of tested models, incorporate behavioral data from version control systems, and explore different source code representations. The ultimate goal is to improve authorship identification and programmer classification, which can be utilized in educational settings, security applications, and talent acquisition.

ACKNOWLEDGMENT

This work was supported by project KEGA 061TUKE-4/2025 "Building bridges between university and high school ICT education".

REFERENCES

- [1] J. Gray, D. Sgandurra, L. Cavallaro, and J. Blasco Alis, "Identifying authorship in malicious binaries: Features, challenges & datasets," *ACM Computing Surveys*, vol. 56, no. 8, pp. 1–36, 2024.
- [2] V. Kalgutkar, R. Kaur, H. Gonzalez, N. Stakhonova, and A. Matyukhina, "Code authorship attribution: Methods and challenges," *ACM Computing Surveys (CSUR)*, vol. 52, no. 1, pp. 1–36, 2019.
- [3] A. Caliskan-Islam, R. Harang, A. Liu, A. Narayanan, C. Voss, F. Yamaguchi, and R. Greenstadt, "De-anonymizing programmers via code stylometry," in *Proceedings of the 24th USENIX Conference on Security Symposium (SEC'15)*. Berkeley, CA: USENIX Association, 2015, pp. 255–270. [Online]. Available: <http://dl.acm.org/citation.cfm?id=2831143.2831160>
- [4] J. H. Hayes, "Authorship attribution: A principal component and linear discriminant analysis of the consistent programmer hypothesis," *International Journal on Computers and Their Applications*, vol. 15, no. 2, pp. 79–99, 2008.
- [5] M. G. de Oliveira, P. M. Ciarelli, and E. Oliveira, "Recommendation of programming activities by multi-label classification for a formative assessment of students," *Expert Systems with Applications*, vol. 40, no. 16, pp. 6641–6651, 2013. [Online]. Available: <https://www.sciencedirect.com/science/article/pii/S0957417413003916>
- [6] B. N. Pellin, "Using classification techniques to determine source code authorship," White Paper, Department of Computer Science, University of Wisconsin, 2000.
- [7] S. G. Macdonell, A. R. Gray, G. MacLennan, and P. J. Sallis, "Software forensics for discriminating between program authors using case-based reasoning, feedforward neural networks and multiple discriminant analysis," in *Proceedings of the 6th International Conference on Neural Information Processing (ICONIP'99)*, vol. 1, 1999, pp. 66–71.
- [8] G. Frantzeskou, E. Stamatatos, S. Gritzalis, and S. Katsikas, "Effective identification of source code authors using byte-level information," in *Proceedings of the 28th International Conference on Software Engineering (ICSE'06)*. New York, NY: ACM, 2006, pp. 893–896.
- [9] S. Burrows, A. L. Uitdenboger, and A. Turpin, "Application of information retrieval techniques for source code authorship attribution," in *Proceedings of the 14th International Conference on Database Systems for Advanced Applications (DASFAA'09)*. Berlin: Springer-Verlag, 2009, pp. 699–713.
- [10] B. S. Elenbogen and N. Seliya, "Detecting outsourced student programming assignments," *Journal of Computing Sciences in Colleges*, vol. 23, no. 3, pp. 50–57, Jan. 2008. [Online]. Available: <http://dl.acm.org/citation.cfm?id=1295109.1295123>
- [11] I. Krsul and E. H. Spafford, "Authorship analysis: Identifying the author of a program," *Computers & Security*, vol. 16, no. 3, pp. 233–257, 1997.
- [12] H. Ding and M. H. Samadzadeh, "Extraction of java program fingerprints for software authorship identification," *Journal of Systems and Software*, vol. 72, no. 1, pp. 49–57, 2004.
- [13] S. Burrows, A. L. Uitdenboger, and A. Turpin, "Comparing techniques for authorship attribution of source code," *Software: Practice and Experience*, vol. 44, no. 1, pp. 1–32, 2014.
- [14] M. Abuhamad, J.-s. Rhim, T. AbuHmed, S. Ullah, S. Kang, and D. Nyang, "Code authorship identification using convolutional neural networks," *Future Generation Computer Systems*, vol. 95, pp. 104–115, 2019.
- [15] D. Azcona, I.-H. Hsiao, and A. F. Smeaton, "Detecting students-at-risk in computer programming classes with learning analytics from students' digital footprints," *User Modeling and User-Adapted Interaction*, vol. 29, pp. 759–788, 2019.
- [16] A. Caliskan, F. Yamaguchi, E. Dauber, R. Harang, K. Rieck, R. Greenstadt, and A. Narayanan, "When coding style survives compilation: De-anonymizing programmers from executable binaries," *arXiv preprint arXiv:1512.08546*, 2015.

Implementation of PQC algorithm for IoT devices

¹Peter PEKARČÍK (3rd year),
Supervisor: ²Eva CHOVANCOVÁ

^{1,2}Dept. of Computers and Informatics, FEI TU of Košice, Slovak Republic

¹peter.pekarcik@tuke.sk, ²eva.chovancova@tuke.sk

Abstract—Post-quantum cryptography represents a new era of cryptography. Since these algorithms are relatively new, the scientific community is beginning to address the transition from the theoretical realm to the realm of their practical application. Our research addresses the possibility of using PQC algorithms on IoT devices. Since currently available implementations of PQC algorithms are characterized by high memory requirements and IoT devices with limited memory capacity, their implementation on IoT devices represents a real challenge.

Keywords—BIKE, ESP32, IoT, memory optimization, PQC

I. INTRODUCTION

Post-quantum cryptography (PQC), defined by [1], is the development of cryptographic algorithms that are thought to be secure against cryptanalytic attacks performed by a quantum computer. These algorithms rely on other problems, such as the difficulty of integer factorization, discrete logarithm, or the elliptic curve discrete logarithm problem.

When we want to ensure data security against quantum computers, quantum-safe algorithms must replace algorithms like *RSA*, *AES*, or *ECC*. Migration from the quantum-vulnerable cryptography used to PQC will be time-consuming and resource-intensive. In August 2024, the first PQC standards were published by the National Institute of Standards and Technology (NIST), making the next phase in the PQC migration [2]. While it is challenging to estimate the exact cost of PQC migration, it is clear that every organization will need to allocate resources [3]. The next problem is hardware requirements. IoT devices have limited memory, processing power, and battery capacity [4].

II. INITIAL STATE OF PROBLEM

Unfortunately, all candidates for PQC standards have large keys, signatures, or cipher text sizes [5]. In our research, we looked at the 4th round of the PQC challenge algorithms¹:

- **BIKE** is a code-base key encapsulation mechanism based on Quasi-Cyclic Moderate Density Parity-Check codes²;
- **Classic McEliece** is the first code-based key encapsulation mechanism based on binary Goppa codes³;
- **HQC** is code-base public key encryption scheme based on hardness of decoding random quasi-cyclic codes in the Hamming metric⁴.

¹<https://csrc.nist.gov/Projects/post-quantum-cryptography/round-4-submissions>

²<https://bikesuite.org/>

³<https://classic.mceliece.org/>

⁴<https://pqc-hqc.org/index.html>

III. IMPLEMENTATION PROCESS

We initially have three candidates for implementing the Post-quantum algorithm for IoT devices. All implementations are available on the NIST web page⁵.

A. Initial assessment of the situation

We measured the time and memory consumption of *Reference implementations*. The results of measurements were these findings:

• BIKE

- **Pros:** lower public key size (~1-2 kB for Level 1); time-efficient key generation, encapsulation, and decapsulation;
- **Cons:** decapsulation requires iterative decoding, which can be unpredictable in run time;

• HQC

- **Pros:** more deterministic runtime to BIKE;
- **Cons:** a larger public key (~5-7 kB for Level 1); higher decryption latency;

• McEliece

- **Pros:** extreme security, based on code-based cryptography; fast encapsulation and decapsulation;
- **Cons:** huge public keys (~261 kB for Level 1 security); difficulty of implementation for IoT devices.

After considering these findings and our knowledge about IoT devices, we decided to experimentally implement the *BIKE* algorithm. The decisive factor was the size of the public keys in the *HQC* and *McEliece*.

For implementation, we chose the microchip *ESP-Wroom-32*. *Table 1* introduces the most important features.

Feature	Specification
Processor	32-bit dual-core Xtensa LX6
Clock Speed	160 or 240 MHz
RAM	520 KB
ROM	448 KB
Wireless Communication	2.4 GHz (802.11 b/g/n)
Bluetooth	Version 4.2

TABLE I: ESP-Wroom-32 Specification⁶

Initially, it was primarily intended as a standalone micro-controller, allowing the development team to focus on other goals.

⁵<https://csrc.nist.gov/Projects/post-quantum-cryptography/round-4-submissions>

⁶https://docs.ai-thinker.com/_media/esp32/docs/nodemcu-32s_product_specification.pdf

B. Changes in implementation of BIKE

In the beginning, we had reference implementation of the *BIKE* available⁷. This implementation had to go through a series of changes like:

- replacing functions from *ntl* and *OpenSSL* libraries with publicly available implementations;
- breaking large functions into smaller ones to optimize compiler performance;
- marking some functions as *static*;
- removing variables that store data that does not need to be explicitly stored in variables;
- moving some variables and fields to global variables and marking them as *static*;
- exploring the possibility of replacing variables with smaller data types;
- performing all possible operations with an array in place, etc.

Moreover, both memory requirements and security of the algorithm depend on the setting of security parameters:

- **R_BITS**: represents the length of the code's block size;
- **DV**: denotes the weight of the parity-check matrix;
- **T1**: the number of errors the code can detect and correct.

These parameters are set in *defs.h*. Unfortunately, they affect not only the security, but also the size of fields used in key pair generation, encapsulation, and decapsulation, and thus, the overall memory footprint. For different security levels, *NIST* recommended setting of parameters mentioned in *TABLE II*.

Security level	R_BITS	DV	T1
Level 1	12 323	71	134
Level 3	24 659	103	199
Level 5	40 973	137	264

TABLE II: BIKE NIST recommended security parameters

The largest of the values is the *R_BITS*. It affects the size of the arrays, the number of loop iterations, the algorithm's security, and, unfortunately, also the overall memory consumption.

As shown in *Figure 1*, the key generation and encapsulation process or original implementation was completely running for the *R_BITS* value of 713. This is the reason why we had to make the next experimental changes; examples are:

- design of more memory-efficient implementation of the hash function (*sha3_384()*);
- design of more memory-efficient implementation of decomposition of a polynomial into its constituent parts (*ntl_split_polynomial()* function);
- implementation of matrix multiplication using *Karatsuba's algorithm*⁸.

IV. OBTAINED RESULTS AND FUTURE PLANS

With the changes described in section III B, we increased the *R_BITS* to 5900. *Figure 1* describes the changes in the *R_BITS* value after applying the modifications.

As you can see, the current *R_BITS* is 5900. This is far from the goal of 12323. However, we decided to use *Karatsuba's algorithm* for matrix multiplication. We hope that after successfully integrating Karatsuba's algorithm, we will be able to perform all steps of the BIKE algorithm on ESP32.

⁷<https://csrc.nist.gov/csrc/media/Projects/post-quantum-cryptography/documents/round-4/submissions/BIKE-Round4.zip>

⁸<https://people.cs.uchicago.edu/~laci/HANDOUTS/karatsuba.pdf>

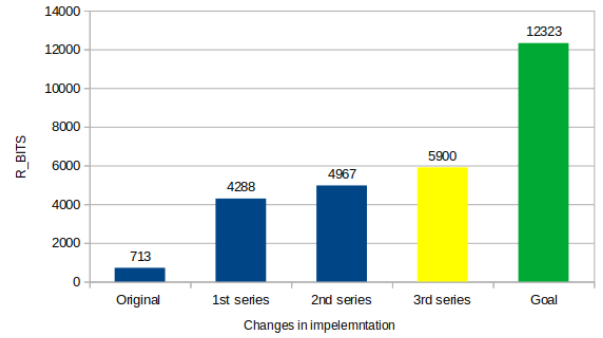


Fig. 1: Increasing of R_BITS value

V. CONCLUSION

Since PQC is a new concept, there are still unresolved questions regarding its practical application. If PQCs are adopted as standard, they will be used across a wide range of diverse devices. Achieving their lower time and memory requirements will enable their implementation on more economically available microprocessors and, thus, their higher availability. In order to achieve the possibility of their use on a wide range of devices, these algorithms must undergo extensive research and optimization.

Unfortunately, the performance metrics of our solution cannot be provided now because it is still in the development phase. This solution's main advantage will be its ability to run on memory-constrained devices. Until today, no implementation of an encryption algorithm exists that is resistant to attacks performed by quantum computers and, at the same time, possible to run on IoT devices.

We have set ourselves the goal of developing a memory-efficient implementation of the *BIKE* that can run on a 32-bit microprocessor. Assuming that the algorithm is entirely secure, this goal seems impossible, but we are gradually approaching it by carefully examining the individual operations.



REFERENCES

- [1] D. J. Bernstein, J. Buchmann, E. Dahment. *Post-Quantum Cryptography*, Springer, 2009. Available at: <https://link.springer.com/book/10.1007/978-3-540-88702-7>
- [2] A. Amadori, T. Attema, M. Bombar, J. D. Duarte, V. Dunning, S. Etinski, D. van Gent, M. Lequesne, W. van der Schoot, M. Stevens. *The PQC Migration Handbook*, Cryptology Group and TNO - Applied Cryptography and Quantum Algorithms, 2024. Available at: <https://publications.tno.nl/publication/34643386/fXcPVHsX/TNO-2024-pqc-en.pdf>
- [3] M. Smith. *The Challenges of IoT (Internet of Things)*, 2024, Available at: https://papers.ssrn.com/sol3/papers.cfm?abstract_id=4993855
- [4] D. T. Dam, T. H. Tran, V. P. Hoang, C. K. Pham, T. H. Hoang. *A Survey of Post-Quantum Cryptography: Start of a New Race*, Survey of Cryptographic Topics, 2023, Available at: <https://doi.org/10.3390/cryptography7030040>
- [5] B. Lonc, A. Auruby, H. Bakhti, M. Christofi, H. A. Mehrez. *Feasibility and Benchmarking of Post-Quantum Cryptography in the Cooperative ITS Ecosystem*, IEEE Vehicular Networking Conference (VNC), 2023, Available at: <https://hal.science/hal-04050027/document>

Optimization of Discrete-event Systems

¹Nikola GECIOVÁ (1st year),
Supervisor: ²Helena MYŠKOVÁ

^{1,2}Department of Mathematics and Theoretical Informatics, FEI TU of Košice, Slovak Republic

¹nikola.geciova@tuke.sk , ²helenamyskova@tuke.sk 

Abstract—Discrete-event systems play a crucial role in various domains, including manufacturing, transportation, and distributed computing. The optimization of these systems often relies on max-plus algebra, a mathematical framework that facilitates modeling synchronization and scheduling problems. This paper presents a review of optimization techniques for max-plus linear systems, discussing global and local optimization approaches, solvability conditions, and computational challenges. Additionally, recent advancements in interval max-plus algebra are explored to address uncertainties in real-world applications. The study highlights the need for efficient algorithms and scalable computational techniques to enhance the practical applicability of max-plus optimization in industrial and engineering systems.

Keywords—discrete-event systems, max-plus algebra, optimization

I. INTRODUCTION

Discrete-event systems represent a class of dynamic systems in which state transitions occur at discrete time instances. These systems are widely applied in manufacturing, transportation networks, and distributed computing. One of the fundamental challenges is optimizing performance under synchronization constraints, where traditional linear algebraic methods often fall short. To address this, researchers have developed max-plus algebra, a mathematical framework well-suited for modeling discrete-event systems characterized by synchronization and concurrency.

Max-plus algebra operates over the max-plus semiring, where addition is replaced by the maximum operator and multiplication corresponds to conventional addition. This framework enables the formulation of optimization problems as max-plus linear equations, facilitating efficient scheduling and resource allocation. Over the years, numerous studies have explored global and local optimization techniques for max-plus linear systems, developing solvability conditions, algorithms, and computational strategies.

Despite significant theoretical advancements, practical implementation remains challenging due to computational complexity and real-world uncertainties. The integration of interval max-plus algebra has introduced robust methods for handling imprecise data, further expanding the applicability of max-plus optimization techniques. However, scalability issues and the need for efficient algorithms persist.

This paper provides a comprehensive review of optimization methods for discrete-event systems using max-plus algebra. It discusses fundamental concepts, existing optimization approaches, recent advancements, and future research directions. The goal is to bridge the gap between theoretical developments and practical applications, highlighting potential avenues for improving computational efficiency and scalability.

II. PRELIMINARIES

This section introduces fundamental concepts and notations from max-plus algebra [1] that are essential for understanding the optimization problems explored in this study. Max-plus algebra operates over the set

$$\mathbb{R}_{\max} = \mathbb{R} \cup \{-\infty\},$$

where the addition and multiplication operations are defined as:

$$a \oplus b = \max(a, b)$$

and

$$a \otimes b = a + b$$

Define $\varepsilon = -\infty$ and $e = 0$. The max-plus algebra has following properties [2]:

- Associativity:

$$\forall x, y, z \in \mathbb{R}_{\max} : x \oplus (y \oplus z) = (x \oplus y) \oplus z$$

and

$$\forall x, y, z \in \mathbb{R}_{\max} : x \otimes (y \otimes z) = (x \otimes y) \otimes z.$$

- Commutativity:

$$\forall x, y \in \mathbb{R}_{\max} : x \oplus y = y \oplus x$$

and

$$\forall x, y \in \mathbb{R}_{\max} : x \otimes y = y \otimes x.$$

- Distributivity of \otimes over \oplus :

$$\forall x, y, z \in \mathbb{R}_{\max} : x \otimes (y \oplus z) = (x \otimes y) \oplus (x \otimes z).$$

- Existence of a zero element:

$$\forall x \in \mathbb{R}_{\max} : x \oplus \varepsilon = \varepsilon \oplus x = x.$$

- Existence of a unit element:

$$\forall x \in \mathbb{R}_{\max} : x \otimes e = e \otimes x = x.$$

- The zero is absorbing for \otimes :

$$\forall x \in \mathbb{R}_{\max} : x \otimes \varepsilon = \varepsilon \otimes x = \varepsilon.$$

- Idempotency of \oplus :

$$\forall x \in \mathbb{R}_{\max} : x \oplus x = x.$$

A max-plus linear system is a system of equations where the operations follow max-plus algebra [1]. The set of all $m \times n$ matrices over \mathbb{R}_{\max} is denoted by $\mathbb{R}_{\max}^{m \times n}$, and the set of all n -dimensional vectors is denoted by \mathbb{R}_{\max}^n . Given a matrix

$$A \in \mathbb{R}_{\max}^{m \times n},$$

and a vector

$$x \in \mathbb{R}_{max}^n$$

their product where $i = 1, 2, 3, \dots, m$ and $j = 1, 2, 3, \dots, n$ is defined as:

$$(A \otimes x)_i = \max_j (a_{ij} + x_j).$$

A fundamental problem in max-plus algebra is solving equations of the form:

$$A \otimes x = b,$$

where $b \in \mathbb{R}_{max}^m$. The solution set determines feasible schedules and optimization configurations in various applications. The Kleene star operation, denoted as A^* , is used to analyze long-term behavior and is defined as:

$$A^* = I \oplus A \oplus A^2 \oplus A^3 \oplus \dots$$

where I is the max-plus identity matrix. These foundational principles of max-plus algebra provide a mathematical basis for studying and optimizing discrete event systems. The next section formulates the global and local optimization problems within this framework.

III. RELATED WORK

Max-plus algebra with its foundational operations of maximization and addition, has emerged as a powerful framework for modeling discrete-event systems characterized by synchronization and concurrency-free dynamics. Max-plus linear systems have been extensively studied in various fields, including manufacturing systems, transportation networks, and discrete event systems. One of the earliest contributions in this field was made by Cohen et al. [3], who introduced the use of dioid algebras for modeling Discrete Event Systems. Their work laid the foundation for analyzing synchronization and timing in event-driven systems. The fundamental theory of max-plus algebra has been developed in works such as Baccelli et al. [4], Butkovič [5], and Cuninghame-Green [6], which provide the mathematical foundation for modeling synchronization phenomena in these systems. Further studies on max-plus algebra have explored its application in control, optimization, manufacturing, traffic management distributed computing and robustness analysis (Heidergott et al. [2], Gaubert et al. [7], Hardouin et al. [8]). These studies laid the groundwork for translating system behaviors into max-plus linear equations and inequalities, forming the basis for optimization and control strategies.

In the area of optimization of max-plus linear systems, several approaches have been proposed to address solvability and computational efficiency. Beaumont [9] examined global optimization problems in the max-plus setting, introducing algorithms for finding globally optimal solutions. Lee and Grossmann [10] extended this work by incorporating additional constraints into the optimization framework. Tao et al. [11] further generalized these approaches by considering max-plus functions with affine constraints and deriving conditions for the existence and uniqueness of globally optimal solutions. However, their work restricted coefficients to unity, limiting applicability to real-world scenarios where heterogeneous constraints naturally arise. Recent efforts, such as Xu et al. [12], introduced efficient approximation methods for nonlinear max-plus optimization but did not fully resolve the challenges of exact global solutions under general affine constraints.

The specific problem of global optimization of max-plus linear systems was directly considered by Tao and Wang [13], who introduced a method for determining globally optimal solutions and applied it to distributed system load balancing. Their work demonstrated that while global optimization can provide an ideal theoretical framework, practical constraints often necessitate local optimization strategies. Later extended these results, providing a corrigendum that refined the conditions under which global optimization solutions exist and remain unique.

Other studies have focused on solving max-plus equations and inequalities as a means of optimizing max-plus linear systems. Research by De Schutter and De Moor [14], [15] addressed minimal realization problems in max-plus algebra, while Adzkiya et al. [16] and Wang et al. [17] explored reachability, observability, and optimal input design. Moreover, interval analysis techniques have been employed to assess the robustness of solutions [18], [19].

Recent works have also applied global optimization techniques to distributed computing and scheduling problems. Shang et al. [20] proposed algorithms for high-throughput screening systems. The application of max-plus optimization to distributed systems has been further explored by Necoara et al. [21], who investigated robust control strategies.

The study by Tao and Wang [13] builds upon these previous efforts by providing new polynomial algorithms for checking solvability and finding globally optimal solutions in max-plus linear systems with affine constraints. Additionally, their work extends the theoretical framework by considering non-negative constraints, which are particularly relevant in practical applications such as scheduling and resource allocation in distributed systems.

Recent advancements have focused on the practical applications of these theories in complex systems. Candido et al. [22] explored the reachability of uncertain max-plus systems, highlighting the challenges posed by system variability. Additionally, Farahani et al. [23] developed stochastic optimization techniques for max-min-plus-scaling systems, broadening the scope of max-plus algebra in control applications.

Another work by Wang and Tao [1] builds upon these foundational and applied studies by further refining the conditions for global and local optimization in max-plus linear systems. It addresses gaps in previous formulations by explicitly defining operations involving infinity elements and real numbers and simplifying the discriminant conditions for global optimization. Moreover, their study applies the developed methods to distributed system load balancing, extending the applicability of max-plus optimization beyond theoretical constructs into practical engineering solutions.

Interval uncertainty in max-plus systems has been addressed in recent years, motivated by the need to handle imprecise data in real-world applications. Myšková and Plavka [24], [25], [26] contributed significantly to interval max-plus matrix theory, developing methods to solve interval equations and analyze regularity. Their work highlighted the challenges of verifying solvability under interval uncertainty, particularly when dependencies between matrix rows or columns must be preserved. These studies provided a foundation for extending optimization problems to interval data, as demonstrated in the current work.

Another article by Myšková and Plavka [27] builds on these foundations by addressing two key gaps. First, it generalizes

Tao and Wang's [13] global optimization framework to include interval matrices, enabling robustness analysis in systems with uncertain parameters. Second, it introduces non-negativity constraints, which are critical in practical applications like load distribution in distributed systems, where execution times and resource allocations must remain non-negative. The proposed algorithms for solvability verification, both for deterministic and interval cases, advance prior methods by efficiently handling combinatorial complexity through structured linear programming approaches.

Applications in distributed systems, such as task scheduling with precedence constraints, further contextualize the theoretical contributions. The example of load redistribution across processors aligns with real-world challenges in high-performance computing, where balancing workloads while minimizing completion times is essential. Their practical focus extends earlier theoretical studies, bridging the gap between abstract algebraic results and operational optimization in engineering systems.

Muijsenber [28] expanded the field by proposing a general modeling framework for Switching Max-Plus Linear (SMPL) systems, focusing on a systematic approach to routing, ordering, and synchronization constraints using topology graphs. Additionally, the novel application of this framework to baggage handling systems, which had not been previously described in the literature as an SMPL system, represents a key contribution.

IV. DISCUSSION

The study of dynamic systems with inaccurate data in extremal algebras, particularly in the max-plus algebraic framework, has garnered significant attention due to its applicability in synchronization and optimization problems across various domains, including manufacturing, transportation networks, and distributed computing. The foundational theories of max-plus algebra have been well-established at the end of the last century in works which provide mathematical frameworks for analyzing synchronization phenomena in discrete event systems. These studies laid the groundwork for modeling and computational approaches to solving problems in extremal algebras.

In terms of optimization of max-plus linear systems, early contributions focused on algorithmic solutions for finding globally optimal solutions under max-plus constraints. More recently, these methods were expanded to include affine constraints, though practical limitations in real-world applications necessitate further refinements. Later, approximation methods were introduced for nonlinear max-plus optimization, addressing the computational complexity but were still facing challenges related to exact global solutions.

Significant strides in global optimization techniques for max-plus linear systems were made recently, applying max-plus algebra to distributed system load balancing. This research demonstrated that while global optimization is theoretically desirable, local optimization strategies are often required due to real-world constraints. More contribution was made by incorporating interval uncertainty into max-plus algebra, enhancing robustness analysis and addressing challenges in systems with imprecise data.

Recent studies have also expanded on interval analysis techniques for solving max-plus equations under uncertainty.

These methods provide improved solvability conditions and computational techniques for handling max-plus linear systems under varying degrees of data accuracy.

Despite these advancements, several challenges remain in this field. While various optimization methods have been proposed, the computational cost of solving max-plus systems, particularly under interval uncertainty, remains a significant hurdle.

Another challenge is scalability. Applying global optimization techniques to large-scale distributed systems introduces scalability concerns that require further research in parallel and distributed computing frameworks. While theoretical advancements have been made, practical implementation in industrial and engineering applications remains limited. More work is needed to integrate max-plus optimization techniques into real-time decision-making systems.

The heterogeneous nature of real-life systems poses another obstacle. Existing optimization frameworks often assume homogeneous constraints, whereas real-world problems involve complex, heterogeneous constraints that require more flexible mathematical formulations. While recent advancements attempt to bridge these gaps by extending max-plus optimization to interval matrices and incorporating non-negativity constraints, which are crucial for practical applications such as resource allocation and scheduling in distributed systems, more work needs to be done.

V. FUTURE RESEARCH

Future research should prioritize the development of novel algorithms or hybrid optimization methods that can reduce computational costs while maintaining accuracy in solving max-plus systems. Improving computational efficiency remains a key challenge, as the current methods still suffer from high complexity, limiting their applicability in large-scale problems. One promising direction is exploring approximation techniques and machine learning-based approaches to accelerate computations while preserving solution quality.

Scalability is another important area that needs further investigation. Applying parallel and distributed computing techniques could mitigate the challenges associated with large-scale optimization problems. Advances in cloud computing and edge computing may also provide new opportunities for implementing scalable max-plus optimization solutions.

The integration of theoretical advances into practical applications is a crucial step toward making max-plus algebra a standard tool in industrial optimization. To achieve this, research should focus on developing software tools and real-time decision-making systems that leverage max-plus optimization techniques. These tools could be tailored for applications in logistics, manufacturing, and network scheduling, making max-plus algebra more accessible to practitioners in engineering and operations research.

A further challenge is expanding the framework to accommodate heterogeneous constraints found in real-world optimization problems. Future work should focus on developing more flexible mathematical models that can incorporate diverse constraint types, including time-varying constraints, stochastic elements, and multi-objective optimization criteria.

In conclusion, while the theoretical foundation and algorithmic advancements in max-plus algebra have progressed significantly, addressing computational complexity and real-world constraints remains an open research avenue. Future

research should emphasize refining optimization algorithms, exploring scalable computational techniques, and developing robust frameworks for integrating these methods into real-world industrial and engineering applications.

VI. CONCLUSION

The optimization of discrete-event systems using max-plus algebra has been extensively studied due to its applicability in synchronization, scheduling, and resource allocation problems. This review has explored fundamental concepts of max-plus algebra, existing optimization techniques, and recent advancements in solving max-plus linear systems, particularly under uncertainty.

Global and local optimization approaches have provided significant theoretical insights, with applications in distributed computing, manufacturing, and transportation networks. However, computational challenges remain, especially in solving large-scale systems efficiently. Recent developments in interval max-plus algebra have introduced methods to handle uncertainty, but further improvements are needed to enhance robustness and practical implementation.

Future research should focus on developing scalable algorithms that can efficiently optimize max-plus systems while addressing real-world constraints. Integrating machine learning techniques, parallel computing, and hybrid optimization methods may provide new solutions to computational bottlenecks. Additionally, expanding the applicability of max-plus algebra to heterogeneous and multi-objective optimization problems will further strengthen its role in industrial and engineering applications.

Finally, while max-plus algebra has proven to be a powerful mathematical framework for optimization, continued research is required to bridge the gap between theory and practice. By advancing computational techniques and addressing practical limitations, max-plus optimization can become a standard tool for solving complex synchronization and scheduling challenges across various domains.

REFERENCES

- [1] C. Wang and Y. Tao, "Locally and globally optimal solutions of global optimisation for max-plus linear systems," *IET Control Theory & Applications*, vol. 16, no. 2, pp. 219–228, 2022.
- [2] B. Heidergott, G. J. Olsder, and J. Van Der Woude, *Max Plus at work: modeling and analysis of synchronized systems: a course on Max-Plus algebra and its applications*. Princeton University Press, 2014, vol. 48.
- [3] G. Cohen and J. Quadrat, *Discrete event systems*. Springer, 1994.
- [4] F. Baccelli, G. Cohen, G. J. Olsder, and J.-P. Quadrat, *Synchronization and linearity*. Wiley New York, 1992, vol. 1.
- [5] P. Butkovič, *Max-linear systems: theory and algorithms*. Springer Science & Business Media, 2010.
- [6] R. A. Cuninghame-Green, *Minimax algebra*. Springer Science & Business Media, 2012, vol. 166.
- [7] S. Gaubert, P. Butkovic, and R. Cuninghame-Green, "Minimal (max,+) realization of convex sequences," *SIAM Journal on Control and Optimization*, vol. 36, no. 1, pp. 137–147, 1998.
- [8] L. Hardouin, Y. Shang, C. A. Maia, and B. Cottenceau, "Observer-based controllers for max-plus linear systems," *IEEE Transactions on Automatic Control*, vol. 62, no. 5, pp. 2153–2165, 2016.
- [9] N. Beaumont, "An algorithm for disjunctive programs," *European Journal of Operational Research*, vol. 48, no. 3, pp. 362–371, 1990.
- [10] S. Lee and I. E. Grossmann, "New algorithms for nonlinear generalized disjunctive programming," *Computers & Chemical Engineering*, vol. 24, no. 9–10, pp. 2125–2141, 2000.
- [11] Y. Tao, G.-P. Liu, and W. Chen, "Globally optimal solutions of max–min systems," *Journal of Global Optimization*, vol. 39, pp. 347–363, 2007.
- [12] J. Xu, T. van den Boom, and B. De Schutter, "Optimistic optimization for model predictive control of max-plus linear systems," *Automatica*, vol. 74, pp. 16–22, 2016.
- [13] Y. Tao and C. Wang, "Global optimization for max-plus linear systems and applications in distributed systems," *Automatica*, vol. 119, p. 109104, 2020.
- [14] B. De Schutter and B. De Moor, "Minimal realization in the max algebra is an extended linear complementarity problem," *Systems & Control Letters*, vol. 25, no. 2, pp. 103–111, 1995.
- [15] —, "A note on the characteristic equation in the max-plus algebra," *Linear Algebra and Its Applications*, vol. 261, no. 1–3, pp. 237–250, 1997.
- [16] D. Adzkiya, B. De Schutter, and A. Abate, "Computational techniques for reachability analysis of max-plus-linear systems," *Automatica*, vol. 53, pp. 293–302, 2015.
- [17] C. Wang, Y. Tao, and H. Yan, "Optimal input design for uncertain max-plus linear systems," *International Journal of Robust and Nonlinear Control*, vol. 28, no. 16, pp. 4816–4830, 2018.
- [18] H. Myšková, "Interval max-plus systems of linear equations," *Linear algebra and its applications*, vol. 437, no. 8, pp. 1992–2000, 2012.
- [19] W. Leela-Apiradee, P. Thipwiwatpotjana, and A. Gorka, "Closed form of l-localized solution set of max-plus interval linear system and its application on optimization problem," *Journal of Computational and Applied Mathematics*, vol. 317, pp. 113–127, 2017.
- [20] Y. Shang, L. Hardouin, M. Lhommeau, and C. A. Maia, "An integrated control strategy to solve the disturbance decoupling problem for max-plus linear systems with applications to a high throughput screening system," *Automatica*, vol. 63, pp. 338–348, 2016.
- [21] I. Necoara, B. De Schutter, T. J. van den Boom, and H. Hellendoorn, "Robust control of constrained max-plus-linear systems," *International Journal of Robust and Nonlinear Control: IFAC-Affiliated Journal*, vol. 19, no. 2, pp. 218–242, 2009.
- [22] R. M. F. Cândido, L. Hardouin, M. Lhommeau, and R. S. Mendes, "Conditional reachability of uncertain max plus linear systems," *Automatica*, vol. 94, pp. 426–435, 2018.
- [23] S. S. Farahani, T. van den Boom, and B. De Schutter, "On optimization of stochastic max–min-plus-scaling systems—an approximation approach," *Automatica*, vol. 83, pp. 20–27, 2017.
- [24] H. Myšková, "Interval max-plus matrix equations," *Linear Algebra and its Applications*, vol. 492, pp. 111–127, 2016.
- [25] H. Myšková and J. Plavka, "Regularity of interval fuzzy matrices," *Fuzzy Sets and Systems*, vol. 463, p. 108478, 2023.
- [26] —, "Regularity of interval max-plus matrices," *Linear Algebra and its Applications*, vol. 680, pp. 28–44, 2024.
- [27] —, "Interval global optimization problem in max-plus algebra," 2024.
- [28] M. Van den Muijsenberg, "Scheduling using max-plus algebra," 2015.

Sparse Wars: Nyquist Strikes Back

¹Antónia KOVÁČOVÁ (2nd year)
Supervisor: ²Ján ŠALIGA

^{1,2}Dept. of Electronics and Multimedia Communications, FEI, Technical University of Košice, Slovak Republic

¹antonia.kovacova@tuke.sk, ²jan.saliga@tuke.sk

Abstract—In this paper two methods of compressed sensing are described. The first one is a compressed sensing method of ECG (electrocardiogram) signals with a DDSS (dynamic deterministic sub-sampling) sensing matrix, which promises one of the most accurate results. The second, a QRS-detection-frames-based approach, offers a compelling alternative, delivering comparable results without the need of transmitting the entire sensing matrix. Also, the author presents her previous work, outlining her goals and further direction of her research.

Keywords—compressed sensing, EKG, signal processing.

I. INTRODUCTION

There are two types of signal compression: lossless and lossy. Lossless compression keeps the exact information of the original signal after decompression, while lossy compression discards some information but remains essential to be suitable for specific applications. Since there is some loss of information, mostly irrelevant, a lossy method shows higher levels of compression ratio. In lossy compression methods, various signals, or data can be recovered from a set of samples taken at Nyquist rate which is a minimal sampling rate that must be twice as high as the highest frequency present in the signal spectral domain [1]. This was considered as the main condition for digital signal processing, until the discovery of compressed sensing (CS).

CS is a lossy compression method exploiting the signal sparsity in time, frequency, or other transformation domains. It gained attention in multiple fields such as signal processing, statistics, computer science and so on [1]. CS allows acquisition and signal reconstruction far below the Nyquist sampling rate [2]. The signal reconstruction is then possible if following necessary conditions are met: the null space property, restricted isometry property, and coherence property [3]. These properties are directly related to the sensing matrix and basis matrix necessary for reconstruction. The functions of discrete orthogonal transformations, such as discrete wavelet transform (DWT), discrete cosine transform (DCT), or discrete Fourier transform (DFT), are frequently used as a basis for CS applications [4]. Choosing a suitable basis depends on the signal structure and the level of sparsity in the transformation domain. Also, the design of an optimal sensing matrix can improve the overall reconstruction.

In this paper, the most promising method in the subject of compressed sensing of ECG (electrocardiogram) signals is described. This method shows a very high compression ratio (CR) with very low PRD (percentage root-mean-square difference). A new method, the QRS-detection-frame-based method is described, which is in the stage of preparation. In the last chapter, the results of authors' work from the past year are summarized and the further goals are set for remaining time of PhD. study.

II. ECG COMPRESSED SENSING WITH DDSS MATRIX

One of the advantages of CS is signal acquisition far below the Nyquist sampling rate. The following method shows that it is possible to get better results in terms of compression and reconstruction accuracy if the Nyquist sampling rate is kept.

In work [5] a dynamic deterministic sub-sampling sensing matrix (DDSS) is proposed. The principle of this matrix lies in the correlation between the frame of n samples, acquired with the fulfillment of Nyquist sampling rate, and the vector p . The vector p is a binary vector whose values depend on the threshold value derived from the centered mean value of samples y . The sample value higher than the threshold assigns the value of one for coefficient of vector p . Otherwise, value zero is assigned. Next, the under-sampling ratio (USR) is set, based on the desired CR. Based on vector p and USR value, the sensing matrix is designed as:

$$\Phi_{DDSS} = \begin{bmatrix} p_1 & p_2 & \cdots & p_n \\ p_{n-USR+1} & p_{n-USR+2} & \cdots & p_{n-USR} \\ \vdots & \vdots & \ddots & \vdots \\ p_{USR+1} & p_{USR+2} & \cdots & p_{USR} \end{bmatrix} \quad (1)$$

As a basis, a Mexican Hat wavelet kernel function is used, proposed in [6]. The experimental results, obtained on ECG records from the MIT-BIH Arrhythmia Database [7], showed that this method shows a better accuracy compared with the other CS methods with the same database.

The better results were published in work [8] where the same principle is used, but instead of single measurement vector (SMV) reconstruction, the multiple measurement vector reconstruction (MMV) is used for CS of the PTB diagnostic database of multiple-lead ECG recordings [9].

The CS based on MMV reconstruction acquires and reconstructs multiple signals simultaneously, instead of individual signal acquisition and reconstruction [1]. This paper shows that MMV reconstruction can be beneficial for computational complexity, as well as for the accuracy of reconstruction. The results show a very low error rate. With $CR = 10$, the average PRD for PTB records was below 6 %. The disadvantage of this method is the necessity to transmit a DDSS sensing matrix to the receiver, where the reconstruction takes place. Since the matrix has a size of $m \times n$, it can lower the overall CR.

In the next chapter, a proposed CS method for ECG signals is described promising similar results in terms of CR and accuracy of reconstruction without the necessity to send the whole sensing matrix.

III. QRS-DETECTION-FRAME-BASED CS METHOD

In work [5] mentioned in the previous chapter shows the comparison with the method proposed in [10] which exploits the basis of DCT functions and deterministic binary block diagonal (DBBD) sensing matrix. This combination of basis and sensing matrix was used in the proposed CS method.

To lower the computational complexity of the reconstruction process, a parametric dictionary learning algorithm based on the DCT functions was used. The parametric dictionary is derived from the overcomplete dictionary for a specific application [4]. Atoms of the dictionary are adapted to the training dataset, retaining functions that best correlate with the training signals. For the dictionary learning process, the MMV-OMP (MMV-Orthogonal Matching Pursuit) reconstruction algorithm was used to train the dictionary for ECG signals.

The DBBD matrix Φ_{DBBD} was used as a sensing matrix in the proposed method. The design of this depends on the desirable CR which is $CR = n/m$, where n and m are lengths of an original signal vector and vector with a reduced number of measurements. The sensing matrix is then constructed as:

$$\Phi_{DBBD} = \begin{bmatrix} \overbrace{1 \dots 1}^{n/m} & 0 & 0 & 0 \dots 0 \\ 0 \dots 0 & \overbrace{1 \dots 1}^{n/m} & 0 & 0 \dots 0 \\ \vdots & \vdots & \ddots & \vdots \\ 0 \dots 0 & 0 & 0 & \overbrace{1 \dots 1}^{n/m} \end{bmatrix} \quad (2)$$

The improvement of this method lies in the frames with samples of ECG signals based on QRS detections. The QRS detector, proposed in [11], was used to detect R-peaks of ECG waveform. The timestamps of those R-peaks are used for deriving frames with one heart cycle so that one R-peak is aligned with other frames. Similarly, as in the method based on the DDSS matrix, keeping the Nyquist sampling rate is necessary to correctly detect R-peaks with QRS detection.

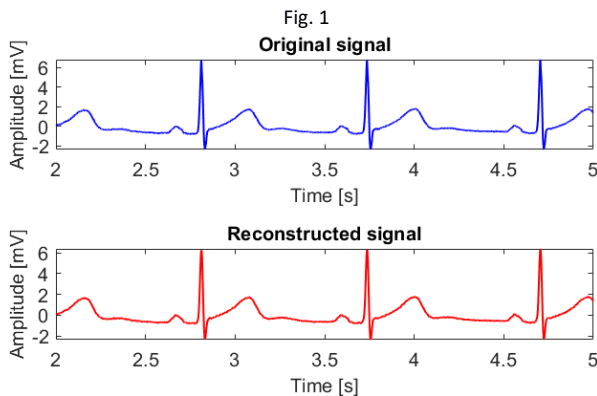


Fig. 1 The comparison of original ECG signal and reconstructed ECG signal for proposed method, database ECGDMLD, set 2001, signal no. 1, lead II.

Fig. 1 shows the result of the CS procedure with the proposed methods. This experiment was performed on record from the database of clinical trial ECGDMLD [12]. This record was sampled at a rate of 1 kHz. For the signal in Fig. 1, the PRD of reconstruction with $CR = 10$ was 4.5 % while the acceptable value of PRD for ECG compression is considered 9 % [8].

IV. PAST, PRESENT AND FUTURE

The author of this paper collaborated on two papers, both published and presented at IMEKO 2024 World Congress in TC4. The first paper [13]: ‘Online impedance estimation of induction motor’ presented a method for the estimation of motor temperature based on the frequency response acquired by compressed sensing. In the second paper [11]: ‘A 12-lead correlation analysis’ where the additional correction algorithm for the Pan-Tomkins QRS detector and correlation analysis of ECG signals for time, DWT and DCT domains was presented.

Currently, the author is working on experiments for the presented proposed method in chapter III and plans to publish it in the special issue of the Measurement journal (Elsevier). This method was proposed during the internship in the Department of Engineering at Università Degli Studi del Sannio in Benevento, Italy. In addition, the student focuses on evaluating the QRS detection accuracy of the algorithm for the Pan Tomkins detector across multiple databases.

In the future, the author wants to further work on compressed sensing of biomedical signals. The main research is focused on the processing of multi-lead ECG signals using MMV reconstruction algorithms.

REFERENCES

- [1] M. A. Davenport, M. F. Duarte, Y. C. Eldar, and G. Kutyniok, “Introduction to compressed sensing,” in *Compressed Sensing*, 1st ed., Y. C. Eldar and G. Kutyniok, Eds., Cambridge University Press, 2012, pp. 1–64. doi: 10.1017/CBO9780511794308.002.
- [2] M. Taghouthi, “Compressed sensing,” in *Computing in Communication Networks*, Elsevier, 2020, pp. 197–215. doi: 10.1016/B978-0-12-820488-7.00023-2.
- [3] M. Khosravy, N. Nitta, K. Nakamura, and N. Babaguchi, “Compressive sensing theoretical foundations in a nutshell,” in *Compressive Sensing in Healthcare*, Elsevier, 2020, pp. 1–24. doi: 10.1016/B978-0-12-821247-9.00006-8.
- [4] I. Tosic and P. Frossard, “Dictionary Learning,” *IEEE Signal Process. Mag.*, vol. 28, no. 2, pp. 27–38, Mar. 2011, doi: 10.1109/MSP.2010.939537.
- [5] F. Picariello, G. Iadarola, E. Balestrieri, I. Tudosa, and L. De Vito, “A novel compressive sampling method for ECG wearable measurement systems,” *Measurement*, vol. 167, p. 108259, Jan. 2021, doi: 10.1016/j.measurement.2020.108259.
- [6] Burke Martin, Nasor Mohamed, “Analysis using the Mexican-Hat Wavelet,” *Advances in scientific computing, computational intelligence and applications, Athens, Greece (2001)*, pp. 26–31.
- [7] G. B. Moody and R. G. Mark, “The impact of the MIT-BIH Arrhythmia Database,” *IEEE Eng. Med. Biol. Mag.*, vol. 20, no. 3, pp. 45–50, Jun. 2001, doi: 10.1109/51.932724.
- [8] P. Daponte, L. De Vito, G. Iadarola, and F. Picariello, “ECG Monitoring Based on Dynamic Compressed Sensing of Multi-Lead Signals,” *Sensors*, vol. 21, no. 21, p. 7003, Oct. 2021, doi: 10.3390/s21217003.
- [9] R. Boussejot, D. Kreiseler, and A. Schnabel, “Nutzung der EKG-Signaldatenbank CARDIODAT der PTB über das Internet,” *Biomedizinische Technik/Biomedical Engineering*, pp. 317–318, Jul. 2009, doi: 10.1515/bmte.1995.40.s1.317.
- [10] A. Ravelomanantsoa, H. Rabah, and A. Rouane, “Compressed Sensing: A Simple Deterministic Measurement Matrix and a Fast Recovery Algorithm,” *IEEE Trans. Instrum. Meas.*, vol. 64, no. 12, pp. 3405–3413, Dec. 2015, doi: 10.1109/TIM.2015.2459471.
- [11] A. Juskova, O. Kovac, J. Kromka, and J. Saliga, “A 12-Lead ECG signal correlation analysis in multiple domains,” *Measurement: Sensors*, p. 101417, Dec. 2024, doi: 10.1016/j.measen.2024.101417.
- [12] L. Johannesen *et al.*, “Late sodium current block for drug-induced long QT syndrome: Results from a prospective clinical trial,” *Clin Pharma and Therapeutics*, vol. 99, no. 2, pp. 214–223, Feb. 2016, doi: 10.1002/cpt.205.
- [13] J. Kromka *et al.*, “Online impedance estimation of induction motor coils using a CS-based measurement method,” *Measurement: Sensors*, p. 101425, Dec. 2024, doi: 10.1016/j.measen.2024.101425.

Decoupling Control of TAB Converter

¹Tomáš BASARIK (2nd year),

Supervisor: ²Milan LACKO

^{1,2}Dept. of Electrical Engineering and Mechatronics, FEI TU of Košice, Slovak Republic

¹tomas.basarik@tuke.sk, ²milan.lacko@tuke.sk

Abstract—This article presents the Triple Active Bridge (TAB) converter and its applications in renewable energy systems, electric mobility and microgrids. The circuit topology and operating principle of the TAB converter are presented. The main contribution is a decoupling approach that linearises the converter, enabling the design of independent linear controllers for each port. This approach simplifies control, increases system stability and improves dynamic performance, making TAB converters a robust solution for modern power applications.

Index Terms—dc-dc converter, triple active bridge converter, power distribution, power flow control

I. INTRODUCTION

The European Union introduced the European Green Deal in December 2019 to deal with climate change and global warming. A key objective of the deal is to achieve decarbonisation by reducing carbon emissions to net zero by 2050. One of the main approaches to achieving this goal is the use of green energy sources and environmentally and energy efficient technologies [1]. To these goals, it is essential to develop power converters that support renewable energy [2], electromobility [3] and microgrids.

The literature [4] presents a power converter that offers all the key features required for these applications. It offers bi-directional power flow, galvanic isolation, high power density and a modular design. However, its main disadvantage is the complexity of control, which is the focus of this article.

II. TRIPLE ACTIVE BRIDGE

The Triple Active Bridge (TAB) converter is shown in Fig. 1. The converter consists of two main parts. The first one is an active bridge and the second one is a high frequency transformer with turns ratio n . Together they create a single module. The TAB converter consists of three of these modules connected together on the secondary side of the transformers. The modularity of the system is achieved by connecting planar transformers in parallel. This method is described in more detail in literature [4]. The literature [5] lists three types of modulation that can be used in active bridge modules:

- Phase shift modulation (PSM)
- Trapezoidal Current Mode Modulation
- Triangular Current Mode Modulation

PSM uses the full power potential of the TAB converter. Disadvantage of this modulation is the circuit current. This increases conduction losses and reduces efficiency.

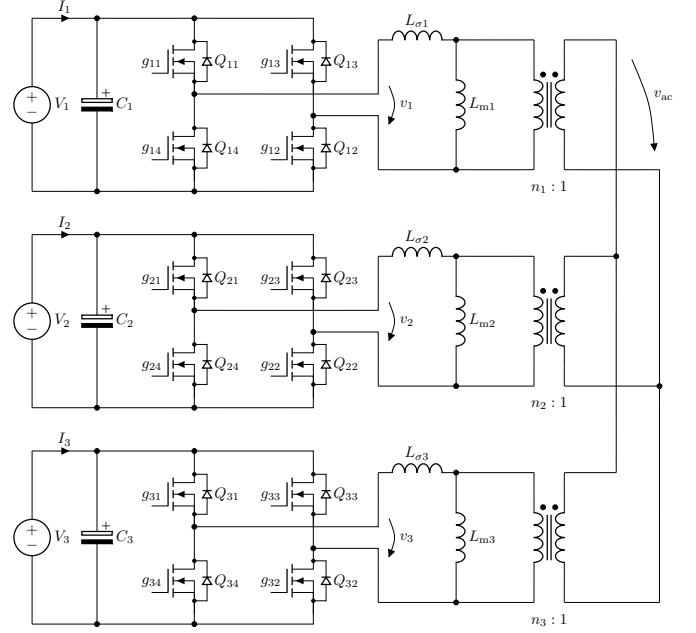


Fig. 1. Topology of TAB Converter with three transformer

The power of an individual module is determined by its voltage V_k and the current flowing into or out of it. The current I_k is defined by the transformer leakage inductance $L_{\sigma k}$. Magnitude of the current is determined by the voltage difference between the module and the AC bus. Current of one module with phase shift modulation can therefore be calculated using the following equation:

$$I_i = \sum_{\substack{j=1 \\ j \neq i}}^k V_j K_{ij} \phi_{ij} (1 - 2|\phi_{ij}|), \quad (1)$$

where k is the number of ports, L_{eq} is equivalent inductance, f_s is switching frequency and

$$K_{ij} = \frac{n_i n_j}{f_s \frac{L_{\sigma i} L_{\sigma j}}{L_{eq}}},$$

$$\phi_{ij} = \phi_i - \phi_j.$$

As can be seen in equation (1) the relationship is nonlinear, which causes problems in converter control and control design.

III. DECOUPLING METHOD

This section describes the decoupling strategy employed to simplify the control of the TAB converter. Because the TAB converter consists of three modules, the number of currents is three. Based on equation (1), it is possible to write a matrix for the TAB converter to calculate the currents of each port, as follows

$$\begin{bmatrix} I_1 \\ I_2 \\ I_3 \end{bmatrix} = \begin{bmatrix} 0 & G_{12} & G_{13} \\ G_{21} & 0 & G_{23} \\ G_{31} & G_{32} & 0 \end{bmatrix} \begin{bmatrix} V_1 \\ V_2 \\ V_3 \end{bmatrix} \quad (2)$$

where

$$G_{ij} = K_{ij}\phi_{ij}(1 - 2|\phi_{ij}|).$$

In the literature [6], the Newton iterative method is used to calculate the inverse model of the MAB converter. This approach allows the determination of correct phase shifts over the entire operating range. The main disadvantage of this method is its dependence on numerical iteration, which requires several iterations of the algorithm to achieve the desired accuracy, for each current change request. To calculate the phase shifts using the Newton iterative method, it is necessary to construct the Jacobian matrix, which contains the partial derivatives of the function f_k . It can be created as follows

$$\begin{bmatrix} \Delta\phi_1 \\ \Delta\phi_2 \\ \vdots \\ \Delta\phi_k \end{bmatrix} = \begin{bmatrix} \frac{\partial f_1}{\partial \phi_1} & \frac{\partial f_1}{\partial \phi_2} & \cdots & \frac{\partial f_1}{\partial \phi_k} \\ \frac{\partial f_2}{\partial \phi_1} & \frac{\partial f_2}{\partial \phi_2} & \cdots & \frac{\partial f_2}{\partial \phi_k} \\ \vdots & \vdots & \ddots & \vdots \\ \frac{\partial f_k}{\partial \phi_1} & \frac{\partial f_k}{\partial \phi_2} & \cdots & \frac{\partial f_k}{\partial \phi_k} \end{bmatrix}^{-1} \begin{bmatrix} -I_1 \\ -I_2 \\ \vdots \\ -I_k \end{bmatrix} \quad (3)$$

where

$$\frac{\partial f_i}{\partial \phi_j} = \begin{cases} V_j K_{ij} \phi_{ij} (4|\phi_{ij}| - 1) & i \neq j \\ \sum_{\substack{j=1 \\ j \neq i}}^k V_j K_{ij} \phi_{ij} (1 - 4|\phi_{ij}|) & i = j \end{cases} \quad (4)$$

At the beginning of the iteration, it is necessary to select appropriate initial values for the phase shifts ϕ_1 , ϕ_2 and ϕ_3 . The closer these initial values are to the desired result, the fewer iterations are required. After defining the initial phase shift values, the individual increments for the phase shifts $\Delta\phi_1$, $\Delta\phi_2$ and $\Delta\phi_3$ are calculated. These increments are then added to the original values, as shown in equation (5), and the iteration process is repeated:

$$\begin{aligned} \phi_1(k+1) &= \phi_1(k) + \Delta\phi_1 \\ \phi_2(k+1) &= \phi_2(k) + \Delta\phi_2 \\ \phi_3(k+1) &= \phi_3(k) + \Delta\phi_3 \end{aligned} \quad (5)$$

The entire iterative process continues until the desired accuracy ε is achieved for all phase shifts of the TAB converter, as expressed by the following condition

$$\Delta\phi_1 < \varepsilon \quad \wedge \quad \Delta\phi_2 < \varepsilon \quad \wedge \quad \Delta\phi_3 < \varepsilon. \quad (6)$$

Adding an inverse model computed via Newton's iterative method maps desired currents to actual currents, decoupling

the TAB converter. This simplifies the system to SISO form, making the transfer matrix equal to the identity matrix.

IV. SIMULATION

The simulation tool PLECS was used to simulate and verify the proposed decoupling. Tab I shows the error of the decoupling method. It depends on the number of iterations. As can be seen, the number of iterations required to achieve precise decoupling is small. For lower precision, two iteration cycles are required.

TABLE I
SIMULATION RESULT

Required current (A)	Iteration Errors (%)		
	1 Iteration	2 Iterations	3 Iterations
−5.0	−8.454	−0.114	$0.885 \cdot 10^{-3}$
−2.5	−8.831	−0.125	$1.752 \cdot 10^{-3}$
+7.5	−8.578	−0.116	$0.531 \cdot 10^{-3}$

V. CONCLUSION

The proposed decoupling method for the Triple Active Bridge (TAB) converter successfully linearizes the system, allowing the design of independent linear controllers for each port. This decoupling approach simplifies control complexity, enhances system stability, and improves dynamic performance. Simulation results confirm that the desired decoupling precision can be achieved with a minimal number of iteration cycles, making the method efficient and practical for real-world applications. Overall, the TAB converter with the decoupling control strategy proves to be a robust and adaptable solution for modern power applications.

ACKNOWLEDGMENT

This work was supported by the Slovak Research and Development Agency under the contracts No. APVV-23-0521 and No. APVV-18-0436.

REFERENCES

- [1] E. Commission, "What is the european green deal?" 2019. [Online]. Available: https://ec.europa.eu/commission/presscorner/api/files/attachment/859152/What_is_the_European_Green_Deal_en.pdf
- [2] B. Chandrasekar, C. Nallaperumal, S. Padmanaban, M. S. Bhaskar, J. B. Holm-Nielsen, Z. Leonowicz, and S. O. Masebinu, "Non-isolated high-gain triple port dc-dc buck-boost converter with positive output voltage for photovoltaic applications," *IEEE Access*, vol. 8, pp. 113 649–113 666, 2020.
- [3] K. Suresh, C. Bharatiraja, N. Chellammal, M. Tariq, R. K. Chakraborty, M. J. Ryan, and B. Alamri, "A multifunctional non-isolated dual input-dual output converter for electric vehicle applications," *IEEE Access*, vol. 9, pp. 64 445–64 460, 2021.
- [4] P. Zumel, C. Fernandez, A. Lazaro, M. Sanz, and A. Barrado, "Overall analysis of a modular multi active bridge converter," in *2014 IEEE 15th Workshop on Control and Modeling for Power Electronics (COMPEL)*. IEEE, 2014, pp. 1–9.
- [5] F. Krismer, "Modeling and optimization of bidirectional dual active bridge dc-dc converter topologies," Ph.D. dissertation, Eth Zurich, 2010.
- [6] P. Wang and M. Chen, "Towards power FPGA: Architecture, modeling and control of multiport power converters," in *2018 IEEE 19th Workshop on Control and Modeling for Power Electronics (COMPEL)*, 2018, pp. 1–8.

Power System Protection Based on Virtual Protection and WAMS

¹Marek Bobček (2nd year)
Supervisor: ²Zsolt Čonka

^{1,2}Dept. of Electric Power Engineering, FEI, Technical University of Košice, Slovak Republic

¹marek.bobcek@tuke.sk, ²zsolt.conka@tuke.sk

Abstract—The research focuses on advancing protection systems in electrical networks by leveraging digital protection relays and virtual protection mechanisms using Phasor Measurement Units (PMUs). Traditional protection systems rely on predefined settings and hardware-based configurations, which can be slow to adapt to dynamic grid conditions. The increasing penetration of renewable energy sources and the growing complexity of modern power systems necessitate more adaptive and intelligent protection schemes. My research aims to address these challenges by developing novel methodologies that enhance system reliability, improve fault detection accuracy, and ensure faster response times in protective relays.

Keywords—Power System Protection, Digitalization in Power Systems, Adaptive Protection, Wide Area Measurement Systems (WAMS).

I. INTRODUCTION

Prior to the past two years, my research was primarily focused on establishing a strong theoretical and practical foundation for improving power system protection using digital solutions. The first step was to critically analyze the limitations of conventional protection methods, which rely on fixed threshold settings and predefined logic. These traditional approaches, while effective in many scenarios, often struggle to adapt to evolving grid conditions, particularly with the increasing penetration of renewable energy sources and the complexities introduced by distributed generation [1]–[6]. The growing demand for real-time data and advanced analytics in power systems has highlighted the necessity of transitioning toward digital protection solutions. The integration of Wide Area Measurement Systems (WAMS) and Phasor Measurement Units (PMUs) has been a key focus, as these technologies provide enhanced situational awareness and enable adaptive protection strategies [7]–[8]. Furthermore, the shift towards digitalization is not only a response to technical challenges but also a critical requirement to meet the rising demand for reliable, data-driven decision-making in modern power networks. In this context, my research has explored the development of protection frameworks capable of leveraging real-time data streams, machine learning algorithms, and automated simulation techniques [9]–[12].

These advancements align with the broader industry trend of digital transformation, ensuring that protection schemes remain robust, flexible, and capable of handling the dynamic nature of future power grids.

II. RESEARCH EXPLANATION

The research has focused on expanding the capabilities of power system protection through digitalization and the use of virtual protection mechanisms based on Phasor Measurement Units (PMUs). With increasing demands for digitalization and data acquisition, protection systems are evolving toward solutions that enable broader utilization of online measurements and advanced analytical methods.

In the initial phase, we conducted research on existing protection systems to analyze their performance and identify opportunities for improvement. Building on this foundation, our current efforts are focused on transitioning towards fully digital protection solutions. This involves the integration of PMUs within Wide Area Measurement Systems (WAMS) to improve real-time data acquisition and enhance situational awareness. The collected data serves as the basis for developing future protection strategies that can leverage advanced analytics and automation. By focusing on real-time monitoring and digital frameworks, this research aims to lay the groundwork for more flexible and adaptive future protection schemes in modern power grids.

A. WAMS & Data Acquisition

In our research, data acquisition is structured around Phasor Measurement Units (PMUs) integrated within the Wide Area Measurement System (WAMS). PMUs continuously measure voltage and current phasors with high accuracy, synchronizing all data using GPS timestamps. These real-time measurements are then transmitted to a Real-Time Automation Controller (RTAC), which serves as a central processing unit within the system. The RTAC is responsible for collecting, time-aligning, and formatting the incoming data, ensuring consistency and reliability before further transmission. The communication between PMUs and RTAC is established using the IEEE C37.118 protocol, which is widely adopted for phasor data transmission. Once processed, the RTAC forwards the data to our central database using the IEC 61850 GOOSE (Generic Object-Oriented Substation Event) protocol. This protocol enables fast and efficient peer-to-peer communication, ensuring that real-time data is readily available for analysis and future application in protection schemes. The database structure allows continuous logging of phasor data while maintaining the capability for rapid retrieval, supporting ongoing research into digital protection solutions and the development of adaptive protection strategies.

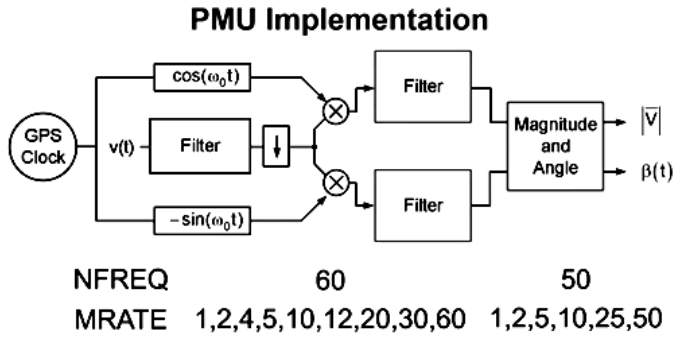


Fig. 1. Example of PMU unit algorithm

NFREQ – nominal frequency, MRATE – measurement rate (reporting rate), $v(t)$ – voltage input in volts, $|V|$ – voltage output in volts, $\beta(t)$ – voltage angle
Output is complex number.

B. Utilization of Data Acquired from PMU and WAMS

The data obtained from PMUs will enable the development of new protection algorithms and the implementation of virtual protection. By utilizing synchronized real-time measurements, it will be possible to enhance the speed and accuracy of fault detection, leading to more adaptive and flexible protection schemes. Unlike traditional solutions based on fixed settings, virtual protection will be able to dynamically adjust to real-time grid conditions, increasing the reliability and resilience of the power system. One of the main research directions will be the development of adaptive protection algorithms that will automatically adjust based on system topology, load conditions, or the presence of distributed energy resources. Real-time PMU data will also enable the implementation of Wide Area Protection schemes capable of coordinating protective responses across multiple substations, helping to prevent cascading failures. Virtual protection, leveraging centralized data processing, will eliminate the need for physical relay modifications, reducing maintenance costs and increasing flexibility in protection strategies. Maybe if not then they could be used like a second layer of protection system in substation with possibility of better data utilization. In the future, integrating the collected data into advanced computational frameworks will allow for the use of predictive analytics, fault localization methods, and automated decision-making to further improve power system protection. This transition to digital and data-driven protection schemes can be a crucial step toward more reliable and resilient power grids.

III. VIRTUAL PROTECTION CONCEPT

Virtual protection, based on data acquired from Phasor Measurement Units (PMU), represents a modern approach to power system protection that differs from traditional methods by relying purely on software-driven analysis rather than physical relay devices. Unlike conventional protection systems, which consist of hardware-based relays, circuit breakers, and sensors, virtual protection operates within a digital environment where data is continuously collected from PMUs distributed across the transmission network. These PMUs provide highly synchronized real-time measurements of voltage, current, and phase angles using GPS timing, allowing for a comprehensive analysis of the power system's state at any given moment [13-14]. Current protection devices are typically housed in metal enclosures with digital displays, buttons, and LED indicators for status monitoring, with no possibility. They feature multiple input and output terminals for connecting to voltage and current transformers, allowing real-time

measurement of electrical parameters. Actual protections are with no possibility to dynamic change of settings from control room. People have to change settings on device at spot. New concept should provide a change settings directly from control room. At fig. 2 is shown the main idea of the research in very simple diagram to understand what is a core of the project.

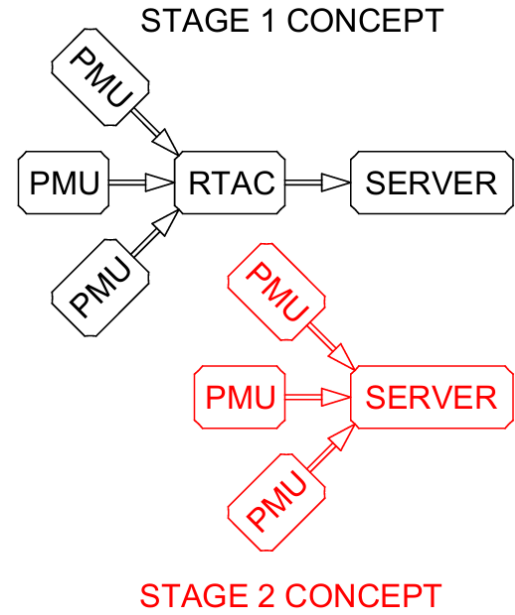


Fig. 2. Example of PMU based protection

In Stage 1, PMUs collect real-time electrical measurements and send data to a Remote Terminal Automation Controller (RTAC), which processes and transmits the information to a central server for analysis and decision-making. The RTAC acts as an intermediary, managing data flow and ensuring system coordination. In Stage 2, the system eliminates the RTAC, with PMUs sending data directly to the server. This streamlined approach reduces latency, enhances real-time monitoring, and simplifies infrastructure, making virtual protection more responsive and efficient. The transition reflects a move toward decentralized and cloud-based protection strategies, leveraging direct data transmission for faster fault detection and system reliability.

IV. FUTURE WORK

A. Completion of algorithms and testing/comparison of current systems with virtual ones

The future direction of this research involves refining and completing the algorithms developed for virtual protection systems. This includes optimizing detection and response mechanisms for various fault scenarios, ensuring real-time operation, and improving interoperability with existing digital protection devices. Additionally, comprehensive testing and benchmarking will be conducted to compare traditional protection systems with the proposed virtual protection framework. The evaluation will focus on response times, reliability, adaptability to different grid conditions, and overall effectiveness in fault mitigation. Through extensive simulations and real-world case studies, the goal is to validate the advantages and limitations of virtual protection and identify areas for further improvement.

B. Development of algorithms for network analysis using modern ML and AI algorithms.

This task focuses on developing advanced algorithms that utilize machine learning (ML) and artificial intelligence (AI) to enhance network analysis in electrical power systems. The objective is to create predictive models capable of detecting, classifying, and responding to faults or disturbances in real time. These algorithms will improve the accuracy of protection schemes by analyzing vast amounts of data from Phasor Measurement Units (PMUs) and other digital sources. By integrating AI-driven techniques, such as deep learning and anomaly detection, the system will dynamically adapt to changing network conditions and optimize protection strategies. Additionally, this will serve as a continuous learning function that refines its responses based on real operational data, including the algorithms developed for virtual protection and manually adjusted settings. By analyzing both historical and real-time data, the system will identify patterns, detect anomalies, and enhance decision-making processes over time. Ultimately, it will recommend the best possible protection settings and adjustments, ensuring optimal performance and increased network reliability.

V. CONCLUSION

This research has demonstrated the potential of digitalization and virtual protection in advancing power system protection. Traditional protection systems, while effective, are limited by predefined settings and hardware constraints, making them less adaptable to modern grid challenges. By integrating Phasor Measurement Units (PMUs) within Wide Area Measurement Systems (WAMS), this study has laid the foundation for real-time monitoring and adaptive protection schemes that respond dynamically to changing grid conditions. The proposed virtual protection approach eliminates the need for physical relay modifications, enabling remote adjustments and reducing maintenance costs while enhancing operational flexibility. The transition from conventional relay-based systems to software-driven virtual protection has been explored through a two-stage concept, where real-time data acquisition and direct server-based decision-making play a crucial role. By leveraging machine learning (ML) and artificial intelligence (AI), the system continuously improves its response capabilities by learning from historical and real-time data. This ensures more accurate and optimized protection settings, and improved overall reliability of the power grid. Future work will focus on refining the developed algorithms, conducting extensive testing, and benchmarking virtual protection against existing systems to validate its efficiency and practicality. Additionally, the integration of AI-driven predictive models will further enhance the adaptability of protection schemes, leading to more resilient and intelligent power networks. The ongoing advancements in digital protection signify a crucial step toward the future of smart grid technologies, ensuring safer, more reliable, and efficient power system operation.

ACKNOWLEDGMENT

The This work was supported by the Ministry of Education, Science, Research and Sport of the Slovak Republic and the Slovak Academy of Sciences under contract no. VEGA 1/0627/24 and Research of systems for semi-autonomous control depending on transient phenomena in the power system using WAMPAC systems under contract no. 08/TUKE/2024.

REFERENCES

- [1] M. Bobcek, R. Štefko, Z. Čonka, "Electrical Protection Systems for the Evolving Microgrid Environment," 2023 Acta Polytechnica Hungarica, Volume 20, Issue 11, pp. 159-178, ISSN: 17858860, doi: 10.12700/APH.20.11.2023.11.10.
- [2] R. Štefko, M. Kolcun, M. Bobcek, D. Mazur, B. Kwiatkowski, "Design of a Protection System for Distributed Energy Sources in Distribution Grids," 2024 Przegląd Elektrotechniczny, Issue 9, pp. 271-276, ISSN: 00332097, doi: 10.15199/48.2024.09.53.
- [3] M. Bobcek, R. Štefko, Z. Čonka, P. Kádár, A. Aamer Bilal and M. Miltner, "Automated Extraction, Simulation, and Smoothing of Load Diagrams in Power Systems Using JSON Data," 2024 IEEE 7th International Conference and Workshop Óbuda on Electrical and Power Engineering (CANDO-EPE), Budapest, Hungary, 2024, pp. 145-150, doi: 10.1109/CANDO-EPE65072.2024.10772965.
- [4] R. Štefko, Z. Čonka, M. Bobček, D. Kurpaš, and M. Kolcun, "Parametrization of the Protection System for a Small Hydropower Plant," Elektroenergetika: International Scientific and Professional Journal on Electrical Engineering, vol. 16, no. 2, pp. 17-21,
- [5] R. Štefko, Z. Čonka, M. Bobček, A. Miháliková, and M. Kolcun, "Impact of Renewable Energy Sources on Power System Operation and the Proposal for Microgrid Creation," Elektroenergetika: International Scientific and Professional Journal on Electrical Engineering, vol. 17, no. 1, pp. 1-4, 2024.
- [6] R. Štefko, M. Bobček, and Z. Čonka, "Microgrids: A Vision for the Future of Distribution Networks," ATP Journal: Industrial Automation and Informatics, vol. 31, no. 10, pp. 32-35, 2024.
- [7] R. Štefko, M. Bobeck and Z. Čonka, "Research of WAMS in Power Systems using SCADA System," 2023 IEEE 6th International Conference and Workshop Óbuda on Electrical and Power Engineering (CANDO-EPE), Budapest, Hungary, 2023, pp. 000053-000058, doi: 10.1109/CANDO-EPE60507.2023.
- [8] Z. Čonka, R. Štefko, M. Bobček, and M. Pavlík, "Application of WAMS Technology in Power System Control," Elektroenergetika: International Scientific and Professional Journal on Electrical Engineering, vol. 16, no. 2, pp. 47-50, 2023.
- [9] M. Bobček, Z. Čonka and J. Palfy, "Neural Network-Based Fault Learning Using Artificial Intelligence and Kalman's Filter," 2024 IEEE 18th International Symposium on Applied Computational Intelligence and Informatics (SACI), Timisoara, Romania, 2024, pp. 000389-000394, doi: 10.1109/SACI60582.2024.10619813..
- [10] R. Štefko and M. Bobček, "Artificial Intelligence and Energy Efficiency Revolution in Electric Consumption Management," 2024 IEEE 18th International Symposium on Applied Computational Intelligence and Informatics (SACI), Timisoara, Romania, 2024, pp. 1-6, doi: 10.1109/SACI60582.2024.10619842.
- [11] M. Bobček, R. Štefko, Z. Čonka and L. Főző, "Adaptive Cloud Movement Prediction for Photovoltaic Systems Using Real-Time Sensor Data and Deep Learning," 2024 22nd International Conference on Intelligent Systems Applications to Power Systems (ISAP), Budapest, Hungary, 2024, pp. 1-5, doi: 10.1109/ISAP63260.2024.10744394.
- [12] M. Bobcek, Z. Conka and J. Simcak, "Machine Learning Techniques for Data Validation in Wide Area Measurement Systems," 2025 IEEE 23rd World Symposium on Applied Machine Intelligence and Informatics (SAMI), Stará Lesná, Slovakia, 2025, pp. 000317-000320, doi: 10.1109/SAMI63904.2025.10883305.
- [13] S.A. Taher, "A new virtual consensus-based wide area differential protection," IET Generation, Transmission and Distribution, vol. 18, no. 9, pp. 1906-1918, May 2024, doi: 10.1049/gtd2.13168.
- [14] R. M. Monaro, A. Q. Santos, S. G. Di Santo, D. V. Coury and A. M. Aguiar, "OpenRelay: Open Source Protection Algorithms for Electric Power System Relays," 2018 IEEE Power & Energy Society General Meeting (PESGM), Portland, OR, USA, 2018, pp. 1-5, doi: 10.1109/PESGM.2018.8586454.

Overview of Sensors for Biosignal Measurement

¹Miroslav JUSKO (1st year),
Supervisor: ²Peter LUKÁCS

^{1,2}Department of Technologies in Electronics, FEI TU of Košice, Slovak Republic

¹miroslav.jusko@tuke.sk, ²peter.lukacs@tuke.sk

Abstract—This paper explores the types and design challenges of electrodes used in biosensing applications, for purpose of continuous blood pressure monitoring. Current biosensors often rely on wet electrolytes to improve body-electrode interface. These electrolytes however can dry out over time, reducing their effectiveness and limiting their usage in wearable type of devices. The goal of this overview is to identify a viable long-term solution for wearable devices that can estimate blood pressure (BP) using pulse wave velocity (PWV).

Keywords—Biosensing, Electrodes, Interface impedance, Bioimpedance, Microneedle array electrode

I. INTRODUCTION

The World Health Organization estimates that cardiovascular disease (CVD) account for roughly 17.9 million deaths every year. In fact, CVDs are considered the leading cause of death globally. Hypertension is most common and potential lethal condition that can result in heart attack, stroke heart failure and many other. Scientists and researchers around the world are therefore working to find ways to combat this issue by continuously monitoring vital body signs such as body temperature, pulse rate, respiration rate, and blood pressure (BP). All of these signs, except for BP, can be continuously monitored without restricting the patients body. Blood pressure, however, can only be precisely monitored using a bulky restraining cuff [1].

Regular and accurate blood pressure monitoring is essential for the early diagnosis of hypertension and risk assessment. For more than 100 years standard way of BP monitoring was in doctor office using auscultatory mercury sphygmomanometer. The basic principle behind this method is to restricting blood flow in the arm using an inflatable rubber cuff. The cuff is inflated above the expected systolic pressure and then slowly deflated. The point at which blood flow resumes represents the systolic pressure. As the pressure is further lowered, the point at which blood flow is no longer detectable [2]. Although this method is precise and reliable, it is not suitable for continuous monitoring, because they are bulky devices not portable or practical for daily or long-term uses

Recently a few methods have been proposed for cuff-less systolic and diastolic BP [3], [4]. One of the most prominent seems to be method based on measuring pulse transition time (PTT). It is based on Moens-Korteweg's formula (1) which states that pulse wave velocity (PWV) is proportional to the square root of the incremental elastic modulus E_{inc} of the vessel wall given constant ratio of wall thickness h to vessel radius r and blood density ρ . Velocity of wave can be substitute by constants divided by time needed for the arterial pulse wave to reach periphery. This time can be calculated by

monitoring the R-wave of the electrocardiogram (ECG) and systolic peak of the photoplethysmography (PPG).

II. DESIGN OF WEARABLE SENSOR FOR MEASURING BIO-Z

To be able to measure bioimpedance, an electrode is needed. A biopotential electrode is transducer that sens the ion distribution on the surface of skin and converts it to the electron current [5]. This conversion is needed due to the fact that current flow in a human body is caused by the ion flow.

A. Measuring Interface Impedance

At the contact of electrode and skin there is an interface impedance. To be able to assets different types of electrode, a model for describing electrode interface impedance is needed. There exist numerous models to describe this interference, such as Helmholtz model, Gouy-Chapman diffuse model, Stern double-layer model, and many others.

For measuring electrode interface impedance its possible to use bipolar measurement, where two electrodes are submerge in phosphate buffered solution. One electrode is the electrode which impedance is measured, so called working electrode. The second electrode, called counter electrode, have much larger area to ensure that its interface impedance is negligible in comparison to working electrode. This however does not allow stable electrode polarization and interface impedance of counter electrode is also measured. Stable electrode polarization is needed because it ensures that electrode-electrolyte interface remains constants through the measurement. In measurement it will behave as varying electrode interface

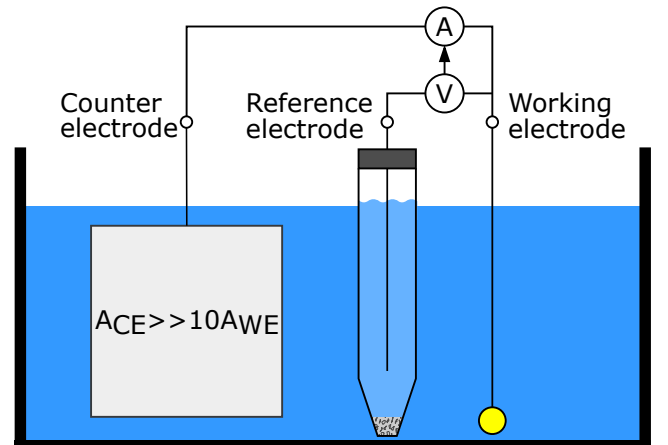


Fig. 1. Three-electrode electrochemical cell for electrode interfacial impedance measurements.

impedance through time. This issues can be overcome by three electrode measurement [6]. This measurement system is shown on Fig. 1.

In three electrode setup, the third electrode called reference electrode is placed in-between working and counter electrode. Reference electrode is non-polarized Ag/AgCl electrode that measures the bias potential which is then used as feedback for ensuring stable current flow through the counter electrode. It provides the most stable and reliable way of measuring electrode interface impedance [7].

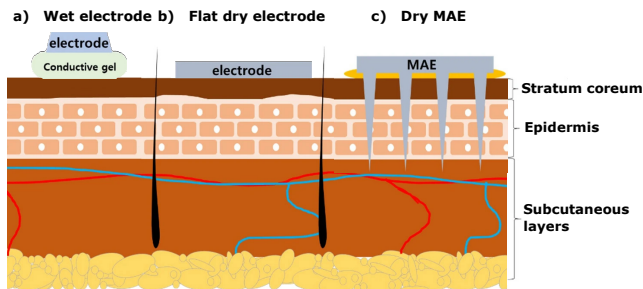


Fig. 2. Images of interface between skin and (a) wet electrode with conductive gel, (b) flat dry electrode, and (c) MAE without conductive gel [8]

B. Types of Electrodes Used in Biosensing Application

Electrodes used for biosensing applications can generally be categorized into two types: wet electrodes and dry electrodes. Wet electrodes are typically made of silver/silver chloride ($Ag/AgCl$). Their work on principle of converting the ion current at the surface of the skin to electron current which can be easily measured by ADC convertor. To reduce interface impedance, a conductive gel based on polyethylene glycol (PEG), polypropylene glycol (PPG), or hydrogel is used. The gel must contain free chloride ions such that the ion charge can be carried through the electrolyte solution.

These electrodes are commonly preferred due to their low cost and low skin-interface impedance. However, their main disadvantage is that their impedance can increase up to three times their original value over time. This occurs because the gel dries out, leading to a degradation in performance. For this reason, wet electrodes are not suitable for long-term measurements [9].

In recent years, scientists have been developing alternatives to wet electrodes. Dry electrodes have emerged as a viable option for long-term bio-signal sensing. As the name suggests, dry electrodes do not require any conductive gel or saline solution to serve as an interface material. Instead, they utilize different materials and technologies to enhance their properties. Their primary advantage is their good biocompatibility, allowing them to be worn for extended periods. Additionally, the inherent air gap between the electrode and the skin provides better breathability. However, this air gap also presents a drawback: it increases interface impedance, which lowers signal amplitude and introduces more noise into the recorded signal.

C. Reduction of Electrode Interface Impedance of Dry Electrodes

Main goal when designing skin contact electrode is to lower interface impedance between an electrode and tissue.

Impedance of human body in contrast to the electrode interface impedance is several magnitude lower. This high impedance can introduce unwanted error into the measurement. By lowering interface impedance it is possible to increase injected current for a set voltage and thus increasing SNR value or for set current lowering power supply voltage which lowers power consumption.

There are many methods for lowering interface impedance. The most popular ones involve use of electrochemical deposition of platinum. Typically a chloroplatinic acid solution H_2PtCl_6 together with lead acetate trihydrate $Pb(C_2H_3O_2)_2$ or lead nitrate $Pb(NO_3)_2$ is used and electrochemical deposition is performed under ultrasonic agitation which is used for removing weakly adhered Pt from the electrode surface. For platinum deposition, 3-electrode cell is usually used, similar as shown on Fig. 1 [7], [9].

Another way is the use of poly(3,4-ethylenedioxythiophene) polystyrene sulfonate (PEDOT:PSS) as a conductive polymer, to directly electropolymerize on electrode surface. Due to its rough surface and high conductivity, the interface impedance can be as much as 2 orders of magnitude higher than Pt electrodes [10].

Third method that can be used involves carbon nanotube (CNT). Single-walled and multi-walled carbon nanotube suspensions with an appropriate surfactant can be electrophoretically deposited on electrodes using a two-electrode cell. Combination of CNT and PEDOT:PSS can outperform both methods achieving roughly 1.29 times smaller impedance than electrodes with PEDOT:PSS films [11]. This kind of electrodes have also greater surface area and better mechanical stability. It is also important to note, that higher pressure applied on the electrode and tissue can improve electrode interface impedance.

D. Microneedle Array Electrode

In Fig 2.c shows invasive type of dry electrode, called microneedle array electrode (MAE). MAE can effectively minimize the influence of stratum corneum, due to the fact, that needles are in direct contact with epidermis layer. This type of dry electrode seems as promising candidate for replacing traditional wet electrodes in ECG, EMG, and EEG monitoring, thanks to their exceptional properties including low impedance, high selectivity, and minimal skin trauma [12]. Microneedle arrays typically have a height and width of several hundred micrometers and are shaped like cones or pyramids, allowing them to penetrate and attach to the skin layers. The design of microneedle electrodes is inspired by small natural structures, such as thorns, which can easily penetrate the human skin's surface with minimal pain and without causing damage.

To ensure optimal conductivity, these electrodes are made from various materials, with silicon being one of the most commonly used. A photolithography process is typically employed to achieve the desired structure. However, rigid silicon has difficulty conforming tightly to the skin, a drawback that can be mitigated by integrating flexible substrates with silicon microneedles [13].

Another material used for microneedle electrodes is metal alloys. For example, in [14], researchers developed microneedle array electrodes (MAE) using a low-melting alloy composed of bismuth, indium, tin, and zinc, integrated with a

polydimethylsiloxane (PDMS) substrate. In addition to silicon and metal alloys, various polymers, such as PEDOT:PSS and lactic-co-glycolic acid (PLGA), have also been explored.

Silicon microneedle electrodes offer high signal acquisition quality and fidelity in initial bioelectrical measurements. However, they have significant drawbacks, including complex, expensive, and environmentally sensitive fabrication processes, as well as fragility during use. These limitations restrict their suitability for long-term human bioelectrical signal monitoring.

In contrast, metal-based microneedle electrodes provide excellent mechanical strength and can be shaped easily, with high conductivity ensuring accurate physiological signal recording. However, their poor biocompatibility makes them unsuitable for long-term monitoring. On the other hand, polymer-based electrodes offer excellent biocompatibility without posing health risks, but they require an additional conductive layer to enhance conductivity [15]. This necessitates extra fabrication steps, such as sputtering, electroless plating, or electrolysis.

One approach involves creating a polymer mold on a glass wafer using photolithography [16]. A wafer is coated with photoresist, onto which a desired pattern is developed. Due to the separation between the mask and the photoresist, a diffraction pattern is formed. By adjusting the wavelength, the distance between the photoresist and the mask, and the shape of features on the mask, the microneedle shape can be modified. Once the master mold is created, a negative mold can be produced from resin. This casting is then used to fabricate MAE from biocompatible conductive resin. In the final step, a thin layer of silver coating is sputtered to enhance signal quality Fig. 3.

Another technique is the magnetization-induced self-assembly method. In this process, epoxy resin is mixed with iron powder and deposited onto a substrate. A magnetic field is then applied to form the microneedle electrode array. Once the resin is cured, a thin titanium coating is deposited, similar to the previous method [17]. Additional manufacturing techniques include 3D stereolithography (SLA) printing, inkjet printing, and micromachining [18].

E. Body Electrode Interface

For electrodes that are in direct contact with the bodily fluids like for example sweat, the current transfer mechanisms are

similar to those in wet electrodes. This similarity exist because bodily fluids act similar to electrolytes rich in positively charge cations and negatively charge anions. The conversion of ionic current to electronic current and vice versa across the interface happens via two types of current transfer mechanisms: faradic and non-faradic [19].

In faradic process current transfer charges ions cross electrode-electrolyte interface by oxidation and Reduction. Oxidation occurs when atom from the electrode loses electron and then travel to electrolyte as cation or when anions from electrolyte transform to a neutral atom. Reversal of this process is called reduction. On the other hand in non-faradic, current transfer never cross this interface but charges accumulate across sides of electrode-electrolyte interface. For faradic process undergoing electrode-electrolyte interface behaves like a resistor known as charge-transfer resistor (R_{CT}) and in non-faradic like a capacitor sometimes called double-layer capacitor (C_{DL}) [20]. Fig. 4 models equivalent circuit models of an electrode-electrolyte interface. These two current transfer mechanisms are shown as parallel combination of R_{CT} and C_{DL} . R_{EL} represents electrolyte resistance and V_{HC} symbolize variable called half-cell potential.

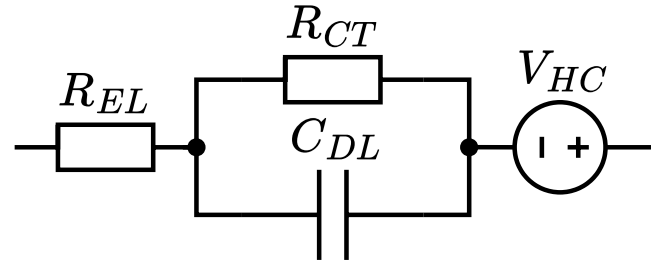


Fig. 4. Equivalent circuit models of an electrode-electrolyte interface supporting both faradaic and non-faradaic processes of current transfer with half-cell potential V_{HC} , and electrolyte resistance R_{EL} .

When an electrode is placed in an electrolyte, charge transfer occurs at the interface through oxidation and reduction reactions. If an imbalance between oxidation and reduction occurs, it leads to unequal charge transfer across the interface. This disturbs the local charge neutrality, causing the electrode to develop a potential difference relative to the electrolyte. This potential difference increases until equilibrium is reached, where the rates of oxidation and reduction balance each other. The resulting equilibrium potential is known as the half-cell potential. Different electrode materials have characteristic half-cell potentials, which depend on their intrinsic electrochemical properties [9]. Some common electrode materials, their reduction reactions and half-cell potentials are listed in Table 1.

TABLE I
HALF-CELL POTENTIAL (V_{HC}) OF ELECTRODES

Electrode	Reduction reaction	V_{HC} [V]
Aluminum	$Al \rightarrow Al^{3+} + 3e^-$	-1.71
Iron	$Fe \rightarrow Fe^{2+} + 2e^-$	-0.41
Nickel	$Ni \rightarrow Ni^{2+} + 2e^-$	-0.23
Lead	$Pb \rightarrow Pb^{2+} + 2e^-$	-0.13
Silver chloride	$Ag + Cl^- \rightarrow AgCl + e^-$	+0.23
Copper	$Cu \rightarrow Cu^{2+} + 2e^-$	+0.34
Silver	$Ag \rightarrow Ag^+ + e^-$	+0.8
Gold	$Au \rightarrow Au^+ + e^-$	+1.68

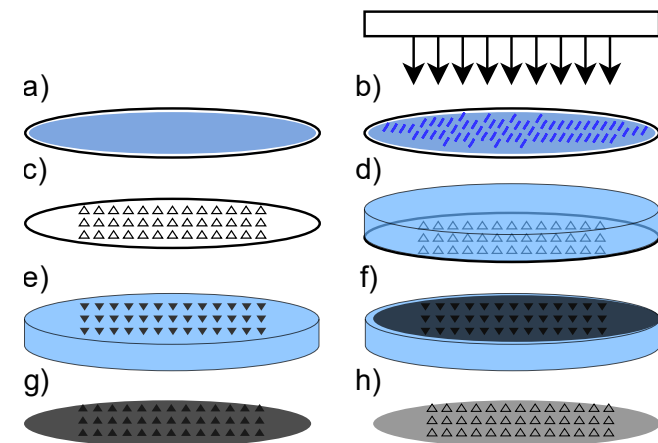


Fig. 3. Proces of manufacturing microneedle array (a) photoresist deposition, (b) UV exposure, (c) developing, (d) resin molding, (e) microneedle molding, (f) backing material, (g) conductive polymer electrode, (h) silver deposition.

III. SUMMARY AND FUTURE WORKS

This work presents a comprehensive assessment of different types of electrodes used for biosignal measurement. The development of human-worn electrodes requires a deep understanding of their underlying mechanisms, working principles, and interactions with the skin. Several types of electrodes are discussed in this study, along with the materials and techniques used in their fabrication. The choice of electrode type significantly impacts the quality, reliability, and long-term stability of biosignal acquisition.

Currently, the majority of electrodes used in medical applications are based on wet electrolytes, which significantly reduce skin-electrode impedance. A better skin-electrode interface allows for lower current usage when measuring impedance to achieve the same voltage, thereby reducing power consumption. Power efficiency is a crucial criterion in body-worn electronics. However, wet electrodes are not suitable for long-term applications because the electrolyte used as an interface medium can dry out over time, leading to unfavorable changes in electrode characteristics. This limitation has driven the development of dry electrodes, which aim to provide stable, long-term signal acquisition without relying on electrolytes.

Currently, two types of electrolyte-free electrodes exist. The first type consists of flat dry electrodes, which use specialized materials to achieve acceptable interface impedance values. Various materials, including conductive polymers, metals, and carbon-based composites, have been explored to improve the interface properties of these electrodes. Nonetheless, achieving low skin-electrode impedance with flat dry electrodes remains a challenge, as their interaction with the skin surface is more limited than that of wet electrodes.

The second type of dry electrode—microneedle array electrodes (MAEs)—represents a more innovative approach to biosignal acquisition. These electrodes consist of small needle-like structures that penetrate the outermost layer of the skin and establish direct contact with deeper skin layers. This penetration significantly reduces interface impedance by bypassing the high-resistance outer skin barrier. As a result, microneedle electrodes can achieve impedance levels comparable to those of wet electrodes while eliminating the need for liquid electrolytes.

Although microneedle array electrodes show promising performance, they also present certain disadvantages. These include complex manufacturing processes, challenges related to mass production, and user discomfort due to trypanophobia (fear of needles). Despite these drawbacks, microneedle array electrodes remain one of the most effective options for continuous biosignal monitoring.

In conclusion, while wet electrodes remain the standard in many biomedical applications, dry electrodes are gaining increasing attention as a promising alternative for long-term, wearable biosignal monitoring.

Future research should focus on the following directions: (i) the use of advanced materials for electrodes, such as graphene, (ii) the integration of dry electrodes directly into textiles and wearable fabrics, (iii) the development of hybrid technologies, for example, combining dry electrodes with hydrogel interfaces, (iv) improving the fabrication process of microneedle array electrodes (MAEs) to reduce production costs and increase yield, and (v) enhancing the durability

and mechanical robustness of dry electrodes to extend their operational lifespan during continuous use.

REFERENCES

- [1] Weltgesundheitsorganisation, Ed., *Cardiovascular Disease Prevention and Control: Translating Evidence into Action*, ser. Cardiovascular Disease Programme. Geneva: World Health Organization, 2005.
- [2] W. Elliott, "Recommendations for Blood Pressure Measurement in Humans and Experimental Animals: Part 1. Blood Pressure Measurement in Humans. A Statement for Professionals From the Subcommittee of Professional and Public Education of the American Heart Association Council on High Blood Pressure Research," *Yearbook of Cardiology*, vol. 2006, pp. 3–4, Jan. 2006.
- [3] R. Mukkamala, G. S. Stergiou, and A. P. Avolio, "Cuffless Blood Pressure Measurement," *Annual Review of Biomedical Engineering*, vol. 24, no. 1, pp. 203–230, Jun. 2022.
- [4] J.-R. Hu, G. Martin, S. Iyengar, L. C. Kovell, T. B. Plante, N. V. Helmond, R. A. Dart, T. M. Brady, R.-A. N. Turkson-Ocran, and S. P. Juraschek, "Validating cuffless continuous blood pressure monitoring devices," *Cardiovascular Digital Health Journal*, vol. 4, no. 1, pp. 9–20, Feb. 2023.
- [5] "Biopotential Electrode Sensors in ECG/EEG/EMG Systems | Analog Devices," <https://www.analog.com/en/resources/technical-articles/biopotential-electrode-sensors-ecg-ecg-emg.html#authors>.
- [6] N. Elgrishi, K. J. Rountree, B. D. McCarthy, E. S. Rountree, T. T. Eisenhart, and J. L. Dempsey, "A Practical Beginner's Guide to Cyclic Voltammetry," *Journal of Chemical Education*, vol. 95, no. 2, pp. 197–206, Feb. 2018.
- [7] P. Kassaros, "Bioimpedance Sensors: A Tutorial," *IEEE Sensors Journal*, vol. 21, no. 20, pp. 22 190–22 219, Oct. 2021.
- [8] H. Gwak, S. Cho, Y.-J. Song, J.-H. Park, and S. Seo, "A study on the fabrication of metal microneedle array electrodes for ECG detection based on low melting point Bi–In–Sn alloys," *Scientific Reports*, vol. 13, no. 1, p. 22931, Dec. 2023.
- [9] M. R. Neuman, *Biopotential Electrodes*, ser. The Biomedical Engineering Handbook: Second Edition. Boca Raton: CRC Press LLC, 2000, 2000.
- [10] X. T. Cui and D. D. Zhou, "Poly (3,4-Ethylenedioxythiophene) for Chronic Neural Stimulation," *IEEE Transactions on Neural Systems and Rehabilitation Engineering*, vol. 15, no. 4, pp. 502–508, Dec. 2007.
- [11] E. Castagnola, L. Maiolo, E. Maggiolini, A. Minotti, M. Marrani, F. Maita, A. Pecora, G. N. Angotzi, A. Ansaldo, M. Boffini, L. Fadiga, G. Fortunato, and D. Ricci, "PEDOT-CNT-Coated Low-Impedance, Ultra-Flexible, and Brain-Conformable Micro-ECOG Arrays," *IEEE Transactions on Neural Systems and Rehabilitation Engineering*, vol. 23, no. 3, pp. 342–350, May 2015.
- [12] X. Tang, Y. Dong, Q. Li, Z. Liu, N. Yan, Y. Li, B. Liu, L. Jiang, R. Song, Y. Wang, G. Li, and P. Fang, "Using microneedle array electrodes for non-invasive electrophysiological signal acquisition and sensory feedback evoking," *Frontiers in Bioengineering and Biotechnology*, vol. 11, p. 1238210, Aug. 2023.
- [13] N. Wilke, C. Hibert, J. O'Brien, and A. Morrissey, "Silicon microneedle electrode array with temperature monitoring for electroporation," *Sensors and Actuators A: Physical*, vol. 123–124, pp. 319–325, Sep. 2005.
- [14] S. Guo, R. Lin, L. Wang, S. Lau, Q. Wang, and R. Liu, "Low melting point metal-based flexible 3D biomedical microelectrode array by phase transition method," *Materials Science and Engineering: C*, vol. 99, pp. 735–739, Jun. 2019.
- [15] S. A. Machekposhti, M. Soltani, P. Najafzadeh, S. Ebrahimi, and P. Chen, "Biocompatible polymer microneedle for topical/dermal delivery of tranexamic acid," *Journal of Controlled Release*, vol. 261, pp. 87–92, Sep. 2017.
- [16] J. Lozano and B. Stoeber, "Fabrication and characterization of a microneedle array electrode with flexible backing for biosignal monitoring," *Biomedical Microdevices*, vol. 23, no. 4, p. 53, Dec. 2021.
- [17] X. Tang, Y. Dong, Q. Li, Z. Liu, N. Yan, Y. Li, B. Liu, L. Jiang, R. Song, Y. Wang, G. Li, and P. Fang, "Using microneedle array electrodes for non-invasive electrophysiological signal acquisition and sensory feedback evoking," *Frontiers in Bioengineering and Biotechnology*, vol. 11, p. 1238210, Aug. 2023.
- [18] S. Rajaraman, J. A. Bragg, J. D. Ross, and M. G. Allen, "Micromachined three-dimensional electrode arrays for transcutaneous nerve tracking," *Journal of Micromechanics and Microengineering*, vol. 21, no. 8, p. 085014, Aug. 2011.
- [19] P. M. Biesheuvel, S. Porada, and J. E. Dykstra, "The difference between Faradaic and non-Faradaic electrode processes," Jan. 2021.
- [20] L. Beckmann, C. Neuhaus, G. Medrano, N. Jungbecker, M. Walter, T. Gries, and S. Leonhardt, "Characterization of textile electrodes and conductors using standardized measurement setups," *Physiological Measurement*, vol. 31, no. 2, pp. 233–247, Feb. 2010.

Design and implementation of a device for supporting the visually impaired with a focus on spatial orientation

¹Richard KRÁL (1st year)
Supervisor: ²Tibor VINCE

^{1,2}Dept. of Theoretical and Industrial Engineering, FEI, Technical University of Košice, Slovak Republic

¹richard.kral@tuke.sk, ²tibor.vince@tuke.sk

Abstract—This paper provides an overview of research focused on the development of assistive technologies for visually impaired individuals, with a particular emphasis on spatial orientation and obstacle detection. The study explores various approaches to wearable haptic feedback systems, LiDAR-based perception models, and energy-efficient sensor integration. It critically examines existing solutions, highlighting their limitations in terms of affordability, size, and accuracy, which serve as the motivation for the development of a novel, custom-designed LiDAR system. This system aims to balance cost-effectiveness, energy efficiency, and compactness while ensuring reliable performance in real-world applications. The paper also presents an in-depth analysis of different feedback modalities, including vibrotactile stimulation, linear actuators, and electroactive polymers, as potential interfaces for user interaction.

Keywords— assistive technology, LiDAR, spatial awareness, haptic feedback, wearable navigation, visually impaired accessibility

I. INTRODUCTION

Visual impairment affects over 285 million people globally, creating significant challenges in their daily lives [1],[2]. While traditional aids like white canes and guide dogs have long supported this community, there's a growing demand for innovative solutions that can enhance their ability to navigate and interact with the world independently. Current technological advances show promise in addressing these needs [3]-[5], yet many cutting-edge devices remain out of reach for most users due to their high cost. Despite the availability of various assistive tools, including mobile apps and specialized equipment, many individuals still face barriers in accurately detecting obstacles, understanding their surroundings, and adapting these tools to their specific needs. This underscores the need for a comprehensive review of existing navigation devices, a thorough analysis of the underlying technologies, and the development of enhancements or entirely novel approaches to improve accessibility and functionality.

Therefore, this paper presents an overview of various approaches to the issue at hand. Next, an analysis of current navigation assistive technologies for visually impaired people, focusing on methods of vision compensation and data acquisition techniques was conducted. Furthermore, an in-

depth analysis of LiDAR technology was performed as a means of collecting input data, and various feedback delivery methods were explored. This study contributes to the further development of more accessible, cost-effective, and inclusive assistive technologies that enhance independence and mobility for visually impaired individuals.

II. LITERATURE REVIEW AND ANALYSIS

A. Related works

Recent innovations combine advanced AI capabilities, body-worn detection systems, and instant data analysis to create tools that help people with visual impairments navigate their surroundings more effectively. These technological solutions aim to improve daily accessibility by providing real-time assistance and environmental information.

Modern technological advances have produced diverse solutions for visual impairment assistance. Smart clothing with integrated sensor systems [6] represents one innovative direction, while connected devices like the IoT-Smart Stick [7] offer enhanced navigation capabilities. More sophisticated systems include RASPV, which creates simulated visual environments [8], and specialized SLAM (Simultaneous Localization and Mapping) techniques for spatial orientation [9].

Text recognition technology has made significant progress through various approaches. These include attention-based neural networks [10] and enhanced VGG (Visual Geometry Group) algorithms designed specifically for visual prosthetics [11].

Safety innovations include real-time hazard detection using wavelet networks [18], while retail accessibility has improved through advanced product recognition systems utilizing the Aquila Optimization Algorithm with deep learning capabilities [12].

Text recognition capabilities have expanded through various technological approaches. Arbitrarily-Oriented Networks can process text from multiple angles [13], while SGBANet employs balanced attention mechanisms with semantic GANs (Generative Adversarial Networks) [14].

Language-specific solutions, particularly for Farsi script, combine traditional classifiers with neural networks [15]. Recent developments include temporal convolutional encoders [16] and established RNN-based (Recurrent Neural Network) approaches for scenic text categorization [17].

These technological developments collectively demonstrate the potential for significantly improving visually impaired individuals' daily experiences through personalized assistive solutions. The subsequent section presents products specifically used for navigation, which are currently available on the market or under development.

B. Current navigation assistive devices for visually impaired people

Analyzing current assistive devices reveals two primary approaches to gathering environmental information: distance sensors and AI-enabled cameras that analyze objects and their proximity to the user. These devices typically employ one or both of two feedback methods: tactile and auditory. Tactile feedback is delivered either through pressure cylinders that apply force proportional to obstacle distance, or through vibrations/electrode stimulation with intensity corresponding to proximity. While audio feedback specifications vary, they generally correlate sound patterns with obstacle distance and position.

The Lumen [18], as illustrated in Fig. 1(a), combines a specialized AI camera with dual feedback systems - audio (including verbal descriptions and obstacle alerts) and tactile patterns - to create a comprehensive navigation aid. It is currently under development.

ForeSight's haptic vest [19], shown in Fig. 1(b), features a front-mounted camera connected to a smartphone. The system processes camera data and transmits it via Bluetooth to electro-mechanical components on the vest's back, creating targeted pressure points for directional feedback. This prototype is not yet commercially available.

The BuzzClip [20], depicted in Fig. 1(c), utilizes ultrasonic sensing technology to detect nearby obstacles and converts this data into vibrational feedback for the user. It costs around 200€.

Vision Pro [21], displayed in Fig. 1(d), consists of a head-mounted digital camera that translates environmental information into electrostimulation delivered through tongue-mounted electrodes. However, due to business restructuring and intellectual property transfer, this system is currently unavailable commercially.

The Sixth Sense device [22], shown in Fig. 1(e), combines a proprietary navigation app with Bluetooth-connected sensors, delivering environmental information through both headphone-based audio and head-mounted tactile feedback.

The SuperBrain [23], illustrated in Fig. 1(f), uses a head-mounted camera system that processes environmental data and conveys spatial information through a forehead-mounted pressure actuator. It costs around 9000€.

The Niira system [24], presented in Fig. 1(g), employs a head-mounted camera to capture environmental data, converting it into spatial audio signals for user navigation. Currently, this device is only available in the Spanish market.

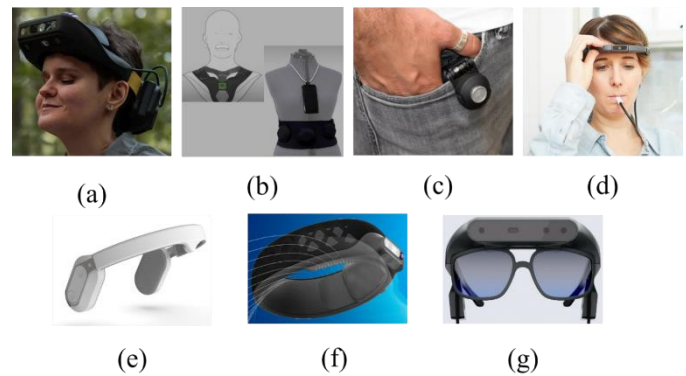


Fig. 1 Navigation assist devices for visually impaired people, (a) - Lumen device, (b) - ForeSight haptic vest, (c) - BuzzClip device, (d) - Vision Pro system, (e) - Sixth sense device, (f) - SuperBrain system, (g) - Niira device

When evaluating acquisition methods for obstacle detection in assistive devices, laser ranging technology demonstrates superior temporal performance compared to ultrasonic sensing systems. However, the integration of current laser measurement devices into wearable applications presents challenges regarding mass and dimensional constraints. Camera-based solutions offer advantages in terms of miniaturization and weight optimization, making them particularly suitable for wearable applications. Nevertheless, questions persist regarding the real-time processing capabilities and reliability of AI-based image/video analysis systems. That's the reason why we prefer LiDAR solution.

In the context of feedback mechanisms, tactile interfaces demonstrate advantages over auditory systems by eliminating the cognitive load associated with sound pattern interpretation and spatial correlation. That is the reason why this approach will be further analyzed. It potentially enables more rapid obstacle response times. However, the implementation of mechanical pressure cylinders presents significant engineering challenges due to their structural complexity. While electrostimulation electrodes offer improved response times and mechanical simplicity, their current tongue-based placement may not optimize the available sensory surface area. Alternative approaches, such as back-mounted electrode arrays, could potentially increase both the quantity of electrodes and feedback precision. This solution, however, faces limitations regarding sustained usage duration, as prolonged intense electrostimulation may have adverse physiological effects on muscle tissue.

Table I Limitations of current assistive devices for visually impaired people.

Company & Product	Vision compensation	Input data from	Limitations
.Lumen	Touch, hearing	Embedded camera	Real-time processing capabilities, reliability of AI-based image/video analysis
Anirban Ghosh, ForeSight	Touch	Smartphone camera	Real-time processing capabilities, reliability of AI-based image/video analysis
iMerciv, BuzzClip	Touch	Ultrasonic sensor	Limited range and accuracy, feedback does not interpret space fast and accurately enough.
BrainPort, Vision Pro	Touch	Embedded camera	Real-time processing capabilities, reliability of AI-based image/video analysis
HopeTech, Sixth sense	Touch, hearing	Sensors	Feedback does not interpret space fast and accurately enough.
7sense, SuperBrain	Touch	Embedded camera	Real-time processing capabilities, reliability of AI-based image/video analysis
Sensotec and Eyesynth, Niira	Hearing	Laser sensor	Feedback does not interpret space fast and accurately enough.

In subsequent sections, we present an in-depth analysis of LiDAR technology as a means of collecting input data, and various tactile feedback delivery methods.

C. Wearable LiDAR

Light Detection and Ranging (LiDAR) technology integration into wearable devices requires optimized systems that prioritize lightweight design and power efficiency while maintaining operational effectiveness. These portable LiDAR implementations enable real-time spatial perception applications, particularly beneficial for enhancing navigation assistance and environmental awareness for visually impaired individuals.

The operational principle of LiDAR systems centers on time-of-flight (ToF) measurements of reflected laser pulses, enabling precise distance determination. LiDAR systems are classified into two primary categories based on their scanning methodology: non-scanning and scanning systems. Flash LiDAR, a non-scanning variant, employs simultaneous full-field illumination with photodetector arrays for ToF detection. While this approach offers mechanical simplicity and vibration resistance, it faces limitations in signal-to-noise ratio and operational range [25].

Canning LiDAR systems utilize either mechanical or non-mechanical beam steering mechanisms. Mechanical systems employ rotating mirrors or motorized components for beam direction, achieving comprehensive coverage despite size and energy constraints. Non-mechanical alternatives, such as optical phased arrays (OPAs), provide beam steering without moving components, enhancing durability and enabling compact design [25] [26].

Microelectromechanical Systems (MEMS) mirrors

represent a significant advancement in scanning LiDAR technology. These hybrid devices combine solid-state and mechanical principles, delivering precise beam control while maintaining compact dimensions and energy efficiency. MEMS mirror technology presents *advantages* for wearable LiDAR applications where size, weight, and power consumption are critical design parameters. Fig. 2, source: [25]

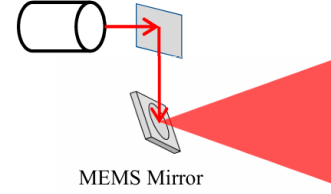


Fig. 2 Working principle of MEMS-based LiDAR

Assessing the performance and applicability of a LiDAR system for specific use cases requires the quantification of several critical parameters.

As we can see in Fig. 3, the minimum divergence angle of the laser beam, denoted as θ_{min} , affects the spatial resolution of the LiDAR system. It is defined as:

$$\theta_{min} = \frac{M^2 \lambda_0}{\pi w_0} \quad (1)$$

where λ_0 represents the laser wavelength, w_0 is the half beam waist (typically limited by the size of the MEMS mirror), and M^2 indicates the beam quality. A lower divergence angle results in better resolution, which is particularly critical for LiDAR applications requiring precision in detailed mapping.

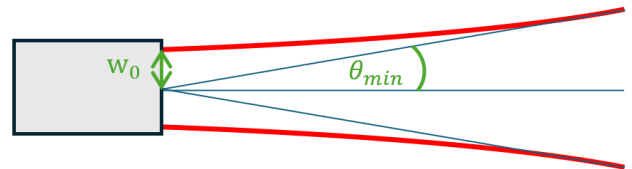


Fig. 3 Half divergence angle and half beam waist of the laser

The resonant frequency f_0 of a MEMS mirror depends on the stiffness k and mass m of the mirror. It is defined as:

$$f_0 = \frac{1}{2\pi} \sqrt{\frac{k}{m}} \quad (2)$$

The quality factor Q is defined as the ratio of the resonant frequency f_0 to the bandwidth Δf . It is expressed as:

$$Q = \frac{f_0}{\Delta f} \quad (3)$$

A higher Q -factor allows for a larger scanning angle at the resonant frequency but may reduce the tolerance to changes in environmental conditions.

D. Haptic feedback delivery methods

Haptic feedback systems are technological solutions designed to provide users with tactile sensations through controlled

mechanical stimulation. These systems utilize actuators such as vibration motors, piezoelectric elements, or electrostatic forces to simulate touch-based interactions. The development of haptic feedback systems for visually impaired individuals aims to convey spatial information about their surroundings through tactile stimuli. One promising approach involves the use of a two-dimensional array of actuators positioned on the back, which can deliver localized sensations corresponding to the proximity of objects in the environment. This section examines three actuator technologies suitable for such applications: linear actuators, vibrotactile motors, and electroactive polymers (EAPs).

Linear actuators operate by mechanically displacing elements to exert pressure on specific areas of the skin. Their primary advantage lies in their ability to produce substantial tactile forces, potentially leading to precise spatial perception. However, the mechanical complexity and high energy consumption associated with linear actuators pose significant challenges for their integration into wearable haptic devices. The bulkiness and power requirements may impede user mobility and device autonomy, limiting their practicality in daily use.

Vibrotactile motors generate tactile feedback through localized vibrations on the skin's surface. These motors are favored for their energy efficiency and straightforward implementation. Nonetheless, the efficacy of vibrotactile feedback in conveying detailed spatial information remains a subject of investigation. The human skin's ability to discern between multiple simultaneous vibrations is limited, which may affect the user's capacity to accurately interpret complex spatial cues solely through vibratory stimuli.

EAPs are materials that undergo shape or size changes in response to electrical stimulation, enabling them to function as actuators in haptic feedback systems. Their advantages include low energy consumption and the potential for creating soft, flexible interfaces that conform to the body's contours. Recent advancements have demonstrated the feasibility of EAP-based soft tactile interfaces for wearable devices, highlighting their potential in delivering nuanced haptic feedback. However, challenges persist regarding the durability, long-term stability, and cost-effectiveness of EAPs, as the technology is still maturing and may involve higher production expenses compared to more established actuator technologies [27].

III. PROBLEM IDENTIFICATION AND FUTURE DIRECTIONS

Given the lack of an affordable, sufficiently lightweight, and compact LiDAR suitable for wearable devices, our goal is to develop a custom LiDAR system with low manufacturing costs, minimal energy consumption, and a form factor optimized for integration into a wearable solution.

We tested commercially available laser distance meters of various sizes and weights that fall within an economically feasible price range (under 40 EUR). Our initial approach involved employing a MEMS mirror to oscillate the laser beam across both horizontal and vertical axes, thereby constructing a three-dimensional representation of the environment in front of the visually impaired user. However, during our experimental validation, we observed significant inaccuracies introduced by the mirrors. Furthermore, MEMS technology falls within the domain of nanotechnology and requires specialized fabrication processes and tools that are not readily accessible. These manufacturing constraints, combined with the high production costs, render MEMS-based solutions unsuitable for the low-cost alternative we aim

to develop. Furthermore, MEMS technology falls within the domain of nanotechnology and requires specialized fabrication processes and tools that are not readily accessible. These manufacturing constraints, combined with the high production costs, render MEMS-based solutions unsuitable for the low-cost alternative we aim to develop.

To overcome this issue, we adopted an alternative approach involving the oscillation of the entire sensor rather than relying on MEMS-based beam steering. The proposed mechanism consists of a rotating magnetic material positioned above two coils, each mounted on opposite sides of the oscillating arm. These coils alternately generate a magnetic field, exerting an attractive force on the magnetic material and inducing oscillatory motion. To enhance and sustain this motion, torsional springs are attached at both ends of the magnetic component along its axis of symmetry. By precisely tuning the spring parameters, we can determine, simulate, and optimize the system's natural oscillation frequency. Continuous actuation of the arm by alternating the magnetic field between the two coils results in sustained oscillations.

Further simulations were conducted to analyze the magnetic force exerted on a metallic plate by a solenoid-type coil (core dimensions: 5 mm thickness, 10 mm length, core material: permalloy) under varying parameters, including the number of windings, direct current passing through the coil, and the coil's distance from the metallic plate.

IV. CONCLUSION

This paper provides an extensive review of the technological landscape surrounding assistive devices for visually impaired individuals, covering aspects such as sensor selection, LiDAR technology, and haptic feedback systems. By addressing the limitations of existing solutions, this research contributes to the development of a novel approach that leverages whole-sensor oscillation as an alternative to traditional MEMS-based beam steering. The study highlights the significance of integrating energy-efficient actuation mechanisms with robust feedback interfaces to improve spatial awareness for visually impaired users. Future research will focus on prototype development, real-world testing, and refinement of sensor-actuator interactions to ensure practical usability and reliability in assistive navigation applications.

REFERENCES

- [1] B. J. Lee and N. A. Afshari, "The global burden of blindness," *Current Opinion in Ophthalmology*, vol. 36, no. 1. Ovid Technologies (Wolters Kluwer Health), pp. 1–3, Dec. 05, 2024. doi: 10.1097/icu.0000000000001099.
- [2] M. Robby, E. Hartoyo, E. Wydiamala, H. Husaini, and S. Arifin, "Meta Analysis: The Relationship of Looking Distance and Long Time of Smartphone use with Myopia," *Jurnal Berkala Kesehatan*, vol. 10, no. 2. Center for Journal Management and Publication, Lambung Mangkurat University, p. 157, Nov. 30, 2024. doi: 10.20527/jbk.v10i2.10947.
- [3] J. Madake, S. Bhatlawande, A. Solanke, and S. Shilaskar, "A qualitative and quantitative analysis of research in mobility technologies for visually impaired people," *IEEE Access*, vol. 11, pp. 82496–82520, 2023, doi: 10.1109/ACCESS.2023.3291074.
- [4] S. Bhatlawande, R. Borse, A. Solanke and S. Shilaskar, "A Smart Clothing Approach for Augmenting Mobility of Visually Impaired People," in *IEEE Access*, vol. 12, pp. 24659–24671, 2024, doi: 10.1109/ACCESS.2024.3364915.
- [5] A. Lo Valvo, D. Croce, D. Garlisi, F. Giuliano, L. Giarré, and I. Tinnirello, "A Navigation and Augmented Reality System for Visually Impaired People," *Sensors*, vol. 21, no. 9. MDPI AG, p. 3061, Apr. 28, 2021. doi: 10.3390/s21093061.

- [6] A. I. Apu, A.-A. Nayan, J. Ferdaous, and M. G. Kibria, "IoT-Based Smart Blind Stick," *Lecture Notes on Data Engineering and Communications Technologies*. Springer Singapore, pp. 447–460, Dec. 04, 2021. doi: 10.1007/978-981-16-6636-0_34.
- [7] A. Perez-Yus *et al.*, "RASPV: A Robotics Framework for Augmented Simulated Prosthetic Vision," in *IEEE Access*, vol. 12, pp. 15251–15267, 2024, doi: 10.1109/ACCESS.2024.3357400.
- [8] M. Bamdad, D. Scaramuzza, and A. Darvishy, "SLAM for Visually Impaired People: a Survey," 2022, arXiv. doi: 10.48550/ARXIV.2212.04745.
- [9] A. A. A. Alshawi, J. Tanha and M. A. Balafar, "An Attention-Based Convolutional Recurrent Neural Networks for Scene Text Recognition," in *IEEE Access*, vol. 12, pp. 8123–8134, 2024, doi: 10.1109/ACCESS.2024.3352748.
- [10] Z. Li, B. Li, S. G. Jahng and C. Jung, "Improved VGG Algorithm for Visual Prosthesis Image Recognition," in *IEEE Access*, vol. 12, pp. 45727–45739, 2024, doi: 10.1109/ACCESS.2024.3380839.
- [11] Z. Yu and M. Hu, "Real Environment Warning Model for Visually Impaired People in Trouble on the Blind Roads Based on Wavelet Scattering Network," in *IEEE Access*, vol. 12, pp. 82156–82167, 2024, doi: 10.1109/ACCESS.2024.3412328.
- [12] M. Alghamdi, H. A. Mengash, M. Aljebreen, M. Maray, A. A. Darem and A. S. Salama, "Empowering Retail Through Advanced Consumer Product Recognition Using Aquila Optimization Algorithm With Deep Learning," in *IEEE Access*, vol. 12, pp. 71055–71065, 2024, doi: 10.1109/ACCESS.2024.3399480.
- [13] Z. Cheng, Y. Xu, F. Bai, Y. Niu, S. Pu, and S. Zhou, "AON: Towards arbitrarily-oriented text recognition," 2017, arXiv:1711.04226.
- [14] D. Zhong, S. Lyu, P. Shivakumara, B. Yin, J. Wu, U. Pal, and Y. Lu, "SGBANet: Semantic GAN and balanced attention network for arbitrarily oriented scene text recognition," in *Proc. Eur. Conf. Comput. Vis.*, 2022, pp. 464–480.
- [15] Y. A. Nanekaran, D. Zhang, S. Salimi, J. Chen, Y. Tian, and N. Al-Nabhan, "Analysis and comparison of machine learning classifiers and deep neural networks techniques for recognition of Farsi handwritten digits," *J. Supercomput.*, vol. 77, no. 4, pp. 3193–3222, Apr. 2021.
- [16] X. Du, T. Ma, Y. Zheng, H. Ye, X. Wu, and L. He, "Scene text recognition with temporal convolutional encoder," in *Proc. IEEE Int. Conf. Acoust., Speech Signal Process. (ICASSP)*, May2020, pp. 2383–2387, doi:10.1109/ICASSP40776.2020.9054269.
- [17] B. Su and S. Lu, "Accurate scene text recognition based on recurrent neural network," in *Proc. Asian Conf. Comput. Vis.*, in *Lecture Notes in Computer Science: Including Subseries Lecture Notes in Artificial Intelligence and Lecture Notes in Bioinformatics*, vol. 9003, 2015, pp. 35–48, doi: 10.1007/978-3-319-16865-4_3.
- [18] Lumen, .Lumen, [quoted 24.07.2024], available on the internet: <<https://www.dotlumen.com/>>
- [19] Anirban Ghosh, ForeSight, [quoted 24.07.2024], available on the internet: <<https://www.anirbanghoshdesign.com/copy-of-gathr>>
- [20] iMerciv, BuzzClip, [quoted 21.07.2024], available on the internet: <<https://neuroticworks.com/projects/wearable-mobility-device/>>
- [21] BrainPort, Vision Pro, [quoted 25.08.2024], available on the internet: <<https://www.wicab.com/brainport-vision-pro>>
- [22] HopeTech, Sixth sense, [quoted 15.08.2024], available on the internet: <<https://www.hopetech.vision/>>
- [23] 7sense, SuperBrain, [quoted 14.09.2024], available on the internet: <<https://7sense.ee/toode/superbrain-i/>>
- [24] Sensotec and Eyesynth, Niira, [quoted 20.09.2024], available on the internet: <<https://www.pro.sensotec.com/post/niira-glasses-launch>>
- [25] Wang, D.; Watkins, C.; Xie, H. MEMS Mirrors for LiDAR: A Review. *Micromachines* 2020, 11, 456. <https://doi.org/10.3390/mi11050456>
- [26] P. F. McManamon *et al.*, "A Review of Phased Array Steering for Narrow-Band Electrooptical Systems," in *Proceedings of the IEEE*, vol. 97, no. 6, pp. 1078–1096, June 2009, doi: 10.1109/JPROC.2009.2017218.
- [27] S. Mun *et al.*, "Electro-Active Polymer Based Soft Tactile Interface for Wearable Devices," in *IEEE Transactions on Haptics*, vol. 11, no. 1, pp. 15–21, 1 Jan.-March 2018, doi: 10.1109/TOH.2018.2805901.

Solving optimization and search problems using D-Wave Systems' Quantum Annealer

¹*Renáta RUSNÁKOVÁ (1st year),*

Supervisor: ²Martin CHOVANEC

^{1,2}Dept. of Computers and Informatics, FEI TU of Košice, Slovak Republic

¹renata.rusnakova@tuke.sk, ²martin.chovanec@tuke.sk

Abstract—Quantum annealing provides a practical approach to solving complex optimization problems by leveraging quantum effects. This paper explores its application using D-Wave's hybrid solver, focusing on the QUBO formulation for shortest path and graph partitioning problems. We compare its performance with classical methods such as A* and METIS and discuss its potential in autonomous mobility, particularly for motion planning and real-time decision-making.

Keywords—D-Wave Systems, Optimization problem, Quantum Annealing, Quantum Computing

I. INTRODUCTION

Quantum computing leverages quantum-mechanical principles to solve problems more efficiently than classical methods. Quantum annealing, pioneered by D-Wave Systems, focuses on solving optimization problems by minimizing a system's energy. This paper explores the QUBO formulation of shortest path and graph partitioning problems, evaluating D-Wave's hybrid solver against classical methods like A* and METIS. Additionally, we discuss its potential in autonomous mobility, particularly for real-time motion planning and lane-changing in congested traffic.

II. CURRENT STATE OF QUANTUM COMPUTING WITH FOCUS ON QUANTUM ANNEALING

With the rapid development of modern quantum computing machines, the need for reformulating classical algorithms for quantum hardware has grown. Here, we introduce the two main quantum computing paradigms:

• Universal Quantum Computing

- Based on quantum gates and circuits operating on qubits, leveraging quantum mechanics principles such as superposition and entanglement.
- Suitable for solving computationally complex problems; algorithms must be specifically designed for quantum hardware, often differing significantly from classical counterparts.
- Developed by companies like Google [1], IBM [2], and Rigetti [3].

• Quantum Annealing

- Utilizes the Adiabatic Theorem and quantum annealing to slowly evolve the system toward the ground state (minimum energy configuration), leveraging superposition and tunneling to escape local minima and find the global optimum (Fig. 1).

- Designed for solving optimization, search, and sampling problems.
- The pioneering company providing commercial quantum annealers is D-Wave Systems [4].

Quantum computers have the potential to significantly reduce computational time and resource requirements for certain problems. As demonstrated in [5], Shor's factoring algorithm provides significant speedup over the best-known classical approaches such as the General Number Field Sieve (GNFS) [6], reducing complexity from sub-exponential to polynomial time.

The following subsections focus on Quantum Annealing, the Quadratic Unconstrained Binary Optimization (QUBO) formulation, and D-Wave Systems' implementation of quantum annealer, as these techniques can be used to solve optimization problems in graph theory and problems in area of autonomous mobility which is our main focus.

A. Quantum Annealing and Adiabatic Theorem

Quantum annealing is a quantum optimization technique that leverages superposition and tunneling to solve combinatorial optimization problems [7]. The process, illustrated in Fig. 2, involves initializing the system in the ground state of a simple Hamiltonian H_0 and then evolving it into a final Hamiltonian H_f that encodes the problem to be solved [8]. If this evolution occurs slowly enough, the system remains in its ground state, corresponding to the optimal solution.

The **Hamiltonian**, an operator describing the total energy of a quantum system, is designed so that its ground state represents the optimal configuration. Initially, the system's state is a superposition of all possible states, allowing exploration of multiple configurations simultaneously. As the system evolves, quantum tunneling facilitates transitions through energy barriers, enhancing the search for the global minimum of the objective function.

The **Objective Function** represents the mathematical formulation of an optimization problem, typically expressed as a cost function that the system seeks to minimize. It is often written in QUBO form, encoding problem constraints and interactions between binary variables. The lowest energy state corresponds to the optimal solution [9], with the objective function being interpreted as the energy function of a quantum system [10].

This demonstrates the correspondence between the objective function, the QUBO formulation, and the system's Hamil-

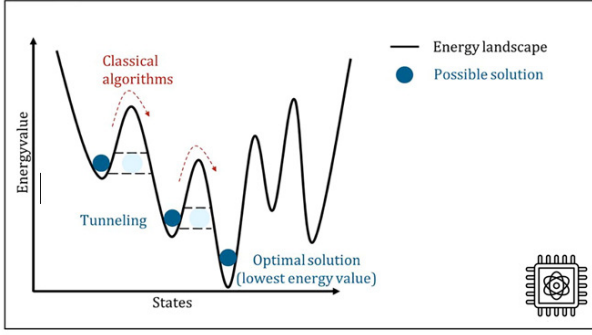


Fig. 1. Energy landscape of the system under adiabatic evolution.

tonian, as they all describe energy minimization but from different perspectives.

The **Adiabatic Theorem** [11] states that if a quantum system starts in the ground state of a Hamiltonian and that Hamiltonian evolves slowly over time, the system will remain in the ground state of the instantaneous Hamiltonian. This is mathematically expressed as:

$$H(t) = (1 - s(t))H_0 + s(t)H_f, \quad (1)$$

where $s(t)$, the function of time, evolves gradually from 0 to 1, ensuring that H_0 is smoothly transformed into H_f . If this transition occurs too quickly, the system may jump to excited states, leading to suboptimal solutions.

Quantum annealing relies on this theorem to ensure that the system reaches the ground state of H_f . However, a trade-off exists: slower evolution improves accuracy but increases runtime.

B. QUBO and Ising Models

Many combinatorial optimization problems can be formulated using either the Ising model or QUBO model, both central to modern quantum computing [9]. These representations enable efficient solutions using quantum annealers.

The **Ising Model**, originating from statistical mechanics, describes ferromagnetism and spin interactions. Each spin takes discrete values $+1$ or -1 and interacts with its neighbors to minimize the system's total energy. Many combinatorial optimization problems can be mapped onto the Ising model [12], leading to the development of Ising Machines. However, classical Ising machines often become trapped in local minima, preventing them from finding the optimal solution [13].

To address this, quantum annealing was introduced, leveraging quantum tunneling to allow the system to escape local minima and search the solution space more effectively [14]. The energy function for the Ising model is:

$$E = - \sum_{i < j} J_{i,j} s_i s_j - \sum_i h_i s_i, \quad (2)$$

where s_i is the spin variable at site $i \in \{-1, 1\}$, $J_{i,j}$ represents the interaction strength between spins i and j , and h_i denotes the external magnetic field applied at spin i .

Since quantum annealers solve optimization problems by minimizing energy (objective) functions, **QUBO models** are often used as an equivalent mathematical framework:

$$Obj(x) = \sum_{i < j} Q_{i,j} x_i x_j + \sum_i Q_i x_i, \quad (3)$$

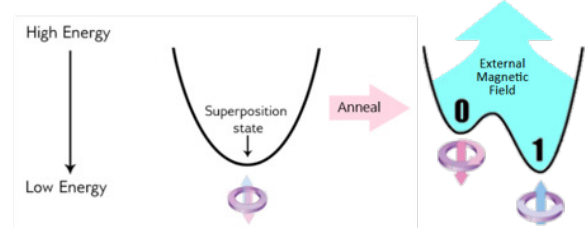


Fig. 2. The annealing process follows an adiabatic evolution, transitioning the system from the ground state of H_0 (a simple Hamiltonian where all qubits exist in superposition) to the ground state of H_f , which encodes the problem's solution. The hardware comprises qubits, structured as superconducting loops made of niobium, influenced by an external magnetic field.

where Q is the symmetric QUBO matrix encoding the problem, and x_i represents the binary variables defining the solution.

Each QUBO/Ising problem—specific optimization task—can be represented by QUBO/Ising Model formulation. Ising problem is known to be NP-hard, meaning that solving it requires exponential time in the worst case [12]. Through polynomial transformations, any Ising problem can be converted into a QUBO problem (and vice versa), making them interchangeable for quantum annealing-based optimization tasks [15].

C. D-Wave System's Hybrid Solver

D-Wave Systems is the first company to develop and commercialize quantum annealers, focusing on solving optimization problems using quantum annealing technology. Unlike gate-based quantum computers that utilize unitary operations, D-Wave's quantum annealers operate based on the adiabatic theorem, transitioning the system into a low-energy configuration that represents an optimal solution [16], [17].

D-Wave's quantum processing units (QPUs) rely on superconducting qubits, which maintain quantum coherence by operating at cryogenic temperatures (approximately 15 millikelvin) [18]. These qubits interact through programmable couplers, and their behavior can be mapped onto an Ising model, allowing optimization problems to be encoded directly onto the hardware.

Due to limitations in qubit connectivity and the available hardware resources, pure quantum annealing cannot efficiently handle large-scale optimization problems. D-Wave's hybrid solvers integrate quantum annealing with classical optimization techniques, partitioning large problems into smaller quantum-accessible subproblems while utilizing classical heuristics to refine and validate solutions [19].

D-Wave's Leap Quantum Cloud Service provides users with access to hybrid solvers that combine classical pre-processing, quantum annealing, and classical post-processing to optimize solutions [20].

Workflow of the Quantum Annealing Hybrid Solver:

- 1) **Problem Decomposition:** The hybrid solver decomposes a large problem into smaller subproblems, ensuring that each subproblem fits within the constraints of the QPU.
- 2) **Quantum Annealing Backend:** Each subproblem is mapped—embedded, onto the QPU in the form of QUBO or Ising model. The annealing process finds solutions by minimizing the energy function.

- 3) **Classical Post-processing:** A classical post-processing stage refines the solutions, applies constraint corrections, and merges subproblem results into a final optimized solution. The classical optimizer also helps handle problem constraints that cannot be easily embedded onto the quantum hardware.

D-Wave's Pegasus topology, an improvement over its predecessor (Chimera), offers higher qubit connectivity and shorter chain embeddings, reducing noise and enhancing problem scalability [17]. In the Pegasus topology, each qubit has a degree of 15, meaning it is directly connected to 15 other qubits. While this topology allows the hybrid solver to tackle larger-scale problems, it still faces scalability limitations, including embedding overhead, problem decomposition costs, and constraint handling.

Despite these challenges, quantum annealing hybrid solvers have shown competitive performance compared to classical solvers like Gurobi and CPLEX, particularly in binary quadratic programming (BQP) problems [21].

D-Wave's hybrid solver framework extends quantum annealing's capabilities, making it a viable tool for solving large-scale optimization problems that would otherwise be infeasible on quantum-only processors. Advancements in embedding techniques, QPU architectures (such as upcoming Zephyr topology), and problem decomposition heuristics are expected to further improve hybrid solver performance, making quantum-classical hybrid computation increasingly relevant for real-world optimization problems.

III. USAGE OF QUANTUM ANNEALING ON SOLVING OPTIMIZATION PROBLEMS

Many real-world problems can be formulated as optimization, search, or sampling problems, where the goal is to find an optimal solution from a large set of possible configurations. Among these, graph-based problems, such as the shortest path problem and graph partitioning, play a significant role in numerous applications, including logistics, network routing, and autonomous mobility.

A. Problem identification

The shortest path problem involves finding the minimum-cost path between two nodes in a graph. Classical algorithms such as Dijkstra's or A* provide efficient solutions in polynomial time for deterministic graphs. However, for large-scale dynamic graphs, where edge weights frequently change due to real-time constraints (e.g., traffic conditions in urban mobility), quantum approaches such as quantum annealing offer potential speedups by encoding the problem as QUBO model.

We have already studied and compared classical and quantum approaches to the shortest path problem, focusing on a QUBO formulation executed on D-Wave's quantum annealing hybrid solver. Our results indicate that while A* search with heuristics achieves linear complexity $O(n)$, the QUBO formulation, despite reducing the problem from $O(4^n)$ to polynomial complexity, faces challenges in accuracy as the number of nodes increases.

For smaller graphs (10–20 nodes), the hybrid solver finds the optimal path with high accuracy (100% for $n = 10$, 80% for $n = 20$), but for larger graphs (50+ nodes), exact matches drop significantly, with only near-optimal solutions found (e.g., for $n = 100$, paths deviate by up to 24.4% from A*). The study

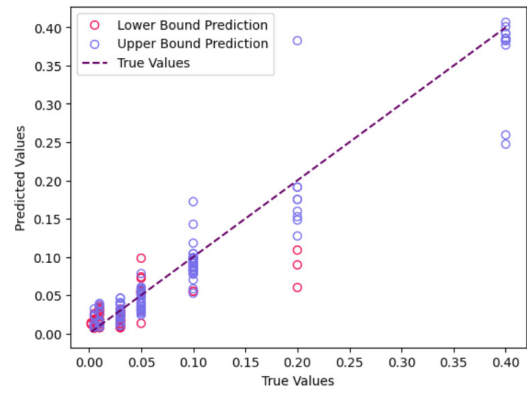


Fig. 3. GBR model predictions for penalty parameter γ based on graph's density and number of nodes compared to true values.

also highlights the impact of penalty parameters, problem embedding, and quantum hardware constraints on solution quality.

Another important optimization problem is graph partitioning, which involves dividing a graph into smaller subgraphs while minimizing edge cuts between them. This problem is particularly relevant in parallel computing, clustering, and transportation networks. It can be used also to minimize V2V communication and reduce computational overhead. In quantum annealing, the graph partitioning problem can be formulated using an QUBO model, where each node is assigned a binary variable, and the system seeks to minimize the total cut weight while maintaining balanced partition sizes. Since graph partitioning is NP-hard, quantum optimization techniques provide a promising alternative to classical heuristics, such as METIS or Kernighan–Lin algorithms.

At the moment, we are focusing on comparing the accuracy and performance of quantum annealing-based graph partitioning with classical methods such as METIS. Our experiments utilized a Gradient Boosting Regression (GBR) model to determine the optimal penalty parameter γ of the QUBO formulation, ensuring a balanced partitioning with minimal inter-edges.

The first analysis (Fig. 3) shows the GBR-predicted penalty parameter compared to actual values, confirming that our model provides reliable estimates.

After determining the optimal γ , we tested quantum annealing against METIS across various graph sizes on around 60 random-generated graphs. The analysis shown in Table I extends the evaluation to graphs with up to 4000 nodes, where the hybrid solver consistently outperformed METIS in terms of partitioning quality, achieving a lower or equal number of inter-edges in all cases. This demonstrates that quantum annealing, when combined with proper penalty parameter tuning, can effectively handle both small and large-scale partitioning tasks, outperforming classical methods.

B. Future directions

In the context of autonomous mobility, optimization plays a crucial role in situations like motion planning and decision-making. For instance, in overtaking scenarios, an autonomous vehicle must evaluate whether it is safe to overtake another vehicle while considering road conditions, lane availability, and surrounding traffic. Lane-changing decisions require real-

TABLE I
COMPARISON OF QA HYBRID SOLVER AND METIS RESULTS ON GRAPH
PARTITIONING PROBLEM

Number of Nodes	QA Hybrid vs METIS (winner)	Absolute Difference ^a (Inter-edges)	Percentage Difference ^b (%)
100	QA Hybrid	6	36.14%
200	QA Hybrid	19.2	48.50%
300	QA Hybrid	58.67	80.75%
400	QA Hybrid	62.43	44.58%
500	QA Hybrid	94.33	20.36%
600	QA Hybrid	141	38.04%
700	QA Hybrid	217.6	36.03%
800	QA Hybrid	180	47.14%
1000	QA Hybrid	249.36	20.89%
1500	QA Hybrid	622	15.08%
2000	QA Hybrid	1243	21.31%
3000	QA Hybrid	1119.25	38.75%
4000	QA Hybrid	1372	36.93%

$$^a |\text{avg}(\text{hybrid_inter_edges}) - \text{avg}(\text{pymetis_inter_edges})|$$

$$^b 100 \times \frac{\text{avg}(\text{pymetis_inter_edges}) - \text{avg}(\text{hybrid_inter_edges})}{\text{avg}(\text{hybrid_inter_edges})}$$

time assessment of the vehicle's position, velocity, and possible obstacles. By leveraging sensor data, quantum annealers can rapidly process information about nearby vehicles and compute optimal maneuvers in congested traffic.

Quantum annealing can also be employed to integrate real-time sensor data to determine the safest and most efficient next move for an autonomous vehicle. This involves dynamically adjusting path planning based on environmental changes, such as sudden braking by nearby cars or shifts in traffic density. By formulating the problem as an optimization task in a QUBO form, quantum processors can explore multiple configurations simultaneously and select the optimal trajectory, reducing computation time in highly dynamic environments.

The integration of quantum optimization techniques into autonomous driving has the potential to enhance safety, efficiency, and decision-making speed, particularly in complex traffic situations. Future research aims to further refine these approaches, incorporating hybrid quantum-classical methods to handle large-scale mobility scenarios with real-world constraints.

IV. CONCLUSION

This paper explored quantum annealing for solving optimization problems using D-Wave's quantum hybrid solvers, with a focus on shortest path and graph partitioning problems. Our findings indicate that, with proper tuning of penalty parameters, quantum annealing can outperform classical heuristics like METIS in partitioning tasks, particularly for mid-sized graphs. Additionally, we examined the potential of quantum optimization in autonomous mobility, highlighting its role in motion planning, overtaking, and lane-changing decisions. Future research will focus on improving hybrid quantum-classical methods to enhance scalability and efficiency in real-world applications.

ACKNOWLEDGMENT

The research was partially supported by the European Health and Digital Executive Agency (HADEA) under the project no. 101133546 — 22-SK-DIG-TUKE 5GSC and Recovery and Resilience Plan of the Slovak Republic under the project no. 17I04-04-V01-00009.

REFERENCES

- [1] H. Neven. (2024) Meet willow, our state-of-the-art quantum chip. [Online]. Available: <https://blog.google/technology/research/google-willow-quantum-chip/>
- [2] J. Gambetta. (2023) The hardware and software for the era of quantum utility is here. [Online]. Available: <https://www.ibm.com/quantum/blog/quantum-roadmap-2023>
- [3] A. Bestwick. (2023) Introducing the ankaa™-1 system — rigetti's most sophisticated chip architecture unlocks a promising path to narrow quantum advantage. [Online]. Available: <https://www.rigetti.com/news/introducing-the-ankaa-1-system-rigetti-s-most-sophisticated-chip-architecture-unlocks-a-promising-path-to-narrow-quantum-advantage>
- [4] D-Wave. (2018) How many qubits do d-wave quantum computers have? [Online]. Available: <https://support.dwavesys.com/hc/en-us/articles/360009868993-How-Many-Qubits-Do-D-Wave-Quantum-Computers-Have>
- [5] H. Li and G. Zhao, "The comparison of the computing ability of quantum and conventional computer," *Highlights in Science, Engineering and Technology*, vol. 5, pp. 68–74, 07 2022.
- [6] C. Pomerance, "A tale of two sieves," *Notices of the American Mathematical Society*, vol. 43, pp. 1473–1485, 1996.
- [7] E. Farhi, J. Goldstone, S. Gutmann, J. Lapan, A. Lundgren, and D. Preda, "A quantum adiabatic evolution algorithm applied to random instances of an np-complete problem," *Science*, vol. 292, no. 5516, p. 472–475, Apr. 2001. [Online]. Available: <http://dx.doi.org/10.1126/science.1057726>
- [8] T. Albash and D. A. Lidar, "Adiabatic quantum computation," *Reviews of Modern Physics*, vol. 90, no. 1, p. 015002, 2018.
- [9] A. Lucas, "Ising formulations of many np problems," *Frontiers in Physics*, vol. 2, p. 5, 2014.
- [10] E. Farhi, J. Goldstone, S. Gutmann, and M. Sipser, "Quantum computation by adiabatic evolution," *arXiv preprint*, 2000.
- [11] M. Born and V. Fock, "Beweis des adiabatsatzes," *Zeitschrift für Physik*, vol. 51, pp. 165–180, 1928, english translation in: V.A. Fock – Selected Works: Quantum Mechanics and Quantum Field Theory, ed. by L.D. Faddeev, L.A. Khalin, I.V. Komarov, Chapman & Hall/CRC, Boca Raton, 2004.
- [12] F. Barahona, "On the computational complexity of ising spin glass models," *Journal of Physics A: Mathematical and General*, vol. 15, no. 10, p. 3241, 1982.
- [13] T. Leleu, Y. Yamamoto, S. Utsunomiya, and K. Aihara, "Destabilization of local minima in analog spin systems by correction of amplitude heterogeneity," *Physical Review Letters*, vol. 122, p. 040607, 2019.
- [14] T. Kadowaki and H. Nishimori, "Quantum annealing in the transverse ising model," *Physical Review E*, vol. 58, no. 5, pp. 5355–5363, 1998.
- [15] R. Hamerly, T. Inagaki, P. L. McMahon, D. Venturelli, A. Marandi, T. Onodera, E. Ng, C. Langrock, K. Inaba, T. Honjo, K. Enbutsu, T. Umeki, R. Kasahara, S. Utsunomiya, S. Kako, K. ichi Kawarabayashi, R. L. Byer, M. M. Fejer, H. Mabuchi, D. Englund, E. Rieffel, H. Takesue, and Y. Yamamoto, "Experimental investigation of performance differences between coherent ising machines and a quantum annealer," *Science Advances*, vol. 5, no. 5, p. eaau0823, 2019. [Online]. Available: <https://www.science.org/doi/abs/10.1126/sciadv.aau0823>
- [16] D-Wave Systems, "D-Wave Hybrid Solver Service: An Overview," D-Wave Whitepaper Series, Tech. Rep., 2020. [Online]. Available: <https://www.dwavesys.com/resources/white-paper/d-wave-hybrid-solver-service-an-overview/>
- [17] K. Boothby, P. Bunyk, J. Raymond, and A. Roy, "Next-generation topology of d-wave quantum processors," *arXiv*, 2020. [Online]. Available: <https://arxiv.org/abs/2003.00133>
- [18] D-W. Systems, "Improving performance of logical qubits by parameter tuning and topology compensation," D-Wave Systems Whitepaper Series, Tech. Rep. QPU-Performance-2021, 2021, accessed from D-Wave Systems documentation. [Online]. Available: <https://www.dwavesys.com/resources/white-paper/qpu-performance-tuning>
- [19] —, "Overview of hybrid solvers for combinatorial optimization," 2020. [Online]. Available: https://docs.dwavesys.com/docs/latest/handbook_hybrid.html
- [20] —, "Leap quantum cloud service: Overview and performance analysis," D-Wave Systems Whitepaper Series, Tech. Rep. LeapCloud-2021, 2021, accessed from D-Wave Systems documentation. [Online]. Available: <https://www.dwavesys.com/resources/white-paper/leap-quantum-cloud-service-overview>
- [21] D. Tadi, K. Sirigeri, and S. Panda, "Quantum annealing vs classical solvers: Performance comparison," *Kalpa Publications in Computing*, 2023.

Modelling and Analysis of Cyber-Physical Systems

¹Dominika LÍŠKOVÁ (1st year),
Supervisor: ²Anna JADLOVSKÁ

^{1,2}Dept. of Cybernetics and Artificial Intelligence, FEEI, Technical University of Košice, Slovak Republic

¹dominika.liskova@tuke.sk, ²anna.jadlovsk@tuke.sk

Abstract—This paper introduces cyber-physical systems (CPS), highlighting their key characteristics, applications, and challenges. The paper presents a modelling approach of hybrid systems considered as CPS, integrating it into a distributed control system (DCS) within the framework of DCAI FEEI TUKE. Moreover, DCS, which can also be considered as CPS with hybrid nature, is compared with DCS implemented at the ALICE experiment at CERN within the research field of the dissertation thesis using the advanced simulation techniques.

Keywords—Cyber-Physical System, Distributed Control System, Detector Control System, Hybrid System

I. INTRODUCTION

Cyber-Physical Systems (CPS) represent a convergence of computation, control, and communication, seamlessly integrating the physical and digital worlds. These systems play a critical role in a wide range of domains, including distributed systems, networked systems, robotics, manufacturing, smart grids, autonomous vehicles, and healthcare systems. The increasing complexity of CPS requires robust modelling, simulation, and control strategies to ensure their efficiency, safety, and reliability [1], [2].

This paper reviews CPS with a focus on modelling, simulation techniques, and their integration within distributed control systems (DCS) as it is the crucial part of my dissertation thesis named *Implementation of Hybrid System Models into the Distributed Control Systems Using Modern Methods and Effective Simulation Tools*. By examining existing methods and applications, we highlight key challenges and future directions to propose a methodology for hybrid systems modelling and their implementation into distributed control systems at the Centre of Modern Control Techniques and Industrial Informatics (CMCT&II) at the Department of Cybernetics and Artificial Intelligence (DCAI), as well as at the ALICE Experiment at CERN [3].

II. CYBER-PHYSICAL SYSTEMS

Cyber-Physical Systems have a fundamental role in Industry 4.0 [4], as they connect the computing and physical processes. CPS can be represented as a large amount of interconnected devices, embedded in the physical world [2]. An essential part of CPS are networks that ensure communication between computational processes as well as actuators and sensors, see Fig. 1. All operations of these physical and engineered systems must be monitored, controlled, and coordinated by the communication and computing core. Because of the CPS's interactions with the physical world, including humans, the behaviour of CPS must be safe, dependable, efficient, and in

real-time. To combine the discrete dynamics of computational processes with the continuous dynamics of physical processes, CPS must address the uncertainty caused by environmental noise, compensate for occasional process faults, and tolerate imperfections in time synchronisation [1].

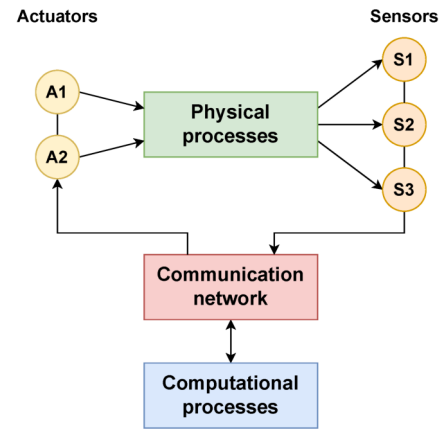


Fig. 1. Schematic representation of the concept of CPS

CPS share some common features with information and communications technology (ICT) systems, including embedded systems, networked control systems (NCSs), the Internet of Things (IoT), and the Industrial Internet. Although from the closed-loop systems perspective, the design, analysis and modelling of CPS differ from the standard ICT systems. The main differences can be found in system modelling, bridging the physical and computational world through sensing, the flexibility in the communication infrastructure, the correct control in real-time and the secure behaviour of the whole CPS [5].

CPS possess several defining characteristics that distinguish them from traditional computing and control systems [6]:

- (a) embedded computation and resource limitations - system resources are limited, but the software is implemented in every embedded or physical component,
- (b) scalability and network connectivity - CPS use wired and wireless network, which are considered distributed systems and provide high level of variability and scalability,
- (c) adaptive reconfiguration - size and complexity of CPS define their requirements for adaptive characteristics,
- (d) closed-loop control and high automation - advanced feedback control is often implemented in the CPS,
- (e) reliability and compliance - as CPS are spacious and

complex systems, it is necessary that the system is secure and reliable, which in some cases includes the certification.

In terms of architecture, CPS can utilise multiple structures, including layered architectures [7], distributed architectures that enable decentralised decision-making [3], service-oriented architectures (SOA) that facilitate modular and flexible system integration and event-driven architectures that respond dynamically to real-time stimuli [8]. The main focus will be on the distributed architectures of CPS, as it represents one of the key parts of my dissertation thesis in terms of modelling and simulation of individual layers and cross-layered relations.

III. HYBRID SYSTEMS

Hybrid systems (HS) are considered a crucial aspect of CPS. The behaviour of HS exhibits both continuous and discrete dynamics, making it suitable for modelling and controlling CPS within the framework of hybrid systems [9]. Subsystems with continuous dynamics are represented by non-linear differential equations with continuous input $u(t)$ and continuous output $y(t)$ of the system, while subsystems with discrete dynamics have discrete input $\sigma(t)$ and discrete output $w(t)$, which can be described by finite-state machines [10]. HS have found applications in various fields, including CPS applications, embedded systems, robotics, etc. There is also significant research interest within the domain of artificial intelligence.

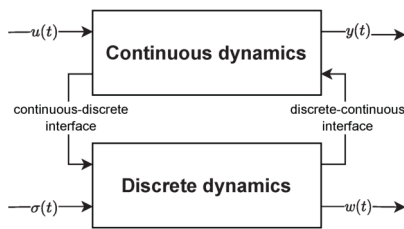


Fig. 2. Interconnection of the continuous and discrete dynamics of HS

The hybrid nature of the system is demonstrated in the structure of the HS, see Fig. 2, which shows the interactions between continuous and discrete dynamics. The continuous subsystem describes the evolution of the continuous state $x(t)$ over time, while the discrete subsystem shows the evolution of the discrete state q_i , see Fig. 3. Since the signals generated in both subsystems operate in distinct signal spaces, an interconnection between the two model components requires two interfaces, called the discrete-to-continuous interface or the continuous-to-discrete interface. The discrete-to-continuous interface, or injector, links discrete signals to continuous subsystems. The continuous-to-discrete interface, or event generator, transforms continuous signals into discrete events based on thresholds or switching surfaces. It defines the events by their name and time and is represented by guards and invariants in hybrid automata [11].

The hybrid character of the system is observable in many different applications, such as systems with more than one continuous dynamics with the discrete condition of switching between those dynamics (e.g. bouncing ball, mechatronic systems). The other approach is hybrid control of physical systems, when the control is done by discrete logic,

switching between local and global control algorithms, or discrete control for continuous system.

The modelling and control design of HS require a mathematical framework that captures both their continuous and discrete dynamics. Various modelling approaches exist, with the most commonly used representations including discrete hybrid automata (DHA), switched systems, piecewise linear/affine models (PWA), timed automata, and timed or hybrid Petri nets [11].

To describe the discrete dynamics of HS, the final-state machine (FSM) is widely used. An FSM represents an abstract mathematical model used to describe a system that can be in exactly one discrete state from a finite set of states at a given time. Providing inputs to the automaton triggers a transition between distinct states governed by a predefined transition function. Despite the fact that FSM is often used, it is insufficient to capture both discrete and continuous dynamics.

In the case of modelling CPS that combine discrete and continuous dynamics, which can be considered HS, it is essential to use a mathematical description that captures both dynamic subsystems. Suitable representation of the HS that captures both dynamics is the concept of hybrid automata (HA), providing a mathematical description of a system and a graphical representation of its behaviour [11]. HA can be defined as a collection $\mathbf{H} = (\mathbf{Q}, \mathbf{X}, \mathbf{f}, \mathbf{Init}, \mathbf{D}, \mathbf{E}, \mathbf{G}, \mathbf{R})$, where the individual elements are \mathbf{Q} - set of discrete states, \mathbf{X} - set of continuous state variables, \mathbf{f} - vector field describing the evolution of the continuous state vector, \mathbf{Init} - initial states of HA, \mathbf{D} - domain constraints, \mathbf{E} - set of boundaries to determine a combination of discrete states between which a transition is possible, \mathbf{G} - determines the boundary conditions of the switches, \mathbf{R} - determines the transition function, i.e. for each edge and the continuous state, the jump of the continuous state during the transition between discrete states [9], [12].

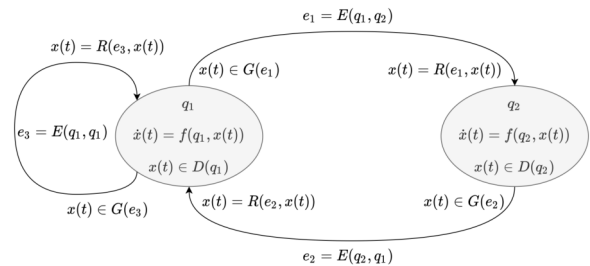


Fig. 3. Graphical representation of hybrid automaton

Fig. 3 presents a graphical representation of a hybrid automaton. This automaton has two discrete states, q_1 and q_2 , and its continuous dynamics vary depending on the discrete state. The automaton also has three edges, e_1, e_2, e_3 , that allow the system to transition between discrete states $q_1 \rightarrow q_2, q_2 \rightarrow q_1$, and $q_1 \rightarrow q_1$. When transitioning along edge e_1 , the continuous state of the system, $x(t)$, reaches a value within the designated region of the state space defined by the function $G(e_1)$. Similarly, when transitioning to the discrete state q_2 , a jump occurs in the continuous state [12].

The concepts described in this section will be further elaborated on in a subsequent section of the paper, which will provide an example of a distributed control system (DCS) within the context of a CPS.

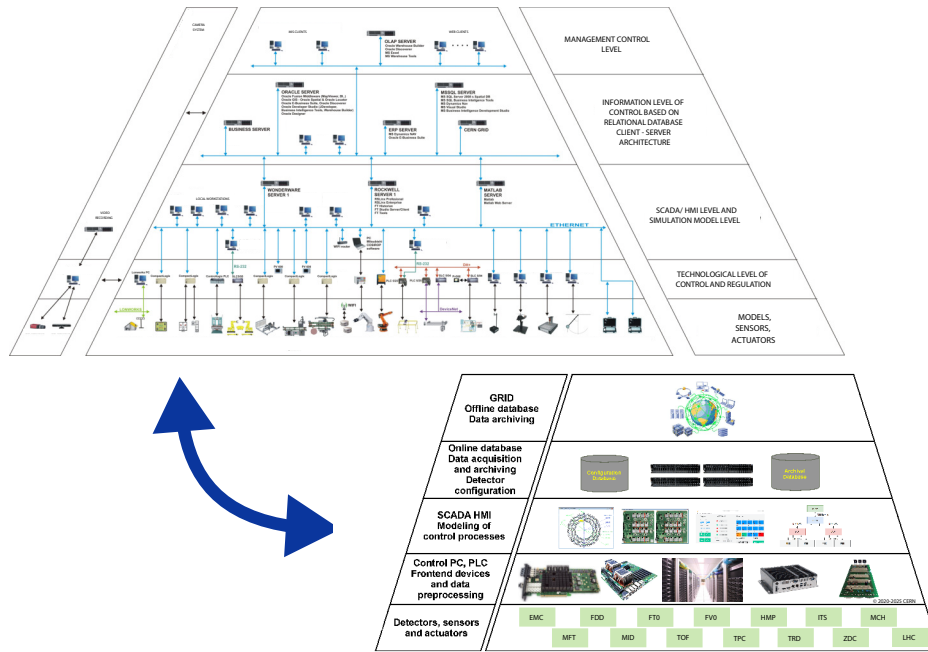


Fig. 4. Architecture of DCS concept at CMCT&II - DCAI, Detector Control System at the ALICE Experiment at CERN

IV. DISTRIBUTED CONTROL SYSTEMS

Distributed Control Systems (DCS) serve as an apt illustration of CPS, as they exhibit numerous characteristics that are commonly found in CPS. DCS is a concept of Network Control Systems (NCSs) frequently used in industrial applications, where the distribution of resources throughout the system offers substantial advantages [13]. The DCS are characterised by a multi-level architecture, where the individual control levels are interconnected via various communication networks, as outlined in the IEC 61499 standard [14].

The DCS is a computer-based control system designed to manage complex processes without the need for a central control node. Individual control and coordination processes are distributed throughout the system, bringing them closer to the controlled process. This characteristic enhances the reliability of the system and, at the same time, reduces initial implementation costs. In addition, supervisory systems monitor and supervise individual subsystems, providing a comprehensive overview of the state of the controlled processes. The DCS architecture is typically categorised into several control/functional levels, as specified in IEC 62264 (ANSI/ISA-95). Variations in level nomenclature and numbering may occur in exact implementations [3], [15], [16].

The example of hierarchical structure and nomenclature employed in the DCS architecture at CMCT&II, DCAI and in the Detector Control System at the ALICE Experiment (ALICE-DCS) at CERN. Firstly, the DCS at CMCT&II is presented by multiple subsystems, each of which can be considered an independent CPS [17]. Together, these subsystems create a DCS representing a complex CPS divided into five hierarchical levels, shown in Fig. 4. The research platform is represented by physical systems such as mechatronic systems modelled as CPS, which can be implemented into the DCS across all levels.

Secondly, the structure of the Detector Control System (ALICE-DCS) of the ALICE experiment (A Large Ion Col-

lider Experiment) at the Large Hadron Collider (LHC) at the European Organization for Nuclear Research (CERN) is presented. The ALICE experiment is studying the physics of strongly interacting matter and the quark-gluon plasma to help understand the formation of the early universe i.e. conditions shortly after the Big Bang, when quarks and gluons could move freely. These conditions are created in the LHC by heavy-ion collisions, which are captured by the ALICE experiment. The ALICE-DCS ensures stable and safe operation of the detectors while ensuring the tasks of control, monitoring, and data acquisition from the detector's electronic [3], [18].

The ALICE-DCS is similar to the DCS at the CMCT&II, DCAI. The author of the paper is a member of the research team which is currently involved in the basic research project entitled *ALICE Experiment at the LHC at CERN: Study of Strongly Interacting Matter in Extreme Conditions* (ALICE-TUKE). The ALICE-DCS is modelled as a HS and is used in the control and diagnostics of individual sub-detectors of the ALICE experiment. The infrastructure of ALICE-DCS (Fig. 4) is defined by 5 levels [19]:

- level of detectors, sensors and actuators,
- level of technological control of sub-detectors at lower level and frontend devices,
- SCADA/HMI level including the visualisation and control managed by WINCC OA, which contains the virtual representation of the system as FSM,
- the information level of control represented by databases containing data from lower level electronics as well as from the sub-detectors,
- management level of ALICE-DCS control consists of a worldwide network of GRID computing centres for experiments implemented within CERN and an archival database connected to the *informational system DARMA* developed by the research team of the project ALICE-TUKE.

The shared characteristics of both structures present the

opportunity to develop a methodology for the analysis, modelling, and simulation of distributed systems within the context of CPS. Within the CMCT&II domain, the main focus is on the modelling and analysis of hybrid systems using effective simulation tools such as MATLAB/Simulink, which will form the main part of the dissertation thesis. Many approaches can be considered within the DCS at CMCT&II, e.g. applications involving mobile robots and other types of mechatronic systems. To illustrate this example, a modular robotic platform named ModBot is used [20]. Different subsystems of mobile robot can be analysed and classified into layers of the DCS structure, given the sensors and actuators at the lowest level, the microcontroller at the level of technological regulation, the third level is associated with the supervisory computer, which sends the data to the database situated at the fourth level of the DCS. In addition to the implementation of a single mobile robot into a DCS structure, applications such as robotic football are also a suitable example for the practical use of CPS modelling, simulation, and control methods, since the robotic football application has the physical subsystem, i.e. sensors and actuators of mobile robots, computational subsystem such as supervisory computer or microcontroller, and a communication network connecting the physical and computational subsystem.

Extending this concept further, another example of CPS implementation is seen in the ALICE-DCS focus area. Considering an increase in real-time data processing and an unbearable load on the Supervisory Control and Data Acquisition (SCADA) system within the ALICE-DCS, the software layer named the ALICE Low-Level Front-End Device (ALFRED) was implemented. ALFRED ensures data processing before being forwarded to the SCADA system while also creating an abstraction layer for detector electronics from the point of view of the SCADA system. The ALFRED system is characterised by a distributed architecture, in which individual components can be classified into distinct levels of the DCS architecture. The lowest level of the ALFRED system consists of detector electronics, including the Readout Unit and Power Board units. These units communicate with higher-level applications via optical lines or CAN bus interfaces, translating messages into the DIM protocol format for communication with FRED applications, which abstracts detector electronics for SCADA/HMI system, unifying communication and reducing computationally intensive data processing [21].

V. CONCLUSION

This paper provides an overview of cyber-physical systems, their characteristics, and specific challenges they present. The hybrid nature of these systems requires advanced modelling and simulation techniques to ensure efficiency and reliability. The methodology that will be developed when solving open problems in context of modelling, simulation and implementation of HS in the DCS within the dissertation thesis will be generalised and used to model and implement different types of HS from the ALICE-DCS framework. The author is also a member of ALICE Collaboration in CERN, which means that the contribution to the ALICE-DCS presents part of the topics of the dissertation thesis.

ACKNOWLEDGEMENT

This work has been supported by the project ALICE experiment at the CERN LHC: The study of strongly interacting

matter under extreme conditions (ALICE TUKE 0410 / 2022).

REFERENCES

- [1] R. R. Rajkumar, I. Lee, L. Sha, and J. Stankovic, "Cyber-physical systems: the next computing revolution," in *Proceedings of the 47th Design Automation Conference*, ser. DAC '10. New York, NY, USA: Association for Computing Machinery, 2010, p. 731–736. [Online]. Available: <https://doi.org/10.1145/1837274.1837461>
- [2] Y. Eslami, C. Franciosi, S. Ashouri, and M. Lezoche, "A review and analysis of the characteristics of cyber-physical systems in industry 4.0," *SN Computer Science*, vol. 4, no. 6, p. 825, 2023. [Online]. Available: <https://doi.org/10.1007/s42979-023-02268-0>
- [3] M. Tkáčik, J. Jádlovský, S. Jádlovská, A. Jádlovská, and T. Tkáčik, "Modeling and analysis of distributed control systems: Proposal of a methodology," *Processes*, vol. 12, no. 1, 2024. [Online]. Available: <https://doi.org/10.3390/pr12010005>
- [4] Plattform Industrie 4.0, "The fourth industrial revolution and the term "industry 5.0" – a critical perspective," 2024, accessed: 2025-02-25. [Online]. Available: https://www.plattform-i40.de/IP/Redaktion/EN/News/Actual/2024/04_Industry50.html
- [5] X. Guan, B. Yang, C. Chen, W. Dai, and Y. Wang, "A comprehensive overview of cyber-physical systems: from perspective of feedback system," *IEEE/CAA Journal of Automatica Sinica*, vol. 3, no. 1, pp. 1–14, 2016. [Online]. Available: <https://doi.org/10.1109/JAS.2016.7373757>
- [6] J. Wan, H. Yan, H. Suo, and F. Li, "Advances in cyber-physical systems research," *TIIIS*, vol. 5, pp. 1891–1908, 01 2011.
- [7] A. Al-Ali, R. Gupta, and A. Al Nabulsi, "Cyber physical systems role in manufacturing technologies," vol. 1957, 04 2018, p. 050007.
- [8] Y. Liu, Y. Peng, B. Wang, S. Yao, and Z. Liu, "Review on cyber-physical systems," *IEEE/CAA Journal of Automatica Sinica*, vol. 4, no. 1, pp. 27–40, 2017.
- [9] D. Vošček, A. Jádlovská, and D. Grigl'ák, "Modelling, analysis and control design of hybrid dynamical systems," *Journal of Electrical Engineering*, vol. 70, no. 3, pp. 176–186, 2019. [Online]. Available: <https://doi.org/10.2478/jee-2019-0026>
- [10] Y. Yang and X. Zhou, "Cyber-physical systems modeling based on extended hybrid automata," in *2013 International Conference on Computational and Information Sciences*, 2013, pp. 1871–1874.
- [11] J. Lunze and F. Lamnabhi Lagarrigue, *Handbook of Hybrid Systems Control: Theory, Tools, Applications*. Cambridge University Press, 2009.
- [12] A. van der Schaft and J. Schumacher, *An Introduction to Hybrid Dynamical Systems*, 2nd ed., 2024.
- [13] X.-M. Zhang, Q.-L. Han, X. Ge, D. Ding, L. Ding, D. Yue, and C. Peng, "Networked control systems: a survey of trends and techniques," *IEEE/CAA Journal of Automatica Sinica*, vol. 7, no. 1, pp. 1–17, 2020.
- [14] E. Monroy Cruz, L. R. García Carrillo, and L. A. Cruz Salazar, "Structuring cyber-physical systems for distributed control with iec 61499 standard," *IEEE Latin America Transactions*, vol. 21, no. 2, pp. 251–259, 2023. [Online]. Available: <https://doi.org/10.1109/TLA.2023.10015217>
- [15] L. Apilioğulları, "Digital transformation in project-based manufacturing: Developing the isa-95 model for vertical integration," *International Journal of Production Economics*, vol. 245, p. 108413, 2022. [Online]. Available: <https://doi.org/10.1016/j.ijpe.2022.108413>
- [16] E. M. Martínez, P. Ponce, I. Macias, and A. Molina, "Automation pyramid as constructor for a complete digital twin, case study: A didactic manufacturing system," *Sensors*, vol. 21, no. 14, 2021. [Online]. Available: <https://doi.org/10.3390/s21144656>
- [17] A. Jádlovská, S. Jádlovská, and D. Vošček, "Cyber-physical system implementation into the distributed control system," *IFAC-PapersOnLine*, vol. 49, no. 25, pp. 31–36, 2016, 14th IFAC Conference on Programmable Devices and Embedded Systems PDES 2016. [Online]. Available: <https://doi.org/10.1016/j.ifacol.2016.12.006>
- [18] S. Chapeland, "Commissioning of the alice readout software for lhc run 3," *EPJ Web of Conferences*, vol. 295, 05 2024. [Online]. Available: <https://doi.org/10.1051/epjconf/202429502007>
- [19] P. Chochula, L. Jiriden, A. Augustinus, G. de Cataldo, C. Torcato, P. Rosinsky, L. Wallet, M. Boccioni, and L. Cardoso, "The alice detector control system," *IEEE Transactions on Nuclear Science*, vol. 57, no. 2, pp. 472–478, 2010. [Online]. Available: <https://doi.org/10.1109/TNS.2009.2039944>
- [20] M. Tkáčik, A. Březina, and S. Jádlovská, "Design of a prototype for a modular mobile robotic platform," *IFAC-PapersOnLine*, vol. 52, no. 27, pp. 192–197, 2019.
- [21] M. Tkáčik, J. Jádlovský, S. Jádlovská, L. Koska, A. Jádlovská, and M. Donadoni, "Fred—flexible framework for frontend electronics control in alice experiment at cern," *Processes*, vol. 8, no. 5, 2020.

Achieving Maximum Efficiency: Critical Factors for Optimizing Phase-Shifted Full-Bridge (PSFB) Converter

¹Daniel Gordan (2nd year)
Supervisor: ²Marek Pástor

^{1,2}Dept. of Electrical Engineering and Mechatronics, FEI TU of Košice, Slovak Republic

¹daniel.gordan@tuke.sk, ²marek.pastor@tuke.sk

Abstract— The paper describes the key factors affecting the efficiency of phase-shifted full-bridge (PSFB) converter and the resulting limitations in increasing the switching frequency. Some of the mentioned factors are also implied in the converter, the efficiency of which is measured under laboratory conditions.

Keywords— dc-dc converter, efficiency, phase shifted full bridge, PSFB, GaN

I. INTRODUCTION

PSFB converter has been known for decades and has found its application in various fields of human activity. The major advantages of the converter are a large range of input and output voltages and currents, simple regulation on the primary side due to the phase shift change and low parts count. On the other side, the disadvantage is the problem with the circulating current and the occurrence of overvoltage on the rectifier components. Transistors based on GaN and SiC technology have caused a significant improvement in PSFB converter parameters, pushed the limits of switching frequency, reduced switching and conduction losses, and improved power density [1]. The development of microcontrollers has made it possible to apply more complex methods of converter control, adaptively changing the times and delays of PWM signals, instead of the classical solution where this was not possible [2].

The paper describes the most important steps to be followed in designing a PSFB converter, some of which are implied in a laboratory model whose efficiency is measured using a power analyzer.

II. KEY FACTORS OF PSFB CONVERTER DESIGN

A. Select a suitable synchronous rectifier

The inverter of the PSFB converter is the same, but in the case of rectifiers, three types can generally be used:

- full bridge rectifier (FB) [3],
- center-tapped rectifier (CT) [2],
- current doubler rectifier (CD) [4], Fig. 1.

The differences between the rectifiers are shown in Tab. 1 [5]. The full bridge is best for higher output voltages because it produces half the over voltage compared to CT and CD rectifiers.

TABLE I
THE DIFFERENCE BETWEEN RECTIFIERS

Rec. type	Num. of sec. windings	Num. of rec. components	Num. of o. inductors
Full bridge	1	4	1
Center tapped	2	2	1
Current doubler	1	2	2

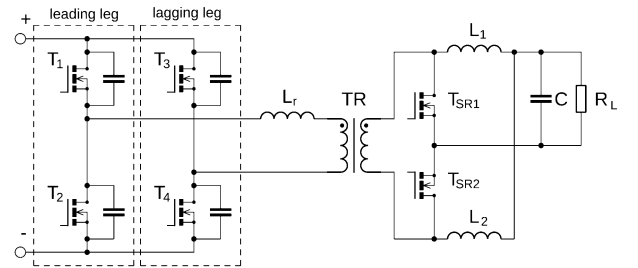


Fig. 1. The schematic of the PSFB converter with current doubler rectifier

Center-tapped rectifiers are disadvantageous in that they require a transformer with two windings. However, only two rectifier components and one filter inductance is required.

Current doubler combines the advantage of two rectifier components and a simpler transformer but requires additional filtering inductance. The extra benefit is that heat is spread more evenly in the CD because half the current flows through the secondary winding of the transformer. Also, because of the two inductances, the current in the filter inductances is half that of CT and FB. So, in general, at higher voltages, it's better to use FB, and at higher currents, CD or CT.

B. Select suitable semiconductors for inverter and rectifier

Achieving high efficiency is greatly affected by achieving ZVS of the primary transistors. In order to achieve ZVS, it is necessary that there is more capacitive energy than inductive energy in the resonance circuit:

$$E_L \geq E_C \quad (1)$$

Where the capacitive energy E_C is formed by the output capacitance of the primary transistors C_{oss} and the parasitic capacitance of the transformer. The inductive energy is different for the leading and lagging leg of the inverter because different currents flow through the transistors when the transistor is turned off, i.e. the resonant event that affects the zero-voltage switching (ZVS). Inductive energy is formed by the transformer leakage inductance and the output filter inductance, but it is different for the two legs of the inverter

because different currents flow through the leading and lagging leg at the time of achieving ZVS. As the frequency increases, the inductive energy decreases (smaller transformer), thus, to achieve ZVS and hence higher efficiency it is necessary to reduce the capacitive energy in the circuit, i.e. Coss. Transistors based on GaN and SiC technology achieve up to 10 times better ratio between output capacitance and series resistance compared to Si mosfet and thus are ideal for use in PSFB inverter [6].

When selecting rectifier transistors, it is mainly important that they should have low series resistance to minimize conduction losses.

C. Implement adaptive control using DSP

The ideal delay time (t_d) affects the ZVS and is different for the two inverter legs (different current=different inductive energy) and is dependent on the output current. A shorter t_d can lead to ZVS loss, a longer time to unnecessary prolongation of the conductivity of the built-in diode, thus increasing conduction losses. The control should be able to set different t_d for both inverter legs and change it depending on the output power.

In the case of a rectifier, the transistor should turn on shortly after its built-in diode starts conducting, to achieve ZVS. Because changing the output current changes the ideal switch-on time, it is necessary to adaptively adjust this time. Further, there are three options for switching the rectifier transistors, and these modes need to be varied depending on the load current, more in the literature [4].

D. Use an additional network to reduce overvoltage

In the rectifier, overvoltage is caused by the resonance between the output capacitance of the rectifier transistors and the leakage inductance of the transformer. This overvoltage will cause the need to use transistors at higher voltages, thus indirectly increasing the conduction losses. By using an additional snubber [6], it is possible to reduce the overvoltage and thus the conduction losses.

E. Use suitable magnetic circuits

If high efficiency is required, magnetic circuits also need to achieve high efficiency, especially the transformer [7].

III. LABORATORY MEASUREMENTS

Based on the recommendations given in the previous chapter (except point D) and the above literature, a prototype converter was built, the schematic is shown in Fig. 1, parameters are shown in Tab. 2. The photo of the converter is in Fig. 2. Efficiency was measured with a LMG500 power analyzer and is shown in Fig. 3.

TABLE II
PARAMETERS OF PSFB WITH CURRENT DOUBLER

Parameter	Value
Supply voltage V_{IN}	390 V
Output current I_O	25 A
Output voltage V_O	24 V
Output power P_2	600 W
Switching frequency f_s	100 kHz
Inverter transistors	GS-065-011-2
Rectifier transistors	IPTG039N15NM5

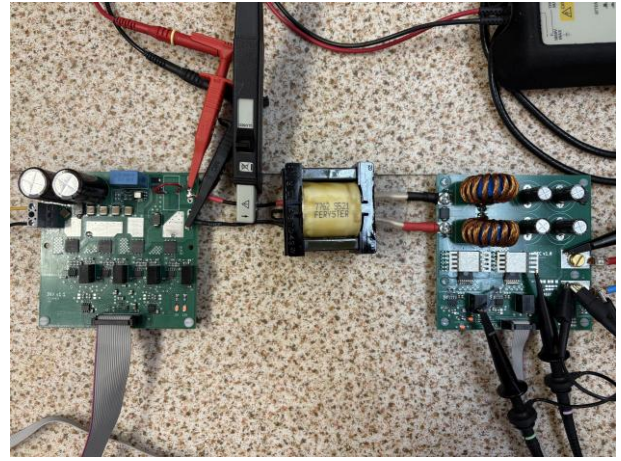


Fig. 2. Photo of PSFB converter, from left to right, inverter, transformer, rectifier

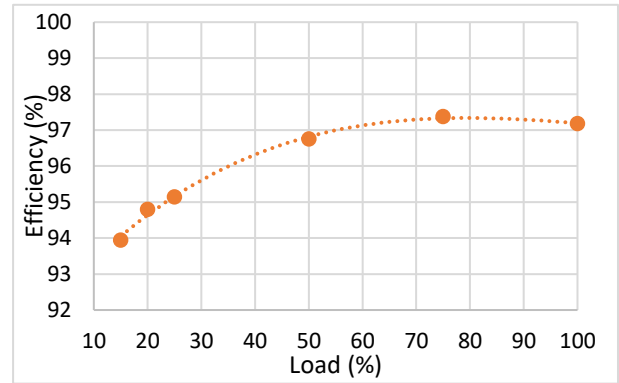


Fig. 3. Measured efficiency of the PSFB converter

IV. CONCLUSION

The paper describes the conditions for achieving high efficiency in a PSFB converter. As a result, relatively high efficiency is achieved in the laboratory conditions. The next step is to use theoretical and practical experience to build an converter operating at a frequency of at least 500 kHz, which will increase the power density many times over, due to the reduction of magnetic circuits.

ACKNOWLEDGMENT

This work was supported by the Scientific Grant Agency of the Ministry of Education of the Slovak Republic under the project APVV-23-0521 and VEGA 1/0584/24.

REFERENCES

- [1] M. Beheshti, "Wide-bandgap semiconductors: Performance and benefits of gan versus sic," in Analog Design Journal, 2020, Texas Instruments.
- [2] T. Instruments, "Phase-shifted full bridge dc/dc power converter design guide," Application note, Texas Instruments, 2014.
- [3] S. Chothe, R. T. Ugale, and A. Gambhir, "Design and modeling of phase shift-ed full bridge dc-dc converter with zvs," in 2021 National Power Electronics Conference (NPEC), 2021, pp. 01–06.
- [4] A.-R. Sam, "Design of phase shifted full-bridge converter with current doubler rectifier," Design note, Infineon, 2013.
- [5] S.-Y. Yu, B. Lough, R. Yin, and Q. Ye, "Phase-shifted full-bridge converter fundamentals," in Power Supply Design Seminar. Dallas, Texas, USA: Texas Istruments, 2024.
- [6] M. Heintze and I. Stefan Butzmann, "A gan 500 khz high current active clamp phase-shifted full-bridge converter with zero-voltage switching over the entire line and load range," in 2018 20th European Conference on Power Electronics and Applications (EPE'18 ECCE Europe), 2018, pp. P.1–P.9.
- [7] D. Lloyd, "Designing planar magnetics," Application note, Texas Instruments.

Artificial Intelligence in Routing for Mobile Multi-Hop Networks in 6G: A Comprehensive Review

¹Jozef Badár (*1st year*),
Supervisor: ²Ján Papaj

^{1,2}Dept. of Electronics and Multimedia Communications, FEI, Technical University of Košice, Slovak Republic

¹jozef.badar@tuke.sk, ²jan.papaj@tuke.sk

Abstract—This paper provides a critical analysis of the current state of research on the application of artificial intelligence (AI) in routing protocols for mobile ad-hoc networks (MANET) within the context of 6G network technologies. Through a systematic review of the existing literature, we identify key resolved and persisting challenges and formulate prospective research directions aimed at optimizing routing efficiency and enhancing network robustness in dynamic environments.

Keywords—AI routing, MANET, 6G networks, swarm intelligence, reinforcement learning

I. INTRODUCTION

The emergence of 6G networks brings significant challenges and opportunities in wireless communication. One of the key aspects of these networks is efficient routing in mobile multi-hop networks (MANET), where nodes must dynamically establish multi-hop communication paths. Traditional routing protocols, such as AODV and DYMO, face challenges related to increasing complexity and the growing demands for low latency, energy efficiency, and adaptability in next-generation networks. Recent research explores the integration of artificial intelligence (AI) into MANET routing to enhance decision-making, optimize network performance, and improve resilience in dynamic environments.

II. LITERATURE REVIEW AND ANALYSIS

A. Directions in MANET in the context of 5G and 6G

The integration of artificial intelligence (AI) into routing protocols for mobile ad-hoc networks (MANET) represents a significant research trend, particularly in the context of increasing complexity in 6G network environments. MANETs are characterized by high topology dynamics and node mobility, which impose specific requirements on routing protocols. Traditional approaches, such as AODV (Ad-hoc On-Demand Distance Vector), DSR (Dynamic Source Routing), and DSDV (Destination-Sequenced Distance Vector), have been extensively analyzed in terms of their performance characteristics under various conditions [1], [2], [3]. The incorporation of AI techniques into these protocols enables improved decision-making mechanisms, enhances the efficient use of network resources, and increases adaptability to constantly changing network conditions.

B. AI-based and hybrid routing approaches

The integration of artificial intelligence (AI) into MANET routing enables the development of advanced mechanisms that leverage machine learning for node mobility modeling and predictive optimization of routing paths. For instance, the use of swarm intelligence (SI), genetic algorithms (GA), and reinforcement learning (RL) has been identified as a promising method to enhance the efficiency of routing decisions in dynamic networks [4], [5]. These techniques allow routing algorithms to respond more effectively to constantly changing network conditions, thereby improving packet delivery ratio, throughput, and latency [1], [6].

Although purely AI-based approaches provide a high level of adaptability and accuracy, their computational complexity and the need for extensive training data present a significant challenge. Therefore, in recent years, there has been increasing interest in hybrid AI approaches that combine artificial intelligence with heuristic methods, such as traditional routing protocols or biologically inspired algorithms. For example, the combination of swarm intelligence (ACO, PSO) with adaptive routing strategies leverages the collective behavior of agents to optimize paths, while adaptive mechanisms help prevent network congestion [7].

Research has shown that hybrid approaches are particularly effective in high-mobility environments, where traditional AI models may struggle with prediction accuracy due to rapid changes in network topology. For instance, adaptive protocols can combine learning from experience with traditional routing rules, achieving a better trade-off between routing accuracy and computational efficiency [8], [9].

Hybrid algorithms combining ACO and OLSR have gained particular attention. This model utilizes ACO to initiate routing tables, where pheromone values are updated based on the quality of discovered paths, while OLSR provides stable proactive routing using Multi Point Relay (MPR). Simulations have shown that such a hybrid approach can improve network stability and reduce overhead compared to purely AI-based solutions [10].

Overall, hybrid AI solutions represent a promising alternative to purely AI-based routing models, as they combine the robustness of heuristic algorithms with the adaptability and predictive capabilities of artificial intelligence.

C. Challenges and limits of AI in MANET

Although AI-based approaches demonstrate significant advantages, their application in MANET also presents several challenges:

- Computational complexity: Training and real-time inference of AI models require substantial computational resources, which can be limiting for nodes with constrained processing power and battery capacity [11].
- Dynamic changes in network topology: While AI models enable better adaptability, the high variability in MANET can lead to inaccurate predictions and suboptimal routing decisions [12].
- Security concerns: AI models may be vulnerable to adversarial attacks that can manipulate routing predictions and compromise network integrity [11].
- Dependence on historical data: Machine learning models are trained on historical data, which may cause issues when dealing with new, previously unseen scenarios [12].

D. Comparison of AI-based Routing Protocols with Traditional Approaches

1) *Traditional Routing Protocols in MANET and Their Limitations:* Traditional routing protocols, such as AODV, DSR, and DSDV, were developed to enable efficient communication in MANET without centralized infrastructure. These protocols employ reactive (AODV, DSR) or proactive (DSDV) routing strategies to establish and maintain paths between nodes [13], [1].

Their main advantages include:

- Simplicity of implementation and low computational requirements.
- Efficiency in small to medium-sized networks with stable topology.

Despite these advantages, traditional protocols have significant limitations that become critical in dynamic MANET environments, especially in the context of 5G and 6G networks:

- High routing overhead – Frequent message forwarding for route maintenance increases network load [1], [2].
- Lack of adaptability – These protocols lack predictive capabilities and respond only to the current network state, leading to frequent connection disruptions [3].
- Weak security – They are not equipped with attack detection mechanisms, making them vulnerable to black hole or wormhole attacks [14].
- Limited energy efficiency – They are not optimized for nodes with constrained energy resources, leading to faster battery depletion [2].

2) *Benefits of AI-based routing protocols:* The deployment of artificial intelligence (AI) in MANET addresses many limitations of traditional protocols. AI enables dynamic decision-making based on the analysis of both historical and real-time network data [15]. The key advantages include:

- 1) Dynamic route optimization – Reinforcement learning (RL) and machine learning (ML) algorithms can predict optimal routes, reducing the number of connection disruptions [10].
- 2) Reduction of routing overhead – AI models can predict and adjust routes without frequent update broadcasts, thereby reducing network overhead [6].

- 3) Enhanced security – AI enables anomaly detection and identification of potential attacks, improving network resilience against black hole attacks and rogue nodes [14].

- 4) Energy efficiency – AI can optimize routing while considering energy consumption, extending the lifespan of nodes with limited battery capacity [2].

3) *Comparison of AI-based and traditional routing protocols:* Although AI-based approaches offer significant improvements, they also face major challenges, particularly:

- High computational complexity – AI models, especially deep learning (DL) and RL, require substantial computational resources, which can be problematic for nodes with limited processing power [11].
- Dependence on historical data – If AI models are not properly trained, they may produce inaccurate predictions, leading to suboptimal routing [16].
- Security risks – AI models are vulnerable to adversarial attacks that can manipulate their predictions and degrade routing performance [17].

Table I provides an overview of the key differences between AI and traditional protocols.

Based on the conducted analysis, it can be concluded that individual AI-based approaches have specific advantages and limitations in the context of mobile multi-hop networks. While reinforcement learning and deep neural networks offer adaptive and accurate routing, their computational complexity can be a limiting factor. Conversely, heuristic algorithms such as ACO and PSO enable efficient route optimization with lower computational requirements but may be sensitive to improper parameter configuration.

The combination of these methods in hybrid models represents a promising solution that integrates the robustness of heuristic algorithms with the accuracy and adaptability of machine learning models. This approach enables routing with higher reliability, efficiency, and scalability, thereby improving the overall performance parameters of MANET in the dynamic conditions of future 6G networks.

E. Challenges and limitations of AI-based routing in MANET

Although AI-based routing in MANET offers significant advantages, its application in real-world scenarios faces several fundamental challenges. These challenges can be categorized into four main areas: computational complexity, adaptability to dynamic networks, security threats, and model reliability. Each of these factors influences the practical implementation of AI-based routing in 5G/6G networks and must be addressed with effective optimization strategies.

F. Computational Complexity of AI Algorithms

AI-based protocols, particularly those utilizing machine learning (ML), reinforcement learning (RL), or deep neural networks (DL), require high computational power for data analysis and optimal route prediction. This factor is especially critical in nodes with limited computational resources, such as mobile devices, sensors, and drones [11] [16].

Main challenges:

- Real-time model inference – RL algorithms must continuously update their decisions based on changing network conditions, increasing the load on the processor and memory [11].

TABLE I
COMPARISON OF SELECTED AI-BASED AND TRADITIONAL ROUTING ALGORITHMS IN MANET [10], [15], [1]

Algorithm	Approach	Advantages	Disadvantages
AODV	Reactive routing	Low routing overhead in static conditions	Increased latency during frequent topology changes
DSR	Source routing	Efficient in small networks, low overhead	Increased control packet overhead in large networks
DSDV	Proactive routing	Stable and predictable routes	High overhead in frequent topology changes
RL	Adaptive decision-making	Improved packet delivery ratio	High computational costs
Neural Networks	Route prediction	Efficient routing	Requires extensive training data
ACO	Pheromone-based optimization	Suitable for dynamic networks	Possible network congestion
PSO	Swarm-based path selection	Low overhead	High sensitivity to parameters
Hybrid models	Combination of AI techniques	High routing accuracy	Complex implementation

- Training and prediction at the network edge – AI models are often trained centrally and then deployed to distributed nodes, causing adaptation issues in new conditions [16].
- Energy consumption – Computationally intensive AI algorithms reduce battery life, which is a significant problem in scenarios where nodes cannot be regularly recharged or have their batteries replaced [2].

Possible Solutions:

- Using lightweight ML models – Reducing model complexity and employing optimized techniques such as quantized neural networks can lower computational overhead.
- Federated learning – Instead of sending raw data to a central node, models are trained locally on nodes and only updated parameters are synchronized, reducing energy consumption and communication costs.

1) *Adaptability of AI models to dynamic networks:* Frequent changes in MANET topology impose high demands on routing algorithms. Traditional AI models rely on historical data, which can lead to incorrect predictions in unforeseen situations. Main challenges:

- Unanticipated changes in network topology – AI models often fail to respond quickly enough to drastic changes in MANET, such as sudden node failures or the emergence of new paths [3].
- Model generalization – Traditional ML models struggle to adapt to new, unseen scenarios, leading to suboptimal routing [16].

Possible Solutions:

- Online learning (continual learning) – Allows models to adapt in real time instead of relying on pre-trained models.
- Combining AI with heuristic methods (hybrid approaches) – The integration of ACO and RL enables better adaptation to network dynamics without requiring constant retraining of models [10].

2) *Security risks of AI-based routing:* AI models are susceptible to adversarial attacks, where an attacker manipulates input data to cause the AI algorithm to make incorrect routing decisions. This vulnerability poses a serious security risk in critical MANET applications, such as military missions or rescue operations. Main Security Threats:

- Adversarial attacks on ML models – An attacker can introduce subtle changes to routing metrics, leading to incorrect route predictions [17].
- Manipulation of RL rewards – An attacker can influence feedback in RL algorithms, training the system to adopt inefficient or even malicious routing strategies [18].

Possible Solutions:

- Adversarial training – AI models can be trained to detect and resist manipulative inputs.
- Hybrid security architecture – Combining AI with traditional security mechanisms, such as intrusion detection systems (IDS), can enhance network protection.

3) *Reliability of AI-based protocols in practice:* Although AI offers predictive routing and performance optimization, its deployment in real-world MANET environments raises questions about reliability and stability [11]. Main Challenges:

- Failure of models in critical situations – If an AI model is not properly trained on rare but critical scenarios, it may fail or behave unpredictably in certain situations [19].
- Catastrophic forgetting problem – DQN and RL models tend to forget old knowledge when learning new strategies, which can lead to routing instability [11].

Possible Solutions:

- Utilization of meta-learning – Techniques such as MAML (Model-Agnostic Meta-Learning) enable rapid adaptation to new conditions without losing previous knowledge.
- Enhancing the robustness of RL algorithms – Combining dual learning and knowledge transfer between RL agents can improve the stability of routing decisions.

III. IDENTIFICATION OF PROBLEMS AND DIRECTIONS FOR FUTURE RESEARCH

A. Solved and unsolved problems

AI-based routing in MANET has brought significant improvements in efficiency, adaptability, and network parameter optimization. Despite these advancements, key challenges remain that limit its widespread deployment:

- Computational complexity and scalability – Most advanced AI models require high computational capacity, which poses a challenge for resource-constrained nodes. Effective deployment requires optimizing computational processes and distributing the computational load among nodes [20].
- Energy efficiency – AI algorithms can predict optimal routing paths with lower energy consumption; however, their real-time implementation can paradoxically increase energy demands. Therefore, more efficient models must be developed to minimize computational overhead while maintaining reliable routing [20].
- Security and resilience against adversarial attacks – AI-driven routing is vulnerable to adversarial manipulations that can affect decision-making mechanisms. Malicious inputs can lead to incorrect routing decisions or overload specific nodes, disrupting network stability. Robust defense mechanisms are therefore essential to protect AI models from such attacks [21].

- Dependence on available data – Machine learning models used for routing are trained on historical data, which may limit their ability to respond to unexpected changes in network topology. Poor generalization leads to increased latency and suboptimal decision-making, particularly in unpredictable MANET scenarios [22].

B. Future research directions

To overcome the aforementioned challenges, future research in AI-driven routing for MANET can focus on the following key directions:

- Development of computationally efficient AI models – Optimization of neural network models for resource-constrained environments by utilizing techniques such as quantization, model pruning, or low-complexity learning methods. The goal is to achieve high performance while minimizing computational and energy consumption [23].
- Federated learning for distributed routing – A decentralized approach to training AI models, allowing nodes to collaboratively learn models without the need for centralized data sharing. This method can ensure higher levels of privacy protection and data security [24].
- Integration of blockchain technologies – Leveraging blockchain to enhance transparency and trustworthiness in routing decisions. Distributed consensus mechanisms can provide protection against malicious tampering with routing tables and improve overall network robustness [25].
- Dynamic real-time adaptation strategies – Applying reinforcement learning (RL) and meta-learning to continuously adjust routing strategies based on real-time network conditions. The goal is to ensure routing protocol flexibility and network performance optimization in dynamic environments [26].
- Hybrid solutions combining heuristic and AI methods – Combining AI with classical heuristic algorithms, such as ACO and PSO, can improve routing adaptability in dynamic networks while maintaining low computational complexity. Hybrid solutions can leverage AI's predictive capabilities alongside the efficiency of biologically inspired algorithms for route optimization [8].

The implementation of these research directions can significantly enhance the efficiency, security, and scalability of AI-driven routing in MANET, opening new possibilities for its deployment in future 6G networks.

IV. CONCLUSION

In conclusion, the application of artificial intelligence in MANET routing represents a promising approach to enhancing network performance and robustness. By leveraging AI techniques, researchers can develop adaptive, efficient, and secure routing protocols that are better suited to the dynamic nature of mobile ad-hoc networks. As the demand for robust communication systems continues to grow, particularly in the context of 6G, integrating AI into routing protocols will be crucial in addressing the challenges posed by mobile and dynamic environments.

ACKNOWLEDGMENT

This research was funded by the Slovak Research and Development Agency, research grant no. APVV-17-0208 and VEGA 1/0260/23.

REFERENCES

- [1] J. Kumar, "Performance analysis of routing protocol in mobile ad-hoc networks," *International Journal of Advanced Research in Computer Science*, vol. 14, pp. 33–38, 2023.
- [2] "Comparison of aodv, dsr and dsdv on different simulators for qos parameters," *International Journal of Science and Research (IJSR)*, vol. 6, pp. 1029–1033, 2017.
- [3] B. C. Mummadiisetty, A. Puri, and S. Latifi, "Performance assessment of manet routing protocols," *International Journal of Communications, Network and System Sciences*, vol. 08, pp. 456–470, 2015.
- [4] C. Shakuntala, "Swarm intelligence based route determination in manet using dsr algorithm."
- [5] F. Sarkohaki, R. Fotuhi, and V. Ashrafi, "An efficient routing protocol in mobile ad-hoc networks by using artificial immune system," *International Journal of Advanced Computer Science and Applications*, vol. 8, no. 4, 2017. [Online]. Available: <http://dx.doi.org/10.14569/IJACSA.2017.080473>
- [6] S. K. Maakar and Y. Singh, "Traffic pattern based performance comparison of two proactive manet routing protocols using manhattan grid mobility model," *International Journal of Computer Applications*, vol. 114, no. 14, 2015.
- [7] A. Manhar and D. Dembla, "Improved hybrid routing protocol (ihrp) in manets based on situation based adaptive routing," *International Journal of Electrical and Electronics Research*, vol. 11, no. 1, pp. 15–24, 2023.
- [8] D. Wang, D. Tan, and L. Liu, "Particle swarmf optimization algorithm: an overview," *Soft computing*, vol. 22, no. 2, pp. 387–408, 2018.
- [9] M. Ciba, "Design of optimization algorithms on ant colony simulation basis," Ph.D. dissertation, Slovak University of Technology in Bratislava, Faculty of Electrical Engineering and Information Technology, Bratislava, Slovakia, 2018.
- [10] M. V. H. B. Murthy and B. P. Rao, "Ants for routing in manet using hybrid aco-olsr algorithm," *International Journal of Electronics Communication and Computer Engineering*, vol. 9, no. 1, pp. 5–11, January 2018.
- [11] T. Zhang, X. Wang, B. Liang, and B. Yuan, "Catastrophic interference in reinforcement learning: A solution based on context division and knowledge distillation," *IEEE Transactions on Neural Networks and Learning Systems*, vol. 34, no. 12, p. 9925–9939, Dec. 2023. [Online]. Available: <http://dx.doi.org/10.1109/TNNLS.2022.3162241>
- [12] T. Fujimoto and A. P. Pedersen, "Adversarial attacks in cooperative AI," *CoRR*, vol. abs/2111.14833, 2021. [Online]. Available: <https://arxiv.org/abs/2111.14833>
- [13] Z. Alom, T. Godder, and M. Morshed, "Performance analysis of routing protocols in mobile ad-hoc network (manet)," 05 2016.
- [14] L. M. Tripathi and K. Sindhuben, "Analysis of black hole attack during route discovery phase of aodv in manet," 2020. [Online]. Available: <https://api.semanticscholar.org/CorpusID:219136003>
- [15] P. Rahul and B. Kaarthick, "Proficient link state routing in mobile ad hoc network-based deep q-learning network optimized with chaotic bat swarm optimization algorithm," *International Journal of Communication Systems*, vol. 36, 2022. [Online]. Available: <https://api.semanticscholar.org/CorpusID:253455137>
- [16] J. Kirkpatrick, R. Pascanu, N. Rabinowitz, J. Veness, G. Desjardins, A. A. Rusu, K. Milan, J. Quan, T. Ramalho, A. Grabska-Barwinska, D. Hassabis, C. Clopath, D. Kumaran, and R. Hadsell, "Overcoming catastrophic forgetting in neural networks," *Proceedings of the National Academy of Sciences*, vol. 114, no. 13, pp. 3521–3526, 2017. [Online]. Available: <https://www.pnas.org/doi/abs/10.1073/pnas.1611835114>
- [17] T. Fujimoto and A. P. Pedersen, "Adversarial attacks in cooperative ai," 2022. [Online]. Available: <https://arxiv.org/abs/2111.14833>
- [18] Y. Lin, Z. Hong, Y. Liao, M. Shih, M. Liu, and M. Sun, "Tactics of adversarial attack on deep reinforcement learning agents," *CoRR*, vol. abs/1703.06748, 2017. [Online]. Available: <http://arxiv.org/abs/1703.06748>
- [19] A. Paleyes, R.-G. Urma, and N. D. Lawrence, "Challenges in deploying machine learning: A survey of case studies," *ACM Comput. Surv.*, vol. 55, no. 6, Dec. 2022. [Online]. Available: <https://doi.org/10.1145/3533378>
- [20] D. Narayanan, M. Shoeybi, J. Casper, P. Legresley, M. M. A. Patwary, V. Korthikanti, D. Vainbrand, P. Kashinkunti, J. Bernauer, B. Catanzaro, A. Phanishayee, and M. Zaharia, "Efficient large-scale language model training on gpu clusters using megatron-lm," 11 2021, pp. 1–15.
- [21] K. Ren, T. Zheng, Z. Qin, and X. Liu, "Adversarial attacks and defenses in deep learning," *Engineering*, vol. 6, 01 2020.
- [22] M. Chen, U. Challita, W. Saad, C. Yin, and M. Debbah, "Machine learning for wireless networks with artificial intelligence: A tutorial on neural networks," *ArXiv*, vol. abs/1710.02913, 2017. [Online]. Available: <https://api.semanticscholar.org/CorpusID:26853250>
- [23] S. Han, H. Mao, and W. J. Dally, "Deep compression: Compressing deep neural networks with pruning, trained quantization and huffman coding," 2016. [Online]. Available: <https://arxiv.org/abs/1510.00149>

- [24] W. Y. B. Lim, N. C. Luong, D. T. Hoang, Y. Jiao, Y.-C. Liang, Q. Yang, D. Niyato, and C. Miao, "Federated learning in mobile edge networks: A comprehensive survey," *IEEE Communications Surveys Tutorials*, vol. 22, no. 3, pp. 2031–2063, 2020.
- [25] P. K. Sharma, M.-Y. Chen, and J. H. Park, "A software defined fog node based distributed blockchain cloud architecture for iot," *IEEE Access*, vol. 6, pp. 115–124, 2018.
- [26] W. Cui, K. Shen, and W. Yu, "Spatial deep learning for wireless scheduling," *IEEE Journal on Selected Areas in Communications*, vol. 37, no. 6, pp. 1248–1261, 2019.

Research on the possibilities of increasing the integration of renewable energy sources into the electric power system

¹Kristián ELIÁŠ (1st year)
Supervisor: ²Lubomír BEŇA

^{1,2}Dept. of Electric Power Engineering, FEI, Technical University of Košice, Slovak Republic

¹kristian.elias@tuke.sk, ²lubomir.bena@tuke.sk

Abstract—Due to the European Union's commitment to achieving climate neutrality by 2050, the use of renewable energy sources is developing rapidly in Europe. The Slovak Republic, as a member of the European Union, must play its part in achieving the set targets, and therefore the share of renewable energy sources in the country's energy mix is also growing in Slovakia. The number of connected electricity sources using renewable energy sources in the electricity system of the Slovak Republic is constantly growing. Such sources represent decentralized generation, which is, however, unstable due to its weather dependency.

At present, mainly small photovoltaic (PV) power plants (up to 10.8 kW) are being connected to low-voltage distribution systems. However, the impact of such decentralized generation on grid operation has not yet been comprehensively studied.

Therefore, this paper discusses ways to determine the adverse impacts of these sources on the power grid, as well as analyzes data measured in a real low-voltage distribution network to which single-phase and three-phase PV power plants are connected.

Keywords—distribution system, electricity quality, photovoltaic power plants, renewable energy sources.

I. INTRODUCTION

Electricity is a product that should meet certain quality criteria [1]. In the case of low-voltage distribution networks, the distribution system operator is responsible for ensuring that the quality of electricity at the point of connection is maintained.

The term "quality of electricity" refers mainly to voltage quality. Voltage quality is ensured if it has a sinusoidal waveform, a constant magnitude, a constant frequency, and, in the case of a three-phase system, if the three-phase voltages are symmetrical [2].

In Europe, the quality of electrical energy is dealt with in the EN 50160 standard. This standard defines, describes, and specifies the main characteristics of the voltages present at the supply terminals of users in public low-voltage, medium, high, and extra-high AC networks under normal operating conditions (it does not apply to exceptional situations such as fault clearance or emergencies) [2], [3].

II. PARAMETERS FOR ASSESSING THE IMPACT OF THE SOURCE ON THE DISTRIBUTION SYSTEM

EN 50160 defines various indicators for assessing the

quality of electricity in the power grid and also lists their permissible values. The connection of a renewable energy source has a complex effect on the quality of electricity in the grid, but the greatest impact can be observed on:

- the voltage magnitude,
- the voltage unbalance.

A. Voltage Magnitude

The normalized nominal voltage (U_n) of a low-voltage electrical network is 230 V between the phase and the neutral conductor in three-phase, four-wire electrical networks [3], [4].

According to the standard STN EN 50160:

- 95 % of the ten-minute average effective values of the voltage must be within $U_n \pm 10$ % during each one-week period,
- all ten-minute average effective values of the voltage must be within $U_n + 10$ % / - 15 % [3].

B. Voltage Unbalance

Voltage unbalance in a three-phase network is a condition where the voltage vectors in the individual phases are not of equal magnitude or do not have the same mutual phase shift [5].

The voltages at the terminals of the generators connected to the power system are symmetrical, i.e. the voltage vectors have the same magnitude and the same mutual phase shift (120°) [5], [6].

If the impedances of the individual elements of the power grid were equal in each phase and all loads connected to the grid were three-phase and symmetrical, the voltages in the power grid would be symmetrical [6].

Asymmetry occurs due to the uneven loading of the individual phases in a three-phase system (presence of single-phase appliances) [2], [7], but also due to the asymmetry of the electrical parameters (R , L , and C), mainly of the external air lines. The occurrence of asymmetry is also caused by disturbances in electrical networks (e.g., two-phase short circuit, connection of one phase to earth, etc.) [2].

Voltage Unbalance Calculation

The voltage unbalance can be calculated in various ways. Among the most commonly used methods are:

1. According to IEEE (Institute of Electrical and Electronics Engineers) - by the ratio of the maximum deviation of phase voltages from the average value of phase voltages and the average value of phase voltages [2], [8], [9]:

$$VU_{IEEE} (\%) = \frac{\max(|\Delta U_{L1}|; |\Delta U_{L2}|; |\Delta U_{L3}|)}{\bar{U}_f} \cdot 100 \quad (1)$$

where:

VU_{IEEE} is the voltage unbalance calculated according to IEEE
 \bar{U}_f is the average value of the phase voltages, calculated according to the relation [2], [10]:

$$\bar{U}_f = \frac{U_{L1} + U_{L2} + U_{L3}}{3} \quad (2)$$

ΔU_{L1} is the deviation of the phase voltage in phase 1 from the average value of the phase voltages, calculated according to the relation [2]:

$$\Delta U_{L1} = U_{L1} - \bar{U}_f \quad (3)$$

This relation (3) is valid by analogy for calculating the deviations in the other two phases [2].

2. According to NEMA (National Electrical Manufacturers Association) – by the ratio of the maximum deviation of the phase-to-phase voltages from the average value of the phase-to-phase voltages to the average value of the phase-to-phase voltages [2], [8], [11]:

$$VU_{NEMA} (\%) = \frac{\max(|\Delta U_{12}|; |\Delta U_{23}|; |\Delta U_{31}|)}{\bar{U}} \cdot 100 \quad (4)$$

where:

VU_{NEMA} is the voltage unbalance calculated according to NEMA

\bar{U} is the average value of the phase-to-phase voltages and is calculated according to the relation [2], [12]:

$$\bar{U} = \frac{U_{12} + U_{23} + U_{31}}{3} \quad (5)$$

ΔU_{12} is the deviation of the phase-to-phase voltage between the first and second phases from the average value of the phase-to-phase voltages and is calculated according to the relation [2]:

$$\Delta U_{12} = U_{12} - \bar{U} \quad (6)$$

This relation (6) is valid by analogy for the calculation of ΔU_{23} and ΔU_{31} [2].

3. as the ratio of the negative phase sequence to the positive phase sequence of the voltage (the "true definition") [2], [8], [13]:

$$k' = \frac{U_{(2)}}{U_{(1)}} \cdot 100 \quad (7)$$

where:

k' is the voltage unbalance factor,

$U_{(2)}$ is the negative phase sequence of the voltage,

$U_{(1)}$ is the positive phase sequence of the voltage.

This definition is based on the theory of decomposing an unbalanced system into symmetrical components (positive, negative, and zero phase sequence). A three-phase unbalanced system can be decomposed into three symmetrical components using Fortescue's method [2], [14].

This method is the most suitable for calculating voltage unbalance because it incorporates both the magnitude and angle of the voltage [6].

Elimination of Voltage Unbalance

It is not possible to completely eliminate voltage unbalance in the electricity grid, but there are several ways to reduce it at least partially. These options include redistributing loads evenly across all three phases of the power network, reducing the unbalance of individual elements of the power network (e.g., lines), or using passive LC elements or active electronic devices (e.g., SVCs). The advantage of active elements over passive ones is that they can dynamically adjust the resulting unbalance [14], [15].

Voltage Unbalance Limit Value

According to the standard EN 50160, 95 % of the ten-minute average effective values of the negative phase sequence of the voltage must be within 2 % of the positive phase sequence of the voltage during each one-week period [3].

III. TECHNICAL REQUIREMENTS FOR CONNECTION TO THE DISTRIBUTION SYSTEM

Only devices that do not endanger the reliability, safety, and operation of the distribution system can be connected to it [16]. Every device connected to the distribution system has certain feedback effects that affect the quality of electrical energy in the distribution system. Therefore, distribution system operators have established the maximum permissible feedback effects from the user on the distribution system.

At the low-voltage level, the following applies:

- the relative change in the RMS voltage caused by connecting a user's device to the distribution system must not exceed $\pm 3 \%$ at the connection point compared to the voltage magnitude when the device is not connected, i.e., $|\Delta u| \leq 3\%$,
- the maximum level of voltage unbalance caused by connecting a single user's device to the network must not exceed 0.7 % [17], [18], [19].

If the distribution system operator determines that the impact of a device connected to the distribution system exceeds the permissible limit, the user responsible for operating the device must take corrective measures. Otherwise, the distribution system operator is authorized to interrupt or restrict the user's connection to the distribution system [20].

IV. ANALYSIS OF THE IMPACT OF PHOTOVOLTAIC POWER PLANTS ON THE LOW-VOLTAGE DISTRIBUTION SYSTEM

On August 13, 2024, a measurement was conducted in a real low-voltage distribution network, to which approximately 60 consumption points are connected, with PV power plants installed at ten of these points. The individual PV power plants differ in installed capacity and the number of phases. Three PV power plants are connected to the distribution network in a single-phase manner, while seven are connected in a three-phase manner. At each consumption point, the voltage of each phase (L1, L2, L3) was measured at ten-minute intervals, as well as the active power supplied to/drawn from the distribution network at fifteen-minute

intervals. (Note: The active power flowing through the connection point of the consumption point to the distribution system was measured continuously, and the average value of the drawn/supplied active power from/to the network was subsequently calculated for the 15-minute time interval. During this time interval, due to the time-varying production of the PV power plant and the time-varying consumption at the consumption point, it could happen that both consumption and supply of active power from/to the grid occurred.)

The aim of the measurement was to obtain data to determine the relationship between the production of the PV power plant and the voltage magnitude at the connection point of the consumption point to the distribution system, as well as to assess whether the voltage magnitude at the connection point is within the permissible limits. According to the EN 50160 standard, the voltage magnitude at the connection point should be in the range of $230 \text{ V} \pm 10 \%$, i.e., between 207 V and 253 V.

In the following section, an analysis is performed for selected consumption points. The graphs are created from the average values of drawn/supplied active power during fifteen-minute intervals and from the average values of phase voltages during ten-minute intervals over a period of one day.

Case 1

This case represents a consumption point with a three-phase PV power plant, where the impact of the source on the voltage magnitude at the connection point did not exceed the permissible limits.

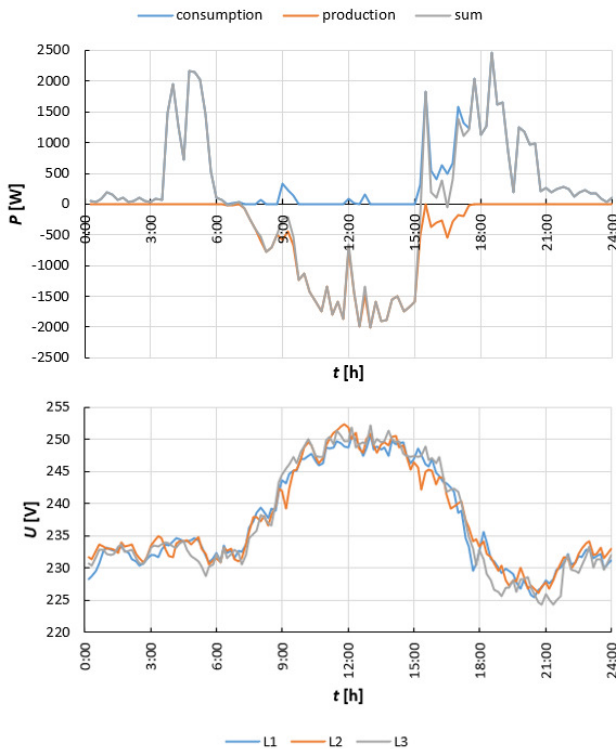


Fig. 1 Time profile of three-phase active power transmitted through the connection point and the voltages of individual phases at the connection point – case 1

Case 2

This case represents a consumption point with a three-phase PV power plant, where the source caused an excessive increase in voltage magnitude at the connection point.

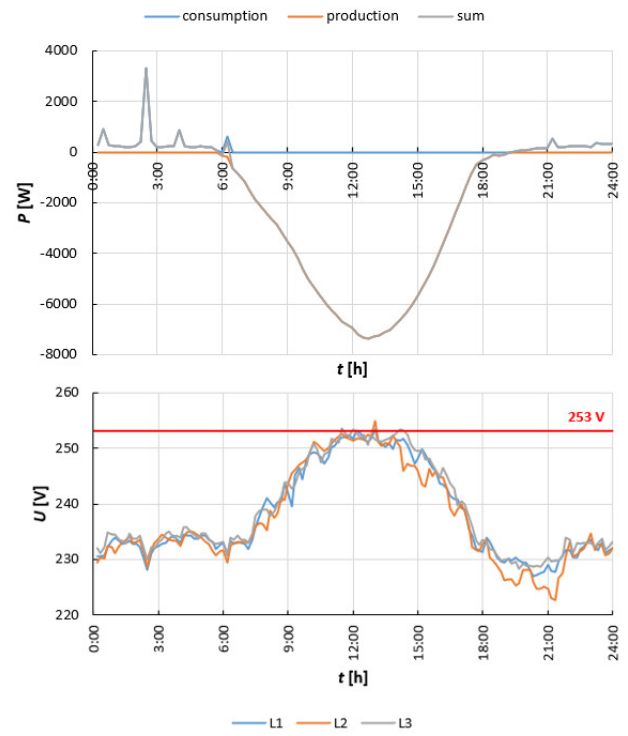


Fig. 2 Time profile of three-phase active power transmitted through the connection point and the voltages of individual phases at the connection point – case 2

Case 3

This case represents a consumption point with a single-phase PV power plant that had an excessive impact on the voltage magnitude at the connection point.

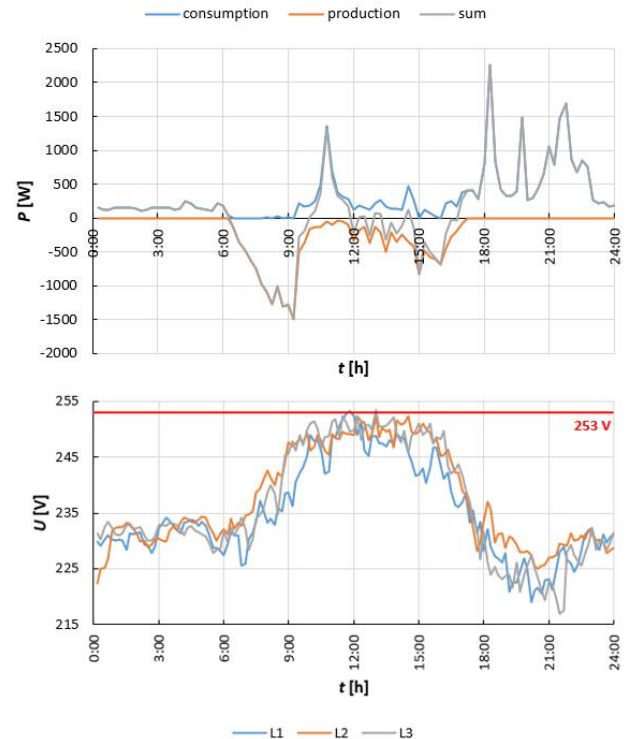


Fig. 3 Time profile of three-phase active power transmitted through the connection point and the voltages of individual phases at the connection point – case 3

In Fig. 1, Fig. 2, and Fig. 3, two graphs are presented:

- the time profile of the three-phase active power (P) transmitted through the connection point of the consumption point over the course of one day,

- the time profile of the voltage (U) in each phase at the connection point of the consumption point over the course of one day.

The graph of active power consists of three curves:

- the blue curve represents the drawn active power from the low-voltage distribution network,
- the orange curve represents the supply of active power to the low-voltage distribution network,
- the gray curve indicates the sum of supplied and drawn active power.

V. SUMMARY OF MEASUREMENT RESULTS

From the graphs in Fig. 1 and Fig. 2, it is evident that the electricity production in the three-phase PV power plant directly affects the voltage magnitude at the connection point. Whether the impact of the PV power plant's operation on the voltage magnitude is within permissible limits depends on various factors, such as the installed capacity of the PV power plant, the draw at the consumption point, the weather, and the location of the consumption point within the electrical network.

From Fig. 2, it can be seen that if the consumption at the consumption point is minimal during the day, weather conditions are favorable, and the installed capacity of the PV power plant is high (e.g., 10.8 kW), the operation of the PV power plant can cause the voltage at the consumption point to exceed the permissible value (i.e., 253 V).

From the voltage time profile in Fig. 3, it can be seen that the electricity production in a single-phase PV power plant primarily causes an increase in the differences in voltage magnitudes across the individual phases, thus increasing the voltage unbalance at the connection point. However, it is not possible to calculate the voltage unbalance factor k' from the measured values, as the measurement data do not contain information about the phase angles of the voltages in the individual phases.

VI. NEXT DIRECTION OF THE WORK

From the analysis of the data obtained from measurements, it follows that the operation of electricity sources using renewable energy sources affects the quality of electrical energy in the distribution system. Under certain circumstances, the impact can be so significant that the electricity in the distribution system will not meet the required quality standards. To prevent such situations, it is essential to thoroughly examine the influence of the operation of electricity sources using renewable energy sources on the distribution system to which they are connected and to adjust the operation of the sources as well as the operation of the distribution system accordingly.

In the upcoming period, I will therefore focus on creating a model of a low-voltage distribution system with integrated PV power plants in a simulation program, with the aim of examining the impact of single-phase and three-phase PV power plants with various operating modes (different installed capacities and different power factors) on selected qualitative indicators of electricity.

ACKNOWLEDGMENT

This paper was supported by the Science Grant Agency of the Ministry of Education, Research, Development and Youth

of the Slovak Republic under the contract VEGA 1/0532/25.

REFERENCES

- [1] Z. Lukasiak and Z. Olczykowski, "Quality and reliability of electricity supply," 2020 *ELEKTRO*, Taormina, Italy, 2020, pp. 1-6, doi: 10.1109/ELEKTRO49696.2020.9130127.
- [2] B. Dolník, J. Pitoňák and L. Beňa, in *Quality and reliability of electricity supply*, 1st ed. Košice, Slovakia: Technical University of Košice, 2022, ISBN 978-80-553-4107 1.
- [3] *Voltage characteristics of electricity supplied by public electricity networks*, STN EN 50160, 2011.
- [4] D. Hlubeň, R. Stolárik and Š. Vaško, "Power quality according to the applicable STN," in *Elektroenergetika*, vol. 5, no. 2, pp. 5-7, 2012, ISSN 1337-6756.
- [5] M. Kanálik and J. Tomčík, in *Transmission and distribution of electricity*, 1st ed. Košice, Slovakia: Technical University of Košice, 2019, ISBN 978-80-553-3376-2.
- [6] Z. Kovács and P. Szathmáry, in *Reliability and quality of electricity*, 2007, ISBN 978 80-8073-864-8.
- [7] A. von Jouanne and B. Banerjee, "Assessment of voltage unbalance," in *IEEE Transactions on Power Delivery*, vol. 16, no. 4, pp. 782-790, Oct. 2001, doi: 10.1109/61.956770.
- [8] "Definitions of Voltage Unbalance," in *IEEE Power Engineering Review*, vol. 21, no. 5, pp. 49-51, May 2001, doi: 10.1109/MPER.2001.4311362.
- [9] A. M. El-Bashbishi and A. A. El-Fergany, "Calculation methods of voltage unbalance factor," 2023 *24th International Middle East Power System Conference (MEPCON)*, Mansoura, Egypt, 2023, pp. 1-6, doi: 10.1109/MEPCON58725.2023.10462408.
- [10] K. Girigoudar, D. K. Molzahn and L. A. Roald, "On the relationships among different voltage unbalance definitions," 2019 *North American Power Symposium (NAPS)*, Wichita, KS, USA, 2019, pp. 1-6, doi: 10.1109/NAPS46351.2019.9000231.
- [11] K. Girigoudar and L. A. Roald, "On the impact of different voltage unbalance metrics in distribution system optimization," *Electric Power Systems Research*, vol. 189, p. 106656, Dec. 2020, doi: 10.1016/j.epsr.2020.106656.
- [12] A. D. Rodriguez, F. M. Fuentes and A. J. Matta, "Comparative analysis between voltage unbalance definitions," 2015 *Workshop on Engineering Applications - International Congress on Engineering (WEA)*, Bogota, Colombia, 2015, pp. 1-7, doi: 10.1109/WEA.2015.7370122.
- [13] F. Shahnia, P. J. Wolfs and A. Ghosh, "Voltage unbalance reduction in low voltage feeders by dynamic switching of residential customers among three phases," in *IEEE Transactions on Smart Grid*, vol. 5, no. 3, pp. 1318-1327, May 2014, doi: 10.1109/TSG.2014.2305752.
- [14] P. Szathmáry and M. Kanálik, "Adverse effects of voltage asymmetry on electrical equipment and ways to eliminate them," *ATP Journal*, vol. 2025, no. 2, pp. 51-53, Feb. 2025, ISSN: 1335-2237.
- [15] F. Shahnia, P. Wolfs and A. Ghosh, "Voltage unbalance reduction in low voltage feeders by dynamic switching of residential customers among three phases," 2013 *IEEE Power & Energy Society General Meeting*, Vancouver, BC, Canada, 2013, pp. 1-5, doi: 10.1109/PESMG.2013.6672798.
- [16] *Operating regulations of the distribution system operator Východoslovenská distribučná, a.s., Východoslovenská distribučná, a.s., Bratislava, Slovakia, 2023*. [Accessed: Feb. 17, 2025]. [Online]. Available: https://www.vsds.sk/mdoc/dso.B6000.A/doc/Prevadzkovy_poriadok_VSD.pdf.
- [17] *Technical conditions of the distribution system operator Východoslovenská distribučná, a.s., Východoslovenská distribučná, a.s., Košice, Slovakia, 2022*. [Accessed: Feb. 17, 2025]. [Online]. Available: https://www.vsds.sk/mdoc/dso.B6000.A/doc/VSD_Technicke_Podmienky_PDS.pdf.
- [18] *Technical conditions of the distribution system operator Západoslovenská distribučná, a.s., Západoslovenská distribučná, a.s., Bratislava, Slovakia, 2024*. [Accessed: Feb. 17, 2025]. [Online]. Available: <https://www.zsdis.sk/Uvod/Spolocnost/Dokumenty/Predpisy-prevadzkovatela>.
- [19] M. Špes, L. Beňa, M. Kostelec, and M. Márton, "Study of power plant connectivity to the HV network," in *Electrical Engineering and Informatics VIII*, Košice, Slovakia: Technical University of Košice, 2017, pp. 154-159, ISBN 978-80-553-3192-8.
- [20] *Technical conditions of the distribution system operator Stredoslovenská distribučná, a.s., Stredoslovenská distribučná, a.s., Žilina, Slovakia, 2022*. [Accessed: Feb. 17, 2025]. [Online]. Available: https://www.ssd.sk/buxus/docs/dokumenty/o_nas/legislativa/Technick%C3%A9%20podmienky%20PDS%20Stredoslovensk%C3%A1%20distrib%C4%8Dn%C3%A1,%20a.s.,%20platn%C3%A9%20od%201.%20decembra%202022.pdf.

Dynamic Allocation of Electric Power Capacities

¹Július ŠIMČÁK (1st year)
Supervisor: ²Dušan MEDVEĎ

^{1,2}Dept. Department of Electric Power Engineering, FEI, Technical University of Košice, Slovak Republic

¹julius.simcak@tuke.sk, ²dusan.medved@tuke.sk

Abstract— The increasing demand for electricity supply quality, along with the expansion of electromobility and decentralized energy production from photovoltaic (PV) systems, pose new challenges for the stability and management of the electrical grid. The necessity of DC to AC voltage conversion significantly affects power quality and grid stability, as charging electric vehicles (EVs) can lead to load imbalances and harmonic distortions. Additionally, overproduction from PV systems can strain the grid, making energy storage solutions essential for balancing supply and demand.

This paper explores the efficient utilization of renewable energy sources and their impact on power quality in distribution networks. Reducing conversion losses can enhance overall system efficiency, particularly by utilizing direct current (DC) for EV charging, which eliminates double conversion losses. The study also examines the behavior of photovoltaic panels using the volt-ampere (V-I) characteristic and discusses approaches modeling approaches.

The role of smart grids is analyzed, highlighting their ability to integrate advanced information and communication technologies and automation for improved grid management. Smart grids enhance reliability, enable bidirectional energy flow, and support demand-side energy management. Furthermore, the paper discusses EV charging models and simulations, considering key parameters such as state of charge (SOC), energy consumption, and charging profiles. Various statistical methods and simulation approaches are explored to optimize EV charging strategies and minimize grid disruptions.

Keywords—DC/AC conversion, Electromobility, Renewable Energy source, Smart grid.

I. INTRODUCTION

The demands for electricity supply quality are constantly increasing. The expansion of electromobility and decentralized energy production, especially from photovoltaic panels, presents new challenges for the stability and management of the electrical grid. The need for DC to AC voltage conversion is essential, affecting the quality of electrical energy and the overall stability of the grid.

Charging electric vehicles can cause an unbalanced load on the grid, which negatively affects its stability. While home charging is convenient, it also comes with risks. The increasing number of rectifiers and inverters required for voltage conversion can complicate the situation, especially due to the injection of harmonic distortion into the grid. This harmonic distortion can lead to a deterioration of voltage quality, increased losses, and compatibility issues with electrical devices.

Photovoltaic panels reduce the electricity consumption from the distribution grid, but their overproduction during peak periods can negatively impact the network. Since

photovoltaic systems generate direct current (DC), its conversion to alternating current (AC) is necessary, and this process can also lead to harmonic distortions. Battery storage systems can help balance the fluctuations and improve the efficiency of renewable energy utilization. [1].

Work describes the issue of efficiently utilizing renewable energy sources and their impact on the quality of electrical energy in the distribution network. Minimizing conversion can increase the overall efficiency of the system. When charging with direct current (DC), double transformation is not required, allowing for the dedicated use of a DC source for charging and an AC source for grid connection or household power supply.

II. PHOTOVOLTAIC ARRAY

To understand the behavior of a photovoltaic panel, it is essential to familiarize oneself with the V-I (volt-ampere) characteristic. This characteristic defines how the current generated by the panel changes depending on the voltage and is influenced by several key parameters. The main factors affecting the energy production of a photovoltaic panel include the photogenerated current (I_{ph}), the diode current under reverse voltage (I_D), the number of series-connected cells (N_s), the parallel resistance (R_p), the series resistance (R_s), and the thermal voltage of the junction (V_t).

$$I = I_{ph} - I_0 \left[e^{\frac{V + IR_s}{N_s V_t}} - 1 \right] - \frac{V + IR_s}{R_p} \quad (1)$$

These parameters determine how the panel behaves at different voltage and current levels, thereby affecting its overall performance. Analyzing the V-I characteristic of the panel is fundamental for optimizing its output under various conditions and for designing efficient photovoltaic systems[2].

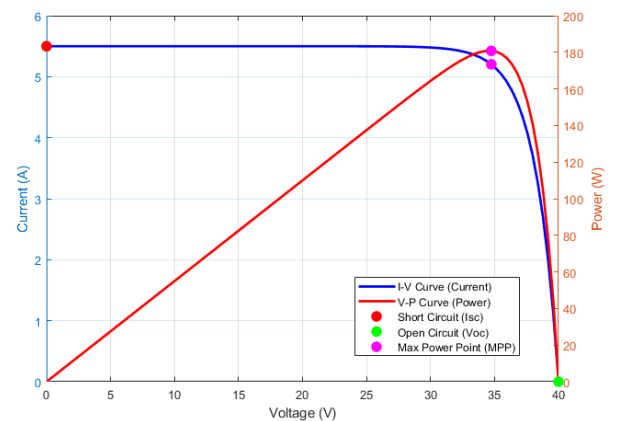


Fig. 1. Volt-ampere characteristic

The goal is to create a model that uses as few parameters as possible while still accurately describing a wide range of curves. Simplified versions of the single-diode model exist, utilizing only four parameters. In this case, a version is used where the series resistance is neglected[3].

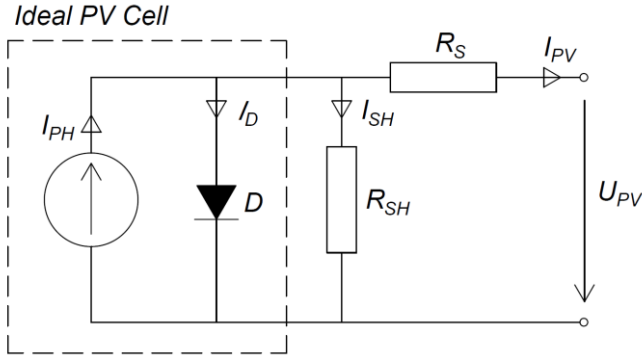


Fig. 2. Model of ideal photovoltaic cell

This model is easy to understand because it simplifies into a combination of linear and exponential functions. By setting $R_S=0$ and using normalized values for current and voltage, where the short-circuit current and open-circuit voltage are set to unit values, the equations are transformed into a more convenient form, making modeling easier[3].

$$i = \frac{I}{I_{sc}}, v = \frac{V}{V_{oc}} \quad (2)$$

After substitution, the equation takes the following form:

$$i = 1 - \frac{I_o}{I_{sc}} \left[e^{\frac{V_{oc}}{N_s V_t} v} - 1 \right] - \frac{V_{oc}}{I_{sc} R_p} v \quad (3)$$

In photovoltaic panels, various faults such as shading or damage to the panel or individual cells can have a significant negative impact on the overall system performance. Shading a single panel can cause a drop in power output, and when panels are connected in series, the failure or shading of one panel can affect the entire string, as all panels in series must operate at the same current. Damaged panels, such as those that are short-circuited, can lead to voltage or current drops, reducing energy production. Even minor damage can have a disproportionately large impact on overall performance, making it crucial to optimize the design and operation of solar systems to minimize these losses[4].

III. SMART GRID

A smart grid is an advanced, computer-controlled, bidirectional energy system capable of self-recovery, adaptability, resilience, and efficient forecasting in unpredictable situations. It is defined as an electrical system that utilizes information technology, bidirectional, cyber-secured communication, and analytical intelligence in an integrated manner across electricity generation, transmission, substations, distribution, and consumption to achieve a system that is clean, secure, reliable, resilient, efficient, and sustainable[5].

Smart grids differ from traditional grids by providing a self-regulating function that enhances their reliability. They integrate modern technologies such as the Internet of Things (IoT), advanced information and communication technologies (ICT), and intelligent algorithms that manage energy demand-side requirements (DSE) in real-time.

A smart grid consists of various components, such as the Energy Management System, Supervisory Control and Data Acquisition system, energy sensors, Static Var Compensators, and intelligent relays. The smart grid can overcome several challenges of traditional grids, such as one-way energy flow, fixed tariffs regardless of consumption, and inefficient energy measurement. [5].

Traditional grids rely on fossil fuels, which produce carbon emissions that harm the environment, so it is necessary to find new, efficient, and innovative solutions. Traditional electrical grids operate on a one-way energy flow and a centralized energy network. This one-way system affects energy distribution on a small scale. Such grids urgently require transformation to address fundamental issues related to energy management and protective schemes[18]. By deploying modern digital information and telecommunications networks, these grids can prevent outages and provide sustainable energy[5].

Smart grids have a crucial role in our society as they utilize renewable energy sources to generate clean electricity. Sustainable renewable energy sources, such as wind and solar, are used to meet the growing demand for electricity. However, renewable energy sources are dependent on weather conditions, which adds complexity to the regular operations of the grid. Therefore, it is necessary to implement various storage systems to balance the fluctuations caused by weather.

Data obtained from smart grids are essential for solar panels and wind farms to supply energy to the grid and optimize its usage to meet the constantly changing energy demands[6].

IV. ELECTRIC VEHICLE CHARGING

Electric vehicles (EVs) are typically divided into three categories: battery electric vehicles (BEV), plug-in hybrid electric vehicles (PHEV), and hybrid electric vehicles (HEV). Charging can be done in three ways: conductive, inductive, and wireless[17]. However, inductive and wireless charging are still in the early stages of development for widespread deployment. The development of chargers whether on-board or off-board has primarily focused on conductive charging, which ensures energy transfer through a physical connection to the vehicle. Most fast-charging stations use one of two configurations – AC or DC bus structures[7].

AC bus structure: The three-phase AC bus operates with a voltage range of 250 V to 480 V (phase-to-phase voltage). Each charging unit contains an AC-DC rectifier and a DC-DC converter, which increases the number of power stages, costs, and system complexity. Nevertheless, this configuration is dominant in fast and ultra-fast charging stations due to the maturity of power electronics and the existing AC distribution infrastructure[7].

DC-based structure: It includes a central AC-DC rectifier connected to an input low-frequency transformer. Photovoltaic sources, battery storage systems, and electric vehicles are then connected to the DC bus via DC-DC converters. This structure provides greater system flexibility and better handles faults on the grid side. Since the number of AC-DC rectifiers[8] is lower, efficiency is higher, and control is simpler. The problem with DC bus stations is the lack of established safety regulations, which becomes critical, especially during the operation of Vehicle-to-Grid (V2G) systems[9].

Designing a model for electric vehicle charging will assist in the development and improvement of the operation of the

power grid and in preparing for the penetration of EVs[9]. Grid operators need to prepare for a high levels of EV penetration into the power system. The EV charging model provides operators with an overview of the impact of EV integration on the distribution network, allowing them to identify and prevent issues such as overload caused by uncontrolled charging. Uncontrolled EV charging can cause various problems, such as voltage fluctuations, transformer overload, power losses, and instability in the power system[9].

When modeling the residential EV charging profile, it is necessary to consider various parameters such as daily energy consumption, driving period, charging start times, charging power levels, EV battery capacity, initial state of charge (SOC₀), and final state of charge (SOC). The patterns of these parameters can be modeled by analyzing historical real data and selecting the most appropriate statistical methods that can model these parameters with matching distribution shapes. Probability density functions (PDFs) are important methods for identifying data distributions, such as gamma distribution, beta distribution, uniform distribution, and others. However, PDF methods sometimes fail to capture the distribution of real parameters precisely. The inverse transformation method can be used to generate random numbers from any probability distribution variable. The distribution of each parameter can be used to develop individual and aggregated EV charging profiles[10].

Several studies have proposed EV charging models based on real data or simulations[15]. For example, a model was created considering the behavior of EV drivers, using data from a North American university network. Monte Carlo simulation was used to model the daily charging profile in non-residential sectors, taking into account parameters such as charging power, initial state of charge, charging start time, and duration. In another study, a model was developed based on data from a Norwegian housing company, which included information on connection duration and the amount of energy charged[10].

Since historical EV charging data has not always been available, many studies had to rely on assumptions and surveys to model the parameters. Some assumed a constant daily driving distance and calculated the initial SOC from that. They also assumed that all EV owners would plug in their vehicles to charge immediately upon arriving home and would not disconnect the vehicle until the next day. Some studies used mathematical analyses to determine charging demand based on travel or charging behavior. However, not all models considered key parameters—for example, the initial battery charge level or daily energy consumption during driving were not included, which could have affected the accuracy of the results[10].

V. EV CHARGING SIMULATION

Charging electric vehicles is a random event, however, certain parameters can be predicted that may help in designing a simulation of a household using renewable energy sources to charge vehicles. key parameters include the electric vehicle battery capacity and energy consumption, state of charge (SOC) when connecting and disconnecting from the charger, and the power of the charging station. From the perspective of the electrical grid, it is important to know the time when the most vehicles connect to the charger, how long it takes to charge the battery to 90% SOC (which extends its lifespan), and the technical design of the charging system – such as

onboard chargers, home charging stations[11], or the number of phases for connection (single, two, or three phases)[16].

To model the battery storage system of an electric vehicle in Matlab/Simulink, a controlled current source is used, which is driven by a signal and represents the equivalent of a current source. The simulation monitors three main factors: the characteristics of the photovoltaic (PV) system production, the characteristics of energy consumption, and the battery state. Input parameters and efficiencies are considered constant during the simulation, which, however, is not the case in reality, as the charging system control dynamically adjusts and modifies the charging power based on current conditions[12].

To maximize the lifespan of battery systems, the SOC value is maintained within the range of 20% to 90%, and for different vehicle models, this value may represent a different capacity. The capacity of a lithium-ion battery (LIB) is considered an indicator of the battery's health (Health Indicator – HI), which reflects the ability of the battery to deliver the required performance compared to a new battery and quantifies the extent of its degradation. Under laboratory conditions, the actual capacity of the battery is determined as the average of three complete charging and discharging cycles[12].

In real-world conditions, however, complete charging and discharging cycles are not practical, so instead of discharging capacity, charging capacity is used, as commercially available batteries have high coulombic efficiency. Therefore, in this study, charging data is used to calculate the battery pack capacity. To calculate the state of charge, the ampere-hour integral method, also known as the coulomb counting method, is employed, and its mathematical expression is given below[13].

$$SOC(t) = SOC(t_0) + \frac{\int_{t_0}^t I(t) dt}{C_{act}} \quad (4)$$

Where SOC(t) and SOC(t₀) represent the state of charge of the battery pack at the time moments t and t₀. I(t) represents the current of the battery pack at the time moment t, and C_{act} is the maximum available capacity of the battery pack. The maximum available capacity of the battery pack can be calculated using the inverse form of equation (4), which is expressed as follows:

$$C_{act} = \frac{\int_{t_0}^t I(t) dt}{SOC(t) - SOC(t_0)} = \frac{Q}{\Delta SOC} \quad (5)$$

It is clear that the key to accurately determining the battery pack capacity is obtaining an accurate SOC value. The capacity Q can be calculated by integrating the current recorded by the Battery Management System (BMS) [14] over time; however, precise determination of the SOC is challenging due to inevitable estimation errors in real-world BMS conditions. To address this issue, this study proposes a labeled capacity acquisition method that combines the inverse form of the ampere-hour integral method with correction methods based on Open Circuit Voltage (OCV) and internal battery resistance [13].

VI. CONCLUSION

The growing integration of electric vehicles (EVs) and decentralized renewable energy systems, particularly photovoltaic panels, into the electrical grid presents both opportunities and challenges for the energy sector. As the demand for high-quality electricity supply increases, the need

for efficient energy conversion and grid stability becomes paramount. The conversion of direct current (DC) to alternating current (AC) plays a critical role in this context, particularly in systems such as home charging stations and photovoltaic arrays, where DC power is generated and must be converted for use within the grid.

The use of photovoltaic energy reduces dependence on the grid, but its intermittent nature and the overproduction during peak periods can strain the system. This highlights the importance of optimizing energy management and minimizing the number of conversions between DC and AC to reduce inefficiencies and the risk of harmonic distortions. Smart grid technologies provide a solution by enhancing grid adaptability and stability, helping to manage renewable energy fluctuations, and improving the quality of electricity delivered to consumers.

For electric vehicle charging, ensuring efficient integration with the grid is essential. Modeling the behavior of EV charging and understanding its parameters, and considering aspects such as the battery state of charge, energy consumption patterns, and charging infrastructure can help mitigate issues like grid overload and energy loss. The development of dynamic, real-time charging control systems and the use of advanced modeling techniques such as probability density functions (PDFs) for realistic simulation provide valuable tools for grid operators to prepare for widespread EV adoption.

In conclusion, the study emphasizes the need for a holistic approach to managing the integration of renewable energy systems, electric vehicles, and energy storage, utilizing technologies such as smart grids, optimized charging systems, and accurate modeling techniques to ensure efficient, reliable, and sustainable energy production and consumption in the future.

NEXT STEPS

In the future, I plan to develop simulations in MATLAB/Simulink to address challenges related to integrating renewable energy sources and electromobility into the power grid. My goal is to compare different types of converters and analyze their impact on the grid through simulations.

I also want to implement Vehicle-to-Grid technology using bidirectional charging at a distribution point. Additionally, I aim to design a hybrid system that combines photovoltaic panels and battery storage for electric vehicle charging.

Another key focus will be analyzing the effects of different EV adoption scenarios on grid stability and efficiency. Lastly, I plan to compare predictions of daily charging cycles to better understand demand patterns and optimize charging strategies.

ACKNOWLEDGMENT

This paper was supported by the Slovak Academy of Sciences under the contract VEGA 1/0532/25.

REFERENCES

- [1] R. Faraji and H. Farzanehfard, "Soft-Switched Nonisolated High Step-Up Three-Port DC-DC Converter for Hybrid Energy Systems," *IEEE Transactions on Power Electronics*, vol. 33, pp. 10101–10111, 2018. doi: 10.1109/TPEL.2018.2826542.
- [2] H. A. Mahdi, "Predicting unparalleled degradation progression in PV module using simulation of shunt resistance experimental data," *Energy Rep.*, vol. 12, pp. 3134–3144, Dec. 2024, doi: 10.1016/j.egy.2024.09.012. Available: <https://www.sciencedirect.com/science/article/pii/S2352484724005857>.
- [3] M. Orkisz, "Estimating Effects of Individual PV Panel Failures on PV Array Output," in *IEEE Transactions on Industry Applications*, vol. 54, no. 5, pp. 4825–4832, Sept.–Oct. 2018, doi: 10.1109/TIA.2018.2841818.
- [4] Jha, V. Mathematical modelling of PV array under partial shading condition. *Sādhanā* 47, 85 (2022). <https://doi.org/10.1007/s12046-022-01853-y>
- [5] S. Baidya, V. Potdar, P. R. Partha, and C. Nandi, "Reviewing the opportunities, challenges, and future directions for the digitalization of energy," *Energy Research & Social Science*, vol. 81, p. 102243, Nov. 2021, doi: 10.1016/j.erss.2021.102243.
- [6] C. Lamnatou, D. Chemisana, and C. Cristofari, "Smart grids and smart technologies in relation to photovoltaics, storage systems, buildings and the environment," *Renewable Energy*, vol. 185, pp. 1376–1391, Feb. 2022, doi: 10.1016/j.renene.2021.11.019.
- [7] M. Safayatullah, M. T. Elrais, S. Ghosh, R. Rezaii and I. Batarseh, "A Comprehensive Review of Power Converter Topologies and Control Methods for Electric Vehicle Fast Charging Applications," in *IEEE Access*, vol. 10, pp. 40753–40793, 2022, doi: 10.1109/ACCESS.2022.3166935.
- [8] G. A. Taylor and S. M. Halpin, "Identifying Trends Between Source Unbalance and Harmonic Emissions of an AC-DC Rectifier," 2023 North American Power Symposium (NAPS), Asheville, NC, USA, 2023, pp. 01–05, doi: 10.1109/NAPS58826.2023.10318690.
- [9] M. El-Hendawi, Z. Wang, R. Paranjape, S. Pederson, D. Kozoriz, and J. Fick, "Electric vehicle charging model in the urban residential sector," *Energies*, vol. 15, no. 13, p. 4901, 2022, doi: 10.3390/en15134901.
- [10] O. Khan, B. Hredzak and J. E. Fletcher, "A Reconfigurable Multiport Converter for Grid Integrated Hybrid PV/EV/Battery System," 2022 IEEE 16th International Conference on Compatibility, Power Electronics, and Power Engineering (CPE-POWERENG), Birmingham, United Kingdom, 2022, pp. 1–6, doi: 10.1109/CPE-POWERENG54966.2022.9880873.
- [11] C. Marinescu, "Progress in the Development and Implementation of Residential EV Charging Stations Based on Renewable Energy Sources," *Energies*, vol. 16, no. 1, p. 179, 2023, doi: 10.3390/en16010179.
- [12] Q. Qi, W. Liu, Z. Deng, J. Li, Z. Song, and X. Hu, "Battery pack capacity estimation for electric vehicles based on enhanced machine learning and field data," *Journal of Energy Chemistry*, vol. 92, pp. 605–618, May 2024, doi: 10.1016/j.jechem.2024.01.047. Available: <https://www.sciencedirect.com/science/article/pii/S2095495624000858>.
- [13] M. Yasko, A. Balint, J. Driesen and W. Martinez, "Future workplace EV charging architectures: DC and AC charging choices," 2023 IEEE International Conference on Electrical Systems for Aircraft, Railway, Ship Propulsion and Road Vehicles & International Transportation Electrification Conference (ESARS-ITEC), Venice, Italy, 2023, pp. 1–7, doi: 10.1109/ESARS-ITEC57127.2023.10114837.
- [14] R. Pakdel, M. Yavarinasab, M. R. Zibad and M. R. Almohaddesn, "Design and Implementation of Lithium Battery Management System for Electric Vehicles," 2022 9th Iranian Conference on Renewable Energy & Distributed Generation (ICREDG), Mashhad, Iran, Islamic Republic of, 2022, pp. 1–6, doi: 10.1109/ICREDG54199.2022.9804549.
- [15] Singla, P., Boora, S., Singhal, P. et al. Design and simulation of 4 kW solar power-based hybrid EV charging station. *Sci Rep* 14, 7336 (2024). <https://doi.org/10.1038/s41598-024-56833-5>
- [16] Y. Xiao, C. Liu and F. Yu, "An Integrated On-Board EV Charger with Safe Charging Operation for Three-Phase IPM Motor," in *IEEE Transactions on Industrial Electronics*, vol. 66, no. 10, pp. 7551–7560, Oct. 2019, doi: 10.1109/TIE.2018.2880712.
- [17] W. Yin and J. Ji, "Research on EV charging load forecasting and orderly charging scheduling based on model fusion," *Energy*, vol. 290, p. 130126, Mar. 2024, doi: 10.1016/j.energy.2023.130126.
- [18] Li, F., Campeau, É., Kocar, I., & Lesage-Landry, A. (2024). Inferring electric vehicle charging patterns from smart meter data for impact studies. *Electric Power Systems Research*, 235, 110789. <https://doi.org/10.1016/j.epr.2024.110789D>

Effect of halloysite content on the quality and mechanical properties of thermoplastic starch-based material

¹Simona SAPAROVÁ (3rd year)
Supervisor: ²Mária KOVALAKOVÁ

^{1,2}Department of Physics, FEEI TU of Košice, Slovak Republic

¹simona.saparova@tuke.sk, ²maria.kovalakova@tuke.sk

Abstract— In this paper, the effect of halloysite content on the quality and mechanical properties of thermoplastic starch-based polymer material was studied using melt flow index measurements and mechanical testing. The results of melt flow index measurements indicate improvement in the quality and an increase in viscosity with increasing filler content in the studied material. The results of mechanical testing confirmed the reinforcing effect of halloysite nanofiller. Deterioration of mechanical properties (tensile strength and elongation at break) was observed with increasing halloysite content.

Keywords— thermoplastic starch-based material, nanocomposite, halloysite, melt flow index, mechanical testing

I. INTRODUCTION

Environmental pollution has become a topical issue nowadays. There is an effort to reduce it by replacing conventional plastics with biodegradable ones [1]. One of the most promising materials is thermoplastic starch (TPS) since it is produced from abundant and renewable raw material – starch, which is present in various plants, e.g. corn, potato and rice. TPS is produced by thermomechanical processing of native starch, in the presence of plasticizers which are needed to destroy hydrogen bonding between starch macromolecules and to create new bonds between starch and plasticizers molecules. The type and amount of plasticizers influence TPS properties [2][3].

In general, TPS mechanical properties are rather poor and not satisfactory for many applications. One of the possible solutions is to blend TPS with other biodegradable polymers (e.g. poly(butylene-adipate-co-terephthalate) or other polyesters) [4]. An example of the mentioned blends is material named AGENACOMP® F40. It has many advantages – it is biodegradable, home-compostable and colorable material with high TPS proportion [5]. However, for some modern applications like 3D printing, AGENACOMP mechanical properties need to be improved to produce long-lived products. Preparation of nanocomposites with AGENACOMP matrix is a promising way to improve properties of the resulting material. There is a large number of nanofillers available – organic and inorganic. Clay materials are often used because of their abundance and price. Halloysite, which is a relatively rare form of kaolinite with a wide range of application [6],[7] was chosen to improve mechanical properties of AGENACOMP® F40.

It is very important to know some characteristics of polymer materials in view of their future processing and applications.

The melt volume rate (MVR) obtained from melt flow index measurements gives information about the flowability of materials. MVR value [8] can help in choosing appropriate of methods for polymer processing, e.g. extrusion, injection molding, blow molding, rotational molding. Mechanical testing belongs to basic experimental methods used for characterization of new polymer materials. Mechanical properties (e.g., elongation at break and tensile strength) acquired from mechanical testing are very important for determination of possible application of the prepared materials [9].

In this paper, the effect of the content of halloysite used as nanofiller in AGENACOMP matrix was studied using melt flow index measurements and mechanical testing.

II. MATERIALS AND METHODS

The studied samples were prepared at the Central European Institute of Technology in Brno, Czech Republic. Material AGENACOMP® F40 (AGRANA Stärke GmbH, Austria) was used as a polymer matrix, halloysite Imerys Premium (Imerys, France) with aspect ratio of 5 was used as a nanofiller and calcium stearate was used as a lubricator. The studied samples were prepared with different halloysite content – 0, 0.1, 0.2, 0.5, 1 and 2 wt. % respectively. The calcium stearate content was 2 wt. %. AGENACOMP, halloysite and calcium stearate were processed in laboratory mixer (Brabender Plastograph EC Plus W50 EHT) for 7 min at 150°C and 60 rpm.

Prepared samples were compression molded at 140°C using one minute preheating without pressure and an additional 3 minutes with the applied force of 100 kN followed by cooling process with duration of 80 seconds. Dogbones type 5A were cut from compression molded samples with the length of 75 mm and the width of 4 mm.

Melt flow index measurements were carried out at 190°C using 2.16 kg load and 2 mm capillary die. Mechanical testing was carried out using tensile machine Zwick Roell Z005 with the preload of 0.1 MPa and rate 1 mm/s and the measurement rate 50 mm/s. All studied samples were tested seven times.

III. RESULTS AND DISCUSSION

The plastogram of AGENACOMP processing without nanofiller is depicted in Fig. 1. In the beginning, three torque peaks are observed due to chamber being filled up in three parts. When the chamber was filled, the torque successively

decreased which can be attributed to the melting of material and at a certain time a constant value is achieved which indicates that the duration of processing is sufficient. Plastograms of other prepared samples are very similar to plastogram of AGENACOMP [10].

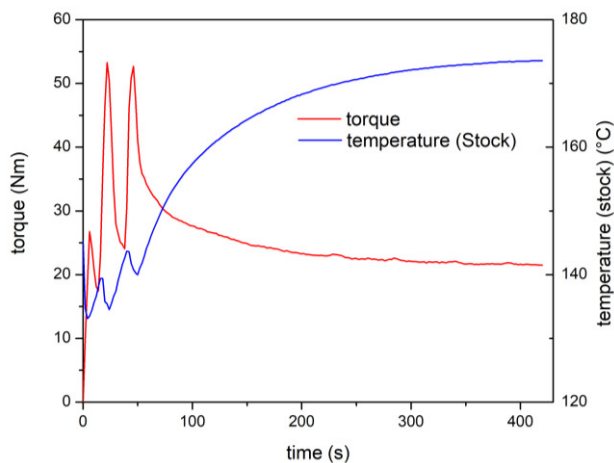


Fig. 1 Plastogram of preparation of AGENACOMP without nanofiller

Melt flow index measurements provide very important information about rheological properties and quality of studied material. MVR value of AGENACOMP® F40 listed in material datasheet is 2 cm³/10 min while the value of material after extrusion is 2.8 cm³/10 min. An increase in MVR value indicates a degradation of initial material which is an undesirable effect. The prepared nanocomposite should have MVR value close to the value in the datasheet which indicates negligible material degradation. The MVR values for all samples studied are between 2 and 3.2 g/10 min (Fig. 2). Materials with this range of MVR values can be processed by extrusion, injection and rotational molding. By addition of 0.1% of halloysite nanofiller, an increase in MVR value is observed. Higher MVR value indicates lower viscosity compared to initial AGENACOMP material. It could be caused by the degradation of polymer material during nanocomposite preparation. With increasing filler content, a decrease in MVR value is observed which indicates an increase in viscosity. A decrease in MVR value also indicates improvement in quality of nanocomposite for samples with 0,2% and higher percentage of halloysite content compared to pure matrix [8], [11], [12].

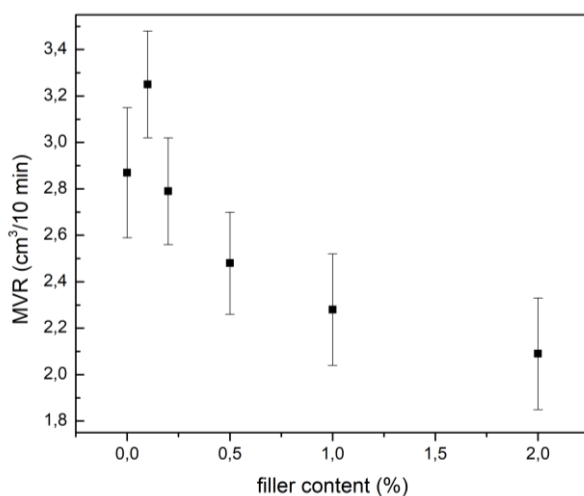


Fig. 2 MVR value vs. filler content of studied samples

Mechanical testing provides information on the elongation at break (ϵ_M) of studied samples (Fig. 3). With increasing

halloysite content, a decrease in elongation at break is observed. A decrease is more conspicuous for samples with 1% and 2% filler content. By the addition of 2% nanofiller, the elongation at break decreases from 111% to 50%. The results of mechanical testing confirmed the reinforcing effect of halloysite nanofiller which is probably due to the appropriate dimensions of halloysite nanofiller which can be incorporated in the AGENACOMP matrix [13], [14].

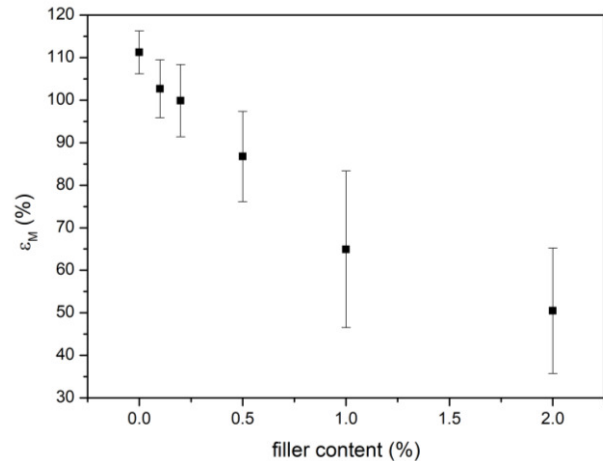


Fig. 3 Results of mechanical testing

IV. CONCLUSION

Melt flow index measurements and mechanical testing were used to study the influence of halloysite nanofiller content on the quality and mechanical properties of AGENACOMP matrix. The results showed that with increasing halloysite content:

- the increase in viscosity is observed,
- the quality of material is improved,
- the halloysite reinforcing effect is confirmed by the decrease in elongation at break.

The future research will be focused on the study of the effect of halloysites with different aspect ratios and other available nanofillers on the quality and mechanical properties of AGENACOMP. The nuclear magnetic resonance measurements will be used to study the influence of nanofiller on structure and molecular mobility of prepared nanocomposites. The obtained data could provide more complex information about prepared nanocomposites and determine their areas of application.

REFERENCES

- [1] M. Megha et al., "Biodegradable polymers – research and applications," in *Physical Sciences Reviews*, vol. 9, no. 2, 2024, 949-972.
- [2] T. Jiang et al., "Starch-based biodegradable materials: Challenges and opportunities," in *Adv. Industrial Engineering Polym. Res.* Vol. 3, no. 1, 2020, 8-18.
- [3] S. B. M. Diah et al., "Towards Sustainable Food Packaging: A Review of Thermoplastic Starch (TPS) as a Promising Bioplastic Material, its Limitation, and Improvement Strategies with Bio-fillers and Essential Oils," in *J. of Adv. Res in Fluid Mechanics and Thermal Sciences*. vol. 119, no. 1, 2024, 80-104.
- [4] A. Surendren et al., "A review of biodegradable thermoplastic starches, their blends and composites: recent developments and opportunities for single-use plastic packaging alternatives," in *Green Chemistry*. vol. 24, 202, 8606-8636.
- [5] AGRANA, AGENACOMP® F40 – Technical Datasheet.
- [6] K. E. Rivadeneita-Velasco et al., "Green Nanocomposites Based on Thermoplastic Starch: A Review," in *Polymers*. vol. 13, no. 19, 2021, 3227.
- [7] K. M. Dang et al., "Morphology and properties of thermoplastic starch blended with biodegradable polyester and filled with halloysite nanoclay," in *Carbohydrate Polymers*, vol. 242, 2020, 116392.

- [8] J. Vlachopoulos, D. Strutt, "Polymer processing," in *Materials Science and Technology*, vol. 19, 2003, 1161-1169.
- [9] D.S. Lai et al., "Mechanical Properties of Thermoplastic Starch Biocomposite Films with Hybrid Fillers," in *J. of Physics: Conference Series*, vol. 2080, 2021, 012011.
- [10] D. Nestler et al., "An innovative production method of a C/CSiC break disc, suitable for a large-scale production," in *International Munich Chassis Symposium*, 2015, 1-23.
- [11] A. V. Shenoy, D. R. Saini, "Melt flow index: More than just a quality control rheological parameter. Part I.," in *Adv. in Polymer technology*. Vol. 6, no. 1, 1986, 1-58.
- [12] A. V. Shenoy, D. R. Saini, "Melt flow index: More than just a quality control rheological parameter. Part II.," in *Adv. in Polymer technology*. Vol. 6, no. 2, 1986, 125-145.
- [13] K. M. Dang et al., "Morphology and properties of thermoplastic starch blended with biodegradable polyester and filled with halloysite nanoclay," in *Carbohydrate Polymers*, vol. 242, 2020, 116392.
- [14] T. S. Gaaz et al., "The Impact of Halloysite on the Thermo-Mechanical Properties of Polymer Composites," in *Molecules*, vol. 22, no. 5, 2017, 838.

Video Compression Using Radiance Fields for V2I Communication

¹Matúš DOPIRIAK (3rd year),

Supervisor: ²Juraj GAZDA

^{1,2}Dept. of Computers and Informatics, FEI, Technical University of Košice, Slovak Republic

¹matus.dopiriak@tuke.sk, ²juraj.gazda@tuke.sk

Abstract—Connected and autonomous vehicles (CAVs) offload tasks to multi-access edge computing (MEC) servers via vehicle-to-infrastructure (V2I) communication, enabling the vehicular metaverse that digitizes physical environments. Physical-to-virtual (P2V) synchronization through digital twins (DTs) relies on ultra-reliable low-latency communication (URLLC). We introduce radiance field delta video compression (RFDVC), employing radiance field encoders and decoders with distributed radiance fields storing compressed photorealistic 3D scenes. By encoding differences between traffic frames and empty scene frames from the same camera positions, our method efficiently transmits data. Experiments show data savings up to 71% over H.264 and 44% over H.265 codecs under varying conditions, including lighting changes and rain.

Keywords—Autonomous driving, edge computing, radiance fields, video compression.

I. INTRODUCTION

Connected and autonomous vehicles (CAVs) utilize advanced perception modules to process vast sensor data for real-time environmental interpretation, executing computationally intensive tasks such as localization and object detection to ensure safe navigation. To meet these high demands, CAVs offload processing tasks to edge computing servers using vehicle-to-infrastructure (V2I) communication. Major technology companies are investing significantly in transforming physical environments into digital spaces within the metaverse, particularly focusing on vehicular applications [1]. A key challenge is physical-to-virtual (P2V) synchronization [2], which relies on V2I communication utilizing multi-access edge computing (MEC) networks [3] and ultra-reliable low-latency communications (URLLC) [4].

We introduce radiance field (RF) delta video compression (RFDVC) to optimize V2I communication between CAVs and MEC servers. By storing static scene elements in distributed RFs on both the sender and receiver, RFDVC eliminates the need to repeatedly transmit this data. Only the differences, Delta-frames, between actual vehicle frames and RF-frames are encoded and transmitted, reducing redundant data and enhancing compression efficiency. This approach achieves notable throughput savings and reduces latency, which is crucial for real-time communication.

II. RELATED WORK

Deep learning techniques have been employed to enhance P2V synchronization and meet communication requirements through video compression [5]. These methods often focus

on compressing intra frames, which significantly contribute to overall bitrate by using standard video codecs for intra-prediction. Other approaches utilize implicit neural representations to transform individual frames [6], [7] or apply learning-based compression to exploit temporal and binocular redundancy in stereo videos [8].

Since 2020, neural radiance fields (NeRFs) [9] have advanced 3D scene reconstruction, enabling digital twin (DT) applications without the need for LiDAR data transmission over MEC networks. By employing implicit depth prediction through volumetric rendering, NeRFs generate novel views from sparse input data, encoded as multi-layer perceptrons (MLPs) and rendered via volumetric ray-marching. Recent developments of RFs, such as instant neural graphics primitives (INGP) [10] and 3D gaussian splatting (3DGS) [11], have reduced training and rendering times while enhancing accuracy.

Traditional RF methods in autonomous driving (AD) face scalability challenges, resulting in visual artifacts and reduced fidelity in large outdoor environments [12]. To address this, Block-NeRF [13] decomposes extensive scenes into multiple compact, independently trained NeRFs. However, recent solutions for large-scale scenes are hindered by significant computational demands [14], [15].

III. EXPERIMENTAL RESULTS

RFDVC provides data savings over H.264 and H.265 codecs via its lossy compression scheme. In URLLC applications, frames are sent in small batches at 30 FPS for real-time communication. Dynamic objects (e.g., vehicles or pedestrians) are segmented as RGB masks, with the background as black pixels, termed Delta-frames. RFDVC uses adaptive quantization to compress black regions efficiently, balancing data reduction and quality. The 3DGS model achieves a peak signal-to-noise ratio (PSNR) of 28.94 and structural similarity index measure (SSIM) of 0.86. Delta-frame encoding with ground truth (GT) RGB masks sets a compression efficiency upper bound, compared to our delta segmentation (DS) algorithm, which uses the segment anything model (SAM) to segment dynamic objects.

Fig. 1 presents a box plot comparing the data savings of RFDVC and video coding (VC) when employing either the DS algorithm or GT masks for transmitting camera sensor data under noon, evening, and wet conditions. The static RF models used do not precisely match the actual conditions, leading to

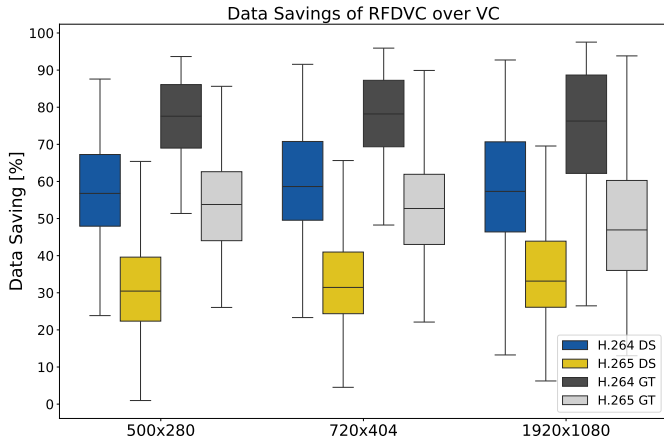


Fig. 1. RFDVC data savings, for both H.264 and H.265-based RFDVC variants, utilizing masks obtained using DS method and GT masks in noon, evening and wet conditions. H.264-based RFDVC savings are measured relative to plain H.264 maskless frame compression, while H.265-based RFDVC savings are measured relative to plain H.265 codec.

lighting discrepancies, especially notable in wet scenarios. For RFDVC with the DS algorithm, the interquartile range of data savings is 48% to 71% with the H.264 codec and 24% to 44% with the H.265 codec; higher resolutions result in greater savings due to more efficient encoding of larger black regions. Using GT masks, data savings range from approximately 65% to 90% with the H.264 codec and 38% to 63% with the H.265 codec.

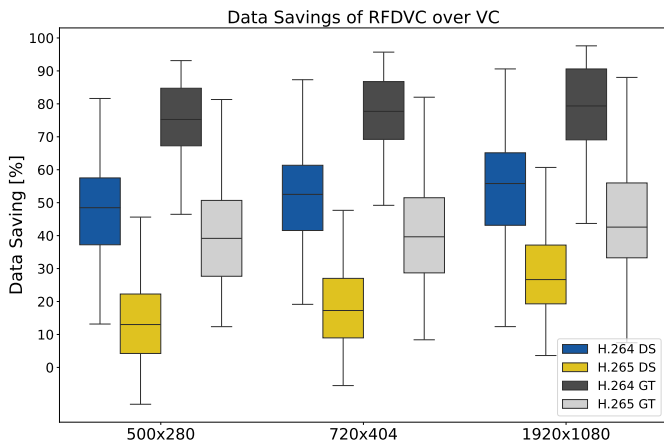


Fig. 2. RFDVC data savings, for both H.264 and H.265-based RFDVC variants, utilizing masks obtained using DS method and GT masks in rainy weather conditions. H.264-based RFDVC savings are measured relative to plain H.264 maskless frame compression, while H.265-based RFDVC savings are measured relative to plain H.265 codec.

Fig. 2 presents the data savings achieved by RFDVC compared to VC under rainy conditions, which are challenging due to significant lighting changes and compression degradation caused by the high-frequency content introduced by heavy rainfall. Despite these difficulties, RFDVC attains data savings within an interquartile range of 39% to 68% using the H.264 codec and 7% to 37% using the H.265 codec. When employing GT masks, the data savings increase to approximately 68% to 90% with H.264 and 29% to 59% with H.265.

IV. CONCLUSION

This work proposes RFDVC approach based on RF-encoder and RF-decoder architecture for V2I communication and P2V

synchronization within the vehicular metaverse. Distributed RFs act as DTs, storing photorealistic 3D scenes in compressed form. The results demonstrate that RFDVC achieves data savings of up to 71% compared to the H.264 codec and 44% compared to the H.265 codec under various conditions, including lighting changes and rain. Future research will focus on pre-processing downstream tasks within the vehicular metaverse and adaptively updating RFs as needed. This strategy aims to minimize latency and improve the accuracy of the virtual environment, thereby optimizing real-time performance for advanced vehicular applications.

ACKNOWLEDGMENT

This work was supported by the Ministry of Education, Science, Research and Sport of the Slovak Republic, and the Slovak Academy of Sciences under Grant VEGA 1/0685/23 and by the Slovak Research and Development Agency under Grant APVV SK-CZ-RD-21-0028 and APVV-23-0512, and by Research and Innovation Authority VAIA under Grant 09I03-03-V04-00395.

REFERENCES

- [1] L. U. Khan, M. Guizani, D. Niyato, A. Al-Fuqaha, and M. Debbah, "Metaverse for wireless systems: Architecture, advances, standardization, and open challenges," *Internet of Things*, vol. 25, p. 101121, 2024.
- [2] M. Xu, D. Niyato, B. Wright, H. Zhang, J. Kang, Z. Xiong, S. Mao, and Z. Han, "EPViSA: Efficient Auction Design for Real-Time Physical-Virtual Synchronization in the Human-Centric Metaverse," *IEEE Journal on Selected Areas in Communications*, vol. 42, no. 3, pp. 694–709, 2024.
- [3] Y. Qiu, M. Chen, H. Huang, W. Liang, J. Liang, Y. Hao, and D. Niyato, "Spotlighter: Backup Age-Guaranteed Immersive Virtual Vehicle Service Provisioning in Edge-Enabled Vehicular Metaverse," *IEEE Transactions on Mobile Computing*, pp. 1–17, 2024.
- [4] H. Alves, G. D. Jo, J. Shin, C. Yeh, N. H. Mahmood, C. H. M. de Lima, C. Yoon, G. Park, N. Rahatheva, O.-S. Park, and et al., "Beyond 5G urllc evolution: New service modes and practical considerations," *ITU Journal on Future and Evolving Technologies*, vol. 3, no. 3, p. 545–554, 2022.
- [5] R. Birman, Y. Segal, and O. Hadar, "Overview of research in the field of video compression using deep neural networks," *Multimedia Tools and Applications*, vol. 79, pp. 11 699–11 722, 2020.
- [6] Y. Zhang, T. van Rozendaal, J. Brehmer, M. Nagel, and T. Cohen, "Implicit neural video compression," *arXiv preprint arXiv:2112.11312*, 2021.
- [7] A. Ghorbel, W. Hamidouche, and L. Morin, "NERV++: An Enhanced Implicit Neural Video Representation," 2024.
- [8] Z. Chen, G. Lu, Z. Hu, S. Liu, W. Jiang, and D. Xu, "LSVC: A learning-based stereo video compression framework," in *Proceedings of the IEEE/CVF Conference on Computer Vision and Pattern Recognition*, 2022, pp. 6073–6082.
- [9] B. Mildenhall, P. P. Srinivasan, M. Tancik, J. T. Barron, R. Ramamoorthi, and R. Ng, "NeRF: Representing Scenes as Neural Radiance Fields for View Synthesis," in *Computer Vision – ECCV 2020*, A. Vedaldi, H. Bischof, T. Brox, and J.-M. Frahm, Eds. Cham: Springer International Publishing, 2020, pp. 405–421.
- [10] T. Müller, A. Evans, C. Schied, and A. Keller, "Instant neural graphics primitives with a multiresolution hash encoding," *ACM Transactions on Graphics (ToG)*, vol. 41, no. 4, pp. 1–15, 2022.
- [11] B. Kerbl, G. Kopanas, T. Leimkühler, and G. Drettakis, "3D Gaussian Splatting for Real-Time Radiance Field Rendering," 2023.
- [12] "Neural Radiance Field in Autonomous Driving: A Survey, author=Lei He and Leheng Li and Wenchao Sun and Zeyu Han and Yichen Liu and Sifa Zheng and Jianqiang Wang and Keqiang Li," 2024.
- [13] M. Tancik, V. Casser, X. Yan, S. Pradhan, B. P. Mildenhall, P. Srinivasan, J. T. Barron, and H. Kretzschmar, "Block-NeRF: Scalable Large Scene Neural View Synthesis," in *2022 IEEE/CVF Conference on Computer Vision and Pattern Recognition (CVPR)*, 2022, pp. 8238–8248.
- [14] R. Li, S. Fidler, A. Kanazawa, and F. Williams, "NeRF-XL: Scaling NeRFs with Multiple GPUs," 2024.
- [15] B. Kerbl, A. Meuleman, G. Kopanas, M. Wimmer, A. Lanvin, and G. Drettakis, "A Hierarchical 3D Gaussian Representation for Real-Time Rendering of Very Large Datasets," *ACM Transactions on Graphics*, vol. 43, no. 4, July 2024.

Optimizing Wireless Robotics Using NeRF and RIS

¹Miroslav IMRICH (*1st year*),
Supervisor: ²Juraj GAZDA

^{1,2}Department of Computers and Informatics, FEI, Technical University of Košice, Slovak Republic

¹miroslav.imrich@tuke.sk, ²juraj.gazda@tuke.sk

Abstract—Achieving full signal coverage for any device or robot, regardless of their location within a factory, would significantly improve operational efficiency and ensure seamless communication in complex industrial environments. In this work, we present dynamic neural radiance fields (NeRF) and reconfigurable intelligent surfaces (RIS), focusing on their fundamental principles and operation, recent advances, and practical applications. The right synergy between these two fields offers enormous potential for optimal wireless communication in the environment of wireless robotics and achieving the aforementioned goal.

Keywords—Dynamic neural radiance fields, reconfigurable intelligent surfaces, wireless robotics.

I. INTRODUCTION

The collaboration of various robotic systems and devices within a factory requires fast and efficient wireless communication. In industrial environments, communication is significantly limited due to the numerous obstacles present in the surroundings. In many cases, direct communication is not possible due to the lack of line-of-sight (LoS) between robotic systems. Since high-frequency wireless communication is difficult to pass through obstacles, it is crucial to find indirect paths, utilizing reflections around obstacles.

To effectively reflect high-frequency electromagnetic waves for wireless communication in the dynamic environment of a factory, it is crucial to know the precise location and timing of the signal receiver. Using dynamic NeRF [1], we can obtain high-quality 3D reconstructions of dynamic scenes and determine the position of the receiver at any given moment.

For optimal communication, RIS [2] can then be employed. Based on the physical properties of waves and the information about the receiver's location, RIS reflects electromagnetic waves directly to the receiver. The implementation of such a synergy between these two fields could be the next step toward achieving an autonomous factory.

II. DYNAMIC NEURAL RADIANCE FIELDS

Dynamic NeRF, like D-NeRF [1], add a temporal component to the original NeRF framework [3] in order to model 3D scenes that change over time. Unlike the static NeRF, which represents fixed scenes by translating the spatial coordinates and the view angle to the radiance and volume density, Dynamic NeRF employs a deformation network that learns a mapping between dynamic spatial coordinates and the canonical space where the object is rendered in the reference position. The second network is responsible for reconstructing the RF out of the canonical space and transforming it to the scene at some time t , which enables representation of the scene in 4D. This enables Dynamic NeRF to capture

and reproduce scenes of objects in rigid or non-rigid motion super realistically without multi-view cameras or ground-truth 3D data. Even more detail and accuracy facilitates real-time scene reconstruction, motion representation, and object tracking through monocular image optimization.

A. Mathematical Formulation

A standard NeRF [3] models a static 3D scene as a continuous function F_{Θ} that maps spatial location and viewing direction to color and density:

$$F_{\Theta} : (\mathbf{x}, \mathbf{d}) \rightarrow (\mathbf{c}, \sigma), \quad (1)$$

where $\mathbf{x} = (x, y, z)$ represents a spatial location in 3D space, $\mathbf{d} = (\theta, \phi)$ represents the viewing direction, $\mathbf{c} = (r, g, b)$ is the color emitted from \mathbf{x} along \mathbf{d} , σ represents the volume density at \mathbf{x} .

A pixel color is rendered by integrating the radiance along a camera ray using the classical volume rendering [4] equation:

$$C(\mathbf{r}) = \int_{t_n}^{t_f} T(t) \sigma(\mathbf{r}(t)) \mathbf{c}(\mathbf{r}(t), \mathbf{d}) dt, \quad (2)$$

where t_n and t_f are near and far bounds, $T(t)$ is the accumulated transmittance defined by the formula:

$$T(t) = \exp\left(-\int_{t_n}^t \sigma(\mathbf{r}(s)) ds\right), \quad (3)$$

which accounts for occlusion and light absorption along the ray.

To model time-dependent deformations in dynamic scenes, D-NeRF [1] introduces time as an additional input t , modifying the radiance field to:

$$F_{\Theta} : (\mathbf{x}, \mathbf{d}, t) \rightarrow (\mathbf{c}, \sigma). \quad (4)$$

Temporal redundancy cannot be properly exploited by just knowing this function. Rather, D-NeRF breaks down the issue into two main blocks:

- 1) Points in the dynamic scene are mapped to a canonical space via a deformation field Ψ_t :

$$\Psi_t : (\mathbf{x}, t) \rightarrow \Delta \mathbf{x}, \quad (5)$$

where $\Delta \mathbf{x}$ is the displacement that transforms the point \mathbf{x} at time t into the canonical space.

- 2) In the canonical frame, a canonical radiance field Ψ_x that predicts color and density:

$$\Psi_x : (\mathbf{x} + \Delta \mathbf{x}, \mathbf{d}) \rightarrow (\mathbf{c}, \sigma). \quad (6)$$

Fig. 1 depicts these two blocks.

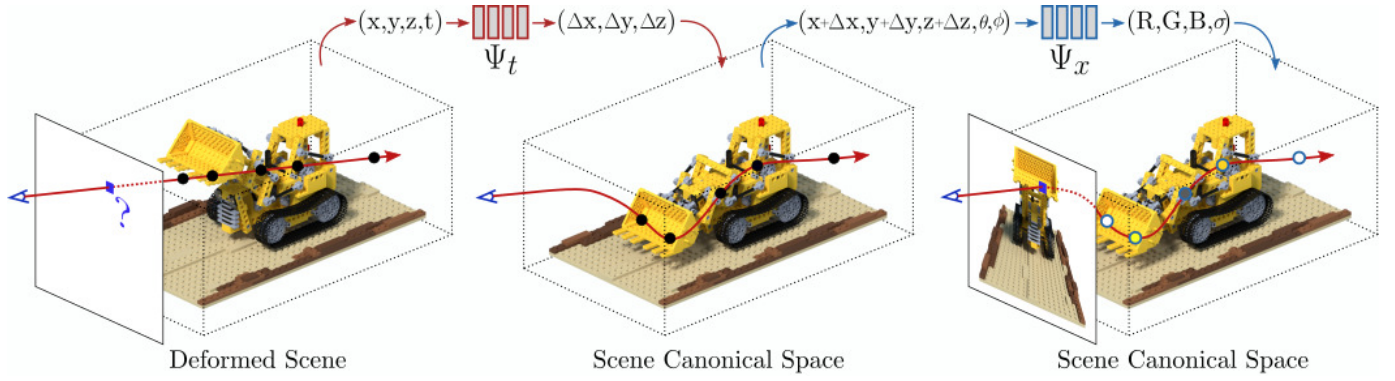


Fig. 1: Main blocks of the D-NeRF model [1]. The model comprises a deformation field Ψ_t , which maps scene deformations to a canonical space, and a canonical field Ψ_x , which predicts volume density and view-dependent color for rendering dynamic scenes.

Instead of directly evaluating the radiance field at a deformed spatial position, D-NeRF first maps the point into a canonical reference frame before querying its radiance and density. The final rendering equation is then formulated by incorporating the learned deformation field, ensuring a more coherent representation of dynamic scenes:

$$C(p, t) = \int_{h_n}^{h_f} T(h, t) \sigma(\mathbf{p}(h, t)) c(\mathbf{p}(h, t), \mathbf{d}) dh, \quad (7)$$

where p is pixel at time t , $\mathbf{p}(h, t)$ is the transformed point in the canonical space and $T(h, t)$ represents the accumulated probability that a ray emitted from traverses the scene without interacting with any particle:

$$\mathbf{p}(h, t) = \mathbf{x}(h) + \Psi_t(\mathbf{x}(h), t), \quad (8)$$

$$T(h, t) = \exp\left(-\int_{h_n}^h \sigma(\mathbf{p}(s, t)) ds\right). \quad (9)$$

A reconstruction loss is used to minimize color discrepancies between synthesized and ground-truth pixels. Specifically, the mean squared error loss is employed, defined as:

$$\mathcal{L} = \frac{1}{N_s} \sum_{\mathbf{r} \in R} \left\| \hat{C}(p, t) - C'(p, t) \right\|_2^2, \quad (10)$$

where $\hat{C}(p, t)$ is the ground-truth pixel color, and $C'(p, t)$ is the predicted pixel color at pixel p and time t . The loss is averaged over N_s sampled rays to ensure accurate color reconstruction and temporal consistency in dynamic scenes.

Scalar input values are mapped into a higher-dimensional space via positional encoding to improve the neural network's representational power. The network can record fine-grained spatial and temporal features thanks to positional encoding, which applies a set of sinusoidal adjustments because typical multilayer perceptrons find it difficult to learn high-frequency fluctuations when using raw coordinate inputs. The encoding function $\gamma(p)$ is defined as:

$$\gamma(p) = (\sin(2^l \pi p), \cos(2^l \pi p))_{l=0}^{L-1}, \quad (11)$$

where p represents the input coordinate, such as spatial location, view direction or time, l is the frequency index. L is the number of frequency bands used in the encoding.

B. Recent Advances

New architectures such as Instant-NGP [5] and FastNeRF [6], which maximize hash encoding and grid-based representations to speed up training and rendering, have greatly increased the efficiency of Dynamic NeRF. These methods enhance the practical application of NeRF by enabling models to deliver realistic, high-quality scene reconstructions in real time.

D-NeRF [1] and Neural Scene Flow Fields [7] use motion fields which can express complex scene deformations more accurately. The advancements of a fully convolutional approach extend this capability to maintain high temporal coherence with realistic moving objects, providing physically accurate representations of reconstructed physical environments.

NeRFflow [8] enhances motion coherence and minimizes artifacts in dynamic settings by incorporating optical flow estimation into NeRF-based systems. NeRFflow improves scene understanding in situations where object motion is irregular or non-rigid by fusing radiance fields with scene flow estimation.

K-Planes [9] is an innovative approach for modeling 3D scenes that is both scalable and extremely effective in the field of neural scene representations. By expanding on the ideas of grid-based representations and tensor decomposition, this method greatly increases memory usage and computing efficiency. K-Planes is a significant advancement in the high-fidelity, real-time representation of complicated 3D environments.

TiNeuVox [10] employs a voxel-based representation that enables real-time updates of NeRF models, significantly improving NeRF's ability to adapt to changes in the environment. Similarly, NeRFPlayer [11] is designed for smooth and interactive dynamic scene rendering, optimizing efficiency through adaptive temporal encoding. By combining TiNeuVox's real-time adaptability with NeRFPlayer's efficient playback, these methods enhance NeRF's usability in robotics, AR/VR, and real-time simulations. Key development in real-time scene perception is the integration of NeRF with simultaneous localization and mapping (SLAM), a development that enhances both spatial understanding and real-time mapping capabilities. NeRF-SLAM [12] synthesizes NeRF's high-fidelity implicit scene representation with SLAM's capability for camera pose estimation and environmental mapping, thereby addressing critical limitations of traditional SLAM methodologies. Conventional SLAM systems, particularly those relying on feature-based methods, often encounter challenges in environments with complex geometries, non-Lambertian surfaces, lighting variations and textureless regions.

III. RECONFIGURABLE INTELLIGENT SURFACES

RIS [2] have become a promising technology to transform wireless communication environments. RIS are almost passive devices that may dynamically modify the phase shifts, reflection angles, and polarization to efficiently control signal propagation.

A. Fundamentals

Electromagnetic wave manipulation serves as the foundation for optimizing wireless communication through RIS. One of the basic principles of RIS is passive beamforming [13], where the surface intelligently reflects incident signals in the direction of interest without active power amplification. This relies on the precise manipulation of phase shifting of discrete elements, leading to constructive or destructive interference for enhancing signal strength or canceling interference. Programmable wavefront engineering [14] is another key principle of RIS, enabling real-time adaptation to changing wireless environments. By applying external control devices such as gateways, microcontrollers, and inter-cell communication networks, combined with advanced optimization algorithms, RIS have the ability to dynamically manage signal reflections to enhance the quality of signals, eliminate interference, and enhance spectral efficiency. This real-time tunability allows RIS to optimize electromagnetic wave propagation, directing signals to their destinations and saving energy.

When the signal arrives at the receiver through two possible paths [15], namely the direct path from the transmitter and the reflected path via a RIS. The RIS consists of N meta-surfaces, each of which can independently adjust the angle and phase of the reflected wave through its reflection coefficient R_i and phase shift $\Delta\phi_i$, the received signal power P_r at the receiver is calculated as follows:

$$P_r = P_t \left(\frac{\lambda}{4\pi} \right)^2 \left| \frac{1}{l} + \sum_{i=1}^N \frac{R_i \times e^{-j\Delta\phi_i}}{r_{1,i} + r_{2,i}} \right|^2, \quad (12)$$

where P_t is the initial power of the signal emitted by the transmitter, signal wavelength is denoted by λ and l represents the direct distance between the transmitter and the receiver. The distances $r_{1,i}$ and $r_{2,i}$ correspond to the path from the transmitter to the i -th meta-surface and from the i -th meta-surface to the receiver, respectively.

B. Design and Architecture

A typical RIS architecture [16] built with metamaterials includes a control unit that can be either single-layer or multi-layer, as well as a planar surface, as illustrated in Fig. 2 a). A three-layer RIS design [17], for example, consists of a bottom circuit board that controls the reflection coefficients using a smart processor, such as a field programmable gate array (FPGA), a middle copper layer that stops signal and energy leakage, and an outer layer with several reflecting elements printed on a dielectric substrate to manipulate incident signals. Typically, the base station (BS) uses channel state information (CSI) to determine the ideal reflection coefficients, which are then sent to the RIS controller via a feedback link. Frequent changes are not necessary because the CSI updates take place over a far longer duration than the transmission of data symbols. Each reflecting element, as shown in Fig. 2 a), incorporates a positive-intrinsic-negative (PIN) diode. By

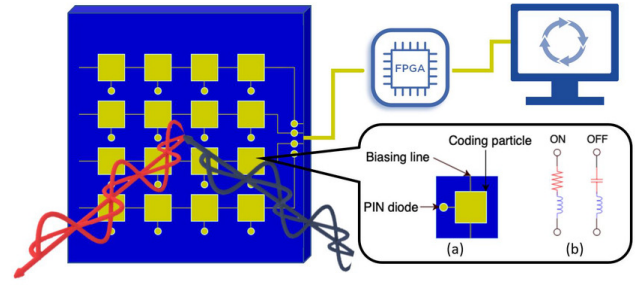


Fig. 2: RIS's architecture [16] with reflecting elements controlled by PIN diodes to produce a phase shift of π radians.

adjusting the biasing voltage, the PIN diode switches between "on" and "off" states, producing a phase shift of π in radians [18], as illustrated in Fig. 2 b). To achieve more precise phase control, multiple PIN diodes can be integrated into a single reflecting element.

C. Current Applications

Robust wireless communication is crucial for mobile robots in industrial settings [19], but obstacles like walls and machinery disrupt signals, causing unreliable connectivity. Traditional solutions, such as additional base stations, increase complexity and energy use. RIS offers an efficient alternative by intelligently reflecting signals to optimize pathways, ensuring stable connections. Strategically placed RIS panels enhance mmWave communication, reducing energy consumption while maintaining seamless connectivity. This technology improves both data transmission and real-time control, essential for autonomous robotic operations.

Accurate localization [20] is essential for autonomous systems in indoor settings like warehouses and smart factories, but traditional methods suffer from signal degradation due to multipath interference. RIS technology enhances positioning by optimizing signal reflections, reducing errors, and enabling precise tracking of robots and vehicles. This is particularly beneficial in logistics and healthcare, where real-time asset tracking is crucial. Studies show RIS-assisted localization can achieve sub-meter accuracy, outperforming conventional methods.

In hybrid aerial and ground-based vehicular communication [21], RIS fall under the wireless communication technologies that enhance efficient wireless communication, particularly on high-frequency bands. This solution has the ability to boost coverage, lower out of factors that result in outages, and maximize the reliability of the connection by intelligently redirecting signals, especially in urban settings. The integration of RIS with intelligent transportation systems allows for dynamic network optimization through the strategic deployment of RIS on vehicles, unmanned aerial vehicles and fixed infrastructure.

IV. SYNERGY OF DYNAMIC NeRF, RIS AND FUTURE DIRECTIONS

The synergy of dynamic NeRF and RIS enables intelligent real-time adaptation of the environment, with dynamic tracking of objects to optimize signal direction even in challenging non-line-of-sight (NLoS) environments. Their integration enhances wireless communication quality, enables more efficient reconstruction of scenes, and enables the development of new applications in autonomous systems, intelligent networks

and immersive technologies. This approach offers new opportunities for precise signal control, lowering computational complexity, and enriching physical-digital world interaction.

With dynamic NeRF, most of the problems have been addressed, significantly improving existing implementations that were previously solved less effectively. The biggest improvements have been in realistic rendering of dynamic scenes, where dynamic NeRF can successfully reconstruct dynamic objects with high quality and without artifacts. The other major progress is also efficient depiction of movement, allowing continuous rendering of deforms and natural transformations in an environment without separate rendering of each frame. Dynamic NeRF have also greatly increased data compression and storage as, instead of requiring a huge amount of input images, they learn with a neural network from merely a few frames without the requirement for large storage space and its resultant computational costs.

The application of RIS has managed to address most of the fundamental wireless communication issues that previously limited the reliability and efficiency of networks. One of the most significant RIS accomplishments is overcoming NLoS limitations, enabling signal redirection through obstacles, thus eliminating traditional losses through buildings, walls or cars. Another issue addressed is reducing network energy consumption. RIS operates passively with no requirement for signal amplification, thus offering less power consumption than active relay stations and amplifiers. Spectral efficiency has also been enhanced because RIS supports intelligent steering of signals to the receiver, which creates negligible interference and increased usage of available bandwidth in closely packed networks. In addition, RIS has enabled precise beamforming for authorized users with better network capacity planning and higher quality of connection even in mobile and dynamic networks. All these improvements have already improved the performance of satellite and mobile networks, provided more stable links to IoT devices, and built a basis for 6G network construction and intelligent communication systems.

The integration of dynamic NeRF and RIS is a promising but not yet fully investigated area that can significantly enhance existing implementations and facilitate new application scenarios. In this combination, we see future research being used in dense indoor settings such as factory plants and industrial areas, where numerous devices, robots, and mobile workers generate dynamic and challenging wireless communication environments. By reconstructing normal motion patterns of individual objects using models of dynamic NeRF, their trajectories can be predicted more precisely in real time. With this information, RIS would then be able to smartly direct wireless signals towards objects in motion, offering stable and high-quality links even in very dense settings with constant changes. Future research may focus on optimizing wireless network efficiency and sensor reliability in dynamic environments through this integration.

V. CONCLUSION

This paper highlighted the fundamentals of dynamic NeRF and RIS. Since this synergy has not yet been extensively explored, it presents the idea for future research and work, suggesting that their integration could offer highly effective solutions to practical challenges in complex environments.

ACKNOWLEDGMENT

This work was supported by the Ministry of Education, Science, Research and Sport of the Slovak Republic, and the Slovak Academy of Sciences under Grant VEGA 1/0685/23 and by the Slovak Research and Development Agency under Grant APVV SK-CZ-RD-21-0028 and APVV-23-0512, and by Research and Innovation Authority VAIA under Grant 09I03-03-V04-00395.

REFERENCES

- [1] A. Pumarola, E. Corona, G. Pons-Moll, and F. Moreno-Noguer, "D-NeRF: Neural Radiance Fields for Dynamic Scenes," 2020.
- [2] Y. Liu, X. Liu, X. Mu, T. Hou, J. Xu, M. Di Renzo, and N. Al-Dhahir, "Reconfigurable Intelligent Surfaces: Principles and Opportunities," *IEEE Communications Surveys & Tutorials*, vol. 23, no. 3, pp. 1546–1577, 2021.
- [3] B. Mildenhall, P. P. Srinivasan, M. Tancik, J. T. Barron, R. Ramamoorthi, and R. Ng, "NeRF: Representing Scenes as Neural Radiance Fields for View Synthesis," 2020.
- [4] J. T. Kajiya and B. P. Von Herzen, "Ray Tracing Volume Densities," in *Proceedings of the 11th Annual Conference on Computer Graphics and Interactive Techniques*, ser. SIGGRAPH '84. New York, NY, USA: Association for Computing Machinery, 1984, p. 165–174.
- [5] T. Müller, A. Evans, C. Schied, and A. Keller, "Instant Neural Graphics Primitives with a Multiresolution Hash Encoding," *ACM Transactions on Graphics*, vol. 41, no. 4, p. 1–15, Jul. 2022.
- [6] S. J. Garbin, M. Kowalski, M. Johnson, J. Shotton, and J. Valentin, "FastNeRF: High-Fidelity Neural Rendering at 200FPS," 2021.
- [7] Z. Li, S. Niklaus, N. Snavely, and O. Wang, "Neural Scene Flow Fields for Space-Time View Synthesis of Dynamic Scenes," 2021.
- [8] Y. Du, Y. Zhang, H.-X. Yu, J. B. Tenenbaum, and J. Wu, "Neural Radiance Flow for 4D View Synthesis and Video Processing," 2021.
- [9] S. Fridovich-Keil, G. Meanti, F. Warburg, B. Recht, and A. Kanazawa, "K-Planes: Explicit Radiance Fields in Space, Time, and Appearance," 2023.
- [10] J. Fang, T. Yi, X. Wang, L. Xie, X. Zhang, W. Liu, M. Nießner, and Q. Tian, "Fast Dynamic Radiance Fields with Time-Aware Neural Voxels," in *SIGGRAPH Asia 2022 Conference Papers*, ser. SA '22. ACM, Nov. 2022.
- [11] L. Song, A. Chen, Z. Li, Z. Chen, L. Chen, J. Yuan, Y. Xu, and A. Geiger, "NeRFPlayer: A Streamable Dynamic Scene Representation with Decomposed Neural Radiance Fields," *IEEE Transactions on Visualization and Computer Graphics*, vol. 29, no. 5, pp. 2732–2742, 2023.
- [12] A. Rosinol, J. J. Leonard, and L. Carlone, "NeRF-SLAM: Real-Time Dense Monocular SLAM with Neural Radiance Fields," 2022.
- [13] Q. Wu, S. Zhang, B. Zheng, C. You, and R. Zhang, "Intelligent Reflecting Surface-Aided Wireless Communications: A Tutorial," *IEEE Transactions on Communications*, vol. 69, no. 5, pp. 3313–3351, 2021.
- [14] M. Di Renzo, A. Zappone, M. Debbah, M.-S. Alouini, C. Yuen, J. de Rosny, and S. Tretjakov, "Smart Radio Environments Empowered by Reconfigurable Intelligent Surfaces: How It Works, State of Research, and The Road Ahead," *IEEE Journal on Selected Areas in Communications*, vol. 38, no. 11, pp. 2450–2525, 2020.
- [15] E. Basar, M. Di Renzo, J. De Rosny, M. Debbah, M.-S. Alouini, and R. Zhang, "Wireless Communications Through Reconfigurable Intelligent Surfaces," *IEEE Access*, vol. 7, pp. 116 753–116 773, 2019.
- [16] C. Pan, H. Ren, K. Wang, J. F. Kolb, M. Elkhassan, M. Chen, M. Di Renzo, Y. Hao, J. Wang, A. L. Swindlehurst, X. You, and L. Hanzo, "Reconfigurable Intelligent Surfaces for 6G Systems: Principles, Applications, and Research Directions," *IEEE Communications Magazine*, vol. 59, no. 6, pp. 14–20, 2021.
- [17] Q. Wu and R. Zhang, "Towards Smart and Reconfigurable Environment: Intelligent Reflecting Surface Aided Wireless Network," *IEEE Communications Magazine*, vol. 58, no. 1, pp. 106–112, 2020.
- [18] T. Cui, M. Qi, X. Wan, J. Zhao, and Q. Cheng, "Coding Metamaterials, Digital Metamaterials and Programmable Metamaterials," *Light: Science & Applications*, vol. 3, p. e218, 2014.
- [19] Z. Liu, Y. Liu, and X. Chu, "Reconfigurable-Intelligent-Surface-Assisted Indoor Millimeter-Wave Communications for Mobile Robots," *IEEE Internet of Things Journal*, vol. 11, no. 1, pp. 1548–1557, 2024.
- [20] S. T. Shah, M. A. Shawky, J. ur Rehman Kazim, A. Taha, S. Ansari, S. F. Hasan, M. A. Imran, and Q. H. Abbasi, "Coded Environments: Data-Driven Indoor Localisation with Reconfigurable Intelligent Surfaces," *Communications Engineering*, vol. 3, p. 66, 2024.
- [21] K. Heimann, B. Sliwa, M. Patchou, and C. Wietfeld, "Modeling and Simulation of Reconfigurable Intelligent Surfaces for Hybrid Aerial and Ground-based Vehicular Communications," 2021.

Correlation Between AMS-02 Data and Space Weather Parameters for Machine Learning Prediction

¹Martin NGUYEN (3rd year),

Supervisor: ²Ján GENČI, Consultant: ³Pavol BOBÍK

^{1,2}Dept. of Computers and Informatics, FEI TU of Košice, Slovak Republic

³Department of Cosmic Physics, Institute of Experimental Physics SAS Kosice, Slovak Republic

¹martin.nguyen@student.tuke.sk, ²jan.genci@tuke.sk, ³bobik@saske.sk

Abstract—The AMS-02 daily proton spectra captured from 2011 to 2019 provide the most precise and comprehensive cosmic rays dataset. The data set consists of almost 3-thousand data points and covers a broad energy range. The availability of such an extensive dataset offers an opportunity to train machine learning algorithms to complement or replace the traditional methods for approximating the cosmic ray proton spectrum. This study examines the linear correlation between the AMS-02 dataset and space weather parameters obtained from NMDB and OMNIWeb. If there is a linear correlation, correlation-based feature selection can be applied and also linear machine learning models may be suitable for our use case.

Keywords—Linear Regression, AMS-02, Correlation Analysis, Machine Learning

I. INTRODUCTION

Cosmic rays play an important role in space physics. They are high-energy particles that have implications in various areas, including satellite operations [1], [2], human [3], [4], [5] and astronaut safety [6], [7], and communication systems [8]. Because of that, predicting and understanding their behavior could be beneficial. One of the most reliable sources for daily cosmic ray spectra is the AMS-02 detector onboard the International Space Station [9].

Forecasting cosmic ray flux has the potential to complement traditional physics-based methods [10], which often struggle with the complexities of the data. This study aims to test, whether there is a linear correlation between the AMS-02 data and space weather parameters. The data sets used in the study focus on solar, interplanetary, and Earth's magnetosphere parameters within the time range that aligns with the AMS-02 data, from 2011 to 2019. The parameters were extracted from the OMNIWeb¹ and the NMDB database², which offers data from the Oulu neutron monitor (NM).

II. CORRELATION-BASED FEATURE SELECTION

Feature selection is a critical step in the machine learning process. In Table I, we present the correlation values between the AMS-02 intensity data and the space weather parameters from OMNIWeb and NMDB for the first bin, corresponding to rigidities from 1.00 GV to 1.16 GV. The table shows that some

space weather parameters correlate significantly with the target AMS-02 intensity data, achieving correlation values higher than 0.70. By using these highly correlated features, whether positively or negatively, during model training, we can enhance the performance of linear algorithms. This approach is known as correlation-based feature selection.

TABLE I
CORRELATION OF FEATURES WITH AMS-02 INTENSITIES FOR THE 1. BIN
(RIGIDITIES 1.00-1.16 GV).

Parameter	Correlation with 1. bin (Rigidities 1.00-1.16 GV)
NM Intensity	0.939
Lyman_alpha	-0.869
R (Sunspot No.)	-0.718
Dst-index, nT	0.210
sigma-theta V, degrees	-0.197
RMS_BZ_GSE, nT	-0.191
Scalar B, nT	-0.190
Vector B Magnitude, nT	-0.169
RMS_field_vector, nT	-0.138
RMS_BY_GSE, nT	-0.116
sigma-phi V, degrees	-0.110
ap_index, nT	-0.064
Long. Angle of B (GSE)	0.059
sigma-T, K	-0.059
Kp index	-0.057
BY, nT (GSE)	-0.052
BY, nT (GSM)	-0.049
SW Plasma Speed, km/s	0.040
E electric field	0.040
RMS_BX_GSE, nT	-0.036
Lat. Angle of B (GSE)	-0.033
BZ, nT (GSM)	-0.033
RMS_magnitude, nT	-0.031
SW Plasma flow lat. angle	-0.029
SW Plasma flow long. angle	0.025
SW Plasma Temperature, K	-0.021
BZ, nT (GSE)	-0.013
sigma-V, km/s	-0.003
BX, nT (GSE, GSM)	0.002

We can see a high positive correlation with the feature "NM Intensity" from the Oulu neutron monitor, with a strong positive correlation of 0.939. It indicates a direct and substantial linear relationship. Feature "Lyman_alpha", indicating solar radiation variations, shows a strong negative correlation of -0.869, suggesting that as the Lyman Alpha index decreases, the intensity measured in the first bin increases. Similarly, the parameter for the sunspot number "R" has a negative

¹<https://omniweb.gsfc.nasa.gov/form/dx1.html>

²<https://www.nmdb.eu/>

correlation value of -0.718. This suggests that lower sunspot numbers correspond with higher intensities in the provided bin.

We can see the moderate positive relationship in the "Dst-index, nT" parameter, known as the intensity of geomagnetic storms, with a decent value of 0.210. Even though it is much lower than the first three parameters, it is still a good candidate for inclusion because it suggests it will affect the prediction accuracy. Features like "BX, nT (GSE, GSM)" and "BZ, nT (GSE)", known as components of the magnetic field given in both Geocentric Solar Ecliptic (GSE) and Geocentric Solar Magnetospheric (GSM) coordinates, have correlation values close to zero, suggesting they have almost no linear impact on the target bin. In the correlation-based feature selection, we exclude those features based on the desired threshold.

It is notable that correlations do not imply causation and a high correlation between two variables does not necessarily mean that one causes the other. Other external variables might also influence the feature and the target measurement, and the correlation analysis can overlook potential nonlinear relationships between variables. In a follow-up study, we can recognize such complex interactions with causality feature selection techniques or exploratory data analysis [11].

III. LINEAR REGRESSION FOR APPROXIMATING AMS-02 DATA

Linear regression is a foundational algorithm that aims to find relationships between the independent and target variables through a simple linear equation. We include only the most relevant features with significant relationships in the linear regression model by correlation-based feature selection. By applying linear regression to predict AMS-02 energy bin intensities, we gain a straightforward comparable benchmark against more complex models like XGBoost.

This approach may not capture complex interactions in the data, but it allows us to establish a baseline performance. Even such a simple algorithm can tell how well basic linear assumptions hold in our dataset. When working with multiple features, as is our case, these variables can exist on vastly different scales. To solve this, we employ a preprocessing step to scale the feature space; in our case, we add a pipeline with StandardScaler. This preprocessing step transforms each feature into a mean of zero and a standard deviation of one. Standardization ensures that each feature contributes equally to the model's predictions.

The table II provides a comparison between the R^2 test scores for the linear model using multiple features ($N = 15$) and a single feature ($N = 1$), where we used only the highest correlating NM Intensity feature. As can be seen, when we feed the linear model by multiple features ($N = 15$), it consistently shows higher test R^2 scores across all bins compared to the linear model of single feature ($N = 1$). The performance of the multi-param linear model is very accurate in 8th to 22nd bin, where results surpass the R^2 score of 0.95.

For higher bin numbers, test R^2 scores decrease across both models. Despite lower overall scores for the linear model with single feature ($N = 1$), it performs sufficiently in many bins, especially the initial ones. Having only one feature balances complexity and accuracy. The simplicity of using only one feature, NM Intensity, reduces training and computational complexity.

TABLE II
 R^2 SCORES COMPARISON ON TEST DATA OF 2 LINEAR MODELS FOR DIFFERENT FEATURE SETS COMPARED TO AMS-02 DATA

Bin	N = 15 Linear R^2	N = 1 Linear R^2
1	0.9105	0.8682
2	0.9192	0.8771
3	0.9263	0.8852
4	0.9327	0.8940
5	0.9382	0.9009
6	0.9437	0.9082
7	0.9473	0.9142
8	0.9520	0.9212
9	0.9551	0.9268
10	0.9593	0.9345
11	0.9623	0.9410
12	0.9665	0.9492
13	0.9707	0.9569
14	0.9735	0.9633
15	0.9758	0.9688
16	0.9777	0.9727
17	0.9785	0.9760
18	0.9786	0.9774
19	0.9755	0.9754
20	0.9733	0.9721
21	0.9665	0.9631
22	0.9534	0.9460
23	0.9385	0.9263
24	0.9204	0.8956
25	0.8603	0.7957
26	0.7355	0.6120
27	0.4930	0.2926
28	0.2436	0.0357
29	0.1179	-0.0004
30	0.0579	0.0058

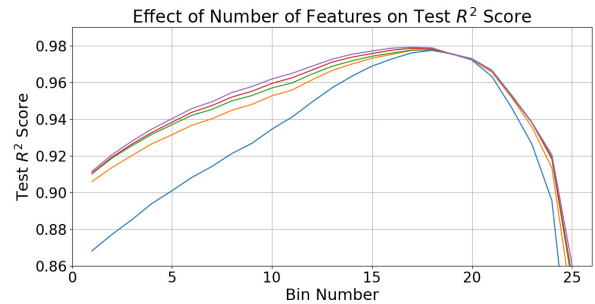


Fig. 1. Effect of number of features on Test R^2 score, where blue indicating $N=1$ features, orange $N=3$, green $N=4$, red $N=15$ and purple $N=25$

In the figure 1 we evaluated the impact of increasing the number of features on model performance across various data bins. By monitoring the Test R^2 scores, we identified specific points where adding more features led to significant improvements. For most bins, a transition from a single feature to two or three features resulted in immediate improvement in performance. From the 4 features, the improvements in the higher number of features were not that significant. This suggests that initial feature additions capture substantial additional information that benefits model predictions, but less correlating parameters do not affect the results that much.

IV. CONCLUSION

Our study explored the relationship between AMS-02 cosmic ray data and various solar and geophysical parameters, aiming to improve the prediction accuracy of cosmic ray intensities through machine learning approaches. Using correlation-based feature selection, we successfully identified critical parameters such as NM Intensity and Lyman Alpha,

which exhibited very strong relationships with the AMS-02 cosmic ray flux.

Linear regression can serve as a baseline for comparing performance with more sophisticated machine learning methods. It effectively captured linear relationships and demonstrated strong results. The linear model utilizing multiple features achieved higher accuracy than the single-feature model, with the R^2 score exceeding 0.95 in several bins. An analysis of the feature count revealed that improvements in prediction scores occur when more than three features are incorporated. Adding more than four features continues to enhance the prediction score, but these improvements become less substantial.

This study's findings indicate that even basic feature selection methods can be highly effective. Future research should investigate more advanced machine learning models, such as XGBoost or neural networks, alongside causality-driven feature selection techniques to uncover deeper correlations between cosmic rays and their complex interactions with solar and geophysical phenomena.

REFERENCES

- [1] H. Köksal, N. Demir, and A. Kilcik, "Analysis of the cosmic ray effects on sentinel-1 sar satellite data," *Aerospace*, vol. 8, no. 3, p. 62, Mar 2021.
- [2] J. Feynman and S. Gabriel, "On space weather consequences and predictions," *Journal of Geophysical Research*, vol. 105, pp. 10 543–10 564, 05 2000.
- [3] F. A. Cucinotta, M. Alp, F. M. Sulzman, and M. Wang, "Space radiation risks to the central nervous system," *Life Sciences in Space Research*, vol. 2, p. 54–69, Jul 2014.
- [4] E. Cekanaviciute, S. Rosi, and S. V. Costes, "Central nervous system responses to simulated galactic cosmic rays," *International Journal of Molecular Sciences*, vol. 19, no. 11, p. 3669, Nov 2018.
- [5] M. Shea and D. Smart, "Cosmic ray implications for human health," *Space Science Reviews*, vol. 93, no. 1/2, p. 187–205, 2000.
- [6] V. S. Kokhan and M. I. Dobynde, "The effects of galactic cosmic rays on the central nervous system: From negative to unexpectedly positive effects that astronauts may encounter," *Biology*, vol. 12, no. 3, p. 400, Mar 2023.
- [7] X. Chen, S. Xu, X. Song, R. Huo, and X. Luo, "Astronaut radiation dose calculation with a new galactic cosmic ray model and the ams-02 data," *Space Weather*, vol. 21, no. 4, Apr 2023.
- [8] S. K. Höeffgen, S. Metzger, and M. Steffens, "Investigating the effects of cosmic rays on space electronics," *Frontiers in Physics*, vol. 8, Sep 2020.
- [9] M. Aguilar, L. Ali Cavazonza, G. Ambrosi, L. Arruda, N. Attig, F. Barao, L. Barrin, A. Bartoloni, S. Başğömez-du Pree, J. Bates, and et al., "The alpha magnetic spectrometer (ams) on the international space station: Part ii — results from the first seven years," *Physics Reports*, vol. 894, p. 1–116, Feb 2021.
- [10] M. Potgieter, "Solar modulation of cosmic rays," *Living Reviews in Solar Physics*, vol. 10, 2013.
- [11] K. Yu, X. Guo, L. Liu, J. Li, H. Wang, Z. Ling, and X. Wu, "Causality-based feature selection," *ACM Computing Surveys*, vol. 53, no. 5, p. 1–36, Sep 2020.

Power Module Packaging Technology Trends

¹Peter NEMERGUT (1st year)
Supervisor: ²Alena PIETRIKOVÁ

^{1,2}Dept. of Technologies in Electronics, FEI, Technical University of Košice, Slovak Republic

¹peter.nemergut@tuke.sk, ²alena.pietrikova@tuke.sk

Abstract— The biggest challenges in power module packaging are to ensure high level of module reliability, to achieve the best possible thermal management and heat dissipation, to miniaturize the modules and to optimize the resulting product price. This article reviews the current technological solutions in the field of power module packaging and describes the individual technological operations. Also, it discusses the current trends in the field of power module packaging and identifies some individual problems.

Keywords—power module, power electronics, packaging, DBC, solder foil

I. INTRODUCTION

Currently, we can see that the areas of use of power electronics are increasing. Frequently used devices are power modules. The power electronic module, or power module for short, consists of several power components that create a functional unit. The power module may also include thermal protection or additional electronics. The use of power modules is especially in high-power applications, such as high-power converters for electric (EV) and hybrid vehicles (HEV), energy storage systems (ESS), solar electricity production, motor and traction drives, uninterruptible power supplies (UPS) and smart systems.

II. LITERATURE REVIEW AND ANALYSIS

Power modules are the basis of many applications that require high performance. Power modules can have different size, shape and construction according to the type of use and function (e.g., IGBT, MOSFET, diode or thyristor) [1].

The basic structure of the power module (Fig. 1) consists of several dies (silicon chips), solders, DBC (direct bonded copper) substrates, solder foils (preform), TIM (thermal interface material), heatsink, wire bonds and terminals.

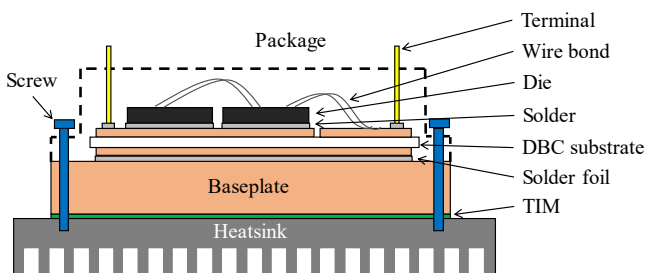


Fig. 1 Typical structure of the power module.

The subject of power module packaging research is to solve several problems. Among them we can include the distribution of temperature fields, the incompatibility of materials due to

different coefficients of thermal expansion (CTE) (Tab. I) and many other material-technological aspects.

TABLE I
CTE OF POWER MODULE COMPONENTS [2]

Component	Material	CTE (10 ⁻⁶ /K)
Bond wire	Aluminum	23
Metallization layer	Aluminum	23
Die	Si/SiC	3/3.4
Die solder	96.5Sn3.0Ag0.5Cu	21
DBC	Copper	17
	Ceramics (Al ₂ O ₃ /AlN)	6.5/5.2
	Copper	17
Substrate solder	96.5Sn3.0Ag0.5Cu	21
Baseplate	Cooper	17
TIM	-	-
Heatsink	Aluminum	23

The manufacturing process includes several technological processes, with each procedure having specific requirements. A solder is used as the basic connection element of individual components in power modules, which is a long-term reliable solution. The solder paste is used between the die and the DBC substrate, which is applied to the DBC substrate with a stencil. After fitting the die on the solder paste, the solder paste is reflowed. After cooling, a joint is formed between die and the DBC substrate.

The electrical wiring between the dies (e.g., IGBT and diode) or die and DBC is provided by Al or AlSi ultrasonic wire bonding process [2]. The solder foil is used to create a large-area joint between the DBC substrate and the baseplate.

The baseplate serves as a mechanical support for the power module and can be connected to a heatsink by means of screws for heat removal [3]. The TIM is used between the heatsink and the baseplate for better thermal conductivity. The finished module is closed with housing and filled with silicone gel or epoxy.

A. Substrate

The substrates are mechanical support for dies, ensure electrical insulation and significantly contribute to the heat dissipation process from the power components. The substrates typically consist of insulating material (ceramics) and two conductive layers on the upper and lower sides of the insulating material.

The substrate is based on ceramic material that is characterized by defined thermal conductivity, temperature expansion, density, strength, fracture toughness and Young's modulus. In the formation of substrates, ceramics materials aluminum nitride (AlN), aluminum oxide (Al₂O₃), silicon nitride (Si₃N₄) and zirconia toughened alumina (ZTA or Zr-

Al_2O_3) (Tab. II) are used, on both sides of which a metal layer of defined purity and thickness is attached. These materials are characterized by good resistivity (insulating properties), high thermal conductivity and resistance to cyclic temperature changes, low dielectric loss, good adhesive properties, high strength, and thermal stability.

TABLE II
SELECTED PARAMETERS OF CERAMICS [4],[5]

Material	Bending strength (MPa)	Dielectric strength (kV/mm)	CTE ($10^{-6}/\text{K}$)	Thermal conductivity (W/mK)
Al_2O_3	500	15	7 - 9	24
AlN	450	15	5 - 6	170
ZTA	700	25	7 - 10	27
Si_3N_4	700	25	3 - 4	90

A common type of substrate used for power electronics is DBC. The DBC substrate is made by combining ceramic (typically made of Al_2O_3 or AlN) with copper plates on both sides (Fig. 2). The manufacturing process consists of heating the materials in a nitrogen atmosphere to the eutectic point temperature (1063 - 1083 °C). After cooling, a solid bond is formed between the materials. These substrates provide high thermal conductivity, excellent electrical insulation, and superior reliability, making them ideal for high-power applications such as electric vehicles, power modules, and renewable energy systems. A similar procedure is also used to create DBA substrates, but the temperature of the eutectic point is lower (around 650 °C).

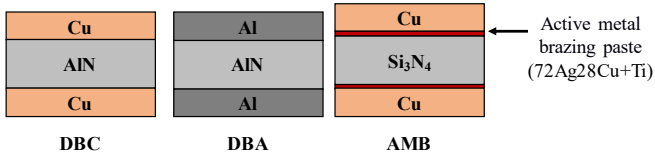


Fig. 2 Structure of DBC, DBA and AMB substrates.

Another type of substrate is AMB (Active Metal Brazing). It is an advanced technology in the field of substrate fabrication for power electronics. A eutectic alloy (e.g. 72Ag28Cu) supplemented with a small amount (2 - 8%) of an active element (e.g. titanium) is used to join the ceramic material (typically Si_3N_4 , but Al_2O_3 or AlN are also used) and the metal layer (most often copper). AMB substrates achieve bonding through a chemical reaction between ceramics and active metal brazing paste at high temperatures (750 - 1000 °C) in vacuum atmosphere [6].

The advantages of using AMB, especially with Si_3N_4 ceramics over DBC are higher mechanical strength and resistance to cracking. Also, AMBs reduce the risk of delamination and have increased resistance to thermal stress. The advanced bonding method minimizes defects, improving the reliability and durability of power modules.

B. Die attach

Attaching a die is the process of attaching a die to a substrate. It is the connection of the die (made of Silicon - Si, Silicon Carbide - SiC or Gallium Nitride - GaN) to the top copper layer of the substrate (e.g., DBC) in dependence on the electrical wiring. The connection between the die and the substrate can be made using a eutectic bond, solder or adhesive. The most used method of making the connection is by using solder in the form of solder paste using a screen-printing process or stencil printing process. Lead-free and especially void-less paste based

on SAC305 or SnAg3.5 is used as standard. Reflow solder paste is usually realized by Vapour Phase Soldering process with a maximum reflow temperature of approximately 260 °C. The basic requirement is almost zero voids. The soldering process is dependent on the amount of paste applied, which must not penetrate beyond the die surface after reflowing. The joints are formed in a precisely controlled process. The dies go through the soldering process twice (the first time when the dies are mounted and the second time when the substrates are mounted). It is important to ensure that the die surface finish is not damaged, and the die delaminated after the second reflow.

A new trend in the field of dies attach is the use of sintering solder paste based on silver particles (nano-Ag paste). [7] The first step in the sintering process (Fig. 3) is to clean the input materials (dies and substrates). The second step is to apply the nano-Ag paste to the substrate surface by screen printing. The third step is to mount the die on the applied nano-Ag paste. After the die is mounted, the thickness of the applied paste may change, which must be considered in the second step. The last step is thermal treatment in two stages: debinding (or paste drying) and sintering (either, with or without pressure) [8].

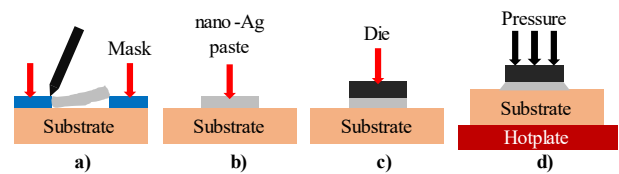


Fig. 3 Sintering die attach process a) dispensing the nano-Ag paste b) nano-Ag paste before die attach c) die attach d) sintering.

The use of nanoparticles reduces the temperature (generally about 300 °C) and pressure during the sintering process. Nano-Ag paste offers better thermal (200 - 250 W/mK) and electrical conductivity over standard solder, improving thermal dissipation and efficiency. It withstands higher temperatures (more than 800 °C) and enables power modules to operate above 200 °C. The sintering process creates void-free, strong, and reliable joints, reducing failure risks. Nano-Ag is lead-free, environmentally friendly, and more fatigue resistant than standard solder paste. It also enables higher performance and better adhesion to materials like Si, SiC, and Cu. Lower processing temperatures (150 - 300 °C) make it suitable for advanced semiconductor applications [9].

C. Electrical interconnection

Wire bonding is a specific type of electrical interconnection where wires (Al, AlSi, Cu, Au) with diameter about of 300 μm , are used to connect the die to the substrate, terminals or lead frame (Fig. 4).

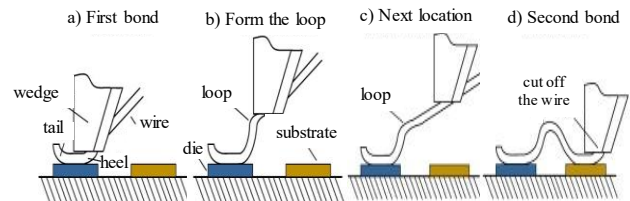


Fig. 4 Standard bonding process [2].

The wires provide electronic interconnection of the individual power components depending on the required function. Because bond wired joints are subjected to thermal cyclic loading, it is important to properly optimize parameters such as material, shape, and wire diameter [3].

Copper generally has higher electrical and thermal conductivity than aluminum. The use of copper results in improved heat dissipation and reduced resistive losses. It has a higher mechanical strength which improves the reliability joint under cyclic thermal loading and increases the life of the module. The use of copper wire bonds also allows the use of smaller diameter wires, making it possible to make a smaller power module design. However, the use of higher force and a precisely defined controlled atmosphere is required when making copper wire connections. The disadvantage of copper is rapid oxidation on the surface. The process of using copper wires is higher in cost. Also, there are special applications where the use of thick wires is required (typically ribbon bonds). For this purpose, the use of copper wire bonds is not suitable due to their hardness [10].

D. Baseplate

The baseplate (thickness 2.5 – 5 mm) is used to provide heat dissipation from the substrate to the external heatsink. It also provides mechanical support for the power module. The most commonly used material for the base plate is high purity copper (>99.95%) with a nickel coating (thickness around 20 μm) that prevents copper oxidation and improves solderability [11]. The surface of the base plate is required to have as little roughness as possible to ensure a good joint formation without voids. Voids create areas of higher temperature which can cause damage to the power module. The baseplates are manufactured with a precisely defined deflection to eliminate the influence of different CTE and to avoid delamination after the remelting process.

The use of copper as the base material for the baseplate is the best solution so far, as copper has very good thermal conductivity. In the past, materials such as aluminum-copper (AlCu) [12] or aluminum silicon carbide (AlSiC) [13] have been investigated. However, the use of nickel-plated copper due to better solderability has proven to be the most optimal.

E. Substrate attach

This is the process by which a bond is formed between the substrate (after wire bonding) and the baseplate. The joint between the substrate and the baseplate is formed by solder, most often in the form of solder foil. Solder foil is a solder alloy (typically flux-less solder) in the form of a ribbon with a precisely defined thickness (50 - 300 μm). The advantage of using a solder foil is to ensure a constant solder thickness under the substrates. Surface unevenness or deformation of the baseplate is caused by the reflowing process. This is due to the large surface area of the baseplate and the internal stresses of the materials.

To reduce thermal resistance, a layer of TIM is applied between the baseplate and the heatsink. The purpose of the TIM is to fill the voids created by the unevenness of the baseplate surface. The greater the deformation of the baseplate, the greater the thickness of the TIM to be applied. However, the TIM has low thermal conductivity (around 3 W/mK) compared to the materials used (Cu - 398 W/mK or Al - 273 W/mK). Greater thickness of TIM increases thermal resistance and reduces cooling efficiency. For this reason, it is important to achieve a flat base plate surface after the reflow process [14]. The second alternative is not to use the baseplate and TIM and to mount the substrates directly on the heatsink (Baseplate-less power module) [15].

A new trend, similar to die attach, is the use of sintering technology as a substrate attach is being explored [7]. Sintering joints between the substrate and base plate in power module devices offer advantages, including improved thermal conductivity, enhanced mechanical strength, and better long-term reliability. However, creating void-free joints remains a challenge, as incomplete sintering or insufficient pressure can lead to voids in the joint, compromising its strength and thermal conductivity. Achieving a void-free joint is crucial for maximizing the performance and reliability of power modules.

F. Encapsulation

Epoxy or epoxy molding compound (EMC) is often preferred over silicone gel for encapsulating power modules because it has higher mechanical strength, thermal conductivity, and long-term stability, which is critical in power modules. Additionally, epoxy tends to have better adhesion to a variety of materials, improving the overall reliability and durability of the power modules. While silicone gel offers flexibility and ease of application, epoxy's robustness and enhanced performance in high-stress applications make it a more reliable choice for power module encapsulation [16],[17].

III. PROBLEM IDENTIFICATION AND FUTURE DIRECTIONS

The goal of research in power module packaging is to ensure the highest level of reliability, improving thermal management, downsizing of packages and optimizing manufacturing costs of the final power modules [18]. The main problem in packaging power electronics is soldering process. The problems are voids, scraps, fjord voids, delamination, and cracks. All these failures have a major impact on long-term reliability of power modules.

A. Voids in solder joints

The main cause of void formation in large area joints is the presence of fluxes in the solder alloy. Fluxes are substances of a non-metallic nature that remove oxide coatings from soldering places, prevent their re-formation and improve wetting and melting of molten solder at soldering places. Therefore, the fluxes in the solder are replaced using vacuum, an inert atmosphere (N_2), forming gas (N_2H_2) or formic acid (HCOOH) as the reducing agent in the reflow process (Fig. 5).

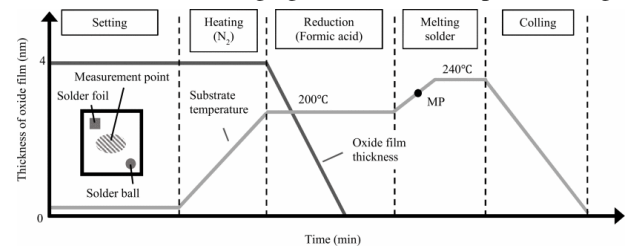


Fig. 5 Example of reflow profile using formic acid [19].

The main area of research is to properly optimize the soldering profile so that no voids are created in the solder. At the same time, the solder alloy type, thickness, cooling method, and other parameters must be considered.

B. Delamination

Delamination is a phenomenon where after the process of soldering the substrate to the baseplate, they are separated. This is mainly due to the large, soldered area and the different CTE of the materials (Tab. I). Different coefficients cause large internal stress in individual materials. This problem occurs when the materials are not cooled properly after the soldering

process. This phenomenon may also occur between the die and the substrate after the second reflow process.

C. Simulation programs

Simulation programs allow simulation and optimization of production processes. Also, they make it possible to simulate the behavior of the power module during operation. Simulations are important when analyzing voids in the solder as well as in optimizing soldering processes to understand the behavior of the material in individual production processes. Experiments in normal operation of industry are not possible. Simulation programs are used as a key tool to optimize processes that allow examination of materials in production processes. These are programs that allow structural analysis of materials (FEA – Finite Elements Analysis) under the influence of heat and pressure. Software such as SimScale, Ansys (Fig. 6), Comsol, Solid Edge and others can be used [20].

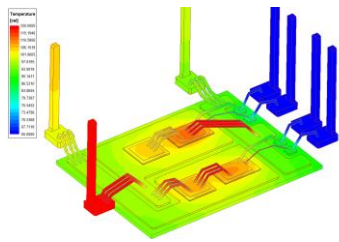


Fig. 6 The thermal distribution in the power module [20].

The main advantage of using simulation programs is more efficient optimization of parameters, setting the correct reflow profile and early detection of potential problems.

IV. CONCLUSION

Significant trends in power module packaging are needed due to the increasing number of electric vehicles. This requires adapting manufacturing processes (Fig. 7) to ensure good thermal conductivity and high durability of the power modules.

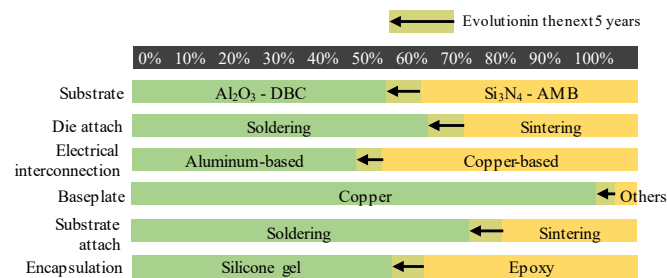


Fig. 7 Summary of power module packaging trends [18].

A critical area of investigation and one of the many challenges in power module packaging is creating new packaging structures and cooling methods that help improve power module lifetime.

REFERENCES

- [1] "Power Modules," Semikron Danfoss. Accessed: Feb. 20, 2025. [Online]. Available: <https://www.semikron-danfoss.com/products/power-modules>
- [2] L. Xie *et al.*, "State-of-the-art of the bond wire failure mechanism and power cycling lifetime in power electronics," *Microelectronics Reliability*, vol. 147, p. 115060, Aug. 2023, doi: 10.1016/j.microrel.2023.115060.
- [3] E. Santi, S. Eskandari, B. Tian, and K. Peng, "6 - Power Electronic Modules," in *Power Electronics Handbook (Fourth Edition)*, M. H. Rashid, Ed., Butterworth-Heinemann, 2018, pp. 157–173. doi: 10.1016/B978-0-12-811407-0.00006-4.
- [4] "Technical Ceramics Substrates," CeramTec GmbH. Accessed: Feb. 22, 2025. [Online]. Available: <https://www.ceramtec-industrial.com/en/products-applications/substrates>
- [5] "Overview of Ceramic Substrates," Rogers Corporation. Accessed: Feb. 22, 2025. [Online]. Available: <https://www.rogerscorp.com/blog/2022/Overview-of-Ceramic-Substrates>
- [6] "Ceramic Substrate Series-Performance and Application of AMB Active Metal," XIAMEN MASCERA TECHNOLOGY CO.,LTD. Accessed: Feb. 22, 2025. [Online]. Available: <https://www.mascera-tec.com/news/ceramic-substrate-series-performance-and-application-of-amb-active-metal>
- [7] S. Daryanani, "Large-area sintering advances improve power module performance," *Power Electronics News*. Accessed: Feb. 24, 2025. [Online]. Available: <https://www.powerelectronicsnews.com/large-area-sintering-advances-improve-power-module-performance/>
- [8] L. Navarro, X. Perpiñà, M. Vellvehí, and O. Aviñó, "Electrical Behaviour of Ag Sintered Die-attach Layer after Thermal Cycling in High Temperature Power Electronics Applications," Sep. 2019. Accessed: Feb. 23, 2025. [Online]. Available: https://www.researchgate.net/publication/346785787_Electrical_Behaviour_of_Ag_Sintered_Die-attach_Layer_after_Thermal_Cycling_in_High_Temperature_Power_Electronics_Applications
- [9] M. Calabretta, M. Renna, V. Vinciguerra, and A. A. Messina, "Power Packages Interconnections for High Reliability Automotive Applications," in *ESSDERC 2019 - 49th European Solid-State Device Research Conference (ESSDERC)*, Sep. 2019, pp. 35–39. doi: 10.1109/ESSDERC.2019.8901742.
- [10] "Aluminum Bonding Wire and Copper Bonding Wire (ALU and CU) - TOLL MOSFET." Accessed: Feb. 23, 2025. [Online]. Available: <https://community.infineon.com/t5/Knowledge-Basis-Articles/Aluminum-Bonding-Wire-and-Copper-Bonding-Wire-ALU-and-CU-TOLL-MOSFET/ta-p/464145>
- [11] "COPPER BASE PLATE | POWER MODULE | jem industries." Accessed: Feb. 24, 2025. [Online]. Available: <https://power-module.com/copper-base-plate/>
- [12] "A new base plate concept on the basis of aluminium-copper clad materials," ResearchGate. Accessed: Feb. 24, 2025. [Online]. Available: https://www.researchgate.net/publication/285689294_A_new_base_plate_concept_on_the_basis_of_aluminium-copper_clad_materials
- [13] "AlSiC Baseplates for Power IGBT Modules: Design, Performance and Reliability," ResearchGate. Accessed: Feb. 24, 2025. [Online]. Available: https://www.researchgate.net/publication/237471109_AlSiC_Baseplates_for_Power_IGBT_Modules_Design_Performance_and_Reliability
- [14] B. Rabay and A. Stelzer, "Large surface area substrate attach in power module applications," in *CIPS 2022; 12th International Conference on Integrated Power Electronics Systems*, Mar. 2022, pp. 1–4. Accessed: Feb. 24, 2025. [Online]. Available: <https://ieeexplore.ieee.org/document/9862013>
- [15] "Examining the Benefits of Baseplate-Less Power Modules - Industry Articles," Accessed: Feb. 24, 2025. [Online]. Available: <https://eepower.com/industry-articles/power-modules-baseplate-less-power-modules-offer-thermal-resistance-and-robustness/>
- [16] S. Daryanani, "Package Innovations for SiC Power Devices," *Power Electronics News*. Accessed: Feb. 24, 2025. [Online]. Available: <https://www.powerelectronicsnews.com/package-innovations-for-sic-power-devices/>
- [17] "Next-Generation SiC Power Module Development," WASEDA UNIVERSITY. Accessed: Feb. 24, 2025. [Online]. Available: <https://www.yoshida.mech.waseda.ac.jp/powermodule-details.html>
- [18] "Status of the Power Module Packaging Industry 2024," Yole Group. Accessed: Feb. 19, 2025. [Online]. Available: <https://www.yolegroup.com/product/report/status-of-the-power-module-packaging-industry-2024/>
- [19] N. Ozawa, T. Okubo, J. Matsuda, and T. Sakai, "Sn- and Cu-oxide reduction by formic acid and its application to power module soldering," in *2018 IEEE 30th International Symposium on Power Semiconductor Devices and ICs (ISPSD)*, May 2018, pp. 248–251. doi: 10.1109/ISPSD.2018.8393649.
- [20] "Multiphysics Analysis of Power Electronic Module Econ Engineering - Blog," Econ Engineering. Accessed: Feb. 26, 2025. [Online]. Available: <https://econengineering.com/en/blog/multiphysics-analysis-of-power-electronic-module/>

Hardware Construction of Capacitor-Based Active Cell Balancer

¹Daniel MARCIN (3rd year)
Supervisor: ²Milan LACKO

^{1,2}Department of Electrical Engineering and Mechatronics, FEI TU of Košice, Slovak Republic

¹daniel.marcin@tuke.sk, ²milan.lacko@tuke.sk

Abstract—This study explores capacitor-based active cell balancing techniques to enhance the performance and longevity of electric vehicle battery systems. Using MATLAB Simulink simulations, we analysed three balancing circuits: switched capacitors, double-tiered switched capacitors, and an enhanced configuration incorporating an additional capacitor. To validate the simulation results, we developed a real-world prototype, requiring the design and fabrication of custom circuitry. This involved constructing a battery module, a control module, and a balancer module. This article primarily focuses on the design, implementation, and evaluation of the balancer module.

Keywords—Balancer, battery management system, active cell balancing, Li-ion, switched-capacitors.

I. INTRODUCTION

The growing adoption of electric vehicles (EVs) is driven by the need to reduce reliance on fossil fuels and lower the environmental impact of transportation. At the heart of EV performance and reliability is the battery system (BS) [1], [2]. A well-optimised BS not only extends driving range but also improves efficiency and longevity.

A key component of any EV battery system is the battery management system (BMS), which ensures safe operation and peak performance. By monitoring cell states and managing voltage, temperature, and fault detection, the BMS plays a crucial role in protecting the battery pack and maximising its lifespan [3].

One of the most important functions of a BMS is cell balancing, which ensures an even charge distribution across all cells in the battery pack. Keeping cells balanced prevents excessive wear on individual cells, helping to maintain performance and reduce safety risks [4].

Active cell balancing is a more efficient approach compared to traditional passive methods, as it redistributes energy between cells rather than dissipating excess charge as heat. This process relies on PWM-controlled switches and various energy storage components, including capacitors, inductors, transformers, and DC/DC converters [5]. Among these, capacitors are particularly effective, as they allow for fast and efficient charge transfer, helping to maintain cell voltage equilibrium and improve overall battery performance.

In this paper, we present an overview of the hardware used for active cell balancing circuits based on switched capacitors, double-tiered switched capacitors, and an enhanced variant that incorporates an additional capacitor into the second circuit. This involved designing and constructing a battery module, a control module, and a balancer module. The primary focus of

this paper is on the balancer module. Additionally, our aim is to provide insights into the advantages and limitations of each circuit, highlighting their potential applications in battery management systems.

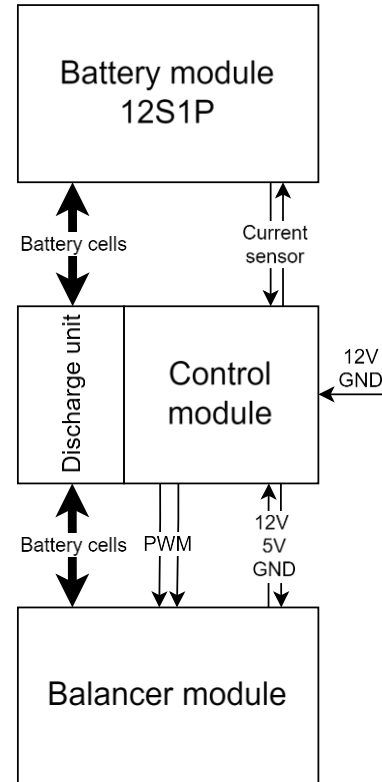


Fig. 1 Battery module, control module, balancer module interconnections

II. HARDWARE REQUIREMENTS AND SOLUTION ANALYSIS

To verify the accuracy of our simulation results [6], we developed and constructed hardware for the balancer. To ensure modularity, adaptability, and ease of modification, the hardware is divided into three distinct DPS modules: the battery module, the control module, and the balancer module (Fig. 1). These modules will be interconnected using necessary wiring. The control module plays a vital role in real-time monitoring, creates controlled imbalances in individual cells to establish consistent initial test conditions, and gathering data during charging and discharging cycles. Additionally, it controls the operation of the balancer module. One of the key benefits of this design is that a single control module can support multiple balancing circuit configurations in future modifications.

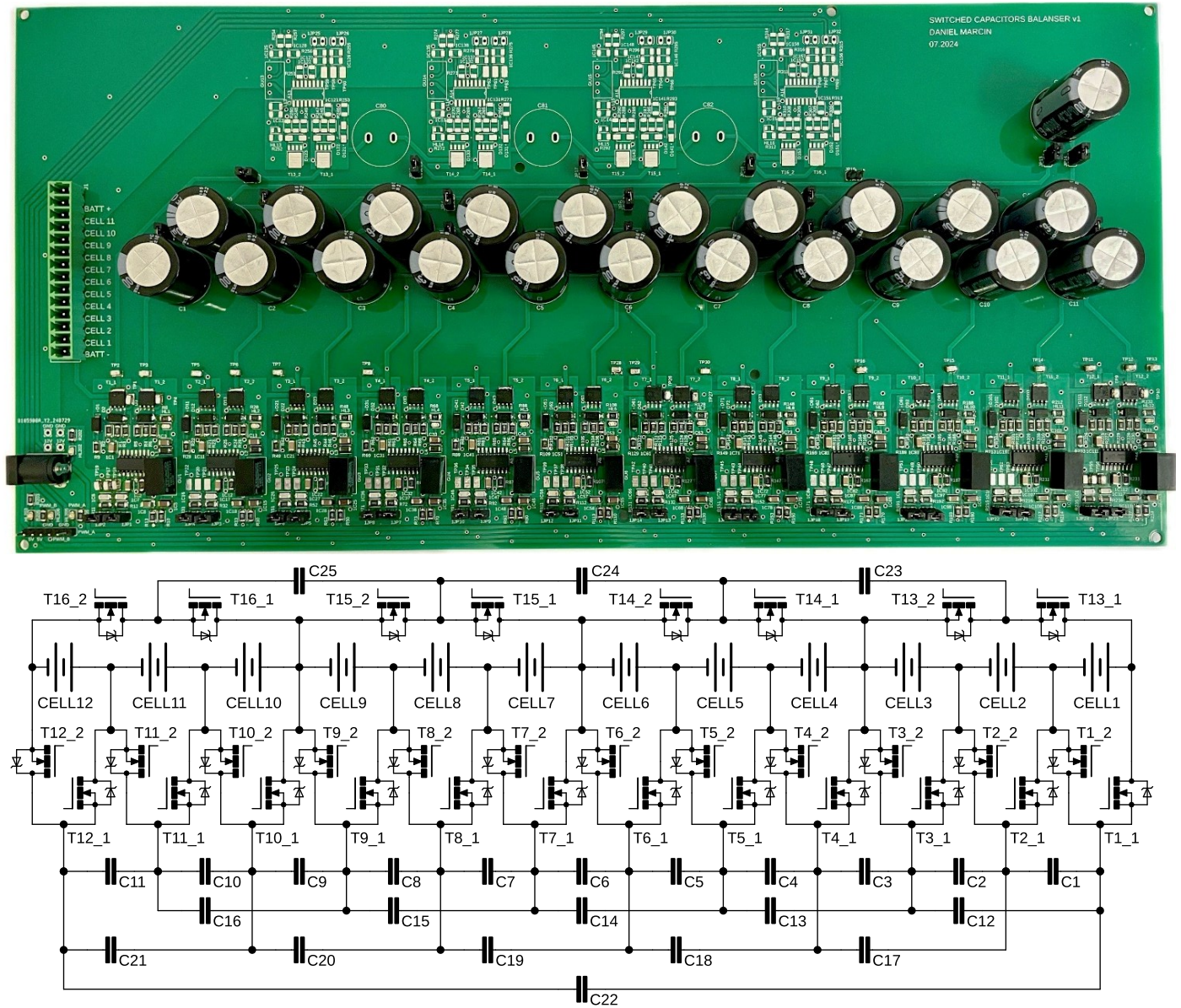


Fig. 2 Balancer module board, basic electrical schematic of balancer module

A. Battery module

The battery module features series-connected cell holders, each linked to a connector for voltage sensing and balancing. SMD fuses rated at 3 A protect these connections. An additional 6 A fuse safeguards the entire module. An ACS712-05 current sensor, measuring -5 A to 5 A with a 5 V supply, is integrated with a connector for microcontroller processing. This design also allows easy cell replacement. LFP-based APR18650M1B cells from Lithium Werks are used.

B. Control module

The control module consists of two primary sections: the control unit and the discharge unit. The control unit integrates a microcontroller, signal processing components, data storage, a real-time clock (RTC) circuit, a programming connector, and interfaces for external devices and HMI. The second section manages the initial voltage levels of battery cells using discharge resistors connected through switching relays. Based on user settings, the microcontroller directs specific cells to connect with discharge resistors until the target voltage is achieved.

The system operates on a 12 V power supply, primarily for relay switching, with a voltage regulator stepping down to 5 V

for microcontroller operations. The microcontroller selected for this design is the AVR128DB64 from Microchip, offering 128KB flash memory, a 24 MHz maximum frequency, and multiple communication options, including I2C and SPI. It supports 22 differential 12-bit ADC channels, providing sufficient capability for monitoring and control.

The microcontroller connects to essential components, including relays, buttons, a potentiometer, and analog inputs for cell voltage and temperature monitoring. I2C communication links the microcontroller to both the LCD display and the RTC circuit. User interaction is facilitated through four buttons, a potentiometer and 20x4 character LCD display with PCF8574 module. These enable program navigation, resets, confirmations, and other control tasks. The RTC module, DS1307, ensures accurate timekeeping even during power failures using a coin-cell battery backup. It supports I2C communication and features an external oscillator for clock precision.

Data storage is managed through SPI communication with a microSD card, providing logging of current, voltage, and timestamps for accurate monitoring.

Voltage sensing for individual battery cells presented a challenge due to the series connection of 12 cells, which resulted in high cumulative voltages. Initially, this was addressed using two HEF4067BT.653 analog multiplexers to ensure that only one cell is connected to the microcontroller at a time. However, due to connection issues, the system was upgraded with the INFINEON TLE9012DQU Evaluation Board. This dedicated board should improve voltage sensing process and accuracy.

The discharge unit is designed to prepare cells for experimentation by bringing them to a desired initial state. Each discharge path incorporates a $3.3\ \Omega$, 5 W AX5W-3R3 resistor, limiting the discharge current to 1C (1.1 A). Relays (AZ943-1AH-12DE) switch the resistors on or off.

C. Balancer module

The balancer module (Fig. 2) is primarily composed of switches and capacitors and it is designed for flexibility and adaptability in possible future research applications. It integrates multiple capacitor-based active cell balancing topologies within a single board, allowing modification of different configurations through jumpers. These jumpers enable reconfiguration for various balancing topologies or adjusting the number of capacitors involved in the process. Two N-channel MOSFETs (P140LF4QL) per cell, serve as switches, managing the current flow for both directions. Each cell connects to the balancer circuit via a multi-pin connector for secure and efficient connection with other modules.

To ensure precise measurements during balancing research, auxiliary circuits are not powered by the battery cells but by two dedicated power supplies. A 12 V supply controls the MOSFET gates, while a 5 V supply powers the driver circuits. These power supplies are shared with the control unit. Balancing operations are controlled by PWM signals from the microcontroller. It is two complementary PWM signals (PWM_A and PWM_B).

Each MOSFET pair is driven by an isolated dual-channel gate driver (UCC21330BDR) with programmable dead time. This driver uses the 5 V supply for input logic and serves as a reference for the PWM signals. RC filters are applied at both the PWM signal and power supply inputs, following manufacturer specifications. A 56 k Ω resistor (RDT) sets the dead time to approximately 500 ns. The high-voltage side is powered by 12 V-to-12 V isolated DC/DC converters, which also charge the bootstrap capacitor. Turn-on resistance is managed by a 15 Ω R_{ON} resistor, while turn-off is facilitated by a Schottky diode and a 3.3 Ω R_{OFF} resistor. This schematic design is replicated 12 times to operate 12 battery cells.

As previously outlined, various capacitor-based active cell balancing topologies are incorporated into the electrical schematic shown in Fig. 2 using jumpers. The system supports four distinct balancing configurations:

- Switched capacitors (SC)
- Double-tiered switched capacitors (DTSC)
- Double-tiered switched capacitors with an additional capacitor (DTSCAC)
- Modular switched capacitors (MSC)

This modular system ensures adaptability for different experimental setups and enhances research capabilities by allowing easy switching between balancing topologies within a single hardware design. The design prioritizes flexibility, accuracy and efficiency, what makes it suitable for advanced studies in battery management and active cell balancing. Depending on the specific balancing strategy, some capacitors

connect in parallel across one, two, or three cells, thus capacitors with various voltage ratings must be used.

III. CONCLUSION

This paper explored capacitor-based active cell balancing methods designed for electric vehicle battery systems. After building on earlier simulations and theoretical research [6], a hardware prototype was developed to test these concepts in practice. The balancer combines various capacitor-based topologies: SC, DTSC, DTSCAC, and MSC in a flexible, adaptable setup.

The hardware was built with scalability and precision in mind. A dedicated voltage sensing board was implemented to improve monitoring accuracy, ensuring reliable data collection during tests. Discharge unit in control module allows for consistent cell preparation and repeatable testing.

Initial tests show that the balancer handles real-time voltage equalization effectively, which offers a solid foundation for future development. Its modular design makes it easy to switch between different balancing strategies, opening doors for future research.

Next steps will focus on programming the software, aiming for automated balancing and a deeper dive into the energy efficiency of different topologies. Further testing under various conditions will find better battery performance, efficiency, and safety for electric vehicle applications.

In conclusion, the hardware developed in this study offers a strong, adaptable platform for advancing capacitor-based active cell balancing, laying the groundwork for future research and practical use in electric vehicle battery management systems.

ACKNOWLEDGMENT

This work was supported by projects APVV-18-0436, VEGA 1/0363/23 and KEGA 059TUKE-4/2024.

REFERENCES

- [1] M. A. Hannan, Md. M. Hoque, A. Hussain, Y. Yusof, and P. J. Ker, "State-of-the-Art and Energy Management System of Lithium-Ion Batteries in Electric Vehicle Applications: Issues and Recommendations," *IEEE Access*, vol. 6, pp. 19362–19378, 2018, doi: 10.1109/ACCESS.2018.2817655.
- [2] P. Nur Halimah, S. Rahardian, and B. A. Budiman, "Battery Cells for Electric Vehicles," *International Journal of Sustainable Transportation Technology*, vol. 2, no. 2, pp. 54–57, Oct. 2019, doi: 10.31427/IJSTT.2019.2.2.3.
- [3] P. Sun, R. Bisschop, H. Niu, and X. Huang, "A Review of Battery Fires in Electric Vehicles," *Fire Technol*, vol. 56, no. 4, pp. 1361–1410, Jul. 2020, doi: 10.1007/s10694-019-00944-3.
- [4] G. L. Plett, *Battery management systems, Volume II: Equivalent-circuit methods*. Artech House, 2015.
- [5] D. Andrea, *Battery Management Systems for Large Lithium-Ion Battery Packs*. Artech House, 2010.
- [6] D. Marcin, M. Lacko, D. Bodnár, and L. Pancurák, "Capacitor-Based Active Cell Balancing for Electric Vehicle Battery Systems: Insights from Simulations," *Power Electronics and Drives*, vol. 9, no. 1, pp. 317–330, Jan. 2024, doi: 10.2478/pead-2024-0020.

Structural Transitions in Ferronematics Under Electric and Magnetic Fields

¹Dmytro Miakota (4th year)
Supervisor: ²Natália TOMAŠOVIČOVÁ

^{1,2}Institute of Experimental Physics of the Slovak Academy of Sciences, Košice, Slovak Republic

¹dmytro.miakota@tuke.sk, ²nhudak@saske.sk

Abstract— This work presents observations on structural transitions in ferronematics (FNs) based on the liquid crystal E7 doped with magnetic goethite nanoparticles. The dielectric properties of the prepared FNs were examined under the influence of an orienting magnetic field and a DC biasing electric field. The findings demonstrate that nanoparticle doping significantly enhances the sensitivity of FNs to external magnetic fields.

Keywords— liquid crystal, magnetic nanoparticles, liquid crystal composites, ferronematics.

I. INTRODUCTION

Liquid crystals (LCs) are a unique class of soft condensed matter, combining the fluidity of liquids with the directional-dependent electrical and optical properties of crystalline solids. This duality makes LCs highly versatile, particularly in liquid crystal displays (LCDs) [1]. Due to their anisotropic mechanical, electrical, and magnetic properties, LCs can be easily oriented, realigned, or deformed by external stimuli such as electric and magnetic fields, temperature variations, mechanical stress, and light. Initially considered a scientific curiosity, LCs have since gained widespread recognition for their adaptability, enabling applications far beyond displays. For example, a small electric field can modulate their optical properties, switching them between transparent and opaque states. Their responsiveness to external influences, including magnetic fields, pressure, and temperature, has opened new possibilities for advanced technologies. Since the 1980s, LC research has expanded into photonics, magneto-optics, nanosensing, biosensing, light valves, tunable lenses, smart windows, and more [2].

A fundamental discovery in LC research was the threshold behavior of their reorientational response to external fields, known as the “Fréedericksz transition”, named after Vsevolod Fréedericksz [3]. This effect demonstrated that LCs can be reoriented using electric or magnetic fields due to their anisotropic dielectric permittivity (ϵ_a) and diamagnetic susceptibility (χ_a). While LCs exhibit relatively large dielectric anisotropy ($\epsilon_a > 1$), allowing reorientation with low voltages (typically a few volts or millivolts), their response to magnetic fields is significantly weaker, with diamagnetic susceptibility values on the order of $\chi_a \sim 10^{-7}$. Consequently, LC reorientation via magnetic fields typically requires strong fields in the tesla range [4].

In 1970, Brochard and de Gennes proposed enhancing the magnetic sensitivity of LCs by doping them with fine magnetic nanoparticles (MNPs), leading to the development of “ferronematics” (FNs) [5]. FNs are colloidal suspensions of ferromagnetic or ferrimagnetic nanoparticles within nematic

LCs, allowing the LC director (\mathbf{n}) to couple strongly with the magnetic moments (\mathbf{m}) of embedded particles. This interaction enables FNs to respond more effectively to magnetic fields. The Brochard–de Gennes theory predicted rigid anchoring of LC molecules on the nanoparticle surfaces, leading to parallel alignment ($\mathbf{n} \parallel \mathbf{m}$). Early studies produced both lyotropic [6,7] and thermotropic FNs [8], while later experiments revealed the possibility of perpendicular alignment ($\mathbf{n} \perp \mathbf{m}$). To account for this, Burylov and Raikher extended the theoretical model [9,10], introducing a parameter (ω) that represents the ratio of anchoring energy (W) at the nematic-nanoparticle interface to the LC’s elastic energy ($\omega = Wd/K$, where d is the particle size and K is the Frank elastic modulus). For $\omega \gg 1$, rigid anchoring enforces $\mathbf{n} \parallel \mathbf{m}$, whereas for $\omega \leq 1$, soft anchoring permits both parallel and perpendicular alignments.

The combination of electric and magnetic fields as bias fields in FNs provides a powerful approach for studying Fréedericksz thresholds. The motivation for investigating combined fields lies in their potential to reveal complex interactions between LC molecules and MNPs. While the electric field interacts with the dielectric anisotropy of LCs, the magnetic field couples to the enhanced magnetic susceptibility introduced by MNPs. This interplay enables precise tuning of the Fréedericksz transition, which is crucial for optimizing low-power devices. By analyzing field-induced reorientation, this approach offers insights into the binding energy between MNPs and LC molecules, shedding light on the fundamental interactions that govern their behavior.

This work presents experimental observations and mathematical analysis of structural transitions in FNs based on E7 LC doped with rod-like goethite MNPs (nanorods) at various concentrations. These systems have been recently studied from both experimental [11] and theoretical [12] perspectives. The dielectric properties of the prepared FNs were investigated under the influence of an orienting magnetic field (B) and a DC biasing voltage (U_{bias}).

II. MATERIALS AND METHODS

E7 is a thermotropic nematic liquid crystal composed of a mixture of four LCs: 5CB (51%), 7CB (25%), 8OCB (16%), and 5CT (8%) [13]. It has a nematic-to-isotropic transition temperature (T_N) of 61°C and a glass transition temperature (T_g) of –62°C, providing a broad nematic range of approximately 120°C. E7 is widely used due to its high anisotropy across a large temperature range [14].

The synthesis of goethite nanoparticles was described in [15]. Their microstructural characterization was performed using transmission electron microscopy (TEM). The goethite nanorods had an average length of 350 ± 100 nm, width of 25 ± 7 nm, and thickness of 10 ± 5 nm. Doping was achieved by adding magnetic nanoparticles (MNPs) to the E7 LC in its isotropic phase while continuously stirring. The resulting ferronematic (FN) suspensions contained MNPs at concentrations of $\phi_1 = 10^{-3}$, $\phi_2 = 5 \times 10^{-4}$, and $\phi_3 = 10^{-4}$. To ensure stability, the mixtures were sonicated in a bath for 30 minutes.

Structural transitions were investigated through dielectric measurements. Samples of undoped E7 and E7 doped with goethite MNPs were filled into capacitors with indium-tin-oxide (ITO) electrodes, each with an area of approximately $0.5 \text{ cm} \times 0.5 \text{ cm}$ and a thickness of $D = 50 \text{ }\mu\text{m}$. The samples, introduced in the isotropic phase via capillary forces, were aligned using a rubbed polyimide coating on the electrodes to ensure planar orientation. Measurements were conducted at 30°C under the influence of either a magnetic or electric field, both oriented perpendicular to the sample cell. The capacitor was placed in a thermostat system with a temperature stability of $\pm 0.05^\circ\text{C}$. Capacitance was measured at a frequency of 1 kHz using a TiePie Handyscope HS5 instrument with a sinusoidal voltage signal of root-mean-square value of $U = 0.3 \text{ V}$.

III. RESULTS

The structural transitions induced by combined electric and magnetic fields were monitored. A DC bias voltage (U_{bias}) and a magnetic field (B) were applied perpendicular to the initial director orientation. Since the electric and magnetic fields were parallel, they induced the same type of distortion due to the identical sign of dielectric anisotropy (ϵ_a) and magnetic susceptibility anisotropy (χ_a).

Figure 1 shows how the reduced capacitance ($(C - C_{\min}) / (C_{\max} - C_{\min})$) (where C , C_{\min} and C_{\max} are the sample capacitance, its value at $B = 0$ and $B = 0.85 \text{ T}$, respectively) of the undoped E7 and E7 doped with goethite nanorods depends on the external magnetic field B , measured at no bias voltage ($U_{\text{bias}} = 0 \text{ V}$). Doping with MNPs led to a decrease in the critical magnetic field.

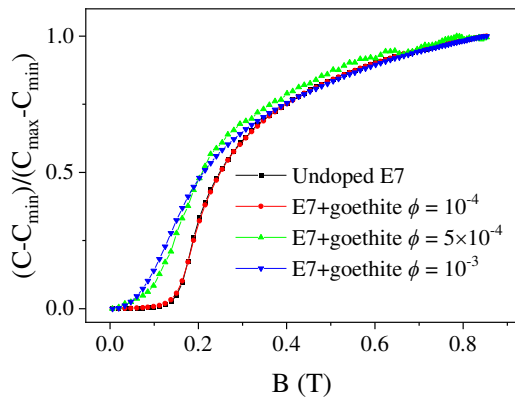


Fig. 1. Reduced capacitance for undoped E7 and E7 doped with goethite nanorods in three concentrations, plotted against the magnetic field.

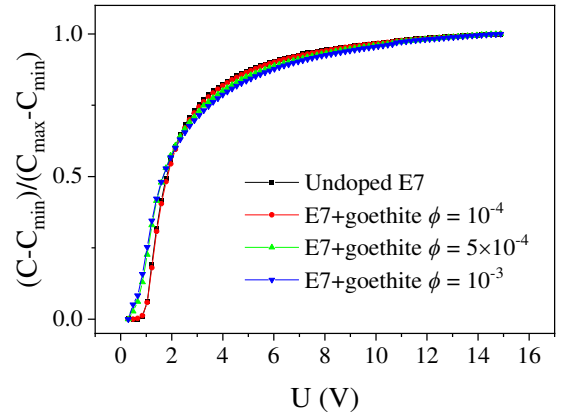


Fig. 2. Reduced capacitance for undoped E7 and E7 doped with goethite nanorods in three concentrations, plotted against the electric field.

Figure 2 presents the reduced capacitance as a function of the external electric field (U) at zero bias magnetic field ($B_{\text{bias}} = 0 \text{ T}$). Similarly, doping E7 with goethite nanorods resulted in a decrease in the critical electric field. Figure 3 demonstrates the capacitance dependence on external magnetic field B for doped E7 ($\phi = 10^{-4}$) under various bias voltages (U_{bias}). As the bias voltage increased, the critical magnetic field (B_F) for the magnetic Fréedericksz transition decreased, as described by Equation (1):

$$\left(\frac{U_{\text{bias}}}{U_F}\right)^2 + \left(\frac{B_c}{B_F}\right)^2 = 1, \quad (1)$$

where $U_F = U_{LC}$, $B_F = B_{LC}$ for liquid crystal, and $U_F = U_{FN}$, $B_F = B_{FN}$ for composites.

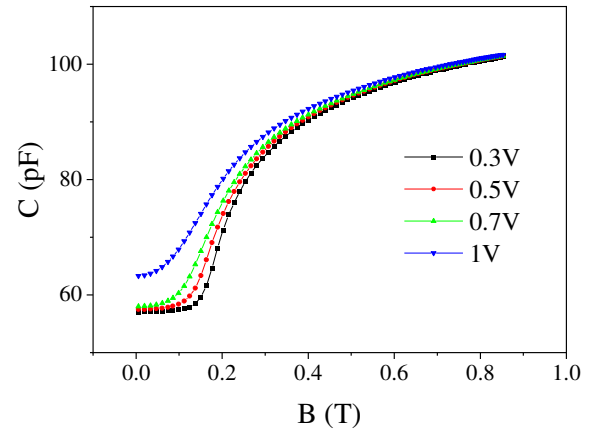


Fig. 3. Capacitance vs. the external magnetic field bias voltages $U_{\text{bias}} = 0.3, 0.5, 0.7$ and 1 V for E7 doped with MNPs with concentration $\phi = 10^{-4}$.

The Fréedericksz threshold at $U = 0$, with the magnetic field applied perpendicular to the cell surface, can be calculated using the standard formula:

$$B_F = \frac{\pi}{D} \sqrt{\frac{\mu_0 K_1}{|\chi_a|}}, \quad (2)$$

where D represents the cell thickness and K_I is the Frank elastic modulus. In their investigation of the magnetic Fréedericksz transition, Burylov and Raikher [10] derived

a theoretical relationship between the threshold magnetic induction of thermotropic FNs (B_{FN}) and that of the host LC (B_{LC}). Assuming homeotropic anchoring of LC molecules on the MNP surfaces, they proposed the following approximate formula:

$$B_{FN}^2 - B_{LC}^2 = \pm \frac{2\mu_0 W \phi}{\chi_a d} \quad (3)$$

The sign in this equation depends on the initial orientation of the magnetic moment (\mathbf{m}) relative to the director (\mathbf{n}): a positive sign corresponds to parallel alignment ($\mathbf{m} \parallel \mathbf{n}$), while a negative sign corresponds to perpendicular alignment ($\mathbf{m} \perp \mathbf{n}$). The critical magnetic induction in our experimental geometry follows directly from Equation (1).

Since both B_{FN} and B_{LC} were experimentally measured, Equation (3) was used to estimate the anchoring energy density (W) at the nematic–magnetic particle boundary. The susceptibility anisotropy of E7 was calculated from Equation (2) as $\chi_a = 2.66 \times 10^{-6}$. For all FN composites with different nanorod concentrations, the anchoring energy density was estimated at approximately $W \approx 10^{-7}$ N/m. The parameter $\omega = Wd/K_I$ was then calculated, where for E7 at the measurement temperature, $K_I = 10.8$ pN [16]. This yielded $\omega \approx 10^{-4}$, indicating soft anchoring of the nematic director on the goethite nanorod surfaces in E7-based FNs.

Figure 4 consolidates the experimental data, showing the dependence of the critical magnetic field (B_c) on the applied bias voltage (U_{bias}) for both undoped E7 and E7-based FNs. In FNs, the lower the MNP concentration, the steeper the measured slope, indicating that the electric field facilitates LC molecule rotation along the field lines. The presence of MNPs enhances FN sensitivity to low magnetic fields, with the highest MNP concentration reducing the critical field by approximately ~ 2.5 times.

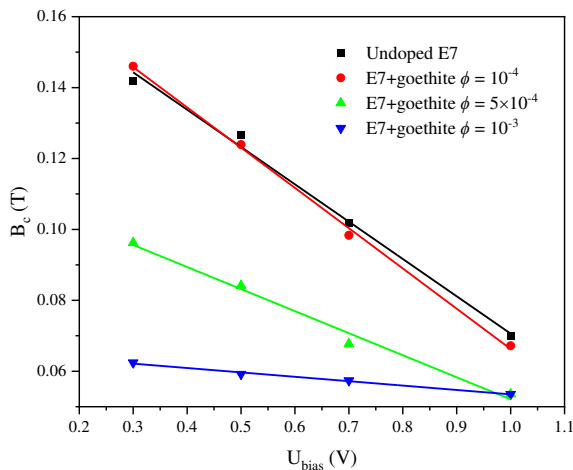


Fig. 4. The dependence of the critical magnetic field B_c on the voltage U_{bias} for the undoped E7 and for E7 doped with goethite nanorods.

IV. CONCLUSIONS

Our experimental results confirm the presence of soft anchoring at the MNP–LC interface, enabling both parallel and perpendicular orientations between the nanorod magnetic moment (\mathbf{m}) and the LC director (\mathbf{n}). Furthermore, the observed decrease in the critical reorienting magnetic field (B_c) strongly indicates an initial $\mathbf{m} \parallel \mathbf{n}$ alignment. In conclusion, the prepared

FNs, based on E7 LC, which features an exceptionally wide nematic phase range ($\sim 120^\circ\text{C}$, from -62°C to 61°C), emerge as promising candidates for magnetically sensitive materials capable of operating under extreme temperature conditions.

The results presented in this work have been published in [17].

REFERENCES

- [1] J. Jung, et al., “Recent progress in liquid crystal devices and materials of TFT-LCDs, Journal of Information Display, vol. 25, pp. 121–142, 2023.
- [2] J. P. Lagerwall, G. Scalia, “A new era for liquid crystal research: Application of liquid crystals in soft matter nano-, bio- and microtechnology”, Curret Applied Physics, vol. 12, no. 6, pp. 1387–1412, 2012.
- [3] V. Freedericksz and V. Zolina, “Forces causing the orientation of an anisotropic liquid,” Transactions of The Faraday Society, vol. 29, pp. 919-930, 1970.
- [4] P. G. de Gennes and J. Prost, The Physics of Liquid Crystals, Oxford: Clarendon Press, 1993.
- [5] F. Brochard and P. d. Gennes, “Theory of magnetic suspensions in liquid crystals,” J. Phys. France, vol. 31, no. 7, pp. 691-708, 1970.
- [6] P. G. de Gennes and J. Prost, The Physics of Liquid Crystals, Oxford: Clarendon Press, 1993.
- [7] F. Brochard and P. d. Gennes, “Theory of magnetic suspensions in liquid crystals,” J. Phys. France, vol. 31, no. 7, pp. 691-708, 1970.
- [8] S.-H. Chen and N. M. Amer, “Observation of Macroscopic Collective Behavior and New Texture in Magnetically Doped Liquid Crystals,” Phys. Rev. Lett., vol. 51, pp. 2298-2301, 1983.
- [9] S. V. Burylov and Y. L. Raikher, “On the orientation of an anisometric particle suspended in a bulk uniform nematic,” Physics Letters A, vol. 149, pp. 279-283, 1990.
- [10] S. V. Burylov and Y. L. Raikher, “Macroscopic Properties of Ferromagnetics Caused by Orientational Interactions on the Particle Surfaces. II. Behavior of Real Ferromagnetics in External Fields,” Molecular Crystals and Liquid Crystals Science and Technology, vol. 258, pp. 123-141, 1995.
- [11] S. V. Burylov, et al., “Ferromagnetic and antiferromagnetic liquid crystal suspensions: Experiment and theory”, Journal of Molecular Liquids, vol. 321, p. 114467, 2021.
- [12] D. A. Petrov and I. A. Chupeev, “Antiferromagnetic liquid- crystal suspensions of goethite nanorods: three mechanisms of magnetic field influence on orientational structure”, The European Physical Journal E, vol. 47, 2024.
- [13] G. Vijayakumar, M. J. Lee, M. Song, S.-H. Jin, J. W. Lee, C. W. Lee, Y.-S. Gal, H. J. Shim, Y. Kang, G.-W. Lee, K. Kim, N.-G. Park and S. Kim, “New liquid crystal-embedded PVdF-co-HFP-based polymer electrolytes for dye-sensitized solar cell applications,” Macromolecular Research, vol. 17, pp. 963-968, 2009.
- [14] A. Bouriche, L. A. Bedjaoui and U. Maschke, “Phase behaviour and electro-optical response of systems composed of nematic liquid crystals and poly (2-ethylhexylacrylate),” Liquid Crystals, vol. 45, no. 5, pp. 656-665, 2018.
- [15] P. Kopčanský, V. Gdovinová, S. Burylov, N. Burylova, A. Voroshilov, J. Majorošová, F. Agresti, V. Zin, S. Barison, J. Jadzyn and N. Tomašovičová, “The influence of goethite nanorods on structural transitions in liquid crystal 6CHBT,” Journal of Magnetism and Magnetic Materials, vol. 459, pp. 26-32, 2018.
- [16] J. M. Hind, A. A. T. Smith and C. V. Brown, “Transient capacitance study of switching in the nematic Freedericksz geometry,” J. Appl. Phys., vol. 100, p. 094109, 2006.
- [17] D. Miakota, V. Lacková, K. Kónyová, M. Jarošová, A. Juríková, P. Kopčanský, N. Tomašovičová, Physics of Particles and Nuclei, (2025) – accepted.

Effect of magnetic anisotropies on the properties of magnetic microwires

¹Martin ELIÁŠ (1st year)
Supervisor: ²Jozef ONUFER

^{1,2}Dept. of Physics, FEI, Technical University of Košice, Slovak Republic
¹RVmagnetics, a.s., Boženy Němcovej 30, 040 01 Košice, Slovak Republic

¹martin.elias@tuke.sk, ²jozef.onufer@tuke.sk

Abstract—This manuscript provides a comprehensive analysis of the current state-of-the-art approaches for tailoring anisotropy, magnetostriction, and domain wall dynamics in microwires produced by rapid solidification techniques such as the Taylor–Ulitsky method. It discusses how intrinsic material properties, internal stresses, and chemical composition – particularly the role of rare-earth elements like terbium – affect the magnetostriction behavior and effective magnetic anisotropy in these materials. In addition, the review examines various thermal processing techniques, including annealing and stress-annealing, which facilitate atomic diffusion and relax internal stresses, thereby altering the short-range atomic order and modulating the magnetic response. The mechanisms governing the switching field distribution, arising from both magnetoelastic and defect-related pinning, are also critically analyzed. The paper highlights key challenges and suggests future research directions aimed at optimizing microwire performance for sensor and memory applications.

Keywords—Magnetostriction, Magnetoelastic anisotropy, Microwire, Switching field distribution

I. INTRODUCTION

Magnetic microwires fabricated by rapid solidification techniques such as the Taylor–Ulitsky method are promising for sensor and memory applications due to their excellent soft magnetic properties and unique domain structures [1], [2], [3]. Their properties are governed by magnetic anisotropies, which set the preferred magnetization direction and influence key phenomena like giant magnetoimpedance (GMI) and domain wall (DW) dynamics [4]. Various thermal processing techniques, including stress annealing, modify the internal stress distribution and thereby the effective magnetic anisotropy [5]. For instance, a temperature gradient during annealing can induce graded anisotropy along the wire, while current annealing and magnetic field-assisted processing further refine anisotropy characteristics [5], [6]. However, a comprehensive review of these methods is still lacking. This paper reviews state-of-the-art approaches for tailoring anisotropy and discusses their impact on the functional properties of microwire devices.

II. LITERATURE REVIEW AND ANALYSIS

A. Anisotropies in Microwires

Glass-coated microwires exhibit multiple anisotropy contributions. The amorphous metallic core has negligible

magnetocrystalline anisotropy but develops significant stress-induced (magnetoelastic) anisotropy during rapid quenching. Residual stresses from the mismatch in thermal expansion between the core and glass, combined with shape anisotropy from the wire’s geometry, determine the effective easy and hard magnetization axes [4], [7], [8], [9], [10]. These factors are crucial for controlling domain structure, coercivity, and GMI response.

B. Magnetostriction and Its Implications

Magnetostriction – the change in dimensions caused by an external magnetic field – plays a pivotal role in these microwires [4], [11]. In amorphous wires, magnetostriction is primarily an intrinsic material constant determined by the alloy’s composition. However, the internal stresses generated during rapid quenching interact with this inherent magnetostriction to modify the magnetoelastic energy. Because magnetostriction can be either positive or negative, it dictates whether the magnetic moments within the material align parallel or perpendicular to the applied or residual stresses. This alignment, in turn, affects the effective magnetic anisotropy, thereby influencing domain wall (DW) propagation and the giant magnetoimpedance (GMI) effect [4]. Fine-tuning the interplay between intrinsic magnetostriction and internal stresses is therefore essential for optimizing the sensitivity and performance of microwire-based sensors.

C. Effect of Terbium on Magnetostriction

Substituting a fraction of the transition metal in amorphous alloys with rare-earth elements – particularly terbium – significantly enhances magnetostriction [11]. Terbium possesses a large single-ion anisotropy and an inherently high magnetostriction coefficient, which allows it to impose substantial strain on the host alloy lattice when magnetized [12]. As a result, incorporating Tb frequently leads to higher overall magnetostriction values in amorphous systems compared to their Tb-free counterparts [12].

When Tb is added to amorphous transition-metal alloys (e.g., Fe-, Co-, or FeCo-based), it introduces localized 4f electronic states that couple strongly with the 3d band of the transition metals [13]. This coupling modifies both the exchange interactions and the local anisotropy fields in the material [14]. Terbium’s strong spin–orbit coupling induces significant distortions in the amorphous structure, altering the arrangement of atoms on the short-range order level [13].

While terbium increases magnetostriction, a higher proportion of Tb in an amorphous alloy can sometimes result in increased brittleness and reduced saturation magnetization (due to Tb's inherently lower magnetic moment compared to some 3d transition metals) [12]. Compositional optimization is therefore crucial to balance mechanical robustness, saturation magnetization, and magnetostriction [14].

D. Thermal Processing

Thermal processing is a critical tool for modifying the magnetic properties of amorphous glass-coated microwires. During rapid quenching (as in the Taylor–Ulitzky method), high residual stresses are "frozen" into the metallic core due to the abrupt temperature drop and the mismatch in thermal expansion between the metal and its glass coating [4]. Annealing provides thermal energy that enables atomic diffusion and stress relaxation. This atomic diffusion not only relaxes internal stresses but also alters the short-range atomic order. As a consequence, annealing leads to several specific effects [15], [16]:

- **Reduction of Magnetoelastic Anisotropy:** The magnetoelastic anisotropy constant K_{me} is given by $K_{me} = \frac{3}{2}\lambda\sigma$, where λ is the magnetostriction coefficient and σ the internal stress. Thermal annealing reduces σ by allowing atoms to rearrange and relieve strain, thereby decreasing the effective anisotropy field H_k [4]. This, in turn, lowers the energy barrier for DW propagation, increasing DW mobility.
- **Decrease in Coercivity:** As internal stresses are relaxed, the coercive field H_c decreases [15]. The uniform reduction in magnetoelastic anisotropy leads to narrower hysteresis loops (Fig. 1), with annealed samples often exhibiting similar coercivities, indicative of homogenized magnetic properties [15].

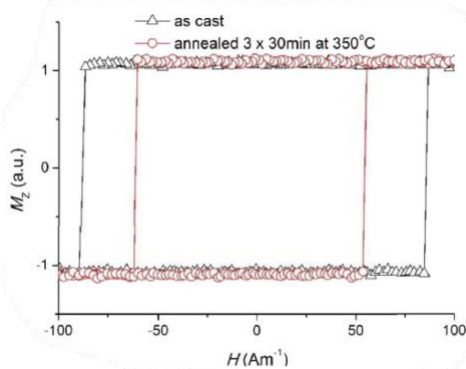


Fig. 1 Hysteresis loops of as-quenched wire and after annealing 3 x 30 min at 350°C [16].

- **Modification of Domain Structure:** Annealing promotes a more uniform domain structure by reducing inhomogeneities in the anisotropy axis that arise from residual stresses [15].
- **Stress-Annealing:** Stress annealing is a post-processing technique in which an external mechanical load is applied during thermal treatment to further modify the internal stress distribution and induce a tailored magnetic anisotropy. This process not only enhances stress relaxation but also promotes the formation of a transverse magnetic anisotropy, leading to significant reductions in coercivity and a

transformation of hysteresis loops – from rectangular to a more linear shape. These changes contribute to enhanced GMI response and improved DW dynamics, optimizing the performance of soft magnetic materials for sensor and memory device applications [17], [18].

E. Switching Field Distribution and Domain Wall Potential

In bistable amorphous microwires, the typical domain structure consists of a large central axial domain, which is magnetized along the wire axis and separated from closure domains located at the wire ends. These closure domains minimize magnetostatic energy and act as initial pinning sites for domain walls. When the applied magnetic field exceeds a critical threshold, a single domain wall depins from the closure region and propagates rapidly along the wire, producing the characteristic Barkhausen jump. However, rather than exhibiting a single, well-defined switching field (H_{sw}), these microwires display a distribution of switching fields. This distribution provides key insights into the energy landscape governing DW depinning and reflects the underlying physics of magnetoelastic and defect-related pinning mechanisms [19], [20], [21], [22], [23].

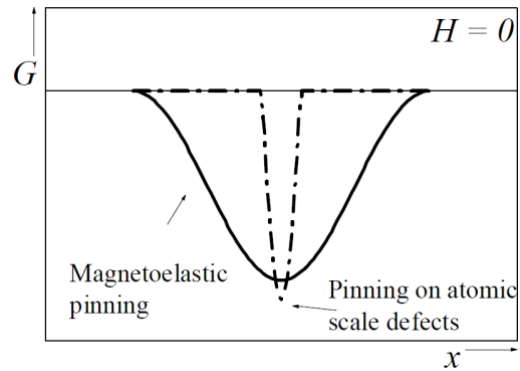


Fig. 2 Schematic view of the two domain-wall potentials that contribute to the switching mechanism [22].

Contributions to the Switching Field Distribution

Several studies have demonstrated that the switching field in amorphous microwires is controlled by two main contributions (Fig. 2) [19], [20], [21], [22], [23]:

Magnetoelastic Pinning:

Residual internal stresses – frozen into the metallic core during rapid quenching – generate a magnetoelastic potential that anchors the DW at the closure domain structure. In Fe-based microwires, which generally exhibit high positive magnetostriction, the magnetoelastic contribution to H_{sw} can be described by a relation of the form [20], [22]:

$$H_{sw,\sigma} \propto c_p M_s^{3/2} [1 + r(\Delta T)]^{1/2}, \quad (1)$$

where M_s is the saturation magnetization, c_p is a constant proportional to the residual stress σ_r , and $r \approx E(\alpha_g - \alpha_m)/\sigma_r$ accounts for additional temperature-dependent stresses arising from mismatched thermal expansion coefficients [19], [20], [21], [22]. This term reflects the “volume” pinning effect due to the overall stress distribution within the microwire. ΔT is the temperature change.

Defect (Atomic-Scale) Pinning:

In addition to the volume magnetoelastic effects, local

atomic-scale defects and structural inhomogeneities provide additional pinning sites. These defects produce local energy barriers that the DW must overcome to depin. The defect-related contribution is often modeled as [19], [20], [21], [22], [23]:

$$H_{sw,p}(T) \propto \frac{1}{M_s} \frac{\epsilon_p^2 \rho_p}{kT} F(T, t), \quad (2)$$

where ϵ_p is the interaction energy between defects and the spontaneous magnetization, kT represents the thermal energy, ρ_p is the density of the mobile defects and $F(T, t) = (1 - e^{-t/\tau})$ is a relaxation function describing the time-dependent dynamics of defect rearrangement, where t is the time of measurement and τ is the relaxation time of mobile defects. This contribution becomes particularly significant at low temperatures, where defect mobility is reduced, thereby increasing the effective switching field.

The total switching field is then expressed as the sum of these two contributions [19], [20], [21], [22], [23]:

$$H_{sw}(T) = H_{sw,\sigma} + H_{sw,p}(T). \quad (3)$$

This superposition model has been validated by fitting experimental data obtained over a broad temperature range [20], [22].

Thermoactivated Depinning Model

The switching of the DW can be understood as a thermally activated process. In the absence of an external magnetic field, the DW resides in a potential well determined by the combined magnetostatic and magnetoelastic energies. When a magnetic field is applied, the total free energy of the DW is given by [19], [20], [21], [22], [23]:

$$G(x) = W(x) - 2\mu_0 M_s H A x, \quad (4)$$

where $W(x)$ represents the intrinsic potential energy, μ_0 is the vacuum permeability, A is the effective area of the DW, and x is its position. As the applied field approaches H_{sw} , the energy barrier ΔG decreases until, at $H = H_{sw}$, it vanishes, allowing the DW to depin (Fig. 3). Thermal fluctuations enable the DW to overcome this barrier even at fields below H_{sw} , resulting in a distribution of switching fields.

The probability dp for the domain wall to depin within a reduced field interval $\Delta H = (H_{sw} - H)/H_{sw}$ is typically modeled by a relation of the form [22]:

$$\frac{dp}{d(\Delta H)} = A' \exp\left(-\frac{\Delta G(\Delta H)}{kT}\right), \quad (5)$$

where A' is a normalization constant. Detailed studies have shown that the logarithm of this probability density often exhibits a 3/2-power law dependence on the reduced field, expressed as [20], [22], [23]:

$$\ln\left(\frac{dp}{d(\Delta H)}\right) = b - a(\Delta H)^{3/2}, \quad (6)$$

with the parameter a directly related to the curvature of the potential well. The parameter b is a constant that arises from the normalization condition and reflects the inherent characteristics of the DW potential. This linear behavior in a plot of $\ln(dp/d(\Delta H))$ versus $(\Delta H)^{3/2}$, enables us to extract important information about the domain wall potential shape and the relative contributions of magnetoelastic and defect pinning.

Frequency and Stress Dependence

In addition to temperature, the switching field distribution is influenced by the frequency of the applied magnetic field and external mechanical stress [23]. Studies on CoFeSiB microwires have shown that at higher frequencies the measured switching field increases linearly with frequency, suggesting that dynamic effects (such as viscous damping of the domain wall) become prominent. Conversely, at low frequencies, additional relaxation effects due to atomic-scale defect stabilization can lead to deviations from the simple model.

Furthermore, the application of external stress has been observed to modify the DW potential [23]. When tensile or compressive stress is applied, the magnetoelastic contribution to the pinning potential is altered, which in turn changes both the mean switching field and the width of its distribution. For example, under applied mechanical load, the internal stress component increases, thereby enhancing the magnetoelastic pinning and shifting the switching field to higher values. Such stress-dependent measurements are crucial for understanding the interplay between mechanical and magnetic phenomena in these complex materials.

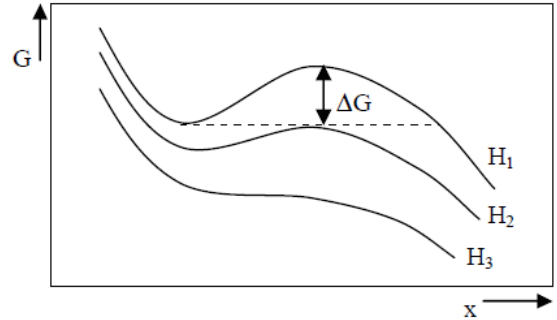


Fig. 3 Schematic representation of the thermoactivated mechanism model. Dependence of the free energy of the DW on its position at applied fields [22].

III. PROBLEM IDENTIFICATION AND FUTURE DIRECTIONS

Although progress has been made in reducing coercivity and homogenizing magnetic properties through thermal processing and alloying, several challenges remain:

1. *Decoupling Pinning Mechanisms:* While current models express H_{sw} as the sum of magnetoelastic and defect-related contributions [19], [20], [21], [22], [23], quantitative separation of these effects under varying processing conditions is still unclear. This separation could be achieved by combining temperature- and stress-dependent measurements. At elevated temperatures, defect-related pinning is expected to weaken due to increased defect mobility, while applying external mechanical stress can selectively enhance the magnetoelastic contribution. By analyzing the switching field distribution under these varying conditions and fitting the results to thermoactivated models, it may be possible to isolate and quantify the individual contributions of each mechanism.
2. *Optimizing Alloy Composition:* The enhancement of magnetostriction by terbium via strong 4f–3d coupling is promising, but the optimal concentrations that maximize magnetic softness without degrading mechanical properties have not been established [11],

[12], [13], [14]. Similarly, the influence of gallium on anisotropy and DW dynamics is underexplored. Systematic alloying studies are required.

3. *Refining Thermal Processing*: Although annealing reduces coercivity and promotes uniformity [15], the ideal temperatures and durations to achieve optimal magnetic properties without triggering crystallization remain unresolved. A more quantitative understanding of thermal energy, stress relaxation, and DW potential evolution is necessary.
4. *Modeling Mechanical Stress Effects*: External mechanical stress alters the H_{sw} distribution and DW potential [23], yet a comprehensive model that predicts these effects accurately is lacking. Controlled temperature- and stress-dependent measurements are needed to decouple magnetoelastic and defect-related contributions.

Addressing these challenges through systematic experimental studies and integrated theoretical modeling will enhance our understanding of magnetization reversal in amorphous microwires and facilitate the design of next-generation magnetic sensors and memory devices with tailored anisotropy and improved performance.

IV. CONCLUSION

In summary, magnetic microwires represent a versatile class of materials whose properties can be finely tuned by controlling magnetic anisotropy, magnetostriction, and DW dynamics. By understanding the interplay between composition, internal stresses, and processing techniques, we can optimize the performance of these microwires for a range of technological applications. Continued research in this area is critical for the development of advanced soft magnetic materials.

ACKNOWLEDGMENT

This research was supported by the Slovak Research and Development Agency under contract No. APVV-16-0079 and VEGA Grant No. 1/0350/24 from the Scientific Grant Agency of the Ministry for Education of the Slovak Republic.


REFERENCES

- [1] V. S. Larin, A. V. Torcunov, A. Zhukov, J. González, M. Vázquez, and L. Panina, "Preparation and properties of glass-coated microwires," *Journal of Magnetism and Magnetic Materials*, vol. 249, no. 1–2, Elsevier BV, pp. 39–45, Aug. 2002. doi: 10.1016/S0304-8853(02)00501-2.
- [2] M. Vázquez and A. P. Zhukov, "Magnetic properties of glass-coated amorphous and nanocrystalline microwires," *Journal of Magnetism and Magnetic Materials*, vol. 160, Elsevier BV, pp. 223–228, Jul. 1996. doi: 10.1016/0304-8853(96)00212-0.
- [3] A. Zhukov, J. González, J. M. Blanco, M. Vázquez, and V. Larin, "Microwires coated by glass: A new family of soft and hard magnetic materials," *Journal of Materials Research*, vol. 15, no. 10, Springer Science and Business Media LLC, pp. 2107–2113, Oct. 2000. doi: 10.1557/jmr.2000.0303.
- [4] V. Zhukova et al., "The Magnetostriction of Amorphous Magnetic Microwires: The Role of the Local Atomic Environment and Internal Stresses Relaxation," *Magnetochemistry*, vol. 9, no. 10, MDPI AG, p. 222, Oct. 20, 2023. doi: 10.3390/magnetochemistry9100222.
- [5] V. Zhukova et al., "Optimization of Magnetic Properties of Magnetic Microwires by Post-Processing," *Processes*, vol. 8, no. 8, MDPI AG, p. 1006, Aug. 18, 2020. doi: 10.3390/pr8081006.
- [6] V. Zhukova et al., "Grading the magnetic anisotropy and engineering the domain wall dynamics in Fe-rich microwires by stress-annealing," *Acta Materialia*, vol. 155, Elsevier BV, pp. 279–285, Aug. 2018. doi: 10.1016/j.actamat.2018.05.068.
- [7] G. Herzer, "Amorphous and Nanocrystalline Soft Magnets," *Magnetic Hysteresis in Novel Magnetic Materials*. Springer Netherlands, pp. 711–730, 1997. doi: 10.1007/978-94-011-5478-9_77.
- [8] A. Zhukov, M. Ipatov, P. Corte-León, L. Gonzalez-Legarreta, J. M. Blanco, and V. Zhukova, "Soft magnetic microwires for sensor applications," *Journal of Magnetism and Magnetic Materials*, vol. 498, Elsevier BV, p. 166180, Mar. 2020. doi: 10.1016/j.jmmm.2019.166180.
- [9] G. Herzer, "Anisotropies in soft magnetic nanocrystalline alloys," *Journal of Magnetism and Magnetic Materials*, vol. 294, no. 2, Elsevier BV, pp. 99–106, Jul. 2005. doi: 10.1016/j.jmmm.2005.03.020.
- [10] A. Zhukov et al., "Advanced functional magnetic microwires for technological applications," *Journal of Physics D: Applied Physics*, vol. 55, no. 25, IOP Publishing, p. 253003, Apr. 04, 2022. doi: 10.1088/1361-6463/ac4fd7.
- [11] Q. Xing, T. A. Lograsso, M. P. Ruffoni, C. Azimonte, S. Pascarelli, and D. J. Miller, "Experimental exploration of the origin of magnetostriction in single crystalline iron," *Applied Physics Letters*, vol. 97, no. 7, AIP Publishing, Aug. 16, 2010. doi: 10.1063/1.3481083.
- [12] R. D. Greenough, T. J. Gregory, S. J. Clegg, and J. H. Purdy, "Magnetostriction and magnetomechanical coupling in amorphous rare earth-iron compounds," *Journal of Applied Physics*, vol. 70, no. 10, AIP Publishing, pp. 6534–6536, Nov. 15, 1991. doi: 10.1063/1.349898.
- [13] F. Jerems, C. M. Mahon, A. G. Jenner, and R. D. Greenough, "Amorphous magnetic materials for transducers," *Ferroelectrics*, vol. 228, no. 1, Informa UK Limited, pp. 333–341, May 1999. doi: 10.1080/00150199908226146.
- [14] J. J. Rhyne, J. H. Schelleng, and N. C. Koon, "Anomalous magnetization of amorphous TbFe₂, GdFe₂, and YFe₂," *Physical Review B*, vol. 10, no. 11, American Physical Society (APS), pp. 4672–4679, Dec. 01, 1974. doi: 10.1103/physrevb.10.4672.
- [15] I. Baraban, S. Leble, L. V. Panina, and V. Rodionova, "Control of magneto-static and -dynamic properties by stress tuning in Fe-Si-B amorphous microwires with fixed dimensions," *Journal of Magnetism and Magnetic Materials*, vol. 477, Elsevier BV, pp. 415–419, May 2019. doi: 10.1016/j.jmmm.2018.12.017.
- [16] J. Onufer, J. Ziman, P. Duranka, and M. Kládiová, "The influence of annealing on domain wall propagation in bistable amorphous microwire with unidirectional effect," *Physica B: Condensed Matter*, vol. 540, Elsevier BV, pp. 58–64, Jul. 2018. doi: 10.1016/j.physb.2018.04.011.
- [17] P. Corte-León et al., "Engineering of Magnetic Softness and Domain Wall Dynamics of Fe-rich Amorphous Microwires by Stress- induced Magnetic Anisotropy," *Scientific Reports*, vol. 9, no. 1, Springer Science and Business Media LLC, Aug. 27, 2019. doi: 10.1038/s41598-019-48755-4.
- [18] V. Zhukova, J. M. Blanco, M. Ipatov, M. Churyukanova, S. Taskaev, and A. Zhukov, "Tailoring of magnetoimpedance effect and magnetic softness of Fe-rich glass-coated microwires by stress- annealing," *Scientific Reports*, vol. 8, no. 1, Springer Science and Business Media LLC, Feb. 16, 2018. doi: 10.1038/s41598-018-21356-3.
- [19] R. Varga, "Switching field fluctuations in bitable microwires," *Physica B: Condensed Matter*, vol. 343, no. 1–4, Elsevier BV, pp. 403–409, Jan. 01, 2004. doi: 10.1016/j.physb.2003.08.077.
- [20] K. L. Garcia, R. Varga, and M. Vazquez, "Influence of the magnetoelastic mechanism on the fluctuating switching field of Fe-based amorphous microwires," *IEEE Transactions on Magnetics*, vol. 41, no. 10, Institute of Electrical and Electronics Engineers (IEEE), pp. 3256–3258, Oct. 2005. doi: 10.1109/tmag.2005.854669.
- [21] R. Varga, K. L. Garcia, M. Vázquez, A. Zhukov, and P. Vojtanik, "Switching-field distribution in amorphous magnetic bistable microwires," *Physical Review B*, vol. 70, no. 2, American Physical Society (APS), Jul. 02, 2004. doi: 10.1103/physrevb.70.024402.
- [22] R. Varga, K. L. Garcia, A. Zhukov, M. Vazquez, and P. Vojtanik, "Temperature dependence of the switching field and its distribution function in Fe-based bistable microwires," *Applied Physics Letters*, vol. 83, no. 13, AIP Publishing, pp. 2620–2622, Sep. 29, 2003. doi: 10.1063/1.1613048.
- [23] R. Varga, A. Zhukov, J. M. Blanco, J. Gonzalez, V. Zhukova, and P. Vojtanik, "Stress dependence of the domain wall potential in amorphous CoFeSiB glass-coated microwires," *Physica B: Condensed Matter*, vol. 372, no. 1–2, Elsevier BV, pp. 230–233, Feb. 2006. doi: 10.1016/j.physb.2005.10.055.

Applications of Homomorphic Encryption in Biometric Data Protection

¹Eva Kupcová (2nd year),
Supervisor: ²Matúš Pleva

^{1,2}Dept. of Electronics and Multimedia Telecommunications, FEI TU of Košice, Slovak Republic

¹eva.kupcova@tuke.sk , ²matus.pleva@tuke.sk 

Abstract—Biometric authentication provides a secure method for identity verification, but protecting sensitive data remains a challenge. Homomorphic encryption (HE) offers a privacy-preserving solution by enabling computations on encrypted biometric data without decryption, reducing the risk of breaches. This paper explores HE applications in biometric security, including secure authentication, multimodal fusion, and large-scale indexing. Our research focuses on using HE to encrypt biometric data stored in databases, ensuring secure authentication while maintaining data protection and privacy.

Keywords—Homomorphic encryption, biometric authentication, data protection

I. INTRODUCTION

BIOMETRIC systems are widely used for identity verification in sectors like law enforcement, healthcare, and finance. Unlike passwords, they rely on unique traits such as fingerprints or facial features, making them harder to forge. However, the permanence of biometric data means breaches cannot be undone, raising significant security risks. High-profile data leaks underscore the need for enhanced protection.

As cyber threats evolve, biometric systems require advanced cryptographic methods to protect data throughout its lifecycle. Homomorphic encryption (HE) enables computations on encrypted biometric data, preserving privacy without exposing sensitive information. Unlike traditional encryption, HE operates directly on ciphertexts, with results accessible only to authorized parties. This makes HE ideal for cloud-based biometric systems, where data security is critical. Despite the computational overhead, ongoing improvements enhance its feasibility [1]. Figure 1 illustrates the core concept of HE.

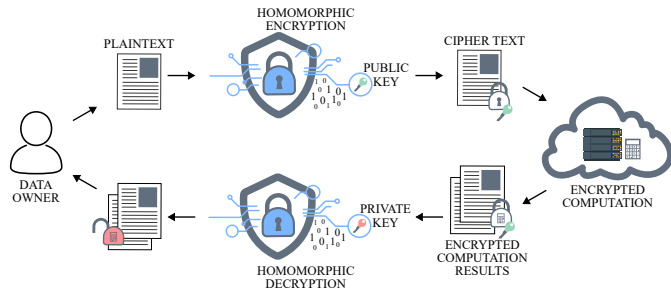


Fig. 1. Basic scheme of HE: computations are performed on encrypted data without decryption, ensuring secure processing.

II. OVERVIEW OF HOMOMORPHIC ENCRYPTION

Homomorphic encryption is an advanced cryptographic technique that allows operations on encrypted data without the

need for decryption. This is especially valuable for privacy-sensitive applications like biometric authentication, where user data must remain confidential throughout the entire processing stage. By performing computations directly on encrypted data, HE ensures that sensitive information remains secure, even during processing [2].

HE schemes are classified based on their computational capabilities, specifically the types and number of supported operations [1]:

- *Partially Homomorphic Encryption* (PHE): Supports one operation (addition or multiplication) on encrypted data. While efficient, it is limited to simple computations and is typically used when only one operation is needed, such as in early encryption schemes for small datasets.
- *Somewhat Homomorphic Encryption* (SHE): Supports both addition and multiplication on encrypted data, but only for a limited number of operations before noise accumulates, potentially causing errors. Techniques like noise management or bootstrapping are needed to preserve encryption integrity. SHE is more flexible than PHE and suits applications with multiple simple operations.
- *Fully Homomorphic Encryption* (FHE): Supports unlimited operations on encrypted data, but noise accumulation during operations is managed using techniques like bootstrapping. It is computationally expensive and resource-intensive.

Table I compares different HE schemes, outlining their supported operations and examples of commonly used cryptographic algorithms.

TABLE I
COMPARISON OF HOMOMORPHIC ENCRYPTION SCHEMES

Type	Supported Operations	Examples
PHE	Addition (Paillier) or Multiplication (RSA)	RSA, Paillier
SHE	Limited Addition and Multiplication	BV, GHS
FHE	Unlimited Addition and Multiplication (via bootstrapping)	Gentry, BFV, CKKS

Mathematically, an HE scheme consists of several components. First, a pair of *public* and *private keys* is generated during the key generation phase. Next, encryption takes place, where a plaintext biometric sample m is encrypted using the public key, resulting in ciphertext $c = \text{Enc}(m)$. Then, computation occurs, where a function f is applied to the

ciphertext c , producing $c' = f(c)$ without needing to decrypt the data. Finally, decryption is performed with the private key, yielding the result $f(m)$ [1].

III. STATE OF THE ART

Recent advancements in HE have led to various methods for securing biometric data, enabling operations on encrypted templates. These approaches aim to enhance security, computational efficiency, and resistance to quantum attacks.

The study in [3] presents a hybrid approach combining HE with cancelable biometrics, enhancing security by protecting biometric templates even if encryption keys are compromised. Techniques like BioHashing and Multi-Layer Perceptron hashing improve efficiency in encrypted-domain comparisons.

In [4], the authors focus on FHE-based biometric matching for border control, addressing privacy concerns under GDPR. They propose a system that integrates hash expansion with FHE, reducing execution time through parallel processing. Their proof-of-concept in SMILE effectively preserves privacy.

HE-based fingerprint authentication secures biometric templates and enables matching in the encrypted domain, protecting against attacks. The trade-off between computational efficiency and accuracy is analyzed and validated on the FVC2002 DB2 database, proving its suitability for high-security applications [5].

Multimodal biometric authentication, such as iris and facial recognition fusion, benefits from homomorphic encryption (HE). Studies show HE secures template fusion while maintaining high true acceptance rates, including 96.41% for iris and 100% TAR for face and iris fusion [6].

To address quantum threats, researchers combine HE with Classic McEliece, ensuring long-term security for secure biometric authentication. This method reduces storage, enhances accuracy, and resists attacks, with real-time execution and a 90.5% storage reduction [7].

For large-scale biometric identification, HE enables encrypted domain indexing, ensuring privacy. However, auxiliary indexing data may leak sensitive information. The study proposes the HEBI framework, which protects indexing with post-quantum security and low computational overhead [8].

The research [9] explores the use of FHE to secure iris biometric templates, enabling matching in the encrypted domain while preserving privacy. It also investigates machine learning techniques for improved accuracy and reduced execution time, with CKKS ensuring confidentiality.

An innovative application explored in this study is the fusion of encrypted biometric modalities, such as fingerprint and iris data, using FHE to enhance authentication accuracy and improve privacy protection, as demonstrated by the HEFT framework [10].

Privacy-preserving biometric matching using lattice-based FHE ensures post-quantum security, preserves recognition accuracy, and significantly reduces computational workload in encrypted-domain identification [11].

Moreover, template protection techniques using FHE have been refined to minimize computational overhead, support operations on real-valued feature vectors, and enable one-shot user enrollment while improving biometric security standards and matching performance by 3% [12].

IV. CONCLUSION AND FUTURE RESEARCH DIRECTIONS

HE has significantly advanced biometric data protection, enabling secure and privacy-preserving authentication across diverse applications, from biometric matching at border controls to large-scale biometric indexing and post-quantum security. By allowing computations on encrypted data, HE reduces the risk of data breaches while ensuring data integrity and user privacy. Despite its advantages, challenges such as computational overhead and scalability remain key concerns.

Our research explores the use of HE to protect biometric data stored in databases, ensuring privacy during authentication. Specifically, we analyze the efficiency of HE schemes in real-time biometric matching, the trade-offs between security and computational complexity, and the feasibility of integrating HE with secure multiparty computation to enhance privacy. Future research will focus on optimizing HE-based biometric authentication for Internet of Things environments, addressing computational constraints while maintaining security.

ACKNOWLEDGMENT

The research was partially supported by the Ministry of Education, research, development and Youth of the Slovak Republic under the projects KEGA 049TUKE-4/2024 & VEGA 2/0092/25, by the Slovak Research and Development Agency under the projects APVV-22-0414 & APVV-22-0261 as well as by the Erasmus+ MetaCog 2024-1-FI01-KA220-HED-000247530 project.

REFERENCES

- [1] W. Yang, S. Wang, H. Cui, Z. Tang, and Y. Li, "A review of homomorphic encryption for privacy-preserving biometrics," *Sensors*, vol. 23, no. 7, p. 3566, 2023.
- [2] C. Gilbert and M. Gilbert, "The effectiveness of homomorphic encryption in protecting data privacy," *International Journal of Research Publication and Reviews*, vol. 5, pp. 3235–3256, 11 2024.
- [3] H. O. Shahreza, C. Rathgeb, D. Osorio-Roig, V. K. Hahn, S. Marcel, and C. Busch, "Hybrid protection of biometric templates by combining homomorphic encryption and cancelable biometrics," in *2022 IEEE International Joint Conference on Biometrics (IJCB)*, 2022, pp. 1–10.
- [4] F. O. Catak, S. Y. Yayilgan, and M. Abomhara, "A privacy-preserving fully homomorphic encryption and parallel computation based biometric data matching," *Preprints*, 2020.
- [5] W. Yang, S. Wang, K. Yu, J. J. Kang, and M. N. Johnstone, "Secure fingerprint authentication with homomorphic encryption," in *2020 Digital Image Computing: Techniques and Applications (DICTA)*. IEEE, 2020, pp. 1–6.
- [6] S. Singh, L. Igene, and S. Schuckers, "Securing biometric data: Fully homomorphic encryption in multimodal iris and face recognition," in *2024 International Conference of the Biometrics Special Interest Group (BIOSIG)*. IEEE, 2024, pp. 1–6.
- [7] R. Arjona, P. López-González, R. Román, and I. Baturone, "Post-quantum biometric authentication based on homomorphic encryption and classic mceliece," *Applied Sciences*, vol. 13, no. 2, p. 757, 2023.
- [8] P. Bauspieß, M. Grimmer, C. Fougner, D. Le Vasseur, T. T. Stöcklin, C. Rathgeb, J. Kolberg, A. Costache, and C. Busch, "Hebi: Homomorphically encrypted biometric indexing," in *2023 IEEE International Joint Conference on Biometrics (IJCB)*. IEEE, 2023, pp. 1–10.
- [9] P. Chitrapu and H. K. Kalluri, "A survey on homomorphic encryption for biometrics template security based on machine learning models," in *2023 IEEE International Students' Conference on Electrical, Electronics and Computer Science (SCECS)*. IEEE, 2023, pp. 1–6.
- [10] L. Sperling, N. Ratha, A. Ross, and V. N. Boddeti, "Heft: Homomorphically encrypted fusion of biometric templates," in *2022 IEEE International Joint Conference on Biometrics (IJCB)*. IEEE, 2022, pp. 1–10.
- [11] P. Bauspieß, J. Kolberg, P. Drozdowski, C. Rathgeb, and C. Busch, "Privacy-preserving preselection for protected biometric identification using public-key encryption with keyword search," *IEEE Transactions on Industrial Informatics*, vol. 19, no. 5, pp. 6972–6981, 2022.
- [12] A. K. Jindal, I. Shaik, V. Vasudha, S. R. Chalamala, R. Ma, and S. Lodha, "Secure and privacy preserving method for biometric template protection using fully homomorphic encryption," in *2020 IEEE 19th international conference on trust, security and privacy in computing and communications (TrustCom)*. IEEE, 2020, pp. 1127–1134.

Intrusion Detection Systems and Attack Graphs

¹Jaroslav MARKO (1st year),
Supervisor: ²Anton BALAŽ

^{1,2}Dept. of Computers and Informatics, FEI, Technical University of Košice, Slovak Republic

¹jaroslav.marko@tuke.sk, ²anton.balaz@tuke.sk

Abstract—The security of computer systems is becoming increasingly important, with intrusion detection systems (IDS) playing a crucial role in safeguarding computer networks. In this article, we explore the significance of IDS in network security and examine how they operate. We provide an overview of the basic classification of IDS. In the second part of the paper, we discuss graph models in cybersecurity, adopting a classification approach based on previous research. We analyze five graph models that meet our selected criteria and highlight alternative approaches to graph modeling. Additionally, we investigate how attack graphs can enhance the effectiveness of IDS. Finally, we identify existing challenges and propose future research directions and open questions.

Keywords—intrusion detection systems, attack graph models, network vulnerabilities

I. INTRODUCTION

Security in computer networks is increasingly important with growing informatization and automation. The rising number of connected devices demands robust network protection, with Intrusion Detection Systems (IDS) playing a key role by detecting abnormal activity and attacker behavior patterns.

Graph-based models effectively describe attacks, from simple to complex scenarios, including parallel processes. These models help predict attacker steps and strengthen network defenses. Combined with IDS, they enhance threat detection, analyze network relationships, and provide critical insights into attack progression, highlighting their vital role in cybersecurity.

II. INTRUSION DETECTION SYSTEMS

IDS is a system that can detect security breaches in real time, regardless of whether the attacker is external or internal, who is just trying to exploit the privileges that have been granted to him. IDS is based on the hypothesis that exploitation of vulnerabilities in the network or on endpoint devices involves abnormal activity or unusual use of the system [1], [2].

Nowadays, an IDS is associated with a software or hardware system that automates the process of monitoring a network and the events that occur on it. These events are analyzed for traces of intrusions [3].

A. Components of IDS

Intrusion detection systems consist of several basic components that work together to identify security threats [4].

According to the work of Thakkar and Lohiya [4], the most important components include (i) network monitoring, which captures network packets in order to gather information about

potential attack patterns (ii) collecting device-specific data, on which an attack is likely to be carried out (iii) packet detail analysis, where during this phase the IDS scans network packets for sensitive information (iv) identification and storage of fingerprints or descriptions of attack patterns (v) finally, generation of alerts for the security administrator.

B. Taxonomy of IDS Classification

The IDS Classification Taxonomy provides a structured and consistent approach to categorising these systems. According to the selected existing reviews [4], [5], [6] we have selected three classifications based on:

- 1) Information Source,
- 2) Analysis Strategy,
- 3) Architecture.

It is these categories that help experts to select the most effective solution. The selected classifications are not all available or used, but for the purposes of this article, it is not necessary to discuss all of them. Further classifications can be found in the review articles sorted by publication date from the most recent [7], [4], [8], [6], [9], [3].

1) *Classification Based on Information Source*: IDSs are classified into several categories, which include a division based on the source of the information [4] or the technology [8] that handled the events. Host-based IDS (HIDS) is installed on a local device or system. It examines and inspects data that originates from the host system and audits sources such as operating system, service logs, firewall logs, application logs, and others [10], [6]. Network-based IDS (NIDS) are devices installed on a network in contrast to the previous category. This type of system accesses the network communication and then analyzes this traffic data. NIDS can be further divided into two other subcategories packet-based and flow-based [11], [4]. Some sources give other classifications in this category but they are not relevant for this review. These include, for instance, Application-based IDS [3], Wireless IDS [8] or Network Behavior Analysis [7].

2) *Classification Based on Analysis Strategy*: The second most important classification of IDS is based on Analysis Strategy. Detection systems analyze traffic based on two approaches in terms of the strategy used. The first of these approaches is Anomaly-based IDS (AIDS), which works by analyzing and looking for patterns of behavior in the network and trying to detect anomalies. Both static and dynamic approaches can be used. The static one focuses on unchanging elements of systems such as the configuration of critical software components or hardware components. The dynamic analysis monitors network traffic in real time. It evaluates

system logs and user behavior. This approach is also effective in identifying zero-day attacks and other unknown intrusions [4], [12]. The second approach is Misuse-based IDS (MIDS) also referred to as Signature-based IDS (SIDS). Later in the paper, when we refer to this approach, we will use the acronym SIDS [8], [12]. SIDS is a simpler detection method than AIDS. The system compares a database of known fingerprints or also signatures, and looks for that attack type or which particular attack is being carried out. SIDS are very effective for detecting already known attacks and intrusions. The disadvantage of this strategy is that in order to achieve a high success rate, we need to have a database of all types of attacks even with their different variants that contain outliers. Such a database must be maintained and updated regularly [8]. Both AIDS and SIDS approaches have their advantages and disadvantages. However, the most optimal results come from using a combination of the two in one system. This kind of system is called Hybrid-based IDS.

3) *Classification Based on Architecture*: An IDS can be implemented in three ways in terms of architecture. The first IDS systems were exclusively implemented on a single device or within a network and were isolated from other data inputs [9]. Over time, communication between multiple IDS systems was tested and the following three approaches were developed:

- Centralized CIDS,
- Decentralized CIDS,
- Distributed CIDS.

Such systems consist of monitoring and analysis units that communicate with each other to more efficiently solve network intrusion detection problems. Centralized IDS is built on a single node that collects network traffic from multiple monitoring nodes. The central node analyzes this data and triggers alerts [13]. In a Distributed IDS architecture, each entity in the network is able to detect and respond to intrusions independent of the others. As an advantage of this architecture, there is no single point of failure [4]. The last approach to IDS systems architecture is Decentralized IDS. This architecture uses a hierarchical approach where preprocessing and correlation of monitored data is done according to the hierarchy before data and results are sent to higher level centralized units. The advantage is that the performance bottleneck is reduced but still the whole result relies on the central analysis unit [9].

III. GRAPH BASED MODELS IN CYBERSECURITY

Graph models have been used in security since the mid-1990s. They provide useful methods for visualization and analysis of security scenarios. They help in finding vulnerabilities in systems and organizations. A great advantage of such graphical models is the possibility of qualitative and quantitative analyses [14].

For the purpose of this graph model review, we analyzed several scientific papers by [15], [16], [14] and selected several graph models from them. In this section, we describe the classification of attack graphs as defined by Wachter [15] in his survey of attack models. In the course of his work, he selected 70 different attack graphs that had a specific name defined and not just the generic name "Attack Graph".

A. Classification of Attack Graph Based on Meta-Types

From past reviews of [17], [18], [14], Wachter was able to identify 5 splits (i) Tree models vs. general graph models

(ii) Stateful models vs. stateless models (iii) Node- and Edge Semantics (iv) Attack vs. Asset view (v) Exploit-oriented Meta-Types [15].

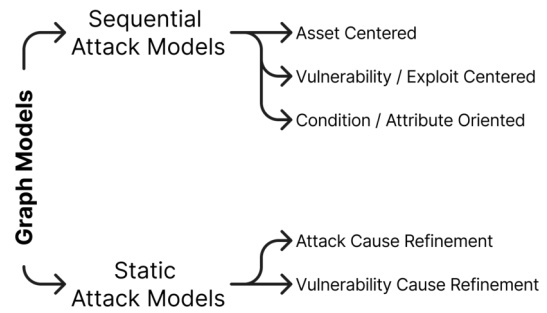


Fig. 1. Attack Graph formalism categories [15]

1) *Sequential vs. Static Attack Models*: We start right away with the first division, which divides all the analyzed models into two groups. Sequential models and causal dependency models. Sequential models contain both sequential and causal dependencies in their edges while causal dependency models (Static Attack Models) show common dependencies between nodes [14].

2) *Sequential Models -> Node Semantics*: Sequential attack models are further classified based on the semantics of their nodes into three main types [15]: (i) Models that focus on system components and help to identify vulnerable targets. (ii) Vulnerability-centric models, these are particularly effective in prioritizing vulnerabilities for patch management. (iii) Condition-specific models, which highlight configurations that could lead to compromise of systems.

3) *Sequential Models -> Attack vs. Vulnerability*: At the second level, for static attack models, formalisms are categorized based on the refinement provided by [15]: (i) Attack cause refinement models, which show the causal relationships between events or elements leading to an attack. They are useful in the context of threat modelling. (ii) Vulnerability cause refinement models focus on the causal relationships between the events or elements that cause vulnerabilities.

B. Attack and/or Defense Modeling

The classification of models according to their approach from the 1 figure is not the only classification. Kordy et al. in their paper [14] also pointed out a division according to the perspective from which a given model/graph is built and modeled. A graph modeling an attack focuses on attacker activity and system vulnerabilities. A defensive model concentrates on defensive aspects such as detection, reaction, response and prevention. In some cases, there are models that focus on the interaction of the two models. In this case, the concept of agents (attacker, defender) is used to define what a given view of the modeling graph looks like [15].

The authors of the review articles aim to categorize all available and analyzed attack charts according to this aspect. Thanks to this, it is possible to choose the right formalism for a particular case.

C. Attack Graph Usage in IDS

Graph models are designed to support practical applications in security. According to the authors, the formalisms are made to help with Simulation, Security Quantification and Intrusion

Detection. It is the last area that is important for improving detection functionality. These models are used within the fourth (iv) point in the chapter Components of IDS (II. Intrusion Detection Systems).

In our opinion, an important component is the ability to automatically generate graphs based on formalisms, network information, and the results of vulnerability scans. This will simplify the integration of graph models and improve the detection capability of IDS systems [19].

We applied these criteria to the attack graphs analyzed in the [15] review. We found 5 graph formalisms out of 70 that satisfy our chosen criteria:

- Hyper-alert Correlation Graphs (2003) [20]
- Hyper-Alert Graphs (2006) [21]
- Alert Dependence Graph (2011) [22]
- Activity Graph (1996) [23]
- Scenario Attacks; Requires-Provides Model (2001) [24]

D. Alternative Approaches

However, there are other alternative models that were not appropriate to include within the main objective of the selected graphical models. However, for completeness of the review, it was important for us to mention these methods as well.

Petri nets were first mentioned in the thesis of [25]. Later these networks were extended with additional attributes and are called Colored Petri Nets [26]. Some authors combine the concepts of security patterns or attack trees together with Petri nets. Interestingly, Zakrzewska and Ferragut [27] present models of extended Petri nets in their work, and they showed that extended Petri nets are more readable compared to attack graphs.

While not primarily designed for attack modeling, approaches derived from UML diagrams are more suited for capturing threats and malicious behavior [14]. However, they can still be used to model attacks although their limitation when used in IDS is somewhat more limited.

IV. CONCLUSIONS

We analyzed several scientific publications in the field of network security. We have described the needs for the use of IDS and its operation. We have pointed out the most important IDS classifications chosen by us, such as Information Source, Analysis Strategy and Architecture. Previous works have shown the importance and effectiveness of Decentralized IDS in the network, although there are still weaknesses and drawbacks identified in this area, which opens opportunities for further research and improvements of these systems.

In the second part of the paper, we took a closer look at the processing of attacks and patterns that are directly or indirectly exploited by IDS systems. These patterns are written in graph formalisms or models. We briefly described the history and classification of graph models according to previous research and works. We highlighted the importance of using graph models in IDS and selected five formalisms based on our chosen criteria. The attack graph must support the IDS by its functionality and at the same time it must be possible to generate these graphs automatically. Finally, we also pointed out alternative models for security incidents and attacks.

The identification of problems and future directions will be primarily devoted to graph models, as we believe that this is where further research needs to be devoted in order for these

models to act as a basis for continuous improvement of IDS systems.

A. Problem Identification

During the analysis of graph-based models used in intrusion detection systems (IDS), several persistent problems and research gaps were identified. These gaps, which have also been noted in previous literature, limit the practical deployment and development of graph-based detection techniques in the context of modern cybersecurity.

1) *Lack of Standardization in Formalisms:* Most existing formalisms - such as attack graphs, attack trees, and Petri nets - suffer from the lack of a standardized structure for representing and analyzing attacks. Although visual model syntaxes such as attack trees or Petri nets have been partially standardized (e.g., as per the reference in [17]), there is no universally accepted standard for graph-based IDS models. The result is a fragmented research environment in which many models differ only slightly, yet are treated as separate entities, as referenced in [15] and [14].

Research gap: There is a lack of a unified framework or ontology to support consistent generation, interpretation and evaluation of graph models across different ITS implementations.

2) *Out of Date Formalisms:* As noted in the Using Attack Graphs in IDS section, most of the models that meet our selection criteria are from 2011 or earlier. These models were developed to represent known attack behavior at the time, and often lack the ability to represent newer types of threats, such as threats involving polymorphic malware, lateral movement in cloud environments, or attacks generated by artificial intelligence.

Research gap: There has been limited recent work on updating classic attack graphs to reflect modern threats or to adapt them to today's complex and dynamic systems.

B. Future Directions

Based on the findings presented in this paper and insights from previous research, we have identified several promising areas for further research. These areas are currently underexplored in the literature, but have great potential for advancing the field of proactive cybersecurity, particularly in the context of graph-based analytics and artificial intelligence. Our future work will focus on the following three directions, with specific approaches listed below:

1) *Defender model with automatic generation:* As pointed out by Wachter [15] in his work, most existing models of attack graphs focus on the attacker, with limited emphasis on the defender's view. Furthermore, there is currently no widely adopted framework that allows for the automatic generation of such defense-oriented graph models. In our future research, we aim to fill this gap by designing and implementing a defense graph model that integrates nodes representing defensive assets (e.g., firewalls, IDS sensors), detection capabilities, and mitigation responses.

Our planned approach involves analyzing system architecture descriptions, firewall rules, and network topology data to extract and encode defense configurations. Based on this input data, we will create a graph generation engine that will automatically produce a visual and analyzable structure. This model will also take into account defensive countermeasures

and detection points, allowing for the simulation of different attack scenarios from the defender's perspective. The generated graphs will support a variety of use cases including blue team planning, incident response simulation, and risk assessment.

2) *large language models*: The use of large language models (LLMs), such as GPT, in cybersecurity is a relatively new trend, but is gaining increasing attention. Recent work by [28] has shown that LLMs can support security-related tasks such as vulnerability identification or code analysis. In our future work, we intend to explore two specific ways in which LLMs can extend the use of attack graphs:

- **Graph generation**: LLMs can be used to parse unstructured threat reports, CVE descriptions, and security recommendations to automatically generate attack graphs. We plan to create a pipeline that uses prompt engineering and structured output formatting (e.g. JSON, GraphML) to translate textual threat data into graph structures. This will reduce the amount of manual work and improve scalability.
- **Natural Language Interaction**: Our goal is to develop a prototype that allows system administrators and analysts to query attack graphs using natural language, e.g., "Which paths lead to elevated privileges from host X?" or "What are possible mitigation strategies for vulnerability Y?". This approach increases usability for non-experts and bridges the gap between complex graph structures and operational security knowledge.

3) *Attack variant detections*: Another important future direction is to explore the use of graph models to detect new and variant forms of cyber attacks that traditional signature-based systems may not detect. We propose to focus on graph similarity analysis and subgraph matching techniques that can reveal structural similarities between known attack paths and new threats.

To support this, we plan to develop a framework for feature extraction that converts attack graphs into numerical representations suitable for machine learning algorithms. Techniques such as graph embeddings (e.g., Node2Vec, GraphSAGE) and graph neural networks (GNNs) will be evaluated to detect anomalous or suspicious graph structures. This method could significantly improve the proactive detection capabilities of intrusion detection systems, especially in identifying zero-day exploits or polymorphic malware behavior.

ACKNOWLEDGMENT

This work was supported by KEGA Agency of the Ministry of Education, Science, Research, and Sport of the Slovak Republic under Grant No. 015TUKE-4/2024 Modern Methods and Education Forms in the Cybersecurity Education.

REFERENCES

- [1] D. E. Denning and P. G. Neumann, "Requirements and model for ides-a real-time intrusion detection system," Computer Science Laboratory, SRI International, Menlo Park, CA, Technical Report, 1985.
- [2] D. E. Denning, "An intrusion-detection model," *IEEE Transactions on Software Engineering*, vol. SE-13, no. 2, pp. 222–232, Feb 1987.
- [3] R. Bace and P. Mell, "Nist special publication on intrusion detection systems," *National Institute of Standards and Technology*, vol. 16, 2001.
- [4] A. Thakkar and R. Lohiya, "A survey on intrusion detection system: feature selection, model, performance measures, application perspective, challenges, and future research directions," *Artificial Intelligence Review*, vol. 55, no. 1, p. 453–563, Jan. 2022.
- [5] H. Liu and B. Lang, "Machine learning and deep learning methods for intrusion detection systems: A survey," *Applied Sciences*, vol. 9, no. 2020, p. 4396, Jan. 2019.
- [6] A. Khraisat, I. Gondal, P. Vamplew, and J. Kamruzzaman, "Survey of intrusion detection systems: techniques, datasets and challenges," *Cybersecurity*, vol. 2, no. 1, p. 20, Jul. 2019.
- [7] D. P. F. Möller, *Intrusion Detection and Prevention*. Cham: Springer Nature Switzerland, 2023, p. 131–179. [Online]. Available: https://doi.org/10.1007/978-3-031-26845-8_3
- [8] M. Ozkan-Okay, R. Samet, Aslan, and D. Gupta, "A comprehensive systematic literature review on intrusion detection systems," *IEEE Access*, vol. 9, p. 157727–157760, 2021.
- [9] E. Vasilomanolakis, S. Karuppayah, M. Mühlhäuser, and M. Fischer, "Taxonomy and survey of collaborative intrusion detection," *ACM Comput. Surv.*, vol. 47, no. 4, pp. 55:1–55:33, May 2015.
- [10] P. Deshpande, S. C. Sharma, S. K. Peddoju, and S. Junaid, "Hids: A host based intrusion detection system for cloud computing environment," *International Journal of System Assurance Engineering and Management*, vol. 9, no. 3, p. 567–576, Jun. 2018.
- [11] E. Altulaihian, M. A. Almaiah, and A. Aljughaiman, "Anomaly detection ids for detecting dos attacks in iot networks based on machine learning algorithms," *Sensors*, vol. 24, no. 22, p. 713, Jan. 2024.
- [12] S. Agrawal and J. Agrawal, "Survey on anomaly detection using data mining techniques," *Procedia Computer Science*, vol. 60, p. 708–713, Jan. 2015.
- [13] S. R. Snapp, J. Brentano, G. V. Dias, T. L. Goan, L. T. Heberlein, C.-L. Ho, K. N. Levitt, B. Mukherjee, S. E. Smaha, T. Grance *et al.*, "Dids (distributed intrusion detection system)-motivation, architecture, and an early prototype," in *Proceedings of the 14th national computer security conference*, vol. 1. Washington, DC, 1991, pp. 167–176.
- [14] B. Kordy, L. Piètre-Cambacédès, and P. Schweitzer, "Dag-based attack and defense modeling: Don't miss the forest for the attack trees," *Computer Science Review*, vol. 13–14, p. 1–38, Nov. 2014.
- [15] J. Wachter, "Graph models for cybersecurity – a survey," Nov. 2023, arXiv:2311.10050 [cs]. [Online]. Available: <http://arxiv.org/abs/2311.10050>
- [16] J. Zeng, S. Wu, Y. Chen, R. Zeng, and C. Wu, "Survey of attack graph analysis methods from the perspective of data and knowledge processing," *Security and Communication Networks*, vol. 2019, no. 1, p. 2031063, 2019.
- [17] H. S. Lallie, K. Debattista, and J. Bal, "A review of attack graph and attack tree visual syntax in cyber security," *Computer Science Review*, vol. 35, p. 100219, Feb. 2020.
- [18] P. Mell, R. Harang *et al.*, "Minimizing attack graph data structures," in *The Tenth International Conference on Software Engineering Advances*, 2015.
- [19] S. Roschke, F. Cheng, and C. Meinel, "Using vulnerability information and attack graphs for intrusion detection," in *2010 Sixth International Conference on Information Assurance and Security*, Aug. 2010, p. 68–73. [Online]. Available: https://ieeexplore.ieee.org/document/5604041?utm_source=chatgpt.com
- [20] P. Ning and D. Xu, "Learning attack strategies from intrusion alerts," in *Proceedings of the 10th ACM conference on Computer and communications security*, 2003, pp. 200–209.
- [21] B. Zhu and A. A. Ghorbani, "Alert correlation for extracting attack strategies," *Int. J. Netw. Secur.*, vol. 3, no. 3, pp. 244–258, 2006.
- [22] S. Roschke, F. Cheng, and C. Meinel, "A new alert correlation algorithm based on attack graph," in *Computational Intelligence in Security for Information Systems: 4th International Conference, CISIS 2011, Held at IWANN 2011, Torremolinos-Málaga, Spain, June 8-10, 2011. Proceedings*. Springer, 2011, pp. 58–67.
- [23] S. Staniford-Chen, S. Cheung, R. Crawford, M. Dilger, J. Frank, J. Hoagland, K. Levitt, C. Wee, R. Yip, and D. Zerkle, "Grids-a graph based intrusion detection system for large networks," in *Proceedings of the 19th national information systems security conference*, vol. 1. CiteSeer, 1996, pp. 361–370.
- [24] S. J. Templeton and K. Levitt, "A requires/provides model for computer attacks," in *Proceedings of the 2000 workshop on New security paradigms*, 2001, pp. 31–38.
- [25] M. Dacier, "Vers une évaluation quantitative de la sécurité informatique," Ph.D. dissertation, Institut National Polytechnique de Toulouse-INPT, 1994.
- [26] S. Kumar and E. H. Spafford, "A pattern matching model for misuse intrusion detection," 1994.
- [27] A. N. Zakrzewska and E. M. Ferragut, "Modeling cyber conflicts using an extended petri net formalism," in *2011 IEEE Symposium on Computational Intelligence in Cyber Security (CICS)*. IEEE, 2011, pp. 60–67.
- [28] Y. Zhang, T. Du, Y. Ma, X. Wang, Y. Xie, G. Yang, Y. Lu, and E.-C. Chang, "Attackg+: Boosting attack graph construction with large language models," *Computers Security*, vol. 150, p. 104220, Mar. 2025.

Use of XAI methods and its evaluation in various domains

¹Miroslava MATEJOVÁ (3rd year)
Supervisor: ²Ján PARALIČ

^{1,2}Dept. of Cybernetics and Artificial Intelligence, FEI, Technical University of Košice, Slovak Republic

¹miroslava.matejova@tuke.sk, ²jan.paralic@tuke.sk

Abstract—Explainable artificial intelligence (XAI) is desperately needed, as seen by the growing use of advanced machine learning algorithms. This paper explores the development and evaluation of XAI methods, focusing on stakeholder needs and the application of different explanation methods in the medical and social media domains. In the medical field, we created a Multi-layer Perceptron classifier model and conducted a user study with students and doctors to compare explanation methods such as LIME, SHAP, ANCHORS, and PDP. Using a questionnaire, we examined the metrics: Understandability, Usefulness, Trustworthiness, Informativeness and Satisfaction and evaluated methods for different user groups. In the social media domain, we used CNN, XGBoost and BERT models to detect hate speech and implemented SHAP and LIME explainability methods. In this case, the DoX method was used to evaluate explainability.

Keywords— Explainability, explainable artificial intelligence, medical data, social media, user study

I. INTRODUCTION

Artificial intelligence (AI) systems have become essential for solving complex problems in various industries, including finance [1], social media [2], and healthcare [3]. However, it is increasingly important to understand the logic and functioning of AI models as they have a greater impact on vital systems and decision-making processes. Users are unable to trust and understand the decisions of AI models due to their opacity and lack of transparency. Explainable AI is therefore becoming a key field of study in AI.

The problem is the complexity of AI models, which often appear very incomprehensible to the user, which can affect credibility. We refer to these models as "black boxes." In the context of AI, the term black box refers to models whose internal mechanisms and decision-making processes are incomprehensible or inaccessible to humans. It is difficult to gather or examine information regarding how outputs are produced from input data in these models. Deep neural networks are examples of extremely complicated "black boxes" that include millions of parameters that are impossible for the average person to comprehend. However, they frequently attain a great degree of accuracy and therefore find use in numerous fields.

Moral and ethical accountability for judgments is essential in fields where choices have a direct impact on people's lives. A clear and understandable method enables us to promptly determine the cause and fix any errors that may arise. In many

instances, this can help the system continue to evolve and prevent repeated mistakes that would do more harm than good.

II. BACKGROUND AND PROGRESS

The aim of our research is to design and verify a generalized methodology for deploying interpretable models. To create the right methodology, it is important to select appropriate aspects that influence the choice of the right XAI method in a specific scenario. In the article [4], we examined the basic division of XAI methods and defined essential questions that are important to answer when implementing XAI solutions: Who? What? How?

- **Who?** - focus on the type of stakeholder, his knowledge, limitations, domain, form of explanation, applicability of explanation, etc.
- **What?** - stakeholder needs, task type.
- **How?** - technical parameters of methods, data types, evaluation of explanation.

Our further research focused mainly on the stakeholder aspect, since explanations are created specifically for them. In the paper [5] we focused on the types of stakeholders, their division according to different studies and different needs. An important part of using XAI solutions is also their evaluation. Doshi-Velez and Kim [6] propose three main levels of explainability assessment: application-grounded, human-grounded, and functionally-grounded. Application-grounded evaluation uses end-user experiments to test on a real-world task. Human-grounded evaluation tests are also used in practice; the only distinction is that lay participants are used in these studies. The functionally-grounded level employs a formal definition of explainability as a model of explanatory quality, but it does not call for human evaluation. One category of human-centered evaluations can be created by combining application-grounded evaluation and human-grounded evaluation. We have further used this knowledge in medical research and in the fight against hate speech.

III. MEDICAL DOMAIN

As mentioned above, medicine is a field that is very sensitive to the use of artificial intelligence, as it directly relates to decisions about human lives. In article [7], we examined how XAI models perform from the perspective of their users. Two target groups participated in the user study we conducted: 25 students and 5 doctors. The aim of the research was a comparison of different explanation methods,

including LIME (Local interpretable model-agnostic explanations) [8], SHAP (Shapley additive explanations) [9], Anchors [10] and PDP (Partial dependence plot) [11], on a selected set of medical data. Specifically, it was the Pima Indians Diabetes Database, which is used in the field of gestational diabetes research.

The ratio of 70 to 30 was used to split the training and testing sets. The data has undergone appropriate pre-processing. Neural network (Multi-layer Perceptron classifier), logistic regression, decision tree, and random forest models were developed. With a 78% precision, the neural network produced the best results. This model was used to classify using explainability techniques.

We focused on human-centered evaluation of explanations and examined five metrics: Understandability, Usefulness, Trustworthiness, Informativeness and Satisfaction. All five have been part of several research papers regarding XAI evaluation [12], [13], and can be used for evaluation by asking the following questions:

- **Understandability:** From the explanation, does the user understand how the model makes a decision?
- **Usefulness:** Is the explanation useful to the user, to make better decisions or to perform an action?
- **Trustworthiness:** Does the explanation increase the user's trust in the model?
- **Informativeness:** Does the explanation provide sufficient information to explain how the model makes decisions?
- **Satisfaction:** Does the explanation of the model satisfy the user?

We collected answers from the participants using a questionnaire and Likert scores (1-5) that contained various scenarios in which the methods were presented. We calculated the resulting score as the average of the individual ratings. The resulting score was calculated for both groups separately.

The LIME approach received the highest ratings for understandability, usefulness, informativeness (for this metric, a lower result was better), and satisfaction from the student target population, while SHAP was praised for being trustworthy (Table 1). Subsequent analysis revealed that respondents' tastes varied and that there is no one-size-fits-all answer for XAI techniques. Certain measurements with high standard deviations show that different pupils perceive and interpret explanations differently. The local (LIME, SHAP, Anchors) and global (PDP) approaches do not differ statistically significantly.

TABLE 1
THE TARGET GROUP OF STUDENTS' AVERAGE SCORE AND VARIANCE

	LIME	SHAP	ANCHORS	PDP
Understandability	4.2±0.91	3.76±0.97	3.76±0.72	3.68±1.18
Usefulness	3.88±0.73	3.6±0.96	3.6±0.87	3.76±0.88
Trustworthiness	3.96±0.89	4.04±0.79	3.72±0.89	3.64±0.95
Informativeness	2.8±1.0	3.2±1.22	2.96±0.98	3.08±1.15
Satisfaction	4.0±0.91	3.68±0.95	3.44±1.03	3.84±1.11

We discovered that the doctors in the focus groups preferred methods that offered straightforward and unambiguous explanations. The LIME method stood out in terms of understandability, informativeness, and satisfaction, while the PDP was rated as the most dependable and helpful (Table 2). The findings showed that medical professionals' perceptions of various XAI techniques vary widely among the population. The study identified no discernible differences between local and global XAI approaches, despite presumptions that they might be seen differently.

All of these user study results highlight how crucial it is to customize XAI tools to end users' requirements and preferences in order to optimize their potential, encourage their adoption, and ensure their efficient application in real-world scenarios.

TABLE 2
VARIANCE AND AVERAGE SCORE AMONG A TARGET GROUP OF DOCTORS

	LIME	SHAP	ANCHORS	PDP
Understandability	4.0±1.22	3.8±1.1	3.4±1.52	3.2±1.64
Usefulness	2.8±1.3	2.8±0.84	2.6±1.34	3.0±1.22
Trustworthiness	3.8±0.84	3.8±0.84	3.0±1.0	4.0±0.71
Informativeness	3.2±1.3	3.2±1.3	3.6±1.52	3.6±1.52
Satisfaction	3.0±1.41	2.8±1.3	2.6±1.52	2.8±0.84

IV. SOCIAL MEDIA DOMAIN

Hate speech on social media can have serious consequences for individuals and communities, which raises the need for effective tools for its recognition and analysis. XAI plays a key role in this process, as it allows not only to identify problematic content, but also to understand the reasons why a certain text was classified as hateful or offensive. Toxic speech is negative or harmful statements that can be offensive, derogatory, racist or otherwise inappropriate. Our research [14] in this area copies the CRISP-DM (Cross-industry standard process for data mining) methodology, supplemented by additional phases dedicated to the explainability of the models and its evaluation.

A. Business understanding

The research focuses on creating models that would be able not only to accurately classify texts, but also to provide an explanation for their decisions, thereby contributing to the transparency and understanding of artificial intelligence in hate speech processing applications. This will not only allow a better understanding of how the models work, but also provide a basis for further improvements in the field of automatic recognition.

B. Data understanding

HateXplain [15] is a hate speech dataset that contains word and phrase-level annotations, including justifications for the labels. The posts come from Twitter (9,055 posts) and Gab (11,093 posts). The annotation was performed using workers from Amazon Mechanical Turk. These annotators classified each post as hate speech, offensive, or normal, and identified

the target communities to which the posts apply. Each post was annotated by three annotators, and the final classification was determined by majority vote.

C. Data Preparation

We split the data into a training and testing part in a ratio of 80:20. The dataset does not contain missing values, and the data is cleaned of punctuation marks. The text in our dataset is already divided into tokens in advance. The next step is the vectorization process using the TF-IDF (term frequency–inverse document frequency) method, which we chose because of models like XGBoost.

D. Modeling and Evaluation

In this phase, we focus on the training of the models themselves, which is a key part of the process. The CNN, XGBoost, and BERT models were chosen. The BERT model achieved the best results, namely 75% accuracy in classifying normal posts, 54% accuracy in classifying offensive posts and 73% in classifying hate posts.

E. Explainability

For this purpose, we used a combination of different explainability models and techniques, namely XGBoost with SHAP, CNN with SHAP, BERT with LIME. In our paper [14], we analyzed in more detail three specific sentences selected from the dataset, which represent different types of textual inputs, using the SHAP and LIME methods.

F. Explainability evaluation

We used a metric called Degree of Explainability (DoX)[16], drawing inspiration from Ordinary Language Philosophy and Achinstein's theory of explanations. It assumes that the degree of explainability is directly proportional to the number of relevant questions that a piece of information can correctly answer. This evaluation works with SHAP values, so it is focused only on CNN and XGBoost models. Explainable aspects represent different components or characteristics of predictions that we want to analyze in detail. In the context of the DoX metric, these aspects provide the basis for measuring the explainability of the model, we chose attributes, SHAP values, prediction values and a reference point (average value of predictions). The result is an evaluation of questions related to explainable aspects. The average DoX value for all questions and aspects is 0.322, which indicates a medium level of explainability, meaning that the model is able to provide relatively understandable explanations, but there is room for improvement. However, this evaluation method is complicated and only suitable for certain types of tasks and text explanations.

V. CONCLUSION

The studies described differed in the models and data types used. In the medical field, we evaluated the use of explainability methods using user study, where the LIME method dominated, which was successful in both user groups. In the social media field, we used the DoX tool for evaluation, which assessed that the solution had a medium level of explainability. Comparing the aforementioned studies, we see that human-centered evaluations provided us with more useful information. It will be useful to compare XAI methods across

different domains and task types using additional metrics. Our next goal is to work with image data and use explainable methods and evaluate them. It will also be important to explore other aspects of the appropriate methodology for selecting XAI methods.

ACKNOWLEDGMENT

This work was supported by the Slovak Research and Development Agency under the contract No. APVV-20-0232 and contract No. APVV-22-0414.

REFERENCES

- [1] J. Černevičienė and A. Kabašinskas, "Explainable artificial intelligence (XAI) in finance: a systematic literature review," *Artificial Intelligence Review* 2024 57:8, vol. 57, no. 8, pp. 1–45, Jul. 2024, doi: 10.1007/S10462-024-10854-8.
- [2] V. U. Gongane, M. V. Munot, and A. D. Anuse, "A survey of explainable AI techniques for detection of fake news and hate speech on social media platforms," *J Comput Soc Sci*, vol. 7, no. 1, pp. 587–623, Apr. 2024, doi: 10.1007/S42001-024-00248-9/FIGURES/11.
- [3] Z. Sadeghi et al., "A review of Explainable Artificial Intelligence in healthcare," *Computers and Electrical Engineering*, vol. 118, p. 109370, Aug. 2024, doi: 10.1016/J.COMPELECENG.2024.109370.
- [4] M. Pavlusová, "The way to the methodological choice of explainability and interpretability methods," in *SCYR 2023: 23rd Scientific Conference of Young Researchers*, Košice: Faculty of Electrical Engineering and Informatics, 2023, pp. 185–188.
- [5] M. Matejová, "The human aspect of explainable machine learning models," in *SCYR 2024: 24th Scientific Conference of Young Researchers*, Košice: Faculty of Electrical Engineering and Informatics, Technical University of Košice, 2024, pp. 58–59.
- [6] F. Doshi-Velez and B. Kim, "Towards A Rigorous Science of Interpretable Machine Learning," Feb. 2017, doi: 10.48550/arxiv.1702.08608.
- [7] M. Matejová, J. Paralič, and L. Gojdičová, "A study comparing explainability methods: a medical user perspective," *Acta Electrotechnica et Informatica*, 2025 (Accepted).
- [8] M. T. Ribeiro, S. Singh, and C. Guestrin, "“Why Should I Trust You?”: Explaining the Predictions of Any Classifier," in *Proceedings of the 22nd ACM SIGKDD International Conference on Knowledge Discovery and Data Mining*, in KDD '16. New York, NY, USA: Association for Computing Machinery, 2016, pp. 1135–1144. doi: 10.1145/2939672.2939778.
- [9] S. M. Lundberg and S. I. Lee, "A Unified Approach to Interpreting Model Predictions," *Adv Neural Inf Process Syst*, vol. 2017-December, pp. 4766–4775, May 2017, Accessed: Jan. 22, 2024. [Online]. Available: <https://arxiv.org/abs/1705.07874v2>
- [10] M. T. Ribeiro, S. Singh, and C. Guestrin, "Anchors: High-Precision Model-Agnostic Explanations," *Proceedings of the AAAI Conference on Artificial Intelligence*, vol. 32, no. 1, Apr. 2018, doi: 10.1609/aaai.v32i1.11491.
- [11] J. H. Friedman, "Greedy function approximation: A gradient boosting machine," *Ann Stat*, vol. 29, no. 5, pp. 1189–1232, 2001, doi: 10.1214/AOS/1013203451.
- [12] R. R. Hoffman, S. T. Mueller, G. Klein, and J. Litman, "Metrics for Explainable AI: Challenges and Prospects," Dec. 2018, Accessed: Mar. 28, 2025. [Online]. Available: <https://arxiv.org/abs/1812.04608v2>
- [13] J. Aechtner, L. Cabrera, D. Katwal, P. Onghena, D. P. Valenzuela, and A. Wilbik, "Comparing User Perception of Explanations Developed with XAI Methods," *IEEE International Conference on Fuzzy Systems*, vol. 2022-July, 2022, doi: 10.1109/FUZZ-IEEE55066.2022.9882743.
- [14] M. Matejová, J. Paralič, and A. Kováč, "Nenávistné prejavy na sociálnych sieťach a ich detekcia pomocou vysvetliteľných modelov," in *Electrical Engineering and Informatics 15*, Košice: Faculty of Electrical Engineering and Informatics Technical University of Košice, 2024, pp. 228–234.
- [15] B. Mathew, P. Saha, S. M. Yimam, C. Biemann, P. Goyal, and A. Mukherjee, "HateXplain: A Benchmark Dataset for Explainable Hate Speech Detection," *35th AAAI Conference on Artificial Intelligence*, AAAI 2021, vol. 17A, pp. 14867–14875, 2021, doi: 10.1609/AAAI.V35I17.17745.
- [16] F. Soprano and F. Vitali, "An objective metric for Explainable AI: How and why to estimate the degree of explainability," *Knowl Based Syst*, vol. 278, p. 110866, Oct. 2023, doi: 10.1016/J.KNOSYS.2023.110866.

Digital twin of mechatronic system: An Overview

¹Matej HRIC (1st year)
Supervisor: ²František ĎUROVSKÝ

^{1,2}Dept. of Electrical Engineering and Mechatronics, FEI TU of Košice, Slovak Republic

¹matej.hric@tuke.sk, ²frantisek.durovsky@tuke.sk

Abstract—The concept of Digital Twin (DT) has gained significant attention in the field of mechatronic systems, providing a virtual representation that mirrors the behavior and characteristics of physical assets in real time. This paper presents a comprehensive review of Digital Twin technology, comparison of digital twin to other similar technologies and showing possible solutions for digital twin. The review highlights the advantages of DT in predictive maintenance, performance optimization, and lifecycle management. The paper concludes with future research directions, emphasizing the potential of DTs in mechatronic systems.

Keywords— Digital twin, mechatronic system, data-driven, model-based

I. INTRODUCTION

Simulation serves as a modeling tool for establishing an infrastructure that monitors the properties of a real-world system by transferring data from the physical environment to a virtual one. By enabling traceability in manufacturing processes, it provides advantages in terms of time efficiency, cost reduction, and risk management. The primary objective of simulation is to predict outcomes within a virtual environment, facilitating necessary preparations. A successful simulation is achieved by accurately replicating every aspect of the physical system in the digital world [1]. The concept of Digital Twin (DT) has emerged as a transformative paradigm that bridges the gap between the physical and digital realms in an ever-evolving technological landscape. A "Digital Twin" is a virtual representation of a physical system, process, or object, created by collecting and integrating real-time data from multiple sources [2]. This digital counterpart serves as a powerful tool for monitoring, analyzing, and replicating the behavior of its real-world equivalent. By providing a dynamic mirror of physical entities, DT enhances understanding, enables predictive insights, and support informed decision-making across various industries. DT encompass not only the geometric characteristics of a physical object but also its functional and behavioral attributes. By using real-time data from sensors, simulations, and historical records, they provide a dynamic representation of their physical counterparts. This enables data analysts and IT specialists to simulate and refine designs before manufacturing physical devices. Beyond their applications in production, digital twins play a crucial role in advancing technologies such as the Internet of Things (IoT), artificial intelligence (AI), and data analytics[1],[3].

II. DEFINITION AND EVOLUTION

The concept of DT has its origins in NASA's use of

computer models to simulate and manage space missions in the 1960s [4]. DT on the other hand become well-known recently because of an improvement in sensor technologies, data analytics and cloud computing. The idea of DT was created because of the convergence of various technologies, which made it possible to gather, integrate and analyze data in real time. DT, as we know today was introduced in early 2000s by Michael Grieves in a course presentation for product life management [4]. Despite introducing this term much earlier, it took a few years to see it in use, where NASA used DT technology to mirror conditions in space to be able to perform tests for flight preparation [6]. Throughout the development of the DT model and its properties, various related concepts have emerged, including 'ultra-high fidelity' [7], 'cradle-to-grave' [8], 'integrated' model [8], and 'integral digital mock-up' (IDMU) [8]. These terms played a crucial role in shaping the evolution of the DT concept. However, given the widespread adoption and growing significance of DT, establishing a unified, comprehensive definition would offer considerable advantages. At its core, a DT is a digital counterpart of a physical entity. While the term "digital twin" may appear straightforward, its definition has been the focus of ongoing discussion and refinement. For instance, Abramovici et al. [9] and Schroeder et al. [10] view the DT as the final product, whereas Gabor et al. [12] and Rosen et al. [13] interpret it as encompassing the entire product lifecycle. Grieves [14] initially introduced the concept of DT with three core components: the digital (virtual) counterpart, the physical entity, and the connection between them. However, this model has since evolved, with Tao et al. [15] expanding it to five components by incorporating data and service as integral parts of a DT. Additionally, Tao et al. [16] identify verification, validation, and accreditation (VV&A) as key components, emphasizing that "DTs are characterized by the seamless integration between the cyber and physical spaces."

A very important part of describing DT technology is comparing it to other technologies which were either predecessors or are very similar to digital twin technology and with that comparison we can understand the main advantages of digital twin technology.

DT stands at the forefront of real-time system representation, providing a dynamic, data-driven digital counterpart to physical systems. Unlike traditional simulations, which are often static and scenario-specific, DT continuously updates using real-world sensor data, enabling predictive maintenance, performance optimization, and advanced decision-making. The integration of IoT plays a crucial role in feeding live data into DT models, enhancing their accuracy and relevance.

On the other hand, Simulation serves as a widely adopted tool for analyzing system behavior under various conditions without real-world intervention [17]. While both simulation and DT rely on computational models, simulations are typically used for discrete event analysis or scenario testing without necessarily maintaining a continuous link to the physical counterpart. Simulation is fundamental in engineering, manufacturing, and logistics, where evaluating system performance under hypothetical conditions is critical.

Closely related to simulation is Optimization, which focuses on refining system parameters to achieve maximum efficiency, cost reduction, or improved performance. Unlike a DT, which can mirror a system in real-time, optimization employs mathematical and heuristic algorithms to determine the best possible system configuration under given constraints. It is widely applied in supply chain management, resource allocation, and energy-efficient system design.

For systems with decentralized interactions, Agent-Based Modeling (ABM) provides a unique simulation approach where individual entities (agents) operate autonomously and interact within a defined environment. This method is particularly useful for studying emergent behaviors in complex systems such as traffic networks, swarm robotics, and economic models. Compared to traditional simulation techniques, ABM offers deeper insights into adaptive and self-organizing system dynamics [18].

In contrast, Machine Learning (ML) and Artificial Intelligence (AI) play an important role in enabling data-driven decision-making and automation. Unlike simulation and optimization, which are rule-based, ML learns patterns from large datasets and improves over time. ML techniques are frequently embedded in DT frameworks to enhance predictive analytics, fault detection, and autonomous decision-making [19]. However, ML is dependent on vast amounts of training data and often lacks transparency in decision processes, posing challenges in critical applications.

Another key concept is the Digital Prototype, which serves as a virtual model of a product or system used for design validation and testing before physical production [20]. While like a DT in representing a digital version of a system, a digital prototype is usually static and serves pre-development and testing purposes. It is widely used in product design, automotive engineering, and aerospace industries to accelerate innovation and reduce costs.

As industries move toward higher levels of autonomy, Autonomous Systems are gaining prominence. These systems operate with minimal human intervention and are often empowered by AI and real-time decision-making algorithms. Autonomous vehicles, industrial robots, and smart infrastructure rely on a combination of ML, simulation, and DT technologies to enhance adaptability and safety. However, ensuring reliability in unpredictable real-world environments remains a significant challenge.

While all the above technologies share overlapping applications, their core functionalities slightly differ. DTs are essential for real-time system integration, while simulation, optimization, and ABM serve as analytical and predictive tools. ML enhances data-driven intelligence, digital prototyping supports early-stage design validation, and autonomous systems represent the future of independent decision-making and operation. The interplay among these technologies is driving innovation in smart industries, digital manufacturing, and intelligent system design, highlighting the necessity of interdisciplinary research in engineering and computer science.

Table 1 shows a summary of listed technologies and lists their key features.

Table 1 Comparison of DT to other technologies

Technology	Key features
Digital twin	Real-time, twinning
Simulation	Static, one-directional
Optimization	Static, finds best solution
Agent based modelling	Static, no twinning
Machine learning	No twinning,
Digital prototype	Simplest, static
Autonomous systems	No self- learning (learning from past outcomes)

To get to know DT technology it is also important to describe several types of digital twin which are shown at *Figure 1*. Main difference between them is scale of coverage. While some solutions may represent the smallest units of the production line, others might imitate the whole factory.

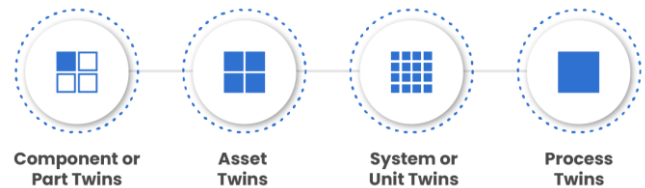


Figure 1 DT types [21]

The component twin, also referred to as the parts twin, represents the most fundamental level of DT technology. It corresponds to the smallest elements within a system, such as a sensor, switch, valve, or any other individual component of the equipment or product. By creating a virtual representation of these smart parts, it becomes possible to monitor their performance and simulate real-time conditions, allowing for comprehensive testing of their endurance, stability, and efficiency [22]. Although this type of DT replicates the manufacturing layout on a smaller scale, it significantly enhances the ability to oversee equipment components and ensure their timely maintenance. This, in turn, contributes to the overall stability of the production process and helps maintain high product quality.

A product or asset DT represents the next level in the hierarchy of this technology. It is typically composed of multiple components twins or utilizes data from part twins to create a virtual model of a more complex asset, such as an engine, a pump, or an entire building. By providing a detailed representation of the asset, an asset twin enables analysis of how individual components interact and function together as a unified system. The adoption of assets or product DT allows engineers to gain valuable insights into equipment performance and identify areas for potential improvement. This, in turn, drives enhancements in productivity, optimizes key operational metrics such as mean time between failures (MTBF) and mean time to repair (MTTR), and contributes to more efficient resource utilization [23].

System twins operate at the system level, replicating how multiple assets interact and function together as cohesive units. This is why they are sometimes referred to as "unit twins." By offering a large-scale perspective of an entire factory or plant, system twins enable the testing of various system configurations to maximize efficiency and uncover new business opportunities, including potential revenue streams. A system twin encompasses a network of assets involved in a

specific operation, such as energy distribution or the production of a particular base product within a facility [23]. Unlike simpler DTs focused on individual components or assets, system twins provide real-time monitoring and advanced simulations that go beyond detecting malfunctions or failures. Instead, they offer valuable insights for strategic decision-making, enabling businesses to optimize operations, improve process visibility, and drive long-term improvements in efficiency and productivity.

At the highest level of DT technology, process twins integrate multiple system twins into a unified model, providing a comprehensive view of how different systems collaborate and synchronize. This advanced approach offers the most extensive perspective on workflows and processes within a plant or factory, enabling a deeper and more dynamic analysis of overall performance and output.

Process twinning allows for the adjustment of key input variables, such as raw material feed rates or production temperatures, while simultaneously collecting data on resulting outputs. This can be done without interrupting actual manufacturing operations or lowering product quality. As a result, executives can safely and efficiently test various business scenarios, monitor critical performance metrics, and make informed, data-driven decisions rather than relying on intuition or guesswork [22].

III. DIGITAL TWIN PROPOSAL

To develop DT, it is important to choose a physical object and define the objective we aim to achieve using DT technology. There are two different approaches that can be used, each offering unique advantages depending on the type of application and available data.

A. Model-Based DT

Model-based simulation approach (MBS) is a structured methodology for defining requirements, designing, analyzing, and verifying complex systems [24]. It centers on using models to represent physical systems, whether natural, experimental, or application-based, comprising interconnected components performing specific functions. Simulating such systems with MBS relies on fundamental physical laws and engineering principles. The strength of MBS lies in its deep understanding of the system or process, using well-established scientific relationships. Model-based DTs extend MBS by incorporating enhanced sensors and AI-driven tools. Various studies demonstrate the implementation of model-based DTs across different applications. Korondi et al. [25] developed a DT of mechatronic drive based on the optimal control model of BLDC motor. Bachelor et al. [26] applied model-based DT to an aircraft ice protection system using Dassault Systems Dymola platform. Ward et al. [27] designed a machining DT for a CNC machine tool using MATLAB/Simulink.

These examples highlight that model-based DTs are most applicable to systems with well-defined physical properties, relying on conventional modeling and simulation platforms, AI techniques, and IoT integration. However, their effectiveness is limited by the need for model simplifications, as they cannot fully capture infinite system complexities. Additionally, they struggle to account for unknown variables and noisy data, which pose significant challenges in high-complexity applications.

B. Data-Driven DT

The implementation of DTs allows operators to monitor production, test deviations in a controlled virtual environment, and enhance the security of process industries [28]. However, with the exponential growth of process data, traditional model-based approaches struggle to accurately describe complex system states. As a result, data-driven modeling has emerged as a viable alternative for developing DTs. This approach identifies relationships between system variable input and output—without requiring exact knowledge of the system's physical behavior. Compared to conventional empirical models, data-driven methods offer significant advancements across various applications. Data-driven modeling depends on large, high-quality datasets to accurately characterize a system. These data enable key tasks such as classification, pattern recognition, associative analysis, and predictive analytics. The literature demonstrates the extensive application of data-driven DTs, particularly in complex systems. Wang et al. [29] developed a data-driven DT framework for a three-domain mobility system—including humans, vehicles, and traffic—using Amazon Web Services (AWS). Nwoke et al. [30] designed FPGA-based digital twin for mechatronic system monitoring, this setup eliminates the need for big data and cloud upload, ensuring data privacy and faster, efficient implementation and update. Another article [31] is about digital twin case study on automotive production line, highlighting benefits of DT for optimizing whole production process. These studies emphasize the strong correlation between data-driven DTs and highly complex systems with vast amounts of data. Furthermore, they highlight that AI and Big Data platforms are commonly used to develop data-driven DTs, distinguishing them from traditional model-based approaches. Base comparison of Data-Driven and Model-Based digital twin is listed in Table 2.

Table 2 Comparison of Model-Based and Data-Driven DT

Comparison	Model-Based DT	Data-Driven DT
Basis	Mathematical equations (model simulations)	Data collected from sensors
Cost	More expensive	Less expensive
Time of creation	shorter	Longer
Applications	Modellable physical systems	Complex systems

Data-driven and model-based DTs serve different purposes depending on the application. Model-based DTs, which rely on physics-based simulations, are particularly useful for the design and optimization of new products, allowing engineers to test and refine system behavior before physical prototyping. In contrast, data-driven DTs, which are using machine learning and big data analytics, are better suited for predictive maintenance and anomaly detection, as they can continuously learn from real-time sensor data to identify patterns and potential failures. While model-based DTs provide a deep understanding of system dynamics, data-driven DTs excel in handling complex, high-variability environments where precise physical modeling is challenging. In many cases, a hybrid approach combining both methods offers the most comprehensive solution, but it is also more difficult to design.

IV. FUTURE WORK

Digital twin plays a crucial role in mechatronics systems. It brings together benefits that can help with designing and monitoring such systems. Currently our focus will be choosing a mechatronic system, most probably a flying shear machine used for cutting to length on material processing lines. This process is very short and dynamic, and it is very challenging to set the control algorithm properly. By developing a digital twin of flying shears, we would like to focus on predictive maintenance possibilities, most likely on monitoring of knife dulling, because the cutting knife plays an important role in such an application and can affect quality, efficiency of a cutting process and cost of a final product. To implement a DT technology, we will have to monitor important parameters during the cutting process- cutting force and motor torque. Based on these parameters, we will be able to determine the knife's condition.

ACKNOWLEDGMENT

This work was supported by the project from Research Grants for Young Scientists at TUKE, project no. 05/TUKE/2025: Design of a Digital Twin of Flying Drum Shears as a Platform for the Development of Control Algorithms and the Needs of Predictive Maintenance Using Artificial Intelligence Tools.

REFERENCES

- [1] O. Korhan, M. Fallaha, Z. M. Çınar, and Q. Zeeshan, *The Impact of Industry 4.0 on Ergonomics*, London, UK: Intech Open, 2023. doi: [10.5772/intechopen.108864](https://doi.org/10.5772/intechopen.108864)
- [2] Crespi N, Drobot AT, Minerva R. The digital twin: What and why? In: N. Crespi, A. T. Drobot, and R. Minerva, "The digital twin: What and why?," in *The Digital Twin*, Cham: Springer, 2023, pp. 3–20.
- [3] M. Soori, B. Arezoo, and R. Dastres, "Digital twin for smart manufacturing, a review," *Sustainable Manufacturing and Service Economics*, vol. 2, 100017, 2023. doi: [10.1016/j.smse.2023.100017](https://doi.org/10.1016/j.smse.2023.100017).
- [4] E. H. Glaessgen and D. S. Stargel, "The Digital Twin Paradigm for Future NASA and US Air Force Vehicles," in *AIAA/ASME/ASCE/AHS/ASC Structures, Structural Dynamics, and Materials Conference*, Honolulu, HI, USA, 2012, pp. 2012–4343
- [5] Grieves, Michael. "Digital twin: manufacturing excellence through virtual factory replication." White paper 1.2014 (2014): 1-7.
- [6] Shafto, Mike, et al. "Draft modeling, simulation, information technology & processing roadmap." *Technology area 11* (2010): 1-32.
- [7] K. Reifsnider and P. Majumdar, "Multiphysics stimulated simulation digital twin methods for fleet management," in *54th AIAA/ASME/ASCE/AHS/ASC Structures, Structural Dynamics, and Materials Conference*, 2013. doi: [10.2514/6.2013-1578](https://doi.org/10.2514/6.2013-1578)
- [8] E. Tuegel, "The Airframe Digital Twin: Some Challenges to Realization," in *53rd AIAA/ASME/ASCE/AHS/ASC Structures, Structural Dynamics and Materials Conference*, 2012. doi: [10.2514/6.2012-1812](https://doi.org/10.2514/6.2012-1812)
- [9] J. Rios, J. C. Hernández, M. Oliva, and F. Mas, "Product avatar as digital counterpart of a physical individual product: Literature review and implications in an aircraft," *Advances in Transdisciplinary Engineering*, vol. 2, pp. 657–666, 2015. doi: [10.3233/978-1-61499-544-9-657](https://doi.org/10.3233/978-1-61499-544-9-657)
- [10] M. Abramovici, J. C. Göbel, and H. B. Dang, "Semantic data management for the development and continuous reconfiguration of smart products and systems," *CIRP Annals—Manufacturing Technology*, vol. 65, pp. 185–188, 2016. doi: [10.1016/j.cirp.2016.04.051](https://doi.org/10.1016/j.cirp.2016.04.051)
- [11] G. N. Schroeder, C. Steinmetz, C. E. Pereira, and D. B. Espindola, "Digital Twin Data Modeling with AutomationML and a Communication Methodology for Data Exchange," *IFAC-PapersOnLine*, vol. 49, pp. 12–17, 2016. doi: [10.1016/j.ifacol.2016.11.115](https://doi.org/10.1016/j.ifacol.2016.11.115).
- [12] T. Gabor, L. Belzner, M. Kiermeier, M. T. Beck, and A. Neitz, "A simulation-based architecture for smart cyber-physical systems," in *2016 IEEE International Conference on Autonomic Computing (ICAC)*, pp. 374–379.
- [13] Rosen, R., Von Wichert, G., Lo, G., Bettenhausen, K.D., 2015. About the importance of autonomy and digital twins for the future of manufacturing, in: *IFAC-PapersOnLine*, pp. 567–572. doi: <https://doi.org/10.1016/j.ifacol.2015.06.141>.
- [14] M. Grieves, "Digital Twin: Manufacturing Excellence through Virtual Factory Replication," White Paper, 2015. [Online]. Available: http://www.aprison.com/library/Whitepaper_Dr_Grieves_Digital_Twin_ManufacturingExcellence.php.
- [15] Tao, F., Cheng, J., Qi, Q., Zhang, M., Zhang, H., Sui, F., 2018. Digital twin-driven product design, manufacturing and service with big data. *The International Journal of Advanced Manufacturing Technology* 94, 3563–3576. doi: [10.1007/s00170-017-0233-1](https://doi.org/10.1007/s00170-017-0233-1).
- [16] Tao, F., Zhang, H., Liu, A., Nee, A.Y., 2019. Digital Twin in Industry: State-of-the-Art. *IEEE Transactions on Industrial Informatics* 15, 2405–2415. doi: [10.1109/TII.2018.2873186](https://doi.org/10.1109/TII.2018.2873186)
- [17] Martin, D. (2023, October 17). Simulation 101—What Is It, and How Can It Benefit You? PTC. <https://www.ptc.com/en/blogs/cad/simulation-101-what-is-it-and-how-can-it-benefit-you>
- [18] Salgado, M., & Gilbert, N. (2013). Agent Based Modelling. In T. Teo (Ed.), *Handbook of Quantitative Methods for Educational Research* (pp. 247–265). Sense Publishers. https://doi.org/10.1007/978-94-6209-404-8_12
- [19] Ayodele, T. O. (2010). Machine Learning Overview. In *New Advances in Machine Learning*. IntechOpen. <https://doi.org/10.5772/9374>
- [20] Autodesk. (2009). Digital Prototyping: Design. Visualize. Simulate. Retrieved from https://images.autodesk.com/adsk/files/dp10_indmach_industry_bro_fin_al.pdf
- [21] Vidyatec. (n.d.). The 4 levels of the Digital Twin technology. Retrieved February 27, 2025, from <https://vidyatec.com/blog/the-4-levels-of-the-digital-twin-technology/>
- [22] Program-Ace, "Types of digital twins: Explained in detail," Program-Ace. [Online]. Available: <https://program-ace.com/blog/types-of-digital-twins/>. [Accessed: 22-Feb-2025].
- [23] IBM, "What is a digital twin?" IBM. [Online]. Available: <https://www.ibm.com/think/topics/what-is-a-digital-twin>. [Accessed: 22-Feb-2025]
- [24] S. Kousar, F. Rehman, and M. A. Khan, "Overview of Digital Twin Platforms for EV Applications," *ResearchGate*, Jan. 2023. [Online]. Available: https://www.researchgate.net/publication/367465526_Overview_of_Digital_Twin_Platforms_for_EV_Applications.
- [25] P. Korondi, T. Haidegger, and L. Kovács, "Digital twin of mechatronic drive based on the optimal control model of BLDC motor," *ResearchGate*, Dec. 2020. [Online]. Available: https://www.researchgate.net/publication/347184908_Digital_twin_of_mechatronic_drive_based_on_the_optimal_control_model_of_BLDC_motor.
- [26] G. Bachelor, E. Brusa, D. Ferretto, and A. Mitschke, "Model-Based Design of Complex Aeronautical Systems Through Digital Twin and Thread Concepts," *IEEE Systems Journal*, vol. 14, no. 2, pp. 1568–1579, Jun. 2020. doi: [10.1109/JSYST.2019.2925627](https://doi.org/10.1109/JSYST.2019.2925627).
- [27] Ward, R., Sun, C., Dominguez-Caballero, J. et al. Machining Digital Twin using real-time model-based simulations and lookahead function for closed loop machining control. *Int J Adv Manuf Technol* 117, 3615–3629 (2021). <https://doi.org/10.1007/s00170-021-07867-w>
- [28] S. Tao, J. Qi, and X. Liu, "Digital Twin and Big Data Towards Smart Manufacturing and Industry 4.0: A Review," *Journal of Manufacturing Systems*, vol. 58, pp. 346–361, Jan. 2021. [Online]. Available: <https://www.sciencedirect.com/science/article/pii/S2212827120314797?via%3Dihub>
- [29] Ziran Wang. Mobility Digital Twin with Connected Vehicles and Cloud Computing. *TechRxiv*. February 01, 2022
- [30] J. Nwoke, M. Milanese, J. Viola and Y. Q. Chen, "FPGA-Based Digital Twin Implementation for Mechatronic System Monitoring," 2023 5th International Conference on Industrial Artificial Intelligence (IAI), Shenyang, China, 2023, pp. 1–6, doi: [10.1109/IAI59504.2023.10327502](https://doi.org/10.1109/IAI59504.2023.10327502).
- [31] Mendi, A.F. A Digital Twin Case Study on Automotive Production Line. *Sensors* 2022, 22, 6963

Research and development of artificial intelligence for document indexing and structuring

¹Sylvia Mat'ašová (1st year),

Supervisor: ²Martin Chovanec

^{1,2}Dept. of Computers and Informatics, FEI, Technical University of Košice, Slovak Republic

¹sylvia.matasova@tuke.sk, ²martin.chovanec@tuke.sk

Abstract—In an era of exponential growth of digital data, efficient document organization and processing is crucial. Traditional methods of indexing and structuring often fail to handle the volume and complexity of modern data. Therefore, it is essential to develop new approaches that enable fast and accurate processing of large volumes of text. Research in the field of artificial intelligence (AI) offers promising solutions through innovative methods of indexing and structuring text data. These methods use modern machine learning algorithms, such as deep neural networks and natural language processing (NLP) models, which enable more accurate analysis of the context of documents and their semantic relationships. In this article, we focus on an overview of the current state of AI for document indexing and structuring, with an emphasis on classical methods, the use of artificial intelligence and machine learning, the advantages of deep learning, and existing systems and solutions. The goal of our research is to optimize these techniques with an emphasis on the speed and accuracy of processing large volumes of data. The proposed methods contribute to more efficient access to information in various domains, such as digital archives, legal documents, and scientific publications. In this paper, we present our results and discuss the potential of these methods for future applications.

Keywords—Artificial Intelligence, Machine Learning, Natural Language Processing, Indexing Document, Structuring Document, Deep Learning, Neural Networks, BERT, Transformer models, Information Search, Big Data.

I. INTRODUCTION

In the current era of digital transformation and the exponential growth of textual data, we face the challenge of efficiently organizing and processing documents. Traditional indexing and structuring methods often struggle to handle the volume and complexity of modern data. Therefore, it is essential to develop new approaches that enable fast and accurate processing of large text corpora.

Research in the field of artificial intelligence (AI) offers promising solutions through innovative methods of indexing and structuring textual data. These methods leverage advanced machine learning algorithms, such as deep neural networks and natural language processing (NLP) models, which allow for more precise analysis of document context and their semantic relationships.

The goal of our research is to optimize these techniques with a focus on speed and accuracy in processing large volumes of data. The proposed methods contribute to more efficient access to information in various domains, such as digital archives, legal documents, and scientific publications. In this paper, we present our findings and discuss the potential of these methods for future applications.

II. OVERVIEW OF THE CURRENT STATE OF ARTIFICIAL INTELLIGENCE FOR DOCUMENT INDEXING AND STRUCTURING

Currently, we are witnessing the dynamic development of artificial intelligence (AI) methods applied to document indexing and structuring. These technologies are revolutionizing the ways we organize and retrieve information in digital environments. From process automation to deep semantic understanding, AI opens new possibilities for more efficient document management.

A. Document Indexing and Structuring in the Context of Digitization

Digitization has advanced rapidly in recent years. Amiraslani [1] analyzes this trend and highlights the importance of efficient indexing and structuring methods in online databases. Key techniques, such as inverted indexing and signature files [2], play an indispensable role in organizing and searching within digital environments.

B. Definitions of Documents in the Digital Age

In the digital age, having a clear definition of a document is crucial. Amiraslani [1] states that a document can be anything that provides information. This definition aligns with the Merriam-Webster dictionary, which also includes computer files. Briet's definition [1] expands the concept of a document to any object that represents a certain phenomenon. In the context of digitization, it is therefore essential to understand documents in their broader sense, encompassing various forms of digital content.

C. Challenges and Opportunities

The use of AI in document indexing and structuring presents numerous challenges and opportunities. Key challenges include:

- **Language complexity:** Natural language processing is complex, especially in cases of multilingual and non-standard texts.
- **Dynamic nature of information:** Digital content constantly changes and evolves, requiring continuous updates and adaptation of indexing and structuring methods.
- **Security and data protection:** In digital environments, it is crucial to ensure the protection of sensitive information and data.

Despite these challenges, AI also offers numerous opportunities:

- **Automation:** AI enables the automation of document indexing and structuring processes, leading to time and cost savings.
- **More efficient search:** AI allows users to find relevant information more quickly and accurately.
- **Personalization:** AI can help tailor search results and document organization to individual user needs.

III. CLASSICAL METHODS FOR DOCUMENT STRUCTURING AND INDEXING

This chapter explores traditional methods of document indexing and structuring, which serve as the foundation for efficient information organization and retrieval. These approaches, originally developed in library and archival environments, have gradually been adapted to meet the needs of digital systems.

A. Database Searching

Effective indexing is crucial for the fast and accurate retrieval of documents. The Web of Science database, which covers a wide range of languages, includes 248 indexed journals in the field of Library and Information Sciences [1]. In the context of database limitations, Amiraslani [1] analyzed the Taylor & Francis Online platform (with 2,700 journals) and SAGE Journals (with 1,000 titles), identifying differences in research availability.

B. Search Criteria

Global search engines utilize sophisticated algorithms to process user queries, ensuring result relevance [1]. These algorithms consider various factors, such as keyword frequency, semantic similarity, and document popularity.

C. Document Types

Documents can be categorized based on their content, format, and purpose. Amiraslani [1] identified up to 120 different document types, including academic texts, electronic books, audiovisual materials, and more. This diversity necessitates specific approaches to indexing and processing.

D. Document Properties

Key document properties include format, length, creation method, management, and distribution [1]. Different formats, such as PDF and HTML, require specific indexing methods [2].

1) *Production and Administration:* The document creation process involves identifying contributors, assessing their productivity, and ensuring digitization. Content quality directly impacts indexing efficiency [2]. The current trend points to the digitization of document management, archives, and platforms [1].

2) *Distribution:* Document distribution is closely linked to copyright issues and visibility. Digital tools such as Creative Commons licenses and Turnitin help address originality and content protection concerns [1].

E. Digitization

Digitization enhances document preservation efficiency and reduces management costs. This aspect is particularly beneficial for libraries and institutions with limited budgets [1].

F. Documentation and Societal Impacts

High-quality documentation significantly improves efficiency and decision-making across various fields, from medicine to business. The preservation of documents plays a crucial role in maintaining cultural heritage and supporting innovation [1].

IV. UTILIZATION OF ARTIFICIAL INTELLIGENCE AND MACHINE LEARNING IN NATURAL LANGUAGE PROCESSING

We are currently witnessing a significant rise in artificial intelligence (AI) and machine learning (ML) applications in natural language processing (NLP). This chapter provides an overview of key methods and models that yield promising results in various NLP tasks.

A. Hybrid Models and Ensemble Methods

Hybrid models that combine multiple deep learning algorithms overcome the limitations of traditional models. Jia et al. [3] emphasize that these approaches improve accuracy and flexibility in NLP tasks. Young et al. [4] analyze the challenges associated with deep learning implementation in NLP, highlighting the importance of embeddings such as Continuous Bag of Words (CBOW) and n-gram embeddings for better representation of polysemous words. In the context of enhancing NLP model robustness, Jia et al. [3] highlight the effectiveness of ensemble methods such as bagging, boosting, and stacking.

B. Convolutional Neural Networks (CNN)

Convolutional neural networks (CNN) have proven to be effective tools for extracting spatial and hierarchical patterns in text, which is essential for tasks such as sentiment analysis and text classification [3]. Young et al. [4] state that CNN effectively respond to linguistic nuances and can be combined with recurrent neural networks (RNN) to achieve even better results. The use of CNN in sentiment analysis is further explored in [5].

C. Recurrent Neural Networks (RNN) and LSTM

Recurrent neural networks (RNN) and their variants, such as Long Short-Term Memory (LSTM) networks, are optimized for processing sequential data. Due to their ability to maintain context, they are suitable for tasks such as machine translation and sentiment analysis [3]. LSTM networks address long-term dependency issues through a gating mechanism [4]. The study [5] describes the combination of RNN and CNN to achieve better accuracy in NLP models.

D. BERT and two-way text processing

The BERT model (Bidirectional Encoder Representations from Transformers) introduces a new approach to text processing by reading it bidirectionally, significantly improving contextual understanding [4]. The use of word masking allows BERT to better represent language [3]. BERT achieves high accuracy in various NLP tasks, such as text classification and question answering [5]. This model sets new standards in NLP and paves the way for further research.

V. EXISTING SYSTEMS AND SOLUTIONS UTILIZING DEEP LEARNING IN NLP

Deep learning empowers various NLP systems. Key examples include:

- Elasticsearch: Real-time search and indexing using fuzzy matching and relevance analysis.
- Google AI: Transforming unstructured data for machine learning-driven content analysis [6].
- Transformer Models: Revolutionizing NLP tasks like translation and summarization through advanced sequence processing.

These examples represent traditional search (Elasticsearch), commercial AI (Google AI), and modern deep learning (Transformer models). Deep learning enhances indexing and NLP across many systems [7], enabling intelligent language applications.

VI. ARTIFICIAL INTELLIGENCE METHODS FOR DOCUMENT INDEXING AND STRUCTURING

The use of artificial intelligence (AI) in document indexing and structuring processes brings efficiency in handling vast volumes of data [2]. Automated AI-based systems can analyze and classify documents based on their content, significantly improving search accuracy.

A. Indexing in the Context of Big Data

In the Big Data environment, effective indexing is crucial to ensure fast access to large data sources. Traditional indexing methods, such as B-trees and hashing, face limitations when dealing with dynamically changing data [8]. In contrast, AI-based methods, such as Latent Semantic Indexing (LSI) and Hidden Markov Models (HMM), can identify hidden patterns in data, improving indexing accuracy. To achieve scalability, collaborative techniques combining machine learning advantages with distributed data processing capabilities are increasingly employed.

B. Automated Indexing

Automated indexing serves as an alternative to manual document tagging. It utilizes machine learning methods and controlled vocabularies (KOS) [9]. The automated indexing process typically involves text preprocessing (stop-word removal, tokenization, lemmatization), term importance evaluation (e.g., using the TF-IDF method), and assigning key vocabulary terms. Various approaches, such as Support Vector Machines (SVM), deep neural networks, and string-matching-based methods, are successfully used in library systems and databases.

C. Modern Approaches to Indexing

In specialized fields such as genomics, specialized tools are developed for indexing vast sequential data. An example is the Pebblescout tool, which combines hashing, compression, and ranking methods for efficient indexing [10]. This system collects 25-mer sequences, encodes them using Feistel cipher, and stores them in B+ trees for fast access. It is used, for example, for identifying genetic markers in metagenomic databases.

D. Natural Language Processing (NLP) and the Advantages of Deep Learning

NLP techniques like tokenization, stemming, lemmatization, and sentiment analysis enhance text indexing [11], [12], [13]. Transformer models improve contextual understanding [14].

Deep learning benefits NLP through:

- Automatic Feature Extraction: Eliminating manual labeling and learning from large datasets [4].
- Diverse Input Processing: Integrating text, images, and audio [5].
- Complex Pattern Handling: Utilizing CNNs and RNNs for better language understanding [4].

E. Text Classification

Various methods are used for text classification tasks, including Support Vector Machines (SVM), decision trees, convolutional neural networks (CNNs), and recurrent neural networks (RNNs) [15]. SVM identifies the optimal boundary between text classes, decision trees provide hierarchical decision-making, and CNN/RNN improve the analysis of sequential data.

The combination of these methods creates robust systems for processing and indexing documents, ultimately leading to better organization and more efficient information retrieval.

F. Automatic Annotation and Summarization of Documents

Transformer models (GPT, BERT, T5) have transformed text summarization. Structural considerations, like using chapters, enhance results [16].

BERT (bidirectional context), GPT (abstractive summaries) [17], and T5 (text-to-text tasks) [18] have revolutionized summarization [19].

These models improve summary quality by understanding context and generating coherent text.

G. Machine Learning Algorithms for Search and Indexing

Machine learning algorithms for document search and indexing are continuously improving. Considering the structure of a document, not just individual words and sentences, brings significant improvements. Liu et al. [16] propose a model that also takes chapters into account and achieves better results compared to traditional approaches.

Machine learning, including models such as GPT and BERT [14], has a significant impact on the accuracy of indexing and searching. Techniques such as TF-IDF, BM25 [20], and embeddings with vector spaces [21] are key for effective search. These methods enable the identification of important terms, consideration of document length, and analysis of semantic relationships between words for improved search results.

1) *Comparison of Traditional and AI-Based Approaches:* TF-IDF, a traditional method, uses word frequency but lacks semantic understanding. AI-based methods, like BERT embeddings, consider context, improving text comprehension.

TF-IDF may return irrelevant documents despite keyword matches, while BERT embeddings identify semantically similar content.

BERT embeddings outperform TF-IDF in information retrieval, particularly where context is vital. Karpukhin et al. [21] demonstrated BERT's superior performance in open-domain retrieval.

2) *Scalability and Computational Costs:* Deep learning, while accurate, demands high computational resources, increasing linearly with dataset size. Indexing large datasets with BERT is costly compared to TF-IDF. Scalability is critical for Big Data.

LLM research addresses computational costs for training and inference. Google's GLaM [22] and other studies [23] focus on scaling and reducing costs through techniques like quantization and sparse models.

Database and information retrieval research [24] compares indexing methods, analyzing scalability and performance. Research aims to optimize models and algorithms for reduced computational costs.

3) *Explainability of AI Models:* AI models' "black box" nature hinders decision interpretation, crucial for indexing. SHAP values and attention visualization clarify model decisions.

SHAP values show input element contributions, while attention visualization highlights key input parts. These methods improve AI indexing transparency.

Attention visualization in transformers shows key words/phrases, and SHAP values reveal influential document features. Research focuses on intuitive AI model explanation in text processing.

Molnar's "Explainable AI: From Black Box to Glass Box" [?] emphasizes explainability for AI trust.

VII. IDENTIFICATION OF PROBLEMS AND FUTURE RESEARCH DIRECTIONS IN AI FOR INDEXING AND DOCUMENT STRUCTURING

Research and development of artificial intelligence (AI) for indexing and document structuring face several key challenges. Despite significant progress, some aspects remain unresolved.

A. Identified Problems and Challenges

The major challenges in this field include:

- **Scalability and efficiency:** Modern AI models can process large amounts of documents, but they are computationally demanding. The challenge is to optimize them to be faster and less resource-intensive while maintaining accuracy.
- **Processing diverse document formats:** Documents exist in various formats, including scanned PDFs, handwritten notes, and structured databases. Ensuring robust indexing across heterogeneous formats remains a persistent problem.
- **Semantic understanding and contextual knowledge:** Current AI systems struggle with nuanced meanings, especially in specialized domains. Ambiguities in text and implicit contextual information can hinder accurate structuring.
- **Privacy protection and security:** AI-driven document processing raises concerns about data security, especially in sensitive sectors such as healthcare and finance. Balancing AI efficiency with regulatory compliance remains challenging.
- **Adaptability to evolving language and terminology:** Language and domain-specific terminology evolve over time. AI systems must be continuously updated to maintain relevance and accuracy in indexing and document structuring.

B. Findings from the Comparison of Existing Solutions

Analysis of current approaches to indexing and document structuring has revealed their strengths and weaknesses. Modern AI systems based on deep learning achieve high accuracy but at the cost of significant computational demands and limited interpretability. Traditional rule-based systems are efficient in specific cases but lack the flexibility needed for application across diverse domains.

Comparative analysis of various AI architectures has highlighted the potential of hybrid models that combine rule-based and learning-based approaches to achieve a balanced trade-off between accuracy and interpretability. Specifically, models integrating symbolic processing and neural networks appear promising for achieving higher accuracy and improved interpretability. These conclusions are based on extensive dataset analysis and experimental studies that compare the performance of various models on standardized benchmarks. For instance, performance analysis on datasets like PubMed for medical texts and LegalBench for legal documents demonstrated that hybrid models outperform both deep learning-only and rule-based models.

C. Potential Solutions and Future Research Directions

For further advancement of AI in indexing and document structuring, research should focus on the following areas:

- **Optimization of AI models:** Implementing techniques such as model reduction, knowledge distillation, and federated learning to improve efficiency and scalability while maintaining accuracy.
- **Multimodal learning:** Integrating text, image, and audio data analysis for more comprehensive processing of diverse document formats.
- **AI techniques for privacy protection:** Using federated learning, differential privacy, and encrypted computation to train models without directly sharing sensitive data.
- **Explainable AI (XAI):** Developing models that provide transparent explanations of their decision-making processes, crucial for adoption in legal and medical applications.
- **Multilingual AI models:** Research on developing models that effectively process and interpret documents in multiple languages while preserving semantic integrity.

Based on these findings, it can be concluded that despite the significant progress that AI has made in the field of document indexing and structuring, there are still open challenges that require further research. Focusing on the above research directions can contribute to the development of more efficient and reliable solutions with practical applications in various industries. These prerequisites for further research are based on an analysis of current trends in the field of AI, as well as on the identified gaps in existing solutions. For example, the need for model optimization stems from the growing volume of data and requirements for real-time processing, while the focus on multimodal learning reflects the need to process complex documents that contain different types of data.

REFERENCES

- [1] F. Amiraslani and D. Dragovich, "A review of documentation: A cross-disciplinary perspective," *World*, vol. 3, no. 1, pp. 126–145, 2022. [Online]. Available: <https://www.mdpi.com/2673-4060/3/1/7>
- [2] E. Singh, A. Asthana, and M. Student, "Review of indexing techniques in information retrieval," 12 2022.

- [3] J. Jia, W. Liang, and Y. Liang, “A review of hybrid and ensemble in deep learning for natural language processing,” 2024. [Online]. Available: <https://arxiv.org/abs/2312.05589>
- [4] T. Young, D. Hazarika, S. Poria, and E. Cambria, “Recent trends in deep learning based natural language processing,” 2018. [Online]. Available: <https://arxiv.org/abs/1708.02709>
- [5] J. Chai and A. Li, “Deep learning in natural language processing: A state-of-the-art survey,” in *2019 International Conference on Machine Learning and Cybernetics (ICMLC)*, 2019, pp. 1–6.
- [6] S. Bouzid and L. Piron, “Leveraging generative ai in short document indexing,” *Electronics*, vol. 13, no. 17, 2024. [Online]. Available: <https://www.mdpi.com/2079-9292/13/17/3563>
- [7] L. Cui, Y. Xu, T. Lv, and F. Wei, “Document ai: Benchmarks, models and applications,” 2021. [Online]. Available: <https://arxiv.org/abs/2111.08609>
- [8] P. K. Sadineni, “Comparative study on query processing and indexing techniques in big data,” in *2020 3rd International Conference on Intelligent Sustainable Systems (ICISS)*, 2020, pp. 933–939.
- [9] K. Golub, “Automated subject indexing: An overview,” *Cataloging & Classification Quarterly*, vol. 59, no. 8, pp. 702–719, 2021. [Online]. Available: <https://doi.org/10.1080/01639374.2021.2012311>
- [10] S. A. Shiryev and R. Agarwala, “Indexing and searching petabase-scale nucleotide resources,” *Nature Methods*, vol. 21, no. 6, pp. 994–1002, Jun 2024. [Online]. Available: <https://doi.org/10.1038/s41592-024-02280-z>
- [11] P. Goyal, S. Pandey, and K. Jain, *Deep Learning for Natural Language Processing*, 01 2018.
- [12] D. Khyani, S. B. S. N. Niveditha, and D. Y. M., “An interpretation of lemmatization and stemming in natural language processing,” *Shanghai Ligong Daxue Xuebao/Journal of University of Shanghai for Science and Technology*, vol. 22, pp. 350–357, 01 2021.
- [13] O. J. Prasad, S. Nandi, V. Dogra, and D. S. Diwakar, “A systematic review of nlp methods for sentiment classification of online news articles,” in *2023 14th International Conference on Computing Communication and Networking Technologies (ICCCNT)*, 2023, pp. 1–9.
- [14] N. Raman, S. Shah, and M. Veloso, “Structure with semantics: Exploiting document relations for retrieval,” *CoRR*, vol. abs/2201.03720, 2022. [Online]. Available: <https://arxiv.org/abs/2201.03720>
- [15] I. Yelmen, A. Gunes, and M. Zontul, “Multi-class document classification using lexical ontology-based deep learning,” *Applied Sciences*, vol. 13, no. 10, 2023. [Online]. Available: <https://www.mdpi.com/2076-3417/13/10/6139>
- [16] Y. Liu, L. Zhang, and X. Lian, “A document-structure-based complex network model for extracting text keywords,” *Scientometrics*, vol. 124, no. 3, pp. 1765–1791, Sep 2020. [Online]. Available: <https://doi.org/10.1007/s11192-020-03542-1>
- [17] M. Asmitha, C. Kavitha, and D. Radha, “Summarizing news: Unleashing the power of bart, gpt-2, t5, and pegasus models in text summarization,” in *2024 4th International Conference on Intelligent Technologies (CONIT)*, 2024, pp. 1–6.
- [18] Unite.AI, “Transformer models for summarization and contextual understanding,” 2020. [Online]. Available: <https://www.unite.ai>
- [19] E. Kotei and R. Thirunavukarasu, “A systematic review of transformer-based pre-trained language models through self-supervised learning,” *Information*, vol. 14, no. 3, 2023. [Online]. Available: <https://www.mdpi.com/2078-2489/14/3/187>
- [20] V. Gulati, D. Kumar, D. E. Popescu, and J. D. Hemanth, “Extractive article summarization using integrated textrank and bm25+ algorithm,” *Electronics*, vol. 12, no. 2, 2023. [Online]. Available: <https://www.mdpi.com/2079-9292/12/2/372>
- [21] V. Karpukhin, B. Oğuz, S. Min, P. Lewis, L. Wu, S. Edunov, D. Chen, and W. tau Yih, “Dense passage retrieval for open-domain question answering,” 2020. [Online]. Available: <https://arxiv.org/abs/2004.04906>
- [22] N. Du, Y. Zhou, W. Chu, A. Saluja, A. Yu, Y. Yang, S. Shakeri, P. Liang, E. H. Chi, L. Hou, and Q. V. Le, “Glam: Efficient scaling of language models with mixture-of-experts,” *arXiv preprint arXiv:2112.06903*, 2022. [Online]. Available: <https://arxiv.org/abs/2112.06903>
- [23] Y. Tay, M. Dehghani, D. Bahri, and D. Metzler, “Efficient transformers: A survey,” *arXiv preprint arXiv:2009.06732*, 2020. [Online]. Available: <https://arxiv.org/abs/2009.06732>
- [24] A. Andoni, R. Pagh, I. Razenshteyn, and E. Waingarten, “Approximate nearest neighbor search in high dimensions,” in *Proceedings of the Thirtieth Annual ACM-SIAM Symposium on Discrete Algorithms*, 2018, pp. 1095–1112. [Online]. Available: <https://dl.acm.org/doi/10.1137/1.4000000.109>

Split Computing and Early Exiting for Computer Vision Tasks in Autonomous Vehicles

¹Róbert RAUCH (4th year),

Supervisor: ²Juraj GAZDA

^{1,2}Dept. of Computers and Informatics, FEI, Technical University of Košice, Slovak Republic

¹robert.rauch@tuke.sk, ²juraj.gazda@tuke.sk

Abstract—This paper addresses the computational limitations of connected autonomous vehicles (CAVs) by optimizing deep learning workload distribution between CAVs and edge servers. We present a cooperative multi-agent deep deterministic policy gradient (MADDPG) approach to determine optimal split points, exit strategies, and autoencoder selection for compression. Our evaluation compares this methodology against Edge ML, Edge AI, and traditional server offloading approaches, demonstrating significant performance advantages in vehicular edge computing environments. Additionally, we explore the application of split computing and early exiting techniques for Transformer-based architectures and evaluate the efficacy of split computing for reinforcement learning models in autonomous driving scenarios.

Keywords—autonomous vehicles, computer vision, early exiting, edge computing, split computing

I. INTRODUCTION

Connected autonomous vehicles (CAVs) represent a significant advancement in intelligent transportation systems with the potential to revolutionize how we commute [1]. However, the computational requirements for autonomous operation are often extremely high for the onboard processing capabilities available in these CAVs [2]. Consequently, recent research demonstrates a clear shift toward offloading computation-intensive tasks to nearby edge servers [3]. This approach builds upon mobile edge computing (MEC), which has been extensively researched for mobile devices. When adapted for vehicular contexts, this paradigm is known as vehicular edge computing (VEC). VEC extends traditional MEC by addressing vehicle-specific challenges, particularly higher mobility and more stringent latency requirements for safety-critical autonomous driving functions [4].

While full offloading has received more research attention, autonomous applications frequently employ deep learning (DL) approaches to perceive and interpret the surrounding environment. These DL models are typically structured in layers, and as shown in [5], such models can be strategically split to distribute computation between the vehicle and edge server. This approach has been shown to increase edge server throughput (i.e., how many CAVs it can simultaneously serve). Furthermore, when incorporating autoencoders for compression, as in [6], this method can also reduce overall task latency, as transmitting the compressed intermediate layer outputs can be significantly more efficient than offloading the complete input images.

However, it is often advantageous to maintain some capability for completing computation onboard the CAV, particularly

when connection to the edge server is degraded. To address this challenge, we can implement early exiting techniques, as shown in [5], where execution of the DL model can be terminated at intermediate points based on available computational resources. While these earlier exits trade accuracy for efficiency, they provide a crucial fallback mechanism when network conditions deteriorate. As [7], [8] demonstrates, the highly dynamic nature of the VEC environment makes it beneficial to adaptively determine execution strategies for DL models, specifically deciding which exit point to utilize and where to position the computational split. This dynamic approach allows the system to respond effectively to changing network and computational conditions.

In this paper, we present our state-of-the-art approach for determining optimal split points, exit strategies, and intermediate compression sizes using a cooperative multi-agent deep deterministic policy gradient (MADDPG) algorithm. We benchmark our proposed methodology against leading approaches, specifically Edge ML [7], which employs a DDPG algorithm, and Edge AI [8], which utilizes a heuristic approach. Additionally, we compare our results against the conventional method of fully offloading tasks to the edge server. Furthermore, we evaluate split computing and early exiting techniques separately on advanced computer vision models, particularly transformer architectures, as well as in reinforcement learning contexts.

II. SYSTEM MODEL

Our system model comprises a set of vehicles \mathcal{V} , where each vehicle $v \in \mathcal{V}$ is connected to a single base station b . Each vehicle generates $N_{\mathcal{Z}_{t,v}}$ tasks within a t time interval. Each task $z \in \mathcal{Z}_{t,v}$ contains specific information about the computational requirements to be processed on the CAV and base station, as well as the volume of data that needs to be uploaded and downloaded between these entities.

To calculate latency for task z we use [9]:

$$t_z = \frac{I_z^{\text{CAV}}}{\eta_v^{\text{CAV}}} + \frac{I_z^{\text{ES}}}{\eta^{\text{ES}}} + \frac{c_z^{\text{UL}}}{r_{t,v}^{\text{UL}}} + \frac{c_z^{\text{DL}}}{r_{t,v}^{\text{DL}}} + t_z^{\text{wait}}, \quad (1)$$

where I_z^{CAV} and I_z^{ES} represent the computational complexity to be executed on the CAV and edge server respectively (calculated as in [9]), η_v^{CAV} and η^{ES} are the processing capabilities of the CAV and edge server, c_z^{UL} and c_z^{DL} denote the data sizes for upload and download, $r_{t,v}^{\text{UL}}$ and $r_{t,v}^{\text{DL}}$ are the uplink and downlink data rates at time t for vehicle v calculated according to [9], and t_z^{wait} accounts for any queuing delay.

III. PROPOSED APPROACH

In this section, we will first detail our proposed decision-making framework using MADDPG. Then, we will examine the implementation of split computing and early exiting in transformer-based models. Finally, we will explore the application of split computing for models in reinforcement learning scenarios. It is important to note that our analyses of transformer-based models and reinforcement learning applications do not incorporate the decision-making mechanisms discussed in the MADDPG framework.

A. MADDPG Framework

As discussed in our paper [9], we first modify our DL model by incorporating early exits and splits, where each split contains multiple autoencoders for different compression sizes. Each autoencoder is a small convolutional neural network (CNN) that compresses the number of channels. Note that papers such as [6] also compress spatial dimensions (i.e., width and height); however, in our case, we use small image sizes, and therefore compressing spatial dimensions doesn't prove beneficial. Nevertheless, our proposed approach can be applied in a similar fashion to spatial compression.

Subsequently, we execute our DL model and dynamically select which split, autoencoder, and exit to utilize. This decision process is implemented using MADDPG, where the reward function is defined as a weighted sum of achieved accuracy and latency—as defined in [9]. This is significant because, while other works such as [7] only choose rewards based on which exit is selected (i.e., preferring later exits, but assigning large negative rewards if a task exceeds its deadline), our approach must also account for different compression sizes, which additionally impact accuracy. We utilize MADDPG, an actor-critic approach specifically designed for continuous action spaces. However, since our approach only requires three discrete values, we implement Gumbel-Softmax, which was specifically developed for DDPG algorithms in discrete action environments.

B. Split Computing and Early Exiting for Transformer-based Models

A key limitation of our approach in [9] is its exclusive use of CNNs for image classification. This is restrictive as transformer-based models now outperform traditional CNNs and offer better capabilities for autonomous vehicles. For CAVs, image classification alone inadequately represents real-world scenarios, where semantic segmentation provides more comprehensive environmental understanding.

We implemented a transformer-based model for semantic segmentation with integrated splits using CNN autoencoders for compression. Although transformer outputs contain richer information than convolutional layers, they remain compressible numerical data. The transformer architecture's depth naturally provides intermediate outputs used during training, which serve as ideal locations for implementing early exit branches.

C. Split Computing for Reinforcement Learning algorithms

While previous works focus on computer vision tasks, these models typically function as components of larger pipelines that manage autonomous driving operations. Here, we utilize a DL model to handle highway lane-switching decisions and

apply split computing techniques to this model. For this application, we exclusively use CNN networks for two key reasons: first, they are more extensively researched in the context of split computing, and second, they are commonly employed in vehicle control scenarios. We also implement small CNN architectures as autoencoders for compressing the intermediate outputs at split points.

IV. NUMERICAL RESULTS

In this section, we will examine each study and present key research findings.

A. Results for MADDPG Framework

Fig. 1 presents a comparison of our proposed approach against other state-of-the-art methods. We used the VGG-16 [10] architecture on the CIFAR-10 dataset as our benchmark task for CAV computation. The results demonstrate that our approach outperforms competitors in both latency and accuracy metrics. It's important to note that tasks exceeding their deadlines are counted as misclassified. The data suggests our proposed approach has a significantly lower task drop rate compared to alternative methods. For more comprehensive research results we refer readers to [9].

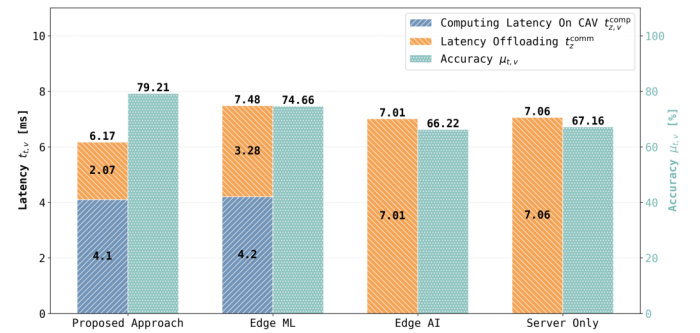
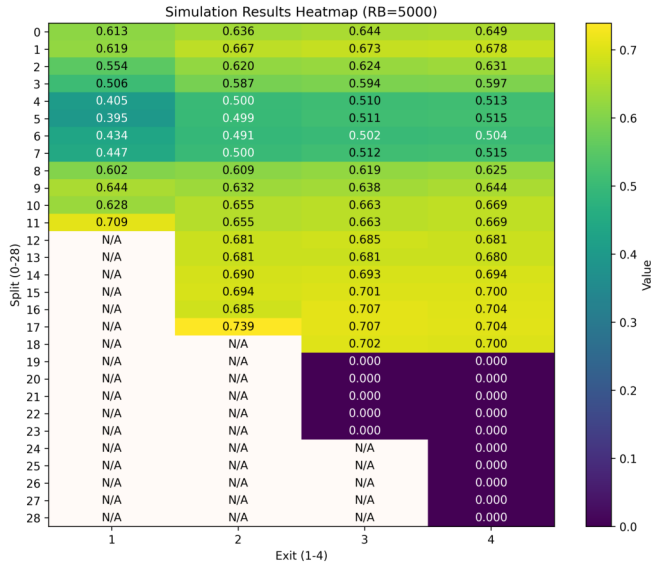


Fig. 1: Results for MADDPG proposed approach comparing against state of the art with accuracy weight of 0.5 and latency weight of 0.9 and $N_{Z_{t,v}} = 165$ tasks generated per second.

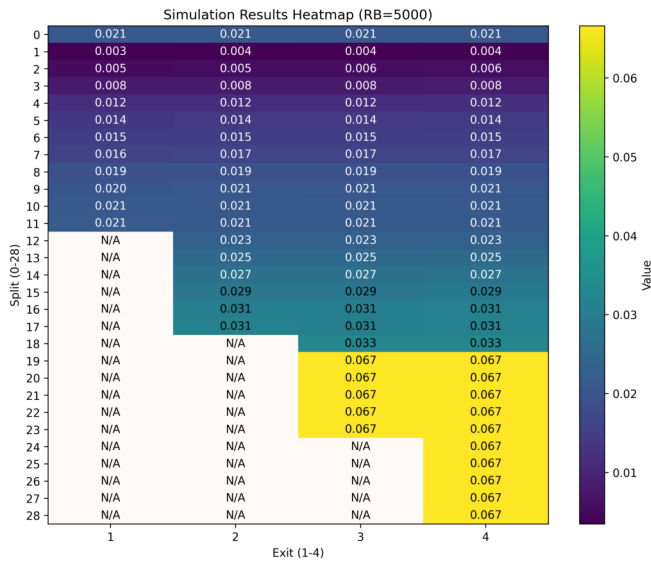
B. Transformer-based results

Here, we evaluate split computing and early exiting for a transformer-based model, specifically the Segmentation Transformer (SETR) [11]. In this scenario, our CAVs perform semantic segmentation using the Cityscapes dataset. Fig. 2 presents a map of all possible strategies with their corresponding latency and accuracy results. Note that N/A fields indicate invalid strategies (i.e., when the split occurs after the early exit point where execution terminates).

As shown in Fig. 2, early exits often achieve better accuracy when the CAV can execute these exits compared to split computing. This advantage stems from the additional accuracy loss caused by compression in split computing. However, early splits significantly outperform in terms of latency. These maps demonstrate the importance of selecting an appropriate strategy based on environmental conditions (e.g., a CAV with limited computational power may be unable to execute any exit). Note that the 19th split and beyond achieves 0 accuracy with 0.067s latency because all tasks are dropped, as CAVs cannot execute that many layers onboard.



(a) Achieved accuracy to current strategy



(b) Achieved latency in seconds to current strategy

Fig. 2: Results for split computing and early exiting for SETR model

C. Results for Reinforcement Learning Algorithm

We evaluate split computing for reinforcement learning using the Highway environment from OpenAI Gym, which provides a bird-eye view for lane switching—a perspective actively researched for CAVs (see e.g., [12]). Unlike conventional approaches that train autoencoders using MSE loss, we train ours by freezing other network layers and optimizing directly with the reinforcement learning reward function. Figure 3 demonstrates that split computing significantly reduces offloaded data size while impacting reward performance.

V. CONCLUSION

In this paper, we have demonstrated that our MADDPG Framework outperforms state-of-the-art approaches through its cooperative multi-agent design. By incorporating autoencoder selection, we enabled more flexible strategy optimization despite increased training complexity. We also highlighted the importance of split computing and early exiting for both Transformer-based models and reinforcement learning. Future

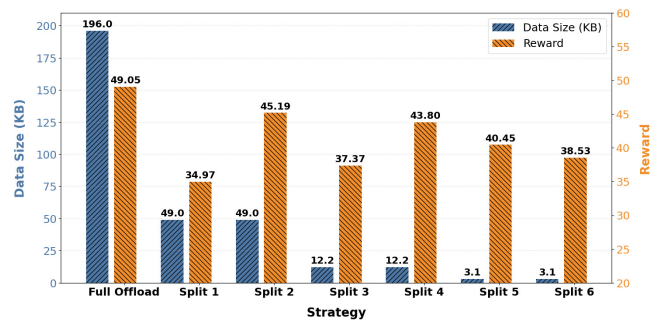


Fig. 3: Results for reinforcement learning model showing data size after compression and impact on reward

work will include comprehensive evaluation of reinforcement learning split computing and development of specialized decision-making algorithms for these architectures.

ACKNOWLEDGMENT

This work was supported by The Slovak Research and Development Agency project no. APVV SK-CZ-RD-21-0028, APVV-23-0512 and the Slovak Academy of Sciences project no. VEGA 1/0685/23.

REFERENCES

- [1] M. N. Ahangar, Q. Z. Ahmed, F. A. Khan, and M. Hafeez, “A survey of autonomous vehicles: Enabling communication technologies and challenges,” *Sensors*, vol. 21, no. 3, p. 706, 2021.
- [2] A. Fauzi, S. Rahayu *et al.*, “Computational challenges and innovations in autonomous vehicle technologies,” *Journal of Advanced Computing Systems*, vol. 5, no. 1, pp. 18–25, 2025.
- [3] G. Yan, K. Liu, C. Liu, and J. Zhang, “Edge intelligence for internet of vehicles: A survey,” *IEEE Transactions on Consumer Electronics*, 2024.
- [4] S. Raza, S. Wang, M. Ahmed, and M. R. Anwar, “A survey on vehicular edge computing: architecture, applications, technical issues, and future directions,” *Wireless Communications and Mobile Computing*, vol. 2019, no. 1, p. 3159762, 2019.
- [5] Y. Matsubara, M. Levorato, and F. Restuccia, “Split computing and early exiting for deep learning applications: Survey and research challenges,” *ACM Computing Surveys*, vol. 55, no. 5, pp. 1–30, 2022.
- [6] A. E. Eshratifar, A. Esmaili, and M. Pedram, “Bottleneck: A deep learning architecture for intelligent mobile cloud computing services,” in *2019 IEEE/ACM International Symposium on Low Power Electronics and Design (ISLPED)*. IEEE, 2019, pp. 1–6.
- [7] Z. Zhao, K. Wang, N. Ling, and G. Xing, “Edgempl: An automl framework for real-time deep learning on the edge,” in *Proceedings of the international conference on internet-of-things design and implementation*, 2021, pp. 133–144.
- [8] E. Li, L. Zeng, Z. Zhou, and X. Chen, “Edge ai: On-demand accelerating deep neural network inference via edge computing,” *IEEE transactions on wireless communications*, vol. 19, no. 1, pp. 447–457, 2019.
- [9] R. Rauch, Z. Becvar, P. Mach, and J. Gazda, “Cooperative multi-agent deep reinforcement learning for dynamic task execution and resource allocation in vehicular edge computing,” *IEEE Transactions on Vehicular Technology*, 2024.
- [10] K. Simonyan and A. Zisserman, “Very deep convolutional networks for large-scale image recognition,” *arXiv preprint arXiv:1409.1556*, 2014.
- [11] L. Zhang, J. Lu, S. Zheng, X. Zhao, X. Zhu, Y. Fu, T. Xiang, J. Feng, and P. H. Torr, “Vision transformers: From semantic segmentation to dense prediction,” *International Journal of Computer Vision*, vol. 132, no. 12, pp. 6142–6162, 2024.
- [12] T. Choudhary, V. Dewangan, S. Chandhok, S. Priyadarshan, A. Jain, A. K. Singh, S. Srivastava, K. M. Jatavallabhula, and K. M. Krishna, “Talk2bev: Language-enhanced bird’s-eye view maps for autonomous driving,” in *2024 IEEE International Conference on Robotics and Automation (ICRA)*. IEEE, 2024, pp. 16 345–16 352.

Cybersecurity Awareness Through Gamification

¹*Lenka BUBENKOVÁ (1st year),*

Supervisor: ²Emília PIETRIKOVÁ

^{1,2}Dept. of Computers and Informatics, FEI TU of Košice, Slovak Republic

¹lenka.bubenkova@tuke.sk, ²emilia.pietrikova@tuke.sk

Abstract—Cybersecurity education is essential as digital threats evolve, yet traditional training methods often fail to engage diverse learners or drive meaningful behavioral change. Passive, compliance-based instruction does not effectively address the needs of individuals with limited technical skills or critical thinking abilities. This paper examines the limitations of current cybersecurity education and explores gamification as a strategy to enhance engagement, knowledge retention, and real-world application. Gamified learning methods, such as cybersecurity escape rooms, phishing awareness games, and adaptive simulations, provide an interactive alternative to traditional instruction. While gamification offers many advantages, challenges remain, including measuring long-term behavioral impact and ensuring accessibility for all learners. This study reviews existing solutions and outlines future directions for integrating game-based learning into cybersecurity training programs.

Keywords—cybersecurity, gamification, education, game-based learning

I. INTRODUCTION

Cybersecurity education must prepare diverse learners, including children, older adults, and non-technical users [1], yet current programs often fail to engage those with limited critical thinking or technical skills. The main challenges in cybersecurity education remain: first, creating awareness about security threats, and second, equipping individuals with practical skills to protect themselves. Recent research highlights the interdisciplinary nature of cybersecurity education and calls for age-appropriate training starting as early as primary school. Essential competencies such as phishing detection, password security, and privacy awareness should become part of early education, especially given the increasing digital exposure among children [2].

Despite this, many curricula still treat cybersecurity merely as a subtopic of computer science rather than an essential life skill. Moreover, Crabb et al. [3] reveals that only 16% of 50 reviewed studies compare instructional methods, mainly focusing on content delivery instead of how learners acquire cybersecurity competencies. This gap is particularly critical for non-technical users. Although Digital Game-Based Learning has shown potential benefits, it also faces known limitations such as limited long-term impact assessment and varying instructional quality [4], [5]. Similarly, while serious games have been used successfully to teach programming concepts [6], [7], not all of them foster deep understanding, as noted by Livovsky et al. [8]. In light of these challenges, gamification emerges as a promising approach to improving cybersecurity education engagement and knowledge retention. Studies confirm that game-based learning significantly boosts motivation and retention [9], and applying Bloom's Taxonomy

to game-based scenarios has been shown to enhance critical thinking in security contexts [10].

Building on these observations, this paper examines the current state of cybersecurity education, focusing on its persistent challenges and the potential of gamification to address them. It explores how gamification can make security training more accessible, inclusive, and practical, particularly for those struggling with conventional learning methods. It analyzes existing frameworks, identifies their limitations, and discusses gamification techniques like escape rooms, phishing awareness games, and decision-based simulations to improve cybersecurity education for diverse audiences.

II. GENERAL CHALLENGES IN CYBERSECURITY EDUCATION

Some studies and recent reviews suggest that future research should focus on two aspects: (1) understanding the long-term behavioral impact of gamified cybersecurity education, and (2) establishing clear evaluation criteria for assessing its effectiveness. Cybersecurity competitions, such as the Pacific Rim Collegiate Cyber Defense Competition, have been explored as alternative learning strategies, providing real-world training opportunities for cybersecurity students [11]. Gamification offers an opportunity to address this challenge by providing hands-on training for learners who might struggle with abstract or technical cybersecurity concepts. While cybersecurity threats require analytical thinking and problem-solving, many individuals, such as young children, elderly users, and people without technical backgrounds, struggle with recognizing deception tactics, such as phishing scams or social engineering attacks. Traditional training methods assume a baseline level of analytical ability, which can lead to gaps in learning for those who do not naturally think critically about security risks. Gamification and interactive learning experiences can help bridge this gap by training pattern recognition and decision-making skills in a controlled, risk-free environment. Instead of relying solely on abstract knowledge, game-based training immerses learners in practical cybersecurity scenarios, allowing them to practice identifying threats without requiring deep prior knowledge. Future work should explore how cybersecurity games can be designed specifically for learners who struggle with traditional security awareness training. This could include decision-tree-based learning, gamified risk simulations, and challenges that adjust difficulty based on the learner's skill level.

III. THE HUMAN FACTOR IN CYBERSECURITY

Recent events highlight that even highly skilled users fall victim to cyber threats, often due to behavioral factors rather than a lack of technical knowledge [12]. According to Verizon's 2024 Data Breach Investigations Report, phishing and pretexting tactics constitute 73% of social engineering breaches [13], confirming that human error remains a leading cause of cybersecurity failures [14], with frequent issues like social engineering, misconfigurations, and poor password practices increasing vulnerability. A Study by Kweon et al. [15] highlights that many organizations invest in advanced security infrastructure while neglecting the human element, which leads to persistent security gaps. Iuga et al. [16] found that users detected phishing attempts with an average accuracy of 65.63%, with pop-up-based attacks being particularly deceptive. Despite anti-phishing training, participants' detection scores only improved marginally (67.10% vs. 65.55%), and none achieved a perfect score, highlighting the limitations of conventional training methods. Additionally, demographic factors such as gender and PC experience influenced phishing detection success. These findings reinforce prior research suggesting that experience and exposure to cybersecurity risks influence awareness levels, underscoring the urgent need for more effective interactive training approaches, such as gamified learning, to enhance decision-making in real-world phishing scenarios. Catal et al. [17] emphasize the growing complexity of cyber threats and argue that traditional security training must evolve to integrate human-centered cybersecurity education. This aligns with research on gamified learning, which aims to make cybersecurity training more adaptive and engaging.

A. The Need for Behavior-Oriented Cybersecurity Training

Traditional security training programs typically rely on passive learning methods, such as video tutorials and compliance checklists. However, recent research suggests that interactive, gamified learning approaches can significantly improve knowledge retention and security behaviors, as stated by Daineko et al. [18]. Practical cybersecurity training should incorporate real-world attack simulations, interactive gamification strategies, and adaptive learning models tailored to individual risk profiles. By integrating interactive and game-based methodologies, cybersecurity education can become more effective in reducing human errors and strengthening organizational security. Catal et al. [17] suggest that gamification and adaptive training models can bridge the gap between cybersecurity education and industry needs by making security awareness an interactive, ongoing process rather than a one-time compliance exercise.

IV. GAMIFICATION IN CYBERSECURITY TRAINING

Gamification has been widely recognized for its ability to enhance engagement in cybersecurity education. Research by Faith et al. [19] suggests that incorporating game elements like points, levels, and interactive scenarios significantly improves both learning outcomes and student motivation. Furthermore, studies, including those by Ros et al. [20], indicate that realistic game design and contextualization are critical for fostering engagement and retention in cybersecurity courses. Similarly, the benefits of game-based learning extend to other technical disciplines, with research showing improvements in

motivation and learning outcomes in areas such as robotics [21] and computational thinking [22]. The effectiveness of gamified cybersecurity training is typically assessed through a combination of quantitative and qualitative measures, such as pre- and post-test knowledge scores, phishing detection rates [16], self-reported motivation [20], and observed behavior changes [23]. However, the literature reveals a lack of standardized methods for evaluating whether improved awareness translates into secure real-world behavior, especially over time.

Examples of Successful Gamified Cybersecurity Education

Several cybersecurity education programs and gamified approaches have been developed to enhance learning engagement and retention. This section reviews key existing solutions, examining their effectiveness and limitations.

1) *Cybersecurity Escape Rooms*: Escape rooms have been introduced as an innovative method for cybersecurity education. Buckley and Buckley [24] developed a cybersecurity-themed escape room using the EscapED framework. Similarly, Bullee and Koning [25] incorporated Bloom's Taxonomy principles into their escape room design. The training engages participants across cognitive skill levels by aligning escape room puzzles with Bloom's Taxonomy: remember, understand, apply, analyze, evaluate, and create. This structured learning approach ensures that participants gain theoretical knowledge and retain and apply it in realistic cybersecurity scenarios. Additionally, integrating privacy principles into cybersecurity escape rooms is essential to make training relevant to real-world concerns. The effectiveness of cybersecurity escape rooms highlights their potential as an engaging and interactive training method. However, while short-term engagement and knowledge retention are high, further research is needed to assess their long-term behavioral impact in real-world cybersecurity practices.

2) *Phishing Awareness Games*: Gamified approaches have also been applied to phishing awareness training. Arachchilage and Love [26] proposed a game design framework focused on educating users to identify and avoid phishing attacks. Their research emphasized the role of threat perception in cybersecurity education, suggesting that interactive gaming scenarios can improve user awareness.

3) *Cryptography Education Through Games*: Huitema and Wong [27] explored the use of a gamified approach in cybersecurity education programs, specifically for teaching cryptographic concepts. Their study demonstrated that integrating gamification into cryptography training helped students understand fundamental encryption algorithms while maintaining engagement.

4) *Cyber-Hero: A Gamified Cybersecurity Awareness Framework*: Cyber-Hero is a gamification framework designed to enhance cybersecurity awareness among high school students. Developed by Qusa and Tarazi [28], the platform allows students to create individual accounts within their schools, granting them access to a series of cybersecurity-focused serious games. These games cover essential topics like password security, phishing recognition, and cybersecurity awareness. Each game session is brief and is designed to be repeated periodically, reinforcing acquired knowledge through repetition. Cyber-Hero also incorporates an evaluation system that assesses students' cybersecurity awareness levels based on predefined criteria. The platform continuously measures

progress and long-term behavioral change in cybersecurity practices. The research highlights that gamification effectively alters human behavior, particularly in improving password selection and encouraging safer digital habits. The framework demonstrates how structured gamification can contribute to a more cyber-aware generation.

V. ONLINE SAFETY PROGRAMS

Beyond traditional gamification, roleplaying-based gamification has shown promise in improving students' ability to apply cybersecurity knowledge in real-world scenarios [29]. Cybersecurity education can extend beyond theory by immersing students in interactive roleplaying exercises and promoting practical decision-making skills.

1) *Google's "Be Internet Awesome"*: Google's "Be Internet Awesome" program was designed to teach children about online safety through interactive lessons and activities. A study by Jones et al. [30] evaluated its effectiveness using a cluster randomized controlled trial. The results showed that students who participated in the program exhibited improved knowledge of online safety concepts and increased confidence in handling online challenges. However, the study found no significant impact on behaviors related to online privacy, cyberbullying, or parental engagement in addressing online issues. Seale and Schoenberger [31] critically analyzed the program and pointed out that while it addresses fundamental internet safety principles, it lacks depth in discussing the broader implications of data usage and privacy beyond individual user responsibility. They argue that it presents Google as an authoritative source on internet safety without fully addressing systemic privacy concerns.

2) *IBM's Cybersecurity Escape Room*: IBM has developed a cybersecurity escape room designed to train employees on best practices in cybersecurity. Research on similar escape room methodologies [24], [25] suggests that such interactive training environments enhance learning retention and engagement. The gamification elements in these programs have been shown to foster motivation and collaboration, making complex cybersecurity concepts more accessible.

These implementations serve as practical case studies demonstrating how gamification strategies can be aligned with the proposed evaluation criteria, highlighting both their benefits and limitations when applied to different target groups.

Challenges of Gamification in Cybersecurity Education

Despite its advantages, gamification in cybersecurity education faces several limitations. Research suggests that while gamified approaches increase engagement and short-term knowledge retention, their long-term effectiveness in changing user behavior remains uncertain [23]. Many cybersecurity training games emphasize threat recognition rather than real-time decision-making, limiting their impact beyond controlled learning environments [26]. Moreover, gamification does not work equally well for all users. These issues also pose challenges to the scalability of gamified approaches, especially when addressing diverse audiences such as children, older adults, or non-technical users with lower digital literacy. Putz and Treiblmaier [32] found that individual personality traits, such as intrinsic vs. extrinsic motivation, significantly affect engagement levels in cybersecurity games. Older adults and individuals with lower digital literacy levels often struggle with game-based training, limiting the scalability of these solutions.

VI. SECURE PROGRAMMING AND RISK-FREE LEARNING

Cybersecurity training should not be limited to general awareness. It must also include secure coding practices, particularly for software developers who directly impact system security. Poor programming practices have led to significant cybersecurity failures, emphasizing the need for proactive security education integrated into software development curricula. Developers often lack sufficient exposure to security-oriented code reviews, which are critical for identifying vulnerabilities before deployment. Traditional education methods rely heavily on theoretical knowledge, but research suggests that interactive, hands-on learning experiences are far more effective in instilling secure coding practices.

A. Game-Based Approaches for Secure Programming

A game-based approach, such as the To Kill a Mocking Bug serious game by Iosif et al. [33], has been developed to train programmers in identifying software security risks and vulnerabilities by simulating real-world debugging scenarios. This gamified training framework aligns with industry security standards, such as IEC 62443 and CWE, ensuring that programmers are not only aware of security threats but are also equipped with practical skills to mitigate them. Further supporting this approach, article from Iosif et al. [34], about DuckDebugger has been introduced as a cybersecurity-oriented code review tool, utilizing game mechanics to engage developers in analyzing and correcting security flaws in software projects. Empirical evaluations indicate that serious games significantly enhance secure coding awareness among programmers, leading to improved software quality and security posture.

B. Gamification for Secure Coding

The integration of gamification into secure programming education has been demonstrated through various initiatives. A study on serious games for industrial cybersecurity has shown that interactive game-based training can enhance developers' understanding of cyber threats in industrial control systems while reinforcing secure programming techniques [35]. By placing programmers in simulated attack scenarios, such training allows them to practice defensive coding strategies in a controlled, risk-free environment. Given the increasing complexity of software security threats, it is crucial to expand beyond static learning models and incorporate interactive cybersecurity simulations into programming education. The use of cybersecurity-focused game environments has proven effective in improving not only developers' awareness but also their ability to apply security measures in real-world coding projects. This evidence reinforces the importance of gamified cybersecurity training for programmers, ensuring that secure development practices become second nature. Future research should explore adaptive game-based learning models that cater to different experience levels among developers, allowing for personalized cybersecurity education paths.

VII. CONCLUSION

Gamification has shown promising results in improving engagement and knowledge retention. However, its long-term influence on behavior and scalability across diverse learner groups remains an open challenge. Factors such as varying

levels of digital literacy and learner motivation further affect its practical effectiveness. By analyzing existing frameworks, this paper identifies limitations of traditional cybersecurity education, while future research should focus on developing adaptive gamified platforms tailored for vulnerable user groups, including learners with low digital literacy. Additionally, there is a need for longitudinal studies that measure not only knowledge acquisition but also persistent behavioral changes and real-world application of cybersecurity skills.

ACKNOWLEDGMENT

This work was supported by project KEGA 061TUKÉ-4/2025 "Building bridges between university and high school ICT education".

REFERENCES

- [1] I. M. Venter, R. J. Blignaut, K. Renaud, and M. A. Venter, "Cyber security education is as essential as "the three r's"," *Heliyon*, vol. 5, no. 12, p. e02855, December 2019.
- [2] A. Ibrahim, M. McKee, L. F. Sikos, and N. F. Johnson, "A systematic review of k-12 cybersecurity education around the world," *IEEE Access*, vol. 12, p. 59726–59738, 2024.
- [3] J. Crabb, C. Hundhausen, and A. Gebremedhin, "A critical review of cybersecurity education in the united states," in *Proceedings of the 55th ACM Technical Symposium on Computer Science Education V. 1*. Portland, OR, USA: ACM, March 2024, p. 241–247.
- [4] A. All, E. Nunez Castellar, N. Castellar, and J. Looy, "Measuring effectiveness in digital game-based learning: A methodological review," *International Journal of Serious Games*, vol. 1, May 2014.
- [5] P. Battistella and C. G. Von Wangenheim, "Games for teaching computing in higher education – a systematic review," *IEEE Technology and Engineering Education*, vol. 9, no. 1, p. 8–30, 2016.
- [6] W. Y. Seng, M. H. M. Yatim, and T. W. Hoe, "Learning object-oriented programming paradigm via game-based learning game – pilot study," *International Journal of Multimedia & Its Applications (IJMIA)*, vol. 10, p. 181–197, 2018.
- [7] S. Abbasi, H. Kazi, and K. Khowaja, "A systematic review of learning object-oriented programming through serious games and programming approaches," in *2017 4th IEEE International Conference on Engineering Technologies and Applied Sciences (ICETAS)*, 2017.
- [8] J. Livovský and J. Porubán, "Learning object-oriented paradigm by playing computer games: Concepts first approach," *Central European Journal of Computer Science*, vol. 4, no. 3, p. 171–182, 2014.
- [9] Z. Zainuddin, S. K. W. Chu, M. Shujahat, and C. J. Perera, "The impact of gamification on learning and instruction: A systematic review of empirical evidence," *Educational Research Review*, vol. 30, p. 100326, June 2020.
- [10] G. Witeck, A. Alves, and M. Bernardo, "Bloom taxonomy, serious games and lean learning: What do these topics have in common?" in *Learning in the Digital Era*, ser. IFIP Advances in Information and Communication Technology. Springer, Cham, 2021, vol. 610.
- [11] G. Fink, D. Best, D. Manz, V. Popovsky, and B. Endicott-Popovsky, "Gamification for measuring cyber security situational awareness," in *International Conference on Augmented Cognition*, ser. Lecture Notes in Computer Science, vol. 8027. Springer, 2013, p. 656–665.
- [12] European Union Agency for Cybersecurity, *ENISA threat landscape 2024: July 2023 to June 2024*. Publications Office, 2024.
- [13] Verizon Communications Inc., "2024 data breach investigations report (dbir)," Verizon, Technical Report, 2024.
- [14] K. Amoresano and B. Yankson, "Human error - a critical contributing factor to the rise in data breaches: A case study of higher education," *HOLISTICA – Journal of Business and Public Administration*, vol. 14, no. 1, p. 110–132, June 2023.
- [15] E. Kwon, H. Lee, S. Chai, and K. Yoo, "The utility of information security training and education on cybersecurity incidents: An empirical evidence," *Information Systems Frontiers*, vol. 23, no. 2, p. 361–373, April 2021.
- [16] C. Iuga, J. R. C. Nurse, and A. Erola, "Baiting the hook: Factors impacting susceptibility to phishing attacks," *Human-centric Computing and Information Sciences*, vol. 6, no. 1, p. 8, December 2016.
- [17] C. Catal, A. Ozcan, E. Donmez, and A. Kasif, "Analysis of cyber security knowledge gaps based on cyber security body of knowledge," *Education and Information Technologies*, vol. 28, no. 2, p. 1809–1831, February 2023.
- [18] L. V. Daineko, N. V. Goncharova, E. V. Zaitseva, V. A. Larionova, and I. A. Dyachkova, *Gamification in Education: A Literature Review*, ser. Lecture Notes in Networks and Systems. Cham: Springer Nature Switzerland, 2023, vol. 830, p. 319–343.
- [19] B. F. Faith, Z. A. Long, and S. Hamid, "Promoting cybersecurity knowledge via gamification: An innovative intervention design," in *2024 Third International Conference on Distributed Computing and High Performance Computing (DCHPC)*, 2024.
- [20] S. Ros, S. González, A. Robles, L. L. Tobarra, A. Caminero, and J. Cano, "Analyzing students' self-perception of success and learning effectiveness using gamification in an online cybersecurity course," *IEEE Access*, 2023.
- [21] M. e. a. Mendonça, "Initial experiments using game-based learning applied in a classical knowledge robotics in in-person and distance learning classroom," *Advances in Science, Technology and Engineering Systems Journal*, 2021.
- [22] T. Turchi, D. Fogli, and A. Malizia, "Fostering computational thinking through collaborative game-based learning," *Multimedia Tools and Applications*, vol. 78, no. 10, p. 13649–13673, 2019.
- [23] R. Matovu, J. C. Nwokeji, T. Holmes, and T. Rahman, "Teaching and learning cybersecurity awareness with gamification in smaller universities and colleges," in *2022 IEEE Frontiers in Education Conference (FIE)*, 2022, pp. 1–9.
- [24] T. Buckley and O. Buckley, "Cracking the code: A cyber security escape room as an innovative training and learning approach," in *Human Factors in Cybersecurity. AHFE (2024) International Conference*, ser. AHFE Open Access, A. Moallem, Ed., vol. 127. AHFE International, USA, 2024.
- [25] J.-W. Bullee and L. Koning, "Cybersecurity on the move: Investigating the efficacy of a movable escape room as an educational tool for healthcare employees," *European Conference on Games Based Learning*, vol. 18, no. 1, pp. 525–533, oct 2024.
- [26] N. A. G. Arachchilage and S. Love, "A game design framework for avoiding phishing attacks," *Computers in Human Behavior*, vol. 29, no. 3, pp. 706–714, 2013.
- [27] D. Huitema and A. Wong, "A case study in gamification for a cybersecurity education program: A game for cryptography," *arXiv preprint arXiv:2502.06706*, no. arXiv:2502.06706, feb 2025, arXiv:2502.06706 [cs].
- [28] H. Qusa and J. Tarazi, "Cyber-hero: A gamification framework for cyber security awareness for high schools students," in *2021 IEEE 11th Annual Computing and Communication Workshop and Conference (CCWC)*, 2021, pp. 0677–0682.
- [29] A. Pereira and M. Wahi, "Development and testing of a roleplaying gamification module to enhance deeper learning of case studies in an accelerated online management theory course," *Online Learning*, vol. 25, no. 3, p. 101–127, 2021.
- [30] L. M. Jones, K. J. Mitchell, and C. L. Beseler, "The impact of youth digital citizenship education: Insights from a cluster randomized controlled trial outcome evaluation of the be internet awesome (bia) curriculum," *Contemporary School Psychology*, vol. 28, no. 4, pp. 509–523, dec 2024.
- [31] J. Seale and N. Schoenberger, "Be internet awesome: A critical analysis of google's child-focused internet safety program," *Emerging Library & Information Perspectives*, vol. 1, may 2018.
- [32] L.-M. Putz, F. Hofbauer, and H. Treiblmaier, "Can gamification help to improve education? findings from a longitudinal study," *Computers in Human Behavior*, vol. 110, p. 106392, September 2020.
- [33] A.-C. Iosif, T. Espinha Gasiba, U. Lechner, and M. Pinto-Albuquerque, "To kill a mocking bug: Open source repo mining of security patches for programming education," *OASICs, Volume 122, ICPEC 2024*, vol. 122, pp. 16:1–16:12, 2024.
- [34] A.-C. Iosif, U. Lechner, M. Pinto-Albuquerque, and T. E. Gasiba, "Serious game for industrial cybersecurity: Experiential learning through code review," in *2024 36th International Conference on Software Engineering Education and Training (CSEE&T)*. Würzburg, Germany: IEEE, July 2024, p. 1–6.
- [35] A.-C. Iosif, U. Lechner, M. Pinto-Albuquerque, and T. Espinha Gasiba, "Code review for cybersecurity in the industry: Insights from gameplay analytics," *OASICs, Volume 122, ICPEC 2024*, vol. 122, pp. 14:1–14:11, 2024.

Automated Evaluation of University Tests Quality

¹Tomáš BUČEK (2nd year),
Supervisor: ²Ján GENČI

^{1,2}Dept. of Computers and Informatics, FEI TU of Košice, Slovak Republic

¹tomas.bucek@tuke.sk, ²jan.genci@tuke.sk

II. BACKGROUND

Abstract—Manual evaluation of students' knowledge is an inherently time-consuming and labor-intensive process, which can often lead to inconsistencies and delays in feedback. The automation of this process offers a promising solution, particularly through the use of tests and practical assignments that are evaluated automatically. Such automation can significantly improve efficiency, accuracy, and the timeliness of feedback provided to students. A key to developing these automated evaluation systems lies in the construction of well-designed and reliable educational tests. These tests can be created using either classical test theory or item response theory (IRT). Item response theory, in particular, provides a more sophisticated approach to test design, as it accounts for varying levels of difficulty and individual student abilities, ensuring a more detailed evaluation.

In this paper, we explore the current state of research and practice in the field of educational test development, specifically focusing on the use of IRT for the automated evaluation of students' knowledge. We delve into the principles of test theory, emphasizing the advantages of using IRT over traditional methods. Additionally, we discuss our work in developing an application for the automated evaluation of tests based on IRT, which aims to streamline the assessment process for practical assignments in software engineering. This paper provides insights into the potential of such system to enhance the objectivity and efficiency of educational evaluations, ultimately benefiting both students and instructors.

This research contributes to the development of efficient and objective methods for assessing students' knowledge, enabling more accurate diagnostics of their abilities. By introducing IRT into automated testing, it advances educational practice toward data-driven and individualized evaluation.

Keywords—Automation, Item Response Theory, Test Quality Evaluation

I. INTRODUCTION

Effective assessment of test results is an integral part of the educational process. For instructors, it is crucial not only to evaluate students' abilities, but also to analyze the quality of test questions in order to improve the objectivity of the assessment. One of the key methods for evaluating test quality is the calculation of the KR-20 coefficient [1], which measures the internal consistency of the questions and provides insights into the overall reliability of the test.

Currently, most instructors work with test results exported from the Moodle system, which offers basic statistical summaries. However, these summaries are limited and do not provide the ability to analyze advanced statistics, such as KR-20, in detail. Calculating this value often requires manual data processing using external tools, which can be time-consuming and prone to errors. These limitations highlight the need for a tool capable of automating such operations and presenting them to instructors in an intuitive and efficient format.

Item Response Theory (IRT) is a framework used to model the relationship between a student's latent ability and their performance on individual test items [2]. Unlike classical test theory, which assumes that all test items have the same difficulty for all test-takers, IRT allows us to use a more detailed approach [3]. IRT considers the varying difficulty levels of items and the probability that a test-taker with a certain ability will correctly answer a particular item [4]. This model is essential for creating tests that are more accurate in measuring student ability across diverse populations. IRT has found widespread use in fields like educational assessment, psychology, and health measurement, as it provides valuable insights into both the quality of test items and the reliability of the test itself [5].

One of the most commonly used reliability measures in educational testing is the KR-20 coefficient. The KR-20 (Kuder-Richardson Formula 20) is a special case of the Cronbach's alpha coefficient, designed specifically for dichotomous items (i.e., items with only two possible responses, such as correct or incorrect answers), but can be applied to other item types as well. The KR-20 coefficient is used to assess the internal consistency or reliability of a test [1], which indicates the degree to which all items on the test measure the same underlying construct. The value of KR-20 ranges from 0 to 1, where a higher value suggests better internal consistency and thus higher reliability of the test. A value of 0.7 or above is generally considered acceptable for most tests, as it is presented on table I.

The KR-20 coefficient is calculated using the formula:

$$KR - 20 = \frac{k}{k - 1} \left(1 - \frac{\sum p_i(1 - p_i)}{\sigma^2} \right)$$

where k is the number of items on the test, p_i is the proportion of correct responses for item i , and σ^2 is the variance of total test scores. This formula allows for an evaluation of how well the items on a test work together in terms of measuring a single construct. A high KR-20 score suggests that the items are consistent in assessing the same ability or trait, while a low score indicates that the test may need to be revised for better reliability.

III. SYSTEM DEVELOPMENT

We have developed an application designed to automate the evaluation of test quality within the Moodle platform. This tool is intended to streamline and accelerate the process of analyzing test results, ultimately improving the quality of

TABLE I
EXAMPLE OF RELIABILITY COEFFICIENT VALUES

KR-20 Value Range	Reliability Interpretation
0.00 - 0.10	Negligible Reliability
0.10 - 0.39	Weak Reliability
0.40 - 0.69	Moderate Reliability
0.70 - 0.89	Strong Reliability
0.90 - 1.00	Very Strong Reliability

assessments in the educational context. The application is capable of efficiently processing and analyzing data generated within Moodle, specifically from test reports exported in CSV format. This format allows the application to easily extract relevant data, such as student responses, scores, and various statistical information, all of which are crucial for evaluating test quality.

The evaluation process begins with the import of CSV files generated by Moodle after each test. These files contain detailed information on test results, which can be analyzed using various statistical methods. The application automatically processes the data, performs the analysis, and provides an assessment of the quality of individual tests. One of the key features is the calculation of the KR-20 reliability coefficient, which measures the internal consistency of test items and provides valuable insights into the overall reliability of the test.

The application offers an intuitive interface that allows instructors to easily upload CSV files and obtain comprehensive statistics on test quality. Additionally, it enables the generation of reports containing key metrics, such as KR-20 values and other relevant indicators (discrimination index, facility index), which help instructors in evaluating and refining their tests. In this way, the application supports continuous improvement in the quality of testing within Moodle, significantly enhancing the efficiency and accuracy of student assessments, as we managed to identify 5 broken test items within 3 exams.

The application also provides detailed insights into the quality of individual test questions, using item response theory (IRT) metrics to assess their performance. Specifically, it highlights questions that may have a poor discrimination index, which refers to how well a question distinguishes between students with different levels of ability. A low discrimination index indicates that a question might not be effective in differentiating high-performing students from low-performing ones, which can negatively affect the test's overall quality. The application clearly flags these questions, allowing instructors to identify and improve them for better assessment reliability.

In addition to the discrimination index, the tool also evaluates the facility index of each question. The facility index measures the percentage of students who answer a question correctly, providing insight into how easy or difficult a particular question is. A question with a very high facility index may be too easy and fail to effectively assess students' knowledge, while a very low facility index might indicate that the question is too difficult or confusing. By analyzing these indices, instructors can make informed decisions about which questions to modify, replace, or remove to improve the overall test quality.

With these statistical insights at their disposal, instructors can directly modify the test questions within the application.

They can adjust the wording, change answer options, or even remove problematic questions based on the IRT analysis and other metrics. After making these adjustments, the tool immediately updates the statistics, allowing instructors to see how the changes impact the overall test quality. This immediate feedback enables continuous refinement of the test, ensuring that it provides a more accurate and fair evaluation of students' knowledge.

Furthermore, the application supports the comparison of different versions of the test. By analyzing and comparing the statistical results of multiple test versions, instructors can identify any significant differences in performance and adjust their tests accordingly. This feature is particularly useful for tracking changes over time or when experimenting with different question formats or difficulty levels. By using the application's powerful analytics, instructors can optimize their tests and ensure that they are consistently assessing students in the most effective way possible.

IV. FUTURE WORK

In the future, we plan to further develop the application so that it will no longer require manual data exports from Moodle. Our goal is to integrate this tool directly as an add-on within the Moodle system, making the entire process even more seamless and efficient. Instructors will be able to access test statistics directly from within the Moodle interface, without the need to download and upload CSV files. This smooth access to data will allow for immediate retrieval of results and analytical insights during test creation and management, significantly speeding up and simplifying the entire assessment process.

Integrating the tool as an add-on within Moodle will also provide greater flexibility and convenience when working with tests and statistics. Instructors will be able to make direct adjustments to the tests based on the displayed analyses and immediately see the impact of these changes on the test quality.

V. CONCLUSION

Automated evaluation of students' knowledge is a crucial step towards improving the efficiency, accuracy, and reliability of educational assessments. In this paper, we have explored the benefits of using Item Response Theory (IRT) for test quality evaluation and the calculation of the KR-20 reliability coefficient. Our developed application streamlines the process by automating the analysis of test results exported from Moodle, enabling instructors to gain deeper insights into test reliability and student performance. By integrating automated statistical evaluations, our system minimizes manual effort and reduces errors in test assessment. Future work will focus on expanding the application's capabilities, incorporating additional psychometric measures, and refining the user experience to further enhance the objectivity and effectiveness of automated student evaluation.

The presented work demonstrates that integrating item response theory into automated assessment systems can significantly enhance the objectivity and precision of evaluating students' knowledge. These findings highlight the potential of data-driven and individualized testing approaches to improve the overall quality and effectiveness of educational evaluation.

REFERENCES

- [1] G. F. Kuder and M. W. Richardson, "The theory of the estimation of test reliability," *Psychometrika*, vol. 2, no. 3, pp. 151–160, 1937.
- [2] F. M. Lord, *Applications of Item Response Theory to Practical Testing Problems*. Hillsdale, NJ: Lawrence Erlbaum Associates, 1980.
- [3] D. Thissen, "Multidimensional item response theory," in *Handbook of Item Response Theory*, vol. 1, D. N. Chang and J. C. Carver, Eds. Boca Raton, FL: CRC Press, 2003, pp. 43–61.
- [4] S. E. Embretson and S. P. Reise, *Item Response Theory for Psychologists*, 2nd ed. New York: Psychology Press, 2013.
- [5] F. B. Baker, *The Basics of Item Response Theory*, 2nd ed. ERIC Clearinghouse on Assessment and Evaluation, 2001.

Data Augmentation with Large Language Models for Minority Languages: A Review

¹Kristián SOPKOVIČ (1st year),
Supervisor:²Matúš PLEVA

^{1,2}Dept. of Electronics and Multimedia Communications, FEI TU of Košice, Slovak Republic

¹kristian.sopkovic@tuke.sk, ²matus.pleva@tuke.sk

Abstract—The application of large language models (LLMs) to natural language processing (NLP) tasks has yielded remarkable advancements. However, performance often lags significantly when these models are deployed on low-resource or minority languages due to the scarcity of available training data. Data augmentation, a technique used to artificially expand datasets, has become a critical tool in mitigating this limitation. This paper reviews research on employing LLMs for data augmentation in the context of low-resource languages. It critically analyzes existing methodologies, focusing on their strengths and weaknesses, and identifies remaining challenges. The review further examines the feasibility of addressing these challenges and proposes directions for future research, aiming to facilitate the development of more robust and effective NLP solutions for under-represented languages.

Keywords—Data Augmentation, Large Language Models, Minority Languages, Natural Language Processing, Low-Resource Languages.

I. INTRODUCTION

Large language models (LLMs) have revolutionized natural language processing (NLP), achieving impressive results in tasks like machine translation and text summarization. However, their performance relies heavily on large, high-quality training datasets, a significant challenge for low-resource or minority languages where such data is scarce. This scarcity limits LLM performance on these languages, creating a digital divide that impacts access to information, education, and cultural preservation.

Data augmentation, artificially expanding datasets, is crucial for mitigating this problem. Traditional methods like back-translation and synonym replacement, while helpful, often produce synthetic data lacking the fluency and coherence of natural language, potentially hindering model performance. LLMs offer a promising alternative. Their ability to generate realistic and diverse text presents the opportunity to create higher-quality synthetic data, specifically tailored to the nuances of low-resource languages.

This review critically analyzes current research on using LLMs for data augmentation in low-resource languages. We discuss the strengths, limitations, and potential biases of existing approaches, identify key challenges, and propose promising directions for future research. The goal is to foster innovation towards more robust and equitable NLP solutions for under-represented languages, improving their performance and accessibility.

II. LITERATURE REVIEW AND ANALYSIS

The scarcity of labeled data for low-resource languages poses a significant hurdle for training effective NLP models. Traditional data augmentation techniques, such as back-translation, synonym replacement, and random insertion, have been widely used to address this problem. However, these methods often generate synthetic data that lacks the fluency and coherence of natural language, potentially leading to suboptimal model performance [1].

The advent of LLMs has opened new avenues for data augmentation. LLMs can be used to generate synthetic data that is more realistic and diverse than that produced by traditional methods. By far, we know several augmentation approaches:

A. Zero-shot Data Augmentation

This involves prompting an LLM to generate text in a specific style or domain without providing any examples. For example, an LLM could be prompted to generate news articles in a specific low-resource language. Studies have shown that zero-shot data augmentation can improve the performance of downstream NLP tasks, such as text classification and machine translation. However, the quality of the generated data can be highly variable, and careful filtering and validation are often required. Furthermore, zero-shot generation may perpetuate biases present in the LLM's pre-training data, which can be particularly problematic for low-resource languages. The lack of explicit guidance can lead to outputs that are either too generic, failing to capture the nuances of the target language, or that hallucinate information, creating factually incorrect or nonsensical data. Researchers are exploring methods to mitigate these issues, such as using more specific and constrained prompts, incorporating knowledge retrieval mechanisms, and employing adversarial training techniques to improve the robustness and accuracy of zero-shot generated data. The effectiveness of zero-shot augmentation also heavily depends on the LLM's inherent understanding of the target language and domain, which can vary significantly across different LLMs and language pairs. Therefore, careful selection of the LLM and rigorous evaluation of the generated data are crucial for successful implementation [2].

B. Few-shot Data Augmentation

This involves providing the LLM with a small number of examples (e.g., 5-10) and then prompting it to generate more

data that is similar to the examples. This approach can be more effective than zero-shot generation, as it provides the LLM with more context and guidance. For example, the LLM could be provided with a few examples of question-answer pairs in a low-resource language and then prompted to generate more question-answer pairs. A critical aspect here is the quality of the seed examples – noisy or unrepresentative examples can lead to the generation of poor-quality synthetic data. Selecting diverse and representative examples is crucial for ensuring that the generated data reflects the true distribution of the target language and domain. Furthermore, the number of examples provided can significantly impact the quality and diversity of the generated data. While a few examples may be sufficient to guide the LLM, providing more examples can often lead to more accurate and nuanced outputs. Researchers are also exploring techniques for automatically selecting the most informative and representative examples from a larger dataset to optimize the performance of few-shot data augmentation. Active learning strategies can be employed to iteratively select examples that maximize the model's learning gain, leading to more efficient and effective data augmentation [3].

C. Back-Translation with LLMs

Back-translation is a widely used data augmentation technique that involves translating text from a source language to a target language and then translating it back to the source language. LLMs can be used to improve the quality of back-translation by generating more accurate and fluent translations. The use of LLMs as translation engines can be particularly beneficial for low-resource languages, where traditional machine translation systems may be less accurate. However, back-translation can also introduce noise and artifacts into the data, which can negatively impact model performance. LLMs, with their ability to capture contextual nuances and generate more natural-sounding translations, can significantly reduce the amount of noise introduced during back-translation. However, it is important to carefully select the source language and the LLM used for translation, as different LLMs may exhibit different biases and strengths in different language pairs. Furthermore, techniques such as noise injection and iterative back-translation can be employed to further improve the diversity and robustness of the augmented data. Noise injection involves adding small perturbations to the source text before translation, which can encourage the LLM to generate more diverse and robust translations. Iterative back-translation involves repeatedly translating the text back and forth between the source and target languages, which can further refine the quality and fluency of the generated data [4].

D. Prompt Engineering for Controlled Generation

A growing area focuses on careful prompt engineering to guide LLMs to generate specific types of data. This includes techniques like specifying the desired length, style, and topic of the generated text. For instance, one might prompt an LLM to **"Translate the following sentence into [Minority Language] and then rephrase it in three different ways, maintaining the original meaning."** This allows for more control over the augmented data and can be tailored to specific NLP tasks. Effective prompt engineering involves carefully crafting prompts that provide clear and concise instructions to the LLM, specifying the desired characteristics of the

generated data. This includes specifying the desired length, style, tone, and topic of the generated text, as well as providing examples of the desired output format. Researchers are also exploring techniques for automatically generating prompts that maximize the quality and diversity of the generated data. This includes using reinforcement learning algorithms to optimize the prompt based on feedback from downstream NLP tasks, as well as using generative models to generate diverse and creative prompts that can elicit novel and informative responses from the LLM. The key to successful prompt engineering is to understand the capabilities and limitations of the LLM and to craft prompts that effectively leverage its strengths while mitigating its weaknesses [5].

E. Fine-tuning LLMs for Specific Augmentation Tasks

In this approach, LLMs are fine-tuned on a small set of high-quality data from the low-resource language to specialize their augmentation capabilities. This might involve fine-tuning on parallel corpora to improve back-translation quality or on a dataset of paraphrases to enhance sentence generation diversity. Fine-tuning can significantly improve the relevance and quality of the generated data, but it requires careful selection of the fine-tuning dataset and computational resources. The choice of fine-tuning data is crucial for ensuring that the LLM learns the specific characteristics of the target language and domain. Fine-tuning on parallel corpora can improve the accuracy and fluency of back-translation, while fine-tuning on a dataset of paraphrases can enhance the diversity and creativity of sentence generation. However, it is important to carefully evaluate the performance of the fine-tuned LLM on a held-out dataset to ensure that it is not overfitting to the fine-tuning data. Techniques such as regularization and early stopping can be used to prevent overfitting and to improve the generalization performance of the fine-tuned LLM. Furthermore, transfer learning techniques can be used to leverage knowledge from pre-trained LLMs in other languages to accelerate the fine-tuning process and to improve the performance of the fine-tuned LLM on the low-resource language [6].

F. Commentary and Assessment

While LLMs offer exciting possibilities for data augmentation in low-resource languages, several challenges remain.

Data Quality: The quality of the synthetic data generated by LLMs can be highly variable. It is crucial to carefully filter and validate the generated data to ensure that it is accurate, fluent, and relevant to the target NLP task. Automated metrics like BLEU, ROUGE, and BERTScore can be used to assess the quality of generated text, but human evaluation is still necessary to ensure its suitability for downstream tasks [7].

Bias Amplification: LLMs are trained on massive datasets that may contain biases. Data augmentation with LLMs can inadvertently amplify these biases, leading to unfair or discriminatory outcomes. It is essential to be aware of potential biases in the generated data and to take steps to mitigate them [8].

Computational Cost: Training and deploying LLMs can be computationally expensive. Data augmentation with LLMs may require significant computational resources, which can be a barrier for researchers and practitioners working with low-resource languages [9].

Lack of Evaluation Benchmarks: There is a lack of standardized evaluation benchmarks for assessing the effectiveness of data augmentation techniques for low-resource languages. This makes it difficult to compare different approaches and to track progress in the field [10].

Ethical Considerations: The use of LLMs for data augmentation raises several ethical considerations, such as the potential for misuse of generated data and the need to ensure that the generated data is respectful of the cultures and values of low-resource language communities [11].

III. PROBLEM IDENTIFICATION AND FUTURE DIRECTIONS

Despite the progress made in recent years, several problems remain unsolved in the field of data augmentation with LLMs for low-resource languages.

A. Proposed Future Directions

Research should explore several promising avenues. One is **Active Learning for Data Augmentation**, which combines active learning with LLM-based generation to maximize the use of limited annotation resources. In this setup, an LLM produces synthetic data, and active learning strategically selects the most informative examples for human annotation, subsequently refining the LLM's performance. This requires specific research into active learning strategies tailored for LLM-generated data [12]. Another direction is **Cross-lingual Transfer Learning**, leveraging linguistic knowledge from high-resource languages to boost NLP model performance for resource-scarce ones. Pre-training LLMs on multilingual datasets and then fine-tuning them on low-resource language data can be enhanced by incorporating language-specific information, though research is needed on optimal alignment techniques and mitigating negative transfer effects [13]. **Meta-Learning for Data Augmentation** offers a way to automate the design and optimization of augmentation strategies specifically suited for different low-resource languages. A meta-learner could identify patterns between language characteristics and effective techniques, reducing manual effort. Further research should focus on meta-learning architectures and methods for encoding linguistic knowledge [14]. **Incorporating Linguistic Knowledge** into the augmentation process can improve the quality, relevance, and diversity of generated data, ensuring it follows grammatical rules and cultural nuances through rule-based, constraint-based, or feature-based methods, while balancing linguistic accuracy and data diversity remains a challenge [15]. The **Human-in-the-Loop Data Augmentation** approach involves human annotators reviewing and editing LLM outputs to enhance quality, reliability, and cultural appropriateness, with their feedback guiding the LLM's learning; effective interfaces and workflows, along with research on integrating and quantifying the impact of this feedback, are key [12]. Finally, **Federated Data Augmentation** uses federated learning to allow collaborative augmentation without sharing raw data, addressing privacy concerns, which is beneficial for fragmented or sensitive low-resource language data. Research must tackle challenges like communication overhead, data heterogeneity, and potential biases [16].

B. Realistically Solvable Problems

While challenges like completely eliminating bias are inherently complex, several issues are likely addressable in the near

future. These include **developing more effective prompt engineering techniques** to generate high-quality synthetic data, focusing on strategies to elicit specific linguistic variations, control style and tone, and minimize irrelevant output [17]. It is also feasible to **create more robust filtering and validation methods** for identifying and removing low-quality or biased data, involving automated quality metrics, machine learning models for bias detection, and human validation processes [18]. Progress can also be made in **developing more efficient algorithms** for training and deploying LLMs on devices with limited resources, exploring techniques like model compression, knowledge distillation, and hardware-aware optimization [19]. Lastly, **creating standardized evaluation benchmarks** specifically for assessing data augmentation techniques for low-resource languages is achievable. These benchmarks should cover diverse tasks, datasets, and metrics relevant to these languages to provide a fair basis for comparison [20].

IV. CONCLUSION

Data augmentation with LLMs holds significant promise for improving the performance of NLP models in low-resource languages. However, several challenges remain, including the need to improve the quality of synthetic data, mitigate bias, reduce computational cost, and develop evaluation benchmarks. By addressing these challenges and pursuing the future directions outlined above, we can unlock the full potential of LLMs for empowering low-resource language communities and promoting linguistic diversity.

ACKNOWLEDGMENT

The research was partially supported by the Ministry of Education, research, development and Youth of the Slovak Republic under the projects KEGA 049TUKE-4/2024 & VEGA 2/0092/25, by the Slovak Research and Development Agency under the projects APVV-22-0414 & APVV-22-0261 as well as by the Erasmus+ MetaCog 2024-1-FI01-KA220-HED-000247530 project.

REFERENCES

- [1] S. Y. Feng, V. Gangal, J. Wei, S. Chandar, S. Vosoughi, T. Mitamura, and E. Hovy, "A survey of data augmentation approaches for NLP," in *Findings of the Association for Computational Linguistics: ACL-IJCNLP 2021*. Online: Association for Computational Linguistics, Aug. 2021, pp. 968–988. [Online]. Available: <https://aclanthology.org/2021.findings-acl.84>
- [2] C. Ryu, S. Lee, S. Pang, C. Choi, H. Choi, M. Min, and J.-Y. Sohn, "Retrieval-based evaluation for LLMs: A case study in Korean legal QA," in *Proceedings of the Natural Language Processing Workshop 2023*, D. Preotiu-Pietro, C. Goanta, I. Chalkidis, L. Barrett, G. Spanakis, and N. Aletras, Eds. Singapore: Association for Computational Linguistics, Dec. 2023, pp. 132–137. [Online]. Available: <https://aclanthology.org/2023.nlp-1.13/>
- [3] M. Bornea, L. Pan, S. Rosenthal, R. Florian, and A. Sil, "Multilingual transfer learning for qa using translation as data augmentation," *Proceedings of the AAAI Conference on Artificial Intelligence*, vol. 35, no. 14, pp. 12583–12591, May 2021. [Online]. Available: <https://ojs.aaai.org/index.php/AAAI/article/view/17491>
- [4] A. Poncelas, G. M. d. B. Wenniger, and A. Way, "Adaptation of machine translation models with back-translated data using transductive data selection methods," in *Computational Linguistics and Intelligent Text Processing*, A. Gelbukh, Ed. Cham: Springer Nature Switzerland, 2023, pp. 567–579.
- [5] B. Meskó, "Prompt engineering as an important emerging skill for medical professionals: Tutorial," *J Med Internet Res*, vol. 25, p. e50638, Oct 2023. [Online]. Available: <https://www.jmir.org/2023/1/e50638>
- [6] J. Wei, M. Bosma, V. Y. Zhao, K. Guu, A. W. Yu, B. Lester, N. Du, A. M. Dai, and Q. V. Le, "Finetuned language models are zero-shot learners," *CoRR*, vol. abs/2109.01652, 2021. [Online]. Available: <https://arxiv.org/abs/2109.01652>

- [7] A. Wang, A. Singh, J. Michael, F. Hill, O. Levy, and S. R. Bowman, “Glue: A multi-task benchmark and analysis platform for natural language understanding,” 2018. [Online]. Available: <https://arxiv.org/abs/1804.07461>
- [8] J. Zhao, T. Wang, M. Yatskar, V. Ordonez, and K.-W. Chang, “Gender bias in coreference resolution: Evaluation and debiasing methods,” 2018. [Online]. Available: <https://arxiv.org/abs/1804.06876>
- [9] T. Heston and C. Khun, “Prompt engineering in medical education,” *International Medical Education*, vol. 2, no. 3, p. 198–205, Aug. 2023. [Online]. Available: <http://dx.doi.org/10.3390/ime2030019>
- [10] T. Gui, X. Wang, Q. Zhang, Q. Liu, Y. Zou, X. Zhou, R. Zheng, C. Zhang, Q. Wu, J. Ye, Z. Pang, Y. Zhang, Z. Li, R. Ma, Z. Fei, R. Cai, J. Zhao, X. Hu, Z. Yan, Y. Tan, Y. Hu, Q. Bian, Z. Liu, B. Zhu, S. Qin, X. Xing, J. Fu, Y. Zhang, M. Peng, X. Zheng, Y. Zhou, Z. Wei, X. Qiu, and X. Huang, “Textflint: Unified multilingual robustness evaluation toolkit for natural language processing,” 2021. [Online]. Available: <https://arxiv.org/abs/2103.11441>
- [11] S. Abhari, S. Fatahi, A. Saragadam, D. Chumachenko, and P. Pelegriini Morita, *A Road Map of Prompt Engineering for ChatGPT in Healthcare: A Perspective Study*. IOS Press, Aug. 2024. [Online]. Available: <http://dx.doi.org/10.3233/shti240578>
- [12] L. Moles, A. Andres, G. Echegaray, and F. Boto, “Exploring data augmentation and active learning benefits in imbalanced datasets,” *Mathematics*, vol. 12, no. 12, p. 1898, Jun. 2024. [Online]. Available: <http://dx.doi.org/10.3390/math12121898>
- [13] W. de Vries, M. Wieling, and M. Nissim, “Make the best of cross-lingual transfer: Evidence from pos tagging with over 100 languages,” in *Proceedings of the 60th Annual Meeting of the Association for Computational Linguistics (Volume 1: Long Papers)*. Association for Computational Linguistics, 2022, p. 7676–7685. [Online]. Available: <http://dx.doi.org/10.18653/v1/2022.acl-long.529>
- [14] L. Wu, Z. Guo, B. Cui, H. Tang, and W. Lu, “Good meta-tasks make a better cross-lingual meta-transfer learning for low-resource languages,” in *Findings of the Association for Computational Linguistics: EMNLP 2023*, H. Bouamor, J. Pino, and K. Bali, Eds. Singapore: Association for Computational Linguistics, Dec. 2023, pp. 7431–7446. [Online]. Available: <https://aclanthology.org/2023.findings-emnlp.498/>
- [15] W. Ahmad, H. Li, K.-W. Chang, and Y. Mehdad, “Syntax-augmented multilingual bert for cross-lingual transfer,” in *Proceedings of the 59th Annual Meeting of the Association for Computational Linguistics and the 11th International Joint Conference on Natural Language Processing (Volume 1: Long Papers)*. Association for Computational Linguistics, 2021, p. 4538–4554. [Online]. Available: <http://dx.doi.org/10.18653/v1/2021.acl-long.350>
- [16] V. Mathur, T. Dadu, and S. Aggarwal, “Evaluating neural networks’ ability to generalize against adversarial attacks in cross-lingual settings,” *Applied Sciences*, vol. 14, no. 13, p. 5440, Jun. 2024. [Online]. Available: <http://dx.doi.org/10.3390/app14135440>
- [17] M. Kochanek, I. Cichecki, O. Kaszyca, D. Szydło, M. Madej, D. Jędrzejewski, P. Kazienko, and J. Kocoń, “Improving training dataset balance with chatgpt prompt engineering,” *Electronics*, vol. 13, no. 12, p. 2255, Jun. 2024. [Online]. Available: <http://dx.doi.org/10.3390/electronics13122255>
- [18] A. K. Pamidi venkata and L. Gudala, “The potential and limitations of large language models for text classification through synthetic data generation,” *INTERNATIONAL RESEARCH JOURNAL OF ENGINEERING; APPLIED SCIENCES*, p. 8–15, Apr. 2024. [Online]. Available: <http://dx.doi.org/10.55083/irjeas.2024.v12i02002>
- [19] M. Miletic and M. Sariyar, *Large Language Models for Synthetic Tabular Health Data: A Benchmark Study*. IOS Press, Aug. 2024. [Online]. Available: <http://dx.doi.org/10.3233/shti240571>
- [20] V. C. D. Hoang, P. Koehn, G. Haffari, and T. Cohn, “Iterative back-translation for neural machine translation,” in *Proceedings of the 2nd Workshop on Neural Machine Translation and Generation*. Association for Computational Linguistics, 2018. [Online]. Available: <http://dx.doi.org/10.18653/v1/w18-2703>

Implementation Potential of Transparent Intensional Logic in Multi-Agent System Communication

¹Samuel NOVOTNÝ (2nd year),
Supervisor: ²William STEINGARTNER

^{1,2}Dept. of Computers and Informatics, FEI TU of Košice, Slovak Republic

¹samuel.novotny@tuke.sk, ²william.steingartner@tuke.sk

Abstract—This paper explores the use of Transparent Intensional Logic in the formalization and modeling of communication in multi-agent systems, resulting in the development of the TIL-Message Formalization System. This system, unlike others, also provides an abstract description of the background of the communication process, as proved by its application on specific examples, by standing out from the order of other formalisms providing only a kind of syntactic standard.

Keywords—Transparent Intensional Logic, communication, TIL-Message Formalization System

I. INTRODUCTION

Transparent Intensional Logic (TIL)[1] is a logic system designed by Pavol Tichý [2], the priority application domain of which is the logical analysis of natural language [3], a discipline situated at the intersection of logic and computational linguistics. The greatest advantage of TIL compared to other logical systems is undoubtedly its procedural (constructive) nature, which is captured by a hyperintensional partial variant of typed λ -calculus. TIL formulas therefore represent procedures, referred to as constructions [4], whose execution corresponds to the semantic interpretation of formulas in standard logical systems.

Although the procedural nature of TIL constructions may suggest that this logical system is well-suited for real implementation, its applications are primarily centered on its role as a syntactic standard (most commonly in the form of the so-called TIL-Script [5],[6] – the computational variant of TIL). Meanwhile, implementation based on its procedural (constructive) nature has remained largely overlooked. A prime example of this is the work focused on extracting and processing information from natural language [7] or formalizing communication within multi-agent systems [8].

However, one of the exceptions can be considered our work on the formalization and modeling of communication within multi-agent systems (MAS) based on TIL [9], where we developed the so-called TIL-Message Formalization System (TIL-MFS). This system exhibits both the characteristics of a syntactic standard built upon the apparatus of TIL and an abstract description of communication implementation based on the procedural nature of this logical system. A more detailed presentation of TIL-MFS will be provided after introducing the fundamental concepts of TIL in the following section.

II. FOUNDATIONS OF TIL

Since TIL is based on a certain variation of the typed λ -calculus, it also has a type system, specifically Tichý's theory

of types [10], elementary types of which typically include:

- ι – the type of individuals,
- o – the type of truth values,
- τ – the type of time moments (real numbers),
- ω – the type of possible worlds (temporal sequences of world states, referred to as *world moments* or simply *w-moments*).

Based on this set of elementary types, one can inductively define compound types $(\alpha_0\alpha_1\ldots\alpha_n)$, which represent types of n -ary partial functions $\alpha_1 \times \ldots \times \alpha_n \rightarrow \alpha_0$.

The syntax of TIL is defined through the following grammar in Backus–Naur form (1), where the nonterminal C represents a construction, the nonterminal O denotes a non-constructive object, and the nonterminal X refers to any object (either a construction or a non-construction).¹

$$\begin{aligned} C &::= x \mid {}^0X \mid \lambda x \ldots xC \mid [C \ldots C] \\ X &::= O \mid C \end{aligned} \quad (1)$$

A detailed explanation of the individual kinds of constructions is presented below.

- Variable x is an elementary construction that, based on a valuation, constructs a specific object X . Its analogy in λ -calculus is a variable term.
- Trivialization 0X is (potentially) a composed construction that constructs the object X without any change. Its analogy in extended λ -calculus is a constant or reference.
- Closure $\lambda x_1 \ldots x_n C$, where $n \in \mathbb{N}$, is a composed construction that constructs an n -ary function by abstracting over the variables x_1, \ldots, x_n within the object constructed by the construction C . Its analogy in λ -calculus is an λ -abstraction term.
- Composition $[C_0 C_1 \ldots C_n]$, where $n \in \mathbb{N}$, is a composed construction that constructs the result of applying an n -ary function constructed by the construction C_0 to arguments successively constructed by the constructions $C_1 \ldots C_n$. Its analogy in λ -calculus is an application term.

III. TIL-MESSAGE FORMALIZATION SYSTEM

The message, as a bearer of information and thus the central object in the communication process, is expressed within the TIL-MFS framework as the structure (π, φ) , where:

¹The standard definition of TIL syntax consists of six kinds of constructions, as presented, for example, in the work of Duží et al. [1]. However, for our purposes, this simplified definition suffices.

- π represents the provocativeness of the message, capturing the difference between its interrogative (questioning) form, which stimulates conversation, and its non-interrogative (informative) form, which does not stimulate further conversation²,
- φ is the content of the message, expressed by TIL constructions.

This specification of the message is based on Tichý's work [11], where he argued that although a syntactic difference can be observed between a non-interrogative expression (providing certain information) and an interrogative expression (finding out certain information), its logical duality does not exist within the analysis of these linguistic expressions in TIL. This difference is therefore situated outside of logic. It must be represented within the message through the additional information π , which determines how the content of the message will be processed by its recipient, the agent of MAS.

The focus now shifts specifically to interrogative messages in the context of MAS, which are more commonly referred to as queries and which assume a response as a consequence of their existence. Based on the work of Duží, Číhalová, and Menšík [12], in the case of an empirical query expressing a construction that constructs a $((\alpha\tau)\omega)$ function i.e. intension, the response can be understood as a linguistic expression representing a construction that constructs an object of type α . The actual α -object, i.e., the extension corresponding to the answer to a given query, is obtained by the agent executing the construction, i.e., the abstract procedure corresponding to the query in the actual world w_A and time t_A , as illustrated by the following example.

Query: Has agent Ag_A ever been at the position 2.1?

TIL-MFS: $(?, \lambda w \lambda t [\exists \lambda t' [{}^0 \wedge [{}^0 < t' t] [{}^0 Be_at w] t'] {}^0 Ag_A [{}^0 Pos {}^0 2 {}^0 1]]])$

$[[\lambda w \lambda t [{}^0 \exists \lambda t' [{}^0 \wedge [{}^0 < t' t] [{}^0 Be_at w] t'] {}^0 Ag_A [{}^0 Pos {}^0 2 {}^0 1]]] w_A] t_A] \rightarrow_v T$

Answer: Yes.

TIL-MFS: $(., {}^0 T)$

TIL-MFS thus represents a communication model for MAS based on TIL. Interrogative messages, or queries, within this model therefore represent constructions – abstract procedures. By executing these on local resources (i.e., the current possible world and time), the recipient (agent) can formulate responses to these queries and thereby complete the communication act. However, the question arises: What can be understood by the term possible world within the context of MAS? A partial answer to this question is provided in our subsequent work [13], which focuses on the modal-temporal analysis of MAS based on TIL. In the first phase of this work, we undertook the logical interpretation of two basic concepts of MAS, namely:

- state of the environment as a w-moment and
- run, i.e., an alternating sequence of environment states and agent actions as a possible world.

Based on the second of the aforementioned interpretations, it is clear that when executing the abstract procedure corresponding to the query addressed to it, the agent must provide

local resources in the form of a logical description of its run, i.e., the actual possible world and time. This actual possible world, however, is necessarily subject to certain limitations, as it typically represents an apriori determined temporal sequence of w-moments that perfectly describe individual time moments of the real world. This would imply that each agent has perfect and thus identical knowledge of this world, based on which there would be no difference between the execution of a query by its recipient and by the sender. The existence of a separate communication mechanism between individual agents would be redundant, as the environment would serve as a perfect communication intermediary.

IV. CONCLUSION AND FUTURE RESEARCH

In this paper, we presented the application of TIL in the modeling of communication within MAS, leading to the synthesis of the TIL-MSF. Rather than serving merely as a syntactic standard, this communication model should be understood as an abstract framework that captures the underlying dynamics of the communication process.

Building on this foundation, future research will focus on designing a general logical model for an agent system based on TIL, facilitating integration of the TIL-MFS communication model. Since implementing such a model inherently depends on the implementation potential of TIL, this issue will represent a parallel research line. The goal is therefore not only to provide another formalism for the logical description of agent systems but also a new approach to their implementation, thereby fulfilling the fundamental purpose of formal models in computer science – supporting software development by application model-driven development approach.

ACKNOWLEDGMENT

This work was supported by the project 030TUKE-4/2023 “Application of new principles in the education of IT specialists in the field of formal languages and compilers”, granted by Cultural and Education Grant Agency of the Slovak Ministry of Education.

REFERENCES

- [1] M. Duží, B. Jespersen, and P. Materna, *Procedural Semantics for Hyperintensional Logic: Foundations and Applications of Transparent Intensional Logic*. Dordrecht, The Netherlands: Springer, 2010, vol. 17.
- [2] P. Tichý, *The Foundations of Frege's Logic*. Berlin: De Gruyter, 1988.
- [3] L. T. F. Gamut, *Logic, Language, and Meaning. Intensional Logic and Logical Grammar*. Chicago: The University of Chicago Press, 1990.
- [4] P. Tichý, “Constructions,” *Philosophy of Science*, vol. 53, no. 4, pp. 514–534, 1986.
- [5] N. Ciprich, M. Duzi, and M. Košinár, “T il-script: Functional programming based on transparent intensional logic,” pp. 37–42, 01 2007.
- [6] N. Ciprich, M. Duzi, and M. Košinár, “The til-script language,” vol. 190, 01 2008, pp. 166–179.
- [7] M. Mensik, A. Albert, P. Rapant, and T. Michalovský, *Heuristics for Spatial Data Descriptions in a Multi-Agent System*, 2023, pp. 68–80.
- [8] T. Frydrych, O. Kohut, and M. Košinár, “Til in knowledge-based multi-agent systems,” pp. 31–40, 01 2008.
- [9] S. Novotný, M. Michalko, J. Perháč, V. Novitzká, and F. Jakab, “Formalization and modeling of communication within multi-agent systems based on transparent intensional logic,” *Symmetry*, vol. 14, no. 3, 2022.
- [10] J. Raclavský, “Explicace a dedukce: od jednoduché k rozvětvené teorii typů,” *Organon F*, no. 20, pp. 37–53, 2013.
- [11] P. Tichý, “Questions, answers, and logic,” *American Philosophical Quarterly*, vol. 15, no. 4, pp. 275–284, 1978.
- [12] M. Duží, M. Číhalová, and M. Menšík, “Communication in a multi-agent system; questions and answers,” in *13th SGEM GeoConference on Informatics, Geoinformatics And Remote Sensing*, 2013, pp. 11–22.
- [13] S. Novotný, W. Steingartner, J. Perháč, V. Novitzká, and Z. Bilanová, “Agent systems: From the markov property to the logical principle of persistence – til approach,” *Journal of Logic, Language and Information*, 2024, submitted.

²The symbols . and ? are used within the schematic designation of non-interrogative and interrogative messages.

Procedural Content Generation in Computer Graphics - A Survey

¹*Peter POPRÍK (1st year),*
Supervisor: ²Branislav MADOŠ

^{1,2}Dept. of Computers and Informatics, FEI TU of Košice, Slovak Republic

¹peter.poprik@tuke.sk, ²branislav.mados@tuke.sk

Abstract—The paper deals with the problematics of procedural content generation as a tool for rapid content generation while minimizing financial costs, time costs and human resources within different fields, including computer graphics in general, computer games, augmented and virtual reality, visualizations in landscape and garden architecture and other fields. The paper provides insight into the definition of procedural content generation as such and classifies its various categories and approaches related to content generation in the field of computer games. The paper also discusses challenges, which are present in balancing automation with control, and integrating machine learning generation methods to create non-repetitive and non-trivial content.

Keywords—procedural content generation, artificial intelligence, computer graphics

I. INTRODUCTION

Different perspectives on the field of procedural content generation (PCG) address different aspects of this issue, which is then reflected in the very definition of what PCG entails. One of the definitions states, that PCG can be defined as a collection of techniques, which enable creation of content algorithmically with limited or no human input [1]. Some authors include randomness as a defining characteristic of PCG. In [2] it's defined as the “programmatic generation of game content using a random or pseudo-random process that results in an unpredictable range of possible game play spaces” and [3] defines it as a “methodology for automatic generation of content of an entity, typically a game using algorithms or processes which can produce, due to their random nature, a very wide range of possible content related to the considered entity”. The author of [4] refers to PCG as the *automatic* creation of content and later in [5] concludes the PCG is not necessarily random, automatic or adaptive, which leaves the broad definition stated at the beginning of this section. On the one hand, this definition encompasses all of PCG, but on the other it opens questions, like for example, whether content created by a player within a game - using an in-game tool such as a character creator or map editor - can be considered procedurally generated.

Procedural content generation finds its greatest application in computer games, where it can be used to generate visual content like textures, 3D models, terrain, but also game levels, systems or rules. The main goal of PCG is to improve efficiency by reducing the time, cost, and human resources needed for content creation. This is especially important in the context of computer games, where large amounts of content

are required and development time is limited. Moreover, modern 3D games are expected to have graphically detailed, but also unique and diverse content, which proves challenging to human designers, as with increasing visual fidelity, repetitive content becomes more noticeable. While PCG can alleviate the resource demands, there remains the persistent problem of ensuring that generated content consistently matches the quality and style of human designers. Achieving playable and reliably error-free content also continues to pose a challenge.

This paper aims to review the current state of procedural content generation, first by describing the methods used to generate content in section II, followed by a description of the types of content that can be generated in section III.

II. METHODS OF PROCEDURAL CONTENT GENERATION

There is a variety of methods which can be used to generate content procedurally. A taxonomy based on the properties of methods is given in [1], [6], which classifies methods based on determinism, controllability and iterativity. Further based on the role of the PCG algorithm, methods are divided based on autonomy and adaptivity.

Search-based methods are based on the idea of searching a space for possible qualifying solutions to a problem - “finding” content that satisfies certain conditions. The core components of search-based methods are: a *search algorithm*, responsible for traversing the search space, a *content representation*, which defines the form of content, and an *evaluation function* which determines the quality of the content. A search-based approach is useful in creating content with strict constraints, like game rules or levels [7].

In the context of PCG, grammar-based methods are utilized for generating structured content like text, plants, buildings, levels by defining a production system. A grammar is a formal system that defines a set of rules for rewriting strings. One well-known class of grammars are L-systems [8], which are used to model the growth of plants.

Noise algorithms are used to generate content like textures or terrains. Noise functions are mathematical functions that generate random-like values, but are deterministic and continuous. The use of noise texturing can have multiple advantages. Firstly, a noise function is very compact compared to the size of texture images. Secondly, noise functions can be parameterized to create a variety of related textures. Thirdly, noise functions can create infinite non-repeating textures. Finally, a noise texture has no fixed resolution, so it can be used on any

surface without loss of detail [9]. For a more detailed overview of noise functions see [10].

A promising trend in PCG is the use of machine learning (ML) methods for generating content. Recent advances in deep neural networks like Generative Adversarial Networks (GAN) [11] have shown great potential in generating images. However, creating necessary game content presents problems because of the constraints that must be satisfied [6]. A comprehensive survey of PCG via ML can be found in [12].

III. TYPES OF GENERATED CONTENT

This section describes the types of content that can be generated procedurally, with methods used to generate them. In [1], [6], the authors classify the type of generated content used in computer games solely on whether it is necessary or optional. Necessary content is such that is required and must be correct for the game to function correctly, while optional content can be avoided or ignored. An example of necessary content can be a game level, which must be completable, while an example of optional content can be a collectible item, which is not required, but can provide an additional challenge. The taxonomy given by [13] provides a more detailed classification of content types, dividing them into 6 classes: game bits, game space, game systems, game scenarios, game design and derived content. This section will describe the methods used to generate textures, game levels and terrain.

A. Textures

Textures in computer graphics are images applied to 3D geometry to add realism without increasing scene complexity. They typically serve a purely visual role rather than altering geometry or functionality. A texture can define various mappings: *albedo* (base color without shadows or lighting), *metalness* (reflectiveness), *roughness* (light scattering), and *normal* (surface normals for added depth).

Traditional, non-procedural textures are applied to 3D models using a technique called UV mapping, where each vertex of the 3D surface corresponds to a point on the 2D texture. Essentially this means that the 3D model is unwrapped into a 2D plane and then the texture is applied. Unfortunately, this method may introduce problems like stretching, or seams.

A typical method for generating textures is the use of noise functions such as Perlin noise[14]. While a noise texture can be mapped to a 3D model using UV mapping, this might still introduce the inherent problems of UV mapping. An alternative approach is to use *solid texturing*, which avoids these problems by defining a texture directly in 3D space. In this case, any point $P(x, y, z)$ can be directly assigned a color from the texture $T(x, y, z)$. One can think of this as carving the object out of a solid block of texture as opposed to wrapping it around the object. This approach is especially useful for materials like marble, wood, or clouds, which are intrinsically 3D [15]. In [16] a lazy solid texturing is presented, which synthesizes only required parts of the texture volume, with the goal of reducing memory usage and computation time.

Another approach is cellular texturing, which is based on randomly distributed *feature points* in a space. Any location x has a feature point closest to it than any other feature point. The boundaries where the closest feature point changes divide the space into cells (see Figure 1). The resulting patterns often resemble natural textures like scales, stone or

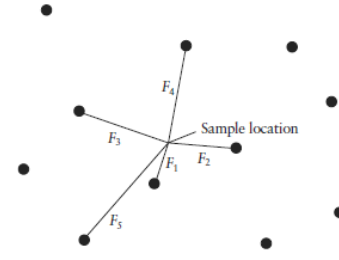


Fig. 1. Visualization of closest feature points in cellular texturing [9].

water [9]. One well-known example of both solid and cellular texturing is presented by [17], which complements Perlin noise. This approach divides space into a grid of uniformly spaced cubes and each cube can be represented by its integer coordinates, which allows assigning any point in space to a cube by flooring its coordinates. A different cellular texturing method is presented in [18], which allows texturing complex architectural models by adapting generated patterns to different features of the model.

B. Game levels and maps

A Level (or map) in a game is the space which a player traverses while experiencing and interacting with its content. Levels can be linear or non-linear. Unlike purely graphical content like textures, levels are required to adhere to game rules and constraints. Most games feature some sort of level or map, which are a necessary content type. The main condition is that the level must be completable, and certain conditions, depending on the design, must be achievable by the player.

An overview of methods used for generating game levels is provided by [19], in which the authors describe space partitioning. A space partitioning method like Binary Space Partitioning (BSP) recursively divides a space into two subsets, arranging them into a *space-partitioning tree*. Another method is the use of agent-based dungeon generation, where agents create spaces by carving out rooms and corridors. This results in more natural, looking dungeons, as opposed to the space partitioning method, but is also more unpredictable and harder to control. Cellular automata (CA) can also be used to generate levels. CA are a grid of cells, where each cell can be in a finite number of states. The cells change their state based on the states of their neighbors [20]. An approach for generating a complete 2D cave map is presented in [21], where cells have two possible states: floor and rock. There are four parameters: r - initial percentage of rock cells, n - number of CA iterations, T - neighborhood value threshold that defines a rock, and M - Moore neighborhood size.

The grid is first initialized with floor cells, then based on r the floor cells are replaced with rock cells. The CA is then iterated n times, where the state of each cell is set to rock if the number of rock cells in its Moore neighborhood is greater than or equal to T , otherwise it is set to floor. After the CA is finished, cells with at least one neighboring floor cell are designated as wall cells (see Figure 2).

A method proposed by [22] uses Generative Adversarial Networks (GAN) [11] to generate levels for the game Super Mario Bros. The GAN is trained on images of an existing Super Mario Level of a standard size of 28 tiles wide and 14 tiles high. Input images were created by sliding a window of this size over a single level one tile at a time. A Mario level

is represented as a 2D array of integers, where each integer represents a tile type. The GAN is trained with the WGAN algorithm [23]. After training, the output of the generator is converted to a 2D array of integers, which can be decoded to create a level. Testing has shown that the basic structure of a level can be generated, which are not just replications of the training data. A limitation of this method is visual artifacts, which are sometimes present in the generated levels.

Another method using ML is proposed by [24]. The authors introduce a PCG framework called Generative Playing Networks (GPN), which is set up as a competition between two networks. The first one is an agent playing the game and modeling the probability of success at every game-state. The second network is a generator, which learns the distribution of game-states and generates challenging levels for the agent. This is similar to the Generative Adversarial Networks (GAN) [11], with the difference that GPN defines a symbiotic relationship between the two networks. The advantage of this method is that it doesn't require any existing data (levels) for training, neither does it require any domain knowledge about the game, on the other hand, it is computationally expensive. Recent approaches [25] also utilize reinforcement learning to automatically balance competitive game levels, improving player experience with simulation-driven adjustments.

C. Terrain

A terrain or landscape refers to the surface of a game world, which can have both a visual and functional role. In a linear game, terrain can serve as a backdrop, while open-world games allow terrain to be traversed and otherwise interacted with. Similarly to textures, terrain can be represented as a 2D matrix of real numbers, where the width and height of the matrix represent the x and y dimensions of the surface, while the individual values represent the height of the terrain at that point. This representation is called a *heightmap*, which can be represented as a function $h : \mathbb{R}^2 \rightarrow \mathbb{R}$, where $h(x, y)$ is the elevation of the terrain at point (x, y) . One limitation of this method is its inability to represent overhangs or caves, as each (x, y) point can only have one height value. This can be avoided by instead using a 3D grid of values - a voxel grid, which allows these features to be represented, but at the cost of increased storage [6]. Volumetric models like this can be defined by a function $\mu : \mathbb{R}^3 \rightarrow M$, where $M \subset \mathbb{N}$ is the set of material indices. In a simple case, M can be a set of two values, $M = \{0, 1\}$, where 0 represents empty space and 1 represents solid material [26].

Fractal subdivision methods like the midpoint displacement algorithm [27], [28] or the diamond square algorithm [29] can be used to generate terrain. The midpoint displacement algorithm begins with a line, which it repeatedly divides and moves the midpoints of the resulting segments by a random value. The diamond square algorithm extends the concept to a 2D grid with two steps: the diamond step, where the midpoint of a square is set to the average of its corners plus a random value, and the square step, where the four cells in between corners are set to the average of its surrounding corners plus a random value (see Figure 3).

Fractal and noise-based methods are relatively simple and fast, but not very controllable. For a greater degree of control over the generated terrain, an agent-based approach can be used. One example is [30], where six types of agents are used

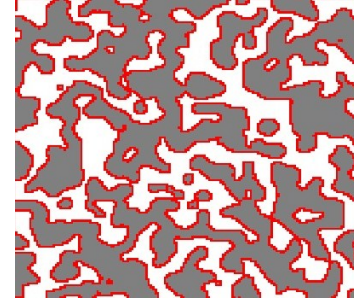


Fig. 2. CA generated map by [21]. Grey cells are rock, white cells are floor, red cells are walls. Parameter values: $r = 50\%$, $n = 4$, $T = 13$, $M = 2$.

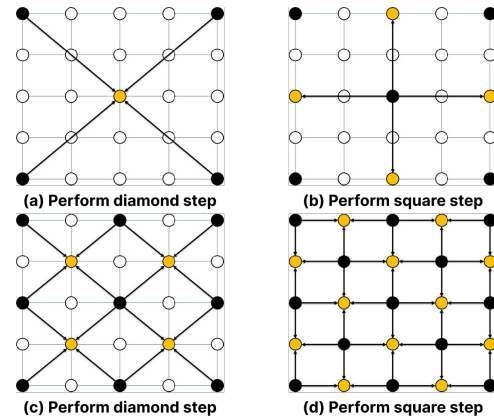


Fig. 3. Diamond square algorithm with 2 repetitions. (a) and (c) show the diamond step, (b) and (d) show the square step. [6]

to create different features of the terrain. First, the coastline agents draw the outline of the landscape. Next, the smoothing agents alter the shape to remove rapid elevation changes by averaging the height of neighboring cells. Beach agents then smooth the transition between land and water. Mountain and hill agents create the main features of the terrain and finally, the rivers agents carve out the riverbeds. The agents are controlled by a set of parameters, which can be used to control the shape of the terrain.

A method proposed by [31] introduces a terrain generator using example-based synthesis with Conditional Generative Adversarial Networks (CGAN) [32]. The generator is trained on a dataset of terrain examples and the user provides a sketch of the desired features of the terrain. The generator then outputs a realistic terrain in a matter of milliseconds.

IV. CONCLUSION

The main goal of PCG is to provide a time and cost-efficient way to create content. Noise and fractal-based methods provide an efficient way to generate content but lack control. Agent-based and search-based methods provide a greater degree of control but are more complex and computationally expensive. There is currently active research and great progress in machine learning in general and in PCG, with deep learning methods like GANs showing potential in generating content. However, applying these methods to PCG presents a different challenge, like the lack of publicly available training data and the requirement of strict constraints. Data scarcity could be addressed by self-supervised learning, where the model requires no training examples. Expanding the generation methods of non-visual content like audio, dialogue and narrative is also a promising direction. Large Language Models (LLMs) could

inherently generate text-based content, and could also provide text to content generation, which would provide an intuitive alternative for creating content with specific attributes without parametrization or exhaustive content space searching.

ACKNOWLEDGMENT

This work was supported by KEGA Agency of the Ministry of Education, Science, Research, and Sport of the Slovak Republic under Grant No. 015TUKE-4/2024 Modern Methods and Education Forms in the Cybersecurity Education.

REFERENCES

- [1] J. Togelius, N. Shaker, and M. J. Nelson, "Introduction," in *Procedural Content Generation in Games*, N. Shaker, J. Togelius, and M. J. Nelson, Eds. Cham: Springer International Publishing, 2016, pp. 1–15. [Online]. Available: https://doi.org/10.1007/978-3-319-42716-4_1
- [2] A. Doull, "The Death of the Level Designer: Procedural Content Generation in Games - Part One," Jan. 2008. [Online]. Available: <https://roguelikedev.blogspot.com/2008/01/death-of-level-designer-procedural.html>
- [3] A. Amato, "Procedural Content Generation in the Game Industry," in *Game Dynamics: Best Practices in Procedural and Dynamic Game Content Generation*, O. Korn and N. Lee, Eds. Cham: Springer International Publishing, 2017, pp. 15–25. [Online]. Available: https://doi.org/10.1007/978-3-319-53088-8_2
- [4] J. Togelius, G. N. Yannakakis, K. O. Stanley, and C. Browne, "Search-Based Procedural Content Generation," in *Applications of Evolutionary Computation*, C. Di Chio, S. Cagnoni, C. Cotta, M. Ebner, A. Ekárt, A. I. Esparcia-Alcazar, C.-K. Goh, J. J. Merelo, F. Neri, M. Preuß, J. Togelius, and G. N. Yannakakis, Eds. Berlin, Heidelberg: Springer, 2010, pp. 141–150.
- [5] J. Togelius, E. Kastbjerg, D. Schedl, and G. N. Yannakakis, "What is procedural content generation? Mario on the borderline," in *Proceedings of the 2nd International Workshop on Procedural Content Generation in Games*, ser. PCGames '11. New York, NY, USA: Association for Computing Machinery, Jun. 2011, pp. 1–6. [Online]. Available: <https://doi.org/10.1145/2000919.2000922>
- [6] G. N. Yannakakis and J. Togelius, "Generating Content," in *Artificial Intelligence and Games*, G. N. Yannakakis and J. Togelius, Eds. Cham: Springer International Publishing, 2018, pp. 151–202. [Online]. Available: https://doi.org/10.1007/978-3-319-63519-4_4
- [7] J. Togelius, G. N. Yannakakis, K. O. Stanley, and C. Browne, "Search-Based Procedural Content Generation: A Taxonomy and Survey," *IEEE Transactions on Computational Intelligence and AI in Games*, vol. 3, no. 3, pp. 172–186, Sep. 2011. [Online]. Available: <https://doi.org/10.1109/TCIAIG.2011.2148116>
- [8] P. Prusinkiewicz, "Graphical applications of L-systems," in *Proceedings on Graphics Interface '86/Vision Interface '86*. CAN: Canadian Information Processing Society, Aug. 1986, pp. 247–253.
- [9] D. S. Ebert, Ed., *Texturing & modeling: a procedural approach*, 3rd ed. Amsterdam ; Boston: Academic Press, 2003.
- [10] A. Lagae, S. Lefebvre, R. Cook, T. DeRose, G. Drettakis, D. Ebert, J. Lewis, K. Perlin, and M. Zwicker, "A Survey of Procedural Noise Functions," *Computer Graphics Forum*, vol. 29, no. 8, pp. 2579–2600, 2010. [Online]. Available: <https://doi.org/10.1111/j.1467-8659.2010.01827.x>
- [11] I. Goodfellow, J. Pouget-Abadie, M. Mirza, B. Xu, D. Warde-Farley, S. Ozair, A. Courville, and Y. Bengio, "Generative Adversarial Nets," in *Advances in Neural Information Processing Systems*, vol. 27. Curran Associates, Inc., 2014. [Online]. Available: https://proceedings.neurips.cc/paper_files/paper/2014/hash/5ca3e9b122f61f8f06494c97b1afccf3-Abstract.html
- [12] A. Summerville, S. Snodgrass, M. Guzdial, C. Holmgård, A. K. Hoover, A. Isaksen, A. Nealen, and J. Togelius, "Procedural Content Generation via Machine Learning (PCGML)," *IEEE Transactions on Games*, vol. 10, no. 3, pp. 257–270, Sep. 2018. [Online]. Available: <https://doi.org/10.1109/TG.2018.2846639>
- [13] M. Hendriks, S. Meijer, J. Van Der Velden, and A. Iosup, "Procedural content generation for games: A survey," *ACM Trans. Multimedia Comput. Commun. Appl.*, vol. 9, no. 1, pp. 1:1–1:22, Feb. 2013. [Online]. Available: <https://doi.org/10.1145/2422956.2422957>
- [14] K. Perlin, "An image synthesizer," *SIGGRAPH Comput. Graph.*, vol. 19, no. 3, pp. 287–296, Jul. 1985. [Online]. Available: <https://doi.org/10.1145/325165.325247>
- [15] J. M. Dischler and D. Ghazanfarpour, "A survey of 3D texturing," *Computers & Graphics*, vol. 25, no. 1, pp. 135–151, Feb. 2001. [Online]. Available: [https://doi.org/10.1016/S0097-8493\(00\)00113-8](https://doi.org/10.1016/S0097-8493(00)00113-8)
- [16] Y. Dong, S. Lefebvre, X. Tong, and G. Drettakis, "Lazy Solid Texture Synthesis," *Computer Graphics Forum*, vol. 27, no. 4, pp. 1165–1174, 2008. [Online]. Available: <https://doi.org/10.1111/j.1467-8659.2008.01254.x>
- [17] S. Worley, "A cellular texture basis function," in *Proceedings of the 23rd annual conference on Computer graphics and interactive techniques*, ser. SIGGRAPH '96. New York, NY, USA: Association for Computing Machinery, Aug. 1996, pp. 291–294. [Online]. Available: <https://doi.org/10.1145/237170.237267>
- [18] J. Legakis, J. Dorsey, and S. Gortler, "Feature-based cellular texturing for architectural models," in *Proceedings of the 28th annual conference on Computer graphics and interactive techniques*, ser. SIGGRAPH '01. New York, NY, USA: Association for Computing Machinery, Aug. 2001, pp. 309–316. [Online]. Available: <https://doi.org/10.1145/383259.383293>
- [19] N. Shaker, A. Liapis, J. Togelius, R. Lopes, and R. Bidarra, "Constructive generation methods for dungeons and levels," in *Procedural Content Generation in Games*, N. Shaker, J. Togelius, and M. J. Nelson, Eds. Cham: Springer International Publishing, 2016, pp. 31–55. [Online]. Available: https://doi.org/10.1007/978-3-319-42716-4_3
- [20] J. Kari, "Theory of cellular automata: A survey," *Theoretical Computer Science*, vol. 334, no. 1, pp. 3–33, Apr. 2005. [Online]. Available: <https://doi.org/10.1016/j.tcs.2004.11.021>
- [21] L. Johnson, G. N. Yannakakis, and J. Togelius, "Cellular automata for real-time generation of infinite cave levels," in *Proceedings of the 2010 Workshop on Procedural Content Generation in Games*, ser. PCGames '10. New York, NY, USA: Association for Computing Machinery, Jun. 2010, pp. 1–4. [Online]. Available: <https://doi.org/10.1145/1814256.1814266>
- [22] V. Volz, J. Schrum, J. Liu, S. M. Lucas, A. Smith, and S. Risi, "Evolving mario levels in the latent space of a deep convolutional generative adversarial network," in *Proceedings of the Genetic and Evolutionary Computation Conference*, ser. GECCO '18. New York, NY, USA: Association for Computing Machinery, Jul. 2018, pp. 221–228. [Online]. Available: <https://doi.org/10.1145/3205455.3205517>
- [23] M. Arjovsky, S. Chintala, and L. Bottou, "Wasserstein Generative Adversarial Networks," in *Proceedings of the 34th International Conference on Machine Learning*. PMLR, Jul. 2017, pp. 214–223. [Online]. Available: <https://proceedings.mlr.press/v70/arjovsky17a.html>
- [24] P. Bontrager and J. Togelius, "Learning to Generate Levels From Nothing," in *2021 IEEE Conference on Games (CoG)*, Aug. 2021, pp. 1–8. [Online]. Available: <https://doi.org/10.1109/CoG52621.2021.9619131>
- [25] F. Rupp, M. Eberhardinger, and K. Eckert, "Simulation-Driven Balancing of Competitive Game Levels With Reinforcement Learning," *IEEE Transactions on Games*, vol. 16, no. 4, pp. 903–913, Dec. 2024, conference Name: IEEE Transactions on Games. [Online]. Available: <https://doi.org/10.1109/TG.2024.3399536>
- [26] E. Galin, E. Guérin, A. Peytavie, G. Cordonnier, M.-P. Cani, B. Benes, and J. Gain, "A Review of Digital Terrain Modeling," *Computer Graphics Forum*, vol. 38, no. 2, pp. 553–577, 2019. [Online]. Available: <https://doi.org/10.1111/cgf.13657>
- [27] F. Belhadj and P. Audibert, "Modeling landscapes with ridges and rivers: bottom up approach," in *Proceedings of the 3rd international conference on Computer graphics and interactive techniques in Australasia and South East Asia*, ser. GRAPHITE '05. New York, NY, USA: Association for Computing Machinery, Nov. 2005, pp. 447–450. [Online]. Available: <https://doi.org/10.1145/1101389.1101479>
- [28] F. Belhadj, "Terrain modeling: a constrained fractal model," in *Proceedings of the 5th international conference on Computer graphics, virtual reality, visualisation and interaction in Africa*, ser. AFRIGRAPH '07. New York, NY, USA: Association for Computing Machinery, Oct. 2007, pp. 197–204. [Online]. Available: <https://doi.org/10.1145/1294685.1294717>
- [29] A. Fournier, D. Fussell, and L. Carpenter, "Computer rendering of stochastic models," *Commun. ACM*, vol. 25, no. 6, pp. 371–384, Jun. 1982. [Online]. Available: <https://dl.acm.org/doi/10.1145/358523.358553>
- [30] J. Doran and I. Parberry, "Controlled Procedural Terrain Generation Using Software Agents," *IEEE Transactions on Computational Intelligence and AI in Games*, vol. 2, no. 2, pp. 111–119, Jun. 2010. [Online]. Available: <https://ieeexplore.ieee.org/abstract/document/5454273>
- [31] E. Guérin, J. Digne, E. Galin, A. Peytavie, C. Wolf, B. Benes, and B. Martinez, "Interactive Example-Based Terrain Authoring with Conditional Generative Adversarial Networks," *ACM Transactions on Graphics*, vol. 36, no. 6, 2017, publisher: Association for Computing Machinery. [Online]. Available: <https://hal.science/hal-01583706>
- [32] M. Mirza and S. Osindero, "Conditional Generative Adversarial Nets," Nov. 2014. [Online]. Available: <http://arxiv.org/abs/1411.1784>

Photovoltaic Systems and Their Influence on Power System Management

¹Kamil ŠEVC (*1st year*)
Supervisor: ²Marek PAVLÍK

^{1,2} Dept. of Electric Power Engineering, FEI TU of Košice, Slovak Republic

¹kamil.sevc@tuke.sk, ²marek.pavlik@tuke.sk

Abstract - The increasing integration of renewable energy sources has become a pivotal subject across various sectors, including energy, construction, economics, and digitalization. A comprehensive analysis of photovoltaic (PV) systems and their influence on electricity generation is essential, given the contemporary relevance of this topic and the numerous unresolved challenges it presents. This review critically examines renewable energy sources, evaluates the current legislative and regulatory framework governing electricity system management in response to PV integration, and highlights key areas requiring further investigation. The article concludes with a forward-looking perspective on the evolving role of photovoltaics in modern power systems.

Keywords - renewable energy sources, photovoltaic systems, distribution networks, electricity generation management.

I. INTRODUCTION

Renewable energy sources (RES) refer to naturally replenishing energy flows that sustain themselves during utilization. These energy reserves occur naturally near the Earth's surface and are replenished at a rate equal to or faster than their consumption. Their potential for extraction theoretically extends for billions of years, essentially as long as the Sun continues to emit energy. RES primarily include solar radiation and its derivatives—wind and hydropower—alongside tidal energy, geothermal energy, and biomass. While solar and wind power remain the most widely deployed renewable technologies, these sources often face criticism regarding their intermittency and aesthetic impact. Nevertheless, the global market for renewable energy has demonstrated substantial growth in recent years, driven by technological advancements and increasing environmental awareness.

Renewable energy is a topic of extensive discourse from energy, ecological, and economic perspectives. As traditional fossil fuel reserves continue to diminish, the imperative to develop renewable energy sources has become increasingly urgent. The key challenge lies in ensuring efficient electricity production while maintaining environmental sustainability. Beyond nuclear power, energy generation from renewable sources fulfills these criteria, providing a viable alternative for long-term energy security and emissions reduction.

A comprehensive analysis of the global renewable energy landscape is essential. The International Energy Agency (IEA) continuously monitors trends in the energy sector and projects

future developments. According to the *World Energy Outlook*, the global energy market is expected to undergo significant transformations by 2040. The adoption of the Paris Agreement on climate change further solidifies the global economic shift towards energy sources that facilitate CO₂ emissions reduction. This trend has been evident for several years, marked by declining investments in oil and natural gas and a concurrent *increase in investments in renewable energy sources*. Energy demand is projected to continue rising, although the contribution of various energy sources to overall production will shift significantly. The increasing share of renewable energy sources is expected to drive profitability by 2040, even in the absence of state subsidies, *with wind and solar energy experiencing the most substantial growth*. However, this transition is unlikely to result in full independence from fossil fuels, as oil and natural gas are expected to retain a dominant position, in contrast to the continued decline of coal [1].

II. ANALYSIS

Renewable energy sources harness naturally occurring phenomena that are continuously replenished, ensuring their long-term availability. These sources include solar, wind, hydro, biomass, and geothermal energy. The primary driver for transitioning to renewables is the finite nature and progressive depletion of fossil fuel reserves. Additionally, several other factors accelerate this shift, including rising environmental pollution, the decentralization of energy production, the equitable distribution of natural resources, and the high costs associated with energy imports [2].

A. General Requirements for Resource Connection

Currently, the integration of new electricity generation sources into distribution networks is primarily centered on renewable energy, particularly household photovoltaic (PV) power plants. As the cost of photovoltaic systems continues to decline, their accessibility is increasing, necessitating additional considerations from distribution network operators. It is essential to incorporate these developments into legislation to establish clear regulations and standardized procedures for connecting small-scale energy sources alongside household electrical installations.

The growing number of decentralized energy sources, such as photovoltaic systems (PVS), is significantly altering the operational and management dynamics of electricity networks.

This shift demands heightened attention, as it is crucial to assess the current state of electrical infrastructure and proactively define, expand, or restrict conditions for the seamless integration of additional energy systems into existing networks.

B. Specific connection requirements

The technical documentation issued by regional distribution system operators in the Slovak Republic governs the management, operation, and development of the distribution network within their respective territories. These documents outline specific conditions and key electrical indicators that must be adhered to within prescribed limits to determine the appropriate placement and connection of energy sources. Compliance with these regulations is essential to assess and mitigate potential feedback effects on the distribution system. In general, the voltage increase resulting from the integration of new energy sources must not exceed 3% at the connection point for low-voltage (LV) systems under worst-case conditions when compared to baseline voltage levels in the absence of these sources [3].

It is necessary to minimize the feedback effects of the sources on the distribution system in which the source is connected, so that several generators are not switched on simultaneously at one point of connection. The solution is available, for example, in the time grading of individual switching, which is dependent on induced voltage changes at the maximum permissible generator output of at least 1.5 minutes. Another possibility, when the apparent power of the generator is half the permissible value, a gap of 12 seconds is sufficient. An important note is that with a very low frequency of switching, for example once a day, the distribution system operator can allow larger changes in the switching voltage, if the conditions in the network allow it [3].

C. Power quality

Photovoltaic power plants must comply with the requirements of the network to which they are connected, especially concerning power quality issues. The factors that affect the disturbance in photovoltaic energy are the size of the photovoltaic plant, connection voltage, short-circuit power in the interconnection and the degree of penetration of the system. Photovoltaic generation shares the characteristics of other distributed generation units. Distributed generation means a change in the way distribution networks are operated since introduces the possibility of bidirectional power flows in networks designed for unidirectional flows. Besides, there may be a significant impact on transmission losses, network reliability and voltage profiles depending on the penetration level, size and location [4].

Two key challenges that may constrain the penetration of distributed generation are its contribution to short-circuit current—affecting circuit breakers, albeit with minimal impact on photovoltaic (PV) systems—and its influence on voltage fluctuations (EPRI). Additionally, the impact on overall network power quality must be considered. Any generation unit, by virtue of its connection to the grid, introduces some degree of influence on network parameters. This impact is determined by several factors, including the technological characteristics of the system, the nature of the primary energy source, installed capacity, nominal network voltage, and short-circuit power at the point of interconnection. In the case of photovoltaic power plants, the primary power quality issues are illustrated in Fig. 1 [4].

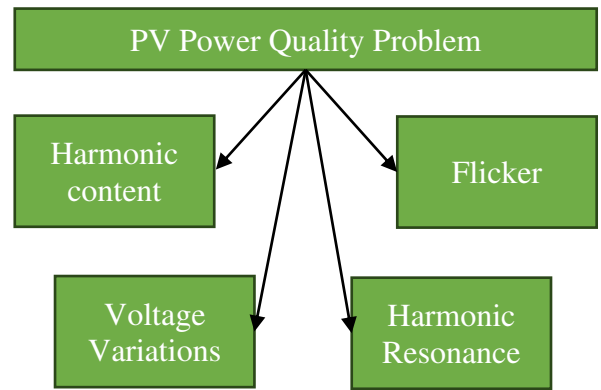


Fig. 1. Main power quality problems

D. Voltage stability

Voltage stability is a critical factor influencing the overall performance of power systems. It refers to the system's ability to maintain acceptable voltage levels across all buses under both normal operating conditions and contingency scenarios. When a disturbance or an increase in load results in a progressive and uncontrollable voltage drop, the system enters a state of voltage instability, which can compromise its reliability and operational integrity [5].

From a voltage stability analysis perspective, the relationship between load and voltage is a critical area of study. In this context, P-V curves, also referred to as 'nose' curves, are widely employed in analytical assessments. As depicted in Fig. 2, the nose point represents the critical operating condition, delineating the boundary between stable and unstable operation. When load demand surpasses this threshold, power control becomes unstable. Additionally, points in the lower segment of the curve exhibit inverse P-V sensitivity, wherein an increase in load power results in a corresponding rise in voltage. The distance, measured in MW, between the current operating point (P_0) and the critical point is defined as the voltage stability margin [5].

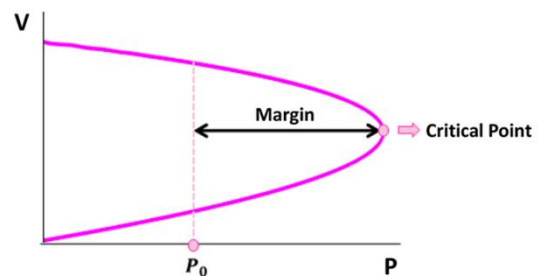


Fig. 2. PV characteristics [5]

E. Production and consumption correlation

The increasing adoption of micro-installations, particularly photovoltaic systems, driven by declining costs, appears inevitable. Consequently, various technical challenges are expected to arise, with voltage impact being among the most critical. This issue primarily stems from power flows directed from the connection points of these systems toward medium-voltage/low-voltage (MV/LV) substations. The underlying cause is the weak correlation between the power generated by these systems and actual demand. Empirical data indicate that peak solar generation often does not coincide with periods of maximum electricity consumption. This mismatch is problematic, as it leads to reverse power flows toward MV/LV transformers, thereby exacerbating the "voltage boosting" effect—an inverse phenomenon of voltage drop [6].

F. Three-phase unbalance

Modern power systems face numerous challenges, including weak voltage and frequency regulation, significant fluctuations in source-load power, and suboptimal power quality indices in distribution networks. Key power quality indicators include harmonics, voltage deviation, and three-phase unbalance. Three-phase unbalance occurs when the amplitude of three-phase voltage or current differs or when the phase angles deviate from the ideal 120° separation. This imbalance poses several risks to the distribution system, primarily in the following six areas:

1. Increased power loss in distribution transformers, leading to overheating or potential transformer failure;
2. Higher line losses, negatively impacting the safety and economic efficiency of network operations;
3. Reduced service life of household appliances, resulting in a higher likelihood of electrical malfunctions;
4. Elevated loads on high-capacity lines, escalating security risks;
5. Deterioration of communication equipment stability, affecting network reliability;
6. Potential misoperation of relay protection and automatic protection systems, compromising grid security.

Addressing three-phase unbalance in distribution systems is critical to ensuring both economic efficiency and high-quality power supply. Therefore, urgent and effective mitigation strategies must be implemented to enhance system reliability and stability. [7]

Various strategies have been proposed to address the issue of three-phase unbalance in power distribution systems, which can be categorized into three main approaches: "source," "load," and "network." From a "source" perspective, mitigation measures include optimizing the allocation of distributed generation, adjusting the reactive power of photovoltaic inverters, and integrating active power regulation through energy storage systems. These approaches enhance grid stability and improve overall power quality [7],[8].

G. Electricity Production Statistics in Slovakia

In 2023, electricity production in Slovakia experienced a significant increase compared to 2022, reaching a total output of 29,961 GWh. The distribution of energy production across various sources is presented in Table 1 [9].

Tab. 1. Structure of energy production in SVK 2023

Type	Value [GWh]	Percentage
PV power plants	594	2,0%
Hydroelectric power plants	5 094	17,0%
Fossil fuels	4 409	14,7%
Nuclear power plants	18 344	61,2%
Other renewable sources	1 408	4,7%
Others	113	0,4%

It is important to highlight the decline in electricity generation from renewable energy sources in 2023 compared to 2022, with photovoltaic (PV) production decreasing to 35 GWh (-5,6%). This reduction reflects the economic strategies adopted by electricity market operators, the technical condition of power generation facilities, as well as climatic, hydrological, and other external factors. A graphical representation of the energy production structure is provided in Figure 3: [9]

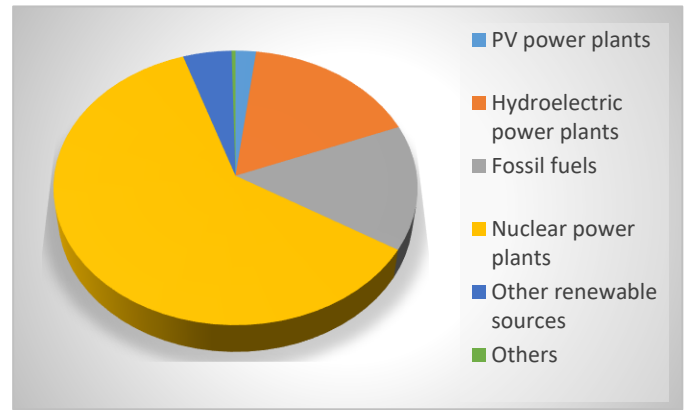


Fig. 3. Structure of energy production in SVK 2023

H. Role of Communication Technology within PV Systems

In power systems, communication technology plays a critical role in ensuring efficient operation, management, and maintenance. Consequently, research in system communication technology is essential for the continuous enhancement and optimization of power system infrastructure [10].

Network communication technology is a crucial component of system communication in power networks, facilitating real-time information exchange and data transmission between power infrastructure components. Currently, the primary network communication technologies employed in power systems include Ethernet, Local Area Networks (LAN), and Wide Area Networks (WAN). Ethernet, a LAN-based communication protocol, enables high-speed data transfer between power devices within a localized setting. While LANs facilitate communication within a restricted geographical area, WANs provide broader coverage, allowing for remote data transmission between power system components [10],[11],[12].

I. Influence of Weather Conditions on Photovoltaic System Management

As decentralized generation systems and electrical loads, such as heat pumps and electric vehicles, continue to expand, the frequency of critical grid states is expected to increase. Various strategies have been proposed to address these challenges. The prevailing approach involves conventional grid expansion, relying on long-term planning and extrapolations based on projected grid growth. However, if actual grid development deviates from forecasts, this expansion strategy may prove insufficient. Consequently, conventional grid planning lacks the flexibility to accommodate unforeseen developments, such as the integration of new generation systems. This limitation is particularly critical given the difficulty in predicting the long-term evolution of local grid loads. A notable example is the ongoing electrification of the heating and mobility sectors, where the full extent of technological advancements and their subsequent impact on low- and medium-voltage grids remains uncertain [13].

Alternative approaches to conventional grid expansion include various grid congestion management strategies, which leverage the flexibility of prosumer power systems to respond to critical grid conditions. One such approach is the implementation of a market-based mechanism known as the local flexibility market, designed to optimize energy distribution and enhance grid resilience [13].

III. FUTURE POSSIBILITIES

The increasing integration of renewable energy sources into electricity generation presents a range of new challenges. Accurate short-term forecasting is essential for effective energy management, including storage, sales, and distribution. However, inaccuracies in predictions can result in substantial financial losses, underscoring the need for advanced forecasting methodologies [14]. The necessity of aligning energy production with real-time demand, already a critical aspect of modern power systems, becomes increasingly complex with the growing prominence of wind and solar energy [15],[16]. The development of robust forecasting methods for electricity production from these sources, considering weather variability, is essential. Additionally, analyzing production capacity across different time intervals plays a crucial role in optimizing energy management. Continuous technological advancements aim to improve predictive accuracy, ensuring both the sustainability and reliability of grid operations in the rapidly evolving renewable energy landscape [17].

Solar photovoltaic (PV) energy is expected to play a pivotal role in future electricity generation. To ensure the safety, reliability, and economic viability of its increasing share in the energy mix, accurate forecasting of PV power generation is essential. However, the inherent variability of solar energy presents challenges such as voltage fluctuations, power factor instability, and grid reliability concerns. The growing prominence of solar energy highlights the need for a comprehensive understanding of its temporal and spatial dynamics, particularly in scenarios where weather data is unavailable [17].

The future of solar energy holds immense potential, driven by continuous technological advancements, evolving policy frameworks, and emerging global trends. The findings presented in this research provide a robust foundation for stakeholders, policymakers, and grid operators to navigate the dynamic energy landscape. In conclusion, this study highlights the long-term viability of solar energy as a reliable and sustainable contributor to the electrical power system. Extensive research has identified key patterns in solar generation, offering a pathway toward a cleaner and more environmentally sustainable energy future. As the transition to renewable energy accelerates, these insights enable informed decision-making, ensuring that the full potential of solar energy is effectively harnessed to support global energy needs [17].

IV. CONCLUSION

In conclusion, this article underscores the critical importance of renewable energy sources, extending beyond photovoltaic systems alone. These energy sources represent a carbon-free future for electricity generation - an increasingly vital necessity in light of environmental concerns, rather than merely a contemporary trend. More specifically, the study has examined the integration of photovoltaic systems within the management of distribution networks and the broader electricity transmission system. Given the rapid expansion of photovoltaic installations in households - driven by increasing affordability and their integration into ON-GRID systems—it is essential to adapt connection requirements, enhance management strategies, and refine maintenance protocols while

ensuring effective long-term planning for distribution system development.

ACKNOWLEDGMENT

This work was supported by the Ministry of Education, Science, Research and Sport of the Slovak Republic and the Slovak Academy of Sciences under the contract no. VEGA 1/0627/24.

REFERENCES

- [1] N. Hlavová, "Obnoviteľné zdroje energie v čínskej ekonomike", Ekonomická univerzita v Bratislave, 2016, p. 444-445.
- [2] M. Pavlík, "Obnoviteľné zdroje a iné netradičné zdroje energie", Technická univerzita Košice, 2019, p. 7
- [3] E. Beňa, et al. "Analýza pomerov pripojiteľnosti 1-fázových a 3-fázových zdrojov v NN sústave", Technická univerzita v Košiciach, Fakulta elektrotechniky a informatiky- Katedra elektroenergetiky, 2023, p. 6
- [4] Luis Hernández-Callejo, Sara Gallardo-Saavedra, Víctor Alonso-Gómez, "A review of photovoltaic systems: Design, operation and maintenance", Solar Energy, Volume 188, 2019, pp. 426-440,
- [5] Sinder Rebecca Laginestra, Lessa Assis, Tatiana Mariano, Taranto Glauco Nery, "Impact of photovoltaic systems on voltage stability in islanded distribution networks", Journal of Engineering-JOE, 2019, p. 5023-5027
- [6] P. Pijarski, S. Adamek, R. Jedrychowski, K. Sereja, "Monitoring the impact of prosumer micro installations on the electrical parameters of low-voltage network systems", PRZEGLAD ELEKTROTECHNICZNY, 2019, p. 59-62
- [7] Min Wang, Huilin Wang, Fanglin Zuo, Jie Zou, Yuan Chen, Zixuan Yu, "A Consideration of the Single-Phase Photovoltaic and Energy Storage Joint Regulation of a Three-Phase Unbalanced Control Strategy in a Power Distribution System", Energies 2023, (16 4817), 2023, p. 1
- [8] C. Yang, "Safety and Economic Evaluation of Three-Phase Unbalance on Low-Voltage Distribution Network", Master's Thesis, University of Jinan, China, 2019
- [9] Ministry of Economy of the Slovak Republic, "POSÚDENIE PRIMERANOSTI ZDROJOV ES SR ZA ROK 2023", Bratislava, 2024
- [10] S. Zhan, S. Yan, Z. Ding and D. Zhuang, "Application of Key Measurement and Control Technologies for Distributed Photovoltaic Grid Connected Systems", 2024 2nd International Conference on Mechatronics, IoT and Industrial Informatics (ICMIII), Melbourne, Australia, 2024, pp. 926-931
- [11] A. M. Mahfuz-Ur-Rahman, Md. Rabiul Islam, Kashem M. Muttaqi, Md. Ashib Rahman and Danny Sutanto, "An Advanced Modulation Technique for Transformerless Grid Connected Inverter Circuits Used in Solar Photovoltaic Systems", IEEE Trans. Ind. Electron, vol. 70, no. 4, pp. 3878-3887, 2023
- [12] Abdessami Soyed, Ameni Kadri, Othman Hasnaoui and Faouzi Bacha, "Direct Power and Voltage Oriented Control Strategies of Grid-Connected Wind Energy Conversion System Based on Permanent Magnet Synchronous Generator", Cybern. Syst, vol. 53, no. 1, pp. 103-125, 2022
- [13] J. Hermanns, K. Kotthaus, S. Pack, M. Zdrallek and F. Schweiger, "Influence of various weather forecast elements on the feed-in prediction of photovoltaic systems", ETG Congress 2021, Online, 2021, pp. 1-5.
- [14] Buwei, W.; Jianfeng, C.; Bo, W.; Shuanglei, F. A, "Solar Power Prediction Using Support Vector Machines Based on Multi-Source Data Fusion", In Proceedings of the 2018 International Conference on Power System Technology (POWERCON), Guangzhou, China, 6-8 November 2018; pp. 4573-4577.
- [15] Paska, J.; Surma, T.; Terlikowski, P.; Zagrajek, K., "Electricity Generation from Renewable Energy Sources in Poland as a Part of Commitment to the Polish and EU Energy Policy", Energies 2020, 13, 4261.
- [16] Yin, L.; Cao, X.; Liu, D., "Weighted fully connected regression networks for one-day-ahead hourly photovoltaic power forecasting", Appl. Energy 2023, 332, 120527
- [17] Saigustia, Candra, and Paweł Pijarski. 2023. "Time Series Analysis and Forecasting of Solar Generation in Spain Using eXtreme Gradient Boosting: A Machine Learning Approach" Energies 16, no. 22: 7

Effectiveness Limits of Benford's Law

¹Ardian HYSENI (2nd year)
Supervisor: ²Jaroslav PETRÁŠ

^{1,2} Department of Electric Power Engineering, FEI, Technical University of Košice, Slovak Republic

¹ardian.hyseni@tuke.sk, ²jaroslav.petras@tuke.sk

Abstract—Big data analytics is a security measure where advanced methods are essential for the operation and increased reliability of increasingly complex electrical distribution grids (EDNs) and for increasing volumes of measurement data. The purpose of this study is to summarize methods for analyzing data in distribution systems. Important areas involve outlier detection, Benford's law (BL) to validate measured data, which helps in using machine learning to solve classification and clustering problems. These methods focus on improving fault detection capabilities, optimizing grid performance indicators, and improving decision-making processes in smart grid environments.

Keywords—Big data, Distribution grids, Data analysis, Benford's law, Machine learning, Anomaly detection.

I. INTRODUCTION

BL, also known as the first-digit law, describes the expected frequency distribution of leading digits in naturally occurring datasets. It is widely used in fraud detection, accounting, and the identification of anomalies [1].

In electricity distribution grids, consumption data typically follows natural distribution under normal conditions. However, artificial interventions, macroeconomic influences, or non-technical losses (e.g., electricity theft) can disrupt this pattern, making the dataset unnatural. BL provides an effective tool for detecting such anomalies in smart metering data [2].

This study investigates the effectiveness of BL-based detection in electricity distribution grids, focusing on its ability to identify dataset changes and determine the threshold at which anomalies remain detectable. No alternative methods are known within the applied scope of BL law. Existing research rarely addresses this threshold, making it a key area of exploration [3].

The main research objectives are:

1. Evaluating BL's effectiveness in detecting non-natural data changes in electricity distribution datasets.
2. Determining the minimum threshold of affected data required for reliable anomaly detection.

II. BACKGROUND AND PROGRESS

BL is used in power engineering to detect anomalies in electricity consumption, identify theft, and optimize forecasting. Its effectiveness depends on factors like dataset size, data type, and statistical tests (e.g., Chi-square, Kolmogorov-Smirnov) [4].

In smart grids, BL helps detect non-technical losses without modifying the grid. Unlike model-based or deep-learning methods, it offers a non-intrusive way to analyze billing data.

It also aids in monitoring electricity production by identifying irregularities and minimizing losses [5].

Despite limitations like small datasets, data distribution issues, and external influences, BL remains a valuable tool for data-driven decision-making in power distribution. This research focuses on [6], [7], [8]:

1. Current challenges in big data evaluation in power systems.
2. Defining analytical goals for distribution grids.
3. Developing and implementing methods for big data analysis.
4. Validating results and assessing their impact.
5. Providing recommendations for future research.

By combining BL with big data analytics, this study aims to improve fraud detection, enhance power system efficiency, and strengthen cybersecurity by identifying data manipulation and potential cyber threats within electricity grids [6].

III. RECENT ACHIEVEMENTS

We used BL for integrity validation of energy data of electricity metering apparatus, and anomaly detection. We tested whether real-world measurement datasets conform to BL, examining the deviations that signal disturbances in natural data generation processes [8].

To test how both sensitive and effective BL is at detecting manipulated values, we performed a subset of experiments that involved creating artificial alterations to the dataset. The dataset itself is not limited; however, the results are summarized due to the scope of the paper. One of the most important analytical tasks in our study was to establish the minimum percentage of manipulated data needed for BL to identify anomalies. It can be concluded from the study that using the proposed approach, anomaly detection in our dataset would take place when the threshold of effectiveness (TE) is between 7% and 9% of the manipulated values. This range was selected based on the results of several simulations and graphs in the paper, with the significance level for the Chi-squared test set at 0.05 according to the literature [8].

Moreover, we assessed the validity of this threshold determination. Our results contribute to the understanding of how BL can be applied in electrical power engineering to verify data integrity and automate the detection of anomalous behavior in distribution grids [8].

In our experiments, we used the Chi-square test to assess the compliance of the energy data with BL. Statistical analysis on deviations of the first-digit distribution was conducted to detect possible anomalies [8].

All p -values are reported at 0.05 (α) level of analysis,

to maintain consistency across all the experiments. We set a threshold value to determine whether the deviations in the dataset are significant and can be used for anomaly detection. We show that this method is highly effective in detecting non-natural changes to electricity metering data, lending further credence to the applicability of BL in the validation of large-scale data sets pertaining to energy [8].

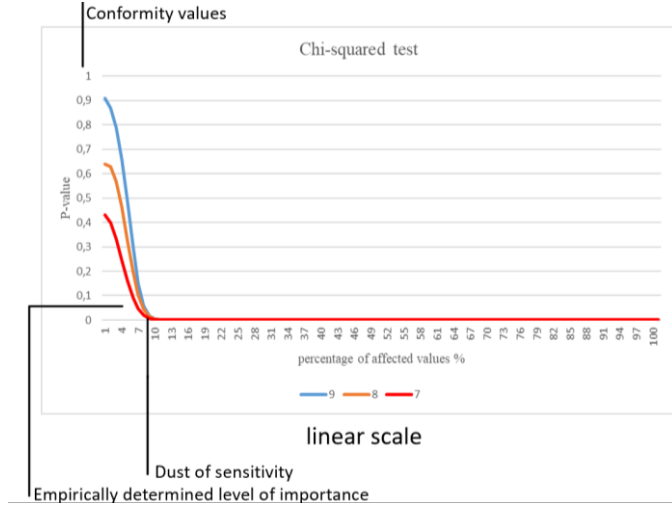


Fig. 1. Chi-square test results of BL distribution comparison from the measuring of all three nodes with different replacement value for each node – linear y-axis

Fig. 1 and 2 show the results of the Chi-square test, analyzing a total of 3 different measurement nodes for BL distribution with different replacement values for all three nodes. The Y-axis in Fig. 1 is on a linear scale, whereas in Fig. 2 it is set to logarithmic to allow for better visualization of the differences, particularly for replacement amounts > 10%.

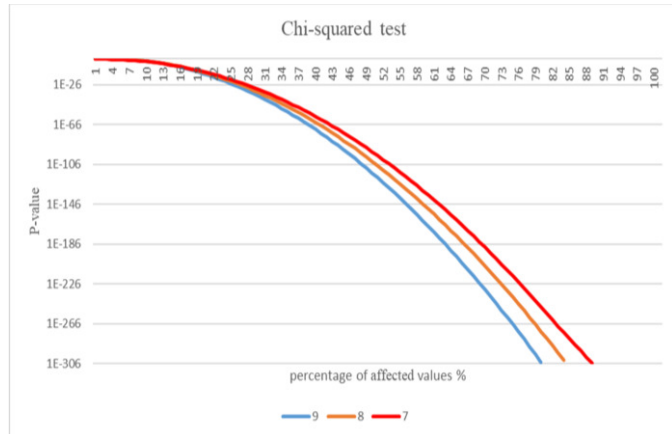


Fig. 2. Chi-square test results of BL distribution comparison from the measuring of all three nodes with different replacement value for each node – logarithmic y-axis

TABLE I

BL application for automated EMS data

Digit	BL Percentages (%)	Data Relative Frequencies (%)	Differences (%)
1	30.2	27.124	2.975
2	17.61	13.581	4.028
3	12.49	11.571	0.918
4	9.69	10.502	0.812
5	7.92	9.405	1.485

6	6.69	8.274	1.584
7	5.8	8.237	2.437
8	5.12	6.442	1.322
9	4.58	4.801	0.23

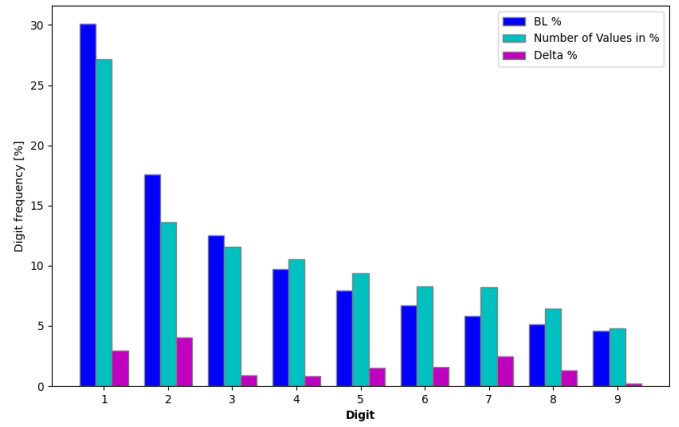


Fig. 3. The image shows a graph from the automation process that was created using a C# program

In Fig. 3 we see a graph that shows the frequency of first digits in a dataset compared to what would be expected based on BL. Again, you can see that y-axis corresponds to percentage frequency of each digit and x-axis is number of the digits (1-9).

Blue bars show the expected distribution according to BL percentages.

The cyan bars are the true distribution of the data.

The Delta % purple bars show the difference between expected and actual values.

This visualization is used in the detection of outliers or unusual observations in datasets; these methods are often used in fraud detection, power system monitoring, and financial audits.

Note: The graph in the image above was generated from an automated process developed in C#, providing a good analysis tool for big data pattern detection. Computational efficiency is not included as part of assessing the method's effectiveness and accuracy.

IV. FUTURE PLANS

We intend to apply for BL in cybersecurity, which plays a crucial role in three phases of big data processing: data acquisition, transmission, and retrieval from storage. Each phase presents potential risk data manipulation during collection, interception during transfer, and unauthorized modifications within storage. By integrating BL-based analysis, we aim to enhance anomaly detection and safeguard metering data integrity.

V. CONCLUSION

Detection of non-technical losses relies heavily on the availability of reliable metering data. Our research upholds the application of BL and seeks to improve detection efficiency with machine learning. The next step is to train a neural network to determine how the data have been modified—whether by multiplication, division, addition, or subtraction. By tuning the model and validating it with real data, we aim to create a valuable tool for distribution grid

operators to identify unauthorized interventions in metering systems.

REFERENCES

- [1] M. A. da Silva, T. Abreu, C. R. Santos-Júnior, and C. R. Minussi, “Load forecasting for smart grid based on continuous-learning neural network,” *Electric Power Systems Research*, vol. 201, p. 107545, 2021. [Online]. Available: <https://doi.org/10.1016/j.epsr.2021.107545>.
- [2] F. Milano and A. Gómez-Expósito, “Detection of cyber-attacks of power systems through Benford’s law,” *IEEE Transactions on Smart Grid*, vol. 12, no. 3, pp. 2741–2744, 2021. [Online]. Available: <https://doi.org/10.1109/TSG.2020.3042897>.
- [3] P. M. Cabeza Garcia, “Application of Benford’s law in fraud detection,” *Revista Universidad y Sociedad*, vol. 11, no. 5, pp. 421–427, Oct.–Dec. 2019.
- [4] M. Rashed, I. Gondal, J. Kamruzzuman, and S. Islam, “State estimation in the presence of cyber attacks using distributed partition technique,” in *2020 Australasian Universities Power Engineering Conference (AUPEC)*, Hobart, Australia, Nov. 29–Dec. 3, 2020.
- [5] J. Petras, M. Pavlik, J. Zbojovsky, A. Hyseni, and J. Dudiak, “Benford’s law in electric distribution network,” *Mathematics*, vol. 11, no. 18, p. 3863, Sep. 2023. [Online]. Available: <https://doi.org/10.3390/math11183863>.
- [6] A. Hyseni, D. Medved, and J. Petras, “Benford’s law in electric power engineering,” in *2024 24th International Scientific Conference on Electric Power Engineering (EPE)*, Kouty nad Desnou, Czech Republic, May 15–17, 2024, pp. 144–149. [Online]. Available: <https://doi.org/10.1109/EPE61521.2024.10559527>.
- [7] M. Pavlik, M. Beres, A. Hyseni, and J. Petras, “Statistical analysis of electricity prices in Germany using Benford’s law,” *Energies*, vol. 17, no. 18, p. 4606, Sep. 2024. [Online]. Available: <https://doi.org/10.3390/en17184606>.
- [8] A. Hyseni, *Research on Big Data in the Distribution Network of Electric Power for Improving Reliability and Efficiency of Distribution*, dissertation exam thesis, Technical University of Košice (TUKE), Košice, 2024, pp. 1–82.

CC 6D SVT: Child Node Mask Compression of 6Dimensional Sparse Voxel Trees

¹Heidar KHORSHIDIYEH (4th year)
Supervisor: ²Branislav MADOS

^{1,2}Dept. of Computers and Informatics, Faculty of Electrical Engineering and Informatics, Technical University of Košice, Letná 9, 042 00 Košice, Slovak Republic

¹heidar.khorshidiyeh@tuke.sk, ²branislav.mados@tuke.sk

Abstract—This paper deals with the problematics of representing the geometry of voxelized 3D scenes in the field of computer graphics through hierarchical data structures based on trees. It follows on from previous research in this area, in which it was found that the transformation of sparse voxel octrees from 3D to higher dimensions allows for the compaction of their binary representation, with an optimum at 6D or 7D sparse voxel trees. When transforming to 6D, the limiting factor for further compression is the size of the child node mask of both internal and leaf nodes, which reaches a size of up to 64b. The analysis showed that the child node masks of internal and also leaf nodes of 6D SVTs contain longer sequences of bits set to the value 0, which made it possible to apply compression to the child node mask and thus create the child node mask compressed 6dimensional sparse voxel trees (CC 6D SVTs) proposed in this research. In tests on 18 voxelized scenes, it was shown that the compactness of the representation of the scene geometry at the binary level increased by using CC 6D SVTs from 1.20 to 1.36 times in comparison to the use of 6D SVTs.

Keywords— voxelized 3D graphics, geometry of the scene, hierarchical data structures, data compression, 6dimensional sparse voxel trees, child node mask compressed 6dimensional sparse voxel trees

I. INTRODUCTION

The use of hierarchical data structures for representing geometry and other properties of both two-dimensional and three-dimensional data in the field of computer graphics has been studied since the 1980s. The use of quadrant trees or directed acyclic graphs for 2D graphics and the use of octant trees or directed acyclic graphs for 3D graphics have been successfully proposed and tested.

Currently, research in this area is underway in connection with the use of advanced graphics cards, which is why the developed hierarchical data structures are referred to as GPU-friendly. Algorithms for constructing Sparse Voxel Octrees (SVOs) have been developed in [1-3]. By modifying SVOs, Efficient Sparse Voxel Octrees (ESVOs) [4, 5] were created, which can represent parts of subtrees economically using the so-called contour information. Clustered Sparse Voxel Octrees (CSVOs) were developed in [6]. While these data structures are primarily intended for representing the geometry of sparse scenes, attention has also been paid to scenes that are densely populated with active voxels [7, 8]. The common subtree merge was used in the design of High Resolution Sparse Voxel Directed Acyclic Graphs (HR SVDAGs) in [9]. In this context,

a version of this data structure, designated as Lossy Sparse Voxel Directed Acyclic Graphs (LSVDAGs), that is able to compress geometry information in lossy manner was introduced in [10]. A further development was the creation of a hierarchical data structure that allows the joining of common subtrees even if it is necessary to implement a mirror transformation. This hierarchical data structure is called Symmetry-aware Sparse Voxel Directed Acyclic Graphs (SSVDAGs) [11, 12]. A hierarchical data structure called Pointerless Sparse Voxel Directed Acyclic Graphs (PSVDAGs) was proposed in [13] and an algorithm for fast transformation between PSVDAGs and SVDAGs was proposed in [14].

II. PROPOSED METHODS WITHIN OUR RESEARCH

Building Sparse Voxel Octrees (SVOs) for a scene with dimensions N^3 voxels, where $N = 2^m$ voxels, means building the corresponding tree with m levels of nodes. Its traversal can stop at any of the m levels of the tree. It means m levels of Level of Details (LOD) can be reached. Each of the internal nodes of the SVO can potentially have 1 to 8 child nodes.

Within our research activity in the last year it has been experimentally found that it is possible, by transforming 3D scenes into scenes with a higher number of dimensions, to create corresponding n-dimensional equivalents of SVOs, referred to as nDimensional Sparse Voxel Trees (nD SVTs). As the number of dimensions increases, the size of the binary representation of these SVTs decreases up to an optimum, which was experimentally found for 6D SVTs or 7D SVTs. Then the size of the binary representation of SVTs starts to increase with increasing number of dimensions. These research results have been formatted into a research paper, which we sent for the publication and is currently in the review process.

A positive effect, enabling the compaction of the binary representation of SVTs is driven by decrease in the number of nodes and pointers to these nodes that form the respective data structure (each node has exactly one pointer pointing to it from the parent node layer, with the exception of the root node, which does not have its own pointer from the parent node layer). A negative effect of increasing the dimensionality of the scene and therefore the respective SVT dimensionality is a significant increase in the size of the child node mask (CHNM) of both internal and leaf nodes of a given SVT. When using 3D SVT, the size of the CHNM is only 8 Header Tags (HTs), where

HT has a size of 1b. In 6D, the CHNM comprises 2^6 HTs, and therefore with 1b HTs it is up to 64b, with a potential number of child nodes ranging from 1 to 64.

As the dimensionality of the scene increases, the number of node layers forming the corresponding nD SVT decreases. If the SVO has m node layers, then the 6D SVT has $m/2$ node layers. This has a positive effect on the speed of tree traversal, but it has a negative effect on the number of Level of Details (LOD), which is also at the level of $m/2$.

Therefore, as a further step, after creating the 6D SVT hierarchical data structure, attention in our research was focused on compacting the binary representation of the child node mask of both the internal and leaf nodes of the 6D SVT.

The analysis revealed that the child node mask in the 6D SVT contains sequences of HTs set to 0. This can be used to compress the child node mask. The compression is implemented so that the 64 HTs are divided into 8 groups of 8 HTs. A separate 8b index is then created, where the n th bit of the index represents the characteristic of the n th group of header tags.

- if the n th group of 8 HTs contains at least one active HT (set to 1), the n th bit of the index is set to 1.
- if the n th group of 8 HTs contains only passive HTs (all

8 are set to 0), the n th bit of the index is set to 0.

For index bits set to 1, the corresponding header tag group is concatenated. The original child node mask with a constant length of 64b (Figure 1a) is thus replaced by a structure with a variable length binary representation, where there is always an 8b index, followed by 1 to 8 header tag groups, where each group consists of 8 header tags (Figure 1b). Fully linearized form of the CHNM can be seen on the Figure 1c.

In the unfavorable case, when all 8 header tag groups are active, the total size of this structure is up to 72b, which is more than 64b. In the case where 7 header tag groups are active, the size of this structure is equal to the size of the original 64b child node mask. In the case where the number of active header tag groups is from 1 to 6, the size of this structure is from 16b to 56b. In the unfavorable case, using child node mask compression will, on the contrary, lead to inflation of the size of the binary representation of the data structure. In the favorable case, compression will occur. The advantage of such a compressed child node mask construction is that it is composed of two levels. The first level is the 8b index and the second level is the header tag groups themselves.

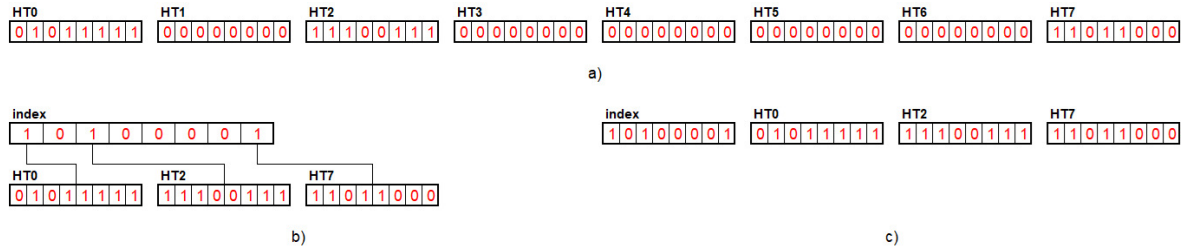


Figure 1 representation of the child node mask of the 6D SVT as a) 64b vector comprising 8 8b HT sets, HT0 to HT7 and as a b) 32b structure comprising 8b index and 3 active 8b HT sets and as a c) linearized form of the compressed child node mask.

TABLE I

Size in KB of the hierarchical data structure SVO HDS, 6D SVT HDS and CC 6D SVT HDS for Angel Lucy, Porsche and Skull model in different resolutions of the scene from 128^3 voxels to 4096^3 voxels. CR_1 represents compression ratio between SVO HDS and 6D SVT HDS, CR_2 represents compression ratio between SVO HDS and CC 6D SVT HDS and CR_3 represents compression ratio between 6D SVT HDS and CC 6D SVT HDS.

	Angel Lucy					
	128 ³	256 ³	512 ³	1024 ³	2048 ³	4096 ³
SVO	53	229	944	3 808	15 600	59 562
6D SVT	15	65	278	1 138	4 574	18 166
CR ₁	3.53	3.52	3.40	3.35	3.41	3.28
CC 6D SVT	12	50	211	855	3 420	13 503
CR ₂	4.57	4.54	4.48	4.45	4.56	4.41
CR ₃	1.29	1.29	1.32	1.33	1.34	1.35
	Porsche					
	128 ³	256 ³	512 ³	1024 ³	2048 ³	4096 ³
SVO	117	540	2 361	9 932	40 700	162 103
6D SVT	29	147	664	2 877	12 021	49 030
CR ₁	4.03	3.67	3.56	3.45	3.39	3.31
CC 6D SVT	24	116	516	2 201	9 094	36 606
CR ₂	4.84	4.64	4.57	4.51	4.48	4.43
CR ₃	1.20	1.26	1.29	1.31	1.32	1.34
	Skull					
	128 ³	256 ³	512 ³	1024 ³	2048 ³	4096 ³
SVO	186	765	3 100	12 413	49 038	189 341
6D SVT	54	225	922	3 727	14 891	58 666
CR ₁	3.44	3.40	3.36	3.33	3.29	3.23
CC 6D SVT	41	171	695	2 794	11 094	43 223
CR ₂	4.52	4.48	4.46	4.44	4.42	4.38
CR ₃	1.31	1.32	1.33	1.33	1.34	1.36

This allows, when traversing the data structure, to traverse the child node mask to the index level or fully up to the header tag group level. The number of LODs is therefore not $m/2$ as in 6D SVT but returns to m , as in SVO.

III. RESULTS

The tests were performed on scenes created by voxelizing three polygonal surface models (mesh) – Angel Lucy, Porsche and Skull. These models were voxelized to a total of six resolutions, from 128^3 to 4096^3 voxels. This resulted into 18 test scenes. The testing was carried out on a Win 11 Home computer, 15.6", 1920×1080 FullHD, IPS, AMD Ryzen 7 7435HS, 3.1GHz, octacore, nVidia GeForce RTX4060 8GB, 16 GB RAM, DDR5, 512 GB SSD. As the test results in Table I show, 6D SVT is 4.52 to 3.23 times more compact than classic SVO, as shown by the CR_1 value, which is the compression ratio between SVO and 6D SVT. When using child node mask compression, i.e. with CC 6D SVT, the compaction rate is achieved at a level of 4.84 to 4.38 times compared to classic SVO. In Table I, it is marked as CR_2 and is calculated as the ratio between the size of SVO and CC 6D SVT. The rate of increase in compaction of the binary representation of the geometry of the relevant scene when using CC 6D SVT versus the use of 6D SVT was achieved at a level of 1.20 to 1.36. It is indicated in Table I as CR_3 and is calculated as the ratio of the size of the 6D SVT and the CC 6D SVT.

IV. CONCLUSIONS

The paper dealt with the issue of representing the geometry of 3D voxelized scenes through hierarchical data structures based on trees, namely Sparse Voxel Trees (SVTs), which were upscaled to 6 dimensions (6D). In previous research, conducted within last year, it was found that by increasing the dimensionality of sparse voxel Trees, it is possible to obtain more compact hierarchical data structures, the minimum size of which is achieved at 6D or 7D. Child Node Masks in the case of 6D SVT increase up to 64b and represent a limiting factor for the compactness of 6D SVT. Therefore, a 64b CHNM of 6D SVT compression was proposed as part of this research. It turned out that, thanks to this modification, it is possible to advance the compression of 6D SVT further. Thus, CC 6D SVTs were created, which are more compact than 6D SVTs. Tests showed that it was possible to achieve 1.20 to 1.36 times higher compression.

V. FUTURE RESEARCH

In our future research we will investigate the use of Common Subtree Merge, which will create 6D SVDAG HDS and CC 6D SVDAG HDS, which should enable further compaction of the geometry representation of voxelized 3D scenes.

Further attention will be paid to the issue of geometry representation of voxelized scenes that are dynamic in time. The possibility of creating Spatio Temporal Sparse Voxel Octrees (ST SVOs), and Spatio Temporal Sparse Voxel Directed Acyclic Graphs (ST SVDAGs) will be investigated.

The influence of the type of scene dynamics on the obtained compression ratio will also be investigated.

ACKNOWLEDGMENT

This work was supported by KEGA Agency of the Ministry of Education, Science, Research, and Sport of the Slovak Republic under Grant No. 015TUKE-4/2024 Modern Methods and Education Forms in the Cybersecurity Education.

REFERENCES

- [1] Baert, J.; Lagae, A.; Dutré, Ph. Out-of-Core Construction of Sparse Voxel Octrees. In Proceedings of the 5th High-Performance Graphics Conference (HPG '13), Anaheim, CA, USA, 19–21 July, 2013, pp. 27–32. <https://doi.org/10.1145/2492045.2492048>.
- [2] Baert, J.; Lagae, A.; Dutré, Ph. Out-of-Core Construction of Sparse Voxel Octrees. *Computer Graphics Forum* 2014, 33, pp. 220–227. ISSN 0167-7055. <https://doi.org/10.1111/cgf.12345>.
- [3] Pätzold, M.; Kolb, A. Grid-free out-of-core voxelization to sparse voxel octrees on GPU. In Proceedings of the 7th Conference on High-Performance Graphics (HPG '15), Los Angeles, CA, USA, 7–9 August 2015, pp. 95–103. ISBN 9781450337076. <https://doi.org/10.1145/2790060.2790067>.
- [4] Laine, S.; Karras, T. Efficient Sparse Voxel Octrees. In Proceedings of the 2010 ACM SIGGRAPH Symposium on Interactive 3D Graphics and Games (I3D '10), Redmond, WA, USA, 19–21 February, 2010, pp. 55–63. ISBN 978-1-60558-938-1. <http://doi.org/10.1145/1730804.1730814>.
- [5] Laine, S.; Karras, T. Efficient Sparse Voxel Octrees—Analysis, Extensions, and Implementation, NVIDIA Technical Report NVR-2010-001, NVIDIA Corporation, Santa Clara, USA, 2010; pp. 30.
- [6] Madoš, B.; Chovancová, E.; Chovanec, M.; Ádám, N. CSVO: Clustered Sparse Voxel Octrees—A Hierarchical Data Structure for Geometry Representation of Voxelized 3D Scenes. *Symmetry* 2022, 14, 2114. <https://doi.org/10.3390/sym14102114>.
- [7] Madoš, B.; Ádám, N.; Štancel, M.; Representation of Dense Volume Datasets Using Pointerless Sparse Voxel Octrees With Variable and Fixed-Length Encoding - 2021. In: SAMI 2021 : IEEE 19th World Symposium on Applied Machine Intelligence and Informatics. - Danvers (USA) : Institute of Electrical and Electronics Engineers pp. 343-348 [online, USB-key]. - ISBN 978-1-7281-8053-3 (online), <https://doi.org/10.1109/SAMI50585.2021.9378675>.
- [8] Madoš, B.; Chovancová, E.; Hasin, M.; Evaluation of Pointerless Sparse Voxel Octrees Encoding Schemes Using Huffman Encoding for Dense Volume Datasets Storage - 2020. In: ICETA 2020 : 18th IEEE International conference on emerging elearning technologies and applications : Information and communication technologies in learning : proceedings. - Denver (USA) : Institute of Electrical and Electronics Engineers s. 424-430 . - ISBN 978-0-7381-2366-0. <https://doi.org/10.1109/ICETA51985.2020.9379265>.
- [9] Kämpe, V.; Sintorn, E.; Assarson, U. High Resolution Sparse Voxel DAGs. *ACM Transactions on Graphics* 2013, 32, pp. 1–13. ISSN 0730-0301. <https://doi.org/10.1145/2461912.2462024>.
- [10] van der Laan, R.; Scandolo, L.; Eisemann, E. Lossy Geometry Compression for High Resolution Voxel Scenes. *Proceedings of the ACM on Computer Graphics and Interactive Techniques* 2020, 3, pp. 13. EISSN: 2577-6193. <https://doi.org/10.1145/3384541>.
- [11] Villanueva, A.J.; Marton, F.; Gobetti, E. Symmetry-aware Sparse Voxel DAGs. In Proceedings of the 20th ACM SIGGRAPH Symposium on Interactive 3D Graphics and Games (I3D '16), Redmond, WA, USA, 27–28 February, 2016; pp. 7–14. ISBN 978-1-4503-4043-4. <https://doi.org/10.1145/2856400.2856420>.
- [12] Villanueva, A.J.; Marton, F.; Gobetti, E. Symmetry-aware Sparse Voxel DAGs (SSVDAGs) for compression-domain tracing of high-resolution geometric scene. *J. Comput. Graph. Tech. (JCGT)*, 2017, 6, pp. 30. <http://jcggt.org/published/0006/02/01>.
- [13] Vokorokos, L.; Madoš, B.; Bilanová, Z. PSVDAG: Compact Voxelized Representation of 3D Scenes Using Pointerless Sparse Voxel Directed Acyclic Graphs. *Computing and Informatics*, 2020, 39, pp. 587-616. ISSN 1335-9150 (print); 2585-8807 (online). https://doi.org/10.31577/cai_2020_3_587.
- [14] Madoš, B.; Ádám, N. Transforming Hierarchical Data Structures—A PSVDAG—SVDAG Conversion Algorithm. *Acta Polytechnica Hungarica*, 2021, 18, pp. 47-66. ISSN 1785-8860. <https://doi.org/10.12700/APH.18.8.2021.8>

Human-Machine Collaboration and Artificial Intelligence in Industry 5.0

¹Maroš KRUPÁŠ (*3rd year*),
Supervisor: ²Iveta ZOLOTOVÁ

^{1,2}Dept. of Cybernetics and Artificial Intelligence, FEEI TU of Košice, Slovak Republic

¹maros.krupas@tuke.sk, ²iveta.zolotova@tuke.sk

Abstract—To enhance production efficiency while keeping humans at the core of manufacturing processes, human-centric manufacturing emphasizes concepts such as artificial intelligence and human-machine collaboration. This paper provides an overview of our research on these topics, focusing primarily on our use cases, with the aim of developing a methodology to support the creation of human-centric human-machine collaboration applications in Industry 5.0. Lastly, it outlines the anticipated future directions of our research in this field.

Keywords—artificial intelligence, human-machine collaboration, human-centric, industry 5.0

I. INTRODUCTION

The rise of Artificial Intelligence (AI) has revolutionized industries by enhancing how systems perceive, interpret, and respond to human inputs. Traditional AI primarily relied on single data sources, but advancements, including multimodal AI, have enabled systems to integrate multiple types of information for more adaptive, context-aware, and intuitive interactions.

At the same time, Human-Machine Collaboration (HMC) aims to blend human and machine capabilities, but existing applications often prioritize efficiency over human-centricity. To bridge this gap, multimodal AI plays a crucial role in creating more natural, responsive, and intelligent HMC systems. By analyzing human behavior across multiple modalities, it enhances collaboration, improving safety, usability, and overall effectiveness.

This paper explores the integration of multimodal AI in HMC, identifying key enabling technologies and methods to foster human-centered AI applications in Industry 5.0. It aims to advance research in designing AI-driven systems that prioritize human adaptability and collaboration and create a methodology to facilitate the systematic creation of these applications while recommending appropriate metrics for both design and evaluation.

II. INITIAL STATUS

Our first study [1] began with the topic of Industry 5.0, its enabling technologies, and their core values, human-centricity, sustainability, and resiliency. Our research focused on human-centricity, which emphasized HMC to enhance work efficiency while keeping humans central to production. First, we identified key challenges and research gaps in this field. Building on these gaps, our research focused on identifying and implementing suitable technologies and methods for human-centered

solutions, focusing on enabling technologies for digital twins (DTs) of HMC in a synergistic way [2].

To develop a systematic approach for designing human-centric applications, we proposed a reference framework [3] for HMC with heterogeneous robots. To enhance this framework, we explored DTs in HMC, identifying key enabling technologies from Industry 5.0 and categorizing them into four groups: (1) DT and simulation for safety, ergonomics, and training; (2) AI for efficiency and decision-making; (3) human-machine interaction using AR/VR, natural interfaces, and sensors; and (4) data transmission and analysis leveraging IoT, cloud, and edge computing. Our review [4] highlights use cases and methodologies supporting human-centric HMC systems.

III. OBJECTIVES SOLVED IN PREVIOUS YEAR

After identifying key enabling technologies for DT-enhanced HMC, we shifted our focus from DTs to multimodal AI use cases, which implemented those technologies while focusing on human-centricity.

In [5], we dealt with ensuring and increasing the safety of mobile robotic systems in human-machine collaboration. The research aimed to design and implement an AI application that recognizes obstacles, including humans, and increases safety. The resulting mobile application (Fig. 1) used a MiDaS neural network model to generate a depth map of the environment from the drone's camera to approximate the distance from all obstacles to avoid the drone's collision. Our work outside of the article continues to implement additional AI to create a multimodal AI solution. After detecting obstacles with MiDaS, the vision-language GPT-4o mini ChatGPT model was used after taking a picture of the environment with the drone's camera to generate the best navigation route and flight commands for the drone in the indoor lab. At the same time, experiments are done in simulation to navigate ground mobile robots in hospital settings with their cameras by using and evaluating different local-based vision-language models.

For our second use case [6], we examined the current application solutions of Large Language Models (LLMs) in education and research and their usability, benefits, and challenges. Through our use case and experimental data on Turtlebot3 education robots, we discussed the potential of different transformer-based LLMs and their limitations to improve educational and research outcomes for students working with robotic systems in laboratory conditions. We also

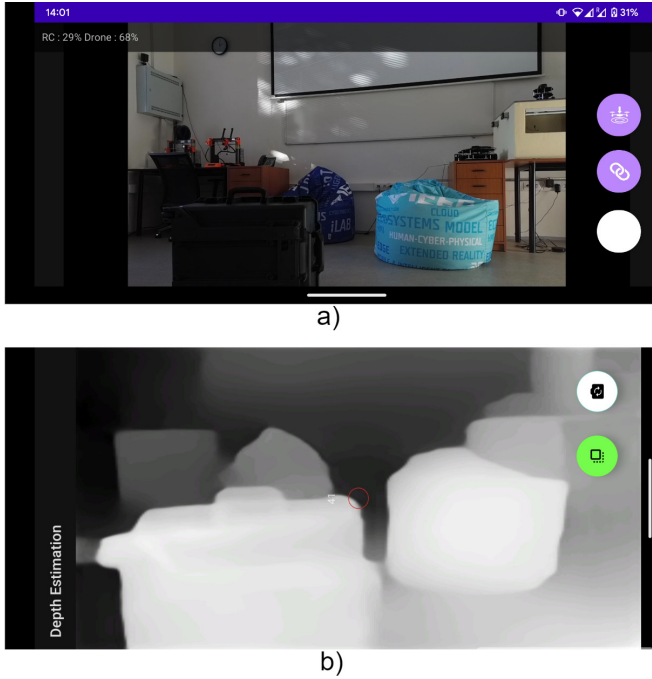


Fig. 1. Application UI: a) drone's camera video stream, b) MiDaS real-time depth estimation

evaluated selected models based on quantitative and qualitative metrics to choose one which was best suited for our AI-based education and research assistant use case.

The third use case [7] explored the integration of ultra-wideband (UWB) technology to improve human localization in augmented reality (AR) applications. As AR becomes increasingly relevant across various fields, it is essential to ensure precise localization. We investigated the potential of UWB to improve localization in AR by evaluating its accuracy through a practical use case. In the paper, we focus on an overview of existing UWB localization systems, discuss their limitations, and then outline the design, implementation, and evaluation of our proposed solution. Besides accuracy for real-time human tracking, our use case also enables human-centric HMC by allowing natural and intuitive AR experiences.

The fourth use case [8] presents the development of an automated landing algorithm that enables a drone to land on a moving platform using computer vision techniques. Our solution is tailored to improve real-time tracking and dynamically adjust the position of the drone, ensuring a precise landing on the ground mobile robot equipped with the landing platform. This advancement facilitates collaboration between unmanned aerial and ground vehicles, thus increasing autonomy and automation. The system was designed and tested in a simulation environment, Webots, and employs the DJI Mavic 2 Pro drone and a four-wheeled ground robot.

The fifth use case involves controlling robotic systems by voice and LLMs with intuitive interfaces. A web app was implemented to control Turtlebot3 mobile robots with ChatGPT models, and a local app was developed to control the Dobot Magician robot arm with Google Gemini using voice commands. Our language models process human voice input to send commands to navigate robots or make them perform specific tasks. In this use case, we can choose to use different modalities, such as voice, text or image to control our robotic systems.

IV. FUTURE WORK AND CONCLUSION

Our research focuses on analyzing suitable technologies and methodologies for developing human-centered human-machine collaboration applications powered by multimodal AI, advancing the understanding of human-centric design in Industry 5.0. By assessing the impact and significance of these enabling technologies in our use cases, we aim to develop a comprehensive methodology applicable across various human-machine collaboration scenarios. This will provide new insights into the role of multimodal AI, expanding knowledge on its applications in diverse industrial contexts.

The next step involves proposing an updated framework for integrating diverse enabling technologies within Industry 5.0, specifically incorporating multimodal AI. This framework will offer a systematic approach to selecting and integrating technologies, ensuring their applicability across different industrial settings to achieve seamless synergy.

Additionally, we will establish criteria, metrics, and guidelines for selecting optimal technology combinations for specific use cases, considering factors such as efficiency, cost-effectiveness, user-friendliness, ease of implementation, and human-centricity. To validate the framework, we will design and develop prototype case studies or experimental applications that emphasize user experience and efficiency in AI-driven human-machine collaboration. These prototypes will help us explore the practical implications, limitations, and benefits of multimodal AI in various industrial environments.

In the final phase, we will assess the performance, scalability, and adaptability of these applications based on predefined criteria and metrics. This evaluation will take place in simulated or real-world environments using technologies such as UAVs or UGVs, ensuring their effectiveness in enhancing human-machine collaboration within Industry 5.0.

ACKNOWLEDGMENT

This publication was supported by the project KEGA 068TUKE-4/2024 - IVI: Internet of Vehicles in the Context of Industry 4.0.

REFERENCES

- [1] M. Krupáš, *23rd Scientific Conference of Young Researchers Proceedings from Conference*. Kosice: Faculty of Electrical Engineering and Informatics, Technical University of Košice, 4 2023, p. 80–83.
- [2] M. Krupáš, S. Chand, Y. Lu, X. Xu, E. Kajáti, and I. Zolotová, "Human-centric uav-ugv collaboration," in *2023 IEEE 19th International Conference on Automation Science and Engineering (CASE)*. IEEE, 2023, pp. 1–6.
- [3] M. Krupáš, *24th Scientific Conference of Young Researchers Proceedings from Conference*. Kosice: Faculty of Electrical Engineering and Informatics, Technical University of Košice, 4 2024, p. 47–48.
- [4] M. Krupáš, C. Liu, E. Kajati, and I. Zolotová, "Towards human-centric digital twin for human-machine collaboration: A review on enabling technologies and methods," *Sensors*, 2024. [in review process].
- [5] M. Krupáš, K. Mykyta, E. Kajáti, and I. Zolotová, "Ai-powered obstacle detection for safer human-machine collaboration," *Acta Electrotechnica et Informatica*, vol. 24, no. 3, pp. 23–27, 2024.
- [6] M. Krupáš, L. Antonets, J. Vaščák, and I. Zolotová, "Ai-based assistant: Lms for effective robotics education and research," in *2024 International Conference on Emerging eLearning Technologies and Applications (IC-ETA)*. IEEE, 2024, pp. 1–6.
- [7] M. Krupáš, V. Orlovský, and I. Zolotová, "Integration of human localization into augmented reality applications," in *2025 IEEE 23rd World Symposium on Applied Machine Intelligence and Informatics (SAMi)*. IEEE, 2025, pp. 000 453–000 458.
- [8] A. Zsetska, Urblik, M. Krupáš, E. Kajáti, and P. Papcun, "Automated landing of a drone on a moving vehicle using computer vision," in *2025 IEEE 23rd World Symposium on Applied Machine Intelligence and Informatics (SAMi)*. IEEE, 2025, pp. 000 385–000 388.

Multimodal Detection of Toxic Behavior in Social Media

¹Viliam BALARA (2nd year)
Supervisor: ²Kristína Machová

^{1,2}Dept. of Cybernetics and Artificial Intelligence, FEI, Technical University of Košice, Slovak Republic

¹viliam.balara@tuke.sk, ²kristina.machova@tuke.sk

Abstract— The main purpose of social networks, as their name suggests, is to connect individuals or groups and thus provide an effective tool for communication. An unwelcome accompanying effect of social networks is the presence of toxic content, which occurs in individual forms. The aim of this work is to explore the various possibilities of detecting toxic content on social networks, whether it is in the form of text or images. The work discusses established methods for text and image classification, as well as the creation of such content with the use of generative artificial intelligence. Furthermore, the work encompasses the topic of sentiment analysis, which is closely associated with the detection of toxic behavior. Finally, the achieved results, experiments, dissertation thesis and the intended methodology for future research are presented.

Keywords— Deepfake; CNN; deepfake detection; GAN; StyleGAN;

I. INTRODUCTION

Due to the potential danger that it presents, toxic content poses a considerable social, economic and reputational risk for societies and individuals alike. Either human-made, or synthetic, with the introduction of social media to everyday life, the spreading of misinformation, hateful content, misleading news or any other form of deceitful message can be easily spread through society. A prime example of it, which have recently found their way into everyday life through social media are Deepfakes, which can occur in form of photorealistic images, videos, or voice recordings. These can be described as type of content that has been algorithmically generated or manipulated often with malicious intent. Common cases of misuse include the dissemination of harmful content by perpetrators on social media with the use of fake videos [1], where they can spread virally, leaving lasting damage to the involved parties even if subsequent legal action is taken (cases of individuals or companies protecting their brand name). Another case of severe misuse of this technology is the creation of illegal sexually explicit content, either breaking the valid laws of particular country, breaching the terms of technology provider or directly attacking particular person [2]. In the majority of cases, it is almost impossible for human users to adequately distinguish between authentic content and a carefully constructed comment, review or video with the naked eye. Even the cases of audio Deepfakes have proven to be hardly discernible for human ear [3]. To produce Deepfake, a variety of methods such as combination, merging, replacement or superimposing of images or videos are used [4], resulting in a realistic

believable content. However, recently the creators generally employ more advanced AI-based techniques, mainly generative adversarial networks (GANs), diffusion models or large language models to create believable content. Often, one type of deepfake modality is accompanied by another to produce more authentic appearing results, as in the case of Deepfake videos where the lips of the speaking person are modified to be synchronized to the Deepfake audio [5].

II. CONDUCTED RESEARCH

To further analyze our problem, we have separated our task into two individual subtasks, the separation criterion being the modality of social media content. The selected modalities are image and text due to their overwhelming prevalence on social media sites. Further, we have set the task as a classification problem, focusing on the detection of images and texts which were created or manipulated through generative AI methods – such as StyleGAN [6] or Stable Diffusion [7]. Individual variations of GAN such as CycleGAN [8] or MaskGAN [9] and others were also included in our research due to their different approach to image modification. We decided to begin our research by assessing the available tools to create deepfakes, available detection methods for text and image classification.

The selected architectures for image classification were:

- VGG-16 [10]
- DenseNet [11]
- ResNet-50 [12]
- YOLOv11 [13]
- MobileNet [14]
- EfficientNet [15]
- ConvNext: [16]

In order to understand the process of deepfake creation, we have analyzed available methods for image and text synthesis, such as various variations of GAN architectures as well as transformers [17] for textual domain.

III. EXPERIMENTS AND RESULTS

In the text domain, we have focused on the application of adapters on GLUE benchmark [18]. The goal was to determine the correct approach for the reduction of training computational requirements, while retaining efficiency. This reduction would significantly improve the adaptation of existing models, especially LLMs, for new types of toxic

content which may be able to circumvent the existing detection mechanisms.

Our research was focused on the replication of the experiments conducted in [19], with the aim of reducing the model training and fine-tuning costs by including the adapters. In the original article, Adapters attained almost state-of-the-art performance in regard to original timeframe, while minimally increasing the number of parameters per individual task. On General Language Understanding Evaluation (GLUE), the attained results were within 0.4% of the performance of full fine-tuning, adding only 3.6% parameters per task. By contrast, fine-tuning necessitates the training of 100% of parameters per task. In our replication of this research, we have focused on the GLUE benchmark and simultaneously added additional variations of BERT [20] architecture to assess the performance of adapters.

We have replicated the research with the use of the original dataset. We have utilized various settings for the models that were used and selected the best performing ones. We have summarized the results and made a comparison to the original paper, with the addition of additional models. The adapter modules have shown significant improvements over fine-tuning while maintaining the required level of performance.

Overall, our results did not achieve the performance that was stated in the original adapter paper. However, the attained performance is close to the original and supports the claim of effectivity of adapter modules. To further support the claim, the additional tested models, depicted in Table 4, have achieved satisfactory performance, thus validating the versatility of adapter modules. However, a significant decrease was achieved in the case of ELECTRA. DeBERTa and DISTILBERT have achieved lower performance than BERT BASE with adapter module. The closest performance to the BERT BASE with adapter module was achieved by DeBERTa.

TABLE 1.
REPLICATED RESULTS

	BERT (Base)	Adapters 64
CoLA	58.2	59.6
SST	92.5	91.8
MRPC	90.6	91.0
STS-B	69.3	89.5
QQP	70.7	70.5
MNLI _m	84.8	83.4
MNLI _{mm}	85.3	83.9
QNLI	89.9	88.3
RTE	69.3	68.9

TABLE 2.
ORIGINAL PAPER RESULTS

	BERT (Base)	Adapters 64
CoLA	60.5	56.9
SST	94.9	94.2
MRPC	89.3	89.6
STS-B	87.6	87.3
QQP	72.1	71.8
MNLI _m	86.7	85.3
MNLI _{mm}	85.9	84.6
QNLI	91.1	91.4
RTE	70.1	68.8

TABLE 3.
ADAPTERS- REPLICATION RESULTS WITH ADDITIONAL ARCHITECTURES

Dataset	CoLA
BERT(Base)	58.2
BERT(Adapters 64)	59.6
DISTILBERT(Adapters	54.1
DeBERTa (Adapters 64)	58.2
ELECTRA (Adapters 64)	49.7

In the image domain, we have focused our experiments especially on the detection of Deepfakes. The idea behind is to detect the cases when the image that contains human face was manipulated, it may suggest the possible intention to deceive. In the case of a social media post made from the combination of image and text, the ability to correctly classify whether the image has been manipulated or synthesized through generative methods increases the chances to correctly assess the overall believability of the social media post. For our experiments, the selected architectures were VGG-16, DenseNet, ResNet, MobileNet, EfficientNet and ConvNext. The used dataset was created as a combination of existing Flickr real face dataset (Flickr-Faces-HQ) provided by Nvidia that were collected for the StyleGAN paper. It also has good coverage of accessories such as eyeglasses, sunglasses, hats, etc. The images were crawled from Flickr, thus inheriting all the biases of that website, and automatically aligned and cropped using dlib. Only images under permissive licenses were collected. Various automatic filters were used to prune the set, and finally Amazon Mechanical Turk was used to remove the occasional statues, paintings, or photos of photos. The part of dataset containing fake faces was created with the use of StyleGAN. The dataset pictures are labeled as real or fake, therefore it is a binary classification task. The whole dataset is publicly available at [21]. The dataset is split into train, test and validation parts. The train contains 50000 samples, test 10000 and validation also 10000, meaning that both classes have equal representation in each subdataset. The images are

colored, have dimensions of 256 x 256 pixels and are focused on the faces. There are no multiple individuals depicted, only single face per picture. The best results were achieved by the EfficientNet architecture with the validation accuracy of 96.76%, followed by ConvNext with 95.72%. The worst performance was attained by the oldest architecture of VGG16, which scored 92.25%. The results are depicted in Table 3.

TABLE 4.
DEEPPAKE CLASSIFICATION RESULTS

Model Name	Validation accuracy
VGG16	0.9225
DenseNet121	0.9528
ResNet50	0.9364
MobileNet	0.9448
EfficientNet	0.9676
ConvNext	0.9572

IV. CONCLUSIONS

Our conclusion is that with rapidly increasing capabilities of DL models and with accessible computing power in combination with the societal impact that the social media have, it is of a high importance to focus on the development of tools to detect artificially generated content. As the models that are used for generation of content constantly improve, the same needs to apply for the detection tools to prevent harmful conduct. The achieved performance of selected architectures was comparable, with the best results achieved by EfficientNet. The accuracy provided by those models was satisfactory, each of them scoring above 90%, which would provide the potential user with a viable chance to detect false content including human faces. The experiments in image domain were conducted successfully considering the initial goal of this work, however, we aim to include additional datasets with broader range of characteristics to ensure the classification quality of our models. We do believe that the rapid development of large language models along with security measures implemented by social media will force the quality of generated content to increase which will in turn create a demand for improved detection models.

V. LIST OF PUBLICATIONS

1. Machová, K., Balara, V., & Mach, M. (2023) Detection of Fake News Relate to CoViD-19. In World Symposium on Digital Intelligence for Systems and Machines (DISA 2023), IEEE, pp. 161-166.
2. Balara, V., Mach, M., & Machova, K. (2023) The Impact of Sentiment in S&P 500 volatility prediction with the use of Deep Learning. In 21st International Conference on Emerging eLearning Technologies and Applications (ICETA 2023), IEEE, pp. 25-30.

3. Balara, V., Machova, K. (2024) Detection of artificially created Faces with convolutional Networks. In 22st International Conference on Emerging eLearning Technologies and Applications (ICETA 2023), IEEE, pp. 40-45.

4. K. Machová, M. Mach, V. Balara, P. Husnaj (2024) Ensemble Learning in the Recognition of Various Types of the Online Toxicity. In 22st International Conference on Emerging eLearning Technologies and Applications (ICETA 2024), IEEE, pp. 419-424.

5. Machová, K., Mach, M., & Balara, V. (2024). Federated Learning in the Detection of Fake News Using Deep Learning as a Basic Method. *Sensors*, 24(11), 3590, CCC, WOS - Q2.

6. Balara, V. (2024) Multimodal detection of antisocial behaviour in social media. In: 24rd Scientific Conference of Young Researchers: proceedings from conference. Košice, Slovakia, Technical University of Košice, 2024, pp. 95-98, ISBN 978-80-553-3474-5.

7. Machová, K., Balara, V., Mach, M., & Kožík, Š. (2025). Selection and evaluation of a set of attributes appropriate for detection of antisocial behavior in online media. *Multimedia Tools and Applications*, 1-39, CCC, WOS - Q2.

VI. FUTURE GOALS

Our future goal is the creation of a comprehensive tool for social media post classification, with the inclusion of explanatory features. For users, the application will highlight the suspicious aspects of particular social media post, accompanied by explanation. We also aim to further incorporate individual LLMs and content generated through them for the enhanced classification in textual domain. In image domain, we aim to improve the versatility of classification by including images that currently deceive the trained classifiers. The last goal is the implementation of the sentiment analysis for the improvement of the achieved classification.

ACKNOWLEDGMENT

This work was supported by the Scientific Grant Agency of the Ministry of Education, Science, Research and Sport of the Slovak Republic, and the Slovak Academy of Sciences under grant no. 1/0685/21 and by the Slovak Research and Development Agency under Contract no. APVV-22-0414.

REFERENCES

- [1] Ajao, O., Bhowmik, D., & Zargari, S. (2019, May). Sentiment aware fake news detection on online social networks. In *ICASSP 2019-2019 IEEE International*
- [2] Hameleers, M., van der Meer, T. G., & Dobber, T. (2024). Distorting the truth versus blatant lies: The effects of different degrees of deception in domestic and foreign political deepfakes. *Computers in Human Behavior*, 152, 108096.
- [3] Dixit, A., Kaur, N., & Kingra, S. (2023). Review of audio deepfake detection techniques: Issues and prospects. *Expert Systems*, 40(8), e13322.
- [4] Amal, N., Ridouani, M., Salahdine, F., & Kaabouch, N. Deepfake Attacks: Generation, Detection, Datasets, Challenges, and Research Directions. *Computers*, 2023. Vol. 12. No. 10.

- [5] Bohacek, M., & Farid, H. (2024). Lost in Translation: Lip-Sync Deepfake Detection from Audio-Video Mismatch. In *Proceedings of the IEEE/CVF Conference on Computer Vision and Pattern Recognition* (pp. 4315-4323).
- [6] Karras, T. (2019). A Style-Based Generator Architecture for Generative Adversarial Networks. *arXiv preprint arXiv:1812.04948*.
- [7] Rombach, R., Blattmann, A., Lorenz, D., Esser, P., & Ommer, B. (2022). High-resolution image synthesis with latent diffusion models. In *Proceedings of the IEEE/CVF conference on computer vision and pattern recognition* (pp. 10684-10695).
- [8] Zhu, J. Y., Park, T., Isola, P., & Efros, A. A. (2017). Unpaired image-to-image translation using cycle-consistent adversarial networks. In *Proceedings of the IEEE international conference on computer vision* (pp. 2223-2232).
- [9] Lee, C. H., Liu, Z., Wu, L., & Luo, P. (2020). Maskgan: Towards diverse and interactive facial image manipulation. In *Proceedings of the IEEE/CVF conference on computer vision and pattern recognition* (pp. 5549-5558).
- [10] Simonyan, K., & Zisserman, A. (2014). Very deep convolutional networks for large-scale image recognition. *arXiv preprint arXiv:1409.1556*.
- [11] Huang, G., Liu, Z., Van Der Maaten, L., & Weinberger, K. Q. (2017). Densely connected convolutional networks. In *Proceedings of the IEEE conference on computer vision and pattern recognition* (pp. 4700-4708).
- [12] He, K., Zhang, X., Ren, S., & Sun, J. (2016). Deep residual learning for image recognition. In *Proceedings of the IEEE conference on computer vision and pattern recognition* (pp. 770-778).
- [13] Redmon, J. (2016). You only look once: Unified, real-time object detection. In *Proceedings of the IEEE conference on computer vision and pattern recognition*.
- [14] Howard, A. G. (2017). Mobilenets: Efficient convolutional neural networks for mobile vision applications. *arXiv preprint arXiv:1704.04861*.
- [15] Tan, M., & Le, Q. (2019, May). Efficientnet: Rethinking model scaling for convolutional neural networks. In *International conference on machine learning* (pp. 6105-6114). PMLR.
- [16] Liu, Z., Mao, H., Wu, C. Y., Feichtenhofer, C., Darrell, T., & Xie, S. (2022). A convnet for the 2020s. In *Proceedings of the IEEE/CVF conference on computer vision and pattern recognition* (pp. 11976-11986).
- [17] Vaswani, A., Shazeer, N., Parmar, N., Uszkoreit, J., Jones, L., Gomez, A. N., ... & Polosukhin, I. (2017). Attention is all you need. *Advances in neural information processing systems*, 30.
- [18] Wang, A., Singh, A., Michael, J., Hill, F., Levy, O., & Bowman, S. R. (2018). GLUE: A multi-task benchmark and analysis platform for natural language understanding. *arXiv preprint arXiv:1804.07461*.
- [19] Houshy, N., Giurgiu, A., Jastrzebski, S., Morrone, B., De Laroussilhe, Q., Gesmundo, A., ... & Gelly, S. (2019, May). Parameter-efficient transfer learning for NLP. In *International conference on machine learning* (pp. 2790-2799). PMLR.
- [20] Devlin, J., Chang, M. W., Lee, K., & Toutanova, K. (2019, June). Bert: Pre-training of deep bidirectional transformers for language understanding. In *Proceedings of the 2019 conference of the North American chapter of the association for computational linguistics: human language technologies, volume 1 (long and short papers)* (pp. 4171-4186).
- [21] Xhlulu. (2020, February 10). *140k real and fake faces*. Kaggle. <https://www.kaggle.com/datasets/xhlulu/140k-real-and-fake-faces>

Exploring the Potential of Docker for Edge AI and IoT Applications

¹*Lubomír URBLÍK*(3rd year),
Supervisor: ²*Peter PAPCUN*

^{1,2}Dept. of Cybernetics and Artificial Intelligence, FEEL, Technical University of Košice, Slovak Republic

¹lubomir.urblik@tuke.sk, ²peter.papcun@tuke.sk

Abstract—With the ever-increasing amount of data produced daily, the need for edge computing increases, too. Processing the data closer to the source allows for faster results, increased privacy, and lower bandwidth. The devices created for these tasks differ significantly and come with issues of incompatible software. Docker offers a way to unify the environments of various devices, significantly increasing their compatibility. These devices are often limited in performance due to low power consumption, which can be both an advantage and a disadvantage. We looked at the performance of various edge computing devices and compared their performance and power consumption. These results were then used to compare the performance of Docker containers versus native.

Keywords—data processing, Docker, edge computing, IoT

I. INTRODUCTION

The onset of edge computing as a solution to cloud computing's issues brings many challenges. The variety of devices alone is not seen in more server-oriented solutions. The devices range from small - smaller than a credit card - SBCs (Single Board Computers) to fully featured Mini-PCs. Devices commonly use AMD64 or ARM64 CPUs, with RISC-V slowly coming onto the scene. The traditional server space is still dominated by AMD64, with more than 95% market share [1]. ARM64 represents only 3.9% market share, with Amazon - more specifically Amazon Web Services - owning around half of all ARM64 server-grade CPUs [2]. Edge environments are the opposite. ARM64 is present in virtually every mobile phone and tablet. The ratio starts to change regarding more PC-like offerings, as many popular devices use either architecture. This leads to an incompatibility with specific software, as running AMD64 software on ARM64 devices and vice versa natively is impossible. There are emulators or translators, but these come with performance penalties. Docker allows us to build cross-platform applications quickly and provides better compatibility with various edge devices.

II. THE INITIAL STATUS

Two years ago [3], we introduced the idea of splitting a data processing workload across multiple devices at the network's edge or in the cloud. The main goal was the reduction of latency, with tasks being divided intelligently. We described different approaches to load balancing, task distribution, and task offloading.

Our initial idea ran into an issue with the monolithic approach to software development currently present in edge computing. We proposed a data processing framework based

on containers to address this issue. We drew inspiration from Directed Acyclic Graphs, where the tasks are represented as nodes and the data flow as edges. This allows for an easy-to-understand visualization of the steps performed to process the data.

The microservice architecture, which became popular with the onset of cloud computing, has services which are anything but micro. To address this inconsistency, nanoservices were created as the tiny parts of a more extensive application [4]. Instead of a service with multiple endpoints, we have multiple services, each with a single endpoint and functionality. Our solution relied on ZMQ as the communication backbone between services hosted in separate Docker containers for easy deployment across devices.

III. THE TASKS SOLVED IN THE PREVIOUS YEAR

We started the last year with a thorough study of different use cases of edge intelligence and edge computing in general across various industries, with the results being published as a review paper [5]. This provided us with a better understanding of the problems arising in different areas of research and development.

We are also actively expanding the services offered by our data processing platform [6]. The first addition was a normalization service. Many tasks require the data to be normalized to prevent skewed results. The user can set the lower and upper boundaries, and the values are normalized before being sent further. The second addition was an expansion of the filtering service. There are cases in which the data sent from the sensor is incorrect, e.g., the temperature sensor showing 999 °C. The user can, therefore, set a lower and upper boundary, and any values outside of this range are ignored. The next addition is the notification service, which allows us to send emails based on detected values. This service works as an extension of the filtering service and allows the user to set values which should trigger the notification email. We originally wanted to implement a self-hosted email server, but this proved too complicated, so we opted for Google Mail. Google offers a Python SDK (Software Development Kit), which can be used to write and send emails, but we did not want our solution to be tied to the email provider used, so we opted for an SMTP (Simple Mail Transfer Protocol) library instead. SMTP is a standard protocol used for sending emails. Google and other email providers provide an API (Application Programming Interface) endpoint to which we can send our data. Another

TABLE I
BENCHMARK SUITE RESULTS

	Raspberry Pi 5	ODROID H4+	Orange Pi 5 Plus	VisionFive 2
Average benchmark duration	557.45 ms	342.50 ms (-38.56%)	638.50 ms (14.54%)	3456.30 ms (520.02%)
Average standard deviation	3.15%	11.66%	3.11%	2.25%
Average benchmark duration (Docker)	-0.41%	-3.69%	0.05%	DNF
Average standard deviation (Docker)	2.74%	2.71%	2.81%	DNF

TABLE II
POWER CONSUMPTION METRICS OF USED DEVICES (NATIVE)

	Raspberry Pi 5	ODROID H4+	Orange Pi 5 Plus	VisionFive 2
Total energy	14.872 Wh	12.539 Wh	11.036 Wh	69.764 Wh
Average duration	10 781 s	6 651 s	11 889 s	67 300 s
Average power consumption	4.97 W	6.79 W	3.34 W	3.73 W

addition was the option of loading the data directly from a database. SQLAlchemy, an object-relational mapper, serves as the core of this service. MySQL and PostgreSQL, the two databases we selected, require different libraries to connect. There are also some slight differences in their respective syntaxes, which we can circumvent using SQLAlchemy.

We are currently working on services for AI models, allowing us to load the model and seamlessly integrate it into our solution. We have already implemented simpler machine learning models, specifically k-means, k-NN, and regression.

Another part of our work is the GUI for deploying the services. We have selected NODE-Red as it provides an easily expandable platform with all the features we require. We are currently adding our custom nodes, i.e. services, and then exporting them in JSON format with all the settings and edges to use in deployment.

Another part of our research focused on the performance comparison of Docker containers versus native deployment. Our understanding of how containers work led us to believe there should be no measurable difference, but our testing showed us something different. We have selected the PyPerformance benchmark suite, which offers various tests that represent typical Python workload and utilize commonly used libraries. The entire suite was run multiple times on Raspberry Pi 5, Orange Pi 5, ODROID H4+, and StarFive VisionFive 2. Each device was running the latest version of the vendor-recommended/provided OS. The runs' results are presented in TABLE I, where the values for Raspberry Pi 5 native are in absolute format and serve as a baseline value. The other values are then compared to the baseline. The Docker values are compared to the native values of each device. The testing compares containers' performance vs native, the performance differences between devices, and their power consumption. Edge devices may be placed in tight spaces, e.g., cars, where they are harder to cool. They might also be powered by batteries or low-wattage power sources. These constraints make the device's power consumption an important factor to consider. Orange Pi 5 Plus had the lowest wattage at 3.34 W. Raspberry Pi 5, one of the most used edge devices, was 14.54% faster, but had an almost 49% increase in wattage, making it harder to cool. The total energy used to run the entire suite was also lower on the Orange Pi 5. ODROID H4+ had the highest wattage at 6.79 W but was also much faster, resulting in total energy usage between Raspberry Pi 5 and Orange Pi 5 Plus. VisionFive 2 was the lowest-performing device in our testing, resulting in high total energy usage, as each suite run took almost 19 hours.

One of the application areas of edge computing is robotics – in our case, drones. We have developed a computer vision-based algorithm for automated drone landing on a moving ground vehicle [7]. The algorithm works by using the drone's camera and utilizing simple computer vision techniques to process the image and find the mark placed on the ground vehicle. Each rotor is controlled separately, and the drone slowly descends, keeping the target in its sights until it lands.

IV. FUTURE WORK

Soon, we would like to finish the features described in the previous section and deploy our platform on multiple edge devices. The testing of our solution will focus on the total latency introduced by splitting the application into multiple parts and deploying it on multiple devices compared to a monolith deployed on a single device. The benchmarks we have performed on our edge devices show us that it is possible to achieve better performance from existing Docker images, so we will optimize them for our use cases.

ACKNOWLEDGMENT

This publication was supported by the APVV grant ENISaC - Edge-eNabled Intelligent Sensing and Computing (APVV-20-0247).

REFERENCES

- [1] B. Bajarín, "Arm in the data center: The dawn of a new era - creative strategies," 10 2024. [Online]. Available: <https://creativestrategies.com/arm-in-the-data-center-the-dawn-of-a-new-era/>
- [2] D. Robinson, "Who has over half all arm server cpus in the world? amazon," 8 2023. [Online]. Available: https://www.theregister.com/2023/08/08/amazon_arm_servers/
- [3] Urblik, "Load distribution in container-based edge computing," in *23rd Scientific Conference of Young Researchers Proceedings from Conference*. Košice, Slovakia: Faculty of Electrical Engineering and Informatics, Technical University of Košice, 2023, p. 158–161.
- [4] J. J. López Escobar, R. P. Díaz-Redondo, and F. Gil-Castiñeira, "Unleashing the power of decentralized serverless iot dataflow architecture for the cloud-to-edge continuum: a performance comparison," *Annals of Telecommunications*, vol. 79, no. 3–4, p. 135–148, 4 2024. [Online]. Available: <https://link.springer.com/10.1007/s12243-023-01009-x>
- [5] L. Urblik, E. Kajati, P. Papcun, and I. Zolotová, "Containerization in edge intelligence: A review," *Electronics*, vol. 13, no. 7, p. 1335, 4 2024. [Online]. Available: <https://www.mdpi.com/2079-9292/13/7/1335>
- [6] L. Urblik, S. Čorbová, E. Kajati, and P. Papcun, "Extending the container of the data processing platform on the edge of the network," *Acta Electrotechnica et Informatica*, 2025.
- [7] A. Zasetska, Urblik, M. Krupáš, E. Kajati, and P. Papcun, "Automated landing of a drone on a moving vehicle using computer vision," in *2025 IEEE 23rd World Symposium on Applied Machine Intelligence and Informatics (SAMII)*, Stará Lesná, Slovakia, 2025.

Calculation of Transient Dynamic Ampacity in the Conditions of the Slovak Electricity Transmission System

¹František Margita (2nd year),
Supervisor: ²Lubomír Beňa

^{1,2}Department of Electric Power Engineering, FEI, Technical University of Košice, Slovak Republic

¹frantisek.margita@tuke.sk, ²lubomir.bena@tuke.sk

Abstract—This article and previous research have highlighted the advantages of applying dynamic line rating (DLR), primarily the deployment of steady-state and transient DLR. Factors such as weather, type, cross-section, and conductor aging affecting ampacity have been addressed. Input parameters for DLR models have been analyzed to ensure the most optimal transmission capacity of OHTLs in the conditions of the Slovak electricity transmission system and to prevent overloading.

Keywords—CIGRE 601, conductor emissivity, HTLS ACCC, transient dynamic ampacity.

I. INTRODUCTION

The transmission capacity of overhead transmission lines (OHTLs) is the primary parameter of the transmission capacity indicator to ensure the efficiency and effectiveness of the transmission system. Increasing demands for reliability, quality and optimization from the point of view of economic, environmental and technical factors bring new opportunities and challenges. The practical and academic community is looking for solutions that will provide fast, safe and easy-to-deploy solutions in the era of expansion and trends in the electric power industry. Increasing ampacity is one of the options to achieve these goals from a long-term perspective [1].

Despite these challenges, the Slovak electricity transmission system is still considering a conservative pragmatic approach of static line rating (SLR) as the current load limits of OHTLs. The deployment of DLR following the example of other transmission systems is a promising way. DLR considers real operational parameters such as geographical, astronomical and meteorological inputs [2].

Our research focuses on DLR under the conditions of the Slovak electricity transmission system using the CIGRE Technical Brochure 601 methodology. The research aims at a model for predicting ampacity in real conditions with high robustness for power transmission on interstate OHTLs [3].

II. BACKGROUND AND PROGRESS

Before this year, our research was focused on gaining knowledge about the thermal behavior of conductors from theoretical knowledge and their subsequent application to real OHTL. The key aspects of our research included [4], [5], [6], [7], [8], [9]:

- 1) Review of international standards for ampacity calculation, specifically CIGRE 601.

- 2) Analysis of the use of wide area monitoring systems (WAMS) for calculating conductor temperature.
- 3) Calculation of SLR according to the STN EN 50341-2-23 standard and steady-state DLR for comparing static limits with dynamically changing ampacity.
- 4) Deployment of alternative conductors, such as high temperature low sag and aluminum conductor composite core (HTLS ACCC), instead of the current aluminum conductor steel reinforced (ACSR) conductors used in the Slovak electricity transmission system.
- 5) Application of this knowledge to the OHTL V427 Rimavská Sobota – Moldava for the preparation of a dynamic ampacity system.

III. RECENT ACHIEVEMENTS

Over the past year, significant progress has been made in creating a mathematical model for calculating transient conductor temperature based on the CIGRE 601 Technical Brochure. This model consists of [3], [9], [10]:

- 1) Algorithm for calculating the steady-state temperature of a conductor (Fig. 1).
- 2) Algorithm for calculating the transient conductor temperature, also known as temperature tracking (Fig. 2).
- 3) The algorithm itself for calculating the transient dynamic ampacity with respect to (Fig. 3):
 - a) Type and cross-section of the conductor.
 - b) Aging of the conductor.
 - c) Meteorological conditions.
 - d) Current load.

The transient DLR was calculated in the conditions of the Slovak electricity transmission system for their most commonly used ACSR conductors and their alternative HTLS ACCC. Initially, it was taken into account against the set parameters of the STN. Subsequently, the impact of meteorological conditions on transient DLR was analyzed, namely the intensity of solar radiation, ambient temperature, direction and wind speed. The model was also extended to include the significance of accurate absorptivity and emissivity measurements in DLR calculations. Finally, the model was used in real meteorological conditions for a selected summer and winter day.

All of this knowledge gained is in the process of being accepted for publication in the journal Electric Power Systems Research.

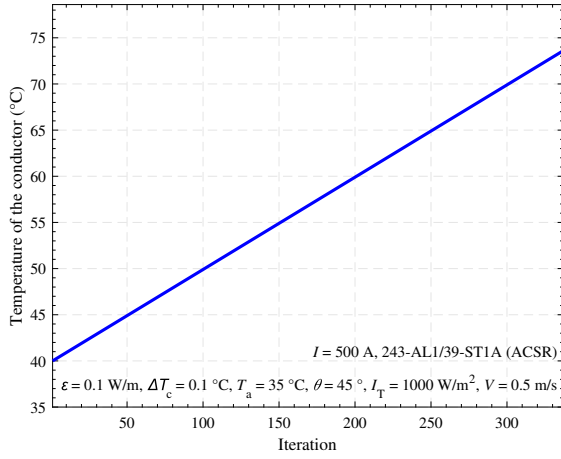


Fig. 1. Calculation of the steady-state temperature of an ACSR conductor under selected meteorological conditions and given calculation accuracy

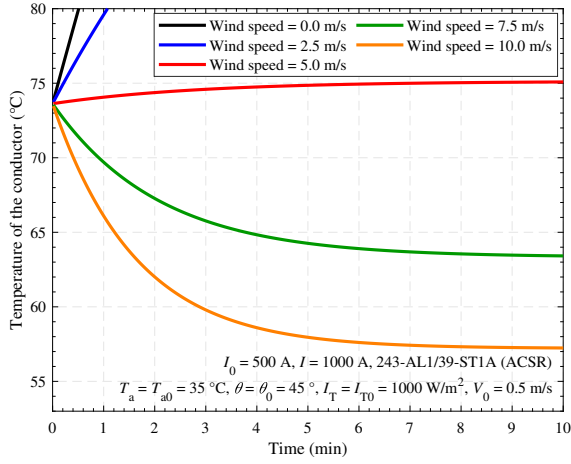


Fig. 2. Determination of transient temperature variations in an ACSR conductor under varying wind speeds over a 10-minute interval

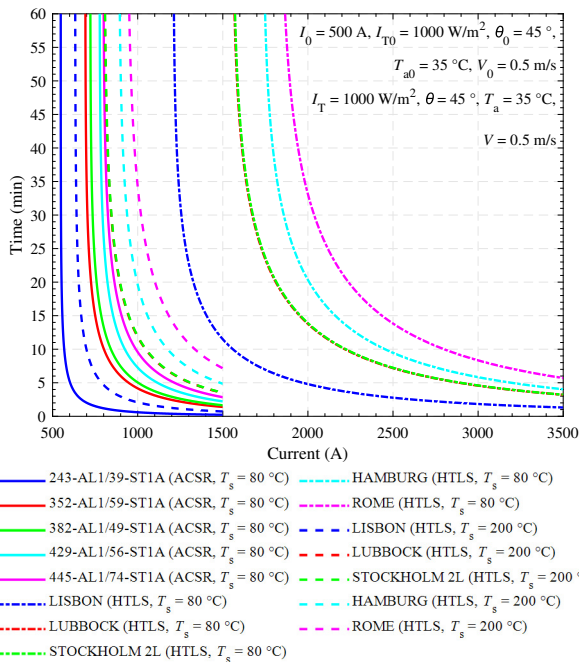


Fig. 3. Transient DLR of ACSR and HTLS ACCC conductors under specified conditions

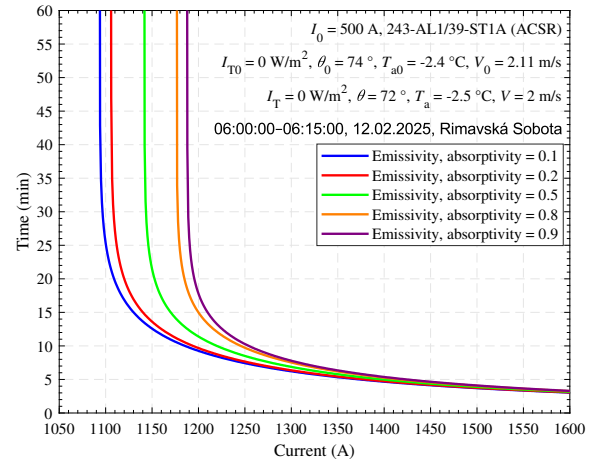


Fig. 4. Calculation of transient DLR for ACSR conductor for different emissivity values on a winter day at a current overload value of 15 minutes

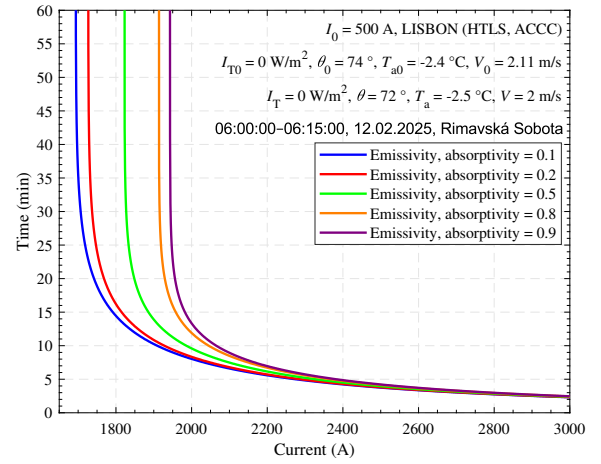


Fig. 5. Calculation of the transient DLR for the HTLS ACCC conductor for different emissivity values on a winter day at a current overload value of 15 minutes

TABLE I
ANALYSIS OF ACSR AND HTLS ACCC CONDUCTOR AMPACITY UNDER TRANSIENT OVERCURRENT CONDITIONS OVER A 15-MINUTE PERIOD, CONSIDERING DIFFERENT EMISSIVITY COEFFICIENTS IN WINTER-DAY OPERATING SCENARIOS

Emissivity, Absorptivity	Ampacity (A)	
	ACSR ($T_s = 80^\circ\text{C}$)	HTLS ACCC ($T_s = 200^\circ\text{C}$)
0.1	1130	1792
0.2	1140	1815
0.5	1170	1886
0.8	1200	1958
0.9	1210	1982

IV. RESULTS

Under SLR conditions, HTLS ACCC conductors are more advantageous than used ACSR conductors in transient DLR, sustaining higher currents for longer durations. ACSR conductors in the specified conditions overheated quickly, limiting overloads to 5–20 minutes, while at 1200–1500 A, duration dropped significantly. HTLS ACCC conductors sustained

2000–2500 A for up to 35 minutes at their maximum temperature of 200 °C (Fig. 3).

Aging of the conductor has been shown to positively affect ampacity (Table I). For a 15-minute overload during winter, ACSR current increased by 7.1% (1130 A to 1210 A, Fig. 4), while HTLS ACCC improved by 10.6% (1792 A to 1982 A, Fig. 5). The consequence of the lower heating of HTLS ACCC conductors is due to their material properties, which have lower resistivity losses R_{AC20C} and a better overall thermal product – consisting of a lower weight m , thermal coefficient of specific thermal capacity β , specific thermal capacity c of the core and conductor sheath.

V. FUTURE PLANS

The following steps of the work and research will deal with:

- 1) Creation of software for determining dynamic steady-state and dynamic transient ampacity based on the proposed mathematical model.
- 2) Technical and economic evaluation of the proposed solutions for increasing the transmission capabilities of lines and recommendations for practice.
- 3) Verification of the developed models and software in real conditions in the OHTL ampacity analysis laboratory at the Lublin University of Technology.

VI. CONCLUSION

This paper and the doctoral student's previous work have highlighted the advantages and benefits of applying DLR and HTLS ACCC as an alternative to ACSR conductors to increase the ampacity of OHTLs. HTLS ACCC has been proven to exceed the limits of ACSR conductors. Their higher thermal resistance allows them to carry higher currents both in steady state DLR conditions and in current overload conditions during transient DLR. Taking these benefits into account opens up the prospect of deploying an economic, technical and environmental solution.

ACKNOWLEDGMENT

This paper was supported by the Science Grant Agency of the Ministry of Education, Research, Development and Youth of the Slovak Republic under the contract VEGA 1/0532/25.

REFERENCES

- [1] W. Malska, "Analysis of current ampacity of the 110 kv overhead transmission line using a multiple regression model," *Electric Power Systems Research*, vol. 236, p. 110939, 2024. [Online]. Available: <https://www.sciencedirect.com/science/article/pii/S0378779624008253>
- [2] J. Bendik, M. Cenky, L. Racz, and B. Nemeth, "Static line rating of overhead power lines in various european countries," in *2024 24th International Scientific Conference on Electric Power Engineering (EPE)*, 2024, pp. 1–5.
- [3] CIGRE Working Group B2.42, "Guide for thermal rating calculations of overhead lines," CIGRE Technical Brochure 601, Tech. Rep., 2014.
- [4] F. Margita, L. Bena, and P. Pijarski, "Calculation of the ampacity of overhead power lines under the conditions of the electric power system of the slovak republic," in *2024 24th International Scientific Conference on Electric Power Engineering (EPE)*, 2024, pp. 1–5.
- [5] F. Margita, L. Bena, W. Malska, and P. Pijarski, "Possibilities of increasing the ampacity of overhead lines using high-temperature low-sag conductors in the electric power system of the slovak republic," *Applied Sciences*, vol. 14, no. 17, p. 7846, 2024. [Online]. Available: <https://doi.org/10.3390/app14177846>
- [6] F. Margita, "Use of wam systems to determine the ampacity of overhead transmission lines," in *24th Scientific Conference of Young Researchers: Proceedings from Conference*. Košice, Slovakia: Technical University of Kosice, 2024, pp. 117–120. [Online]. Available: <https://scyr.fei.tuke.sk/index.php/proceedings>

- [7] F. Margita and L. Bena, "Determination of the ampacity of external lines in the conditions of the electricity system of the slovak republic," *Elektroenergetika: International Scientific and Professional Journal on Electrical Engineering*, vol. 17, no. 1, pp. 23–26, 2024. [Online]. Available: <https://jeen.fei.tuke.sk/index.php/jeen/article/view/558>
- [8] —, "The use of wam systems for determining the ampacity of overhead power lines," *Acta Universitatis Sapientiae, Electrical and Mechanical Engineering*, vol. 16, pp. 96–109, 2024.
- [9] F. Margita, "Utilization of wams for determining the ampacity of overhead transmission lines," Kosice, Slovakia, January 2025.
- [10] J.-R. Riba, Y. Liu, and M. Moreno-Eguilaz, "Analyzing the role of emissivity in stranded conductors for overhead power lines," *International Journal of Electrical Power & Energy Systems*, vol. 159, p. 110027, 2024. [Online]. Available: <https://www.sciencedirect.com/science/article/pii/S0142061524002485>

Phishing Vishing and Deepfake Attacks in the Context of Emerging Cyber Threats

¹Miroslav MURIN (2st year),
Supervisor: Miroslav MICHALKO

^{1,2}Dept. of Computers and Informatics, FEI TU of Košice, Slovak Republic

¹miroslav.murin@tuke.sk, ²miroslav.michalko@tuke.sk

Abstract—The rise of phishing, vishing, hoaxes, and deepfake technologies has intensified cybersecurity challenges, exploiting both human vulnerabilities and AI-driven automation to deceive users and compromise digital security. Traditional defenses are increasingly ineffective as cybercriminals leverage generative AI models like GANs, VAEs, and diffusion models to create hyper-realistic fraudulent content. This research explores AI-driven detection and prevention mechanisms, utilizing machine learning, computer vision, and security analytics to enhance real-time fraud detection. It also assesses the risks associated with AI-powered image generation tools such as Stable Diffusion, Leonardo.Ai, Adobe Firefly, and DALL·E. By integrating advanced AI security solutions, regulatory frameworks, and cybersecurity awareness, this study aims to mitigate digital threats and strengthen trust in online environments.

Keywords—Cybersecurity, Phishing, Deepfake, Generative AI

I. INTRODUCTION

Cybersecurity has become one of the most critical challenges of the digital era, characterized by continuous technological advancements and increasing global connectivity. However, there is also growing reliance on digital platforms and broad availability of information which have resulted in a surge in digital threats. Among the most serious security concerns today are phishing, vishing, hoaxes, and deepfake technologies which exploit human as well as technological vulnerabilities to manipulate and deceive users. These risks and challenges not only erode trust and confidence in the cyberspace but also threaten individuals, corporations, and even national security.

Phishing and vishing represent sophisticated forms of social engineering attacks that rely on psychological manipulation to obtain sensitive information such as passwords, financial data, or authentication credentials. A study [1] shows that phishing and vishing are among the most common forms of attacks, and their sophistication is increasing thanks to modern technologies such as artificial intelligence. As noted in [2], human errors are often the main cause of problems in technology implementations, and humans are generally considered to be the weakest link in information security.

The emergence of deepfake technology, powered by generative models like Generative Adversarial Networks (GANs), Variational Autoencoders (VAEs), and diffusion models, has introduced a new level of complexity in digital fraud. Deepfakes can generate hyper-realistic fake images, videos, and audio, which are often indistinguishable from authentic media. This technology has been exploited for malicious purposes, including misinformation campaigns, impersonation fraud, and

digital identity theft, thereby raising concerns over media authenticity and information credibility. Hoaxes and misinformation disseminated through social media further exacerbate these risks, contributing to public distrust and manipulation.

The primary motivation behind this research is to develop advanced AI-driven detection and prevention mechanisms to combat these cyber threats. By leveraging state-of-the-art machine learning models, computer vision techniques, and AI-driven security analytics, this research aims to enhance real-time fraud detection and strengthen digital trust. In [3], the authors reveal that deep learning techniques outperform traditional rule-based and machine learning methods, achieving higher detection rates with fewer false positives.

II. SOCIAL ENGINEERING ATTACKS

In the modern digitally connected world, the human factor has become the most significant issue in terms of cyber security vulnerability. Social engineering uses psychological manipulation to trick people into divulging confidential information or acting in a way that compromises security. It circumvents technical security controls by exploiting users' underlying trust and behavioural patterns. Of these, phishing and vishing are among the most prevalent forms of social engineering.

A. Phishing

Phishing is a method of cyber-attack that involves sending deceptive messages, usually emails or messages pretending to come from trusted sources. The aim is to trick individuals into divulging sensitive information such as usernames, passwords and credit card details, or to install malware on their devices.

APWG, an organisation that issues regular reports on phishing, said in its Q2 2024 report [4] that it had identified 877,536 phishing attacks. The trend of attacks has been stable for a period of time. They also reported that phishing attacks via phone calls and text messages are increasingly being used to attack bank customers and payment service users. In figure 1, we can see the percentage of the types of phishing attacks.

Pretexting is a social engineering technique in which the attacker creates a false narrative to gain the victim's trust. He or she may pretend to be a bank employee, customer service representative, or other important person to convince the victim that sharing sensitive data is legitimate. According to the authors in [5], the threat of Pretexting is rapidly increasing due to the improving quality of generative AI. Thanks to it, the fake story and text is constantly improving

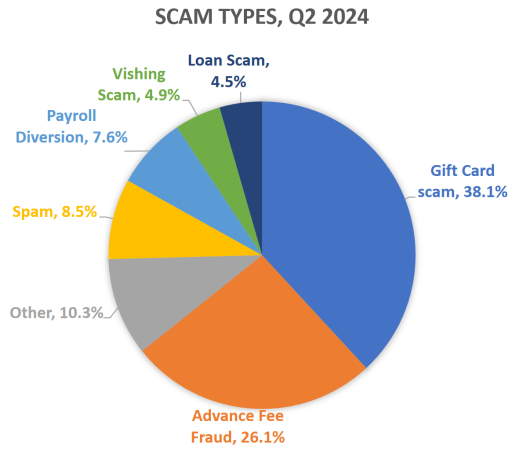


Fig. 1. Types of fraud in Q2 2024 according to APWG [4]

and it is becoming more and more difficult to distinguish it from the real one. According to the authors in [6], only 25% of the people tested out of all 382 participants were able to detect phishing sites from legitimate ones. According to the authors in [7], more educated people are more able to detect phishing sites. Of all the factors contributing to the successful detection of a phishing threat, computer education is the most important. Several studies such as [6] and [8] claim that gender plays a significant role in the success rate of an attack. According to these authors, women are worse at detecting phishing threats than men.

B. Vishing

According to the authors in [9] Vishing and smishing attacks, or voice phishing attacks, are a type of social engineering attack in which attackers use voice communication channels, such as phone calls or text messages, to trick victims into divulging sensitive information or performing actions that compromise their security. Attackers often impersonate trusted entities such as banks, government agencies or technical support services. As the authors in [10] argue, using social engineering techniques, they manipulate victims to divulge personal information such as passwords, credit card numbers, or social security numbers.

III. EXISTING SOLUTIONS FOR IMAGE GENERATION

Today's widely used models for AI-based image generation are Stable Diffusion, Leonardo.Ai, Adobe Firefly and DALL-E. Stable Diffusion is a powerful tool for generating realistic images from text input, with an emphasis on open source and personalization. Leonardo.Ai provides intuitive tools for generating and editing visual content, supported by a wide range of styles and outputs. Adobe Firefly, integrated into Creative Cloud apps, focuses on making visuals legally unobjectionable and easy to generate. DALL-E, with advanced security mechanisms, is specific in its protection against abuse and its ability to create original artwork. The authors in [11] state that deepfake is a technology that uses artificial intelligence (AI) and machine learning to create realistic multimedia content, such as videos, images, or audio recordings, that manipulates or falsifies reality. The term was coined by combining the words deep learning and fake. According to the authors in [12], given the potential misuse of deepfakes for malicious

purposes, the development of detection techniques and policies to mitigate the harmful effects of deepfakes has become an important area of research.

A. Stable Diffusion

Stable Diffusion is an advanced image generation model based on the diffusion model technique, which is used to synthesize high quality and realistic images from text inputs. As stated by the authors in [13], this model has been developed to provide the general public with access to a powerful image generation tool using artificial intelligence, focusing on efficiency, flexibility and scalability.

Stable Diffusion is also very suitable for creating hoaxes. Since it can be run locally, the model has no limitations and it is possible to edit photos as well. In Figure 2 we see a new image generated based on the original one, where we tried to make the businessman a drug addict.



Fig. 2. Converting a photo of a businessman into a drug addict

In Figure 3 we can see again the function to change the selected part of the image. Now, for a change, to demonstrate the possibilities of what can be done with Stable Diffusion we have changed the businesswoman's dress into a swimsuit.

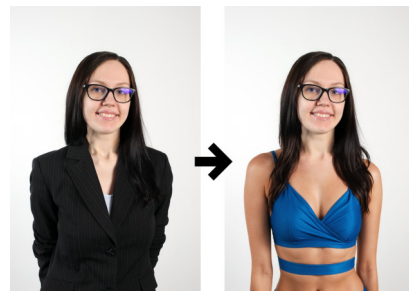


Fig. 3. Use the function to change the selected part of an image

B. Leonardo.Ai

Leonardo.Ai is an advanced platform that uses artificial intelligence to generate high-quality images and videos based on text descriptions. Users can simply enter a description and the platform will create visual content in a variety of styles.

In Figure 4, we can see how we reworked the image by first using the image-to-image tool to dress a particular woman in a formal dress, and then using the canvas editing tool to do the rest of the background. Leonardo.Ai contains several models. The generation of specific elements into the canvas does not always work as expected. For example, it can very easily mess up a hand or generate an object so that it doesn't fit into the background.



Fig. 4. Photo editing with tools in Leonardo.Ai

C. Adobe Firefly

Adobe Firefly is an AI-powered content generation tool developed by Adobe that is integrated into their creative applications such as Photoshop, Illustrator and Adobe Express. It was designed to support the creative process of users by allowing them to generate and edit visual content with simple text input or with visual demos. We also tried to edit the face with AI and do various dirt and a finely grown beard but Firefly can't keep the same face and add details. Every time we tried to edit the face or do detail it generated a face of a completely different person. This is the drawback of Adobe Firefly's artificial intelligence tools

D. DALL-E

DALL-E is an artificial intelligence model developed by OpenAI that generates images based on textual descriptions. The name "DALL-E" is a combination of the name of the artist Salvador Dali and the robot WALL-E, referring to the fusion of the art and technology worlds. When we tried to edit different photos, DALL-E never generated a real photo for us. It would always generate a completely different face in an artistic style even after being tasked to generate a real person without the artistic style. DALL-E has high protection against misuse for illegal activities and therefore DALL-E cannot be used for generating hoaxes.

IV. FUTURE RESEARCH

In future research, we plan to focus on the development and training of advanced machine learning models capable of detecting manipulated or artificially generated content. Specifically, the goal is to create a detection system that can determine whether a given audio recording is authentic or synthetically generated, and similarly, whether an image is real or AI-generated. This will involve the use of deep learning techniques in the fields of audio forensics and computer vision, leveraging large datasets of both genuine and fake samples. The resulting models will aim to combat deepfakes and other forms of digital deception.

V. CONCLUSION

The rapid advancement of digital technologies has brought unprecedented security challenges, with phishing, vishing, hoaxes, and deepfake technologies emerging as significant threats. These attacks exploit both human vulnerabilities and AI-driven automation, eroding trust in digital spaces and endangering individuals, organizations, and national security. The increasing sophistication of phishing and vishing, enabled by AI, makes traditional security measures insufficient, highlighting the need for advanced detection and prevention mechanisms.

Deepfake technology, powered by generative models like GANs and diffusion models, has escalated the risks of misinformation, identity fraud, and media manipulation. The widespread availability of AI-based image generation tools, such as Stable Diffusion and Leonardo.Ai, raises concerns about their potential misuse for hoaxes and digital fraud. As noted in [14], hoax news has long been a problem for society that is quite worrying because receiving hoax news can change a person's point of view to something that is not good, the impact of which is detrimental to many individuals and groups of people. While security measures like metadata analysis and forensic detection have been proposed, continuous innovation in AI-driven detection is crucial to counter these evolving threats.

To mitigate these risks, this research emphasizes AI-enhanced cybersecurity solutions that integrate machine learning, computer vision, and fraud analytics to detect and prevent cyber threats in real time. A combination of technological innovation, policy interventions, and user education is vital to strengthening digital trust and ensuring a more secure cyber environment.

ACKNOWLEDGMENT

This work was supported by Cultural and Educational Grant Agency (KEGA) of the Ministry of Education, Science, Research and Sport of the Slovak Republic under the project No. 004ŽU-4/2024.

REFERENCES

- [1] B. B. Gupta, A. Tewari, A. K. Jain, and D. P. Agrawal, "Fighting against phishing attacks: state of the art and future challenges," *Neural Computing and Applications*, vol. 28, no. 12, pp. 3629–3654, Mar. 2016.
- [2] S. Abraham and I. Chengalur-Smith, "An overview of social engineering malware: Trends, tactics, and implications," *Technology in Society*, vol. 32, no. 3, pp. 183–196, Aug. 2010.
- [3] G. H B and G. H L, "Detection of phishing activities using deep learning approaches," in *2025 17th International Conference on COMMunication Systems and NETWORKS (COMSNETS)*. IEEE, Jan. 2025, pp. 808–810.
- [4] (2024, Q2) Phishing activity trends report. APWG. [Online]. Available: https://docs.apwg.org/reports/apwg_trends_report_q2_2024.pdf
- [5] M. Schmitt and I. Flechais, "Digital deception: generative artificial intelligence in social engineering and phishing," *Artificial Intelligence Review*, vol. 57, no. 12, Oct. 2024.
- [6] C. Iuga, J. R. C. Nurse, and A. Erola, "Baiting the hook: factors impacting susceptibility to phishing attacks," *Human-centric Computing and Information Sciences*, vol. 6, no. 1, Jun. 2016.
- [7] S. M. Albladi and G. R. S. Weir, "User characteristics that influence judgement of social engineering attacks in social networks," *Human-centric Computing and Information Sciences*, vol. 8, no. 1, Feb. 2018.
- [8] T. Halevi, J. Lewis, and N. Memon, "Phishing, personality traits and facebook," 2013.
- [9] Z. H. Phang, W. M. Tan, J. S. Xiong Choo, Z. K. Ong, W. H. Isaac Tan, and H. Guo, "Vishguard: Defending against vishing," in *2024 8th Cyber Security in Networking Conference (CSNet)*. IEEE, Dec. 2024, pp. 108–115.
- [10] M. E. Armstrong, K. S. Jones, and A. S. Namin, "How perceptions of caller honesty vary during vishing attacks that include highly sensitive or seemingly innocuous requests," *Human Factors: The Journal of the Human Factors and Ergonomics Society*, vol. 65, no. 2, pp. 275–287, May 2021.
- [11] S. Alanazi and S. Asif, "Exploring deepfake technology: creation, consequences and countermeasures," *Human-Intelligent Systems Integration*, vol. 6, no. 1, pp. 49–60, Sep. 2024.
- [12] S. Sadhya and X. Qi, "Enhanced deepfake detection leveraging multi-resolution wavelet convolutional networks," in *2024 IEEE International Conference on Big Data (BigData)*. IEEE, Dec. 2024, pp. 8241–8243.
- [13] R. Nikam, M. Chouk, T. Mestry, A. Mahajan, A. Menon, and I. Mathane, *Stable Diffusion: A Robust Approach for Image Generation*. Springer Nature Singapore, 2024, pp. 373–391.
- [14] M. Benedict and E. B. Setiawan, "Hoax detection on social media with convolutional neural network (cnn) and support vector machine (svm)," in *2023 11th International Conference on Information and Communication Technology (ICoICT)*. IEEE, Aug. 2023, pp. 361–366.

Electricity price prediction: Overview, data analysis and future research

¹František KURIMSKÝ (1st year)
Supervisor: ²Roman CIMBALA

^{1,2}Dept. of Electric Power Engineering, FEI, Technical University of Košice, Slovak Republic

¹frantisek.kurimsky@tuke.sk, ²roman.cimbala@tuke.sk

Abstract— The electricity market has become volatile in recent years due to increased renewable energy and geopolitical tensions. This paper reviews existing research on electricity price forecasting, examining key methods such as deep learning, hybrid models, and probabilistic approaches. It also explores various market modeling tools, including PyPSA, Plexos, and OSeMOSYS, assessing their capabilities in market modeling. The study also examines the accessibility of electricity market data from various sources and outlines future research directions, particularly the integration of machine learning with energy market models.

Keywords—Electricity market, Market modeling, Neural networks, Price forecasting, Renewable energy

I. INTRODUCTION

The electricity market has experienced increased volatility, primarily driven by the growth of renewable energy sources like solar, wind, etc. The COVID-19 pandemic and the war in Ukraine have also contributed to this instability. Oil prices have become more unpredictable as Europe relies on LNG delivered via tankers. This shift in energy dynamics has further amplified price fluctuations, making it more challenging for market participants to predict electricity costs accurately. These factors have made electricity pricing more uncertain, requiring new forecasting and market modeling approaches.

Electricity prices in Europe are calculated using the Euphemia algorithm. This algorithm has been developed to solve the optimization problem of coupling day-ahead markets (DAMs) participating in Price Coupling of Regions (PCR) region [1]. Each bidding zone submits its demand and supply bids. Orders are divided into hourly, complex, block orders, and specifically for Italy merit and Prezzo Unico Nazionale (PUN) orders. Euphemia considers network representation and also finds optimal solutions for the maximization of social welfare, it works with intercom constraints, line ramping, balance constraints, tariffs, losses, and net position ramping. The output of Euphemia provides prices and net positions for bidding zones and flows per interconnection.

This paper presents an overview of existing research, explores tools for the future direction of our study, and shows the accessibility of relevant data through multiple providers.

II. ANALYSIS OF CURRENT STATUS

1) Literature Review

When searching the Web of Science database for publications related to electricity price prediction, we found

1629 publications added since 2015 [2]. The most productive year for publications is 2024, which shows rising interest in this topic. In this chapter, we look closely at the most cited publications. In TABLE I, we present the most cited publications on electricity price prediction published since 2015.

TABLE I
MOST CITED PUBLICATIONS WITH TOPIC ELECTRICITY PRICE PREDICTION

Ref.	Key Benefits	Journal Quartile	Cited*
[4]	Probabilistic forecasting, quantile regression, ensemble models, load and price prediction, wind and solar forecasting	Q1	650
[5]	Deep learning, DNN, LSTM, GRU, CNN, feature selection, sMAPE evaluation	Q1	409
[6]	Review, bibliometric analysis, probabilistic methods, forecast uncertainty, methodological guidelines	Q1	378
[8]	P2P trading, decentralized markets, energy management	Q1	394
[7]	Electricity price forecasting, economic impact, closed-loop forecasting	Q2	313
[9]	High-resolution load forecasting, ANN, Bayesian regularization, adaptive training, 15-minute intervals	Q1	294
[11]	Hybrid models, wavelet transform, ARMA, extreme learning machine, market volatility, risk management	Q1	299

*Times Cited in all Databases from Web of Science

In [3], the authors summarized the progress of probabilistic energy forecasting, focusing on Global Energy Forecasting Competition. The main contribution of this article for us is the summary of methods top teams use to forecast solar power, wind power, load, and electricity prices. The goal in load forecasting was to predict the hourly load quantiles for a US utility on an ongoing basis. Team “Tololo”, ranking first in forecasting load, used quantile regression and generalized additive models in the referenced paper. Their approach involved a probabilistic temperature forecast for the medium-term and 800 scenarios for the short-term forecast. The aim of forecasting electricity prices was to predict the probabilistic distribution (in quantiles) of electricity prices for one zone for the next 24 hours. The data provided for the forecast included hourly information such as the locational marginal price, zonal load forecasts, and system load forecasts. The winning team, “Tololo”, created a solution based on quantile regression and generalized additive models. They pre-processed spikes for

some models and used Machine Learning Polynomial aggregation. The goal in the case of wind was to predict wind power generation 24 hours ahead for 10 wind farms in Australia. The best solution from team “kPower”, used nonparametric Gradient Boosting Machines (GBM) organized in two layers.

Overfitting was prevented using cross-validation. The input variables included wind speed and direction at 10 and 100 meters. The probabilistic solar power forecast task was similar to the wind forecast, which predicted solar power generation 24 hours ahead for three solar power plants in a region of Australia. Team “Gang-gang” used nonparametric forecasting models Gradient Boosting and k-Nearest Neighbors. Cross-validation was used to prevent overfitting. This research shows the importance of probabilistic approaches and data-driven modeling and helps us navigate in energy markets.

Authors in the publication [4] proposed 4 deep learning models for electricity price prediction in Belgium’s day ahead market. These are Deep Neural Network (DNN), Long-Short Term Memory Deep Neural Network (LSTM-DNN), Convolutional Neural Network (CNN) and Graded Recurrent Unit Deep Neural Network (GRU-DNN). Input for those models included past prices of electricity, day-ahead load forecast and generation from transmission operators in Belgium and France, and external data such as temperature, gas, and coal prices. Symmetric mean absolute percentage error (sMAPE) was chosen as the key metric for evaluation. Proposed models were compared to 23 forecasting methods, traditional statistical approaches, and machine learning models. In this order, results demonstrated 3 deep learning models (DNN, LSTM-DNN and GRU-DNN). Models with deeper architecture were better at capturing relationships. This research highlights the effectiveness of deep learning in electricity price prediction and helps in terms of model creation.

A comprehensive review article [5] highlights rising interest in electricity price prediction. It provides guidelines for properly using methods, measures, and tests when creating forecasting models. Bibliometric analysis shows development over the years and used methods for this topic. In the third section, the authors introduced probabilistic forecasts and four approaches to their construction: historical simulation, distribution-based probabilistic forecasts, bootstrapped prediction intervals, and Quantile Regression Averaging. Point forecast does not consider the rising uncertainty of future prices, generation, or load. Probabilistic forecasting shows possible future scenarios and their likelihood, recognizing the uncertainty. Another review article [6] highlighted energy forecasting as a rapidly evolving field and pointed out that future research should prioritize closed-loop forecasting and predictions should be able to reflect the economic impact of forecast errors.

Authors in [7] proposed a novel peer-to-peer (P2P) energy market platform that introduces a multiclass energy management framework to differentiate energy based on attributes like source (e.g., renewable, local). This approach allows prosumers to value energy based on financial, social, and environmental factors. The authors demonstrate the platform’s effectiveness on the IEEE European Low Voltage Test Feeder, showing its ability to coordinate trading. Finally, future research could use tools from cooperative game-theory to create fair profit-sharing to encourage prosumer

collaboration.

In [8], the authors proposed a forecasting model for day-ahead electricity usage of buildings per 15 minutes. This approach is well-suited for the recent change in the formation of electricity prices from hour intervals to 15 minutes intervals [9]. The most important predictors for electricity consumption were selected using variable importance analysis. The model used in this study is based on an Artificial Neural Network (ANN) with a Bayesian regularization algorithm. The model’s performance was evaluated using data from a commercial building complex. The study examined how training data size and different training methods, static, accumulative, and sliding window, affect accuracy, showing the benefits of adaptive training in dynamic conditions. This research is beneficial for electricity price prediction due to its focus on high-resolution (15-minute) load predictions, and future work could use crucial parameters for electricity price forecasts.

Article [10] introduced a hybrid electricity price forecasting model combining wavelet transform, optimized kernel extreme learning machine (KELM), and autoregressive moving average (ARMA) to address the complex features of electricity prices, enabling it to handle the complex nature of electricity prices through a multi-faceted approach, leading to more accurate forecasts compared to statistical approaches, which are limited to capture market volatility and non-linear patterns. Better accuracy is crucial for traders, providers, and retailers to make better decisions and manage risk in energy markets.

These articles offer a strong background in electricity price prediction, guiding future research directions by highlighting the need for advanced methodologies to capture market complexities.

B. Recent work

In this chapter, we review recent contributions related to electricity price forecasting. We have curated a selection of noteworthy articles to illuminate the emerging trends and innovative approaches in the recent direction of electricity price forecasting. Articles were selected using the Web of Science search, refining results to show publications from 2024 and 2025, and excluding research articles. In TABLE II we present articles with key benefits of their research for our future work.

Authors in [11] proposed a new method based on the Threshold Select Machine (TSM) and Conditional Time Series Generative Adversarial Network (CTSGAN). CTSGAN learns complex temporal dependencies and generates various electricity price scenarios. TSM is a control mechanism that adjusts the input noise threshold to the CTSGAN and introduces weather factors to raise accuracy, fine-tune the prediction, and meet the needed reliability of nominal coverage probability. Combined TSM-CTSGAN outperformed the separated model CTSGAN. The downside of this model is the architecture of 5 deep networks, which is time-consuming to train, and the model does not respond to fluctuations caused by emergencies. The authors compared the model effectiveness of their solution against established models, Bootstrap, LUBE, and Quantile Regression, and outperformed them.

Article [12] presents the L-NBeatsX, a novel interpretable probabilistic prediction model for electricity prices to deal with prediction stability and poor interpretability. L-NBeatsX integrates NBeatsX with LassoNet, enhancing interpretability and precision by selecting influential features. Skip

connections improve robustness, whereas the instability correction factor in the loss function lends more suppleness for a better probability prediction. Validation over four electricity markets suggests that the model is effective, demonstrating improved accuracy and reliability for decision-making.

Authors in [13] developed a hybrid model EAT that combines Empirical Mode Decomposition (EMD), Autoregressive Integrated Moving Average (ARIMA), and Temporal Convolutional Network (TCN), to forecast short-range electricity prices. In this work, EMD decomposes the price data, ARIMA is used to predict low-frequency trends, and TCN is used to forecast high-frequency fluctuations. The model obtained better results than other competitors, with an increase in MAPE values 13.36-42.35% greater than what the most important benchmark methods achieved. Its accuracy, combined with the ability to withstand extreme values and convergence speed, makes EAT a great solution for electricity market participants.

Publication [14] proposed a mixed-frequency forecasting system that combines data resampling, feature selection, feature importance calculation, and machine learning forecasting. The system analyzes the dynamic influence of four weather conditions in Belgium: temperature, humidity, wind gusts, and wind speed. The forecasting performance of the models is assessed as the root mean square error (RMSE), mean absolute error (MAE), sMAPE. Humidity is the most important feature in price prediction compared to temperature, wind gusts, and wind speed. Overall, the factors of humidity and wind gusts can improve predictions.

Models proposed in articles offer valuable insights for future research by improving forecast stability, integrating external factors like weather, and leveraging hybrid approaches.

TABLE II
RECENT SELECTED PUBLICATIONS RESEARCHING ELECTRICITY PRICE PREDICTION

Ref.	Key Benefits	Journal Quartile	Cited*
[12]	Learns temporal dependencies, generates price scenarios, integrates weather factors, outperforms Bootstrap; LUBE; Quantile Regression, TSM-CTSGAN	Q1	5
[13]	Selects key features, improves interpretability, enhances prediction stability, robust skip connections, adaptable probability forecasting, L-NBeatsX	Q1	0
[14]	Decomposes price data, captures low/high-frequency trends, withstands extreme values, fast convergence, EMD-ARIMA-TCN	Q1	8
[15]	Analyzes weather impact, ranks feature importance, humidity as key factor, Mixed-Frequency Forecasting System	Q1	1

*Times Cited in all Databases from Web of Science

C. Tools modeling energy market

In our research, we want to test the benefits of tools for modeling electricity markets, forecasting prices, and optimizing system operations, such as Plexos, PyPSA-Eur and OSeMOSYS in our future solutions. PyPSA-Eur [15] is an open-access model dataset representing the European energy system at the transmission network level, encompassing the entire ENTSO-E region. It includes data on both demand and supply across all energy sectors. This can aid in the

development of pricing models for electric pricing research. Plexos [16] is a comprehensive simulation and optimization software used for modeling energy systems supporting electricity and gas markets, with advanced capabilities for market price forecasting, capacity expansion, and dispatch modeling, making it a valuable tool for energy system analysis. OSeMOSYS [17] is an open-source modeling system used on various scales for long-term energy planning and integrated assessment. The framework is available in Python for detailed power system analysis. These tools are used in the commercial and academic sector, studying new integrations and future scenarios in the energy market.

III. DATA AND ANALYSIS

Electricity market data in Europe is increasingly accessible due to the European Union's promotion of transparency. In this chapter, we describe the main data providers fitted for our future research. EPEX SPOT [18] provides real-time and historical electricity price data for the power spot market, including intraday and day-ahead markets. Energy Charts [19], operated by the Fraunhofer Institute, offers free access to data on electricity production and prices and provides API service for easy access. Montel [20] delivers in-depth market analysis and price forecasts, with some data available for free or through an academic license. ENTSO-E Transparency Platform [21] provides free access to pan-European electricity system data, including generation, load, and cross-border flows. The JAO Publication Tool [22] provides cross-border electricity trading, allocation constraints, and other market data. It manages capacity allocation and congestion data within the European electricity market. In addition to these major data providers, many local platforms, such as OKTE [23] in Slovakia, offer access to country-specific electricity market data. This variety of sources ensures multiple possibilities for obtaining market information, supporting comprehensive analysis and research.

Data provided by Energy Charts API service were analyzed for number of negative values of electricity prices in Germany. Over the years, the count of negative values has rising trend. Although 2022 has the lowest count of negative price occurrences equal to 70, 2023 and 2024 have encountered rapid rise, reaching 300 and 457 negative prices. In TABLE III cumulative count of negative prices are presented over the years 2015 to 2024.

TABLE III
CUMULATIVE COUNT OF NEGATIVE PRICE OCCURRENCES

Year	15	16	17	18	19	20	21	22	23	24
Count*	110	97	147	133	211	298	139	70	300	457

*Cumulative count of negative prices

Renewable sources of energy are responsible for this market behavior. Renewable energy sources drive this market behavior. The installed capacity of solar and wind power in Germany continues to grow. A Capture Rate (CR) analysis was conducted to evaluate the economic performance of these power plants. The calculation of the CR requires determining the Capture Price (CP) presenting average price at which solar or wind power plants sell electricity. CR, represented as a percentage, demonstrates effectiveness of solar or wind power plants in capturing market value. The formulas for CP and CR are:

$$CP = \frac{\text{Total Revenue}}{\text{Total Amount of Electricity Produced}} \text{ (€/MWh)} \quad (1)$$

$$CR = \frac{CP}{\text{Average Market Price of Electricity}} * 100\% \quad (2)$$

The results displayed in Fig. 1 indicate a decreasing trend in the CR values of Solar over the. For Wind Offshore production, green dotted trend line demonstrates more stable CR over the years analyzed. and Wind Onshore CR demonstrates a slight downward trend. This analysis provides valuable insights of renewable integration, guiding policies to enhance market stability and investment conditions.

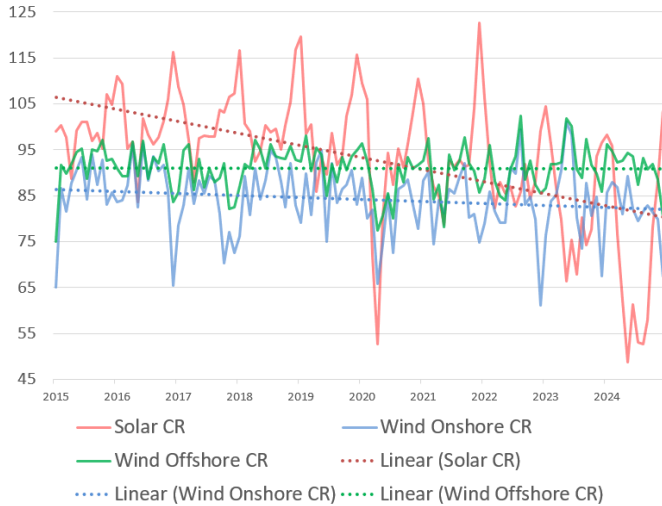


Fig. 1. Capture Rate percentages of solar and wind energy sources in Germany

IV. FUTURE WORK

Our research aims to advance the use of neural networks and machine learning for electricity market predictions, focusing on forecasting solar and wind generation. Convolutional neural networks (CNNs) will be investigated on their applicability for wind generation forecasting based on Copernicus weather data, evaluating their accuracy and reliability compared to conventional methods.

Building upon prior research, electricity price prediction models will be benchmarked against existing methodologies, evaluating their accuracy and robustness. While neural networks will play a key role in our study, our objective is also to analyze the usability of PLEXOS for electricity market modeling, particularly in the context of price forecasting and market optimization.

A critical challenge in our research is the lack of publicly available plant-level production data, which complicates the development of a stack model needed for optimization solution like Euphemia. To overcome this, we will use hourly country-level production data, cross-border transmission capacities, and gas prices to create deep neural network model with aim to calculate net export/import positions between bidding zones. This approach avoids plant-level data modeling by using aggregated national generation and gas price-driven cost assumptions.

Our work will contribute to a deeper understanding of AI-driven forecasting methods while assessing the potential of optimization-based approaches for electricity price prediction.

V. ACKNOWLEDGEMENT

This research was funded by Early Stage Grants (ESG) no. 56/2024/ESGTUKE: Prediction studies on evolving electricity market.

REFERENCES

- [1] "EUPHEMIA Public Description, Single Price Coupling Algorithm." Accessed: Feb. 24, 2025. [Online]. Available: <https://www.nordpoolgroup.com/globalassets/download-center/single-day-ahead-coupling/euphemia-public-description.pdf>
- [2] "electricity price prediction (Topic) – 2,093 – Web of Science Core Collection." Accessed: Feb. 25, 2025. [Online]. Available: <https://www.webofscience.com/wos/woscc/summary/ecf756ad-dbf4-4b6b-b0d4-55f713906e4b-014ca6a7f3/times-cited-descending/1>
- [3] T. Hong, P. Pinson, S. Fan, H. Zareipour, A. Troccoli, and R. J. Hyndman, "Probabilistic energy forecasting: Global Energy Forecasting Competition 2014 and beyond," *Int. J. Forecast.*, vol. 32, no. 3, pp. 896–913, Sep. 2016, doi: 10.1016/j.ijforecast.2016.02.001.
- [4] J. Lago, F. De Ridder, and B. De Schutter, "Forecasting spot electricity prices: Deep learning approaches and empirical comparison of traditional algorithms," *Appl. Energy*, vol. 221, pp. 386–405, Jul. 2018, doi: 10.1016/j.apenergy.2018.02.069.
- [5] J. Nowotarski and R. Weron, "Recent advances in electricity price forecasting: A review of probabilistic forecasting," *Renew. Sustain. Energy Rev.*, vol. 81, pp. 1548–1568, Jan. 2018, doi: 10.1016/j.rser.2017.05.234.
- [6] T. Hong, P. Pinson, Y. Wang, R. Weron, D. Yang, and H. Zareipour, "Energy Forecasting: A Review and Outlook," *IEEE Open Access J. Power Energy*, vol. 7, pp. 376–388, 2020, doi: 10.1109/OAJPE.2020.3029979.
- [7] T. Morstyn and M. D. McCulloch, "Multiclass Energy Management for Peer-to-Peer Energy Trading Driven by Prosumer Preferences," *IEEE Trans. Power Syst.*, vol. 34, no. 5, pp. 4005–4014, Sep. 2019, doi: 10.1109/TPWRS.2018.2834472.
- [8] Y. T. Chae, R. Hoeshe, Y. Hwang, and Y. M. Lee, "Artificial neural network model for forecasting sub-hourly electricity usage in commercial buildings," *Energy Build.*, vol. 111, pp. 184–194, Jan. 2016, doi: 10.1016/j.enbuild.2015.11.045.
- [9] "Transition to 15-minute Market Time Unit (MTU)." Accessed: Feb. 26, 2025. [Online]. Available: <https://www.nordpoolgroup.com/en/trading/transition-to-15-minute-market-time-unit-mtu/>
- [10] Z. Yang, L. Ce, and L. Lian, "Electricity price forecasting by a hybrid model, combining wavelet transform, ARMA and kernel-based extreme learning machine methods," *Appl. Energy*, vol. 190, pp. 291–305, Mar. 2017, doi: 10.1016/j.apenergy.2016.12.130.
- [11] X. Lu, J. Qiu, G. Lei, and J. Zhu, "An Interval Prediction Method for Day-Ahead Electricity Price in Wholesale Market Considering Weather Factors," *IEEE Trans. Power Syst.*, vol. 39, no. 2, pp. 2558–2569, Mar. 2024, doi: 10.1109/TPWRS.2023.3301442.
- [12] H. Jiang, Y. Dong, Y. Dong, and J. Wang, "Probabilistic electricity price forecasting by integrating interpretable model," *Technol. Forecast. Soc. Change*, vol. 210, p. 123846, Jan. 2025, doi: 10.1016/j.techfore.2024.123846.
- [13] H. Zhang, W. Hu, D. Cao, Q. Huang, Z. Chen, and F. Blaabjerg, "A Temporal Convolutional Network Based Hybrid Model for Short-Term Electricity Price Forecasting," *CSEE J. Power Energy Syst.*, vol. 10, no. 3, pp. 1119–1130, May 2024, doi: 10.17775/CSEEJPES.2020.04810.
- [14] X. Du, Y. Cai, and Z. Tang, "Integrating Weather Conditions to Forecast the Electricity Price in Belgium Market: A Novel Mixed-Frequency Machine Learning Algorithm," *J. Syst. Sci. Complex.*, Jul. 2024, doi: 10.1007/s11424-024-3503-7.
- [15] J. Hörsch, F. Hofmann, D. Schlachtberger, and T. Brown, "PyPSA-Eur: An open optimisation model of the European transmission system," *Energy Strategy Rev.*, vol. 22, pp. 207–215, Nov. 2018, doi: 10.1016/j.esr.2018.08.012.
- [16] "PLEXOS Energy Modeling Software." Accessed: Feb. 26, 2025. [Online]. Available: <https://www.energyexemplar.com/plexos>
- [17] "OSEMOSYS," OSEMOSYS. Accessed: Feb. 27, 2025. [Online]. Available: <http://www.osemosys.org/>
- [18] "Home | EPEX SPOT." Accessed: Feb. 27, 2025. [Online]. Available: <https://www.epexspot.com/en>
- [19] P. D. B. Burger, "Energy-Charts." Accessed: Feb. 27, 2025. [Online]. Available: <https://www.energy-charts.info/index.html>
- [20] E. Branding, "Montel | Your guide to navigating energy markets." Accessed: Feb. 27, 2025. [Online]. Available: <https://montel.energy>
- [21] "Transparency Platform." Accessed: Feb. 27, 2025. [Online]. Available: <https://newtransparency.entsoe.eu/>
- [22] "Home Page - publication_tool_common." Accessed: Feb. 27, 2025. [Online]. Available: <https://publicationtool.jao.eu/>
- [23] "Homepage | OKTE, a.s." Accessed: Feb. 27, 2025. [Online]. Available: <https://www.okte.sk/en/>

Innovations and perspectives in Software-Defined Networking

¹*Erika Abigail KATONOVÁ (2nd year),*

Supervisor: ²Peter FECILÁK

^{1,2}Dept. of Computers and Informatics, FEI TU of Košice, Slovak Republic

¹erika.abigail.katonova@tuke.sk, ²peter.fecilak@tuke.sk

Abstract—This article explores the integration of machine learning approaches within Software Defined Networking to address complex challenges in network optimization and management. Machine learning offers significant potential to enhance SDN by providing models capable of realtime decision making and adaptation. This work introduces key ML methods, including reinforcement learning and graph neural networks, and their application to dynamic routing, traffic prediction, and anomaly detection in SDN environments. By integrating ML with SDN, this article highlights improved scalability, reduced computational overhead, and the ability to predict and respond to changing network conditions dynamically.

Keywords—Machine learning, Quality of Service, Reinforcement learning, routing optimization, SDN

I. INTRODUCTION

Software Defined Networking (SDN) represents a revolutionary change in modern networking, offering centralized control, programmability, and flexibility to manage complex network infrastructures. As the demand for efficient traffic management and dynamic resource allocation grows, traditional SDN management approaches face limitations when dealing with diverse and fastly changing network conditions. Machine learning (ML) has proven to be a powerful tool in addressing these challenges, enabling intelligent decision making through models that learn from network behavior.

ML techniques, such as supervised learning, unsupervised learning, and reinforcement learning, bring a new dimension to SDN by automating essential functions like traffic prediction, anomaly detection, and routing optimization. These techniques can adapt to dynamic environments, predict network trends, and optimize resource usage, all while reducing manual intervention. For example, ML models can predict network congestion, optimize routing paths in real time, and maintain compliance with Quality of Service (QoS) standards even under changing traffic conditions.

By combining ML with SDN, networks become more efficient and better suited to manage operations that require minimal delay. The deployment of ML algorithms in SDN settings continues to face significant obstacles with respect to scalability, interoperability, and practical applicability of ML algorithms in SDN environments. The use of advanced ML models enables SDN to reach automated intelligence levels that create intelligent network solutions which can adapt more effectively.

This article explores the research done on role of ML in SDN and reviews existing methods and insights into future

directions for advancing ML enhanced SDN architectures.

II. MACHINE LEARNING MEETS SOFTWARE-DEFINED NETWORKING

Machine learning methodologies, as well as their combined applications with Artificial Intelligence, are becoming more common, in integration with SDN, to execute intelligent network management, enhance performance, and identify or detect anomalies. Italian researchers present significant advancements in federated learning efficiency through their use of Software Defined Networking in their study [1]. Federated learning is a decentralized ML framework where models learn from data stored on multiple devices or servers by exchanging model updates instead of raw data. Each device trains a local model on its data and shares updates, such as weights or parameters, with a central server, which then combines these updates to improve a global model.

The study demonstrates that integrating SDN into federated learning reduces training loss metrics by approximately half the time required compared to environments without SDN support. It proposes a communication architecture optimized for federated learning processes, improving training times without sacrificing performance. This advancement addresses key challenges in next generation network infrastructures.

Furthermore, publication [2] explores how ML technologies are applied to networking, such as traffic prediction, routing optimization, network performance monitoring, and cybersecurity. It also highlights the challenges and potential future opportunities in this field. A significant advantage of ML in networking is its ability to solve essential problems, including classification, regression, clustering, and rule extraction. These methods support automated decision making and network optimization, which are crucial for managing increasing traffic demands and the growing complexity of network infrastructure.

For instance, classification helps in sorting data, such as detecting different types of network attacks, while regression predicts values like upcoming bandwidth requirements. Clustering identifies patterns by grouping similar data points, and rule extraction identifies statistical relationships within network datasets. These capabilities create networks that can adapt to current demands while operating more efficiently.

A. Network traffic prediction

Authors of the paper [3] focus on enhancing QoS aware routing in SDN by proposing a modified version of the *LARAC*

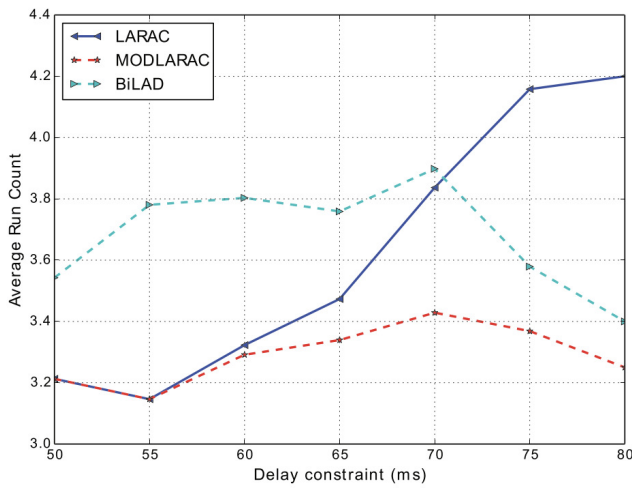


Fig. 1: Average path delay, along with the required flow's delay constraints [3]

(Lagrangian Relaxation-based Aggregated Cost) algorithm, named *MODLARAC*. The study proposes solutions for creating delay sensitive and cost efficient network paths within SDN environments for applications that need strict QoS guaranteed streaming, gaming and critical procedures such as telesurgery.

LARAC is a heuristic algorithm designed to solve the Delay Constrained Least Cost (DCLC) problem, which is a wellknown optimization problem in networking. The goal of LARAC is to find the most cost effective path in a network while satisfying specific delay constraints. This makes it especially relevant for QoS routing in SDN.

The results of this study demonstrate that these methods offer significant advantages compared to traditional methods, particularly in reducing costs in SDN networks and addressing QoS requirements for multimedia applications. The paper also highlights practical implementations, such as experiments using a realistic ISP network topology. These strategies showed that MODLARAC reduces runtime by 20% compared to LARAC and BiLAD, while only slightly increasing path cost by 3% and delay by 7% and ensuring compliance with QoS requirements. MODLARAC demonstrates efficiency and scalability which makes it appropriate for modern SDN use cases while the paper suggests future improvements through additional metrics to optimize computational overhead and accuracy.

B. Efficient routing approaches

Study [4] focused on machine learning and predictive algorithms in network routing processes. The researcher focuses on the application of ML and predictive algorithms to solve the Travelling Salesman Problem (TSP) which refers to the problem of a traveling salesman. The problem involves optimizing the route to visit each location exactly once while minimizing the total distance. Mentioned study shows significant advancements in solving of the TSP problem, especially in environments requiring fast and scalable solutions, since it explored two promising heuristic algorithms: Ant Colony Optimization (ACO) and Q-Learning, what is a reinforcement learning algorithm.

By using the reinforcement learning and graph neural networks, these methods achieve comparable solution quality

to traditional algorithms while drastically reducing the calculation time by 75% in some cases. This combination of accuracy and efficiency makes machine learning a practical alternative for applications used in real scenarios. Furthermore, the importance of solving the optimization problems in large scale networks, highlights the adaptability of these methods. However, the study does not directly address SDN, it demonstrates methods, such as reinforcement learning for dynamic optimization and graph neural networks for complex structure representation, shows strong potential for improving routing and planning in SDN environments.

C. Security concepts in SDN

The topic of security is also an important aspect to consider, and the authors of the paper [5] evaluate exactly the use of ML techniques for enhancing security in SDN. The study highlights how the centralized nature of SDN, while introducing programmability and efficient network management, brings vulnerabilities that attackers can use.

The paper emphasizes how effective can ML Intrusion Detection Systems (IDS) be in detecting anomalies and unauthorized access by learning patterns in network traffic. The authors evaluate four ML algorithms: Support Vector Machine (SVM), Naive Bayes, Decision Tree, and Logistic Regression, in a simulated environment using a dataset created from a DDoS attack scenario. SVM performed the best, achieving an accuracy of 97.5%, followed by Decision Tree and Naive Bayes with over 96% accuracy, while Logistic Regression was slightly behind. The evaluation includes metrics such as precision, sensitivity, specificity, and F1-score, which demonstrate the strong performance of ML algorithms in distinguishing between attack and normal traffic. The authors conclude by emphasizing the potential of ML for IDS in SDN and suggest future work to evaluate the scalability of control platforms with ML integration for real applications.

III. FUTURE STEPS AND RESEARCH PERSPECTIVE

Machine learning mechanisms for monitoring and evaluating network performance parameters present a promising approach to managing modern infrastructures effectively. This approach, appears to be a promising investigation during for future of this research.

Parameters, such as bandwidth, delay, packet loss, can be analyzed to identify potential problems and predict future needs, with the help of machine learning and graph neural networks. Such a dynamic approach would potentially enable networks to adapt to changing conditions, enhancing both reliability and efficiency while ensuring the seamless operation of all services and applications, and therefore fulfill the purpose of the research.

REFERENCES

- [1] A. Mahmod, G. Caliciuri, P. Pace, and A. Iera, "Improving the quality of federated learning processes via software defined networking," in *Proceedings of the 1st International Workshop on Networked AI Systems*, ser. NetAISys '23. ACM, Jun. 2023.
- [2] L. Li, Y. Fan, M. Tse, and K.-Y. Lin, "A review of applications in federated learning," *Computers & Industrial Engineering*, vol. 149, p. 106854, Nov. 2020.
- [3] A. BinSahaq, T. Sheltami, A. Mahmoud, and N. Nasser, "Bootstrapped larac algorithm for fast delay-sensitive qos provisioning in sdn networks," *International Journal of Communication Systems*, vol. 34, no. 11, May 2021.

- [4] P. N. S, “Optimization techniques to solve travelling salesman problem using machine learning algorithms,” *International Journal for Research in Applied Science and Engineering Technology*, vol. 10, no. 1, pp. 274–279, Jan. 2022.
- [5] A. Ahmad, E. Harjula, M. Ylianttila, and I. Ahmad, “Evaluation of machine learning techniques for security in sdn,” in *2020 IEEE Globecom Workshops (GC Wkshps)*. IEEE, Dec. 2020, pp. 1–6.

High-Speed Imaging of Streamer Propagation in Nano-Functionalized Transformer Oils

¹Kristián GLAJC (1st year)
Supervisor: ²Juraj KURIMSKÝ

^{1,2}Department of Electric Power Engineering, FEI, Technical University of Košice, Slovak Republic

¹kristian.glajc@tuke.sk, ²juraj.kurimsky@tuke.sk

Abstract— Dielectric properties of transformer oils can be improved through nano-functionalization, which could help reduce streamers and improve breakdown voltage. TiO₂, SiO₂, Al₂O₃, and ferrite materials are nanoparticles employed to derive electrical discharges in oil, the survey in each of these nanoparticles added to the oil. The streamer behavior and dispersion stability are characterized using high-speed camera and electrical measurements. Nanoparticles could enhance the reliability and performance of insulating media for high voltage applications as the results show.

Keywords— Breakdown voltage, nano-functionalized transformer oil, nanodielectrics, streamer

I. INTRODUCTION

Transformer oils are very important for electrical and cooling of high voltage equipment. Their dielectric properties, however, can be significantly altered by electrical discharges, in particular streamer propagation, which may contribute to the electrical breakdown and failure of insulation properties. As a result, there is a growing need for more reliable and efficient insulating media, and therefore there is a strong motivation to identify innovative approaches to improve the dielectric performance of transformer oils [1].

A promising approach is the modification of transformer oils using nanoparticles. Studies show that nano-functionalized transformer oils can modify the basic mechanisms of streamer propagation thereby inhibiting their development and increasing the breakdown voltage of the insulating medium. Although oxide-based nanoparticles (e.g. TiO₂, SiO₂, Al₂O₃) have been extensively investigated, ferrite nanoparticles represent an exciting option because of their unique magnetic and dielectric properties. Even more effective streaming suppression than regarded for common nanofluids might be supplied by these properties for ferrite-based nanofluids [1] [2].

The focus of this research is the investigation of streamer development and its behavior in transformer oils. Though numerous studies have been performed for nanofluids, this research specifically investigates how streamer propagation and dielectric breakdown may be modified with the addition of ferrite-based nanofluids. A key aspect of this study is the use of a high-speed camera as a primary diagnostic tool to examine how the introduced nanofluid influences the velocity and spread of streamers.

II. THE STATE OF THE ART WITH FOCUS ON STREAMER INVESTIGATION

In the study of streamers, we have decided to use a high-speed camera as the primary observation method. This choice is motivated by the ability of this technology to provide detailed visual information on the dynamics of streamers in real-time, allowing for the analysis of their shape, velocity, and propagation mechanisms. Unlike electrical methods, which provide indirect quantitative analysis of current pulses, or optical emission spectroscopy (OES), which focuses on the chemical composition of discharges, a high-speed camera allows for direct visual representation and comparative analysis of streamers in different insulating media.

This method captures the various phases of streamer development, from initiation to collapse, offering a unique insight into their branching and decay mechanisms. The main disadvantage is significant financial constraints. Compared to electrical measurement techniques, which rely on relatively cost-effective sensors for current and voltage detection, high-speed imaging systems require specialized optics, high-resolution sensors, and advanced data processing capabilities, making them considerably more expensive [11]. Additionally, the need for sophisticated synchronization systems and powerful illumination sources, such as laser or pulsed light setups, further increases the operational costs [20]. As a result, high-speed cameras are often used in conjunction with electrical measurement methods to balance cost-efficiency and data comprehensiveness in streamer research.

Although high-speed imaging provides a powerful tool for visualizing streamer behavior, electrical measurement techniques remain essential for quantifying streamer parameters. Partial discharge (PD) analysis is widely used to detect and evaluate streamer activity by analyzing the electrical signals emitted during discharge events. Studies [3] employed phase-resolved PD (PRPD) patterns to study streamer branching and breakdown initiation under AC voltage conditions, providing valuable insights into the electrical behavior of streamers [3]. Similarly, [4] combined electrical pulse measurements with acoustic emission techniques, which allowed for a more comprehensive understanding of the mechanical and electrical interactions within the discharge process [4]. Additionally, [5] developed a wide-band partial discharge measurement system, enabling the generation of PRPD diagrams, which provide statistical information on streamer formation under different voltage conditions [5].

A high-speed camera is one of several methods for visually analyzing streamers in transformer oils. Approach by [7]

enables their evolution to be recorded with extremely high temporal resolution, in the range of microseconds to nanoseconds. Its applications are broad it enables the study of streamer propagation, classification of different types of streamers based on their visual characteristics such as shape, length, and light emission intensity, and precise determination of their propagation velocity in various dielectric liquids [7]. Additionally, this method allows for the observation of the influence of nanoparticles on streamer development, as well as their interaction with the surrounding medium in various experimental setups with varying electric fields, temperatures, or oil moisture levels [6] [7].

Compared to other methods, a high-speed camera provides a unique experimental approach that facilitates not only the identification of fundamental streamer mechanisms but also their detailed comparison in different insulating fluids. Its ability to visually and temporally analyze streamer development with high precision makes it an indispensable tool for the study of streamers in nanofluid-based transformer oils.

However, its high-precision ability to visually and temporally analyze streamer development makes it an essential tool for studying streamers in nanofluid-based transformer oils.

A. CCD camera (Charge-Coupled Device)

This type of camera uses a CCD sensor to detect light, converting light signals into electrical charges. These cameras provide medium temporal resolution, typically in the range of milliseconds, and are suitable for analyzing slower processes or obtaining high-quality images under sufficient lighting. CCD cameras are used for observing dynamic phenomena where extreme temporal precision is not required, but high image resolution is still needed. In the study [6], CCD cameras were used to analyze streamer propagation along insulation surfaces, providing detailed information about the behavior of streamers under various conditions. Fig. 1-2 captured by CCD camera illustrates typical positive streamers observed in both non-uniform and semi-uniform fields under varying applied voltages. The images capture the final state of the streamer after each impulse shot, clearly showing that streamers originate from the needle tip, where the electric field is at its highest, and predominantly propagate towards the opposing plane electrode [6].

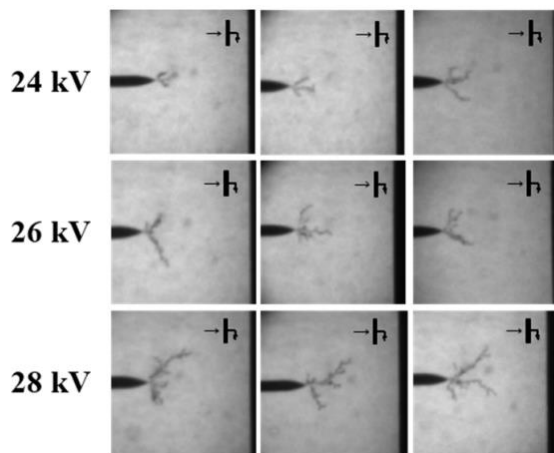


Fig. 1. CCD photos of positive streamers under different voltage levels 24-28kV, $d=10$ mm, $rp=10$ μ m [6].

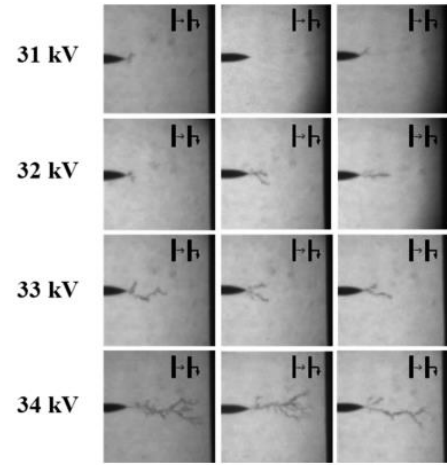


Fig. 2. CCD photos of positive streamers under different voltage levels 31-34kV, $d=10$ mm, $L=8$ mm, $rp=10$ μ m. [6].

B. ICCD cameras (Intensified Charge-Coupled Device)

ICCD cameras usually combine a CCD sensor with a photon intensifier that amplifies weak light signals before detection. This approach allows for capturing very faint light emissions, which is particularly important when studying fast and weak phenomena, such as streamers in dielectric fluids. ICCD cameras provide high temporal resolution, in the range of nanoseconds to microseconds, enabling the capture of very fast events that would otherwise be undetectable with standard cameras. These cameras are ideal for observing fast and weak light phenomena, such as streamers in transformer oil or nanofluids. ICCD cameras allow for detailed observation of streamer dynamics, including their development and interactions with the surrounding environment. In the study [7], ICCD cameras were used to capture the morphology of streamers in pure transformer oil and nano-liquids, providing valuable insights into their shape and behavior under different conditions. The optical characteristics of the streamer in an electrode-plane system within transformer oil were captured using an ICCD camera. The formation and propagation of both positive and negative polarity streamers under applied voltages of 18 kV, 20 kV, and 22 kV are clearly depicted in the images presented in Fig. 3. The ICCD camera was externally triggered by the discharge current, with an exposure time of 10 μ s, allowing for the complete recording of the partial discharge process [7].

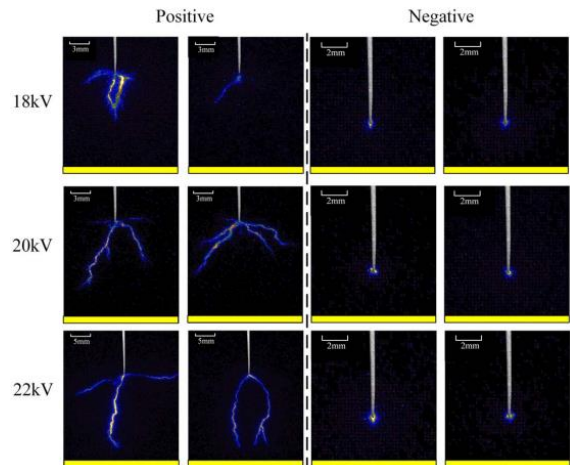


Fig. 3. ICCD photos of streamers under different voltage levels [7].

III. IMPACT ON STREAMER PROPAGATION

A. Nanofluid nature and properties

Streamer propagation in dielectric liquids, such as transformer oil, is a complex process that depends on several factors. The presence of nanoparticles in the liquid, particularly in hybrid nanofluids containing TiO_2 , plays a key role in influencing the dynamics of streamer propagation [8] [19].

According to the study by [8], the presence of TiO_2 nanoparticles in oil leads to the formation of local charge clusters, which deform the electric field, subsequently resulting in slower streamer propagation. This effect has been observed particularly in experiments with hybrid nanofluids, where the propagation velocity of streamers slowed down compared to pure oil [8].

Another important factor affecting streamer propagation is the size and distribution of nanoparticles. In the study by [9], it is stated that smaller nanoparticles can better trap electrons, which slows down streamer propagation. These particles increase the electron trap density in the fluid, affecting the ionization rate and the dynamics of charge propagation in the streamer channel. Particle dispersion in the liquid is also crucial, as homogeneous dispersion contributes to more stable and slower streamer propagation, whereas improper dispersion or clumping of particles may accelerate propagation due to localized increased electric fields [9].

Fig. 4 which [10] obtained during the research, provide representative examples of positive streamers in pure oil and nanofluids during their propagation. In all tested oil samples, the positive streamers exhibit a filamentary structure. However, compared to those in pure oil, streamers in nanofluids appear thicker and more branched. Additionally, under the same camera trigger delay, the length of positive streamers in pure oil is noticeably greater than in nanofluids [10].

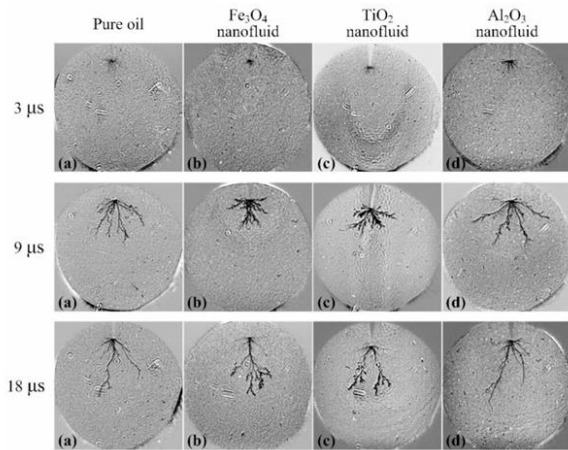


Fig. 4. Positive streamer pattern in pure oil and nanofluids. (a) Pure oil, (b) Fe_3O_4 nanofluid, (c) TiO_2 nanofluid and (d) Al_2O_3 nanofluid [10].

B. Electric field impact

Equally important is the influence of the electric field on the velocity of streamer propagation. Higher electric field intensity accelerates streamer propagation because it increases the energy carried by the charges [11] [12]. The presence of nanoparticles in nanofluids can reduce the electric field ahead of the streamer, thus slowing down its propagation. In systems with hybrid nanofluids, a synergistic effect is observed where

the combination of different types of nanoparticles leads to increased polarizability, causing more intense deformation of the electric field and further slowing of streamer propagation. This effect is emphasized in the study by [12], which shows that in the case of TiO_2 nanoparticles, the streamer propagation velocity decreases due to stronger electric field influences, which affect the speed and stability of streamer growth [12].

In the study by [7], the effect of the permittivity of different nanoparticles (Al_2O_3 , TiO_2 , Fe_3O_4) on the electric field was examined. The findings revealed that the maximum electric field around the nanoparticles could be up to 2.87 times higher than the original field [7]. This local enhancement may affect ionization processes in the oil and alter streamer trajectories. Similarly, [13] analyzed the movement of charged particles in the electric field and demonstrated that polarized nanoparticles can deform the field in their vicinity, thereby influencing the transport of electrons and positive ions in the dielectric liquid. This effect leads to a slowing down of streamers and their possible branching [13].

The research conducted by [14] focused on the interaction between streamers and the surrounding electric field and particles. Simulations indicated that nanofluids containing Fe_3O_4 and TiO_2 exhibit significant electric field distortion, resulting in lower streamer velocity and denser branching compared to pure oil [14].

In the experiment by [15], it was observed that the electric field intensity ahead of the streamer front directly influences its speed and structure, with higher field intensity increasing ionization and leading to faster streamer propagation [15].

Finally, numerical modeling by [16] demonstrated that polarized nanoparticles cause localized enhancement of the electric field, leading to increased charge density and interactions with streamers. This phenomenon could be crucial for improving the insulating properties of transformer oil enhanced with nanoparticles [16].

C. Temperature impact

Temperature has a significant effect on the viscosity and ionization properties of dielectric liquids. Higher temperature reduces the viscosity of the liquid, allowing charges to move more quickly and thus accelerating the propagation of streamers [17]. However, higher temperatures also increase the ionization ability of the liquid, which can affect the stability of the streamers. According to the study [18], the presence of nanoparticles in oil increases its breakdown strength at various temperatures, indicating an improvement in the insulating properties of the oil at higher temperatures. In this way, temperature not only affects the propagation speed of streamers but also the insulating ability of the liquid, which can be crucial for the efficiency of transformers under varying operating conditions [18].

Temperature is crucial factor influencing streamer propagation in dielectric liquids, particularly in nanofluids. Increasing temperature can accelerate streamer propagation but also improve the insulation properties of the oil. Therefore, it is important to examine the optimal temperature conditions to improve the performance and stability of electrical equipment, such as transformers. These findings are supported by the results of studies showing that temperature plays a key role in processes affecting streamer propagation and insulating properties of oils [17] [18].

IV. CONCLUSION

This study focused on selecting the appropriate method for investigating streamers in transformer oil and analyzing the impact of nanofluids on their propagation. High-speed cameras were identified as the optimal experimental technique for visualizing streamer dynamics, allowing for detailed analysis of their shape, velocity, and propagation mechanisms in real-time. The selection of the right camera type is crucial, as different technologies provide varying temporal and spatial accuracy. Among the available options, CCD and ICCD, the ICCD camera was identified as the most suitable for this study. Due to its ability to amplify weak light signals, it enables the recording of very fast and faint light emissions during streamer propagation, providing a more precise analysis of their behavior.

The results demonstrated that nanofluids significantly influence streamer propagation in transformer oil. The presence of nanoparticles, particularly TiO_2 , Al_2O_3 , and hybrid ferrite materials, slows down streamer development by modifying the electric field distribution and enhancing electron trapping. The research confirmed that homogeneous dispersion of nanoparticles contributes to more stable and slower streamer propagation, whereas inhomogeneous dispersion may intensify local electric fields and accelerate propagation.

In addition to the impact of nanofluids, the role of the electric field, temperature, and applied voltage on streamer propagation was also examined. Increasing electric field intensity and voltage accelerates streamer growth, while higher temperatures affect the viscosity of the oil and ionization processes, influencing streamer stability. These factors emphasize the complexity of physical phenomena affecting the insulating properties of transformer oils.

The findings confirm that the application of nanofluids presents a promising approach to improving the dielectric properties of transformer oils. Future research should focus on optimizing nanoparticle concentration, investigating long-term stability, and evaluating the influence of various operational conditions on the reliability and performance of insulating systems. Moreover, selecting the most suitable method for streamer observation particularly the use of ICCD cameras can significantly enhance the accuracy of experimental measurements and provide deeper insights into streamer propagation mechanisms in nano-functionalized transformer oils.

A. Research methods

Based on the acquired knowledge, I have decided to use a high-speed camera as the primary method for visualizing streamer dynamics in my research. The ICCD camera has been identified as the most suitable choice due to its ability to amplify weak light signals and capture rapid processes with high temporal precision. However, the final selection of the camera will depend on the availability of technical and financial resources. Since the necessary high-speed imaging equipment is not locally available, the experimental part of the research will be carried out abroad within the framework of an approved Erasmus+ mobility program. The partner institution provides suitable technical facilities and expertise for conducting high-speed diagnostics of streamer propagation, ensuring the feasibility of the planned measurements. Using a high-speed camera requires access to a specialized experimental setup. Since the necessary equipment is not

locally available, it is essential to perform the research abroad, where suitable technical conditions for conducting the measurements are accessible.

However, the initial experiments will be conducted in collaboration with the Slovak Academy of Sciences (SAV) in their laboratories, focusing on the preparation of nanoparticles, measurement of the dielectric properties of the oil, stability analysis of nanofluid, basic electrical breakdown tests.

B. Materials

In my experiments, I will investigate the influence of ferrite-based nanoparticles, such as Fe_3O_4 , and carbon-based nanoparticles, such as fluorinated nanodiamonds, as potential alternatives to commonly studied oxide nanoparticles like TiO_2 , Al_2O_3 , and SiO_2 . These materials exhibit unique magnetic, dielectric, and environmentally friendly properties, which may significantly impact streamer dynamics and the breakdown voltage of transformer oil.

Additionally, I will evaluate their behavior in different types of insulating liquids, including natural ester-based fluids and conventional mineral transformer oils with well-defined dielectric and thermal properties. These liquids will be selected based on their chemical composition, viscosity, and dielectric strength to assess how nanoparticles interact with different fluid environments. Ferrite-based and carbon-based nanomaterials are considered more environmentally sustainable due to their lower toxicity and recyclability compared to commonly used metal oxide nanoparticles. Ester-based fluids offer additional ecological advantages, as they are biodegradable and present a lower environmental impact than traditional mineral oils.

C. Research objectives

- Ensuring the reproducibility of results and eliminating the influence of external factors.
- Changing the geometric shape of the electrode, which can significantly affect the intensity and distribution of the electric field, subsequently alters the conditions for streamer initiation and propagation.
- Using a thermal imaging camera to eliminate the impact of oil overheating on experimental results.
- Investigating how varying nanofluid concentrations affect streamer velocity, branching, and overall discharge stability.
- Analyzing the branching velocity of streamers and their interaction with nanofluids.
- Identifying the mechanisms through which nanoparticles influence the propagation and development of streamers in transformer oil.

ACKNOWLEDGMENT

Funding: This work is funded by the Slovak Academy of Sciences and Ministry of Education in the framework of project VEGA 1/0380/24, VEGA-2-0029-24 and Slovak Research and Development Agency under contract No. APVV-22-0115.

This publication is the outcome of the already finished project implementation: Innovative Testing Procedures for 21st Century Industry ITMS: 313011T565, by Operational Programme Integrated Infrastructure (OPII) funded by the ERDF.

REFERENCES

- [1] X. Ma, Y. Hu, M. Dong, M. Ren, and Y. Li, "The Streamer Discharge Simulation of Transformer Oil-based Nanofluids," in *Proc. IEEE 20th International Conference on Dielectric Liquids (ICDL)*, Rome, Italy, Jun. 23–27, 2019, pp. 1–4.
- [2] H. Pourpasha, S. Z. Heris, R. Javadpour, M. Mohammadpourfard, and Y. Li, "Experimental investigation of zinc ferrite/insulation oil nanofluid natural convection heat transfer, AC dielectric breakdown voltage, and thermophysical properties," *Scientific Reports*, vol. 14, no. 20721, 2024.
- [3] Y. Li, J. Y. Wen, Y. Liang, J. Wu, S. Qin, and G.-J. Zhang, "Streamer Discharge Propagation and Branching Characteristics in Transformer Oil under AC Voltage: Partial Discharge and Light Emission," in *19th IEEE International Conference on Dielectric Liquids (ICDL)*, Manchester, United Kingdom, Jun. 25–29, 2017, pp. 1–6.
- [4] Y. Zhou, X. Yang, N. Peng, W. Cui, and Z. Wang, "Comparative Studies of Partial Discharge Using Acoustic Emission Method and Optical Spectroscopy," in *Proc. IEEE International Conference on High Voltage Engineering and Application (ICHVE)*, Chongqing, China, Sep. 19–22, 2020, pp. 1–6.
- [5] H. Wang, M. Zhang, C. Liu, Q. Zhang, and L. Xu, "Streamer Discharge Propagation and Branching Characteristics in Transformer Oil under AC Voltage: Partial Discharge and Light Emission," in *Proc. IEEE International Conference on Dielectric Liquids (ICDL)*, Roma, Italy, Jun. 23–27, 2019, pp. 1–4.
- [6] H. Yu, C. Krause, Q. Liu, A. Hilker, and Z. Wang, "Effect of Electric Field Uniformity on Streamer and Breakdown Characteristics in a Gas-to-Liquid Oil under Positive Lightning Impulse," *IEEE Transactions on Dielectrics and Electrical Insulation*, 2020.
- [7] Y. Lv, Y. Ge, L. Wang, Z. Sun, Y. Zhou, M. Huang, C. Li, J. Yuan, and B. Qi, "Effects of Nanoparticle Materials on Prebreakdown and Breakdown Properties of Transformer Oil," *Applied Sciences*, vol. 8, no. 4, pp. 601, Apr. 2018.
- [8] Z. Wang, Y. Zhou, W. Lu, N. Peng, and W. Chen, "The Impact of TiO₂ Nanoparticle Concentration Levels on Impulse Breakdown Performance of Mineral Oil-Based Nanofluids," *Nanomaterials*, vol. 9, no. 4, p. 627, 2019.
- [9] Y. Zhou, N. Peng, Z. Wang, W. Cui, W. Chen, S. Sui, and X. Yang, "Modified propagating behavior of creeping streamers at TiO₂ nanofluid/pressboard interface," *Journal of Molecular Liquids*, vol. 291, p. 111270, 2019.
- [10] Y. Zhou, S. Sui, J. Li, Z. Ouyang, Y. Lv, C. Li, and W. Lu, "The effects of shallow traps on the positive streamer electrodynamics in transformer oil-based nanofluids," *Journal of Physics D: Applied Physics*, vol. 51, no. 10, pp. 105304, Feb. 2018.
- [11] X. Meng, H. Mei, C. Chen, L. Wang, Z. Guan, and J. Zhou, "Characteristics of Streamer Propagation Along the Insulation Surface: Influence of Dielectric Material," *IEEE Transactions on Dielectrics and Electrical Insulation*, vol. 22, no. 2, pp. 1193–1203, Apr. 2015.
- [12] M. Zhang, Y. Zhou, W. Lu, J. Lu, and X. Yang, "Influence of nanoparticles' polarization on the streamer branching and propagation in nanofluids," *Journal of Molecular Liquids*, vol. 392, p. 123474, 2023.
- [13] Y. Li, J. Wu, X. Yang, S. Qin, and G.-J. Zhang, "The Influence of Electric Field on Charge Transport in Transformer Oil-Based Nanofluids," in *Proc. IEEE International Conference on Dielectric Liquids (ICDL)*, Manchester, United Kingdom, Jun. 25–29, 2017.
- [14] H. Wang, M. Zhang, C. Liu, Q. Zhang, and L. Xu, "Streamer Propagation and Electric Field Distortion in Transformer Oil-Based Nanofluids," in *Proc. IEEE International Conference on High Voltage Engineering and Application (ICHVE)*, Chongqing, China, Sep. 19–22, 2019, pp. 1–6.
- [15] Y. Zhou, N. Peng, Z. Wang, W. Cui, and W. Lu, "Electric Field Distribution and Its Impact on Streamer Development in Transformer Oil," *IEEE Transactions on Dielectrics and Electrical Insulation*, vol. 26, no. 4, pp. 1423–1432, Jul. 2019.
- [16] M. Huang, C. Li, L. Zhang, and B. Qi, "Numerical Study on the Influence of Polarized Nanoparticles on the Local Electric Field in Transformer Oil," in *Proc. IEEE International Symposium on Electrical Insulation (ISEI)*, Paris, France, Jul. 3–6, 2019, pp. 1–5. *IEEE Transactions on Dielectrics and Electrical Insulation*, vol. 26, no. 4, pp. 1423–1432, Jul. 2019.
- [17] C. Qin, Y. Huang, L. Liu, H. Liang, J. Shang, and Y. Xue, "Study on Power Frequency Breakdown Characteristics of Nano-TiO₂ Modified Transformer Oil under Severe Cold Conditions," *Applied Sciences*, vol. 13, no. 17, p. 9656, 2023.
- [18] A. M. Abd-Elhady, M. E. Ibrahim, T. A. Taha, and M. A. Izzularab, "Effect of Temperature on AC Breakdown Voltage of Nanofilled Transformer Oil," *IET Science, Measurement & Technology*, vol. 12, no. 1, pp. 138–144, 2018.
- [19] E. G. Atiya, D.-E. A. Mansour, R. M. Khattab, and A. M. Azmy, "Dispersion Behavior and Breakdown Strength of Transformer Oil Filled with TiO₂ Nanoparticles," *IEEE Transactions on Dielectrics and Electrical Insulation*, vol. 22, no. 5, pp. 2463–2470, 2015.
- [20] Y. Zhou, X. Yang, N. Peng, W. Cui, and Z. Wang, "Fractal Analysis of Positive Streamer Patterns in Transformer Oil-Based TiO₂ Nanofluid," in *Proc. IEEE International Conference on Dielectric Liquids (ICDL)*, Manchester, United Kingdom, Jun. 25–29, 2017, pp. 1–6.

Shielding properties and radiation modification of magnetic nanoparticle-functionalized textiles

^{1,2}Kristina ZOLOCHEVSKA (4th year)
Supervisor: ²Peter KOPČANSKÝ

¹Dept. of Physics, FEI TU of Košice, Slovak Republic

²Institute of Experimental Physics of the Slovak Academy of Sciences, Košice, Slovak Republic

¹kristina.zolochovska@tuke.sk, ²kopcan@saske.sk

Abstract—Electromagnetic and nuclear radiation pollution pose significant risks to human health. To address this issue, magnetic nanomaterials have been investigated for their shielding potential in distinct form: textile-based materials embedded with magnetic nanoparticles. This study explores the comparative shielding effectiveness of this approach. Magnetic textile composites, modified with Fe₃O₄ nanoparticles, exhibit promising protective properties against charged radiation (alpha and beta particles) and electromagnetic interference (EMI), frequency-dependent absorption and reflection of electromagnetic fields, making them suitable for shielding electronic components. Experimental analysis of magnetic susceptibility before and after irradiation revealed that textile system experience degradation in magnetic properties due to radiation-induced structural changes. This study provides insights into the application of magnetic nanomaterials in radiation-resistant textiles, offering flexible and adaptable solution for shielding against multiple types of radiation.

Keywords—Electromagnetic absorption, magnetic shielding, magnetic textiles, radiation protection.

I. INTRODUCTION

Electromagnetic and nuclear radiation pollution pose significant risks to both human health and technological systems. The increasing exposure to ionizing and non-ionizing radiation necessitates the development of advanced shielding materials to mitigate these hazards [1]. Traditional shielding methods, including lead-based materials and metal coatings, provide effective radiation protection; however, they present several drawbacks, such as high density, toxicity, and limited flexibility. As a result, alternative materials, particularly textiles embedded with functional nanomaterials, have gained attention due to their lightweight nature, adaptability, and improved protective capabilities [2].

Among various nanomaterials, magnetic nanoparticles, particularly iron oxides (magnetite (Fe₃O₄) and maghemite (gamma-Fe₂O₃)), have demonstrated significant potential in radiation shielding applications. These nanoparticles exhibit unique magnetic properties, such as high saturation magnetization and frequency-dependent absorption of electromagnetic waves, which make them suitable for mitigating electromagnetic interference (EMI) [3]. Furthermore, textile-based composites modified with magnetic nanoparticles offer a flexible and adaptable shielding solution, making them ideal for wearable radiation protection or

electronic component shielding [4]. Compared to conventional metal-based shielding materials, magnetic textiles provide a balance between protection, weight reduction, and breathability, making them more practical for various applications, including healthcare, aerospace, and military defense [5].

By investigating the magnetic behavior and structural integrity of Fe₃O₄-modified textiles, this study aims to enhance the understanding of their potential applications in radiation shielding and to develop strategies for improving their long-term durability and effectiveness. The integration of such innovative materials into everyday protective equipment could revolutionize the field of radiation shielding, making protection more accessible and practical across diverse industries.

II. MATERIALS AND METHODS

2.1 Magnetic Textile Composites

FeSO₄·7H₂O (Penta, Czech Republic), Na₂CO₃·10H₂O (Lachema, Czech Republic). Technical felt TTN (composition: 80% wool, 20% viscose; thickness: 3 mm; density: 0.36 g/cm³) was from Brněnská továrna plstí, s.r.o., Brno, Czech Republic.

Magnetic modification of felt

Felt was magnetically modified using modified direct microwave assisted procedure [6]. Felt was cut to obtain square pieces (6x6 cm), which were then immersed in excess of 20% ferrous sulfate solution for one hour. The modified textile pieces were dried at laboratory temperature for 24 hours and then they were individually put into 250 mL of 10% sodium carbonate solution in one liter beaker and treated in a standard domestic oven (700 W, 2 450 MHz) for 15 min. Then the black colored textile pieces were repeatedly washed with water and dried at laboratory temperature. The amount of magnetic iron oxide bound to textile was measured as a difference of textile mass before and after treatment.

Textile number	Mass before treatment [g]	Mass after treatment [g]	Difference [g]
1	4,095	4,291	0,196
2	3,897	4,062	0,165
3	3,837	3,947	0,110
4	3,607	3,712	0,105
5	3,552	3,721	0,169



Figure 1. Examples of native felt, felt modified with 20% ferrous sulfate solution and magnetic iron oxide particles modified felt (from left to right).

2.2 Measurement Techniques

The magnetic susceptibility was measured by a commercial susceptometer (IMEGO, DynoMag, SE), working at laboratory temperature and frequencies from 1 Hz up to 250 kHz, with a volume susceptibility resolution of 4×10^{-7} . The amplitude of the excitation field was 0.5 mT.

Irradiation was carried out on an electron accelerator M-30 microtron of the Institute of Electron Physics, certified for radiation research, figure 2. The M-30 parameters allow one to smoothly regulate accelerated nuclear particles' energy in the range of 1–25 MeV with mono energy of 0.02% and a beam current value of up to 50 μ A. Conditions for nuclear irradiation of samples were as follows: irradiation was carried out in the air, at room temperature; the irradiation flux density was $3.1 \cdot 10^{11}$ el. ($\text{cm}^{-2} \text{sec}^{-1}$) and not lead to heating of the irradiated samples. Irradiation field homogeneity was more than 80%; irradiated procedure was carried three times with doses of 53 kGy, 100 kGy and 163 kGy. The total time of samples irradiation was 40 min. The contribution of associated photoneutrons and bremsstrahlung gamma radiation was monitored and did not exceed 5%. The energy of the 18.5 MeV particles provided the same irradiation conditions for the entire, as the shadow effects were virtually absent.

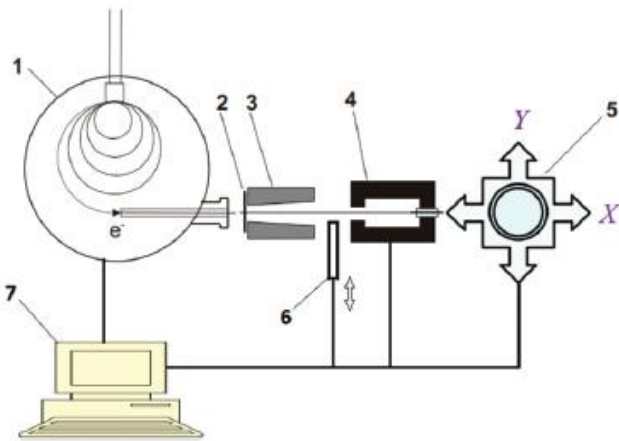


Figure 2. Scheme of the radiation experiment (1) electron accelerator the M-30 microtron; (2) and (3) irradiation field shaper, (4) is Faraday cylinder, (5) the scanner, (6) sample container, (7) the M-30 control and registration panel.

At electron energies above 10 MeV, the maximum energy they give to recoil atoms structure of nanomagnetic textured samples exceeds 10^4 eV, which leads to cascades of atomic displacements, which can also be caused by fast neutrons and heavy charged particles. In this case, the irradiated samples have the local disordered regions with significant damage to the structure of molecules and formations of isolated groups of ionized/excited molecular segments and their structural

complexes, 'spurs', where the primary acts of magnetic interaction and order of the structure can occur.

III. RESULTS AND DISCUSSION

The magnetic susceptibility (χ) of the samples was measured in the frequency range from 1 Hz to 250 kHz. A wide frequency range was covered to understand how magnetic susceptibility depends on frequency. This is particularly important for analyzing nanoparticles, whose behavior can change significantly at high frequencies. Radiation exposure causes defect formation that affects magnetic properties.

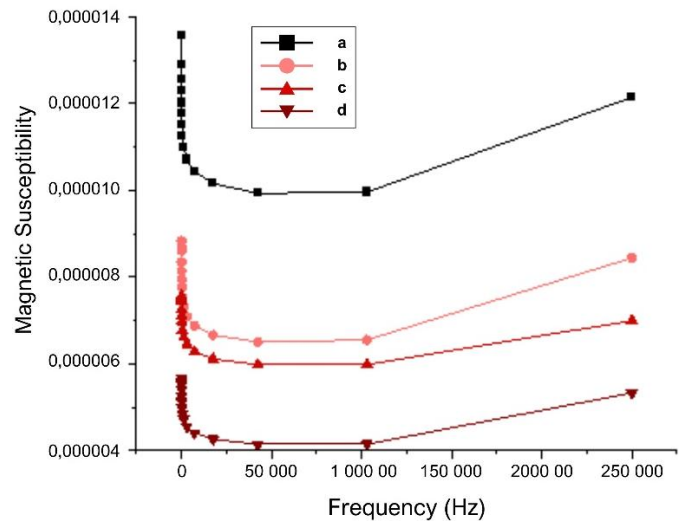


Figure 3. Magnetic susceptibility (Technical felt + $\text{FeSO}_4 + \text{Na}_2\text{CO}_3$) (textile number 1: 0.196g of magnetic nanoparticles per 1 textile square): a: before radiation; b: after irradiation with dose of 53 kGy; c: after irradiation with dose of 100 kGy; d: after irradiation with dose of 163 kGy.

At low frequencies (1 Hz): High susceptibility is expected, as the magnetic moments of the particles can "follow" changes in the field. At high frequencies (250 kHz): Susceptibility may decrease due to dynamic effects (Néel or Brownian relaxation), especially if the nanoparticles are small.

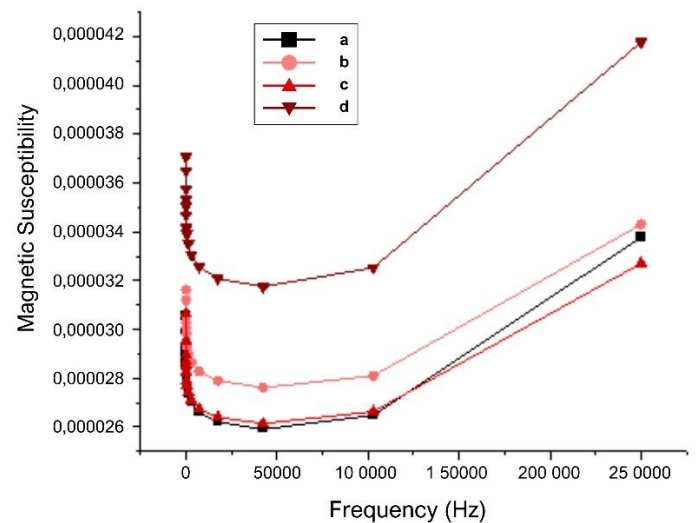


Figure 4. Magnetic susceptibility (Technical felt + $\text{FeSO}_4 + \text{Na}_2\text{CO}_3$) (textile number 1: 0.196g of magnetic nanoparticles per 1 textile square): a: before radiation; b: after irradiation with dose of 53 kGy; c: after irradiation with dose of 100 kGy; d: after irradiation with dose of 163 kGy.

Magnetic textiles demonstrated effective attenuation of EMI, with a notable reduction in susceptibility following radiation exposure. This degradation was attributed to defect formation and the disruption of magnetic domains within the textile matrix. Despite these changes, the fabrics retained a degree of shielding efficiency against charged particle radiation, suggesting potential for application in protective garments.

Radiation increases the number of defects (e.g., vacancies and interstitial atoms), disrupting the alignment of magnetic domains. These defects reduce the material's overall susceptibility to an external magnetic field. If the modifying agent (e.g., magnetic iron oxide) is damaged or altered by radiation, it also affects the magnetic properties.

This material could be useful as an additional layer in a multilayer protective suit, providing protection against secondary radiation effects (e.g., thermal impact or charge decay).

It can be integrated into protective cloaks for:

- **Shielding against charged particles:** Protection from alpha and beta particles.
- **Antistatic effect:** Due to its magnetic properties, the material can reduce the accumulation of electric charges.

IV. CONCLUSIONS

This study highlights the complementary roles of magnetic textiles in shielding against electromagnetic and nuclear radiation. The material can protect against charged particles (alpha and beta radiation) since the magnetic field affects their trajectory.

Applications:

- An additional layer in multilayer protection, reducing secondary radiation effects (thermal impact, charge accumulation).
- Shielding charged particles, for example, in spacesuits or laboratory protective suits.
- Antistatic coating - to prevent the accumulation of electric charge.

While materials experience degradation under radiation exposure, their distinct mechanisms offer potential for hybrid protective solutions. Future work will focus on optimizing material compositions and exploring their applications in wearable protective gear and shielding for sensitive electronics.

REFERENCES

- [1] Mikołajczyk, Z., Nowak, I., Januszkiewicz, Ł., Szewczyk, M., & Junak, J., Modern Electromagnetic-Radiation-Shielding Materials Made Using Different Knitting Techniques. *Materials*, 17(13), 3052. (2024).
- [2] Shahzad, F., & Iqbal, N., Textile fabrics as electromagnetic shielding materials—A review of the current state and future trends. *Fibers*, 11(3), 29. (2022).
- [3] Sparavigna, A. C., Iron Oxide Fe₃O₄ Nanoparticles for Electromagnetic Shielding. *ChemRxiv*. (2023).
- [4] Das, A., & Singh, S., Magnetic nanoparticles application in the textile industry—A review. *Journal of Industrial Textiles*, 49(8), 1061–1095. (2019).
- [5] Liu, X., & Zhang, Y., A review of electromagnetic shielding fabric, wave-absorbing mechanism, and design strategies. *Materials*, 14(3), 583. (2021).
- [6] Safarik, I., K. Horska, K. Pospiskova, Z. Maderova and M. Safarikova, "Microwave Assisted Synthesis of Magnetically Responsive Composite Materials." *IEEE Transactions on Magnetics* 49(1): 213-218. (2013).

Analysis of multiple machine learning approaches in astrophysics

¹*Lenka Kališková (3rd year),*
Supervisor: ²Peter Butka

^{1,2}Dept. of Cybernetics and Artificial Intelligence, FEI TU of Košice, Slovak Republic

¹lenka.kaliskova@tuke.sk, ²peter.butka@tuke.sk

Abstract—This paper presents a comprehensive analysis of multiple machine learning approaches for astrophysical image analysis, focusing on two critical tasks: meteor detection and segmentation of coronal holes and active regions. For meteor detection, the performance of HIC-YOLOv5, YOLO-NAS, DETR, and Faster R-CNN is evaluated to improve accuracy and robustness. In the case of solar image segmentation, YOLOv8-Seg and Pix2Pix are assessed against SCSS-Net to determine their effectiveness in identifying solar structures. The results provide insights into each approach, offering guidance for future applications in astronomical data analysis.

Keywords—Astrophysics, Convolutional Neural Network, Image Segmentation, Object Detection, Pix2Pix, YOLO

I. INTRODUCTION

Machine learning plays a crucial role in processing observational data in astronomy, particularly in image analysis. A key challenge in these fields is the detection and segmentation of celestial and atmospheric phenomena, where deep learning techniques have significantly improved accuracy and efficiency. This study focuses on two critical tasks: meteor detection and segmentation of coronal holes and active regions.

Meteor detection is essential for understanding atmospheric and space phenomena, with applications in meteor shower tracking and near-Earth object studies. Previous work [1] utilized YOLOv5 for detecting meteors in images captured by Slovak AMOS cameras [2]. However, challenges remain in detecting small, fast moving objects with high precision. To address this, we evaluate multiple object detection models, namely HIC-YOLOv5, YOLO-NAS, DETR, and Faster R-CNN, each offering different advantages in terms of accuracy, speed, and robustness against false positives. By comparing these architectures, we aim to refine detection methods and improve overall reliability.

Segmentation of coronal holes and active regions is another crucial task, impacting space weather forecasting and solar activity analysis. Coronal holes, vast regions of open magnetic field lines, contribute to high-speed solar wind streams that influence Earth's magnetosphere. Active regions, characterized by strong magnetic fields, are linked to solar flares and coronal mass ejections [3]. While previous study successfully employed SCSS-Net [4] for coronal hole segmentation, alternative deep learning models such as YOLOv8-Seg and Pix2Pix are explored in this study. Their performance is assessed against SCSS-Net to determine their suitability for solar image segmentation.

By advancing meteor detection techniques and evaluating new segmentation models for coronal holes and active regions, this research aims to improve the accuracy and automation of astronomical image analysis. These findings contribute to more efficient data processing in observational astronomy, supporting both meteor tracking and solar activity studies.

II. PRELIMINARY RESULTS

As previously discussed, various machine learning approaches were selected. Therefore, the following section is dedicated to revisiting these approaches and the associated data.

A. Detection of meteors

This study utilizes a dataset of video frames captured by AMOS cameras in Slovakia. It includes 241 images containing 249 meteors and 35 satellites, annotated with bounding boxes for supervised learning. The dataset originates from the Slovak Video Meteor Network (SVMN), which produces around 40 000 frames annually, many of which contain false positives, primarily satellites. To ensure high-quality training data, only verified meteor detections were included.

Building on prior research [1], this study investigates the performance of several deep learning models to enhance detection accuracy and efficiency.

The dataset remained consistent with the previous study, ensuring a fair comparison. To improve detection performance, we implemented and trained four deep learning models: HIC-YOLOv5, YOLO-NAS, DETR, and Faster R-CNN. Each model was selected based on its potential to refine small-object detection, a critical factor in meteor identification. The training dataset consisted of annotated meteor and satellite images captured by AMOS cameras, following the same annotation format as in the study [1].

- HIC-YOLOv5: A modified version of YOLOv5 designed to improve small-object detection by optimizing network architecture for higher resolution input images [5].
- YOLO-NAS: A neural architecture search (NAS)-optimized model that dynamically adapts its structure to enhance both accuracy and inference speed [6].
- Faster R-CNN: A region-based convolutional neural network known for its precision, leveraging a region proposal network (RPN) to localize objects before classification [7].

- DETR: A transformer-based object detection model that eliminates the need for RPN, leveraging self-attention mechanisms to detect objects across an image [8].

The dataset remained consistent with the previous study, ensuring a fair comparison. Each model demonstrated unique strengths and weaknesses. Faster R-CNN achieved the highest precision and recall, making it the most effective model for meteor detection. However, its complex architecture requires significant computational resources. HIC-YOLOv5, while less accurate, was the fastest and most efficient in terms of resource usage. YOLO-NAS balanced speed and accuracy but showed reduced reliability in certain scenarios. DETR provided the most precise bounding box placements and high detection reliability but struggled with scenes containing multiple meteors.

Faster R-CNN performed best in detecting meteors, achieving 96.5% precision and 98.4% recall. However, satellite detection was less reliable across all models, with lower recall and precision scores. Overall, model performance was strong, but false positives and detection confidence thresholds remain areas for further optimization.

Overall, Faster R-CNN outperformed YOLOv5, achieving higher precision and recall while reducing false detections. YOLO-NAS offered a balanced trade-off between speed and accuracy, while DETR excelled in precision under ideal conditions but struggled with multiple meteors.

B. Segmentation of coronal holes and active regions

The coronal hole is a dark area on the solar disk, appearing as an irregular circle or oval, often several times the size of Earth. Active regions are temporary areas with a stronger magnetic field than their surroundings, affecting space weather and Earth's environment [3].

This study uses extreme ultraviolet (EUV) images from the SOHO satellite's Extreme Ultraviolet Imaging Telescope (EIT), with 195Å images for coronal holes and 171Å for active regions. Annotations from prior studies [4], [9] were used to train and evaluate models.

To improve segmentation of these solar structures, we evaluated two deep learning approaches: YOLOv8-Seg and Pix2Pix.

Evaluation of YOLOv8-Seg [10] model for mentioned solar structures showed that performance is far from optimal. For coronal holes, it achieved a Dice score of 0.59, significantly lower than SCSS-Net's 0.88. In the case of active regions, YOLOv8 demonstrated even greater limitations, highlighting the complexity of accurately segmenting these structures.

Pix2Pix [11] was also tested and demonstrated better performance than YOLOv8, particularly in coronal hole segmentation. It achieved an average Dice score of 0.75 and an IoU of 0.65. The model exhibited strong generalization capabilities, successfully identifying coronal holes even with incomplete annotations. However, despite these improvements, Pix2Pix did not surpass SCSS-Net, which remained the most effective model for this task. The Fig. 1 shows the segmentation of coronal holes by Pix2Pix.

Active region segmentation posed a greater challenge due to the high variability in the data. The model performance remained limited, with average Dice and IoU scores of 0.41 and 0.27, respectively.

For improved evaluation, a visualization technique was employed, overlaying predicted segmentation masks onto original

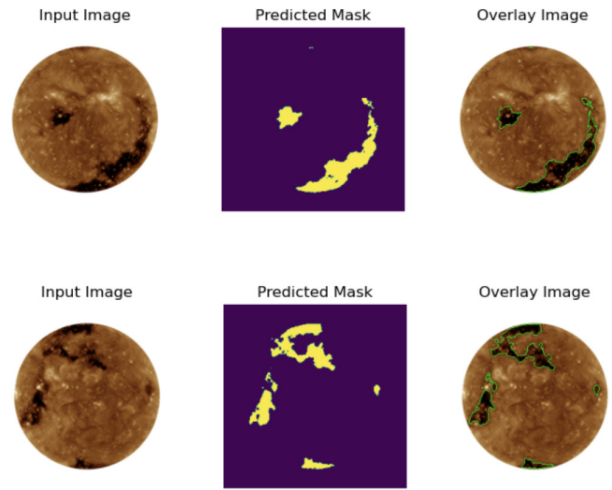


Fig. 1. Segmentation of coronal holes using Pix2Pix. From the left side, input solar images are displayed, then predicted coronal hole masks generated by Pix2Pix, and finally input images overlaid with the predicted coronal hole boundaries are displayed.

images. This facilitated a more detailed analysis of segmentation accuracy and common error patterns. Nevertheless, neither Pix2Pix nor YOLOv8 matched the performance of SCSS-Net.

These findings reinforce the effectiveness of SCSS-Net for coronal hole segmentation and its relative advantage in active region detection. While Pix2Pix demonstrated potential, particularly for coronal holes, further optimization would be required to achieve competitive results.

III. CONCLUSION

In this study, we focused on analyzing observational image data, particularly in the domains of meteor detection and solar structure segmentation. By applying deep learning architectures, we aimed to refine the methods for detecting meteors and segmenting coronal holes and active regions. This research builds upon our previous work and is conducted in collaboration with experts in the physical domain to enhance the processing and analysis of scientific data.

Convolutional neural networks have proven indispensable in our work for detecting and segmenting objects in astronomical images. These models, including YOLO-based architectures, are essential for identifying small and fast-moving objects like meteors as well as complex solar structures. The challenges of detecting small objects and segmenting intricate solar features are compounded by data limitations and variability, making the optimization of deep learning models crucial for success.

Our main motivation is to develop robust solutions for the detection and segmentation tasks associated with meteor identification and solar feature analysis. To achieve this, we focus on improving model quality by exploring various detection architectures and enhancing the ability to handle small-object detection in dynamic conditions. We also emphasize combining different approaches to optimize results, ensuring the development of more accurate and reliable models. Ultimately, the goal is to improve the quality and efficiency of automated astronomical data analysis, contributing to better insights into atmospheric and solar phenomena.

Future research for meteor detection could focus on optimizing detection models and extending them to multi-class

classification. Expanding classification capabilities could improve model adaptability and provide a more comprehensive analysis of atmospheric and astronomical phenomena.

In case of segmentation, future research could focus on improving segmentation models for active regions and coronal holes and exploring new GAN-based architectures. Investigating alternative generative models could lead to more precise and robust segmentation, enhancing the accuracy of space weather forecasting and solar activity analysis.

ACKNOWLEDGMENT

This work was supported by the Slovak Research and Development Agency under the contract No. APVV-22-0414.

REFERENCES

- [1] L. Kališková and P. Butka, "Overview of machine learning methods in astrophysics," *SCYR 2024: 24th Scientific Conference of Young Researchers*, pp. 166–167, 2024.
- [2] J. Tóth, J. Šilha, P. Matlovič, L. Kornoš, P. Zigo, J. Világi, D. Kalmančok, J. Šimon, and P. Vereš, "Amos—the slovak worldwide all-sky meteor detection system," in *Proc. 1st NEO and Debris Detection Conference*, vol. 1, 2019.
- [3] L. van Driel-Gesztelyi and L. M. Green, "Evolution of active regions," *Living Reviews in Solar Physics*, vol. 12, pp. 1–98, 2015.
- [4] Š. Mackovjak, M. Harman, V. Maslej-Krešňáková, and P. Butka, "Scss-net: solar corona structures segmentation by deep learning," *Monthly Notices of the Royal Astronomical Society*, vol. 508, no. 3, pp. 3111–3124, 2021.
- [5] S. Tang, S. Zhang, and Y. Fang, "Hic-yolov5: Improved yolov5 for small object detection," in *2024 IEEE International Conference on Robotics and Automation (ICRA)*, 2024, pp. 6614–6619.
- [6] Deci, "Yolo-nas by deci achieves sota performance on object detection using neural architecture search," *ALGORITHMS*, 2023. [Online]. Available: <https://deci.ai/blog/yolo-nas-object-detection-foundation-model/>
- [7] S. Ren, K. He, R. Girshick, and J. Sun, "Faster r-cnn: Towards real-time object detection with region proposal networks," *Advances in neural information processing systems*, vol. 28, 2015.
- [8] N. Carion, F. Massa, G. Synnaeve, N. Usunier, A. Kirillov, and S. Zagoruyko, "End-to-end object detection with transformers," in *Computer Vision – ECCV 2020: 16th European Conference, Glasgow, UK, August 23–28, 2020, Proceedings, Part I*. Berlin, Heidelberg: Springer-Verlag, 2020, p. 213–229. [Online]. Available: https://doi.org/10.1007/978-3-030-58452-8_13
- [9] E. A. Illarionov and A. G. Tlatov, "Segmentation of coronal holes in solar disc images with a convolutional neural network," *Monthly Notices of the Royal Astronomical Society*, vol. 481, no. 4, pp. 5014–5021, 2018.
- [10] A. A. Alsuwaylimi, "Enhanced yolov8-seg instance segmentation for real-time submerged debris detection," *IEEE Access*, vol. 12, pp. 117 833–117 849, 2024.
- [11] K. Patel, P. Shah, and R. Gajjar, "Semantic segmentation of urban area using pix2pix generative adversarial networks," in *2023 3rd International Conference on Range Technology (ICORT)*, 2023, pp. 1–6.

Thermal stability of thermoplastic starch blends with lignin

¹Leoš ONDRIŠ (3rd year)
Supervisor: ²Olga FRÍČOVÁ

^{1,2}Dept. of Physics, FEI, Technical University of Košice, Slovak Republic

¹leos.ondris@tuke.sk, ²olga.fricova@tuke.sk

Abstract—Plastic waste is a major environmental problem nowadays. Biodegradable materials (e.g. thermoplastic starch) are being developed to replace synthetic plastics. The effect of varying component ratio on the structure and thermal properties of TPS/lignin blends was analyzed using wide-angle X-ray scattering (WAXS), differential scanning calorimetry (DSC) and thermogravimetric analysis (TGA). The results showed that the addition of lignin affects the structure of TPS in blends. The effect of lignin was observed at its contents of 10% and higher, indicating that lignin limits the mobility of starch chains and increases thermal stability of TPS/lignin blends.

Keywords—thermal stability, thermoplastic starch, lignin, wide-angle X-ray scattering, differential scanning calorimetry, thermogravimetric analysis

I. INTRODUCTION

In today's society, plastic materials are an essential part of our daily lives. As a result, the increasing amount of plastic waste and its insufficient recycling are major environmental problems. One possible solution lies in replacing fossil-fuel plastic materials with biodegradable ones. Thermoplastic starch (TPS) represents an environmentally friendly alternative to conventional plastics due to its biodegradability and renewability [1]. However, its mechanical properties (especially low mechanical strength), resistance to water and water vapor, and especially the recrystallisation (retrogradation) process, are often limiting factors for its wider use in industrial applications [2]. One solution to improve these properties is e.g. blending TPS with other (biodegradable) polymer(s) and formation of TPS-based (nano)composites [1][2][3]. In this work, lignin was used to improve TPS properties. Lignin is a natural biodegradable polymer found in plant biomass. It has high stiffness, good adhesive, hydrophobic and thermal properties, which can improve strength, hydrophilicity, (thermal) stability and barrier properties of TPS-based materials [4][5].

This work focuses on the investigation of the effect of different lignin contents on the structure and properties of TPS/lignin blends. Experimental methods such as wide-angle X-ray Scattering (WAXS), differential scanning calorimetry (DSC) and thermogravimetric analysis (TGA) provide information about structure and relaxation transitions in starch-based materials.

This work aimed to optimize lignin content to achieve the best possible balance between mechanical properties, thermal stability and degradability of the resulting material.

II. SAMPLES AND PREPARATION

The studied blends were prepared at the Polymer Institute of the Slovak Academy of Sciences in Bratislava. The lignin content in the samples was 0%, 3%, 5%, 10%, 15% and 20% and respective samples were denoted TPS, TPS3, TPS5, TPS10, TPS15 and TPS20. All measurements were performed 2 months after sample preparation.

III. EXPERIMENTAL METHODS

A. Wide-angle X-ray scattering (WAXS)

X-ray diffractograms were detected on Anton Paar XRDynamics 500, was operated at a voltage of 40.1 kV and a current of 50 mA. Cu K α X-rays with a wavelength of $\lambda=0.154$ nm were used. The sample and the detector were rotated at 2.5°/min and 5°/min, respectively. The method theta-2theta was used for WAXS measurements.

B. Differential scanning calorimetry (DSC)

DSC measurements were performed on a Mettler Toledo DSC-1 instrument equipped with Huber TC100 cooling system. Temperature measurements ran from -80 °C to 350 °C with the heating rate of 10 °C/min under nitrogen gas flow. About approx. 10 mg of the samples were encapsulated in 40 μ l aluminum pans.

C. Thermogravimetric analysis (TGA)

TGA measurements were performed on a Netzsch STA 449 F1 Jupiter instrument. The temperature range of the TGA measurements was 25-600 °C with a heating rate of 10 °C/min in an air atmosphere with a flow rate of 50 ml/min. The sample weight for analysis was approximately 20 mg and samples were placed in a 25 μ l corundum plate.

IV. RESULTS AND DISCUSSION

A. WAXS measurements

Fig. 1 shows X-ray diffractograms of the TPS and TPS/lignin blends with different lignin contents. It should be mentioned that TPS immediately after its preparation is an amorphous material. Several maxima at 7.7°, 13.4°, 17.4°, 20.7°, and 22.7° 2theta can be observed in the diffractograms. The maxima at 7.7°, 13.4° and 20.7° 2theta correspond to starch crystalline regions of V_H-type [6] which are formed by the rearrangement of simple helices of amylose linear chains of starch in a very short time after TPS preparation [7]. The

maxima at 17.4° and 22.7° 2theta correspond to the starch crystalline regions of B-type [6]. The B-type crystalline regions consist of double helices of both polymers in starch – linear amylose and branched amylopectin chains. These crystalline regions are formed in TPS during storage [7].

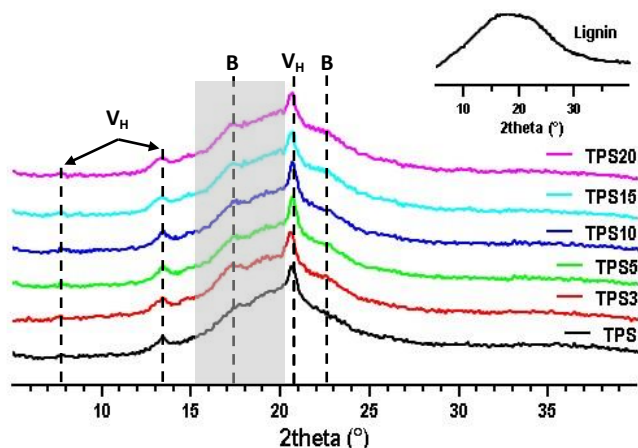


Fig. 1 WAXS diffractogram of the studied samples

Diffractograms for the studied samples differ in the intensity of the shoulder in the range of 15°-20° 2theta (gray area in the graph). This shoulder reflects the structure of lignin, which gives a distinct amorphous maximum at about 18° 2theta [5].

B. DSC measurements

In this work, the DSC method was used to determine the relaxation transitions in the samples, namely glass transition (T_g) and melt temperature (T_m), although most of the available DSC results are inconsistent and sometimes inaccurate. This is due to the multiple phase transformations that starch undergoes during heating as well as the instability of the water molecules entrapped in the starch structure [8].

Fig. 2 shows the temperature dependence of the heat flow (ΔHF) of the samples. All samples show a similar trend, while differing in the intensity of individual thermal transitions. No significant changes are observed in the temperature range from -70 °C to 150 °C. The decreasing part of the curves indicates endothermic processes (samples absorb heat). Glass transitions are expected to occur in this region, causing the change of the curve slope, however, in the obtained results they cannot be detected due to the insufficient sensitivity of the DSC [8][9].

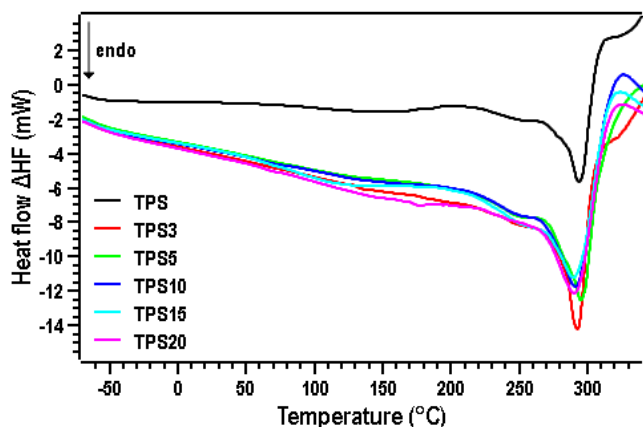


Fig. 2 DSC thermogram of the studied samples

The pronounced endothermic maximum observed at

approximately 292 °C is related to the thermal decomposition of starch, which is observed at approximately the same temperature for all samples. At this temperature, thermal decomposition of the glycosidic bonds occurs and low molecular weight products or other volatile substances are formed [9][10].

C. TGA measurements

The thermal degradation (pyrolysis) and heat resistance of the starch-based samples with different lignin contents were investigated by TGA analysis and the graphical representation of the results is shown in Fig. 3a). The maxima of thermal degradation in specific phases were evaluated from the local maxima of the first derivative of the thermogravimetric curve (DTG) shown in Fig. 3b). Three phases of thermal degradation were detected (gray areas in Fig. 3a) and 3b)). All samples were thermally stable (i.e. their mass did not change) up to a temperature of about 80 °C, with this limit shifting to slightly higher temperatures with an increasing lignin content. The mass of pure TPS was unchanged up to 76 °C, while the TPS20 samples were unchanged up to 85 °C.

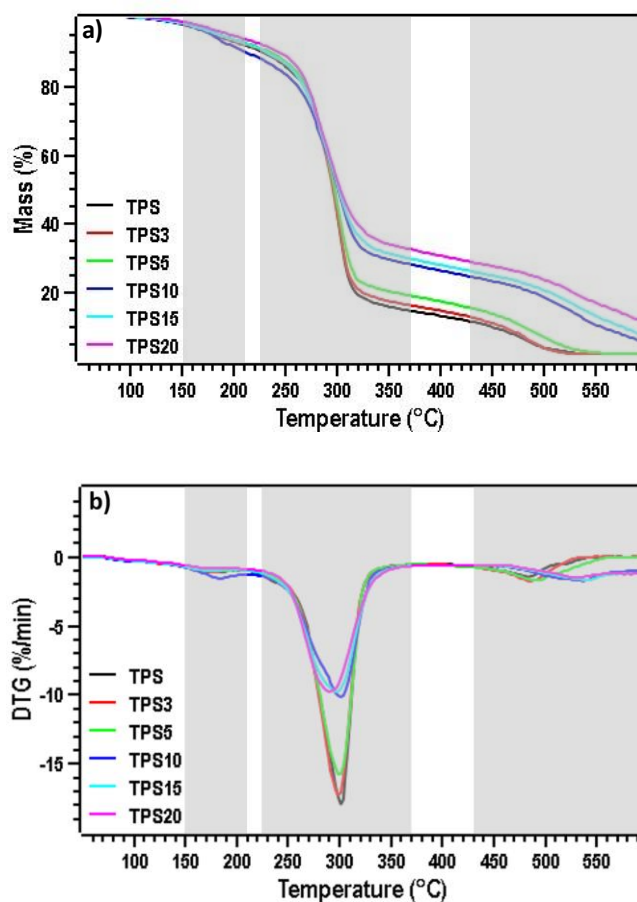


Fig. 3 Temperature dependences of TGA a) and derivative (DTG) b) curves of the studied samples

The first phase of thermal degradation peaked in all samples at approximately 170 °C. Evaporation of (free or/and bound) water followed by glycerol probably occurred at this stage [9][10][11][12]. The mass of all samples was approximately 96.5% of their original mass. Further thermal degradation is observed in the temperature range from 225 °C to 370 °C, with the peak of the main thermal degradation of glycosidic chains (aliphatic groups) of starch and lignin with

evaporation of glycerin and water. This pyrolysis for all samples was observed around 298 °C [9][10][11]. At this temperature, a difference in the thermal stability of the samples can be observed. A lower mass loss was observed with increasing lignin content from 44% for TPS to 62% for TPS20. The last phase of thermal degradation took place from 430 °C to 550 °C with peak degradation at 485 °C with 6.1%, 6.6%, 8.8% for TPS, TPS3, TPS5, respectively. The third phase for TPS10, TPS15, TPS20 samples was shifted to the higher temperature intervals beginning around 450 °C to 560 °C with peak degradation at 530 °C. The residual mass for TPS10, TPS15, TPS20 samples was 13.3%, 15.4%, and 20.4%, respectively. This phase is associated with thermal degradation of lignin and other organic components (mostly burning of carbon) that did not decompose in the second phase [9][12][13]. The TPS, TPS3 and TPS5 samples do not show any change in their masses in the temperature interval of 550 °C to 600 °C. These samples are totally decomposed exothermally to gaseous products resulting in a carbon-rich residue (ash), and their mass was stabilized at about 2.5% of the original mass [13]. It can be argued that these samples have managed to decompose before reaching temperature 600 °C. Slight differences are observed for other samples, where even at 600 °C not all components in the blends with 10% and more lignin content were completely degraded. The TPS10, TPS15 and TPS20 samples at temperature 600 °C showed a mass of 5.5%, 7.1% and 11% compared to the original mass, respectively. From these data, it can be concluded that as the lignin content of the samples increases, thermal stability of the samples increases. This is probably due to the fact that as the lignin content increases, the mobility of the starch chains decreases and the sample becomes stiffer. The lower the mobility of the chains, the higher the degradation temperature. The mobility of chains decreases intermolecular interactions and lowers the dissociation energy [12][14].

V. CONCLUSION

In this work, we investigated the effect of different lignin contents on the structure and thermal stability of thermoplastic starch blends. The WAXS diffractograms revealed that the presence of lignin slightly facilitates the formation of crystalline structure in TPS. TGA analyses showed that lignin addition affects the thermal stability of the material especially at higher lignin contents (10% and more). These results imply that lignin reduces the mobility of starch chains. In further research we would like to study the influence of lignin on the TPS/lignin blends using methods which are sensitive to the changes in their structure and molecular mobility.

ACKNOWLEDGMENT

All measurements (WAXS, DSC and TGA) of the samples were carried out at Department of Polymer Engineering, Faculty of Technology, Tomas Bata University in Zlín as a part of my Erasmus+ mobility. Many thanks to associate prof. Alena Kalendová, Dr. Ondřej Krejčí, and Dr. Jiřina Dohnalová for their help, realization and evaluation of these experiments.

REFERENCES

- [1] M. N. Belgacem, A. Gandini, *Monomers polymers and composites from renewable resources: Starch: Major sources, properties, and applications as thermoplastic materials*, Kidlington: Elsevier Ltd., 2008, ch. 15.
- [2] A. M. Nafchi, M. Moradpour, M. Saeidi, A. K. Alias, "Thermoplastic starches: Properties, challenges, and prospects," in *Starch/Stärke*, vol. 65, 2013, pp. 61-72.
- [3] J. H. Han, *Innovations in Food Packaging: Thermoplastic Starch*, Elsevier Ltd, 2014, ch. 16.
- [4] A. Naseem, et al. "Lignin-derivatives based polymers, blends and composites: A review," in *International Journal of Biological Macromolecules*, vol. 93, 2016, pp. 293-313.
- [5] A. Abe, et al., *Advances in Polymer Science: Biopolymers: Lignin, Proteins, Bioactive Nanocomposites*, Berlin: Springer-Verlag, 2010, ch. 1.
- [6] S. Saporová, et al. "Effects of glycerol content on structure and molecular motion in thermoplastic starch-based nanocomposites during long storage," in *International Journal of Biological Macromolecules*, vol. 253, 2023, pp. 126911.
- [7] M. Paluch, J. Ostrawska, P. Tyński, W. Sadurski, M. Konkol, "Structural and thermal properties of starch plasticized with glycerol/urea mixture," in *Journal of Polymers and the Environment*, vol. 30, 2022, pp. 728-740.
- [8] Y. Zhang, C. Rempel, Q. Liu, "Thermoplastic starch processing and characteristics – A review," in *Critical Reviews in Food Science and Nutrition*, vol. 54, 2014, pp. 1353-1370.
- [9] Midhun Dominic C. D., et al., "Thermoplastic starch nanocomposites using cellulose-rich *Chrysopsis zizanioides* nanofibers," in *International Journal of Biological Macromolecules*, vol. 191, 2021, pp. 572-583.
- [10] E. Stasi, et al., "Biodegradable carbon-based ashes/maize starch composites films for agricultural applications," in *Polymers*, vol. 12, 2020, pp. 524.
- [11] M. Ragoubi, C. Terrié, N. Leblanc, "Physico-chemical, rheological, and viscoelastic properties of starch bio-based materials," in *Journal of Composites Science*, vol. 6, 2020, pp. 375.
- [12] M. Esmaili, G. Pircheraghi, E. Bagheri, "Optimizing the mechanical and physical properties of thermoplastic starch via tuning the molecular microstructure through co-plasticization by sorbitol and glycerol," in *Polymer International*, vol. 66, 2017, pp. 809-819.
- [13] J. Akbar, M. S. Iqbal, S. Massey, R. Masih, "Kinetics and mechanism of thermal degradation of pentose- and hexose-based carbohydrate polymers," in *Carbohydrate Polymers*, vol. 90, 2012, pp. 1386-1393.
- [14] G. S. A. Suleiman, X. Zheng, R. Chakma, I. Y. Wakai, Y. Feng, "Recent advances and challenges in thermal stability of PVA-based film: A review," in *Polymers for Advanced technologies*, vol. 35, 2024, pp. e6327.

Experimental Validation of Direct Speed Predictive Control

¹Lukáš PANCURÁK (3rd year),
Supervisor: ²Karol KYSLAN

^{1,2}Dept. of Electrical Engineering and Mechatronics, FEEI TU of Košice, Slovak Republic

¹lukas.pancurak@tuke.sk, ²karol.kyslan@tuke.sk

Abstract—This paper presents the Finite Control Set Model Predictive Direct Speed Control (FCS-MPDSC) for surface-mounted permanent magnet synchronous motor (SM-PMSM), with a sliding mode observer (SMO) for load torque estimation. The proposed method improves steady state precision under all operating points, excellent dynamic performance and acceptable current ripples, while maintaining simplicity and intuitive controller design. The control algorithm is experimentally validated on a test bench with a hardware-in-loop simulator and offers competitive performance compared to existing solutions.

Keywords—model predictive control, direct speed control, sliding mode observer

I. INTRODUCTION

Model Predictive Control (MPC) is increasingly used in power electronics and motor control due to its ability to predict system behaviour using a mathematical model [1]. It optimizes control inputs via a cost function, enabling flexibility and multi-variable control in one control loop [2]. Finite Control Set MPC (FCS-MPC) is particularly suited for electrical drives, directly selecting optimal switching states, offering fast dynamics and intuitive solution to control non-linear system [3]. However, challenges like variable switching frequency, high current ripples, and load torque estimation remain. This paper introduces and experimentally verifies an FCS-MPDSC method with a sliding mode observer (SMO) for torque estimation [4]. This work builds upon previous simulation-based validation of the method in [5] and the controller sensitivity analysis conducted in [6].

II. FINITE CONTROL SET MODEL PREDICTIVE DIRECT SPEED CONTROLLER

The control algorithm starting with the current and position measurement, estimation of load torque, calculation of predictions, optimization algorithm in the form of a cost function, and lastly selection and application of optimal actuation. The control objectives are represented in the cost function given by (2). Speed control is represented by the first term of a cost function, as the error between the reference ω^* and predicted value ω^p . For maximum torque-per-ampere ratio, current i_d^p is controlled to zero value. Lastly, current i_q^p is controlled regarding the observed value of load torque $\hat{T}_L(k)$ that is converted to

current reference as i_q^* , by equation 1. Weighting factors λ_{1-3} have been selected by trial and error method. Constraints to limit maximum current were also implemented by introducing artificial error i_{OC} into the result of a cost function when current vector $i_s > I_{max}$.

$$i_q^*(k+1) = \frac{B}{k_t}\omega(k) + \frac{1}{k_t}\hat{T}_L(k+1), \quad (1)$$

$$J(k) = \lambda_1(\omega^* - \omega^p(k+1))^2 + \lambda_2(i_d^p(k+1))^2 + \lambda_3(i_q^* - i_q^p(k+1))^2 \quad (2)$$

The controller utilizes estimated values from the SMO and measured currents in dq coordinates as inputs to the predictive model. To implement this, the continuous mathematical model is discretized using the Taylor Series Expansion (TSE). The expansion order is set to $N_j = 1$ for current equations and $N_j = 2$ for the speed equation, resulting in the discrete PMSM model:

$$i_d^p(k+1) = a_1 i_d(k) + a_2 \omega(k) i_q(k) + a_3 u_{di}(k), \quad (3)$$

$$i_q^p(k+1) = a_1 i_q(k) + a_2 \omega(k) i_d(k) - a_4 \omega(k) + a_3 u_{qi}(k), \quad (4)$$

$$\omega^p(k+1) = a_5 \omega(k) + a_6 i_q(k) + a_7 \hat{T}_L(k) + a_8 \omega(k) i_d(k) + a_9 u_{qi}(k), \quad (5)$$

where load torque \hat{T}_L is obtained by SMO and $u_{di}(k)$, $u_{qi}(k)$ are vectors of all possible actuations. The predicted values are then used in a cost function.

III. EXPERIMENTAL RESULTS

The experimental setup consists of a two-level voltage source inverter (2L-VSI) and a real-time hardware-in-loop (HIL) simulator OP5600 from RT-LAB, which includes FPGA-based computational capabilities. The primary machine under test is a synchronous motor whose parameters are listed in Table I. This motor is loaded by an asynchronous motor, which is controlled by a Siemens G120 industrial power converter.

The parameters of the controller are given in Table II. The speed and current responses to a step change in reference speed and application of a load torque are shown in Fig. 1. Small speed ripples can be observed on the actual speed ω_{act} caused by the effect of the speed sensor. Note, that

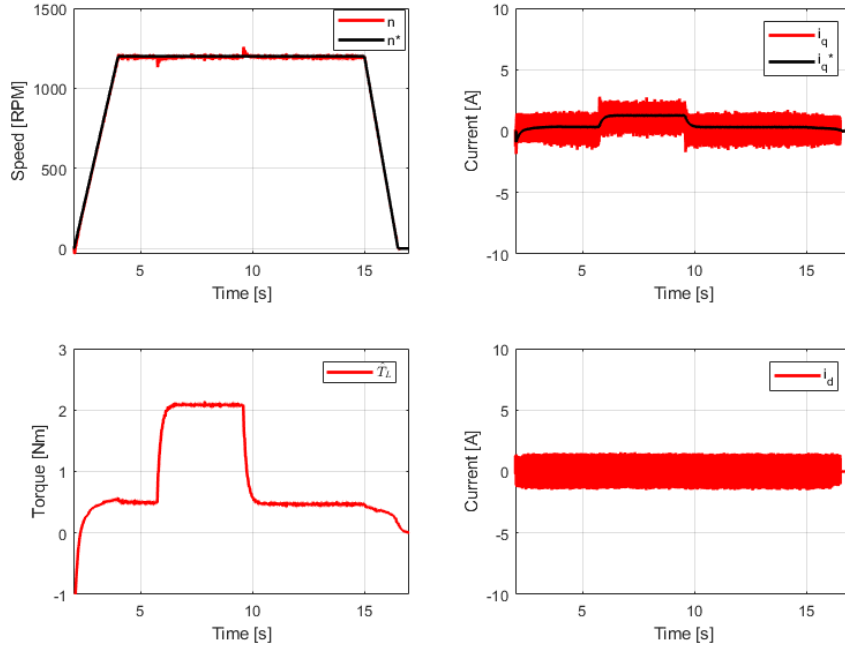


Fig. 1: Experimental response of the drive to speed reference $n^* = 1200 \text{ RPM}$ and load of $\hat{T}_L = 2 \text{ Nm}$.

TABLE I: Synchronous Motor Parameters TGN3-0480

Parameter	Value
Nominal Power (P_N)	1162 W
Nominal Speed (n_N)	3000 RPM
Nominal Current (I_N)	2.8 A
Nominal Torque (T_N)	3.7 Nm
Pole Pairs (p_p)	5

the change in steady state error is very low when applying a load torque, demonstrating the good robustness and performance of the controller and sliding mode observer alike. Furthermore, heavy current ripples can be observed on stator currents Fig. 2 and dq currents alike Fig. 1, which is an inherent trait of model predictive control, however, results are comparable to recent literature [7].

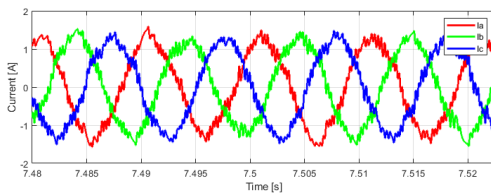


Fig. 2: Phase currents at speed reference $n^* = 1200 \text{ rpm}$ and load of $\hat{T}_L = 2 \text{ Nm}$.

TABLE II: Controller Parameters

Parameter	Value
$\lambda_1 \rightarrow$ weighting factor for ω	8
$\lambda_2 \rightarrow$ weighting factor for i_d	1
$\lambda_3 \rightarrow$ weighting factor for i_q	1

IV. CONCLUSION

The experiments were conducted to experimentally verify the performance of previously simulated results of

FCS-MPDSC. The controller with an SMO load torque observer and calculation of i_q current reference makes for a very intuitive and the simple design, directly controls currents and speed in single control loop. The results showed satisfactory steady-state performance, acceptable current ripples, and excellent dynamic performance.

ACKNOWLEDGMENT

This work was supported by the Scientific Grant Agency of the Ministry of Education, Science, Research and Sport of the Slovak Republic and Slovak Academy of Sciences (VEGA) under the project VEGA 1/0363/23.

REFERENCES

- [1] S. Kouro, M. A. Perez, J. Rodriguez *et al.*, “Model predictive control: Mpc’s role in the evolution of power electronics,” *IEEE Industrial Electronics Magazine*, vol. 9, no. 4, pp. 8–21, 2015.
- [2] C. S. Lim, E. Levi, M. Jones *et al.*, “Fcs-mpc-based current control of a five-phase induction motor and its comparison with pi-pwm control,” *IEEE Transactions on Industrial Electronics*, vol. 61, no. 1, pp. 149–163, 2014.
- [3] M. Preindl and S. Bolognani, “Model predictive direct speed control with finite control set of pmsm drive systems,” *IEEE Transactions on Power Electronics*, vol. 28, no. 2, pp. 1007–1015, 2013.
- [4] C. Gong, Y. Hu, K. Ni, J. Liu, and J. Gao, “Sm load torque observer-based fcs-mpdsc with single prediction horizon for high dynamics of surface-mounted pmsm,” *IEEE Transactions on Power Electronics*, vol. 35, no. 1, pp. 20–24, 2020.
- [5] L. Pancurák, T. Jure, and K. Kyslan, “Finite control set model predictive direct speed control of pmsm,” in *2023 International Conference on Electrical Drives and Power Electronics (EDPE)*, 2023, pp. 1–6.
- [6] L. Pancurák, D. Marcin, and K. Kyslan, “Sensitivity analysis of finite control set model predictive direct speed control of pmsm,” in *2024 ELEKTRO (ELEKTRO)*, 2024, pp. 1–6.
- [7] T. Li, X. Sun, G. Lei *et al.*, “Finite-control-set model predictive control of permanent magnet synchronous motor drive systems—an overview,” *IEEE/CAA Journal of Automatica Sinica*, vol. 9, no. 12, pp. 2087–2105, 2022.

Malware Threat Detection Using Artificial Intelligence And Machine Learning Methods

¹*Dušan ČATLOCH (1st year),*
Supervisor: ²Eva CHOVANCOVÁ

^{1,2}Dept. of Computers and Informatics, FEI, Technical University of Košice, Slovak Republic

¹dusan.catloch@tuke.sk, ²eva.chovancova@tuke.sk

Abstract—The increasing complexity and sophistication of modern malware pose a significant challenge to traditional detection methods. This paper explores the application of artificial intelligence and machine learning techniques in malware threat recognition. By leveraging advanced classification algorithms and behavioral analysis, AI-driven approaches can identify previously unseen threats and adapt to evolving attack patterns. The study compares different machine learning models, highlighting their effectiveness in detecting and mitigating malware infections. Experimental results demonstrate that AI-based methods significantly improve detection accuracy and response times, offering a more robust cybersecurity solution.

Keywords—Malware detection, artificial intelligence, machine learning, cybersecurity, threat recognition, behavioral analysis, anomaly detection, classification algorithms, malware analysis, adversarial attacks.

I. INTRODUCTION

The increasing sophistication and volume of malware attacks pose a significant threat to modern digital infrastructures. Traditional malware detection techniques, such as signature-based and heuristic analysis, have proven effective in identifying known threats but struggle against rapidly evolving malware variants and zero-day attacks. As cybercriminals employ advanced obfuscation and polymorphic techniques, conventional security measures become less effective, necessitating more adaptive and intelligent detection mechanisms.

In recent years, artificial intelligence (AI) and machine learning (ML) have emerged as powerful tools in cybersecurity, enabling dynamic malware recognition based on behavioral analysis, anomaly detection, and predictive modeling. By leveraging AI-driven techniques, security systems can identify previously unseen threats, detect patterns in vast datasets, and respond to cyber threats in real time. Despite their potential, AI-based malware detection systems face challenges, including adversarial attacks, dataset limitations, and interpretability concerns.

This paper provides a comprehensive review of the current state of AI and ML applications in malware detection. It critically analyzes existing research, identifies key challenges, and discusses potential future directions in the field. The goal is to assess the effectiveness of AI-driven malware detection and explore strategies for enhancing the robustness and reliability of these models in real-world cybersecurity applications.

II. LITERATURE REVIEW AND ANALYSIS

Traditional malware detection relies on signatures and heuristics but struggles with evolving threats. AI and ML offer adaptive solutions, improving detection accuracy. This section reviews existing methods, compares AI-driven approaches, and highlights key challenges in the field.

A. Traditional Malware Detection Techniques

Traditional malware detection techniques have evolved from signature-based approaches to more sophisticated heuristic and behavioral methods. Signature-based detection compares files against a database of known malware signatures, making it effective for detecting previously identified threats. However, its reliance on predefined patterns limits its ability to identify polymorphic or zero-day malware, which can evade detection by modifying their structure [1].

Heuristic malware detection identifies threats by analyzing patterns in code execution rather than relying on predefined signatures. It examines features like Application programming interfaces (API) calls, OpCode sequences, and control flow graphs to detect anomalies [2]. This allows it to recognize new and modified malware. API call analysis monitors interactions with system libraries, flagging suspicious behavior. However, obfuscated malware can disguise these calls, making detection harder.

OpCode-based detection analyzes machine instructions to find unusual execution patterns. While effective, it requires high computational resources. Control flow graphs (CFGs) map a program's execution structure to detect malicious patterns. Attackers, however, can modify the graph with code reordering or junk instructions to evade detection. Despite limitations, heuristic methods remain essential, especially when combined with machine learning [2].

Behavioral malware detection identifies threats by monitoring real-time execution, focusing on API calls, file changes, and network activity instead of predefined signatures. This makes it effective against novel malware, but attackers can evade detection by altering behavior in controlled environments.

Dynamic tracing, often using sandboxes like Cuckoo, logs malware actions for classification. Machine learning models, such as Random Forests, improve detection accuracy but require efficient feature selection to reduce computational overhead [3].

While these traditional techniques remain fundamental, the increasing complexity of malware, including polymorphic and metamorphic variants, highlights the need for more adaptive approaches such as machine learning-based detection methods.

B. AI and ML-Based Approaches in Malware Detection

AI and ML enhance malware detection by identifying patterns in large datasets, enabling the detection of novel and obfuscated threats. Unlike traditional methods, ML models learn from data, improving adaptability and accuracy. This section explores supervised and unsupervised learning techniques, deep learning models, and their role in modern cybersecurity.

C. Supervised Learning Models

Supervised learning models are widely used in malware detection, leveraging labeled datasets to classify software as malicious or benign. They learn from features like API calls, OpCode sequences, byte n-grams, and system events, identifying patterns in known malware. Common algorithms include Decision Trees, Random Forests, Support vector machines (SVM), and Neural Networks, achieving high accuracy [4]. In Android malware detection, these models effectively analyze app permissions and behavior to enhance classification [5].

Despite their strengths, supervised models struggle with zero-day malware, as they rely on historical data and fail to detect novel attack patterns. Their performance also depends on high-quality labeled datasets, which are difficult to obtain [4]. To improve adaptability, studies suggest hybrid approaches, feature selection techniques, and semi-supervised learning, which integrates labeled and unlabeled data for better real-world detection [5].

Another challenge in supervised malware detection is selecting the right model. SVM excels in high-dimensional spaces but requires careful tuning and is computationally expensive. Naïve Bayes is efficient for large datasets but assumes feature independence, which may not always hold. kNN is simple and effective for small datasets but struggles with high-dimensional features and requires optimal neighbor selection [6].

Classifier performance depends on dataset characteristics, feature selection, and computational limits. Combining models or optimizing feature representation can improve accuracy. Hybrid approaches integrating supervised learning with heuristic or behavioral analysis help address dataset limitations and enhance adaptability. However, reliance on labeled data and the challenge of robust generalization remain key obstacles in dynamic environments [6].

Supervised learning is used in network-based malware detection, where feature selection enhances accuracy and efficiency. Manzano et al. [7] found that reducing high-dimensional network traffic data with PCA and Logistic Regression filtering improved classification. Among tested models, Random Forest achieved the highest accuracy, highlighting the role of feature selection in optimizing detection while minimizing computational overhead [7].

Supervised learning models classify malware based on features like API calls and OpCode sequences. Algorithms such as Decision Trees, Random Forests, and SVMs achieve high accuracy, especially in Android and network-based detection. However, reliance on labeled data limits adaptability and effectiveness against zero-day threats.

To mitigate these issues, researchers explore hybrid models, feature selection, and semi-supervised learning. Feature selection, particularly in network traffic analysis, improves accuracy and reduces computational costs. Studies show that PCA and Logistic Regression filtering enhance model efficiency, with Random Forest often outperforming others in network-based detection.

Despite advancements, the need for high-quality training data and model generalization remain major challenges. Future research should focus on improving adaptability, integrating multiple detection techniques, and reducing dependence on labeled datasets to enhance scalability and accuracy.

D. Unsupervised Learning Models

Unsupervised learning has been explored in malware detection to identify anomalies without relying on labeled datasets. Tang et al. [8] proposed an approach using hardware performance counters (HPCs) to detect deviations in processor behavior caused by malware. By analyzing execution patterns of common applications like web browsers and Portable Document Format (PDF) readers, they demonstrated that malware exploits introduce measurable anomalies at the hardware level. This method effectively detects zero-day threats, but challenges remain in minimizing false positives and evasion tactics. Malware can be designed to mimic normal execution, reducing detection accuracy. Further research focuses on improving anomaly detection models and integrating them with other techniques to enhance robustness against adaptive malware [8].

Building on the use of unsupervised learning for malware detection, Arora et al. [9] proposed a hybrid approach that combines both supervised and unsupervised learning to improve Android malware detection. Their method integrates static and dynamic features, analyzing both app permissions and network traffic patterns. By applying K-Medoids clustering for initial data grouping and then using K-Nearest Neighbors (KNN) for classification, their model achieved an accuracy of 91.98%, outperforming standalone static and dynamic approaches. This study highlights the advantages of combining different learning techniques to enhance detection accuracy. While static analysis alone struggles with stealthy malware that modifies its behavior over time, dynamic analysis has limitations when dealing with offline malware. The hybrid approach addresses these weaknesses by leveraging both feature sets, demonstrating the effectiveness of integrating supervised and unsupervised learning for more robust malware detection [9].

Mahindru et al. [10] introduced SemiDroid, an unsupervised malware detection framework that leverages feature selection to improve classification performance. Their approach focuses on Android malware detection by analyzing API calls and permissions while utilizing clustering-based machine learning models. The study applied ten distinct feature selection techniques and five unsupervised learning algorithms, demonstrating that the farthest-first clustering algorithm combined with rough set analysis achieved the highest detection rate of 98.8%. This research highlights the importance of feature selection in unsupervised malware detection. SemiDroid reduces feature dimensionality to boost accuracy and efficiency, enabling effective detection of unknown malware without relying on labeled data. [10].

Unsupervised learning helps detect zero-day malware by identifying execution anomalies without labeled data. Tang et al. (2014) used hardware performance counters for detection but faced issues with false positives and evasion. Arora et al. (2018) improved accuracy by clustering malware before classification in a hybrid approach, though it still relied on feature engineering. Mahindru et al. (2020) advanced unsupervised detection with SemiDroid, optimizing feature selection to reduce computational costs while maintaining accuracy. This underscores the role of feature selection in generalization. Future research should refine anomaly detection and integrate behavioral analysis for greater robustness.

E. Combination of Supervised and Unsupervised Learning Models

Combining supervised and unsupervised learning enhances malware detection by leveraging the strengths of both approaches. Comar et al. [11] introduced a two-stage classification framework for detecting zero-day malware. The first stage employs a supervised model to classify known threats, while the second stage applies unsupervised clustering to identify new malware strains. This hybrid approach improves adaptability and detection accuracy by addressing the limitations of purely supervised methods, which struggle with novel threats.

The study also highlights the use of a probabilistic class-based profiling method to refine detection performance. By analyzing network flow characteristics at layers 3 and 4, the framework distinguishes malicious activity from legitimate traffic. It also employs a tree-based feature transformation technique to mitigate data imperfections such as noise and missing values. The results demonstrate that integrating supervised and unsupervised learning improves detection precision, particularly for polymorphic and encrypted malware variants [11].

Combining supervised and unsupervised learning offers a more effective approach to malware detection. Supervised models excel at identifying known threats but fail against zero-day malware. Unsupervised methods detect unknown threats but often generate high false positive rates. A hybrid approach balances these strengths, improving adaptability while maintaining accuracy.

The study by Comar et al. [11] demonstrates that integrating both techniques enhances detection precision, especially for polymorphic malware. However, the effectiveness of such models depends on selecting optimal clustering techniques and reducing computational overhead. Feature selection and anomaly detection improvements are necessary to refine hybrid models further. Future research should focus on optimizing these methods while ensuring scalability and real-time applicability in cybersecurity environments.

F. Deep Learning Approaches

Deep learning has significantly improved malware detection by addressing the limitations of traditional static and dynamic analysis. Shaukat et al. (2023) proposed a novel hybrid approach that transforms malware binaries into colored images. These images are processed using convolutional neural networks (CNNs) to extract deep features, which are then classified using Support Vector Machines (SVMs). This method eliminates the need for manual feature engineering, making detection more efficient and scalable. The proposed

model achieved 99.06% accuracy on the Maling dataset, outperforming traditional machine learning approaches [12].

A key advantage of this approach is its ability to detect malware across different families without requiring extensive handcrafted features. Additionally, the study introduced data augmentation techniques to handle class imbalance, improving model generalization. Despite its success, deep learning-based malware detection faces challenges. Models must be robust against adversarial attacks, where malware is modified to deceive classifiers. Another limitation is high computational cost, making real-time detection more difficult. Future research should focus on improving model efficiency and enhancing adversarial resilience to ensure deep learning remains a viable solution in cybersecurity [12].

Recent advancements in deep learning have significantly improved malware detection. Vinayakumar et al. (2019) proposed a hybrid malware analysis system called ScaleMalNet, which integrates classical machine learning, deep learning, and image processing techniques. This framework uses a two-stage detection process. In the first stage, it applies static and dynamic analysis to identify malicious samples. The second stage categorizes detected malware into specific families. ScaleMalNet demonstrated improved accuracy compared to traditional methods by leveraging deep learning architectures such as CNNs and autoencoders [13].

A key strength of this approach is its scalability, allowing the integration of various data sources for continuous learning. Additionally, the system applies self-learning techniques to refine detection over time. However, the study also highlights challenges, such as computational complexity and the need for substantial training data. Future research should focus on optimizing deep learning models for real-time detection while addressing adversarial robustness [13].

Expanding on deep learning-based malware detection, Rathore et al. (2018) explored the effectiveness of different machine learning and deep learning models for identifying malicious software. Their study compared traditional classifiers, such as Random Forest, with deep neural networks of varying depths. Surprisingly, Random Forest outperformed deep learning models in their experiments, achieving 99.78% accuracy when combined with a variance threshold-based feature reduction technique. This suggests that deep learning models, while powerful, may be overkill for certain datasets, particularly when feature selection is optimized [14].

The study also highlighted the limitations of deep learning in malware detection. Complex models, such as autoencoders and deep neural networks, suffered from overfitting and increased computational costs. This reinforces the need for careful feature selection and model tuning to ensure deep learning methods remain practical for large-scale deployment. Future research should explore how to improve generalization, reduce training complexity, and integrate deep learning with other detection techniques for a more adaptive approach [14].

Ding et al. (2017) proposed a deep learning-based malware detection approach using Deep Belief Networks (DBNs). Their model represents malware as opcode sequences and uses DBNs for classification. Unlike traditional shallow models, DBNs utilize unsupervised pretraining to extract meaningful features from data, improving detection accuracy. The study compared DBNs with Support Vector Machines (SVM), Decision Trees, and k-Nearest Neighbors (kNN), demonstrating that DBNs outperform these conventional classifiers. Addi-

tionally, using unlabeled data for pretraining enhanced model performance, showcasing the potential of deep learning in detecting unknown malware variants while reducing reliance on labeled datasets [15].

Deep learning enhances malware detection by automating feature extraction and improving classification accuracy. CNN-based methods, like Shaukat et al. (2023), achieve high accuracy by converting malware binaries into images. Hybrid models, such as ScaleMalNet, further improve detection by combining static and dynamic analysis. While scalable and adaptable, these methods face challenges like high computational costs and adversarial attacks.

Interestingly, Rathore et al. (2018) found that traditional models, like Random Forest, can outperform deep learning with effective feature selection, highlighting deep learning's limitations in resource-constrained environments. Future research should refine deep learning for real-time deployment, improve generalization, and integrate feature selection for better efficiency and accuracy.

G. Comparison of Machine Learning Approaches in Malware Detection

Machine learning has advanced malware detection, with each approach offering strengths and limitations. Supervised learning excels at identifying known threats but struggles with zero-day attacks and requires frequent updates. Unsupervised learning detects unknown malware by spotting anomalies, making it more adaptable but prone to false positives.

Hybrid models combine both approaches, classifying known threats while clustering unknown malware for further analysis. This improves detection but requires careful tuning to balance accuracy and computational efficiency.

Deep learning automates feature extraction and improves detection rates using CNNs and other architectures to analyze raw data like binary files or network traffic. However, challenges include high computational costs, overfitting, and vulnerability to adversarial attacks.

The optimal approach depends on dataset quality, resources, and detection needs. While supervised learning is effective for known malware, unsupervised and hybrid methods adapt better to evolving threats. Deep learning, though powerful, requires refinement to balance accuracy, efficiency, and resilience. Future research should focus on integrating these methods for scalable, real-time malware detection.

III. PROBLEM IDENTIFICATION AND FUTURE DIRECTIONS

Malware detection faces several critical challenges that hinder the effectiveness of existing models. One significant issue is class imbalance, where datasets often contain more benign samples than malicious ones, leading to biased models that may struggle to detect less common malware variants accurately. Additionally, concept drift poses a challenge, as malware constantly evolves, rendering static models ineffective over time. Adaptive learning techniques are necessary to keep pace with these rapid changes and ensure detection methods remain relevant [16].

Another pressing issue is adversarial attacks, where malware authors intentionally modify malicious code to evade detection. Many machine learning models are vulnerable to such manipulations, reducing their reliability in real-world applications. Additionally, the scalability of malware detection

remains a concern, as the volume of new malware samples continues to grow exponentially. Effective detection systems must process large datasets quickly while maintaining accuracy, requiring improvements in computational efficiency and model optimization [17] [18].

Deep learning models, while highly effective, often lack interpretability, making it difficult for cybersecurity experts to understand and trust their decision-making processes. Transparent and explainable AI models are essential to ensure these systems can be audited and improved upon. Furthermore, data privacy and legal concerns arise when AI-driven detection systems analyze large-scale user data. Striking a balance between robust malware detection and compliance with legal and ethical standards is crucial for practical implementation [19].

To address these challenges, future research should focus on developing adaptive models capable of learning from new threats in real-time. Enhancing model transparency will allow cybersecurity professionals to interpret and validate detection results more effectively. Improving adversarial robustness through advanced training methods can help mitigate evasion techniques used by attackers. Additionally, privacy-preserving AI techniques should be explored to ensure compliance with regulatory standards while maintaining detection performance. Finally, optimizing scalability through efficient algorithms and cloud-based solutions will allow detection systems to process large volumes of malware data without significant performance trade-offs [20].

Some malware detection challenges are easier to solve than others. Class imbalance can be addressed with data augmentation, synthetic samples, and cost-sensitive learning, improving detection of rare malware variants. Concept drift remains a challenge, but adaptive models with real-time updates and reinforcement learning help counter emerging threats.

Adversarial attacks are harder to resolve, as malware authors constantly evolve their techniques. While adversarial training and robust feature extraction help, detection remains an ongoing challenge. Deep learning interpretability is also difficult, with Explainable artificial intelligence (XAI) improving but not fully solving transparency issues. Scalability can be mitigated with cloud-based solutions and model compression, yet real-time processing of vast malware data remains a challenge.

Future research should explore hybrid methods and lightweight deep learning for real-time, efficient malware detection. Privacy-preserving AI, like federated learning, offers secure collaboration. These steps can boost adaptability and defense against emerging threats.

IV. CONCLUSION

The rapid evolution of malware challenges detection systems. Traditional methods struggle with zero-day attacks, while machine learning improves adaptability. Supervised learning offers high accuracy but depends on labeled data, while unsupervised learning detects unknown threats but generates false positives. Hybrid models balance both approaches, and deep learning enhances detection but faces high computational costs and adversarial risks.

Future research should focus on scalability, interpretability, and privacy-preserving AI. Adaptive models that continuously learn from new threats will be crucial for proactive cybersecurity, refining detection and optimizing efficiency.

REFERENCES

- [1] S. K. Sahay, A. Sharma, and H. Rathore, "Evolution of malware and its detection techniques," in *Information and Communication Technology for Sustainable Development*. Springer Singapore, 2020. [Online]. Available: https://link.springer.com/chapter/10.1007/978-981-13-7166-0_14
- [2] Z. Bazrafshan, H. Hashemi, S. M. H. Fard, and A. Hamzeh, "A survey on heuristic malware detection techniques," in *The 5th Conference on Information and Knowledge Technology*, 2013. [Online]. Available: <https://ieeexplore.ieee.org/abstract/document/6620049>
- [3] S. S. Hansen, T. M. T. Larsen, M. Stevanovic, and J. M. Pedersen, "An approach for detection and family classification of malware based on behavioral analysis," in *2016 International Conference on Computing, Networking and Communications (ICNC)*, 2016. [Online]. Available: <https://ieeexplore.ieee.org/abstract/document/7440587>
- [4] I. Santos, J. Nieves, and P. G. Bringas, "Semi-supervised learning for unknown malware detection," in *International Symposium on Distributed Computing and Artificial Intelligence*, 2011. [Online]. Available: https://link.springer.com/chapter/10.1007/978-3-642-19934-9_53
- [5] T. A. Abdullah, W. Ali, and R. Abdulghafor, "Empirical study on intelligent android malware detection based on supervised machine learning," *International Journal of Advanced Computer Science and Applications*, vol. 11, no. 4, 2020. [Online]. Available: https://www.researchgate.net/publication/341071139_Empirical_Study_on_Intelligent_Android_Malware_Detection_based_on_Supervised_Machine_Learning
- [6] M. Kruczkowski and E. Niewiadomska-Szynkiewicz, "Comparative study of supervised learning methods for malware analysis," *Journal of Telecommunications and Information Technology*, 2014. [Online]. Available: <https://jtit.pl/jtit/article/view/1044>
- [7] C. Manzano, C. Meneses, P. Leger, and H. Fukuda, "An empirical evaluation of supervised learning methods for network malware identification based on feature selection," *Complexity*, 2022. [Online]. Available: <https://onlinelibrary.wiley.com/doi/abs/10.1155/2022/6760920>
- [8] A. Tang, S. Sethumadhavan, and S. J. Stolfo, "Unsupervised anomaly-based malware detection using hardware features," in *Research in Attacks, Intrusions and Defenses*, 2014. [Online]. Available: https://link.springer.com/chapter/10.1007/978-3-319-11379-1_6
- [9] A. Arora, S. K. Peddoju, V. Chouhan, and A. Chaudhary, "Hybrid android malware detection by combining supervised and unsupervised learning," in *Proceedings of the 24th Annual International Conference on Mobile Computing and Networking*, 2018. [Online]. Available: <https://doi.org/10.1145/3241539.3267768>
- [10] A. Mahindru and A. L. Sangal, "Semidroid: a behavioral malware detector based on unsupervised machine learning techniques using feature selection approaches," *International Journal of Machine Learning and Cybernetics*, 2021. [Online]. Available: <https://doi.org/10.1007/s13042-020-01238-9>
- [11] P. M. Comar, L. Liu, S. Saha, P.-N. Tan, and A. Nucci, "Combining supervised and unsupervised learning for zero-day malware detection," in *2013 Proceedings IEEE INFOCOM*, 2013. [Online]. Available: <https://ieeexplore.ieee.org/abstract/document/6567003>
- [12] K. Shaukat, S. Luo, and V. Varadharajan, "A novel deep learning-based approach for malware detection," *Engineering Applications of Artificial Intelligence*, 2023. [Online]. Available: <https://www.sciencedirect.com/science/article/pii/S0952197623002142>
- [13] R. Vinayakumar, M. Alazab, K. P. Soman, P. Poornachandran, and S. Venkatraman, "Robust intelligent malware detection using deep learning," *IEEE Access*, 2019. [Online]. Available: <https://ieeexplore.ieee.org/abstract/document/8681127>
- [14] H. Rathore, S. Agarwal, S. K. Sahay, and M. Sewak, "Malware detection using machine learning and deep learning," in *Big Data Analytics*, 2018. [Online]. Available: https://link.springer.com/chapter/10.1007/978-3-030-04780-1_28
- [15] D. Yuxin and Z. Siyi, "Malware detection based on deep learning algorithm," *Neural Computing and Applications*, 2019. [Online]. Available: <https://doi.org/10.1007/s00521-017-3077-6>
- [16] W. Kegelmeyer, K. Chiang, and J. Ingram, "Streaming malware classification in the presence of concept drift and class imbalance," 2013. [Online]. Available: https://www.researchgate.net/publication/262168867_Streaming_Malware_Classification_in_the_Presence_of_Concept_Drift_and_Class_Imbalance
- [17] F. Ceschin, M. Botacin, H. M. Gomes, F. Pinagé, L. S. Oliveira, and A. Grégio, "Fast & furious: Modelling malware detection as evolving data streams," *arXiv preprint arXiv:2205.12311*, 2022. [Online]. Available: <https://arxiv.org/abs/2205.12311>
- [18] Lumenova, "Adversarial attacks on machine learning: Detection and defense strategies," 2024. [Online]. Available: <https://www.lumenova.ai/blog/adversarial-attacks-ml-detection-defense-strategies/>
- [19] A. Paracha, J. Arshad, M. Farah *et al.*, "Machine learning security and privacy: a review of threats and countermeasures," *EURASIP Journal on Information Security*, 2024. [Online]. Available: <https://doi.org/10.1186/s13635-024-00158-3>
- [20] J. J. Hathaliya, S. Tanwar, and P. Sharma, "Adversarial learning techniques for security and privacy preservation: A comprehensive review," 2022. [Online]. Available: <https://onlinelibrary.wiley.com/doi/abs/10.1002/spy2.209>

Advanced Physical Approaches to Presenting Physical Phenomena Using AR

¹Ivana NOVÁKOVÁ (3rd year)
Supervisor: ²Miroslav MICHALKO

^{1,2}Dept. of Computers and Informatics, FEEI, Technical University of Košice, Slovak Republic

¹ivana.novakova@tuke.sk, ²miroslav.michalko@tuke.sk

Abstract— This paper aims to investigate and propose a structured approach to incorporating physical phenomena into AR applications, particularly on industrial environments. Our focus is on developing and implementing an algorithm that seamlessly integrates vSLAM techniques with the advanced modeling of physical processes, enhancing the precision and resilience of augmented reality in complex and demanding production settings.

Keywords—Algorithm, Augmented Reality (AR), Industrial environments, Physical Phenomena, vSLAM

I. INTRODUCTION

Augmented Reality is a rapidly evolving technology that overlays computer-generated imagery onto a user's perception of the real world, offering a blended experience that enhances the understanding of physical phenomena [1]. In contemporary industrial settings, where AR/MR technologies are emerging as pivotal elements in digitalization and process optimization, ensuring exceptional precision and robustness in localization and mapping solutions is imperative. Visual Simultaneous Localization and Mapping (vSLAM) [2] algorithms form the foundation of modern visual navigation systems; however, their efficiency can be significantly compromised by a range of physical phenomena, such as dynamic illumination, mechanical vibrations, and temperature fluctuations. In this context, we propose an extended theoretical framework that integrates additional physical parameters into an adaptive vSLAM model, thereby enhancing the system's resilience and accuracy even under extreme industrial conditions.

II. ASPECTS OF PHYSICAL PHENOMENA

The industrial environment is highly dynamic, characterized by numerous unpredictable changes, large data flows, increased noise levels, dust accumulation, intensified movement of personnel and autonomous machines, high temperatures, and vibrations, which can negatively impact the implementation of augmented reality (AR) technology. To successfully integrate physical phenomena into vSLAM algorithms, it is essential to identify and quantify key factors that directly influence the quality of sensor data and the subsequent interpretation of the environment. The main aspects include:

A. Lighting dynamics and shading

Variability in light intensity, reflections, and shading can cause significant changes in the quality of image data, thereby affecting feature extraction and the robustness of visual analysis. [3] In industrial environments where lighting may be either excessive or insufficient, visual odometry techniques often fail to capture sufficient distinctive features required for accurate mapping and localization of robotic systems. This deficiency can lead to inaccuracies [4] when compared against reference maps created under optimal lighting conditions, which are not always available. To ensure visual comfort in indoor workspaces, minimizing disruptive glare caused by lighting fixtures is essential. The Unified Glare Rating (UGR) method was developed to assess this glare, providing a standardized approach to quantifying potential discomfort caused by indoor lighting. [4] Light intensity I affects the quality of visual data, where $I(x,y)$ represents illumination at point (x,y) . Reflective effects are modeled using the Lambertian reflectance model:

$$I_R = I_0 \cos(\theta)$$

where I_R is reflected light, I_0 is incident light intensity, and θ is the angle of incidence.

B. Mechanical vibration and shocks

Industrial equipment generates significant mechanical fluctuations, which can degrade the accuracy of sensors such as cameras and inertial measurement units (IMU). In an industrial environment, vibrations are significantly increased with various sources such as transportation, vibrations generated during machine or equipment operation, and machine movement. A possible solution involves noise reduction by implementing filters that eliminate noise from sensor data, deploying robust vibration-resistant sensors, developing specialized algorithms, or physically isolating sensors from the vibration source. Acceleration [5] $a(t)$ affects the accuracy of inertial sensors. Mechanical vibrations can be described as harmonic oscillations:

$$A(t) = A \cos(\omega t + \phi)$$

Where A is vibration amplitude, ω angular frequency, and initial phase. To mitigate noise in sensor measurements, the Kalman filter recursively estimates the system state by optimally combining predicted values with real-time sensor

data, effectively reducing uncertainties caused by measurement noise and environmental disturbances.[6]

C. Temperature Fluctuations

Temperature changes significantly affect sensor calibration parameters, potentially leading to systematic deviations in measured data. High temperatures can reduce the accuracy of sensors and SLAM algorithms, accumulating computational errors. Temperature-sensitive sensors may exhibit decreased reliability, negatively impacting algorithm performance. To mitigate these effects, temperature regulation mechanisms, such as active cooling systems and thermal stabilizers, are implemented to ensure optimal operation in extreme conditions.[7] In addition to hardware solutions, algorithm parameters can be adaptively adjusted, for example, by modifying filters or applying automatic sensor calibration to compensate for temperature fluctuations.

IV.

$$T_{\text{corr}} = T_{\text{measured}} - \alpha \cdot \Delta T$$

D. Electromagnetic and Acoustic Interference:

Although their impact is secondary, these phenomena can negatively affect the synchronization and accuracy of multisensor fusion,[8] similar to the effect of fine dust particles in a dusty environment.

III. DESIGN OF ARCHITECTURE OF NEW ALGORITHM

A. Sources and Types of Input Data

To develop an adaptive and robust algorithm, it is essential to synergistically integrate multiple data types, with each source requiring precise calibration and synchronization. Visual data [9] (RGB-D cameras, stereo visual sensors), inertial measurements (IMU for capturing acceleration and angular velocity), physical sensors (temperature, vibration, and acoustic sensors), and geodetic/reference data (GPS and local reference systems) collectively contribute to a comprehensive multisensor input framework.

Table 1. Framework of Processing Input Data

Theoretical Framework for Processing Input Data		
Section	Key aspects	Description
Data Preprocessing	Normalization and Filtering	Improves contrast, reduces noise, and calibrates IMU data for vibrations.
	Sensor	Synchronizes timestamps from all sensors for multisensor
Calibration and Adaptive Models	Calibration Models	Adjusts to temperature, lighting, and vibration changes for optimal algorithm parameters.
	Adaptive Data Weighting	Dynamically adjusts sensor weights based on data quality.
Integration of Physical Phenomena into vSLAM	State Vector Expansion	Adds temperature and vibration parameters to vSLAM.
	Noise Modeling	Uses Kalman or particle filters to compensate for environmental noise.
	Iterative Learning	Applies machine learning for

B. Design of the architecture

The algorithm should consist of the following modules:

Data Collection and Preprocessing: A module responsible for synchronizing, normalizing, and calibrating input data from all sensors.

Multisensor Fusion: A module integrating data from visual, IMU, and physical sensors using adaptive weighting schemes and noise models.

Localization and Mapping: An enhanced version of traditional vSLAM, which, in addition to geometric reconstruction, incorporates corrections based on physical parameters.

Learning and Optimization: A module for continuous learning that utilizes historical data to optimize sensor calibration parameters and weighting adjustments.

IV. AN ADAPTIVE MULTI-PHYSICS ENHANCED VISUAL SLAM FRAMEWORK FOR INDUSTRIAL AUGMENTED REALITY

The proposed Adaptive Multi-Physics Enhanced vSLAM (AMP-vSLAM) algorithm represents a more robust SLAM-based algorithm and offers several advancements to improve AR applications in dynamic industrial environments. It addresses real-world challenges with multi-physics adaptation, self-learning mechanisms, deep understanding of the scene, and resistance to industrial noise.

Table 2. Enhancement vSLAM

Feature	Traditional vSLAM	AMP-vSLAM (Proposed)
Lighting Adaptation	Fixed exposure	Adaptive brightness & Lambertian Reflection
Temperature Compensation	None	Automatic sensor calibration
Vibration Resistance	Limited filtering	Kalman-based compensation & IMU correction
Sensor Weighting	Fixed	Bayesian adaptive weighting
Deep Learning Adaptation	None	CNN-based scene prediction
Object Handling	Basic tracking	Semantic segmentation & occlusion detection
Dust Resistance	None	Infrared-based depth sensing
EMI Compensation	No handling	EMI-aware sensor fusion

Traditional vSLAM systems rely on fixed sensor weighing, which does not work correctly in dynamic industrial environments. The proposed AMP-vSLAM is a self-learning module that automatically adjusts the sensor's importance based on the quality of the incoming data. The system continuously evaluates the reliability of each sensor using Bayesian inference (visual, IMU, thermal, acoustic). Sensors that provide noisy data are automatically filtered out, while more reliable sensors are favored. The system stores historical sensor values and environmental data. Machine learning models analyze this information to predict the optimal weighting for sensors based on past conditions, and the system saves these calculated values. If the industrial site is known to experience significant temperature fluctuations, the system will proactively adjust the thermal correction factors. Real-time

sensor correction is updated every 0.1 seconds based on live sensor feedback.

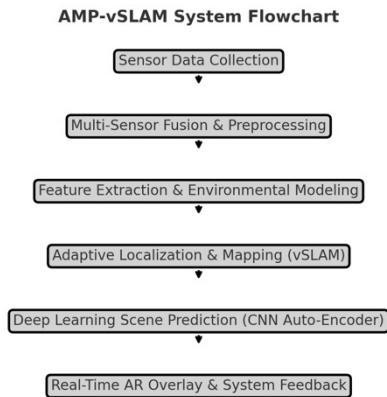


Figure 1.FLOWCHART

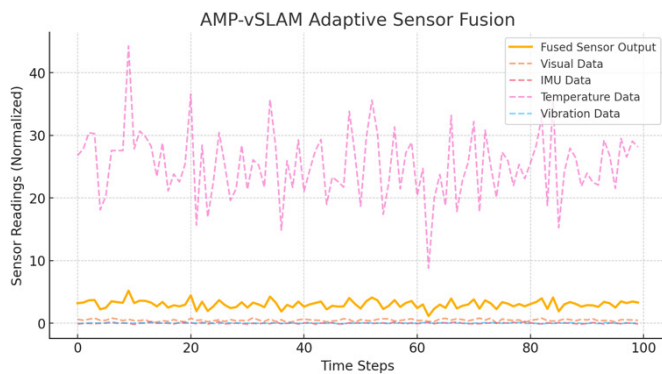


Figure 2.Adaptive Sensor Fusion

V. CONCLUSION

This study provides a theoretical framework for improving algorithms in SLAM by integrating physical factors into augmented reality applications. The proposed AMP-vSLAM is an advanced visual simultaneous localization and mapping framework (vSLAM) designed for industrial augmented reality (AR) applications. It enhances traditional vSLAM by integrating multiphysical modeling designed for dynamic industrial environments.

ACKNOWLEDGMENT

This publication was realized with the support of the Operational Programme Integrated Infrastructure in the framework of the project Intelligent systems for UAV real-time operation and data processing, code ITMS2014+: 313011V422, which was co-financed by the European Regional Development Fund.

REFERENCES

- [1] Li, X., Xie, M., & Chu, J. (2019). Exploring the Application of Serious Game Based on Augmented Reality: A Case Study on Tsingtao Beer Museum. In IOP Conference Series Materials Science and Engineering (Vol. 573, Issue 1, p. 12069). IOP Publishing. <https://doi.org/10.1088/1757-899x/573/1/012069>
- [2] Hamid Taheri and Zhao Chun Xia. 2021.SLAM; definition and evolution.*Engineering Applications of Artificial Intelligence* 97 (2021), 104032.
- [3] Yu, Shun-Yuan & Zhu, Hong. (2017). Low-Illumination Image Enhancement Algorithm Based on a Physical Lighting Model. IEEE Transactions on Circuits and Systems for Video Technology. PP. 1-1. 10.1109/TCSVT.2017.2763180.
- [4] Commission Internationale de l'Eclairage. Discomfort Glare in Interior Lighting, CIEPublication 117. Vienna: CIE, 1995.
- [5] Bhardwaj, Renu & Kumar, Neelesh & Kumar, Vipin. (2017). Errors in micro-electro-mechanical systems inertial measurement and a review on present practices of error modelling. Transactions of the Institute of Measurement and Control. 40. 014233121770823. 10.1177/0142331217708237. Ma'arif, Alfian & Iswanto, & Nuryono, Aninditya & Alfian, Rio. (2020).
- [6] Kalman Filter for Noise Reducer on Sensor Readings. Signal and Image Processing Letters. 1. 11-22. 10.31763/simple.v1i2.2.
- [7] Małek, Maria & Koczyk, Halina. (2024). Influence of Temperature Sensor (Pt100) Accuracy on the Interpretation of Experimental Results of Measuring Temperature on the Surface. Civil and Environmental Engineering Reports. 34. 1-21. 10.59440/ceer/192146.
- [8] Qiu, S., Zhao, H., Jiang, N., Wang, Z., Liu, L., An, Y., Zhao, H., Miao, X., Liu, R., & Fortino, G. (2022). Multi-sensor information fusion based on machine learning for real applications in human activity recognition: State-of-the-art and research challenges. *Information Fusion*, 80, 241–265. <https://doi.org/10.1016/J.INFUS.2021.11.006>
- [9] Cai, Yiyi & Ou, Yang & Qin, Tuanfa. (2024). Improving SLAM Techniques with Integrated Multi-Sensor Fusion for 3D Reconstruction. Sensors. 24. 2033. 10.3390/s24072033.

Author's index

- B**
Badár Jozef 58
Balara Viliam 147
Basarik Tomáš 34
Bobček Marek 36
Bubeňková Lenka 118
Buček Tomáš 122
- Č**
Čatloch Dušan 182
- D**
Dopiriak Matúš 74
- E**
Eliáš Kristián 63
Eliáš Martin 93
- G**
Geciová Nikola 28
Glajc Kristián 166
Gordan Daniel 56
- H**
Horváth Marek 23
Hric Ladislav 10
Hric Matej 106
Hyseni Ardian 139
- I**
Imrich Miroslav 76
- J**
Jusko Miroslav 39
- K**
Kališková Lenka 174
Katonová Erika Abigail 163
Khorshidiyeh Heidar 142
Kmecik Tadeáš 21
Kormaník Tomáš 18
Kováčová Antónia 32
Král Richard 43
Krupáš Maroš 145
Kupcova Eva 97
Kurimský František 159
- L**
Líšková Dominika 52
- M**
Marcin Daniel 87
Margita František 153
Marko Jaroslav 99
Matejová Miroslava 103
Matašová Sylvia 110
Miakota Dmytro 90
Murin Miroslav 156
- N**
Nemergut Peter 83
Nguyen Martin 80
- Nováková Ivana 187
Novotný Samuel 129
- O**
Ondriš Leoš 177
- P**
Pancurák Lukáš 180
Pekarčík Peter 26
Popřík Peter 131
- R**
Rauch Róbert 115
Runsáková Renáta 48
- S**
Saparová Simona 71
Sevc Kamil 135
Sopkovic Kristian 125
- Š**
Šimčák Július 67
- T**
Tomaščík Lukáš 14
- U**
Urblick Eubomír 151
- Z**
Zolochovska Kristina 171



SCYR 2025: 25th Scientific Conference of Young Researchers

Proceedings from Conference

Published: Faculty of Electrical Engineering and Informatics
Technical University of Košice

Edition I, 192 pages
Available Online

Editors:

Assoc. Prof. Ing. Karol Kyslan, CSc.
Assoc. Prof. Ing. Emília Pietriková, PhD.
Ing. Lukáš Pancurák

ISBN 978-80-553-4826-1